Statistical Testing of Downscaled Rainfall Data for Water Security Assessment

by

Nadeeka Parana Manage

A thesis submitted for the degree of Doctor of Philosophy in the field of Environmental Engineering

THE UNIVERSITY OF
NEWCASTLE
AUSTRALIA

December 2016

I hereby certify that this thesis contains no material which has been submitted for the award of any other degree or diploma in any university or other tertiary institution and, to the best of my knowledge work embodied in this thesis is the result of original research.

_____

Nadeeka Parana Manage

Acknowledgements

Undertaking this PhD has been a life changing experience in my life and it would have not been possible without the support and advice from my supervisors, family, friends and colleagues.

To my supervisors, Garry Willgoose, Natalie Lockart and Anthony Kiem, and also George Kuczera, a big thank you for all your help, support and guidance throughout this journey. Your insightful comments and encouragements provided to widen my research from various perspectives. Without your guidance and constant feedback this PhD would not have been achievable.

To my fellow PhD students and friends, thank you for your support and encouragements. A particular thank you to Kamal Chowdhury, Lanying Zhang, Callum Twomey and Nalin Seneviratne for being good friends and helping for my research. I also thank you to all the administrative staff of the School of Engineering.

To my parents, Nelsan and Asilda, and my family, thank you for your blessings towards me to achieve all my life goals, though you all are thousand miles away from me. Thanks for raising me and believing in me.

Last but not the least, Shalika, thank you for your love, understanding and patience during the past three and half years. Words cannot express how thankful I am.

Funding for this project was provided by an Australian Research Council Linkage Grant LP120200494 ("The influence of East Coast Lows on the water security of coastal New South Wales"), the NSW Office of Environment and Heritage, NSW Department of Financial Services, NSW Office of Water, and Hunter Water Corporation.

Table of Contents

Abstract x

Chapter 1 Introduction 1

1.1 General background 1

1.2 Objectives and scope 3

1.3 Overview of the thesis 4

Chapter 2 Background 9

2.1 Introduction 9

2.2 GCM rainfall projections 9

2.3 Climate of Eastern Australia and ECLs 10

2.4 Evaluating GCM projections for the Australian Climate 11

2.5 Downscaling GCMs 20

2.6 Evaluation of RCM simulations 21

2.6.1 Evaluation of RCM simulations outside Australia 22

2.6.2 Evaluation of RCM simulations over Australia 24

2.6.3 NARCliM - High-resolution RCM data for southeast Australia 26

2.6.4 Evaluation of NARCliM RCM simulations 34

2.6.5 Validation needs for NARCliM 40

2.7 Summary and motivations of this thesis 42

Chapter 3 Sites and Data 49

3.1 Introduction 49

3.2 Site description 49

3.2.1 Merriwa site 52

3.2.2 Williams River site 52

3.2.3 Richmond River site 53

3.2.4 Sydney site 54

3.2.5 Bega River site 55
3.3 Data 56
3.3.1 NARCliM Rainfall data 56
3.3.2 Observed rainfall 58
3.3.3 AWAP 65
3.3.4 Elevation data 66
3.3.5 ECL data 66
Chapter 4 Methodology 69
4.1 Introduction 69
4.2 Probability distribution of the rainfall 74
4.3 Spatial variability of the rainfall statistics 74
4.4 Temporal autocorrelation of the rainfall 75
4.5 Spatial correlation of the rainfall 77
4.6 Cross correlation of the rainfall 84
Chapter 5 Statistical Testing of NARCliM reanalysis rainfall data (1950-2009) for the Upper Hunter Region, New South Wales, Australia 87
5.1 Introduction 87
5.1.1 NARCliM and observed rainfall 88
5.1.2 Single grid point analysis 89
5.1.3 Spatial variability of statistics at catchment scale 101
5.2 Conclusions 107
Chapter 6 Testing the rainfall statistics of NARCliM uncorrected and bias-corrected reanalyses using AWAP data for the broader East Coast of Australia 109
6.1 Introduction 109
6.2 Probability distribution of the daily rainfall 112
6.3 Spatial Variability of the rainfall 121
6.3.1 Mean rainfall 121
6.3.2 Coefficient of variation of the rainfall 131

6.3.3 Lag-1 autocorrelation of the rainfall 148

6.4 Autocorrelation Functions of the rainfall 162

6.5 Some insights on the seasonality 177

6.6 Summary and Conclusions 178

Chapter 7 Testing the uncorrected and bias-corrected NARCliM reanalyses data using spatial correlation of the rainfall 181

7.1 Introduction 181

7.2 Spatial correlation of NARCliM reanalyses and AWAP rainfall 187

7.3 Testing the spatial correlation of NARCliM reanalyses and AWAP against rain gauge data 210

7.4 Conclusions 213

Chapter 8 East Coast Low impacts on the relationship between rainfall and elevation…… 215

8.1 Introduction 215

8.2 Mean annual rainfall vs Elevation 216

8.3 Impacts from the East Coast Lows (ECL) 220

8.4 A combined approach: ECL impacts on the relationship between the rainfall and elevation 221

8.5 Assessment of the rainfall in two regions 222

8.6 Conclusions 225

Chapter 9 Testing NARCliM GCM simulations using the probability distribution of the rainfall… 229

9.1 Introduction 229

9.2 Probability distribution of the rainfall 229

9.3 Conclusions 242

Chapter 10 Testing the spatial variability of the NARCliM downscaled GCM uncorrected and bias-corrected rainfall 243

10.1 Introduction 243

10.2 Spatial variability of the rainfall statistics 243
10.2.1 Mean rainfall 243
10.2.2 Standard deviation of the rainfall 251
10.2.3 Coefficient of variation of the rainfall 260
10.2.4 Lag-1 autocorrelation of the rainfall 273
10.3 Conclusions 285
Chapter 11 Testing NARCliM GCM simulations using temporal correlation of the rainfall…… 287
11.1 Introduction 287
11.2 Autocorrelation of the rainfall 287
11.3 Conclusions 300
Chapter 12 Testing NARCliM GCM simulations using spatial correlation of the rainfall…… 301
12.1 Introduction 301
12.2 Spatial correlation of the daily rainfall 301
12.2.1 Williams River site 301
12.2.2 Richmond River site 320
12.2.3 Summary of the spatial correlation analysis 337
12.3 Testing the spatial correlation of NARCliM GCM simulations rain gauge data 338
12.4 Conclusions 342
Chapter 13 NARCliM future climate projections for the East Coast of Australia…… 345
13.1 Introduction 345
13.2 Changes in mean annual rainfall 346
13.3 Changes in the rainfall variability (C_v) 351
13.4 Changes in autocorrelation and spatial correlation of rainfall 356
13.4.1 Autocorrelation 356

13.4.2 Spatial correlation 359
13.5 Conclusions 363
Chapter 14 Synthesis 367
14.1 Introduction 367
14.2 Assessment of NARCliM RCMs current projections 367
14.2.1 Probability distribution of the rainfall 367
14.2.2 Spatial variability of the rainfall statistics 372
14.2.3 Temporal autocorrelation of the rainfall 381
14.2.4 Spatial correlation of the rainfall 384
14.3 Uncertainty of NARCliM Rainfall Simulations 386
14.3.1 Percentile plots 386
14.3.2 Calculation of uncertainty 388
14.4 Assessment of NARCliM RCMs future projections 392
Chapter 15 Conclusions 389
15.1 Introduction 389
15.2 Statistical testing of NARCliM rainfall 389
15.3 Relationship between rainfall and the orography 393
15.4 Performance of the NARCliM RCMs at various sites 393
15.5 Final remarks on NARCliM current rainfall projections 394
15.6 NARCliM future projections 396
15.7 Future work 396
Appendix A 399
A.1 Chapter 6 - Section 6.2 400
A.2 Chapter 9 - Section 9.2 402
A.3 Chapter 10 - Section 10.2 410
A.4 Chapter 10, Section 10.2.3 411
A.5 Chapter 10 - Section 10.2.4 423

A.6 Chapter 12 - Section 12.2 430

References 463

Abstract

Rainfall is the key input for the hydrology predictions used in water supply reservoir simulations. In principal, rainfall data can be obtained from General Circulation Models (GCMs; grid resolution of ~250 km) at the global scale, and at finer resolutions from Regional Climate Models (RCMs). This thesis assesses the ability of RCM simulations to accurately reproduce observed rainfall statistics (temporal and spatial) important for water availability analysis in reservoir simulations. The dynamically downscaled 10 km resolution RCM simulations used in this thesis have been produced by the New South Wales (NSW)/Australian Capital Territory (ACT) Regional Climate Modelling (NARCliM) project. The assessment is performed for four time periods, two current day periods (1950-2009 and 1990-2009) and two future periods (2020-2040 and 2060-2080); four GCMs; three configurations of the RCMs (called R1, R2, R3) for each GCM; and five study regions along the NSW eastern seaboard.

This thesis has three main foci. The first focus was on the assessment of the ability of NARCliM RCM data to generate the correct statistical properties of current day rainfall. Understanding the properties of the NARCliM generated rainfall and how they differ from observed rainfall is important when using the NARCliM data for hydrology modelling, particularly for models calibrated or designed using observed rainfall. Time series and spatial statistics of RCM simulations are compared against the ground based measurements for selected Bureau of Meteorology rainfall stations and 5 km gridded data from the Australian Water Availability Project (AWAP). The second focus was an assessment of the impacts of orography on regional rainfall, both observed and NARCliM rainfall. The third focus was on how the NARCliM rainfall properties will change in the future.

Statistical testing of the NARCliM rainfall performed along the east coast of Australia suggest that bias corrected rainfall from the NARCliM RCMs are better at reproducing the daily rainfall distribution of AWAP rainfall than uncorrected, yet fail to reproduce the entire probability distribution of the rainfall, particularly the probabilities of the light rainfall events (rainfall less than 1 mm). The bias corrected

NARCliM rainfall is able to reproduce both the magnitudes and spatial pattern of distribution statistics such as mean, standard deviation and coefficient of variation. The spatial correlation function of AWAP rainfall is well captured by both uncorrected and bias corrected NARCliM rainfall, however, both AWAP and NARCliM overestimate the correlation between rain gauges by 20-30%. Both the uncorrected and bias corrected NARCliM rainfall fail to reproduce the time series statistics such as autocorrelations of the rainfall. NARCliM overestimates the magnitudes of autocorrelations of AWAP, even though all NARCliM rainfall series are able to capture the seasonal cycle in the autocorrelation. Similar results for both the uncorrected and bias corrected NARCliM rainfall suggest that the bias correction does not influence the time series statistics, particularly the autocorrelations.

The spatial pattern of both the time series and spatial statistics was generally well reproduced by the bias corrected data, though at high elevations there were some significant differences with AWAP. The ability to reproduce the spatial pattern of the rainfall statistics is an important but not sufficient requirement for hydrological studies, particularly reservoir modelling, since many reservoirs are located in areas of localised high rainfall.

The relationship between the mean rainfall and elevation, and impacts from East Coast Lows (ECLs) on this relationship was investigated. The results suggest that there is a statistically significant positive linear relationship between observed rainfall and elevation, in a region close to the coast where the ECL impacts are known to be dominant. When the distance from the coast increases, this relationship becomes weaker. Compared with AWAP, the RCM R2 is best able to replicate the linear relationship between the gauged rainfall and elevation. A relationship for the rainfall combining distance from the coast and elevation difference between two points was also found.

The RCM future projections suggest that mean rainfall will change by approximately -19% to 54% and the monthly rainfall coefficient of variation will change by -19% to 40%. All GCMs, except Commonwealth Scientific and Industrial Research Organisation (CSIRO-Mk3.0) project rainfall increases along the coast. There is a general trend that regions with reduced coefficient of variation for rainfall have a higher mean rainfall and vice versa, for all sites except for Sydney.

Chapter 1
Introduction

1.1 General background

The hydroclimate of the Australian east coast is distinct from other regions of Australia and is characterized by the influence of the Eastern Australian Current and an extended coastal mountain range, known as the Great Dividing Range (Hopkins and Holland, 1997; Kiem and Franks, 2001, Verdon et al., 2004). The coastal area, east of the Great Dividing Range, responds differently to large scale ocean drivers and experiences higher rainfall variability than west of the Great Dividing Range (Kiem and Franks, 2001; Verdon et al., 2004; Risbey et al., 2009; Murphy and Timbal, 2008; Verdon-Kidd et al., 2010, 2016; Callaghan and Power, 2014; Di Luca et al., 2016; Browning and Goodwin, 2016; Kiem et al., 2016). For example, the influence of large-scale modes of variability such as the El Niño/Southern Oscillation (ENSO), the Indian Ocean Dipole (IOD) and the subtropical ridge (STR) is notably different to the region immediately to the west of the Great Dividing Range (Risbey et al., 2009; Timbal, 2010; Timbal and Drosdowsky, 2013; Pepler et al., 2014; Dowdy et al., 2015;). Given that over 50% of Australia's population resides along the east coast of Australia, detailed studies are needed to improve understanding about the rainfall variability that exists in this region, particularly as rainfall is used to assess water security.

The Eastern Seaboard Climate Change Initiative (ESCCI) – East Coast Low (ECL) project is a strategic project initiated and funded by the New South Wales (NSW) government in Australia and aims to understand the climate of the Eastern seaboard (roughly the area between the east-coast and the Great Dividing Range), the effect of climate change on the Eastern seaboard, and the implications for climate change adaptation in this area. ESCCI-ECL project 5 (one of the six projects within ESCCI-ECL) consists of seven subprojects that are carried out by six PhD students and one postdoctoral research fellow. The subprojects are as follows.

- Project 5.1a: Climatological Drivers of Eastern Australia by Callum Twomey (PhD candidate)

- Project 5.1b: Climatological Drivers of Extratropical Cyclones – ECLs by Andrew Magee (PhD candidate)
- Project 5.2: Statistical Testing of Downscaled Rainfall Data for Water Security Assessment by myself (PhD candidate)
- Project 5.3a: Stochastic rainfall and hydrology modelling by AFM Kamal Chowdhury (PhD candidate)
- Project 5.3b: Incorporating ECLs and Climate Change trends into WATHNET by Lanying Zhang (PhD candidate)
- Project 5.3c: Improving hydrologic modelling under climate change by Proloy Deb (PhD candidate)
- Project 5.3d: Stochastic Water Infrastructure Management using WATHNET by Natalie Lockart (Postdoctoral research fellow)

A major motivation for ESCCI is that the relatively narrow (100 km east to west) coastal strip is poorly resolved in current generation General Circulation Models (GCMs; grid resolution of ~250 km × 250 km) so it has proven difficult to infer climate change trends and impacts for the region. However, Regional Climate Model (RCM) simulations which downscale data from GCMs can better resolve regional detail. Therefore, as part of the ESCCI- ECL project 5, this thesis is based on Project 5.2 which aims to validate the dynamically downscaled RCM rainfall data from NARCliM (NSW/Australian Capital Territory (ACT) Regional Climate Modelling project) against ground based rainfall data. NARCliM is a project running parallel with ESCCI (independent of ESCCI but also funded by NSW government) which provides dynamically downscaled climate data for (1) the CORDEX-AustralAsia region at 50 km, and (2) southeast Australia at a 10 km resolution (Evans et al., 2014). NARCliM used three configurations (R1, R2 and R3) of the weather research and forecasting (WRFv3.3) regional climate model (RCM) to generate both reanalysis—driven by National Centers for Environmental Prediction (NCEP)/National Center for Atmospheric Research (NCAR) reanalysis climate data (Kalnay et al. 1996)—and GCM projected (driven by four GCMs) climate data.

In general the 10 km RCM datasets generated by NARCliM have a sufficient resolution to capture the size of many water supply catchments (most are about 100-200 km^2) on the eastern seaboard. But, what is less clear is how well these climate

data will be at replicating the hydrology of a catchment when they are used in hydrology models or in capturing the persistence of runoff that is important in the performance of reservoirs systems. Poor results can be experienced when using stochastic rainfall simulators in hydrology models. Therefore, it is important that the statistical properties of the rainfall dataset are correctly reproduced for the current day data. Therefore the emphasis in this thesis is on rainfall, hence NARCliM rainfall datasets are tested against current day observed rainfall focusing on the statistics such as temporal and spatial correlations, hydrology mean and variability of the rainfall which are important for the correct simulation of runoff and reservoir performance.

1.2 Objectives and scope

This thesis has three main foci. The first focus is on the assessment of the ability of NARCliM RCM data to generate the correct statistical properties of current day rainfall. Understanding the properties of the NARCliM generated rainfall and how they differ from observed rainfall is important when using the NARCliM data for hydrology modelling, particularly for models calibrated or designed using observed rainfall. The second focus is an assessment of the impacts of orography on regional rainfall, both observed and NARCliM rainfall. The third focus is on how the NARCliM rainfall properties will change in the future.

The specific objectives of this thesis are to:

- Test and validate the rainfall statistics of the downscaled RCM data which are important for reservoir modelling and water availability analysis. In order to remove the scale discrepancy between datasets, the downscaled RCM data are tested against point and grid scale observations ;
- Identify the similarities and differences between the performance of NARCliM RCM rainfall to capture the temporal and spatial statistics of observed rainfall for various sites, from north to south along the broader east coast of NSW, and with different orography, exposure to coastal weather systems and ECL occurrence;
- Compare the performance of RCM rainfall with and without bias correction;

- Study the impact of orography on water security. Most of the water supply catchments along the east coast are subjected to orographic rainfall due to proximity of the Great Divide to the coast. Therefore, the relationship between the rainfall and elevation is explored; and
- Determine the future change in NARCliM rainfall properties compared with current rainfall statistics.

1.3 Overview of the thesis

A summary of the main components of the thesis is shown in Figure 1.1.

The organization of the thesis chapters is as follows;

- Chapter 2 - This chapter provides the motivation of this thesis, and a detailed literature review on the background and previous approaches of assessing GCM and downscaled RCM data.
- Chapter 3 – The downscaled RCM data are assessed at various sites along the east coast of Australia. A description of these sites and data used are presented in this chapter.
- Chapter 4 – The general methodology of assessing different statistical measures is presented in this chapter.
- Chapter 5 - The temporal statistics of the NARCliM reanalysis RCMs are tested against observed rainfall as a pilot study in this chapter. The analysis is performed at a study site called Merriwa, located within the Goulburn River catchment in NSW.
- Chapter 6 – In this chapter, the analyses in Chapter 5 are extended for the four selected study sites located along the broader east coast of NSW. The objective of this chapter is to test the time series statistics of uncorrected and bias corrected NARCliM reanalysis RCMs (1950-2009) against Bureau of Meteorology's Australian Water Availability Project (AWAP) rainfall.
- Chapter 7 - The spatial statistics, particularly the spatial correlations of the NARCliM reanalysis RCMs (1950-2009) are evaluated against the observed rainfall in this chapter.

- Chapter 8 - This chapter explores the relationship between the rainfall and orography using both observed and NARCliM reanalysis RCMs (1950-2009).
- Chapter 9, 10 and 11 - Statistical testing of temporal statistics of NARCliM GCM driven RCMs (1990-2009) is presented for the broader east coast sites in these three chapters. The analyses presented in these chapters are similar to that of Chapter 6, however, the main focus is on the performance of NARCliM GCM driven RCMs.
- Chapter 12 – This chapter evaluates the spatial correlation of the NARCliM GCM driven RCMs against the observed rainfall.
- Chapter 13 – Using NARCliM future projections, this chapter determines the projected change in rainfall and its variability for 2060-2079 relative to 1990-2009.
- Chapter 14 - This chapter presents a synthesis on the performance of NARCliM RCM data along the east coast sites studied in this thesis.
- Chapter 15 – This final chapter summarises how the objectives of this thesis were achieved, the major findings and future research directions.

Differentiated by the datasets used, chapters 5-13 are grouped into two sections as Section 1 and 2; in Section 1 (Chapters 5-8), all statistical testings are performed only for NARCliM reanalysis RCMs (1950-2009), while Section 2 (Chapters 9-13) presents results for the 20-year period GCM driven RCMs (1990-2009). More details on these datasets are presented in Chapter 2 and 3. Additionally, in each section, two types of rainfall statistics are assessed; (1) temporal and (2) spatial. The temporal statistics are calculated at individual grid points while spatial statistics are calculated between the grid points at a site.

To conclude, chapters 14-15 are grouped as Section 3 presenting a final synthesis on the performance of NARCliM RCM data (Chapter 14), followed by conclusions (Chapter 15) of this thesis.

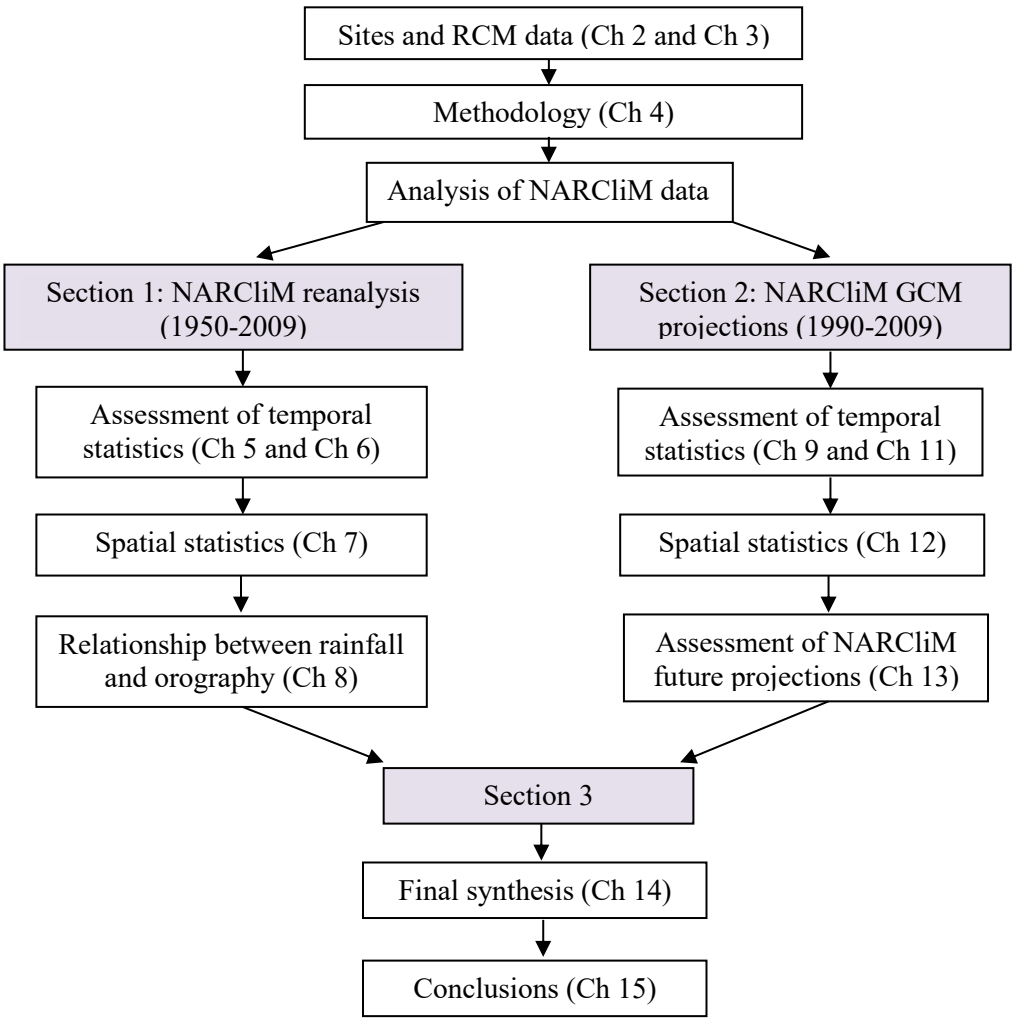

Figure 1.1 Summary of thesis components

As a result of the research work carried out during the course of this thesis, three journal articles, three peer-reviewed conference papers and eight international conference presentations have been published.

Journal papers:

Parana Manage, N., Lockart, N., Willgoose, G., Kuczera, G., Kiem, A. S., Chowdhury, A.F.M.K., Zhang, L. and Twomey, C. (2016), Statistical Testing of Dynamically Downscaled Data for the Upper Hunter Region, New South Wales, Australia, *Journal of Southern Hemisphere Earth System Science*, 66(2), 203-227.

Lockart, N., Willgoose, G. R., Kuczera, G., Kiem, A. S., Chowdhury, A.F.M.K., Parana Manage, N., Zhang, L., and Twomey, C. (2016), Case study on the use of dynamically downscaled GCM data for assessing water security on coastal NSW, *Journal of Southern Hemisphere Earth System Science*, 66(2), 177–202.

Kiem, A.S., Twomey, C., Lockart, N., Willgoose, G.R., Kuczera, G., Chowdhury, A.F.M.K., Parana Manage, N. and Zhang, L. (2016), Links between East Coast Lows and the spatial and temporal variability of rainfall along the eastern seaboard of Australia, *Journal of Southern Hemisphere Earth System Science*, 66(2), 162-176.

Chowdhury, A.F.M.K., Lockart, N., Willgoose, G., Kuczera, G., Kiem, A. S. and Parana Manage, N. (in revision), Development of a decadal and hierarchical Markov Chain daily rainfall model with long-term variability.

Conference papers:

Parana Manage, N., Lockart, N., Willgoose, G., Kuczera, G., Kiem, A. S., and Chowdhury, A.F.M.K. (2015), Testing the Statistics of Dynamically Downscaled Rainfall Data for the East Coast of NSW, *36th Hydrology and Water Resources Symposium*, Hobart, Tasmania, 7-10 December.

Lockart, N., Willgoose, G. R., Kuczera, G., Kiem, A. S., Chowdhury, A.F.M.K., and Parana Manage, N. (2015), Use of NARCliM Rainfall data for Simulating Streamflow in the Williams River Catchment, *36th Hydrology and Water Resources Symposium*, Hobart, Tasmania, 7-10 December.

Chowdhury, A.F.M.K., Lockart, N., Willgoose, G., Kuczera, G., Kiem, A. S. and Parana Manage, N., (2015), Modelling daily rainfall along the east coast of Australia using a compound distribution Markov Chain model, *36th Hydrology and Water Resources Symposium*, Hobart, Tasmania, 7-10 December.

Conference presentations:

Parana Manage, N., Lockart, N., Willgoose, G., Kuczera, G., Kiem, A. S., and Chowdhury, A.F.M.K. (2016), Evaluation of spatial correlations of dynamically downscaled rainfall data for eastern Australia, *European Geosciences Union General Assembly*, Vienna, Austria, 17–22 April (poster presentation).

Chowdhury, A.F.M.K., Lockart, N., Willgoose, G., Kuczera, G., Kiem, A.S., and Parana Manage, N., (2016), Comparison of two stochastic daily rainfall models

and their ability to preserve multiyear rainfall variability, *European Geosciences Union General Assembly*, Vienna, Austria, 17–22 April (oral presentation).

Parana Manage, N., Lockart, N., Willgoose, G., Kuczera, G., and Chowdhury, A.F.M.K. (2015), Statistical Testing of Dynamically Downscaled Rainfall Data for the East Coast of Australia, *European Geosciences Union General Assembly*, Vienna, Austria, 12–17 April (poster presentation).

Chowdhury, A.F.M.K., Lockart, N., Willgoose, G., Kuczera, G., and Parana Manage, N., (2015), Development of a compound distribution Markov Chain model for stochastic generation of rainfall with long term variability, *European Geosciences Union General Assembly*, Vienna, Austria, 12–17 April (oral presentation).

Parana Manage, N., Lockart, N., Willgoose, G., Kuczera, G., Kiem, A. S., and Chowdhury, A.F.M.K. (2015), Statistical validation of dynamically downscaled climate data for the Hunter Region of New South Wales, Australia, *Australian Meteorological and Oceanographic Society Conference*, Brisbane, Australia, 15-17 July (oral presentation).

Chowdhury, A.F.M.K., Lockart, N., Willgoose, G., Kuczera, G., Parana Manage, N., and Kiem, A.S. (2015), A stochastic model for rainfall generation with long-term variability – Calibration to NARCliM data at catchments with characteristic influence of east coast lows, *Australian Meteorological and Oceanographic Society Conference*, Brisbane, Australia, 15-17 July (oral presentation).

Parana Manage, N., Lockart, N., Willgoose, G., Kuczera, G., Kiem, A. S., and Chowdhury, A.F.M.K. (2014), Statistical Testing of Dynamically Downscaled Rainfall Data for the East Coast of Australia, *American Geophysical Union Fall Meeting*, San Francisco, California, 15-19 December (poster presentation).

Chowdhury, A.F.M.K., Lockart, N., Willgoose, G., Kuczera, G., and Parana Manage, N. (2014), Stochastic simulation of rainfall using a Markov Chain model calibrated to dynamically downscaled data, *American Geophysical Union Fall Meeting*, San Francisco, California, 15-19 December (poster presentation).

Chapter 2
Background

2.1 Introduction

Assessments of global and regional rainfall projections to reproduce the current day observed rainfall statistics are important when these projections are used in applications such as agriculture, water resources planning and climate change studies. The following is a comprehensive review on the availability, applicability and previous approaches of evaluating global and regional rainfall projections obtained from GCMs and RCMs. This review supports the importance of evaluating the high-resolution rainfall projections focusing on the statistics which are important for the water security assessments before these projected rainfall datasets are used in hydrology models in generating the runoff.

2.2 GCM rainfall projections

General Circulation Models, also known as Global Climate Models (GCMs) are the primary and most common tool used to simulate present climate worldwide. There are two recent databases of global climate projections; the Coupled Model Intercomparison Project 3 and Project 5 (CMIP3; CMIP5; Meehl et al., 2007; Taylor et al., 2012) which have been produced as an international collaborative effort of worldwide GCM groups. These two databases of global climate projections which describe a large number of GCMs (23 and 47 GCMs by CMIP3 and CMIP5 respectively) (IPCC, 2007; IPCC, 2013) have been widely used to investigate global climate system processes as well as large scale climate change projections. However, as stated in IPCC (2007; 2013) “The confidence of these GCM outputs depends on their physical basis and the ability of reproducing the observed climate”.

Of the climate variables produced by GCMs, rainfall is the key variable required for hydrology predictions used in water supply reservoir simulations (Wigley and Jones, 1985; Sankarasubramaniam et al., 2001; Chiew, 2006). Therefore, this review mainly focuses on the rainfall projections and the assessment of their statistical properties simulated by GCMs. The knowledge of how observed rainfall has been

reproduced by GCMs is important, particularly for a country like Australia where the rainfall is highly variable throughout the year. Therefore, the evaluation of GCM performance for the Australian climate is critically reviewed here. In particular, the focus is on the assessments which cover the east coast of Australia as this region is the region of interest in this thesis. The east coast of Australia is considered as a separate climate entity compared to other regions of Australia and is characterized by the influence of the Eastern Australian Current and an extended coastal mountain range, the Great Dividing Range (Hopkins and Holland, 1997; Kiem and Franks, 2001, Verdon et al., 2004). This chapter will identify research gaps about evaluating GCMs which have not been addressed by previous studies. One major argument in this review is that rainfall projections should be evaluated not only focusing on the biases of the rainfalls, but also the other temporal and spatial statistics such as spatial correlations and autocorrelations which are important for water security assessments.

2.3 Climate of Eastern Australia and ECLs

The general climate of eastern Australia is subtropical and the region experiences more rainfall in the summer than the winter months. During the winter, rainfall is more associated with East Coast Lows (ECLs) and cold fronts (Dowdy et al., 2015). ECLs are intense low pressure systems that occur over the subtropical east coasts of northern and southern hemisphere continents (Verdon-Kidd et al., 2010). Due to the large influence on severe weather conditions and high rainfall volumes generated by ECLs which cause significant inflows into the major water storages along the east coast, there is substantial interest on these ECLs from the research community. Many authors have studied ECLs (Verdon- Kidd et al. 2010, 2016; Kiem and Twomey, 2014; Pepler et al. 2014a, 2014b; Kiem et al., 2016; Browning and Goodwin, 2016). Browning and Goodwin (2013) classified ECL events into five main types (Easterly trough lows (ETL); Southern secondary lows (SSL); Inland troughs (IT); Continental lows (CL) and Extratropical cyclones (XTC)) which affect eastern Australia while Kiem et al. (2016) explained how rainfall pattern and the impacts to the coastal region can vary depending on the type of ECL that occurs. In particular, Kiem et al. (2016) found that there is a large degree of spatial variability in the location of different ECL impacts, therefore, there is a significant geographical spread of the location depending on the type of the ECL. This spatial variability in

the location of different ECL types is particularly important for water resources planning as a small change in the location can directly affect which catchment experiences reservoir filling rainfall. Due to this spatial variability in the ECL locations, assessment on the rainfall variability at different locations along the east coast of Australia is important. Therefore, instead of studying the east coast as a whole, the study in this thesis is performed at various sites along the east coast. One of the major motivations in this project (ESCCI-ECL project 5) is to use the findings in this thesis for the future research on the ECL impacts along the east coast of Australia. However, it should be noted that this thesis does not assess ECL impacts at each site, instead the main focus is on how well the rainfall statistics (ECL or non-ECL) which are important for the water security assessments have been reproduced by the GCM projections.

In the next section, past studies evaluating GCM climate projections over Australia are reviewed. The extent of GCMs' capability to capture the climate variability in the east coast is also investigated in this section.

2.4 Evaluating GCM projections for the Australian Climate

The evaluation of the performance of GCMs at the regional scale is important because performance of GCMs can vary from one region to another, and can simulate different responses to increasing greenhouse gas concentrations at regional scales. This section presents past studies by many authors, which evaluate GCM projections for the climatology of Australia. In particular, the statistical methods and different approaches used in the evaluation of the GCMs are reviewed. Additionally, models which perform best in capturing the observed rainfall for Australia are identified to compare them with the results in this thesis. The review in this section has led to two main conclusions: (1) Some GCMs are able to capture the rainfall variability in regions such as east coast of Australia, yet, none of these models reveal km scale variability in the rainfall (or temperature) within a region because of the coarse resolutions of GCMs, the averaging of the results for large regions over Australia (for example, regions of 10°×10°) and averaging the model skill between all available models, and (2) most of the past studies have evaluated the skill of GCMs' reproduction of observed rainfall or temperature by only focusing on the

distribution statistics such as mean, mean square or mean absolute error, root mean square error, probability distribution, and the spatial patterns of the statistics. None of these studies focused on the temporal or spatial variability of the rainfall which are important for water security assessment studies.

Suppiah et al. (2007) tested the reliability of 23 GCM projections from CMIP3 for the Australia region (110-155ºE, 11-45ºS) for the period of 1961-1990 by comparing observed and simulated patterns of the seasonal mean rainfall. AWAP rainfall data from Australian Water Availability Project (AWAP, Jones et al., 2009; Raupach et al., 2009, 2012; also see Section 3.3.3) was used as the observed dataset in calculating the patterns of rainfall at individual grid points which have been interpolated on to a 0.5°×0.5° grid over Australia. Note that the same AWAP data is used in this thesis as the observed rainfall, but to be consistent with the 10 km resolution NARCliM (NSW/Australian Capital Territory (ACT) Regional Climate Modelling project, see Section 2.6.3) RCM simulations, the 5 km dataset is aggregated up to 10 km resolution (see Section 3.3.3). In the selection of best models, Suppiah et al. used a combined approach of satisfying two statistical measures; pattern correlation coefficient and root mean square error (RMSE) i.e. pattern correlation coefficients of 1.0 indicating a perfect match between the observed and simulated spatial pattern of the rainfall and RMSE error of 0.0 to indicate a perfect match between the observed and simulated magnitudes of the rainfall. The results of Suppiah et al. (2007) showed that there is high rainfall variability along the east coast of Australia during the summer, while in winter the region experiences significant rainfall due to cold fronts and low pressure systems. In particular, the GCMs that capture this rainfall variability had high pattern correlations. According to the results of the statistical tests, 15 models (shown in Table 2.1) including CSIRO-Mk3.0, ECHAM5 and MIROC-M (these three GCMs have been used to produce the downscaled RCMs used in this thesis) were selected as ‘best’ by using a subjective demerit point system (Whetton et al., 2005). The use of a subjective demerit point system in deciding on the ‘best’ performing GCMs has since become a common practice and has been used in several recent studies including the NARCliM design project. In particular, the NARCliM project used the demerit point system of Suppiah et al. (2007) as one criterion for selecting the best

performing GCMs for the east coast of Australia (see Section 2.6.3 and Evans et al., 2014).

Table 2.1 Demerit points based on comparison of observed and simulated MSLP, temperature and rainfall

Originating group(s)	*Model*	*Mean sea-level press-ure*	*Temp eratu-re*	*Rai-nfall*	*Total includin g extra demerit points*
Beijing Climate Centre	BCC	9	3	5	17
Bjerknes Centre for Climate Research	BCCR	0	0	5	5
Canadian Climate Centre	CCCMA T47	6	1	1	8
Canadian Climate Centre	CCCMA T63	5	4	1	10
Meteo-France	CNRM	2	1	1	4
Commonwealth Scientific and Industrial Research Organisation (CSIRO)	CSIRO-MARK3	3	2	2	7
Geophysical Fluid Dynamics Lab	GFDL 2.0	4	0	0	4
Geophysical Fluid Dynamics Lab	GFDL 2.1	0	1	1	2
NASA/Goddard Institute for Space Studies	GISS-AOM	3	4	1	8
NASA/Goddard Institute for Space Studies	GISS-E-H	5	4	5	14
NASA/Goddard Institute for Space Studies	GISS-E-R	4	3	1	8
LASG/Institute of Atmospheric Physics	IAP	0	0	2	2
Institute of Numerical Mathematics	INMCM	1	3	3	7
Institute Pierre Simon Laplace	IPSL	9	1	4	14
Centre for Climate Research	MIROC-H	5	0	2	7
Centre for Climate Research	MIROC-M	6	0	1	7
Meteorological Institute of the University of Bonn, Meteorological Research Institute of KMA	MIUB	1	2	1	4
Max Planck Institute for Meteorology DKRZ	MPI-ECHAM5	1	0	0	1
Meteorological Research Institute	MRI	1	1	1	3
National Center for Atmospheric Research	NCAR-CCSM	1	0	1	2
National Center for Atmospheric Research	NCAR-PCM1	3	3	5	11
Hadley Centre	HADCM3	4	0	2	6
Hadley Centre	HADGEM1	0	2	0	2

One point is given for an rms error greater than 2 or a pattern correlation less than 0.8 in any given season. An extra demerit point was allocated to models with an rms error greater than 4 or a pattern correlation below 0.6. The 15 models with less than eight demerit points are shown by shaded cells (from Suppiah et al. (2007).

However, the pattern correlation used in Suppiah et al. (2007) is an important measure of assessing the ability to correctly distribute the rainfall (or temperature) over a region, but it is not sensitive to the biases between model and observed rainfall and therefore, only explains the spatial similarity of rainfall over a region.

Of past studies performed over Australia, the study by Perkins et al. (2007) is important to this thesis because like Suppiah et al. (2007), their results were also used in Evans et al. (2014) in the design of the NARCliM project when determining the best models that perform well in southeast Australia. Therefore, this study is reviewed in detail here. More details on the NARCliM project design are given in Section 2.6.3.

Perkins et al. (2007) evaluated CMIP3 models for the daily simulation of precipitation, minimum temperature, and maximum temperature (from 1961-2000) by dividing Australia into 12 regions (10°×10°, Figure 2.1) (note that the focus in this review is on the precipitation). The evaluation was based on probability density functions (PDFs). In calculating the PDFs for each variable, all observed data within each 10°×10° region were used to construct the representative distribution for each region. The similarity between the observed and simulated PDFs (Figure 2.2) was evaluated by a skill score (S_{score}) calculated using Equation 2.1.

$$S_{score} = \sum_{1}^{n} \min\left(Z_m, Z_o\right) \quad \ldots\ldots\ldots\ldots (2.1)$$

where n is the number of bins used to calculate the PDF for a given region, Z_m is the frequency of values in a given bin from the model, and Z_o is the frequency of values in a given bin from the observed data. The basis for this evaluation was that if a model simulates the observed conditions perfectly, the skill score will equal one, which is the total sum of the probability at each bin centre in a given PDF whilst a skill score close to zero with negligible overlap between the observed and modelled PDFs shows that the model poorly simulates the observed PDF (Perkins et al., 2007).

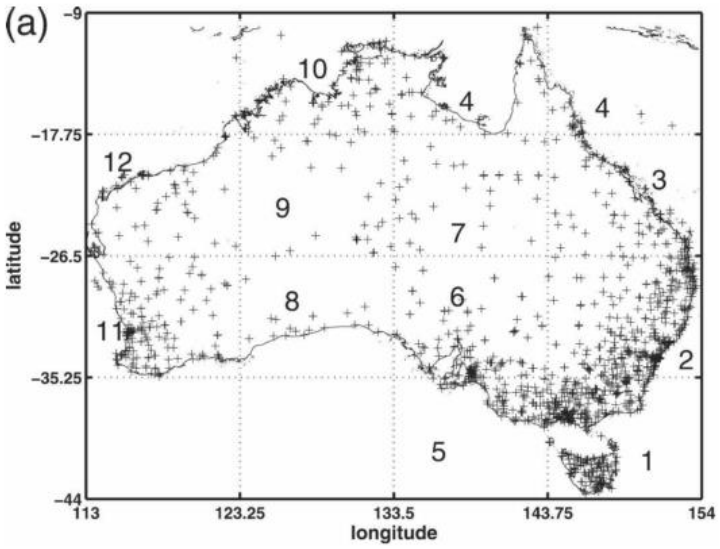

Figure 2.1 Regions used in Perkins et al. (2007)

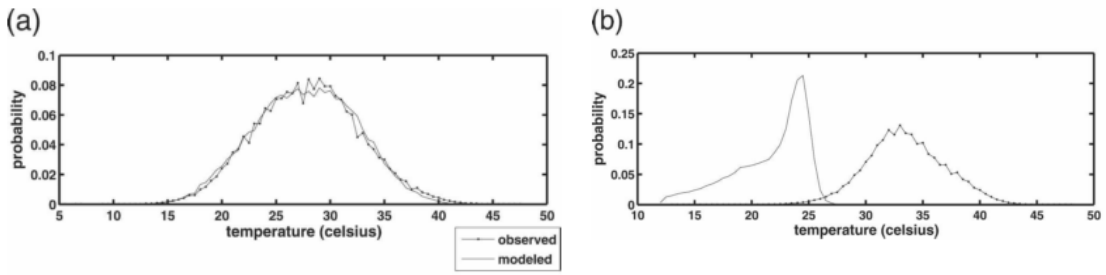

Figure 2.2 Diagrams of modelled vs observed PDF illustrating the total score in (a) a near perfect score test (0.9) and (b) a very poor skill score (0.02) (from Perkins et al., 2007)

Perkins et al. (2007) then ranked the climate models as shown in Table 2.2. They noted that some models show major biases with overestimation of the observed probability of 1-2 mmday^{-1} rainfall values by 2-3 times in many regions. Additionally, there was a tendency of the climate models to simulate too many light rainfall events (a common problem called "GCM drizzle"). However, the ensemble skill score for precipitation of each model averaged over all 12 regions suggested that nine models have an average exceeding 0.7 which was the cut-off for selecting the best models. In particular for rainfall, BCCR, ECHAM, and ECHO-G models were identified as the best models for simulating the observed precipitation across Australia.

Table 2.2 Ranking of climate models for precipitation *P*, maximum temperature *TMAX*, and minimum temperature *TMIN* over all regions of Australia. These results are an average of all 12 regions.

	P	*Rank*	*TMAX*	*Rank*	*TMIN*	*Rank*	*Overall*	*Rank*
MIROC-m	0.77	5	0.87	3	0.84	5	0.83	1
CSIRO	0.73	7	0.80	6	0.88	2	0.80	2
ECHO-G	0.83	3	0.87	2	0.69	12	0.80	3
IPSL	0.65	12	0.85	4	0.83	7	0.78	4
MRI	0.65	11	0.78	8	0.86	4	0.76	5
GISS AOM	0.64	13	0.78	7	0.83	8	0.75	6
FGOALS	0.70	9	0.81	5	0.69	13	0.73	7
CGCM-l	0.60	14	0.68	10	0.86	3	0.71	8
BCCR	0.85	1			0.73	11	0.79	
CGCM-h			0.72	9	0.84	6	0.78	
GFDL2.0	0.79	4					0.79	
GFDL2.1	0.76	6			0.89	1	0.82	
GISS ER	0.73	8			0.80	10	0.76	
MIROC-h			0.87	1			0.88	
ECHAM	0.84	2			0.81	9	0.83	
CCSM	0.67	10					0.67	

The study sites in this thesis fall into region 1 and 2 (see Figure 2.1), with most of the sites falling in region 2 of Perkins et al. (2007). In particular at region 2, ECHAM GCM had a higher skill score of 0.84 than the CSIRO and MIROC-M GCMs which had a skill score of 0.7. Therefore, the performance of ECHAM can be compared with the results in this thesis, though the analysis in this thesis was only based on the cumulative probability distribution (CDF) of the daily rainfall at selected grid points without using any skill score method. There are two main reasons for not using in this thesis the skill methods of Perkins et al. (2007):

(1) In calculating the PDF, Perkins et al. used all data (of either observed or model) available within a region. For example, at region 2, all daily rainfall data available for a large area covering most of NSW was used to construct a single PDF. This method provides the general idea of the model performance within a region, but does not reveal more details at the catchment scale. Therefore, instead of constructing a single PDF for a large area, a method of constructing PDFs of daily rainfall at single

grid points is needed. By doing this, comparisons of simulated and observed PDFs can reveal more details on the temporal variability of the rainfall at a specific location as well as how well the entire rainfall distribution has been captured by GCMs. The ability of GCMs to reproduce the temporal variability in the observed rainfall is important for water security assessments because if GCMs do not reproduce the actual variability of the observed rainfall, the use of these data to genarte catchment average rainfalls to run a rainfall runoff model will cause errors in the simulated runoff; and,

(2) The skill score method (Equation 2.1) used by Perkins et al. (2007) measures the overlap between the simulated and observed rainfall distributions. Measuring the overlap between the model and observed data is important for the atmospheric science studies which intend to identify best GCMs which can be used to generate future climate projections for a specific region. However, this method does not provide enough detail about the time series characteristics of the rainfall or the location where the rainfall event occurred. In other words, this method does not evaluate the differences in the spatial and temporal variability between GCM simulated and observed rainfall. Therefore, in order to test the hydrologic capabilities of GCMs (the ability to capture the observed rainfall time series statistics important for reservoir water availability analysis), more sophisticated analysis methods are required.

Maxino et al. (2008) used a similar methodology as Perkins et al. (2007) for the Murray-Darling Basin, Australia by constructing PDFs for each season for the period from 1980-2000. They recommended three CMIP3 models, CSIRO, IPSL and MIROC-M that captured the observed PDFs of maximum and minimum temperature and precipitation relatively well. However, the ECHAM GCM, which had captured the precipitation better than CSIRO and MIROC-M for eastern Australia in Perkins et al. (2007), had similar performance for the Murray-Darling Basin which is also located in eastern Australia (Maxino et al., 2008).

Smith and Chandler (2010) evaluated 22 CMIP3 models for Australia based on the evaluation method of RMSE and spatial correlation between model and observations used in Suppiah et al. (2007), and found a set of five models (ECHAM5, GFDL2.0 GFDL2.1, MIROC3.2 (hires) and UKMO_HADCM3) that provided good

representations of the Australian rainfall. To find out how these five models performed in future, the percentage change in annual rainfall (2070-2099) versus (1971-2000) for the Murray-Darling Basin had also been calculated. They found that on a seasonal basis, this set of five GCMs tended to agree on the sign of the changes that may occur. These five models simulated different changes in rainfall (with different magnitudes of increases or decreases) compared to the remaining 17 models. The differences between the set of 5 models and the remaining set of 17 models are most evident in winter and spring seasons. However, the similarity between the sign of the mean projected change in rainfall of ECHAM5 and MIROC3.2 found by Smith and Chandler (2010) for the Murray-Darling Basin does not agree with the findings in this thesis (see Chapter 12) where the assessment is for the east coast of Australia (east of the Great Dividing Range). Therefore, their results appear to be only acceptable to the Murray-Darling Basin (west of the Great Dividing Range) so cannot be generalized for east coast of Australia.

Moise et al. (2015) evaluated the mean climate skill score of 47 CMIP5 models and 23 CMIP3 models against AWAP data using M-Statistics (Watterson, 1996; 2008) by interpolating each model to a common 1.5°× 1.5° grid over Australia. In some of their evaluations they studied Australia as five main spatial clusters while some clusters had been further divided into sub-regions. In Watterson (1996) M-statistic is defined as follows.

$$M = 2\arcsin(\rho)/\pi \quad \text{..... (2.2)}$$

ρ is the Mielke's measure of agreement which is defined in Mielke (1984 ; 1991) as;

$$\rho = 1 - \delta/\mu \quad \text{..... (2.3)}$$

where δ is either mean square or mean absolute error calculated between the simulated and observed values of the climate variable and μ is the expected value of δ if the simulated values are distributed randomly over the global grid-points.

However, the skill of models in simulating climatological rainfall across Australia was found to vary strongly (Moise et al., 2015). MIROC-ESM and MIROC-ESM-CHEM were identified as poor models as they did not simulate temperature and rainfall well over Australia and also did not produce monsoon westerlies during the

monsoon season and therefore showed deficient wet season rainfall (spatial distribution). They also found that most of the CMIP5 global climate models were able to reproduce the major climate features (SAM, monsoon, pressure systems, sub-tropical jet and circulation) and modes of variability (seasonal cycle, ENSO, Indian Ocean Dipole) while three models (IPSL-CM5A-MR, IPSL- CM5A-LR and CSIRO-MK3-6-0) showed unusually low skill with respect to the ENSO-rainfall teleconnection which was partly due to their bias in the equatorial sea surface temperatures. In particular for the mean precipitation from 1980-1999, the models (mean CMIP3 models) showed a dry bias along the East coast of Australia compared with AWAP. During the winter, there was a good match between the models and AWAP rainfall suggesting that models are able to capture the higher winter rainfall amounts experienced in the East coast cluster due to ECLs and fronts. However, compared with models used in this thesis the authors only used CSIRO-Mk3.60 and two other versions of MIROC GCM (MIROC-ESM and MIROC-ESM-CHEM).

The results of Moise et al. (2015) contributed to the recent climate projections produced for Australia by Commonwealth Scientific and Industrial Research Organisation (CSIRO) in 2015 (CSIRO and Bureau of Meteorology, 2015). Overall, Moise et al. (2015) assessed the performance of individual models as well as mean CMIP3 models (averaged across 47 models). However, they only used the statistics mean absolute error, and the expected value of mean error between observed and model values in calculating M-statistics. Additionally, the authors have only used the mean daily rainfall averaged over a time period. The approach of calculating a single value as the mean daily rainfall over a long time period hides internal variability within the daily rainfall time series, and therefore, can be considered as a deficiency in their method. Further, M-statistics can be identified as useful for assessing the overall model performance, but does not provide much information on the ability of GCMs to reproduce the hydrologically important statistics such as temporal and spatial variabilities in the rainfall. Bhend and Whetton (2015) evaluated regional trends in daily maximum and minimum temperature, and rainfall in simulations from the CMIP5 archive from 1956-2005 using a z-score defined for the observed and modelled climate variables on a grid (1.5°×1.5°) over Australia. In their study, significant (at the 10% level) differences between simulated and observed trends in rainfall and temperature were found in some areas. In particular, rainfall was

overestimated in north-western Australia in summer and autumn and in north-eastern Australia in spring, while significant underestimates in rainfall were found for large areas of south-eastern Australia in autumn. However, the approach used by Bhend and Whetton (2015) did not reveal much information on the individual performance of each model, since they had used a single z-score which had been averaged across all models for each grid point.

Overall, the review in this section shows that some GCMs are more capable than others to capture the rainfall variability over large regions of Australia, yet, due to the coarse resolution of these GCMs, none of them are able to capture the regional variability in the rainfall. Therefore, there is a need for high-resolution climate projections at regional scales. As a result, researchers have focus on downscaling GCMs, expecting that downscaled high-resolution GCM projections will be able to resolve more regional details in the climate better than the coarse resolution GCMs. Therefore, the following sections of this chapter focus on the regional climate projections produced by downscaling coarse resolution GCMs, and the performance of these projections worldwide.

2.5 Downscaling GCMs

The previous section showed that direct outputs from Global Climate Models (GCMs) fail to capture the internal variability in the climate within small regions. This is because they do not provide realistic daily rainfall at resolutions finer than 200 km (Meehl et al., 2007; Liu and Zuo, 2012) at which hydrological processes are typically assessed (Kundzewicz et al., 2007). Therefore, different downscaling techniques have been developed to produce high-resolution Regional Climate Model (RCM) projections with a focus of resolving the scale discrepancy between current GCMs and the resolution required for hydrological impact assessment (Fu et al., 2011). These downscaling methods can be divided into two types: statistical and dynamical. Statistical downscaling involves deriving statistical relationships between some large scale predictors and the local variable of interest (Buytaert et al., 2010). Dynamical downscaling uses the initial and time-dependent lateral boundary conditions of GCMs to achieve a high spatial resolution by nesting RCMs (Caya and Laprise, 1999). Note that the NARCliM RCM projections used in this thesis have

been produced by the dynamical downscaling method (see Section 2.6.3 for more details on the design process of NARCliM).

There are numerous studies which evaluate these downscaling methods. However, this review does not intend to present more details on the comparison studies between different downscaling methods as it is out of the scope of this thesis. Instead, the next section focuses on the assessment and performance of the RCM simulations downscaled by either dynamical or statistical methods around the globe.

2.6 Evaluation of RCM simulations

An assessment of RCM simulations is necessary to evaluate the reliability of predictions at the hydrological catchment scale. In general, there are many studies with different views and approaches on GCM and RCM evaluation and selection. Some authors (e.g. Kirono and Kent, 2011; Vaze et al., 2011) argue that the evaluation and selection criteria of RCMs can simply be based on the climate variable of interest (for most hydrological applications these variables are rainfall and potential evapotranspiration), while others (e.g. Smith and Chandler, 2010) suggest that there is a need to use of a broader range of variables, including the atmospheric-oceanic climate drivers such as the Southern Annular Mode (SAM) and the El Nino Southern Oscillation (ENSO). This is because climate variables (e.g. rainfall) are mostly associated with the dynamics of climate drivers, and successful simulation and prediction over a wide range of these drivers increases confidence in the GCM used for climate projections in the future (Randall et al., 2007). In general, RCMs are often evaluated with a focus on temperature and precipitation as these are the most commonly observed climate variables.

This section reviews past studies on the evaluation of RCM simulations in and outside Australia, with a focus on various statistical approaches used by different authors worldwide. In the next section, NARCliM RCM simulations, which are used in this thesis, are reviewed in detail followed by a subsection on the pre- and post-evaluation of NARCliM projections over south-eastern Australia. However, note that this section focuses on RCM precipitation projections, as the focus in this thesis is precipitation.

The review in this section has led to two main conclusions: (1) none of the RCM evaluation studies have focused on the time series statistics of the rainfall or the spatial correlation between the rainfalls at two different locations which are two important statistics for the predictions of reservoir water availability analysis, i.e. none of the RCMs have been evaluated in a way that explains how GCMs are capable to capture the regional scale variability (temporal or spatial) in the observed rainfall, and (2) most of RCM evaluation studies have been performed for the aggregated time resolutions such as monthly, seasonal and annual, which can hide the submonthly variability and systematic biases presents in the daily time resolution. Therefore, there is a need to assess the statistics at high temporal resolutions such as daily, weekly and fortnightly.

2.6.1 Evaluation of RCM simulations outside Australia

Evans et al. (2005) investigated the performance of many variables through time simulated using four RCMs (RegCM2, MM5/BATS, MM5/SHEELS, and MM5/OSU) including daily precipitation, seasonal precipitation, runoff, soil moisture and monthly mean temperature. They assessed RMSE and the daily probability distributions of the modelled and observed data in Kansas, United States, but only for a single grid point (20 km × 20 km). They found that all RCMs are able to capture the correct qualitative behaviour of the inter-annual variability, though there are considerable deviations in the magnitudes between models and observations.

The approach in Evans et al. (2005) of assessing the statistics, particularly the rainfall probability distribution at a single grid point provide more insights towards understanding of the daily rainfall probability distribution properties at regional scale, compared with Perkins et al. (2007) who constructed individual PDFs averaged over large regions of 1000 km ×1000 km (10°×10°) over Australia.

Argüeso et al. (2012) evaluated the ability of the Weather Research Forecasting (WRF) RCM to simulate both the mean and extreme precipitation over Spain. The WRF model was driven by ERA-40 and two GCMs (ECHAM5 and CCSM3). In their evaluation, longer term means such as annual, seasonal and monthly precipitation were calculated. Although substantial errors were observed in the

monthly precipitation, especially during the spring, they found that the model was largely able to capture the various precipitation regimes. Further, they found that the major benefits of using WRF were related to the spatial distribution of rainfall and the simulation of extreme events, which are two facets of climate that are difficult to estimate with GCMs (Parry et al., 2007; Randall et al., 2007; Stainforth et al., 2007; Koutsoyiannis et al., 2008; Kiem and Verdon-Kidd, 2011; Stephens et al., 2012). The ability of WRF to capture the spatial distribution of the rainfall was similar to the results of NARCliM simulations in this thesis, which have been downscaled using the WRF RCM. However, note that the spatial resolution of WRF in Argüeso et al. (2012) is 20 km while the resolution of WRF datasets used in this thesis is 10 km.

Comparing the boundary conditions used, Argüeso et al. (2012) found that WRF simulations, driven by ERA-40 better matched with observations than the simulations driven by GCM boundary conditions. The comparison between RCM performances for different boundary condition is useful when selecting datasets for a particular application. The analysis in this thesis also focuses on the performance of WRF model (the same RCM used in Argüeso et al., 2012) driven by two different boundary conditions: NCEP/NCAR reanalysis and four GCMs projections (CSIRO-Mk3.0, MIROC3.2, ECHAM5 and CCCMA3.1).

Salon et al. (2008) focused on monthly averages and seasonal spatial distribution of precipitation in the drainage basin of the Venice lagoon. Their RCM (the ICTP RCM; Giorgi et al. (1993a,b), Pal et al. (2007)) data showed a good agreement between climate observations, monthly area averages, and seasonal spatial distribution of precipitation. Further, they found that frequencies of annual mean distribution of rainfall events with 1-5 days duration were satisfactorily reproduced by the model. Similar to Argüeso et al. (2012), Salon et al. (2008) have also evaluated the rainfall statistics only at the monthly, seasonal and annual time resolutions and none of them used the daily rainfall statistics in their evaluations.

Evans et al. (2004) and Evans (2009) also evaluated RCM performance in the Middle East using monthly, annual and seasonal totals of temperature and precipitation. As in Evans et al. (2005), the model performance was evaluated against observations using several statistics, including the bias, RMSE and the

modified coefficient of efficiency. The RegCM2 RCM which was used in Evans et al. (2004) was able to capture the spatial variability of temperature and precipitation better than European Centre for Medium-Range Weather Forecasts–Tropical Ocean and Global Atmosphere (ECMWF-TOGA) project analyses despite model biases being present. Further, the RCM, based on MM5, used in Evans (2009) showed that the model was able to simulate the precipitation well for most of the domain, while displaying a negative bias in temperature throughout the year. As in Argüeso et al. (2012) and Salon et al. (2008), the longest time resolution used in both Evans' studies (Evans et al., 2004; Evans, 2009) was annual while monthly was the shortest. However, when testing the usefulness of RCM simulations for the reservoir water availability analysis, there is a need to assess the ability of RCMs to capture the observed rainfall statistics at time resolutions such as daily or weekly. Runoff generation responds to daily rainfall and reservoirs of different capacities respond to rainfall differently. Small reservoirs respond to daily variations in rainfall while large reservoirs respond to rainfall variations over weeks or months. Therefore, the lack of knowledge on how RCMs perform at time resolutions such as daily and fortnightly has been addressed in this thesis by evaluating the statistics at four different time resolutions as daily, fortnightly, monthly and annual.

2.6.2 Evaluation of RCM simulations over Australia

To date, few studies involving high spatial-resolution (finer than 30 km) regional climate simulations over Australia have been published. Song et al. (2008) evaluated a 30 year simulation (1961-1990) from the RegCM3 high-resolution climate model at 20 km resolution against the Australian Bureau of Meteorology (BoM) observed rainfall and temperature gridded (0.25° by 0.25°) monthly and daily datasets (these datasets are described in Lavery et al. (1997)). By evaluating the mean bias between RegCM3 and BOM observed rainfall for January and July months, they found that the extent of summer monsoon rainfall, the winter rainfall maximum in the southwest of Western Australia, and the topographically driven high rainfall belt along the Great Dividing Range were well simulated by the RegCM3 model. Over southwest Western Australia and the Murray-Darling Basin, the model was able to reproduce the observed probability distribution functions of daily rainfall, maximum

and minimum temperatures, but the model underestimated probabilities for the light rain events compared with observed.

As explained in Song et al. (2008), the ability of 20 km resolution RegCM3 RCM to resolve the topographically driven high rainfall belt along the Great Dividing Range is important to this thesis, because this suggests that finer resolution RCMs (finer than 20 km) may resolve more regional details if they are used to simulate the climate along the Great Dividing Range.

Additionally, the results in this thesis also show a direct link between the rainfall statistics and topography. Therefore, the relationship between observed rainfall and topography is comprehensively investigated in Chapter 8 in this thesis. Further, while assessing how observed rainfall statistics are related to the topography, the ability of 10 km resolution NARCliM RCMs to replicate this relationship is also investigated.

In a pre-NARCliM assessment, Evans and McCabe (2010) evaluated the WRF RCM data (10 km grid resolution) driven by the lateral boundary conditions of NCEP/NCAR reanalysis (~250 km) against AWAP gridded precipitation and temperature at daily, monthly, inter-annual and multi-annual resolutions for the period from 1985 to 2008, focusing on the Murray-Darling Basin. They evaluated the ability of WRF model simulations to reproduce the PDF of the AWAP rainfall using a similar skill score method used by Perkins et al. (2007) (see Section 2.4). Additionally, using similar statistics used in previous studies such as bias, RMSE, pattern, and anomaly correlations (spatial correlation) of WRF rainfall were compared over the 250 km original NCEP/NCAR reanalysis gridded dataset and finally both 10 km and 250 km RCM datasets were evaluated against AWAP. They also focused on the representation of El Niño-Southern Oscillation (ENSO) and its impact on drought in the Murray-Darling Basin, with the results showing that the WRF simulations were able to capture the drought experienced over the Murray-Darling Basin from ~1997-2010 (for references on this drought see: Verdon-Kidd and Kiem, 2010; Kiem and Verdon-Kidd, 2011 and Gallant et al., 2012). Examining ENSO cycles showed that WRF was able to capture the correct spatial distribution of precipitation anomalies associated with El Niño/La Niña events during their 24 year (1985-2008) testing period. The ability of WRF simulations (driven by

NCEP/NCAR reanalysis) to represent the spatial distribution of the rainfall is consistent with the results in this thesis, even though there are some discrepancies between the observed rainfall and model outputs.

Similar to Evans and McCabe (2010), many authors later evaluated the performance of WRF RCM over south-eastern Australia as pre- and post-NARCliM assessments, with the increasing availability of these high-resolution datasets when the NARCliM project progresses. As explained in the introduction, NARCliM is a project which provides 10 km resolution climate projections for eastern Australia by dynamically downscaling four GCM and one reanalysis datasets using WRF RCM. Since NARCliM are the same datasets used in this thesis, hence, there is a need to understand the technical background as well as the performance of these datasets in capturing the climate variability in Eastern Australia. Therefore, the next two subsections focus on the background to the NARCliM design and the past assessments of these high-resolution projections over south-eastern Australia.

2.6.3 NARCliM - High-resolution RCM data for southeast Australia

There are two recent climate projections available for NSW, Australia: NARCliM (NSW/ACT Regional Climate Modelling) and national climate projections developed by CSIRO and the Bureau of Meteorology (CSIRO and BoM, 2015). However, there are differences between NARCliM and the national climate modelling projections. The national climate projections use GCMs from CMIP5 and provide projections at a coarse resolution of 1.5° latitude/longitude grid (~150 km) for the entirety of Australia (Irving et al., 2012; Bhend and Wetton, 2014) while NARCliM projections use data from the earlier CMIP3 project and provide projections at a finer resolution of 10 km, but only for south-eastern Australia. The national climate projections provide data as time series as well as averages for five different periods: 1986-2005, 2020-2039, 2040-2059, 2060-2079 and 2080-2099. The high-resolution climate projections by NARCliM are also available as current (1990-2009) and future datasets (2020-2039 and 2060-2079).

Of the above two recent climate projections for Australia, NARCliM projections are used throughout this thesis and therefore, the NARCliM project including RCM

selection and GCM selection in Evans et al. (2014) are critically reviewed in this section.

The purpose of NARCliM was to deliver climate change projections for NSW and the Australian Capital Territory (ACT) governments to design their long term climate change adaptation plans (see Evans et al., 2014 and Adapt NSW website: http://climatechange.environment.nsw.gov.au/Climate-projections-for-NSW/About-NARCliM). The project was limited to 12 GCM and RCM ensemble which had been produced by downscaling four GCMS with three different RCMs. Each RCM simulation was produced at 10 km resolution in an inner domain, which was selected within a 50 km resolution domain that covers the CORDEX-AustralAsia region (Figure 2.3). As stated by Evans et al. (2014), "the selection of this 50 km large domain ensures that a future stage of the project using CMIP5 results can take advantage of simulations performed for the CORDEX initiative (Evans et al., 2014; Giorgi et al., 2009) while the inner domain simulates the east-coast climate". As explained in previous sections, this relatively narrow coastal strip, east of the Great Dividing Range, responds differently to the oceanic drivers compared to the west of the Divide (Kiem and Franks, 2001; Verdon et al., 2004; Murphy and Timbal, 2008; Risbey et al., 2009; Verdon-Kidd et al., 2010, 2016; Callaghan and Power, 2014; Di Luca et al., 2016; Browning and Goodwin, 2016; Kiem et al., 2016). In particular, this region is strongly influenced by east-coast lows (Hopkins and Holland, 1997; Speer et al., 2009) and is poorly modelled by the current generation of GCMs (Suppiah et al., 2007), therefore, a better representation of this unique climate was expected from the NARCliM projections.

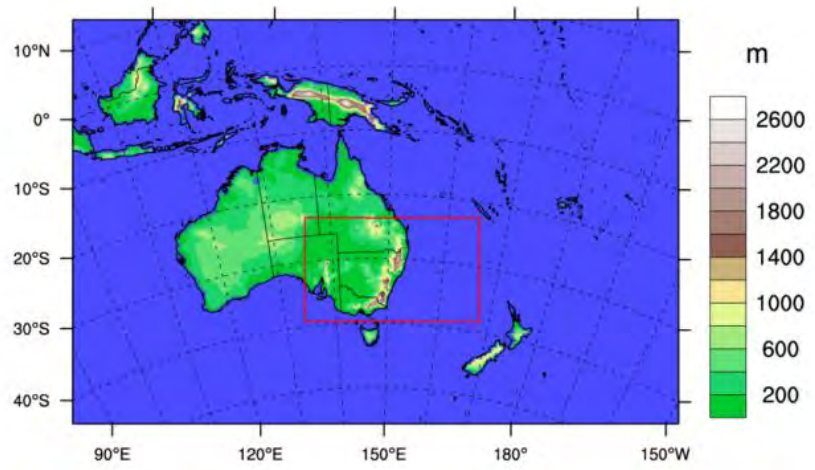

Figure 2.3 Topographic map showing the outer and inner (in red) NARCliM model domain and state boundaries. New South Wales is just to the centre of the inner domain (from Evans et al., 2014).

There are two main phases in the NARCliM project. In the first phase, three RCM configurations of the Weather Research and Forecasting (WRF) model were used to downscale the NCEP/NCAR reanalysis (Kalnay et al., 1996) for the period of 1950 to 2010. The reanalysis was chosen to allow a 60-year long historical simulation (referred as NARCliM reanalysis in this thesis) with the intention of estimating the RCM quality including the systematic biases.

The WRF regional climate modelling system (Skamarock et al. 2008) was developed as a collaborative effort between the National Center for Atmospheric Research (NCAR), the National Centers for Environmental Prediction (NCEP) and the Forecast Systems Laboratory, the Air Force Weather Agency, the Naval Research Laboratory, Oklahoma University, and the Federal Aviation Administration in the United States. In particular in the NARCliM design, the version 3.3 of the WRF was used, with spatial configuration of the model consisting of two one-way nested domains; 50 km and 10 km (Evans and Westra, 2012). The sea surface temperature field was derived from the reanalysis and does not contain any diurnal cycle. The precipitation simulations uses 6 hourly boundary conditions from the NCEP/NCAR ~250 km reanalysis (Evans and McCabe, 2010).

As stated by Evans et al. (2014), the three best WRF RCM configurations were chosen to downscale GCMs from an ensemble of 36 RCMs by following four steps

Note that the description that follows was taken from Evans et al. (2014). See Evans et al. (2014) for more details.

1. The ensemble of 36 RCM configurations were first used to simulate eight different storms observed along the south east region of Australia (Speer et al., 2009; Shand et al., 2010),

2. Then, 30 RCM configurations were chosen by evaluating the ability of each RCM to reproduce the pre- and post-event climate of those storm events, and the climate of storm itself against a range of observations,

3. The chosen RCMs were then ranked based on the method of Bishop and Abramowitz (2013), which defines the model independence based on an averaged covariance matrix of model errors constructed for each variable. For example, if the variable is rainfall, the model independence is evaluated as follows; daily time series of RCM rainfall for each storm event is bias corrected using AWAP observations to produce an anomaly time series. Then, these anomaly series of each event are joined together to construct a single time series used to create the model error covariance matrix. The coefficients, calculated for linear combinations of time series of RCMs that minimize the mean square error are assigned to a covariance matrix constructed for each RCM. The size of these coefficients in the covariance matrix for a given RCM determines the combination of the model performance and the independence. i.e. RCMs with largest coefficients are the best performing and most independent models, and

4. Three top ranked most independent RCMs called R1, R2 and R3 that have been shown to perform well over the region were finally chosen for the design of the NARCliM.

The physics schemes used for R1, R2 and R3 configurations are: WRF Single Moment 5-class microphysics scheme; the Rapid Radiative Transfer Model (RRTM) longwave radiation scheme; the Dudhia shortwave radiation scheme; Monin-Obukhov surface layer similarity; Noah land-surface scheme; the Yonsei University boundary layer scheme and the Kain-Fritsch cumulus physics scheme (Table 2.3).

Table 2.3 The model configuration for the three most independent RCMs (Evans et al., 2014)

NARCliM ensemble member	*Planetary boundary layer physics/ surface layer physics*	*Cumulus physics*	*Micro physics*	*Short-wave/long-wave radiation physics*
R1	MYJ/Eta similarity	KF	WDM5 class	Dudhia/RRTM
R2	MYJ/Eta similarity	BMJ	WDM5 class	Dudhia/RRTM
R3	YSU/MM5 similarity	KF	WDM5 class	CAM/CAM

In the second phase of the NARCliM project, the chosen three RCMs (Table 2.3) were used to downscale four GCMs for three 20-year epochs (1990–2010, 2020–2040, 2060– 2080). The four GCMs from CMIP3 data archive (Meehl et al., 2007) are MIROC-medres 3.2, ECHAM5, CCCMA 3.1 and CSIRO mk3.0 (IPCC, 2007). These four GCMs were identified as performing well for southeast Australia, and were used to set the initial and boundary conditions for the WRF simulations (Evans et al., 2013).

The selection process for these four GCMs is summarized from Evans et al. (2014) as follows.

1. Evans et al. (2014) first built a meta-analysis of GCM evaluation studies (a total of 11) on CMIP3 over Australia, most of which were discussed in Smith and Chandler (2010) and summarized earlier in Section 2.4 in this thesis.

2. Then combining the results in all of these studies, a fractional demerit score was calculated to indicate the models overall performance. The lower the fractional demerit the better the performance. With this argument, six GCMs score 0.5 or higher and were removed from further analysis (See Table 2.4).

3. As was done for assessment of the RCMs, the remaining GCMs were then ranked based on their level of model independence using the measure of Bishop and Abramowitz (2013) (see details on the RCM selection).

Table 2.4 Summary of CMIP GCM assessments (from Evens et al., 2014)

Assessment region		*Australia*							*MDB*		*SE*	
Model	*Fractional demerit*	*A*	*B*	*C*	*D*	*E*	*F*	*G*	*H*	*I*	*J*	*K*
UKMO-HadCM3	0	0	Yes	6	608							179
CSIRO-Mk3.5	0						5	1				207
GFDL-CM2.1	0.111	0	Yes	2	672	Yes			No	Yes	0.72	184
GFDL-CM2.0	0.125	0	Yes	2	671	Yes			No	Yes		252
MIROC3.2 (hires)	0.125	0	Yes	7	608		12	9	Yes			201
CSIRO-Mk3.0	0.182	1	No	7	601	Yes	1	2	Yes	No	0.73	214
UKMO-HadGEM1	0.2	0	No	2	674							163
ECHAM5/MPI	0.222	0	Yes	1	700	Yes			No	No	0.79	173
MIUB-ECHO-G	0.222	0	No	4	632	Yes			Yes	No	0.78	174
INM-CM3.0	0.222	1	No	7	627		9	11		Yes	0.75	192
NCAR CCSM3	0.273	0	No	2	677	No	4	6	No		0.68	245
CNRM-CM3	0.286	0	No	4	542					No	0.73	196
FGOALS-G1.0	0.3	2	No	2	639	No	8	4	Yes		0.66	251
MIROC3.2 (medres)	0.364	2	Yes	7	608	Yes	11	3	Yes	No	0.6	255
CCCM3.1 (T63)	0.375	1		10	478		2	7	No		0.72	241
MRI-CGCM2.3.3	0.455	1	No	3	601	No	10	12	Yes	Yes	0.41	437
CCCM3.1 (T47)	0.455	1	No	8	518	No	3	10	Yes	No	0.77	186
GISS-ER	0.5	0	No	8	515	Yes	6	5	No	No		238
BCCR-BCM2.0	0.5	5		5	590	Yes			No			485
GISS-AOM	0.667	1	No	8	564	No	7	13	Yes		0.6	326
IPSL-CM4	0.8	2	No	14	505	No	13	8	Yes		0.48	394
NCAR PCM	0.833	3	No	11	506						0.64	309
GISS-EH	1	5	No	14	304		14	14				487

A – number of rainfall criteria failed (Smith and Chandler, 2010), B – satisfied ENSO criteria (Min et al., 2005; van Oldenborgh et al., 2005), C – demerit points based on criteria for rainfall, temperature and MSLP (Suppiah et al., 2007), D – M-statistic representing goodness of fit at simulating rainfall, temperature and MSLP over Australia (Watterson, 2008), E – satisfied criteria for daily rainfall over Australia (Perkins et al., 2007), F – order of model based on the total skill scores for each rainfall metric (Kirono et al., 2010), G – order of model based on the total skill scores for each of rainfall and PET metric (Kirono et al., 2010), H – satisfied criteria for daily rainfall over Murray-Darling Basin (MDB) region (Maxino et al., 2008), I – satisfied criteria for MSLP over MDB region (Charles et al., 2013), J – combination of RMSE of mean annual rainfall across south-east Australia and mean NSE (rainfall greater than 1 mm) comparing GCM-simulated and observed daily rainfall distribution with equal weights (Vaze et al., 2011), K – RMSE of mean annual rainfall over Southeast Australia (Chiew et al., 2009).

4. The final step required placement of the GCMs within a future climate change space which was defined by Evans et al. (2014) using two most important climate variables; change in mean temperature in Kelvin, and the percent change in mean precipitation. Figure 2.4 shows the location of the GCMs within this future climate space. The GCMs are represented by their corresponding rank defined in step 3 above.

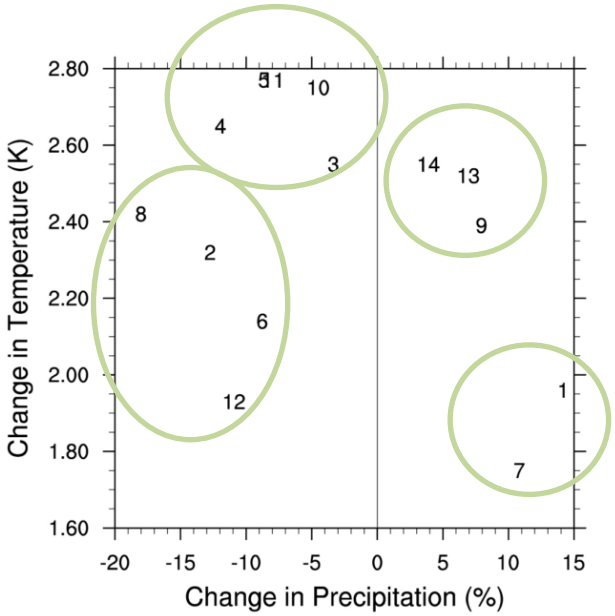

Figure 2.4 Future climate change space for the CMIP3 GCMs numbered by their independence rank. The change is between the mean of 1990–2009 and the mean of 2060–2079 (from Evans et al., 2014). Four groupings of future change in precipitation and temperature are shown in light green circles.

Representing four groupings of future possible changes in temperature and precipitation, four GCMs with the highest independent model ranking were then chosen by Evans et al.: models 3, 9, 2 and 1. However, since some of these GCMs were not able to supply all the required data for various reasons, alternate GCMs were used. Therefore, the final GCM choice used (and their independence model ranking) is MIROC3.2-medres (rank 1), ECHAM5 (rank 5), CCCM3.1 (rank 9), and CSIRO-Mk3.0 (rank 12).

All of the NARCliM downscaled reanalysis and GCM rainfall projections are available as two types: uncorrected and bias corrected. As explained in Evans and Argüeso (2014), the bias correction was based on the 5 km AWAP rainfall data which was aggregated to align with the 10 km WRF grid using inverse distance weighting. The technique used in the bias-correction process is based on Piani et al. (2010a), who explained a method of fitting cumulative distribution function (CDF) of simulated data and observed data to gamma distributions, so that the fitted distributions are matched with each other. The bias correction has been applied at each WRF grid point separately. The bias correction process is described in Evans and Argüeso (2014) as follows.

1. Rain days from both AWAP and simulated (NARCliM) rainfall time series are extracted from a NARCliM grid point by using a threshold of 0.2 mm. However, the threshold value used for the simulated data is slightly larger than 0.2 mm because in general, RCM simulations tend to produce more light rainfall events at coarse resolutions;

2. Using the extracted datasets, two empirical CDFs are calculated for both datasets separately. The empirical CDFs are then fitted to two gamma distributions (F_m and F_o) (Figure 2.5). For a rainfall event i, the simulated rainfall intensity is (M^i) and the corresponding cumulative probability of F_m is (CP_m^i).

3. This (CP_m^i) is used to find the corresponding observed rainfall intensity of AWAP (O^i); and

4. In the last step, M^i is replaced with O^i. Then this correction process is repeated for all grid points in the NARCliM domain.

The statistical testings performed in this thesis use both uncorrected and bias corrected NARCliM simulations and therefore, the improvements and deficiencies of the bias correction process is also discussed in the following chapters.

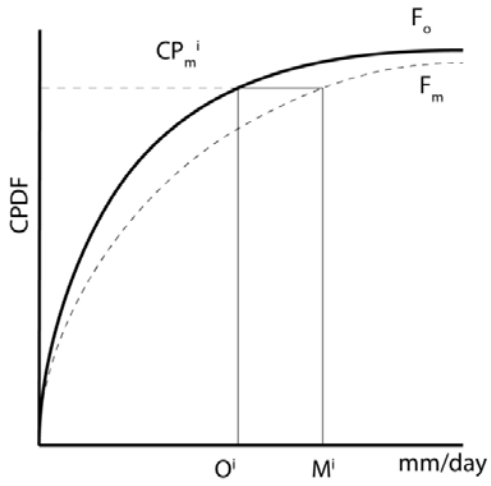

Figure 2.5 Schematic of the bias correction proposed by Piani et al. (2010) (taken from Evans and Argüeso., 2014). M^i is the intensity of the simulated rainfall and O^i is the intensity of the observed event with the same cumulative probability(CP_m^i) as defined by F_m and F_o which are the CDFs for simulated and observed rainfall.

The technical background on NARCliM RCM simulations was presented in this section. The next section focuses on the past studies which have evaluated NARCliM simulations. The main focus is on how these RCMs perform at capturing the observed rainfall statistics in the south east Australia. In particular, the following review identifies research gaps in past studies, while focusing on the assessments required for a better understanding on the use of these RCM datasets in future water resources planning applications.

2.6.4 Evaluation of NARCliM RCM simulations

Since NARCliM high-resolution datasets are fairly new to the research community, most of the applications and evaluations of NARCliM are in progress. Therefore, the published research work on NARCliM projections is relatively limited. However, the most recent publications on NARCliM evaluations are reviewed in this section. It is worth noting that some of the past studies presented in this section are pre-NARCliM assessments which have laid the ground work for the design of NARCliM high-resolution datasets.

As a pre-NARCliM assessment, Evans and McCabe (2010) evaluated the NARCliM RCM data (10 km grid resolution) driven by the lateral boundary conditions of NCEP/NCAR reanalysis (~250 km) against AWAP gridded precipitation over Murray-Darling Basin, Australia and their study was previously presented in Section 2.6.2 under the evaluations of WRF RCM. However, since these datasets are used in this thesis (referred as NARCliM reanalysis) reviewing some of the highlights of their studies is important. In particular, the results of Evans and McCabe (2010) showed that NARCliM reanalysis driven RCMs successfully reproduce daily statistics (bias, RMSE, pattern and anomaly correlations (spatial correlation) and PDF) of AWAP observations. 10 km RCMs had improved results for almost all monthly and interannual spatial distribution of statistics relative to those of the uncorrected NARCliM Reanalysis, which supplied the lateral boundary conditions. NARCliM reanalysis simulations were able to capture the drought experienced over the Murray Darling basin in recent years, except for an overestimation of the negative anomaly in the northernmost part of the domain. Examining ENSO cycles showed that NARCliM reanalysis are able to capture the correct spatial distribution of precipitation anomalies associated with El Niño/La Niña events during this 24 year period (1985-2008).

In another NARCliM evaluation study, Evans and Westra (2012) investigated the ability of reanalysis driven NARCliM RCMs to simulate the diurnal cycle of precipitation over southeast Australia. Their objective was to understand various mechanisms that drive the diurnal variability in the precipitation. The diurnal cycle of a subset of the Australian subdaily rainfall records of 195 gauges located inside the NARCliM domain was compared against the diurnal cycle of NARCliM reanalysis outputs for the period of 1985-2008 using the data from the 10 km ×10 km grid box in which the gauge resides. The 3 hr resolution seasonally averaged number of rainfall occurrence, intensity and the total amounts of rainfall for each season were evaluated in their study. They found that the NARCliM reanalysis tends to simulate too many occurrences and too little intensity for precipitation events at the 3-hourly time resolution, when compared with the gauge rainfall. However, their results showed that the overall precipitation amounts and the diurnal variability in occurrences and intensities of the observed rainfall are well reproduced by NARCliM reanalysis, particularly in spring and summer seasons. For precipitation

intensities, the NARCliM reanalysis had a tendency to overestimate the range of the diurnal cycle during the warmer months, while capturing the rainfall intensities reasonably well during the winter. In winter, the timing of the maxima and minima matched the observed timings well. The spatial pattern of diurnal variability in the NARCliM reanalysis outputs was similar to that of 195 rain gauges used in their study. Compared with other recent evaluation studies of NARCliM, this is the only study which evaluated the ability of NARCliM reanalysis to reproduce the subdaily statistics (occurrence, intensity and diurnal cycle) of the observed rainfall.

As an initial NARCliM assessment, Evans et al. (2013) evaluated the bias in minimum and maximum temperature and precipitation of the reanalysis NARCliM simulations (50 km grid resolution) across Australia by comparing them against the gridded observations of temperature and precipitation of the Bureau of Meteorology's Australian Water Availability Project (AWAP). The results of Evans et al. (2013) showed that WRF-R2 configuration reanalysis (referred as R2 reanalysis in this thesis) produced the best precipitation simulations with only small overestimates of seasonal precipitation along the Great Dividing Range. R1 and R3 were found to overestimate precipitation over eastern Australia and R1 underestimated precipitation over the southwest of Western Australia. Though Evans et al. (2013) evaluated the bias in the rainfall of NARCliM reanalysis compared with AWAP on a seasonal basis, the results for the mean rainfall in this thesis also agree with Evans et al. (2013), showing that R2 reanalysis closely reproduce the spatial distribution of the mean rainfall for all time resolutions studied (daily, fortnightly, monthly and annual), while R1 and R3 reanalyses overestimate the statistics along the east coast of Australia (see Chapter 5 and 6).

Evans and McCabe (2013) evaluated the influence of model resolution on the performance of WRF RCMs which were downscaled from the CSIRO Mk3.5 GCM (~250 km) to 50 km and 10 km resolutions (1985-2009) in three regions of eastern Australia: Murray Basin, Darling Basin and Eastern Seaboard. This study is important to this thesis because the same 10 km resolution dataset is used in this thesis, and referred as CSIRO-Mk3.0 RCM. Using the statistical measures such as mean, bias, RMSE and pattern correlation of the precipitation, they found that increasing spatial resolution of model outputs tended to improve the simulation of

present day climate, with larger improvements in areas affected by mountains and coastlines. In particular on the eastern seaboard, the improvement in the bias in rainfall with increasing resolution was seen for most of the year, except for the period from December to March, when 10 km RCM dataset produce higher rainfall overestimates. The tendency of the CSIRO-Mk3.0 10 km resolution RCM (uncorrected) to produce high rainfall overestimates on the eastern seaboard is consistent with the results in this thesis, keeping in mind that the mean rainfall in this thesis was calculated on the annual basis, but not the seasonal basis. However, most of these systematic biases in the mean rainfall are removed after the bias correction (see Chapter 9).

The results in Evans and McCabe (2013) further indicated that much of the improvement in the RCM performance can be seen in WRF 50 km dataset compared with the performance of 250 km CSIRO-MK3.0 GCM, and there is only a small additional improvement in WRF 10 km dataset. However, in a region like eastern seaboard where there is significant topography and coastlines, there is a need to assess this added value in the improvement of high-resolution RCMs not only considering the distribution statistics such as bias, RMSE and pattern correlation, but also the times series statistics such as temporal and spatial correlations.

Evans and McCabe (2013) also investigated the differences in future climate due to the resolution change in RCMs. They found that largest differences in future projected change in the rainfall are in Murray basin and eastern seaboard where the topography is more complex than the Darling basin. In terms of the magnitudes, high-resolution CSIRO-Mk3.0 RCMs, particularly the 10 km resolution RCM produced changes that are more than double those projected by the raw GCM. However in Evans and McCabe (2013), much of these differences are attributed to the influence of higher topography, which has been better resolved in the 10 km resolution RCM dataset than the original GCM. The ability of 10 km resolution RCMs to better resolve the topography than coarse resolution GCMs is important, yet it is worth to keep in mind that an averaging of the topography within each 10 km grid box is still expected. Due to this averaging effect, the results in this thesis show that NARCliM RCMs have elevations lower than the actual elevations in the ground (see Section 5.1.2).

As in Evans and McCabe (2013), the NARCliM future projections have also been investigated in several other studies.

Ji et al. (2013) investigated the projected changes in the future rainfall of the Sydney metropolitan region through daily and monthly model outputs of 2 km grid resolution dynamical downscaling from CSIRO-Mk3.0 GCM. This 2 km resolution dataset has been produced by the boundary conditions of the 10 km outer domain of CSIRO-Mk3.0 RCM, which was used in Evans and McCabe (2013). However, note that the dataset used in Ji et al. (2013) is bias corrected. By comparing bias corrected projections of rainfall (2040- 2059) with the NCEP/NCAR reanalysis-driven simulation for the period 1990-2009, they found that Blue Mountains, Sydney, Central coast and Illawarra are likely to experience significant increases in the annual rainfall, while Hunter and Southern Highlands experiencing a decrease in the annual rainfall. Note that this 2 km resolution data set only covers a small part of the southern boundary of the Hunter Valley, so could not be used to assess rainfall over the Hunter Water catchments for the Hunter Site used in this thesis, which is on the northern side of the Hunter Valley.

Since there is an overlap between the case study region in Ji et al. (2013) and study sites (Williams River and Sydney) used in this thesis, their results are comparable with the future mean precipitation changes presented in this thesis (Chapter 12). Note that both studies (this thesis and Ji et al., 2013) used RCMs downscaled from the same GCM, but their resolutions are different from each other. Ji et al. (2013) used a 2 km resolution RCM, while the RCM resolution used in this thesis is 10 km. The results in Section 13.2 show that there is a consistency in the expected decrease in the mean annual rainfall simulated by CSIRO-Mk3.0 RCMs in Hunter and Southern Highlands. There is a significant increase in the rainfall predicted by 2 km RCM in Ji et al. (2013) for the Blue Mountains, Sydney, Central coast and Illawarra regions while the results in this thesis only show a slight increase (about 5%) in rainfall for those regions. As explained in Evans and McCabe (2013), the difference in the increases in rainfall appears to be related with the difference between the model resolutions of the same RCM.

Evans et al. (2014a) studied the projected future change in the climate using variables such as precipitation, temperature and wind changes from the present-day

period (1990-2009) to the future period (2060-2079) using the 10 km resolution 12 GCM and RCM ensemble (see Section 2.6.3), and found temperature increases of more than 2ºC in summer but less than this in winter; mean precipitation increases particularly on the northern coast in summer and autumn, and decreases on the southern NSW coast in spring; small decreases in mean wind speed; and increases in maximum wind speeds in summer but decreases in other seasons. Most of these changes in climate variables are presented as the mean change of all 12 ensembles in their study. However, the variability in precipitation within the ensemble was also studied on a seasonal basis and Evans et al. (2014a) found that MIROC3.2 and CCCMA3.1 tend to project increases, while ECHAM5 and CSIRO-Mk3.0 projecting decreases in the mean precipitation, particularly along the east coast during the spring. Though Evans et al. evaluated these changes on a seasonal basis, the general trends in the change in the precipitation for the 12 members of the ensemble is consistent with the results in this thesis (see Section 13.2).

Grose et al. (2015) and Dowdy et al. (2015) compared the projected change in mean rainfall for eastern Australia from the CMIP3 and CMIP5 GCM archives and from three quite disparate downscaling techniques used in the NARCliM and The Climate Projections for Australia's Natural Resource Management Regions (NRM) projects: the NRM project (CSIRO and BoM, 2015) provided projection information and datasets for all of Australia based on CMIP5 and two downscaling methods using CMIP5 as input. The results in these two studies showed that downscaled projections produce different projections than CMIP3 and CMIP5 for the east coast of Australia. In particular, Grose et al. found that NARCliM projections tend to produce wetter projections than their host models (4 GCMs) in most seasons. They further attributed these changes to the interaction between different model components and configurations which are combined with the finer spatial resolution used through the process of downscaling.

The review on NARCliM evaluations in this section shows that NARCliM simulations have mostly been evaluated as pre-NARCliM assessments. Further, the ability of NARCliM RCMs to reproduce the current observed rainfall statistics have only been tested in few studies, while many authors focused on the future climate simulations. Therefore, this highlights a need of evaluating these simulations in more

sophisticated ways to understand the employability of these datasets for water availability studies. In particular this thesis focuses on evaluating the high-resolution NARCliM rainfall projections focusing on the statistics which are important for water security assessments. Therefore, the next section summarizes the validation need for NARCliM simulations before they are used in water security assessments.

2.6.5 Validation needs for NARCliM

The ability of NARCliM to generate the correct observed rainfall statistics is necessary when using these datasets in hydrologic applications such as water security assessments, particularly for generating the runoff in the reservoir water availability analysis. The following key points highlight the validation need for NARCliM before these rainfall projections are used in hydrology models to generate runoff.

1. All the published research are pre-NARCliM assessments and none of those studies compared all 12 RCM-GCM simulations together to identify their individual characteristics and how they capture the current observed rainfall statistics. In particular, many studies have only evaluated the NARCliM reanalysis projections (driven by NCEP/NCAR reanalysis) hence, there is a need to evaluate NARCliM GCM projections for the most recent climate (1990-2009).

2. There are only a few studies which tested the ability of NARCliM to reproduce the current rainfall statistics as many authors focused on the NARCliM future rainfall projections. In these few studies, all evaluation approaches are based on the atmospheric perspective which only considers the distribution statistics such as bias, RMSE, pattern correlation and skill assessments based on the PDFs. None of the studies focused on the time series statistics such as temporal and spatial correlations of the rainfall which are necessary to be reproduced correctly by the RCM projections before these projections are used for the runoff generation. Therefore, while evaluating the ability of NARCliM projections to reproduce the observed rainfall distribution statistics such as mean, standard deviation, coefficient of variation (standard deviation/mean) and daily PDFs, there is a need to study

more sophisticated statistics such as temporal correlations (autocorrelations), spatial correlations and cross correlation of the rainfall which are important for the water security assessments. More details on the statistics used in this thesis are presented in Chapter 4

3. Because the reservoirs of different capacities respond to rainfall differently, there is a need to assess the NARCliM projections, focusing on dam storages and how dams are sensitive to reservoir filling water volumes at different temporal resolutions. Therefore, rainfall statistics should be tested not only based on the daily time resolution, but also on the resolutions aggregated up to longer periods such as weeks, fortnights, months and annual.

4. Instead of studying the RCMs over a large area, there is a need to assess the rainfall statistics of NARCliM projections at various study sites by considering different sizes, aspects of elevations and exposure to the coastal weather systems. Assessments of RCM projections at various catchments are important, particularly for a region like ES, because as explained in Section 2.3 the eastern seaboard does not respond to the climate drivers such as ECLs as one region, instead the ECL impact location on the eastern seaboard varies depending on the type of ECL that occurs at a time.

5. There are only a few published research works on the NARCliM bias corrected projections. Therefore, this highlights a need to assess both bias corrected and uncorrected projections to understand how they perform in capturing the current observed rainfall statistics. The assessment of uncorrected data allows the user to identify the intrinsic characteristics of the RCM simulations. However, it is expected that bias correction will change the PDF of the rainfall, correcting the distribution statistics such as mean and standard deviation, but it is less likely to modify the temporal and spatial relationships present in the observed rainfall. Therefore, there is a need to understand the extent of change caused by the bias correction relative to the uncorrected simulations. To do this more meaningfully, the NARCliM bias corrected and uncorrected rainfall projections should be evaluated based on different hydrologic aspects such as different time resolutions (see key point

3 on the dam related hydrology), topographic conditions and catchment sizes (see key point 4 on the catchment averaging of the rainfall).

By reviewing past studies on evaluation of various GCMs and RCMs in Sections 2.4 to 2.6.4 and identifying the validation approaches need for the NARCliM RCM rainfall, this thesis intends to perform more sophisticated statistical testings on the NARCliM RCMs while filling the research gaps which have not been addressed in the literature. In particular, the focus the statistics which provide information on the employability of these datasets to generate runoff when they are used in rainfall runoff models. The next section presents a summary of this chapter and motivations of the thesis.

2.7 Summary and motivations of this thesis

Climate output from RCMs can be evaluated using a range of different approaches and number of statistical measures such as mean, maximum, minimum, bias, RMSE, PDF, skill and correlation coefficient of the rainfall. However, the selection of these methods to evaluate RCMs often depends on the end application. For example, some of the statistics such as bias, RMSE and model skills can provide information on the climate projections for the atmosphere, but not for the hydrology. When testing RCMs for hydrologic applications there is a need to perform more comprehensive statistical testings which evaluate the spatial and temporal relationships of the rainfall. In particular, this study aims to make advances towards an improved evaluation of RCMs focusing on the hydrology and reservoir modelling applications. This chapter has provided a review of the background, previous work and evaluation methodologies on GCM/RCM projections developed by the research community, and deficiencies of their approaches. By doing so it identified five research gaps which will be addressed by this thesis. The following are the motivations for the objectives of this thesis. A brief summary on the statistics used in this thesis is presented in Objective 1 and more details on each of these statistics are presented in Chapter 4.

- *Objective 1: Test and validate the rainfall statistics of the downscaled RCM data which are important for reservoir modelling and water availability analysis.*

  The NARCliM simulations allow users to do hydrology analysis at the catchment scale with sufficient resolution to capture the size of many water supply catchments. Most recent studies assessing NARCliM showed that the datasets are able to capture the spatial distribution of the rainfall (Evans and McCabe, 2010; Argüeso et al., 2012 on WRF RCMs), but what is less clear is how good these climate data will be at replicating observed rainfall statistics important for hydrology models or in capturing the persistence of runoff that is important in the performance of reservoirs systems. Therefore, it is important to assess if the statistical properties of the observed rainfall are correctly reproduced by these RCM datasets for the current day data. As was studied earlier by Evans and McCabe (2010), Evans and McCabe (2013) and Evans et al. (2013), evaluation of basic statistics such as mean, maximum, minimum, bias, RMSE, PDF and correlation coefficient of the rainfall is necessary for the water resource planning and availability analysis, but not sufficient to understand how accurately the time series properties (e.g time sequencing of rainfall events) of the observed rainfall have been replicated by the RCMs. Therefore, while evaluating the statistics such as mean and coefficient of variation (ratio between standard deviation and mean) of the rainfall, there is a need for more sophisticated assessments focusing on the statistics such as temporal and spatial correlations of the rainfall and their variability with elevation.

  As in Perkins et al. (2007) and Evans and McCabe (2010), the PDFs of RCM daily rainfall are also calculated in this study and validated against observations. However, the validation presented in this study is different to Perkins et al. (2007) and Evans and McCabe (2010), and does not contain any skill assessment (see Section 2.4 for the reasons of not using skill assessment). Instead, cumulative probability distribution (CDF) of the daily rainfall are constructed at selected single grid points, where Perkins

constructed the PDFs for each variable (rainfall, precipitation, etc.) for all modelled and observed data over large regions (10°×10°) of Australia.

In comparison to Evans et al. (2013) who investigated the performance of precipitation on a 50 km grid generated for all of Australia (CORDEX-AustralAsia region), the finer resolution 10 km NARCliM datasets generated only for southeast Australia are used throughout the study in this thesis. As in Evans et al. (2013), the reanalysis driven datasets generated using R1, R2 and R3 model configurations of WRF are used in Section 1 of this thesis, but the focus is on autocorrelations (Evans focused on bias) as reservoir performance can be sensitive to the persistence of runoff. The lag-1 correlation of the rainfall has been studied in McMahon et al. (2008), but they have only focused on lag-1 correlation, whereas this study focuses on lag correlations up to 60 lags (e.g. for a monthly assessment this analysis calculates the correlation between rainfall of the first month and 60th month). Analysing the long term correlation of the rainfall is important as it provides insights about the persistence of the rainfall patterns and seasonal variations throughout a long period of time.

The spatial correlation of the daily rainfall between different grid points (i.e. correlation at a specific time between two different locations) is evaluated in this thesis at the catchment scale. The spatial correlation of the rainfall is important when estimating the rainfall in hydrological and water availability analysis. If the distribution of a rain gauge network is sparse or the available data at a specific location is not highly reliable, an existing spatial correlation of the rainfall can be useful to predict the rainfall. The spatial correlation calculated in this study is different to the spatial correlation (r_s) which was studied by Smith and Chandler (2010), where they calculated the spatial correlation between observed and simulated fields by pairing grid point values across the entire continent and calculating the corresponding Spearman rank correlation coefficient.

The cross correlation between the RCM and observed rainfall is also evaluated at the daily resolution in this study. Similar to Evans et al. (2005), these correlations are calculated at single grid points with contrasting terrain. However, Evans et al. only assessed the root mean square error (RMSE) of

the modelled and observed data and they did not focus on spatial and temporal autocorrelations and cross-correlations between variables. Further, the cross correlation between the rainfall and elevation is also assessed in this thesis.

The gridded NARCliM RCMs can be validated against both gridded and point scale observations. The literature presented so far shows that validation of RCMs against a gridded observed dataset is most common in practice and removes the scale discrepancy between the datasets. However compared with ground-based point scale measurements, there are uncertainties and limitations associated with the gridded observation due to different interpolation techniques used in producing those datasets. Therefore, using point scale measurement and gridded observation in the validation of RCMs has their own pros and cons. To deal with these differences, NARCliM RCM rainfall is evaluated against both rain gauge and gridded observations (AWAP) whenever possible in this thesis. In particular, when an assessment is performed at single grid points, both rain gauge (located within the grid point) and gridded data are used.

- *Objective 2: Identify the similarities and differences between the performance of NARCliM RCM data to capture the temporal and spatial statistics of observed rainfall for various sites, from north to south in the broader east coast of NSW, and with different orography, exposure to the coastal weather systems and ECL occurrence.*

  The review in Section 2.6 showed that high-resolution RCMs are more able to capture regional climate trends than their host GCMs. As was explained in Chapter 1, the major motivation for ESCCI is that the relatively narrow (100 km east to west) coastal strip is poorly resolved in current generation global climate models (grid resolution of ~250 km x 250 km) and it is bounded to the west by a steep escarpment so it has proven difficult to capture the climate change trends and impacts for the region. The purpose of NARCliM was to use RCMs to downscale GCM data to better capture the climate variability along the east coast of Australia. Therefore, detailed investigations on how these RCMs perform along the east coast are needed. Evans and

McCabe (2010) assessed the effect of model resolution on the performance of a subset of NARCliM RCMs (CSIRO-Mk3.0 RCMs) by taking the east coast of Australia as a separate region compared with other regions of Australia. Di Luca et al. (2016) evaluated NARCliM's 15 member ensemble across the 10 km inner domain of NARCliM, but their focus was on assessing the ability of RCMs to reproduce the climatology of ECLs. In contrast, this study evaluates NARCliM RCMs along the broader east coast and their use for water security assessment studies, by performing a range of statistical methods for four main sites. The selection of a range of sites along the east coast renders more regional insights on the rainfall properties along the east coast, and how these properties are replicated when they are subjected to different orography and exposure to coastal weather systems (see Section 2.3). As was explained by Kiem et al. (2016), ECL impacts are not consistent along the east coast, and the impact location tends to vary depending on the type of ECL that occurs. Following this argument, Objective 2 focuses on identifying any possible trends in rainfall properties from north to south of the broader east coast which may be caused by the ECLs or any other climate phenomenon, and therefore the rainfall statistics are investigated for four selected sites along the east coast. Additionally, since the findings from this study are to be used in future water resource planning, each of the sites was selected so that at least one main water supply systems are located within. More details on these water supply systems located in each site are presented in Section 3.2. Moreover, the insights from this study will be useful for water resources planning for the Hunter Water's system located in Williams River site. Additionally, Sydney Catchment Authority is also carrying out similar studies specifically for the Sydney headworks system in an internal project and therefore, insights on the results will be exchanged as the studies conclude. However, it's worth noting that this thesis does not evaluate the runoff generated using NARCliM RCMs and runoff statistics and implications of them on hydrology have been studied in a separate study (see Lockart et al., 2016).

- *Objective 3: Compare the performance of RCM data with and without bias correction*

  With the exception of Ji et al. (2013) (Section 2.7.3) past studies on NARCliM used the uncorrected NARCliM rainfall. This is because the bias corrected data was only generated recently and therefore, bias corrected data were not available during the first two phases of the NARCliM project. However, it is expected that bias correction will improve the PDF of the rainfall, correcting the distribution statistics such as mean and standard deviation, but it is less clear how it might change the temporal and spatial correlations present in the observed rainfall. Therefore, there is a need to understand the extent of improvement caused by the bias correction relative to the uncorrected simulations. Therefore, both uncorrected and bias corrected RCM projections are evaluated throughout this thesis.

- *Objective 4: Study the impact of orography on water security. Most of the water supply catchments along the east coast are subjected to orographic rainfall due to closeness of the eastern edge of the escarpment of the Great Divide to the coast. Therefore, the relationship between the rainfall and elevation is explored.*

  The recent climate projections for Australia issued by CSIRO and Bureau of Meteorology indicate that the degree of confidence in projections of future rainfall in the Eastern Seaboard region is generally not as high as in many other regions of Australia (CSIRO and BoM, 2013). This is due to the significant influence of the fine spatial resolution in topography on rainfall in the east coast region and how it is handled in different models (Evans and McCabe 2013). This suggests that there is a need to explore this relationship between the rainfall and orography further, which was previously found to exist in this region by several authors (McMahon, 1964; Hutchinson, 1998a,b; Anders et al., 2015; Chubb et al., 2016). Therefore, this study will explore the impact of orography on rainfall and assess the impacts of ECLs on this relationship. In general, most water supply catchments located along the broader east coast are subjected to orographic rainfall due to proximity of

the Great Divide to the coast and if wind directions change due to ECLs or other synoptic systems then water security may change even with no change in average rainfall away from the Great Divide.

- *Objective 5: Determine the future change in NARCliM rainfall properties compared with current rainfall statistics*

  Future climate projections are the basis of knowledge used by governments to establish their climate change adaptation plans. The understanding of the RCM/GCM predicted variability in the climate is important and many authors have evaluated the change in precipitation and temperature using NARCliM future projections. Similar to previous studies discussed in Section 2.6.4, the future change in the precipitation is evaluated for 2070 relative to 2000 in this thesis. However, the focus is to identify the differences and similarities between the different NARCliM RCM projections which are certainly caused by the underlying GCMs and RCM configurations.

Chapter 3
Sites and Data

3.1 Introduction

This chapter provides a brief description of the five study sites located on the east coast of Australia and datasets used in this thesis. The sites investigated are Merriwa, Williams River, Richmond River, Sydney and Bega River.

3.2 Site description

As explained by Kiem et al. (2016) (see Section 2.3), the rainfall pattern and the impacts to the east coast of Australia vary depending on the ECL type and time of the year. In fact, results in Kiem et al. (2016) have led to one major conclusion that the rainfall variability along the east coast of Australia is not uniform across the region and can vary from one location to another depending on the type of ECL that occurs. Therefore, there is a need to study this variability in the rainfall at the regional scale. Since the heavy rainfall associated with ECLs often generates reservoir filling water volumes, assessment of the rainfall variability at different study sites where major water supply systems are located can provide directly applicable insights for water security as well as dam safety in those systems. Therefore, instead of studying the eastern seaboard as a whole, the analyses in this thesis are performed at various study sites where main water supply systems are located.

The five study sites used throughout the thesis are shown in Figure 3.1. Note that the Merriwa site is used as a preliminary site and is only used for the analyses in Chapter 5. The remaining four sites; Williams River, Richmond River, Sydney and Bega River are key for the ESCCI-ECL project objectives and, therefore, investigated in more detail throughout this thesis. The summary statistics of each of the five sites are shown in Table 3.1.

Table 3.1 Summary statistics of site locations

Site	*Elevation-m (min, max)*	*Mean annual rainfall-mm (min, max)*
Merriwa	40, 1600	500, 1100
Williams River	0,1600	650, 2000
Richmond River	0,1600	1000,1650
Sydney	0, 2250	600,1700
Bega River	0,2250	750,1050

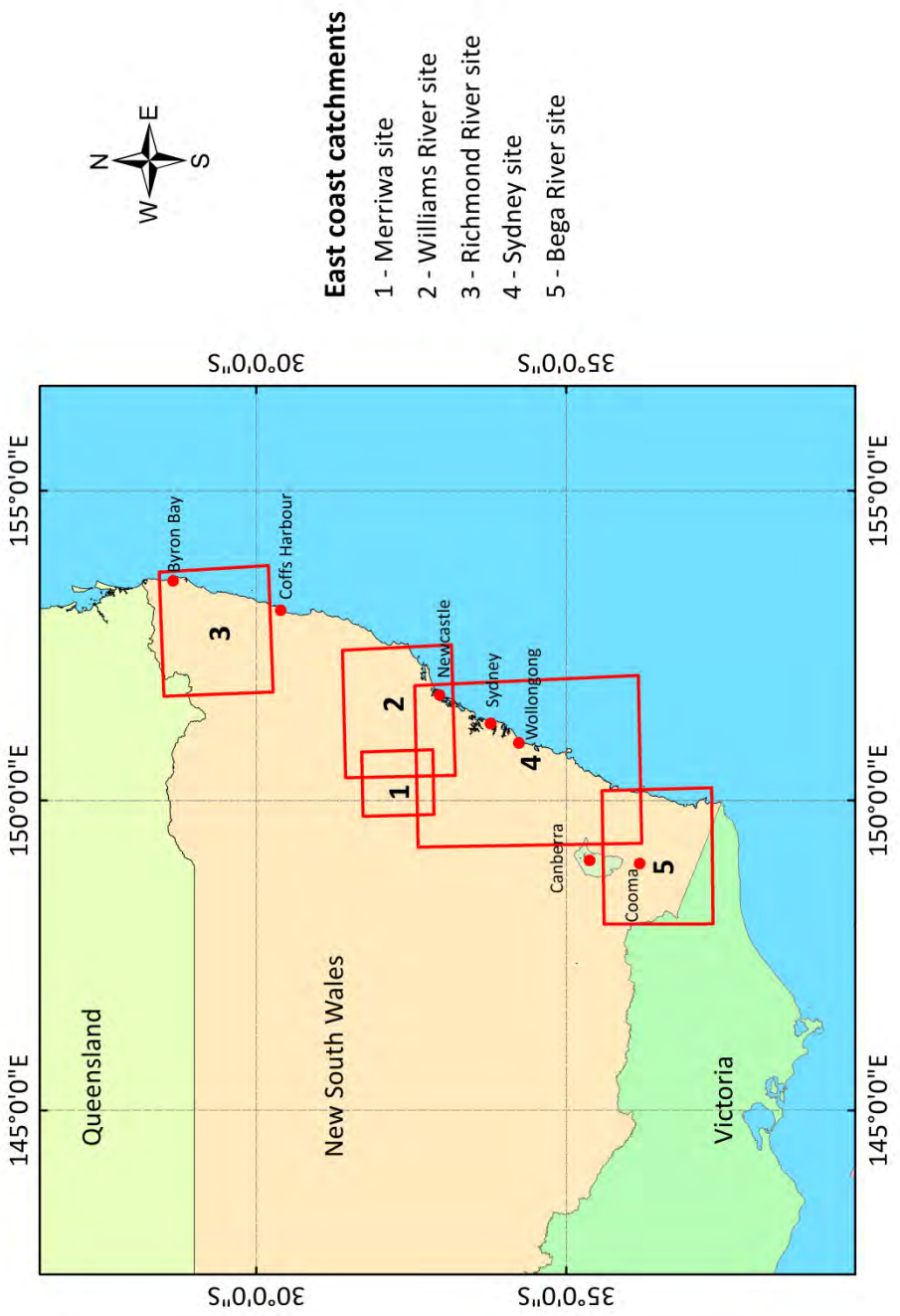

Figure 3.1 Map of site locations

3.2.1 Merriwa site

The Merriwa site has an area of 13,000 km^2 and encompasses the Goulburn River catchment (Figure 3.2) in the Upper Hunter region of NSW, Australia. The climate of the Merriwa site is semi-arid to arid. The average annual rainfall is approximately 650 mm, varying from 500 mm to 1,100 mm spatially depending on the elevation (Chen, 2013). This site has previously been used for a number of hydrology studies and has extensive field instrumentation for monitoring hydrology.

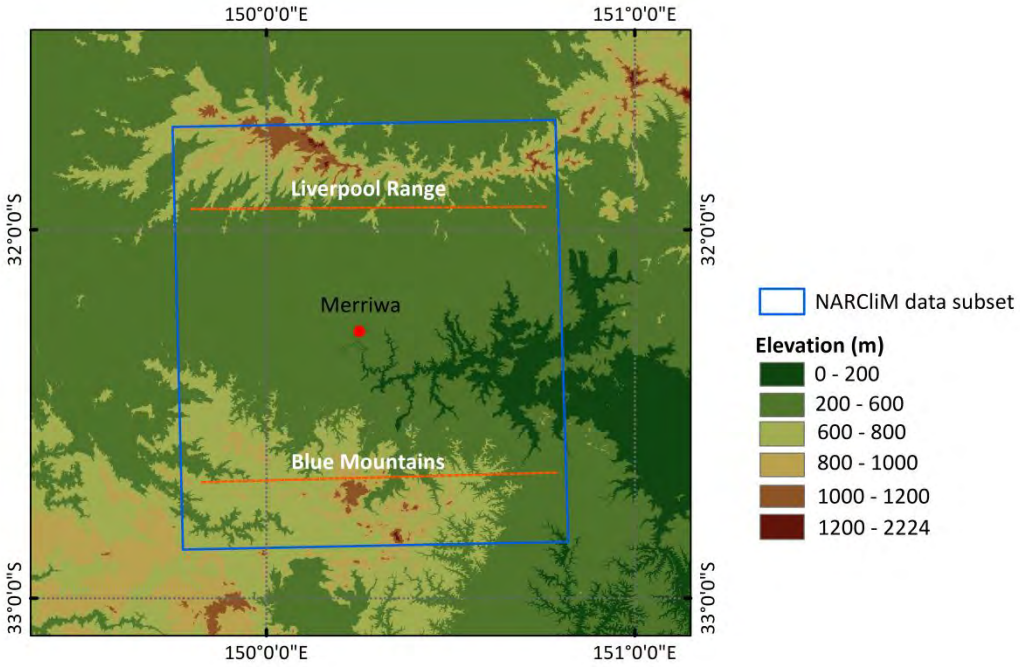

Figure 3.2 Topography map of Merriwa site. The boundary of the site is equal to the boundary of the NARCliM data subset (10×13 pixels with 10 km resolution) outlined in blue.

3.2.2 Williams River site

The topography map of the Williams River site is shown in Figure 3.3. This site, which encompasses the Williams River catchment has an area of 40000 km^2 and is located in the Lower Hunter region of the east coast of Australia. This area has a range of climate types; coastal, inland, rainshadow (west of the Barington Tops) and East Coast Lows. The annual rainfall in the Williams River site ranges from 1,100 mm at Newcastle to only 650 mm at Merriwa and Scone in the upper reaches. Around the Barrington Tops on the northern side of the site, however, annual

precipitation can be as high as 2,000 mm, some of which is snow since July minimum temperatures are often below 0 °C. The Lower Hunter water supply headworks system, which harvests water from the Williams River catchment, is located inside the boundary of the site.

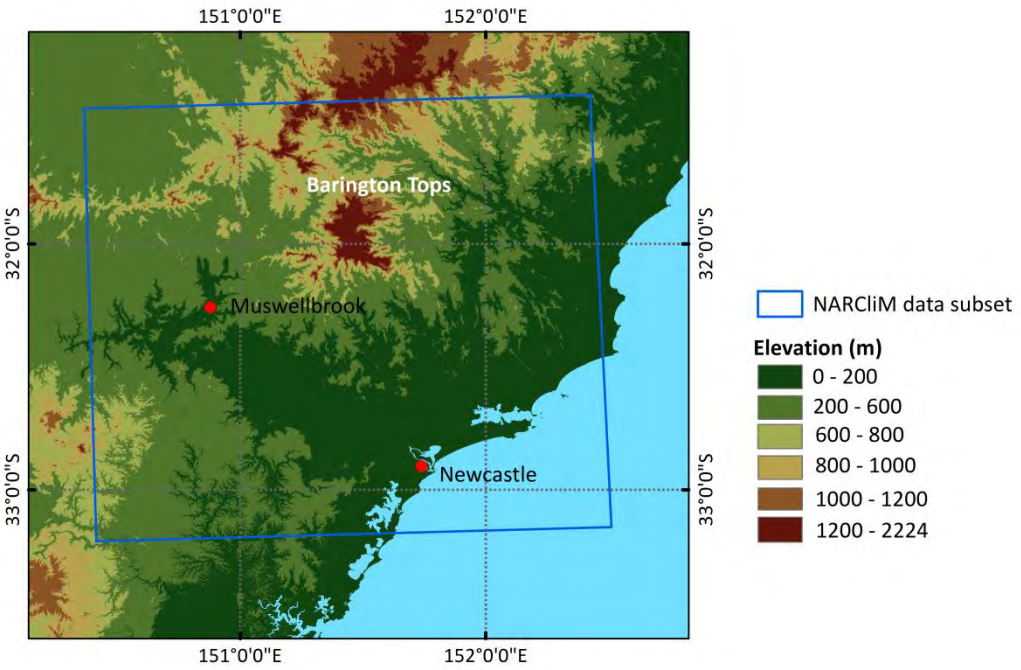

Figure 3.3 Topography map of the Williams River site. The boundary of the site is equal to the boundary of NARCliM data subset (20×20 pixels of 10 km resolution) outlined in blue.

3.2.3 Richmond River site

The Richmond River site, which encompasses the Richmond River catchment shown in Figure 3.4 has an area of 40,000 km^2 and is located on the far north NSW coast. Similar to the Williams River site, the climate types are coastal, inland, rainshadow and East Coast Lows. To the north of the site lies the Border Ranges National Park and other reserves associated with the World Heritage listed Tweed volcanic caldera and its associated Gondwana rainforests. Average annual rainfall in the Richmond River site ranges from 1,650 mm or more along the coast to less than 1,025mm at inland areas.

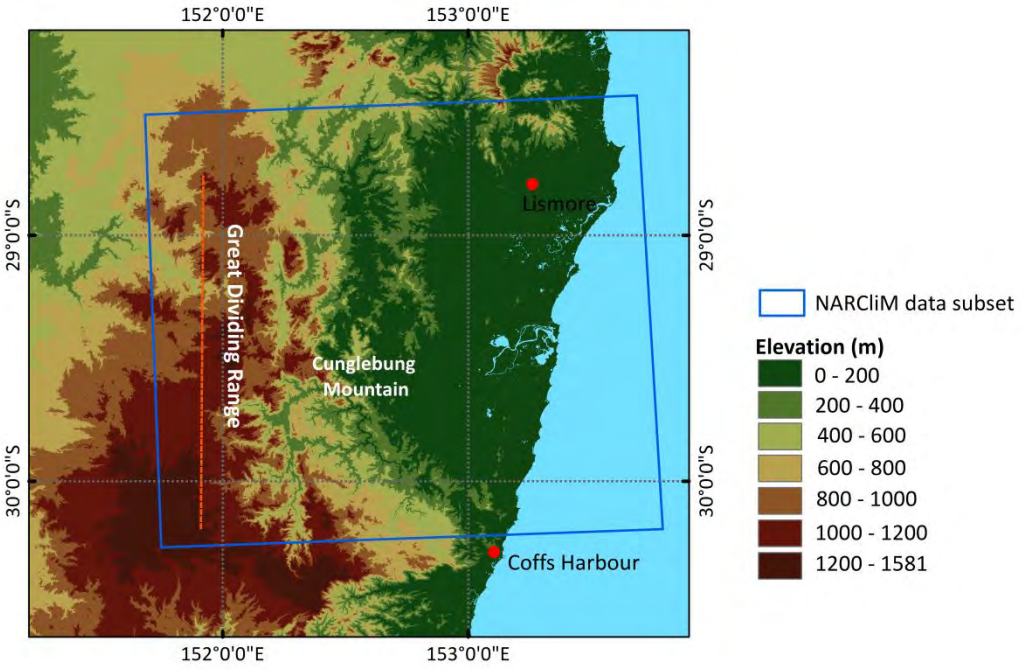

Figure 3.4 Topography map of the Richmond River site. The boundary of the site is equal to the boundary of NARCliM data subset (20×20 pixels of 10 km resolution) outlined in blue.

3.2.4 Sydney site

The Sydney site, which encompasses the Sydney urban water supply catchments, is shown in Figure 3.5 and has an area of 102,500 km^2. The general climatology of the Sydney site is characterized by; coastal, inland, rainshadow and East Coast Low systems. The Blue Mountains range located in the north-west of the site has the highest elevation of 1,215 m. The site has an annual average rainfall of approximately 890 mm. The Sydney water supply system which provides drinking water for about four million residents is located in this site. The drinking water is primarily supplied by surface water sources in the Nepean Hawkesbury river system. Additionally, Sydney Water Supply System incorporates the Shoalhaven System, the Warragamba and Blue Mountains dams, Prospect Dam and Woronora Dam.

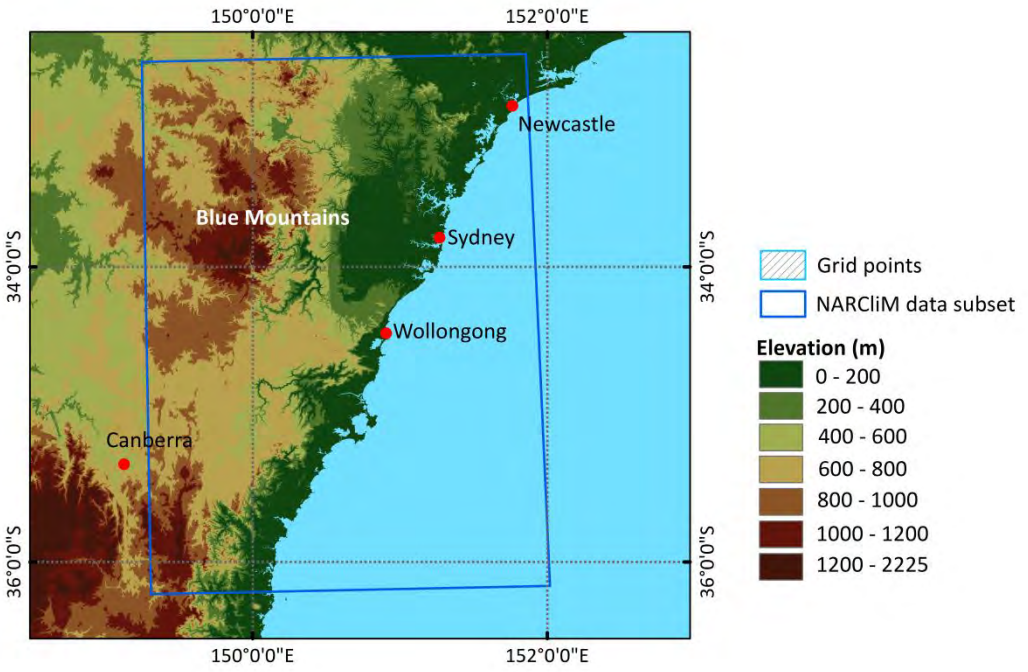

Figure 3.5 Topography map of the Sydney site. The boundary of the site is equal to the boundary of NARCliM data subset (41×25 pixels of 10 km resolution) outlined in blue.

3.2.5 Bega River site

The Bega River site (Figure 3.6) is located on the far south coast of NSW and has an area of 40,000 km^2. The climatology in the site is characterized by warm temperate maritime climate with rainshadows. The escarpment rises gradually to the west of Bega where it attains an elevation of 2,200 m. The highest elevation is at the Australian Alps, which is a segment of the Great Dividing Range. Orographic effects imposed by the escarpment largely control the distribution of rainfall in the high elevation regions of the site. Regional rainfall is greatest in the escarpment zone, where average annual rainfall is in excess of 1050 mm. Rainshadow effects decrease this annual average to around 750-800 mm in the central and lowland sections of the Bega River site (Brooks and Brierley, 1997). Average annual rainfall at the base of the escarpment is between 850-1,000 mm. As the main drinking water supply, Bega River is regulated downstream of Brogo Dam, but the rest of the catchment is unregulated.

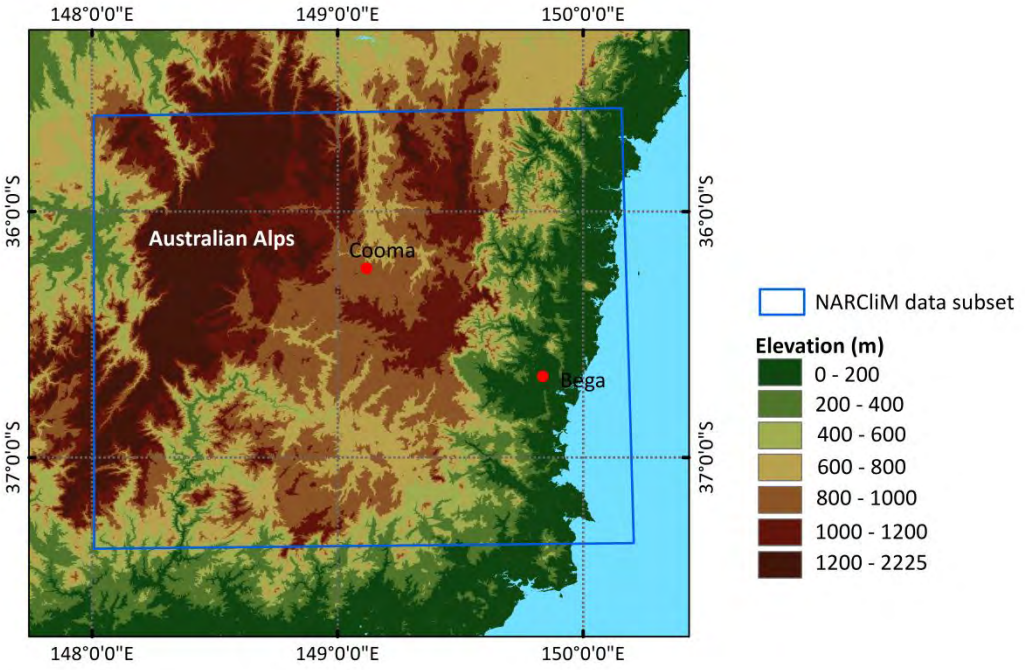

Figure 3.6 Topography map of the Bega River site. The boundary of the site is equal to the boundary of NARCliM data subset (20×20 pixels of 10 km resolution) outlined in blue.

3.3 Data

The rainfall data used in this thesis comprises 1-hourly and daily NARCliM rainfall for one 60 year period (1950-2009) and three 20 year epochs (1990-2009, 2060-2079 and 1950-2009), daily rain gauge rainfall from the Bureau of Meteorology (BoM, 2013) and Australian Water Availability Project (AWAP) 5 km resolution gridded daily dataset.

3.3.1 NARCliM Rainfall data

The climate projection datasets used in this thesis have been produced by the NARCliM (NSW/ACT Regional Climate Modelling) project which provides dynamically downscaled climate data for southeast Australia at 10 km resolution. The NARCliM datasets were reviewed in Section 2.6.3. Therefore, only a summary is presented in this section.

NARCliM has used three configurations of the Weather Research Forecasting (WRF) Regional Climate Model and four different General Circulation Models

(CCCMA 3.1 and CSIRO-Mk3.0, ECHAM5 and MIROC 3.2) from CMIP3 to perform twelve ensembles of twenty year simulations for current (1990-2009) and future climates (2020-2039 and 2060-2079) (Evans et al., 2012; Evans et al., 2014; Ji et al., 2014). In addition to the GCM-driven simulations, three control run simulations driven by the NCEP/NCAR reanalysis for the entire period of 1950-2009 have also been performed by the NARCliM project (Evans et al., 2013; Evans et al., 2014). Including these three control run simulations, there are fifteen different RCM simulations available for south-eastern Australia. Additionally, rainfall data are available in two types: uncorrected and bias corrected.

A summary of the NARCliM datasets used in each chapter is shown in Table 3.2.

Table 3.2 Summary of datasets used in each chapter

Section	*Chapter*	*Datasets used*
Section 1	Chapter 5 Chapter 6 Chapter7 Chapter 8	Uncorrected NARCliM reanalysis rainfall (1950-2009) (referred individually as R1, R2 and R3 reanalysis, and collectively as reanalyses)
Section 2	Chapter 9 Chapter 10 Chapter 11 Chapter 12	1. Uncorrected and bias corrected GCM simulations (1990-2009): CCCMA 3.1, CSIRO-Mk3.0, ECHAM5 and MIROC 3.2 2. Uncorrected and bias corrected reanalysis simulations (1990-2009) (referred individually as CCCMA 3.1 RCM, CSIRO-Mk3.0 RCM, ECHAM5 RCM, MIROC 3.2 RCM and reanalysis, and collectively as RCM simulations)
	Chapter 13	1. Bias corrected GCM simulations (1990-2009): CCCMA 3.1, CSIRO-Mk3.0, ECHAM5 and MIROC 3.2 2. Bias corrected GCM simulations (2060-2079): CCCMA 3.1, CSIRO-Mk3.0, ECHAM5 and MIROC 3.2 (referred individually as CCCMA 3.1 RCM, CSIRO-Mk3.0 RCM, ECHAM5 RCM, MIROC 3.2 RCM and reanalysis, and collectively as RCM simulations)

3.3.2 Observed rainfall

Observed rainfall data have been used for the validation of NARCliM RCM simulations: in particular, rain gauge data are used to assess the statistics of NARCliM simulations at single grid points within a site (see Sections 4.4 to 4.6). The daily rain gauge rainfall data were obtained from the Australian Bureau of Meteorology (BoM) (www.bom.gov.au) for all sites in this thesis. The rainfall data were selected using three criteria: length of record, continuity of record during the NARCliM data period, and location.

In the analysis presented in Chapter 5 for the Merriwa site, three rain gauge stations representing mountainous and flat terrain conditions were chosen, all of which have been in operation for over 60 years and are mostly free of missing data during the years overlapping the NARCliM reanalyses. Details of these stations along with the NARCliM grid points which cover these rainfall stations are shown in Figure 3.7 and Table 3.3.

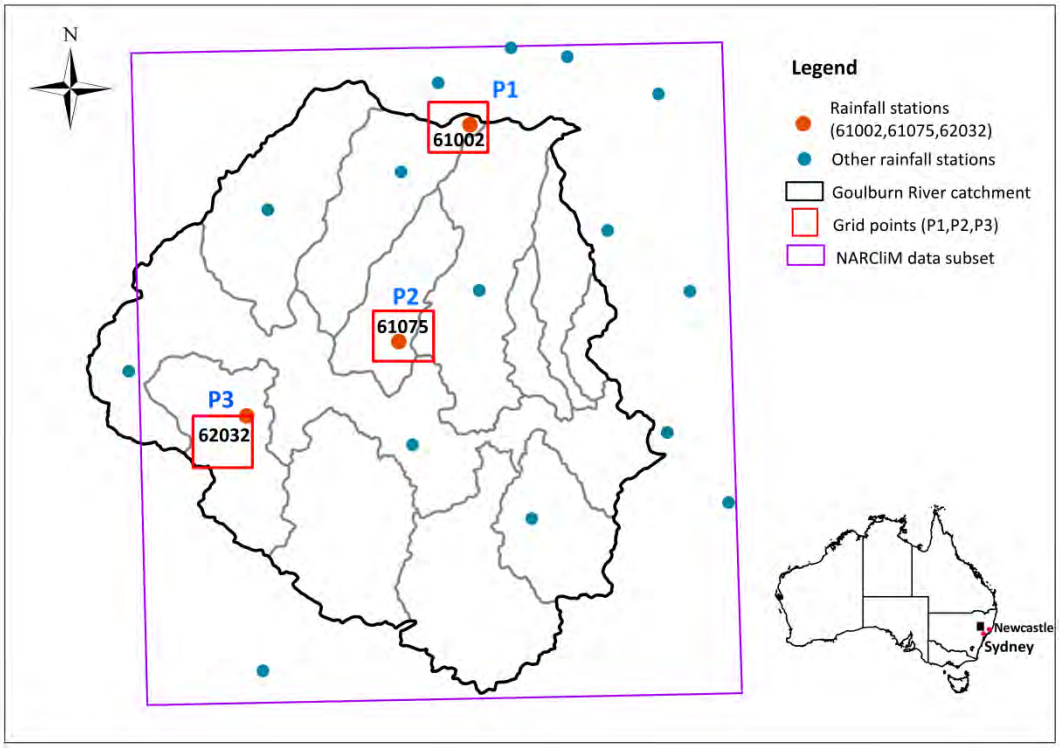

Figure 3.7 Goulburn River catchment and Merriwa site location.

Table 3.3 Statistics of BoM raingauges

Station Number	*Station Name*	*Data availability*	*Annual Minim-um (mm)*	*Annual Maxi-mum (mm)*	*Annual Mean (mm)*	*Terrai-n Condi-tion*	*Elevation of station (m)*	*Corres-ponding NARCl-iM grid point with elevatio n (m)*
61002	Blackville	100	457	1,787	911	Moun-tainous	610	P1, 619.9
61075	Merriwa	98.3	286	1,332	611	rolling hills	380	P2, 308.7
62032	Wollar	98.3	233	1,205	629	flat	366	P3, 546.6

Data availability = % of total days in the 1950-2009 period

Similarly, rain gauges used for the Williams River, Richmond River, Sydney and Bega River sites are shown in Figures 3.8 to 3.11 respectively. The lists of rain gauges used at each site are shown in Tables 3.4 to 3.7 respectively.

As for the Merriwa site, rain gauges which cover the time period of NARCliM data subset were selected at all sites. Additionally, every gauge has an overlap of more than 98% of the duration of the corresponding NARCliM dataset. The missing data were filled with zero rainfall for all sites.

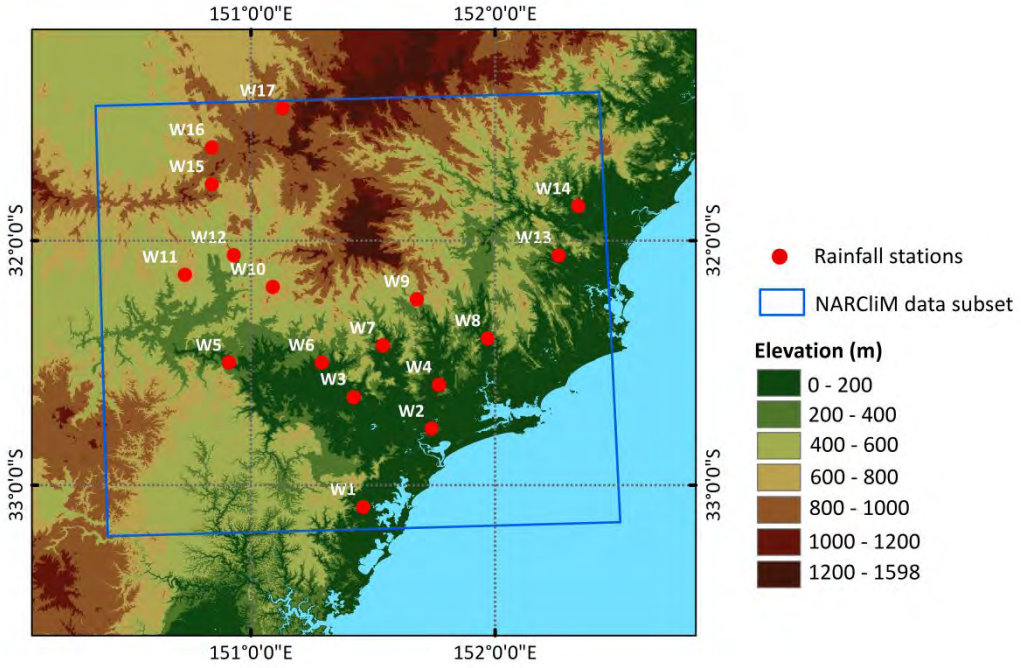

Figure 3.8 Map of the rain gauges at the Williams River site.

Table 3.4 List of BOM raingauges: Williams River site

Station ID (as shown in Figure 3.8)	*Station ID*	*Station name*	*Elevation (m)*
W1	61012	Cooranbong (Avondale)	10
W2	61031	Raymond Terrace (Kinross)	10
W3	61014	Branxton (Dalwood Vineyard)	40
W4	61010	Clarence Town (Prince St)	24
W5	61086	Jerrys Plains Post Office	87
W6	61050	Sedgefield (Bundajon)	73
W7	61024	Gresford Post Office	85
W8	61071	Stroud Post Office	44
W9	61151	Chichester Dam	194
W10	61095	Rouchel Brook (Albano)	305
W11	61065	Aberdeen (Rossgole)	543
W12	61089	Scone SCS	216
W13	60021	Krambach (Firefly Rd)	65
W14	60036	Wingham (Lanark Close)	66
W15	61051	Murrurundi Post Office	466
W16	55066	Wallabadah (Woodton)	640
W17	55041	Nundle Post Office	595

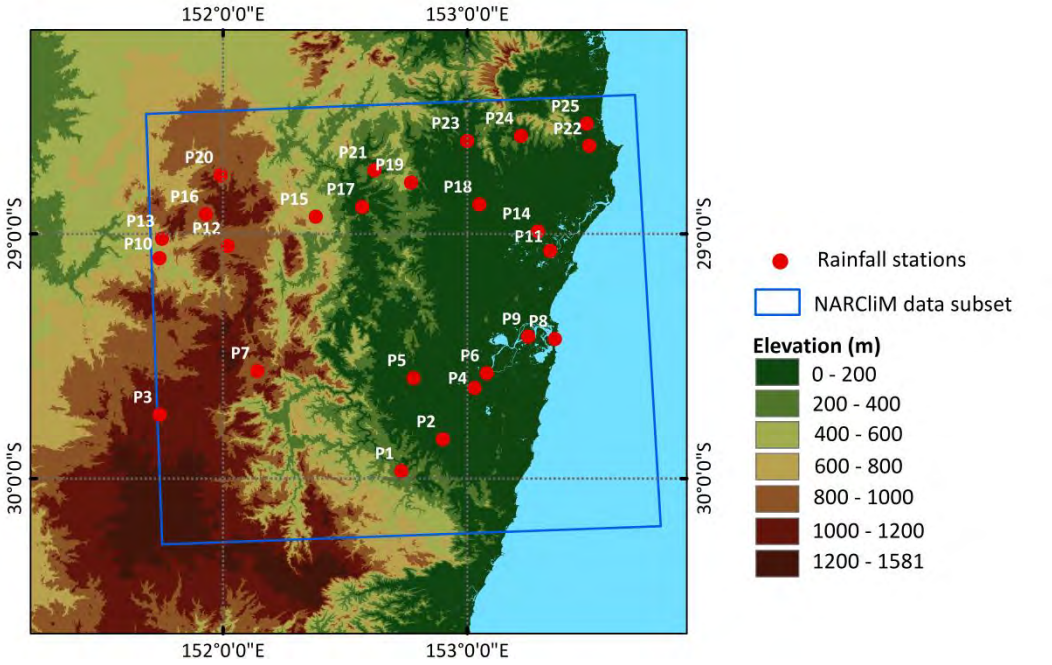

Figure 3.9 Map of the rain gauges at the Richmond River site.

Table 3.5 List of BOM raingauges: Richmond River site

Station ID (as shown in Figure 3.9*)*	*Station ID*	*Station name*	*Elevation (m)*
P1	58045	Nymboida (Armidale Road)	200
P2	58138	Kangaroo Creek (Hayfield)	45
P3	56011	Glen Innes Post Office	1,062
P4	58059	Ulmarra (Newsagency)	5
P5	58014	Copmanhurst Post Office	25
P6	58006	Brushgrove (Clarence St)	8
P7	57014	Glen Elgin (Glenbrook)	895
P8	58012	Yamba Pilot Station	27
P9	58027	Harwood Island (Harwood Sugar Mill)	2
P10	56052	Tenterfield (Mole Station)	440
P11	58061	Woodburn (Cedar St)	5
P12	56032	Tenterfield (Federation Park)	838
P13	56050	Tenterfield (Aberfeldie)	680
P14	58015	Coraki (Union St)	6
P15	57005	Drake (Village Resource Centre)	490
P16	41116	Wallangarra Post Office	875
P17	57018	Tabulam Post Office	130
P18	58063	Casino Airport	26
P19	58004	Mummulgum (Bingeebeebra)	195
P20	41033	Carawatha	938
P21	57003	Bonalbo Post Office	170
P22	58007	Byron Bay (Jacaranda Drive)	3
P23	58032	Kyogle Post Office	80
P24	58044	Nimbin Post Office	70
P25	58040	Mullumbimby (Fairview Farm)	15

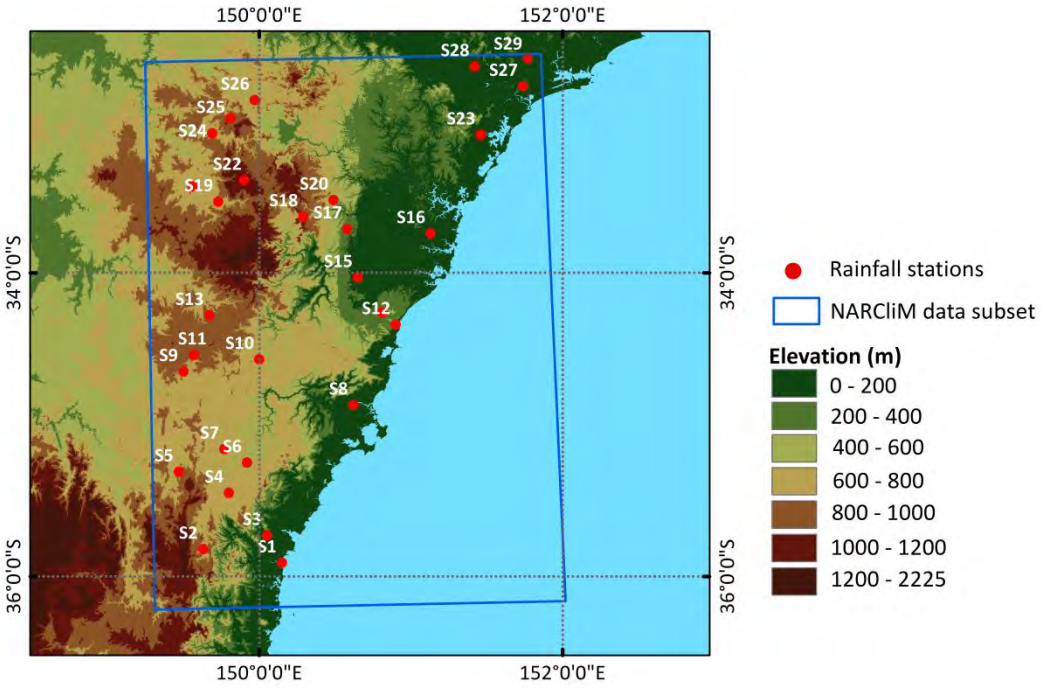

Figure 3.10 Map of the rain gauges at the Sydney site.

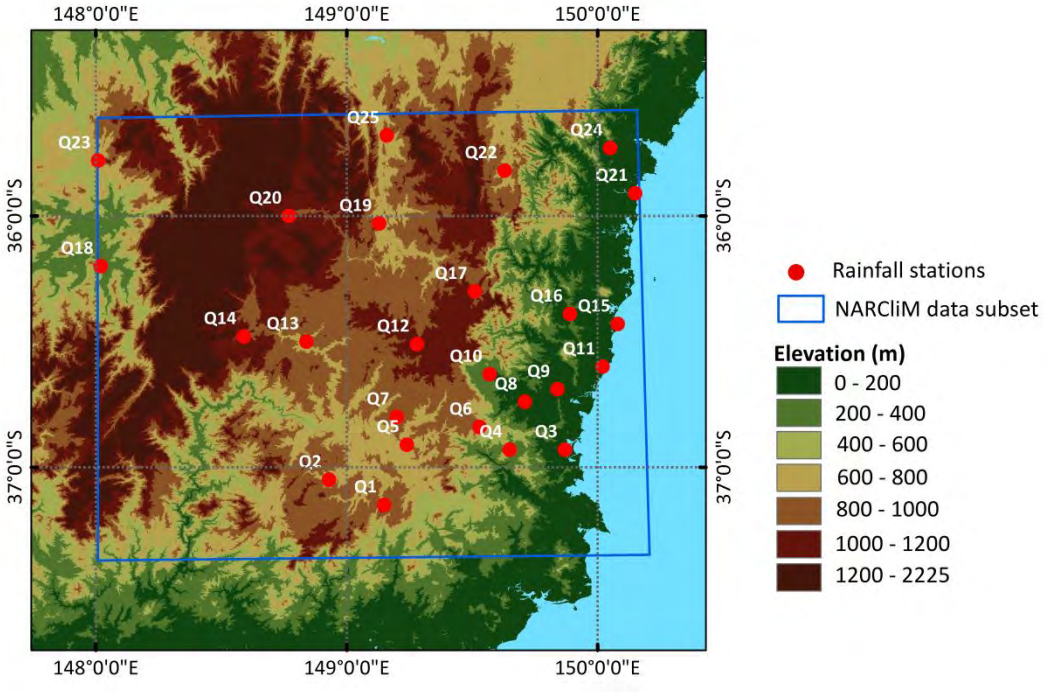

Figure 3.11 Map of the rain gauges at the Bega River site.

Table 3.6 List of BOM raingauges: Sydney site

Station ID (as shown in Figure 3.10)	*Station ID*	*Station name*	*Elevation (m)*
S1	69018	Moruya Heads Pilot Station	17
S2	70057	Braidwood (Krawarree)	730
S3	69052	Batemans Bay - Buckenbowra	30
S4	69010	Braidwood (Wallace Street)	643
S5	70035	Bungendore (Gidleigh)	725
S6	69041	Charleyong (Nerriga Road)	570
S7	70060	Lower Boro (Calderwood)	610
S8	68048	Nowra Treatment Works	10
S9	70071	Goulburn (Pomeroy)	685
S10	70119	Big Hill (Glen Dusk)	648
S11	70069	Crookwell (Gundowringa)	838
S12	68108	Woonona (Popes Rd)	45
S13	63032	Golspie (Ayrston)	855
S14	68016	Cataract Dam	340
S15	68007	Camden (Brownlow Hill)	61
S16	66158	Turramurra (Kissing Point Road)	160
S17	63077	Springwood (Valley Heights)	320
S18	63009	Blackheath (Lawrence St)	1,060
S19	63064	O'Connell (Stratford)	699
S20	63118	Bilpin (Fern Grove)	610
S21	63005	Bathurst Agricultural Station	713
S22	63079	Sunny Corner (Snow Line)	1,225
S23	61012	Cooranbong (Avondale)	10
S24	63076	Sofala Old Post Office	579
S25	62029	Ilford (Tara)	780
S26	62017	Kandos Cement Works	660
S27	61031	Raymond Terrace (Kinross)	10
S28	61014	Branxton (Dalwood Vineyard)	40
S29	61010	Clarence Town (Prince St)	24

Table 3.7 List of BOM raingauges: Bega River site

Station ID (as shown in Figure 3.11)	*Station ID*	*Station name*	*Elevation (m)*
Q1	70326	Craigie (Bondi Forest Lodge)	790
Q2	70107	Delegate Station	765
Q3	69024	Pambula Post Office	10
Q4	69066	Wyndham Post Office	300
Q5	70005	Bombala (Therry Street)	705
Q6	69019	Cathcart (Mount Darragh)	872
Q7	70009	Bukalong Station	78
Q8	69107	Kameruka (Kameruka Estate)	125
Q9	69002	Bega (Newtown Road)	50
Q10	69003	Bemboka Post Office	215
Q11	69032	Wapengo Lake Road	15
Q12	70067	Nimmitabel Wastewater Treatment Facility	1,075
Q13	71005	Dalgety (Hamilton St)	775
Q14	71021	Jindabyne (Glochinbah)	990
Q15	69005	Bermagui South (Young Street)	15
Q16	69014	Cobargo Post Office	85
Q17	69054	Tuross	970
Q18	82060	Towong Upper	280
Q19	70073	Chakola (Riversdale)	716
Q20	71000	Adaminaby Alpine Tourist Park	1015
Q21	69018	Moruya Heads Pilot Station	17
Q22	70057	Braidwood (Krawarree)	730
Q23	72043	Tumbarumba Post Office	645
Q24	69052	Batemans Bay - Buckenbowra	30
Q25	70064	Michelago (Soglio)	758

3.3.3 AWAP

The Bureau of Meteorology's Australian Water Availability Project (AWAP) 5 km resolution gridded daily dataset was also used for the validation of NARCliM rainfall. The AWAP rainfall grids were interpolated from the observed daily rainfall from gauges within the BOM gauging network (up to approximately 7,500 gauges, both open and closed) (Jones et al., 2009).

In the derivation of AWAP, the observed daily/monthly gauge rainfall was decomposed into a monthly average and associated daily/monthly anomaly series, where the anomalies were weakly related to topography. The average and anomaly

series were interpolated onto a grid. The averages were gridded using three-dimensional smoothing splines, and the Barnes successive correction method was used for analysis of the anomalies. The AWAP rainfall grids were then produced by multiplying the climate average and anomaly grids and incorporate an unexplained microscale variance term to allow for observational or measurement error, and hence exact reproduction of gauged rainfall values at each gauge location is not expected (Jones et al.,2009; Tozer et al., 2012).

This 5 km AWAP dataset is used to address the differences in the spatial resolutions of the point scale rainfall stations and the gridded NARCliM datasets. The raw 5 km resolution AWAP gridded data was aggregated up to 10 km to be consistent with the 10 km NARCliM grid, and it is this 10 km data that is used in the comparison in this thesis.

3.3.4 Elevation data

The elevations used are the 10 km resolution elevation data used by the NARCliM project. If the analysis is performed with respect to a rain gauge, the elevation was taken from metadata files provided by BoM. This method removes the discrepancy between scales (point and gridded) of datasets.

3.3.5 ECL data

The average daily rainfall calculated for all Easterly Trough Lows (ETL) ECL events occurring from 1979-2001 is shown in Figure 3.12. This 5 km resolution raster dataset was taken from Kiem et al. (2016) and used in Chapter 8 to identify the ECL impact distance from the east coast. (see Section 8.3).

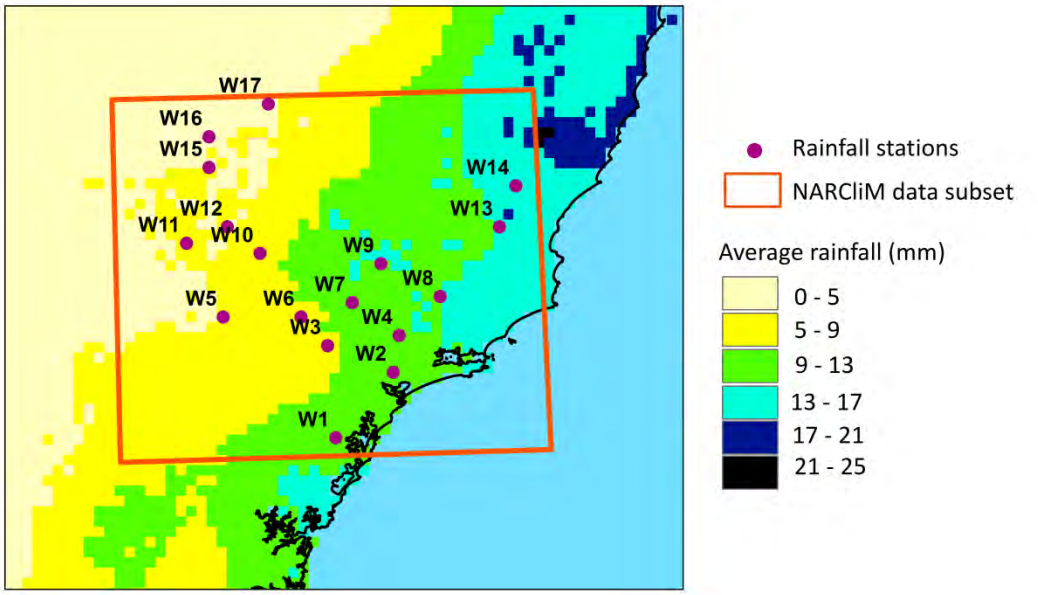

Figure 3.12 Average rainfall associated with Easterly Trough Low-ECL events occurring from 1979-2001 at the Williams River site.

Chapter 4
Methodology

4.1 Introduction

As noted in the literature in Chapter 2, there are different approaches for RCM evaluation and selection. The evaluation approach is critical to understand the performance of individual RCM and often depends on the end application. For example; analyses in this thesis assesses the usefullness of NARCliM RCMs in hydrology models by evaluating how they differ from the observed rainfall. In this chapter, the statistical methods used to evaluate the NARCliM RCM rainfall are presented. The motivation for selecting these methods was previously discussed in Section 2.6.5. The evaluation of the NARCliM rainfall is achieved by comparing the chosen statistical analyses results from NARCliM against those from AWAP and/or rain gauge data. The statistical methods used are divided into two types; (1) temporal and (2) spatial. The temporal statistics are typically calculated at individual grid points while spatial statistics are calculated for all grid points of a site.

The following statistics are calculated for the NARCliM rainfall and compared to the AWAP and/or rain gauge statistics:

1. probability distribution,
2. spatial variability of the rainfall statistics : mean, coefficient of variation and lag-1 correlation,
3. temporal autocorrelation (i.e. correlation at a specific location between two different times),
4. spatial correlation (i.e. correlation at a specific time between two different locations), and
5. cross correlation (i.e. correlation at a specific time between two different properties)

The probability distributions, temporal autocorrelation and cross correlation are calculated at selected grid points only. The selected grid points which are used for these three types of analysis are first presented for each site. The methods of calculating each of these statistics are presented in the following sections.

The grid points selected at the contrasting terrain (low and high elevations) and their corresponding rain gauges for the Merriwa site were previously shown in Figure 3.7 and Table 3.2. The grid points selected for the Williams River, Richmond River, Bega River and Sydney sites are shown in Figures 4.1 to 4.4. A summary of all grid points used is shown in Table 4.1. The grid points are chosen to assess how NARCliM data perform at different elevations. The analyses (probability distribution, temporal autocorrelation and cross correlation) are performed at four selected grid points (two grid points at a high elevation and two grid points at a low elevation) for each site.

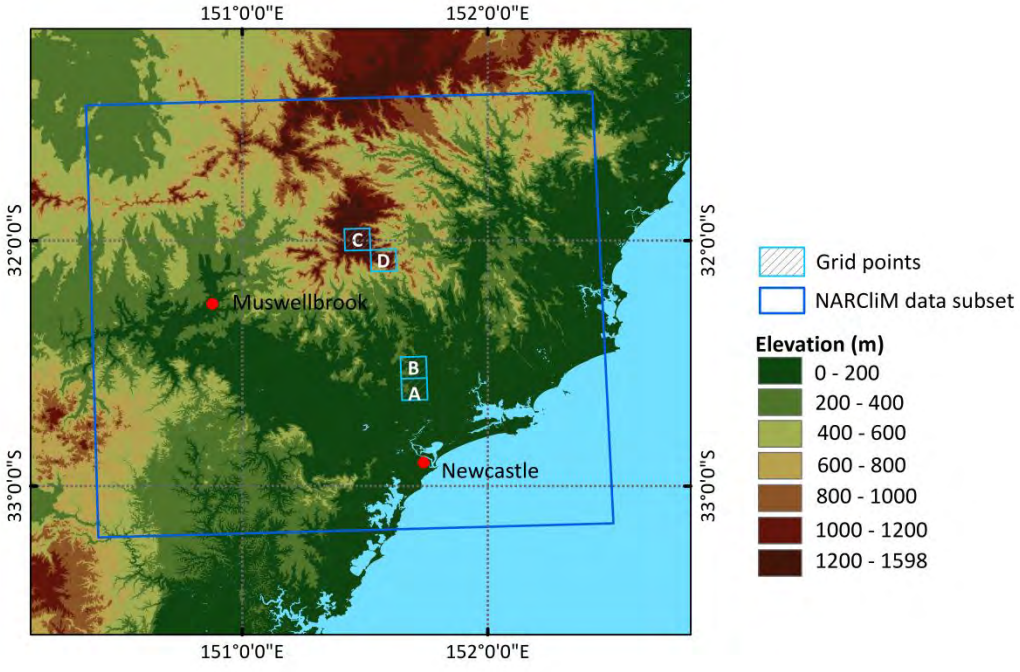

Figure 4.1 Map of the Williams River site with topography. The NARCliM data subset outlined is 20 x 20 grid points (10 km resolution). The grid points A - D are the NARCliM grid points used for comparison.

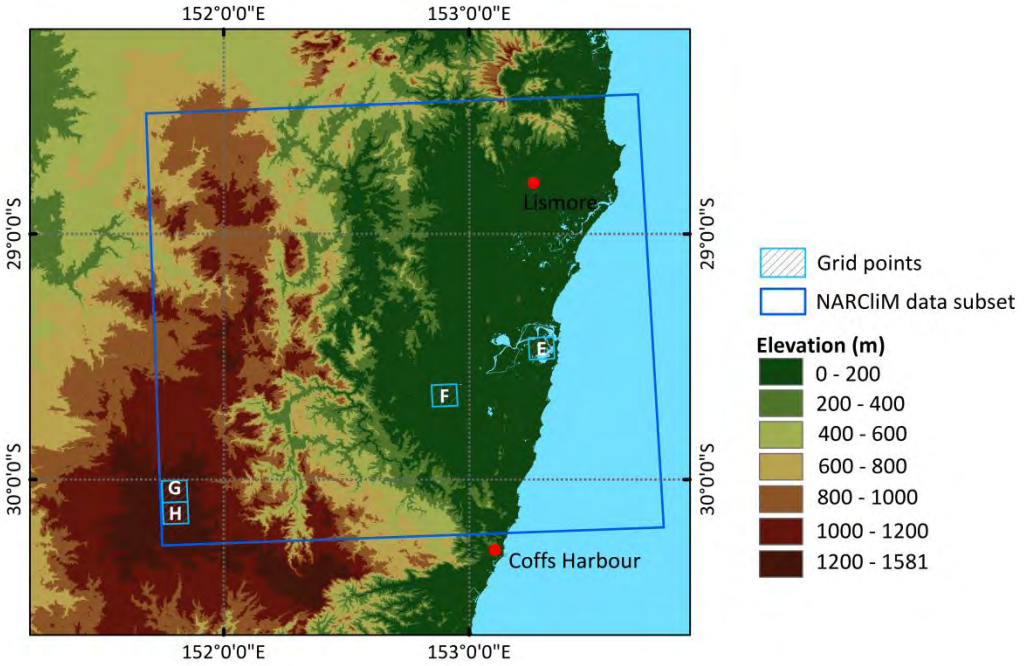

Figure 4.2 Map of the Richmond River site with topography. The NARCliM data subset outlined is 20 x 20 grid points (10 km resolution). The grid points E - H are the NARCliM grid points used for comparison.

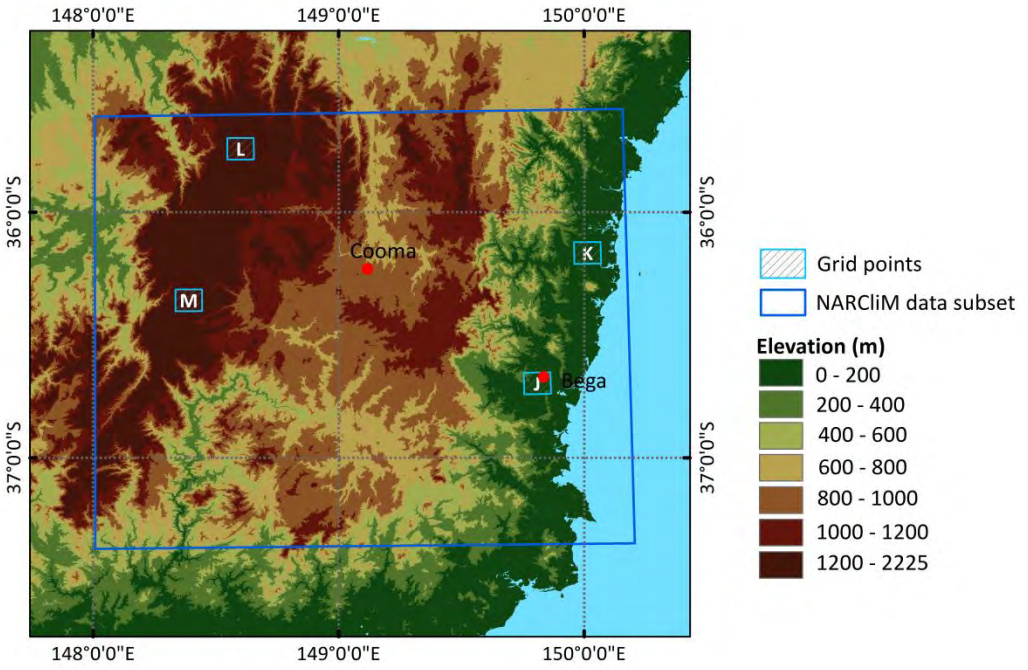

Figure 4.3 Map of the Bega River site with topography. The NARCliM data subset outlined is 20 x 20 grid points (10 km resolution). The grid points J - M are the NARCliM grid points used for comparison.

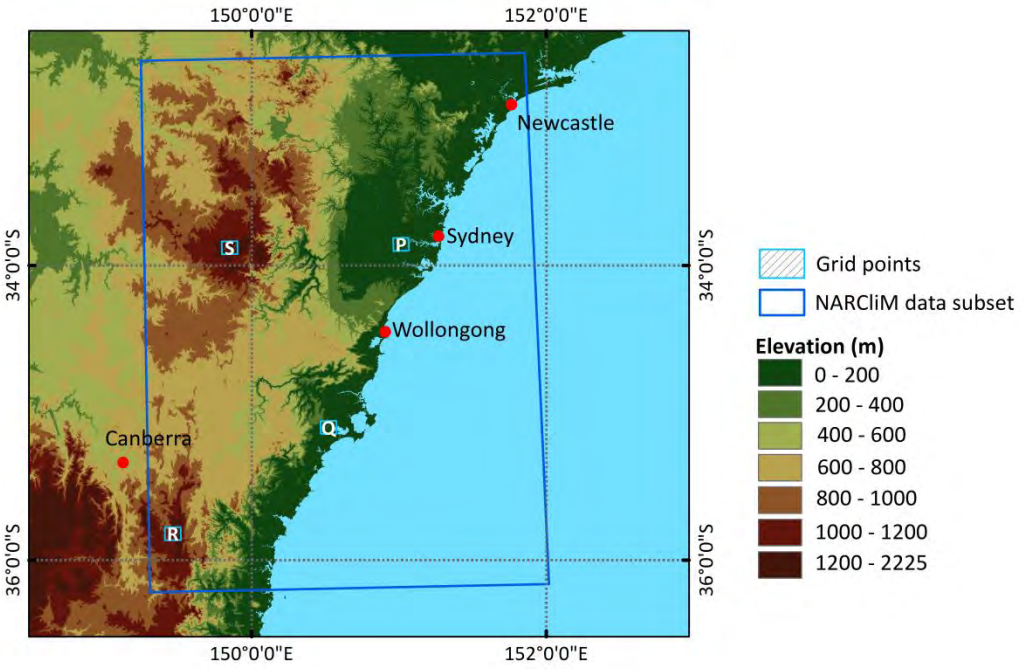

Figure 4.4 Map of the Sydney site with topography. The NARCliM data subset outlined is 41 x 25 grid points (10 km resolution). The grid points P - S are the NARCliM grid points used for comparison.

Table 4.1 Summary of grid points used at each site

Site name	*grid point ID*	*Elevation of the grid point (m)*	*Elevation range*	*NARCliM grid point location (i,j)*	*NARCliM coordinates (lat, lon)*
Williams River	A	35.5	low	172, 90	-32.60, 151.70
	B	86.7	low	172, 91	-32.51, 151.70
	C	959.8	high	170, 97	-31.99, 151.47
	D	615.2	high	171, 96	-32.08, 151.57
Richmond River	E	30.8	low	189, 125	-29.46, 153.29
	F	85.6	low	185, 123	-29.65, 152.89
	G	1097.6	high	174, 119	-30.05, 151.80
	H	1003.7	high	174, 118	-30.13, 151.80
Bega River	J	122.5	low	153, 44	-36.70, 149.81
	K	108.6	low	155, 50	-36.16, 150.01
	L	1298.1	high	142, 55	-35.74, 148.60
	M	1506.0	high	140, 48	-36.36, 148.39
Sydney	P	7.0	low	165, 76	-33.85, 151.01
	Q	35.6	low	160, 62	-35.09, 150.52
	R	1162.6	high	150, 54	-35.82, 149.46
	S	1024.3	high	154, 76	-33.88, 149.85

4.2 Probability distribution of the rainfall

Perkins et al. (2007) evaluated the PDF of the daily rainfall of CMIP4-AR4 climate models. Similarly, the ability of NARCliM RCM data to reproduce the observed daily rainfall probability distribution is assessed as it is important to know how NARCliM RCMs replicate the observed rainfall distribution before these datasets are used in reservoir modelling. The daily probability distribution of rainfall at grid points A to D at the Williams River site, E to H at the Richmond River site, J to M at the Bega River site and P to Q at the Sydney site (shown in Figures 4.1 to 4.4 respectively) are calculated and compared with AWAP. However, in contrast to Perkins et al. (2007), the results here are presented as cumulative probability distributions. Since data aggregation of rainfall can hide biases and systematic errors that can be identified at the daily scale, the main focus is on the daily resolution and therefore, the other aggregated time resolutions (fortnight, month and annual) are not used in this analysis.

A spatial analysis of the mean annual rainfall (averaged across 60 (1950-2009) years for the reanalysis and 20 (1990-2009) years for the GCMs) is performed by constructing a single cumulative probability distribution for each study site using mean annual rainfall values at all grid points in that site. The resulting cumulative probability distributions of the mean annual rainfall of NARCliM RCMs are compared with that of AWAP calculated using the mean annual rainfall of AWAP for each site.

4.3 Spatial variability of the rainfall statistics

One of the major motivations of the ESCCI-ECL project is that the relatively narrow eastern coastal strip of NSW is poorly resolved in current generation GCMs (grid resolution of ~250 km x 250 km). The NARCliM project was performed to address this issue. So, it is important to evaluate the capability of NARCliM RCMs which have a resolution finer than GCMs to capture the rainfall variability that exists in this region. Accordingly, the spatial variability of the rainfall for each site is calculated and the results are compared with the 10 km aggregated AWAP dataset.

The spatial variability of rainfall is assessed using three different measures. The mean, coefficient of variation (C_v, the ratio of standard deviation to mean), the lag-1 autocorrelation and the Box-Cox transformation λ (Equation 4.1) of the NARCliM RCMs and AWAP are computed for each grid cell of each site and the statistical values are mapped spatially. The analysis is similar to McMahon et al. (2008) who investigated the spatial variability of rainfall using the coefficient of variation and lag-1 autocorrelation. The spatial pattern and magnitudes of both NARCliM RCMs and AWAP are compared side by side at the Merriwa site.

According to the preliminary results of the spatial variability of the rainfall statistics at Merriwa site, NARCliM RCMs are significantly different from AWAP. However, the extent of the difference in rainfall magnitudes between the datasets (NARCliM and AWAP) is unknown. This suggests that there is a need to understand how much overestimation or underestimation of the rainfall statistics are being produced by the NARCliM data, particularly along the east coast of Australia. With this argument, spatial variability in the ratio of each statistical measure of the NARCliM RCMs and 5 km resolution AWAP are also calculated for the four main east coast sites as they are the key for the ESCCI project.

4.4 Temporal autocorrelation of the rainfall

The temporal evaluation of the rainfall generated by the NARCliM RCMs is focused on the autoregressive characteristics of the time series, specifically the autocorrelation values at different lags. Autocorrelation is also termed “lagged correlation” or “serial correlation”, and is the correlation between members of a series of numbers arranged in time. A statistically significant non-zero value indicates that the values in the time series are not independent with time while zero value indicates that the time series is uncorrelated (i.e. white noise). The focus is on autocorrelations of rainfall as the reservoir filling water volume is affected by the persistence in runoff caused by the rainfall.

The autocorrelations at the selected NARCliM grid points are evaluated for each site against the ground based gauge measurements and AWAP data. However at Williams River, Richmond River, Bega River and Sydney sites, only AWAP data was used.

The analysis is performed as follows.

Step 1:

The daily rainfall series of each selected grid point of each RCM is aggregated to three different resolutions: fortnightly, monthly and annual. Similarly, the AWAP and daily rainfall series at the selected raingauges are aggregated into the fortnightly, monthly and annual resolutions. Daily autocorrelations are not used due to the large number of days with zero rainfall.

Step 2:

Before comparing the autocorrelations (which requires that the data be approximately Gaussian distributed), each time series is transformed to have a zero skewness (i.e. so that the data are approximately Gaussian distributed) using the Box-Cox power transformation (Box and Cox, 1964; Siriwardena et al., 2006; Chiew et al., 2014). As the Box-Cox power transformation requires that all data be greater than zero, the zero rainfall values of the aggregated datasets are replaced with a value of 0.2 mm prior to the power transformation. A value of 0.2 mm is chosen because Parkinson (1986), referring to the data records of the Australian Bureau of Meteorology, indicated that rainfall values below 0.2 mm d^{-1} are considered to be zero rainfall. This means that rainfall values which are considered as zeros might lie in the range of 0 to 0.2 mm. The Box-Cox power transformation is

$$y = (x^{\lambda} - 1)/\lambda \qquad \text{..... (4.1)}$$

where y is the transformed variate, x is the original data variate, and λ is the Box-Cox power parameter. By selecting a value of λ that results in the skewness of y being close to zero, the distribution of y can be made approximately Gaussian.

Autocorrelations at different lags were then calculated for all RCMs, AWAP and gauge data at each grid point for all three time resolutions.

Step 3:

The autocorrelation of the raw datasets exhibits a seasonal signal. To see if there is any persistence in the seasonal anomalies, the fortnightly and monthly rainfall time series are seasonally detrended, using the mean and standard deviation

$$Z_n = (Y_n - \mu)/\sigma \qquad \text{.....(4.2)}$$

where Z_n is the detrended rainfall, the subscript n refers to the individual data points (monthly or fortnightly series), Y_n is the raw rainfall, μ is the mean rainfall (of each month or fortnight) and σ is the standard deviation (of each month or fortnight).

Step 4:

The autocorrelation analysis is repeated on the detrended rainfall time series. The detrending is only performed for the rainfall at grid points of the Merriwa site in Chapter 5. Since the detrended correlograms at Merriwa site do not show any significant improvement in the results compared with the results generated for the raw data (i.e. there is no consistency in the results that explain the differences between autocorrelations of RCM and observed rainfall) this step was not repeated for the other four sites.

The analysis explained in steps 1-3 is repeated for both uncorrected and bias corrected RCM simulations at all sites because this is an important test which determines whether the raw and bias corrected data exhibits similar or different autocorrelations, where bias correction only adjusts the daily rainfall and not how one day is related to another.

4.5 Spatial correlation of the rainfall

The spatial correlation function (scatter plot of correlation vs distance between two points) at a catchment can be generated between one rain gauge/grid point and all other gauges/grid points. If the catchment properties such as rainfall distribution or topography are not known, the selection of this reference gauge/grid point (out of all the available gauges/grid points) can be arbitary. However, with the knowledge of the terrain and hydrological properties gained in previous chapters, two grid points,

one located at a low and one at a high elevation, were selected as the references at each site (i.e. 8 grid points for all four sites). The selected reference grid points/rain gauges and all other grid points/rain gauges used in the analysis are shown in Table 4.2 and Figures 4.5 to 4.8. Note that the grid points selected for this analysis were different to what was used in the previous analysis (section 4.4). Because the spatial correlation of NARCliM rainfall was evaluated against both rain gauge and AWAP data in this analysis, grid points were selected at rain gauges with continuous data records. In contrast to the analysis in Section 4.4 which only used AWAP data as the observed rainfall, the selection process of grid points in this analysis was based on the rain gauges, therefore, rain gauges were first selected and then corresponding grid points were used for the comparison.

To minimize the confusion between grid point IDs of two gridded datasets (NARCliM RCMs and AWAP) and rain gauges', the rain gauge ID which is located inside the corresponding grid point are used for naming the NARCliM and AWAP grid points. For example, if the rain gauge ID is W1, the corresponding NARCliM grid point is called the 'W1 NARCliM grid point' while AWAP grid point is referred to as 'W1 AWAP grid point'.

Table 4.2 Reference grid points selected at each site

Site name	*Total rain gauges used*	*Reference grid point/rain gauge ID*	*Elevation of the reference grid point (m)*	*Elevation range*
Williams River site	17	W17	595	high
		W4	24	low
Richmond River site	25	P20	938	high
		P9	2	low
Bega River site	25	Q12	1,075	high
		Q3	10	low
Sydney site	29	S22	1,225	high
		S8	10	low

The analysis was in two parts:

(1) Assessment of the spatial correlation of the NARCliM daily rainfall and its variability at the catchment scale between the reference grid point and all other grid points. This part compared the NARCliM against AWAP only.

(2) Testing the NARCliM daily rainfall against the 10 km resolution AWAP and rain gauge data for selected grid points that encompassed the location of the rain gauges. Note that, the Pearson's correlation coefficient (r) (Pearson, 1895) was used for the calculation of daily rainfall correlations between the reference grid point and all other grid points.

The analysis was performed as follows.

- Step 1: The correlation between the daily rainfall of NARCliM grid points (between reference and other grid points) were first evaluated using the Pearson's correlation coefficient. The correlation between all other grid points was calculated with reference to two grid points located at high and low elevations of each site. Then, results were compared with the spatial correlation of AWAP which were calculated using the same method.

  The correlations are presented as spatial plots and scatter plots. In scatter plots, elevation difference (Equation 4.3) between the reference and all other grid points is also shown as a third variable. This elevation difference provides more information on the variability of the correlation in a contrasting terrain.

  $$\text{Elevation difference} = |H_2 - H_1| \quad \text{.....} \quad (4.3)$$

  Where H_1= Elevation of the reference and H_2 = Elevation of the destination grid point.

- Step 2: The spatial correlation of both NARCliM and AWAP gridded data are compared with the observed spatial correlations, calculated for the selected rain gauges within each site. Only grid points (NARCliM/AWAP) which encompassed the location of the rain gauges were used for the comparison. The purpose of this second analysis is to assess the ability of both NARCliM and AWAP to replicate the spatial correlation of rain gauges.

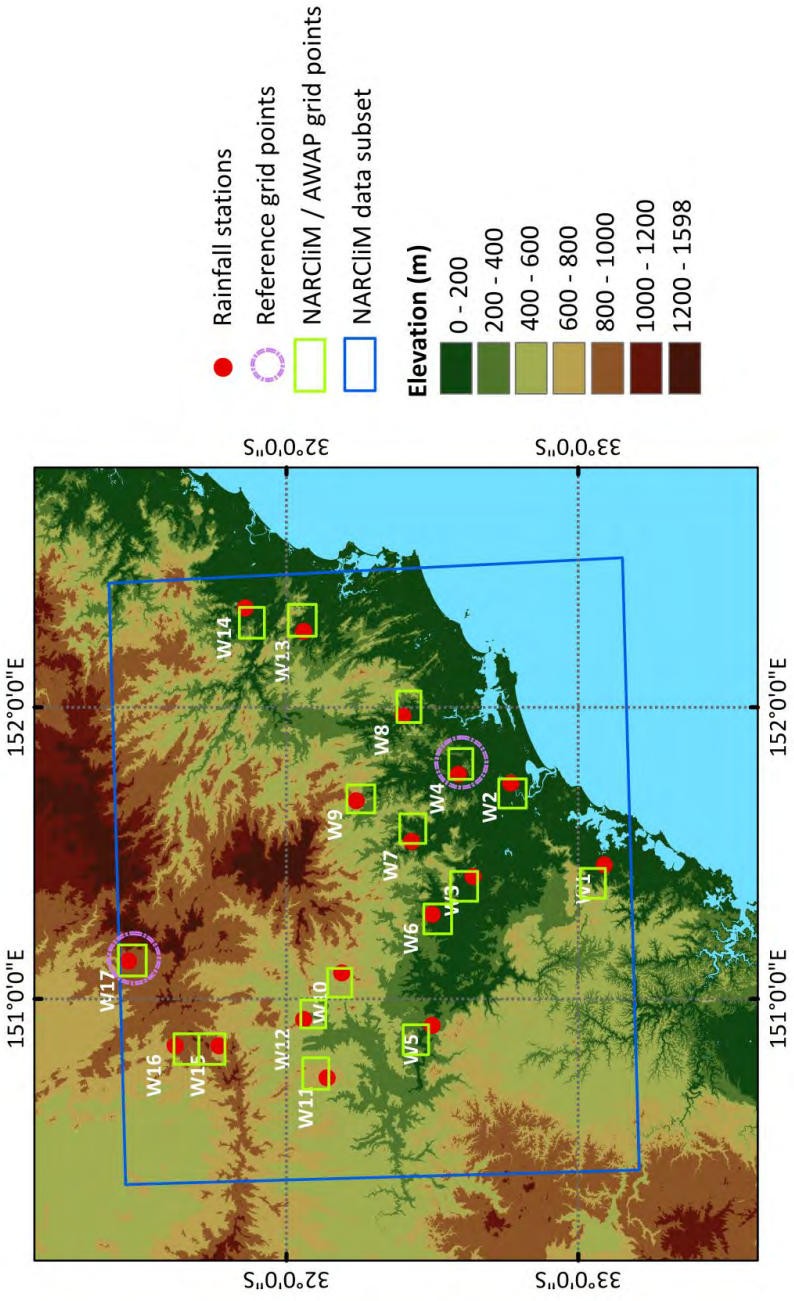

Figure 4.5 Map of the rain gauges and NARCliM/AWAP grid points selected - Williams River site.

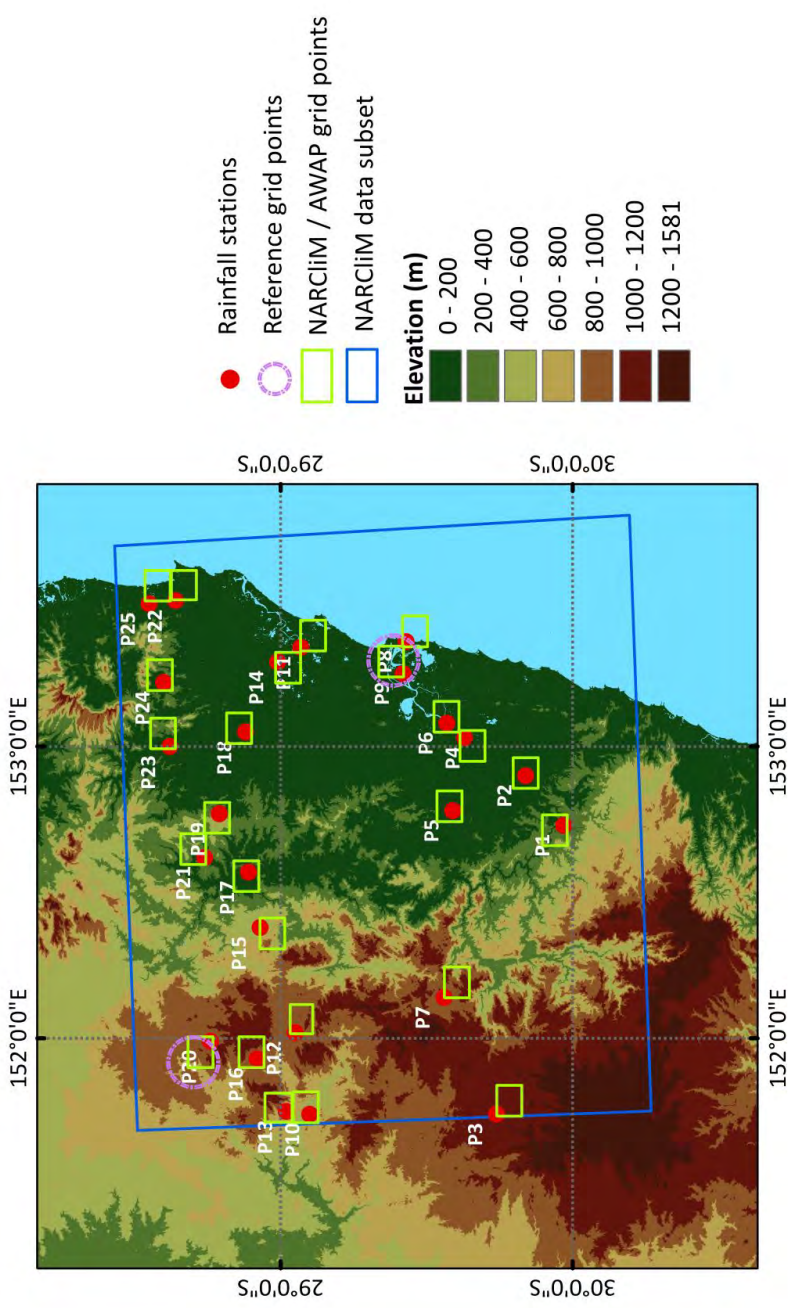

Figure 4.6 Map of the rain gauges and NARCliM/AWAP grid points selected - Richmond River site.

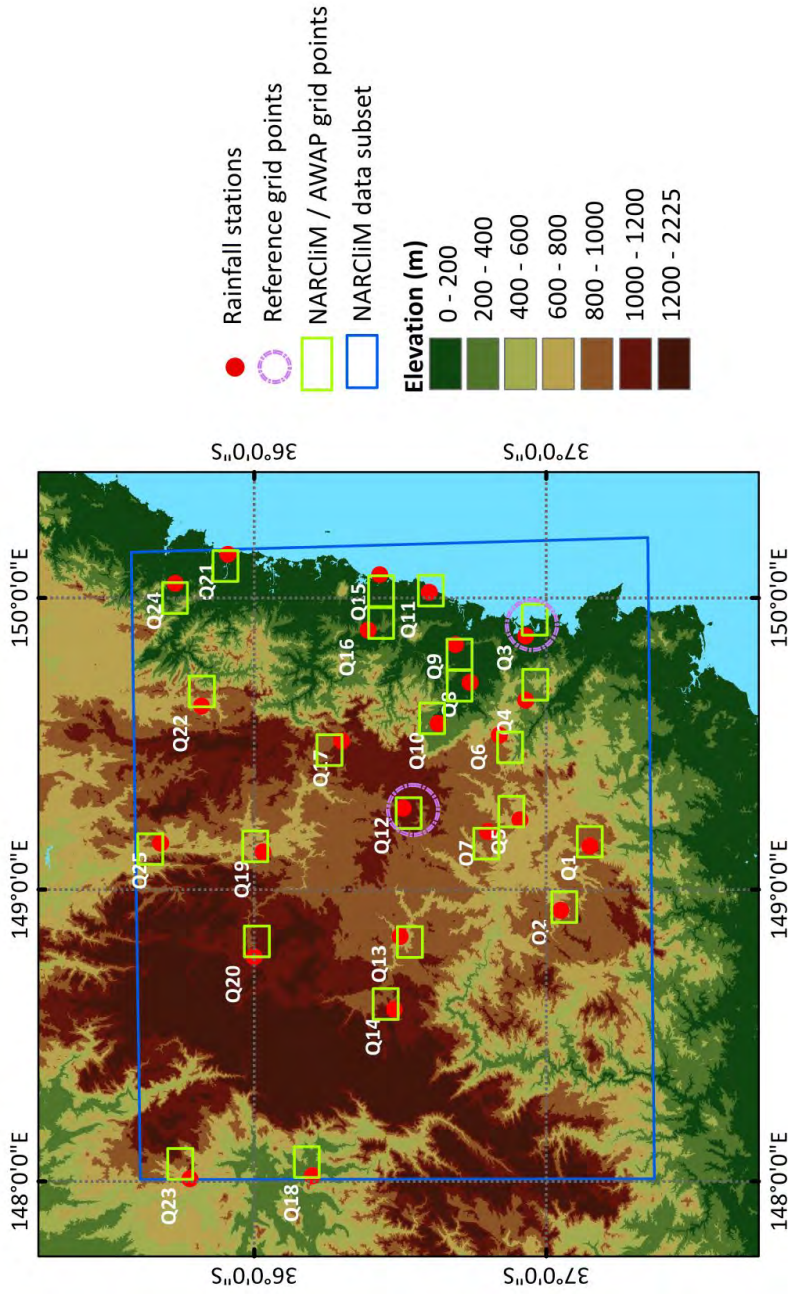

Figure 4.7 Map of the rain gauges and NARCliM/AWAP grid points selected - Bega River site.

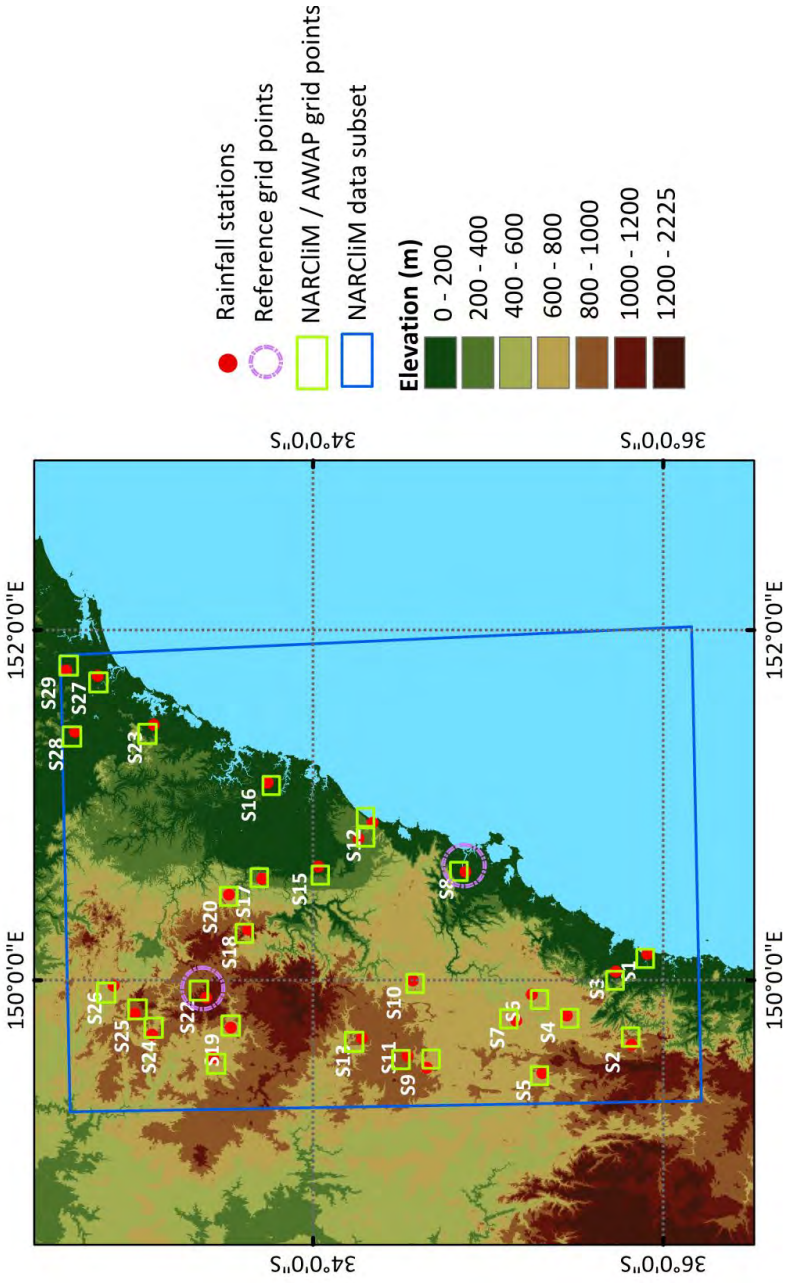

Figure 4.8 Map of the rain gauges and NARCliM/AWAP grid points selected - Sydney site.

4.6 Cross correlation of the rainfall

In order to assess whether the magnitude of NARCliM RCM rainfall is significantly different from observed rainfall, correlations between NARCliM RCM, and gauge and AWAP are calculated for daily, fortnightly, monthly and annual resolutions using Pearson's Correlation Coefficient. The results for the cross correlations are presented as scatter plots. However, the NARCliM RCMs and AWAP rainfall are 10 km gridded datasets while the gauge is a point value, selected to lie inside the corresponding grid box so ignore the averaging over the 10 km pixel

Additionally, to study the relationship between orography and rainfall, a cross correlation analysis between rainfall and elevation is also performed at two sites; Merriwa and Williams River which are located in the Hunter valley region where previous studies (McMahon, 1964) have shown evidence for an orographic effect on rainfall.

Section 1

Assessment of rainfall statistics of NARCliM reanalysis projections (1950-2009)

Section 1 (Chapters 5-8) is an assessment of the ability of the three NARCliM reanalysis datasets to generate the correct statistical properties of current day rainfall. As was explained in Section 2.6.3, three different RCMs (R1, R2 and R3) have been used to downscale the NCEP/NCAR reanalysis (Kalnay et al., 1996) from 1950 to 2009 in the first phase of the NARCliM project, and these three reanalysis datasets are referred to here as R1, R2 and R3 reanalysis. As stated by Evans et al. (2014), these 60 year period reanalysis-driven simulations provide a strong test of the RCMs ability to simulate the strong decadal variability in precipitation which was experienced in Southeast Australia over the second half of the 20th century with particularly wet decades in the 1950s and 1970s. However, it is worth noting that reanalysis do not attempt to deterministically recreate the day to day climate since NCEP/NCAR is only used to specify the climate of the edge of RCM computational domain, and the upper atmosphere lid. Day to day variability at 10 km resolution is largely a result of the internal dynamics of the RCMs, and the topography.

Four statistical methods are used to assess the NARCliM reanalysis: (1) probability distribution of the rainfall (2) spatial variability of the rainfall statistics, (3) temporal autocorrelation of the rainfall, and (4) spatial correlation of the rainfall.

The key focus of this section is to determine the performance of NARCliM reanalyses in capturing the observed rainfall statistics. As three different RCMs have been used to downscale the 60 year reanalysis, evaluation of the performance of each simulation is important to identify the RCMs that best reproduce the observed statistics of the rainfall.

Additionally, there are two types of NARCliM rainfall data: uncorrected and bias corrected. First the statistical testing results for the uncorrected data are presented, and then these results are compared with the results for the bias corrected

simulations. The assessment of uncorrected data allows us to identify the intrinsic characteristics of the RCM simulations, while the comparison between bias corrected and uncorrected data provides insights into how the data have been improved after the bias correction.

Chapter 5
Statistical Testing of NARCliM reanalysis rainfall data (1950-2009) for the Upper Hunter Region, New South Wales, Australia

This chapter is published as Parana Manage, N., Lockart, N., Willgoose, G., Kuczera, G., Kiem, A. S., Chowdhury, A.F.M.K., Zhang, L. and Twomey, C. 2016. Statistical Testing of Dynamically Downscaled Data for the Upper Hunter Region, New South Wales, Australia, *Journal of Southern Hemisphere Earth System Science*, 66, 203-227. It has been slightly modified to maintain the consistency with the rest of the thesis.

5.1 Introduction

As identified in the literature (see Section 2.6.2), few studies involving high spatial-resolution (finer than 30 km) regional climate simulations over Australia have been published. Among these few publications, most of the studies have simply assessed the basic statistics of the dynamically downscaled rainfall such as mean, standard deviation, change of the minimum/maximum, bias and root mean square error against the observed rainfall. However, important time series statistics such as autocorrelation have received less attention from the research community. The autocorrelations between rainfall events are important since reservoir performance can be sensitive to the persistence of runoff. Therefore, in this chapter the ability of NARCliM RCM data to reproduce the autocorrelations of observed rainfall is assessed at the Merriwa site which encompasses the Goulburn River catchment (see Section 3.2.1 for more details). The NARCliM outputs are evaluated against data from BoM raingauges and AWAP.

Additionally, a cross correlation analysis was performed at three grid points located in the contrasting terrain of the Merriwa site. This cross-correlation analysis assesses the performance of the NARCliM rainfall data at capturing observed rainfall depths. Further, it is important to evaluate the capability of NARCliM RCMs which have a resolution finer than GCMs to capture the rainfall variability that exists in this

region. Therefore the spatial variability of the rainfall across the Merriwa site was calculated and the results were compared with the 5 km AWAP dataset.

The analyses presented in this chapter are different from previous studies in a number of ways. Most previous studies which assess RCM precipitation use aggregated monthly, seasonal or annual rainfall. In addition to monthly and annual resolutions, daily and fortnightly resolutions of precipitation were also used for the validation. The major motivation to use these different time resolutions is that reservoirs of different capacities respond to rainfall differently; small reservoirs respond to daily variations in rainfall while large reservoirs respond to rainfall variations over weeks to years.

5.1.1 NARCliM and observed rainfall

Only the three downscaled NARCLIM reanalyses (1950-2009) were used in the analyses. It should be noted that the study presented in this Chapter was carried out as a pilot study, different to the other four east coast sites explained in Chapter 3, therefore only the uncorrected 60 year reanalyses data was used. Further, bias corrected rainfall dataset was not available at the time of the analyses as the bias corrections were supplied during the second phase of the NARCliM project (Evans et al., 2014). A descriptive assessment of the bias corrected data is presented in Chapter 9. However, the assessment of uncorrected data allows us to identify the intrinsic characteristics of the RCMs.

The time series of the NARCliM R1, R2 and R3 reanalyses, AWAP and ground based raingauge measurements were used for the analysis. As explained in Section 3.3.2, rainfall data of P1, P2 and P3 rainfall stations and 5 km resolution AWAP data were used for the validation of rainfall.

The analysis is in two parts; (1) autocorrelation and cross correlation analysis for single grid points, and (2) spatial variability at catchment scale (all grid points) (see Sections 4.3 to 4.6).

5.1.2 Single grid point analysis

5.1.2.1 Autocorrelation analysis

The initial testing of the three NARCliM reanalyses focuses on the autoregressive characteristics of the time series, specifically the autocorrelation values at different lags. The autocorrelations at the three NARCliM grid points P1, P2 and P3 were evaluated against the ground based gauge measurements and AWAP data at three different resolutions: fortnightly, monthly and annual (see Figure 3.7 and Table 3.3). The method explained in Section 4.4 was used to calculate the autocorrelations at each grid point. The results are shown by the correlograms generated for fortnightly, monthly and annual time resolutions. The correlograms for the R1, R2 and R3 reanalyses and AWAP at grid point P1, and rainfall station 61002 are shown in Figure 5.1. The autocorrelations of NARCliM reanalyses at P2 and P3 were compared with the corresponding AWAP pixel and rainfall station (see Table 3.3) and are shown in Figures 5.2 and 5.3 respectively.

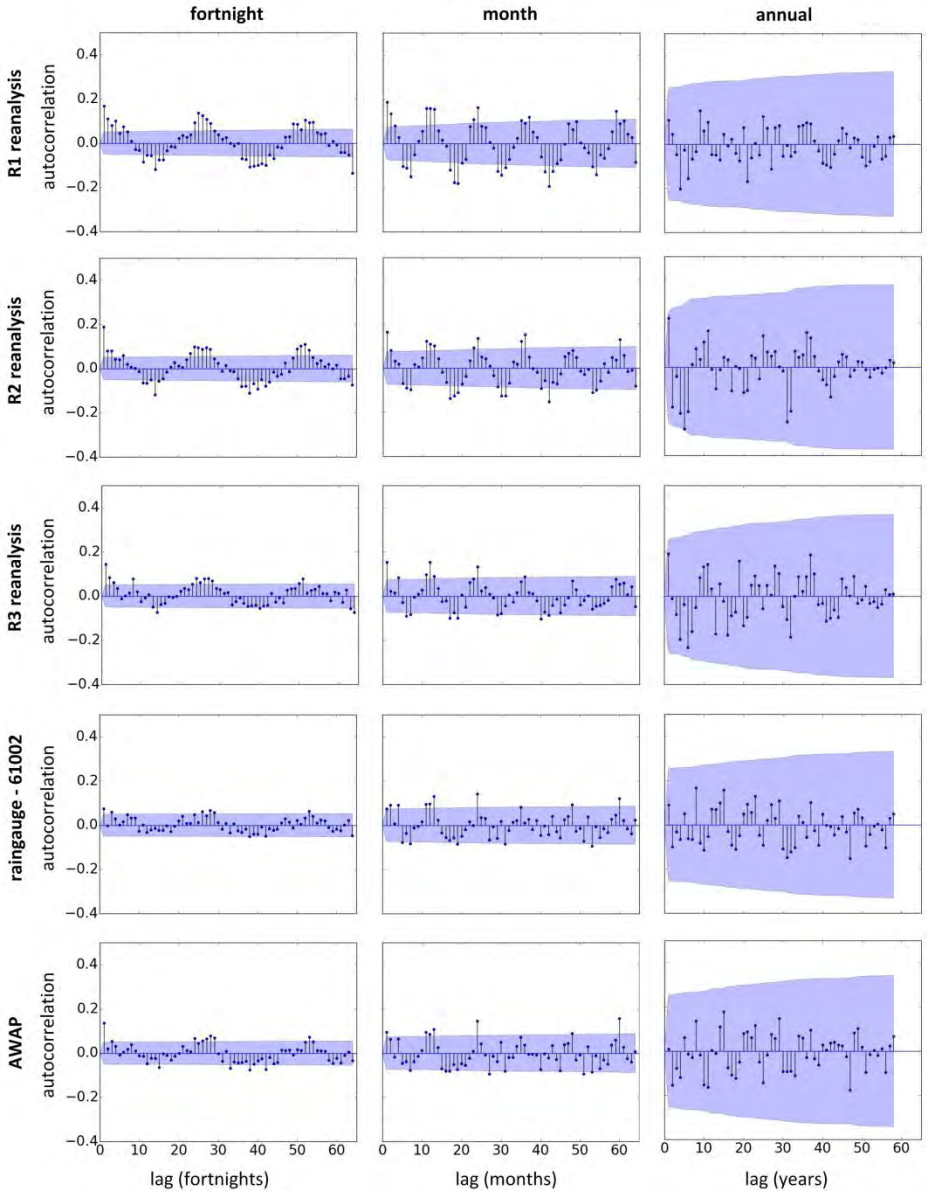

Figure 5.1 Correlograms of NARCliM reanalysis and observed data at grid point P1. The shaded regions are the 95% confidence limits of the null hypothesis (i.e. the correlations are not significantly different from 0).

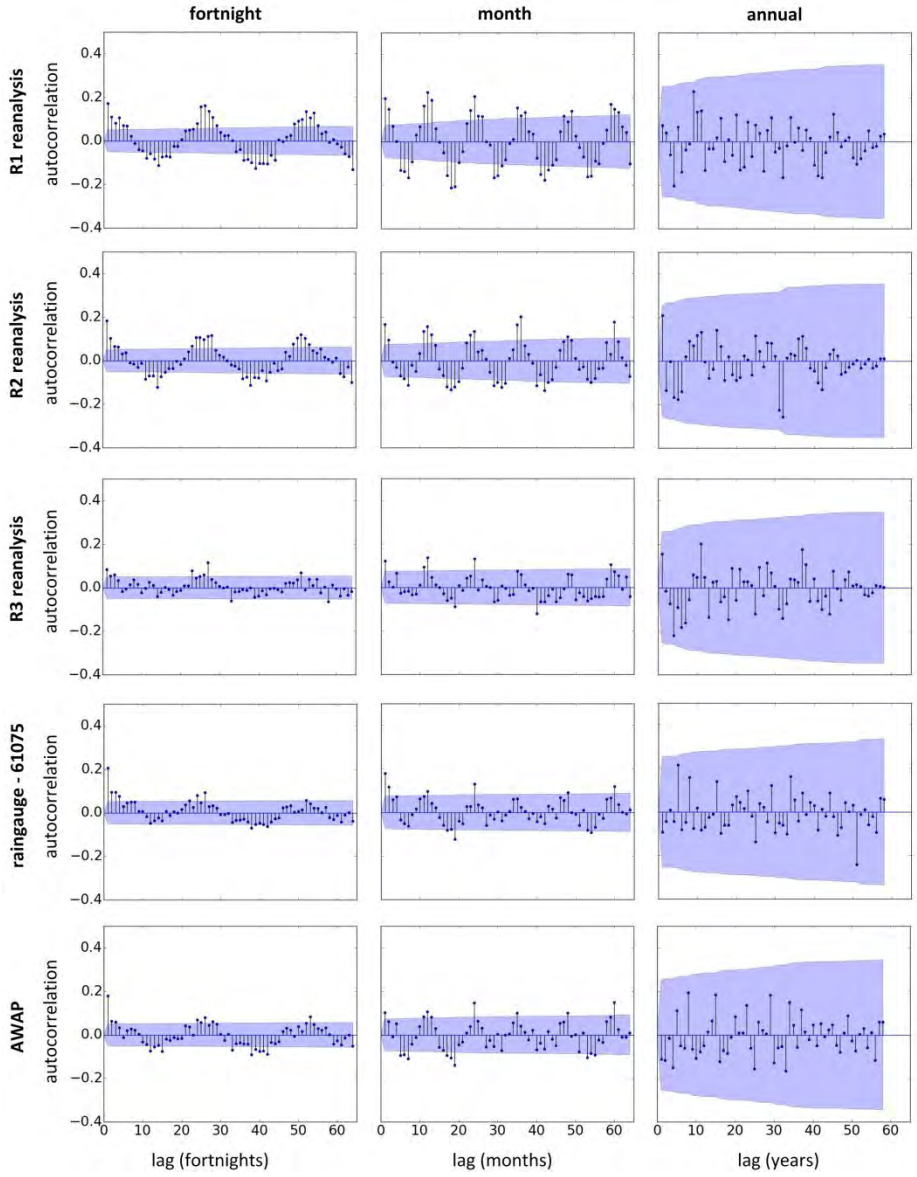

Figure 5.2 Correlograms of NARCliM reanalysis and observed data at grid point P2. The shaded regions are the 95% confidence limits of the null hypothesis (i.e. the correlations are not significantly different from 0).

For each of the three locations (Figures 5.1 to 5.3) the observed gauge and AWAP series have very similar autocorrelation values at all time resolutions. For the fortnight and month resolution, there is a weak seasonal signal, with significant autocorrelations at 1 and 2 years. At the annual resolution, there is no significant signal, with all values falling within the 95% confidence limits of the null hypothesis (i.e. the autocorrelations are not significantly different from 0).

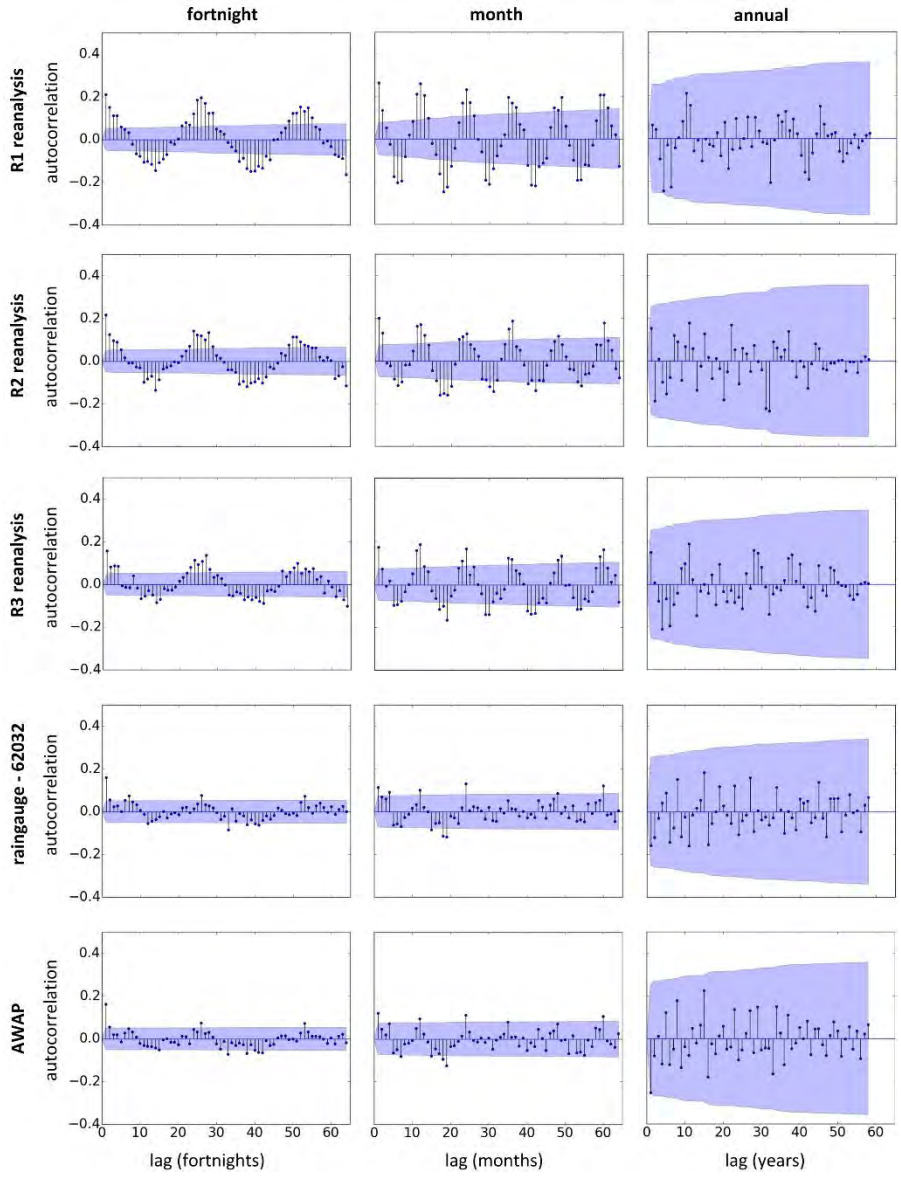

Figure 5.3 Correlograms of NARCliM reanalysis and observed data at grid point P3. The shaded regions are the 95% confidence limits of the null hypothesis (i.e. the correlations are not significantly different from 0).

For the three NARCliM reanalyses, the correlograms in Figures 5.1 to 5.3 show a clear seasonal signal for the fortnight and month resolutions. However, the seasonal signal is much stronger in the R1 and R2 reanalyses compared with the R3 reanalysis.

Due to the strong seasonal cycle, the R1 and R2 reanalyses overestimate the autocorrelation values of the observed gauge and AWAP rainfall. The R3 reanalysis better reproduces the autocorrelations of the gauge and AWAP data than R1 and R2, especially at grid points P1 and P2. These differences in the autocorrelations of R1, R2 and R3, are unsurprising as Evans et al. (2014) selected three configurations of the WRF model that were as independent as possible. At grid point P3 all three NARCliM reanalyses overestimate the autocorrelations of observed gauge and AWAP rainfall. This overestimation of the autocorrelations at grid point P3 could be attributed to the NARCliM RCMs averaging the topography over each grid point. We speculate that a smoother lower resolution topography may result in a lower sensitivity to wind direction and thus any spatially random effects as a result of the orographic influence on rainfall. If the rainfall is a function of elevation (Hutchinson, 1998a,b), this would suggest that NARCliM simulated rainfall series would have been affected by this averaging of topography. Further, elevations shown in Table 3.3 show that elevation of the raingauge (62032) is different to that of the corresponding NARCliM reanalysis grid point. The averaging effect of the topography of NARCliM reanalysis is more pronounced at grid point P3; grid point P3 is located in a flat area surrounded by the nearby steep cliffs and high elevation plateaus while the terrain around grid points P1 and P2 is rolling hills and distant mountains.

The autocorrelation of the raw datasets exhibits a seasonal signal. Therefore, rainfall time series were seasonally detrended using the method explained in Section 4.4. The correlograms generated for the detrended time series of each reanalysis dataset at P1, P2 and P3 grid points are shown in Figures 5.4 to 5.6 respectively. All correlograms show a statistically significant lag-1 correlation, and the value of this correlation in the gauge and AWAP data is well matched by NARCliM. For lags greater than five there are few statistically significant results in either gauge and AWAP, or NARCliM. However, for lags between one and five the results are more varied with some time series showing significant correlations.

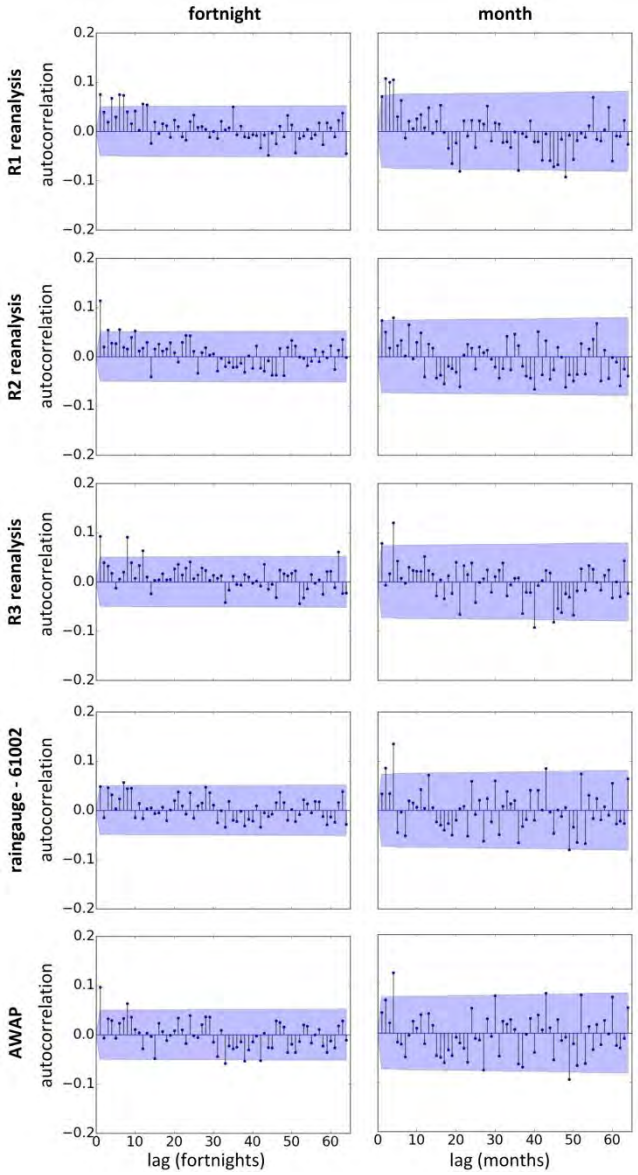

Figure 5.4 Correlograms of detrended NARCliM reanalysis and observed data at grid point P1. The shaded regions are the 95% confidence limits of the null hypothesis (i.e. the correlations are not significantly different from 0).

For monthly data there are generally significant correlations in gauge and AWAP to lag-5 that are sometimes replicated in NARCliM. For the fortnightly data there is no consistent trend either in the gauge and AWAP data, or in NARCliM. The reduction in the number of significant autocorrelations for lags greater than one in the correlograms for the original and detrended data is consistent with a strong seasonal signal. The overly strong seasonal signal of NARCliM reanalyses in Figures 5.1 to 5.3 might be changed by bias correction. The results suggest that, even though the resolution disagreement of using a gridded observed dataset (i.e. AWAP instead of

point raingauges) is eliminated, the results remain the same showing discrepancies between the NARCliM reanalyses and observed data.

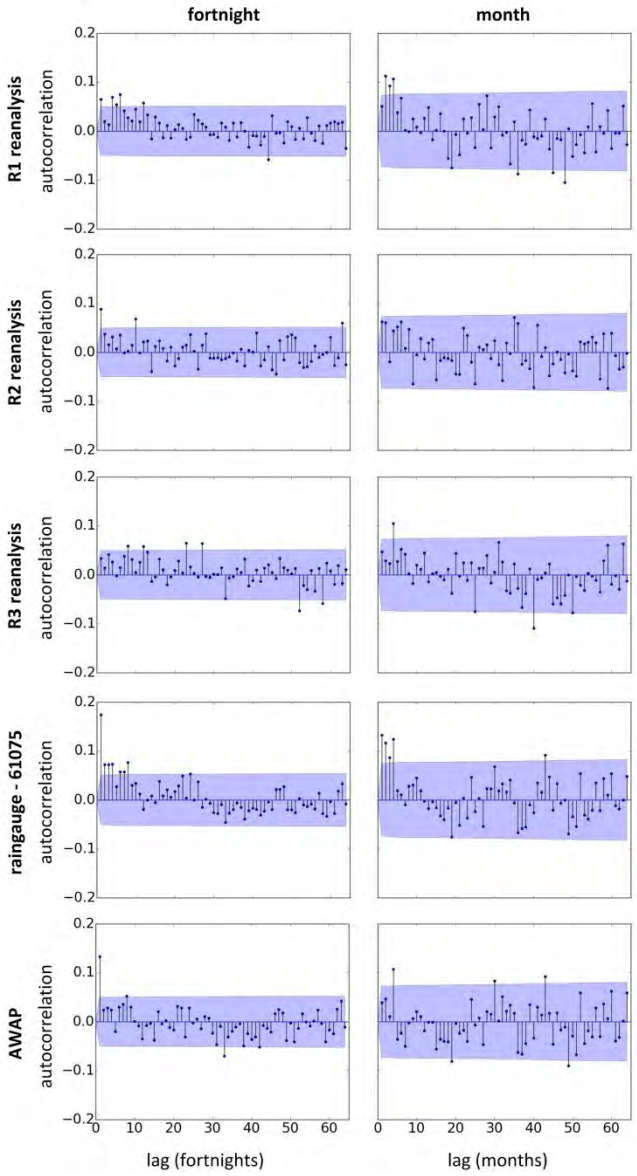

Figure 5.5 Correlograms of detrended NARCliM reanalysis and observed data at grid point P2. The shaded regions are the 95% confidence limits of the null hypothesis (i.e. the correlations are not significantly different from 0).

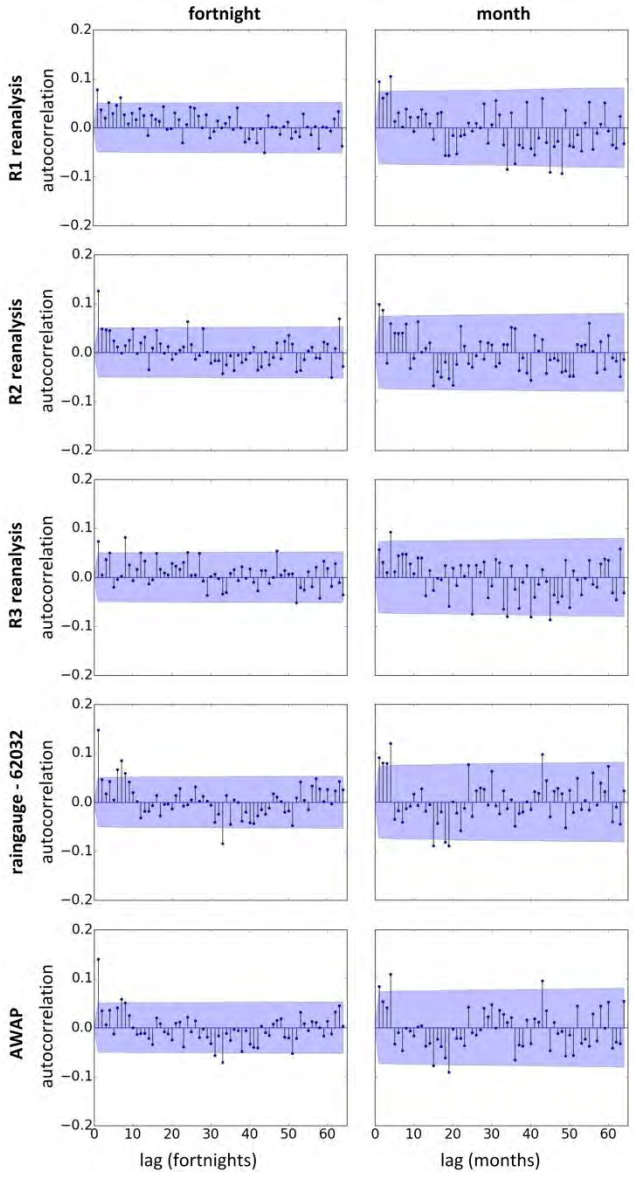

Figure 5.6 Correlograms of detrended NARCliM reanalysis and observed data at grid point P3. The shaded regions are the 95% confidence limits of the null hypothesis (i.e. the correlations are not significantly different from 0).

5.1.2.2 Cross correlation analysis

In order to assess whether the NARCliM reanalyses rainfall are deterministically different from observed rainfall, cross-correlations between reanalysis, and gauge and AWAP were calculated for daily, fortnightly, monthly and annual resolutions using Pearson's Correlation Coefficient (r) (Pearson, 1895). The results for the cross correlations are presented as scatter plots. However, it should be noted that the

reanalyses and AWAP rainfall are 10 km gridded datasets while the gauge is a point value, selected to lie inside the corresponding grid box.

Figures 5.7 and 5.8 show the scatter plots of the NARCliM reanalyses at grid point P1 versus gauge and AWAP rainfall at daily, fortnightly, monthly and annual time resolutions.

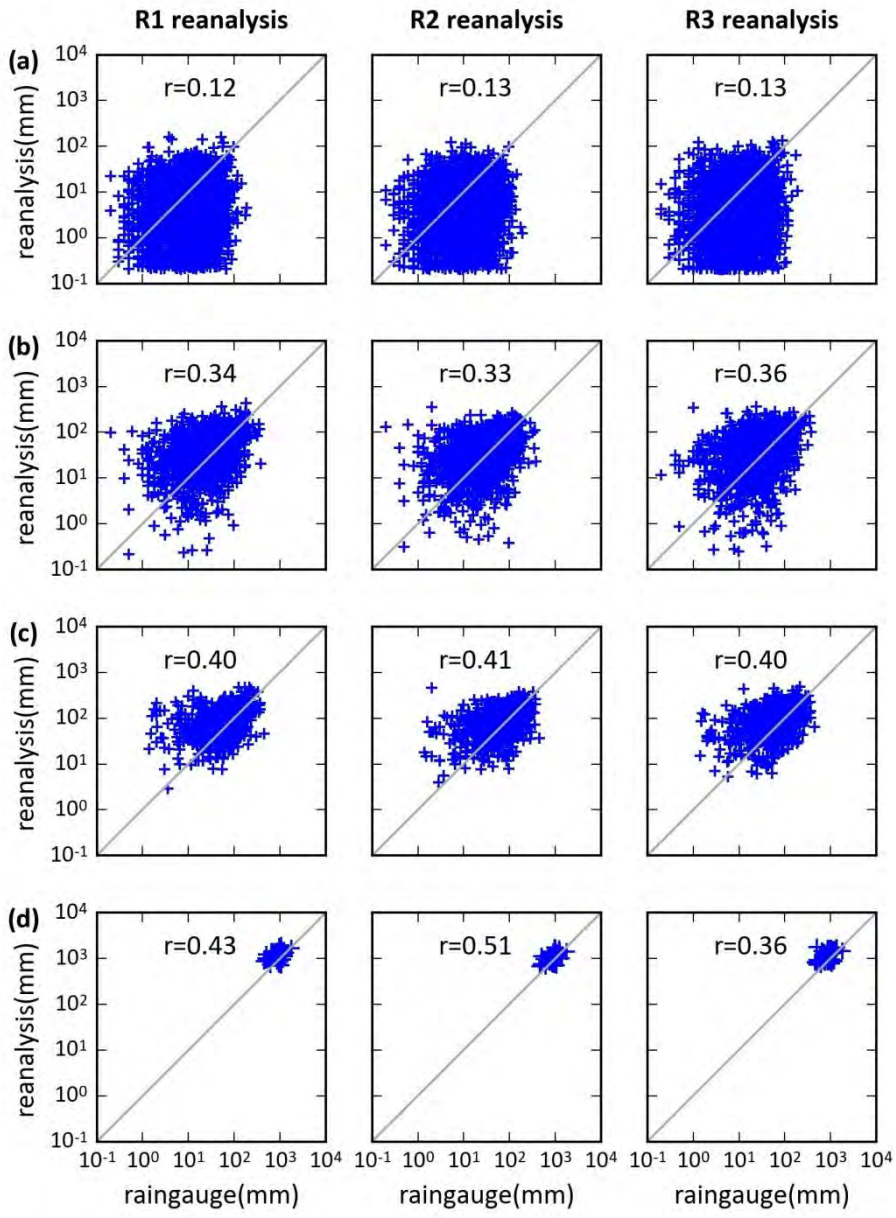

Figure 5.7 Scatter plots of NARCliM reanalysis vs raingauge (61002) in log scale at grid point P1: (a) day, (b) fortnight, (c) month, and (d) annual. Note that only non-zero rainfall values are plotted.

Visual inspection of the scatter plots shows that the rainfall is systematically overestimated by all NARCliM reanalyses for the fortnightly, monthly and annual resolutions. This will likely be corrected in the bias corrected rainfall. The daily rainfall of the NARCliM reanalyses shows a poor agreement to the gauge and AWAP data. The results for P2 and P3 are also similar to those for P1 and are not shown.

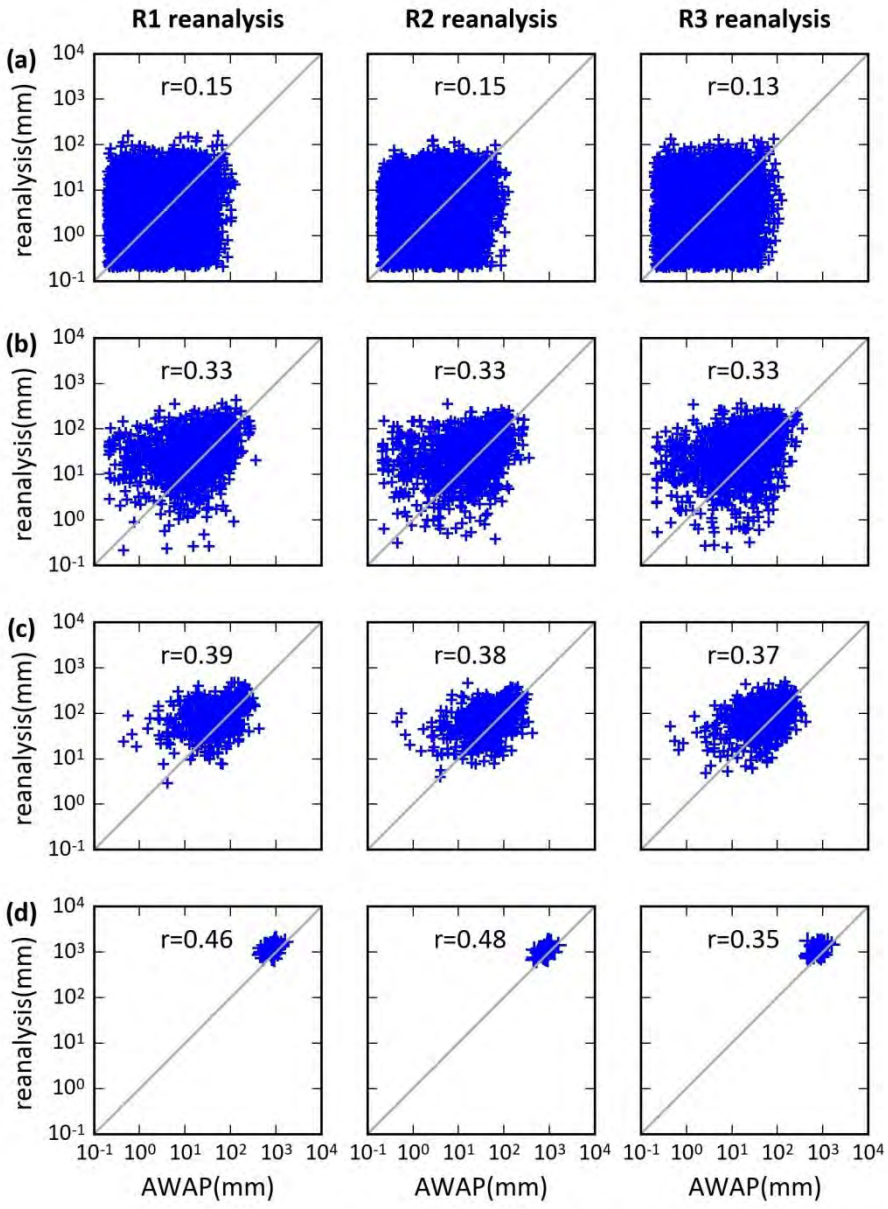

Figure 5.8 Scatter plots of NARCliM reanalysis vs AWAP in log scale at grid point P1: (a) day, (b) fortnight, (c) month, and (d) annual. Note that only non-zero rainfall values are plotted.

To summarise the results, cross correlations (r values) computed for the NARCliM reanalyses versus gauge rainfall and AWAP at grid point P1, P2 and P3 are shown in Figures 5.9a to 5.9c respectively. Correlations ranging from 0.12 to 0.51 show a poor agreement between the reanalyses, and gauge and AWAP data. The highest correlation values are 0.49 (grid point P2 for R1 reanalysis versus AWAP) and 0.51 (grid point P1 for R2 reanalysis versus gauge) for the annual resolution while for the fortnightly resolution R3 reanalysis shows the highest cross correlation of 0.36 at two grid points (grid point P1 for R3 reanalysis versus gauge and grid point P3 for R3 reanalysis versus AWAP). Grid point P1, which represents the mountainous area, shows a better correlation with gauge data compared to the other two grid points located in the flat area, though the improvement is small. Comparing the correlations between the reanalyses, and gauge and AWAP data, the NARCliM reanalyses tend to be slightly more correlated to the AWAP than gauge rainfall for all time resolutions at all grid points.

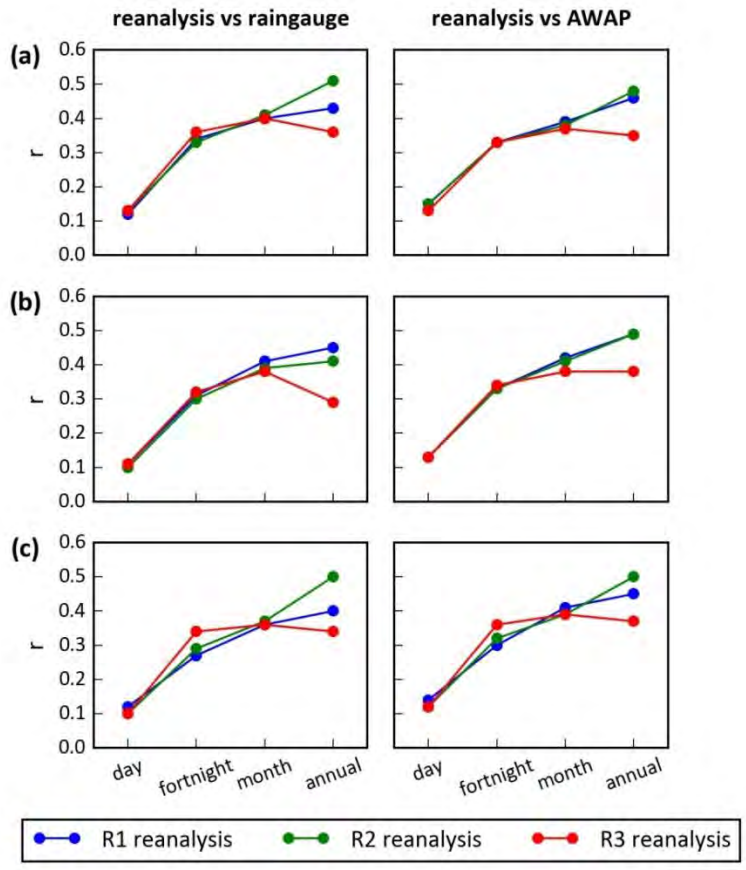

Figure 5.9 Pearson's correlation coefficients (r) at three grid points: (a) P1, (b) P2, and (c) P3.

Correlations between the three NARCliM reanalyses (i.e. R1 versus R2, etc.) were also calculated at grid point P1 (Figure 5.10). The low correlations ranging from 0.3 to 0.6 are similar to the correlations between NARCliM reanalysis, gauge and AWAP (Figures 5.7 and 5.8), and confirm that the RCMs are not highly correlated and thus are conditionally independent from each other. This is consistent with the design of the NARCliM project where Evans et al. (2014) chose 3 RCM configurations that were as independent as possible from each other.

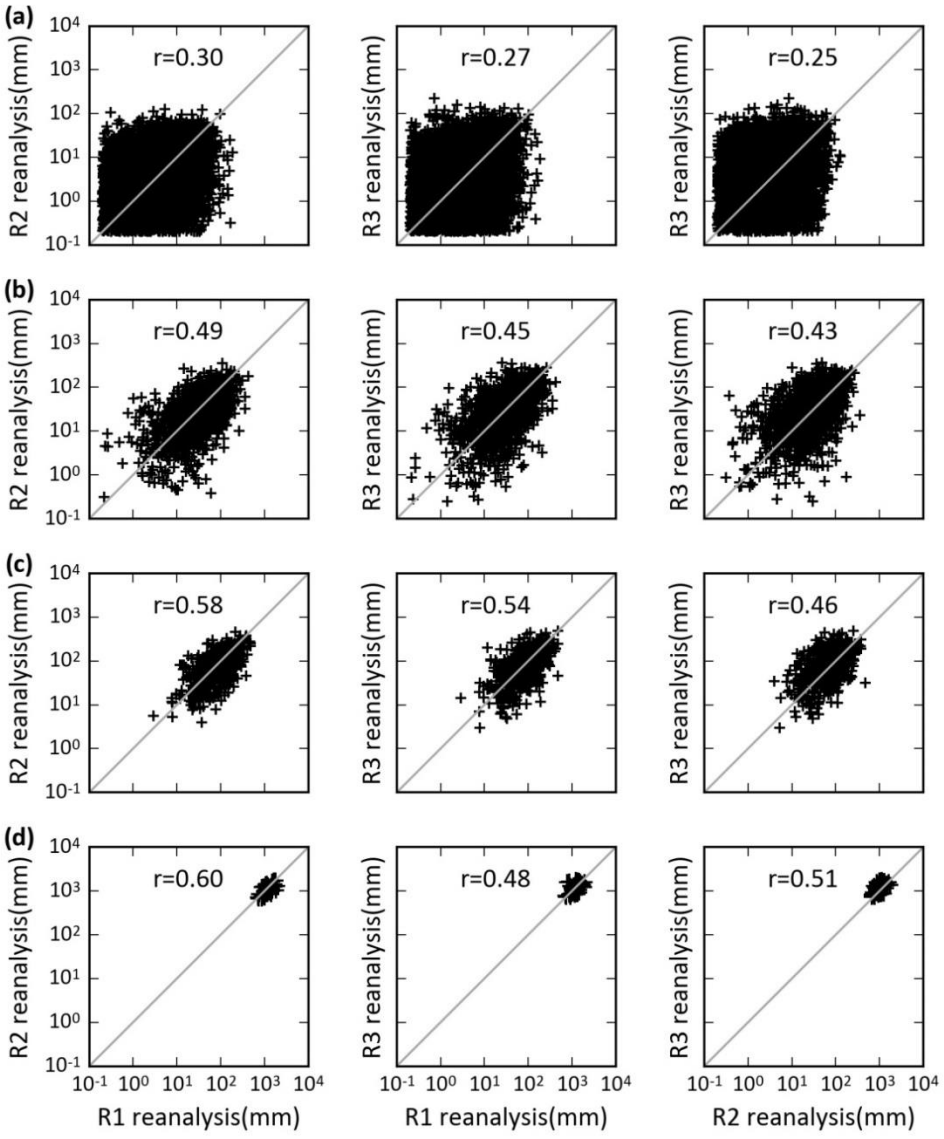

Figure 5.10 Scatter plots between NARCliM reanalyses individual runs in log scale at grid point P1: (a) day, (b) fortnight, (c) month, and (d) annual. Note that only non-zero rainfall values are plotted.

Overall, low correlations (ranging from 0.12 to 0.51) between the NARCliM reanalyses and observed rainfall depths characterise the limited ability of the reanalyses to deterministically reproduce the observed runoff series. Given that the reanalyses were driven at the ~250 km resolution by NCEP/NCAR reanalysis (see Evans et al., 2014 for more details on the design) then at least part of the correlation reflects the ability of NARCLIM to reproduce the rainfall, while part of the correlation reflects the internal dynamics of the RCMs that are used to downscale. No data assimilation of rainfall (gauge rainfall or AWAP) was done during the downscaling, so it is an open question as to how much deterministic fit should be expected from the RCMs, over and above that of NCEP/NCAR, but both the distance from the coast and the topography (which are both better represented in the higher resolution RCM) are likely to condition the spatial patterns of rainfall predicted, though it is unclear how much impact these would have on the temporal characteristics of the rainfall. Figure 5.10 provides some preliminary insight into this question because the difference in the correlations between the reanalyses reflects these internal dynamics. For annual rainfall, the minimum correlation is about 0.3 and the maximum 0.5, so at a minimum NCEP/NCAR accounts for 10% of the variance ($r^2=0.3^2$).

5.1.3 Spatial variability of statistics at catchment scale

The spatial variability of rainfall can be assessed by several measures. In this section the mean, coefficient of variation (C_v) and the lag-1 autocorrelation of the NARCliM reanalyses and AWAP were computed for each grid cell of the entire study area and the statistical values were mapped spatially. The analysis is similar to McMahon et al. (2008) who investigated the spatial variability of rainfall using the coefficient of variation and lag-1 autocorrelation.

The mean, C_v and the lag-1 autocorrelation plots were created at different time resolutions to examine the temporal variability of the rainfall across the study area. Figure 5.11 shows the spatial distribution of mean annual rainfall. Low annual rainfalls (less than 1,200 mm/year) are simulated across much of the centre, east and west of the study area, while the highest rainfalls (up to 2,000 mm/year) generally

are simulated in the northern and southern regions. The mean annual rainfall is noticeably higher in R1 and R3 compared to R2. This is consistent with the relative trends at P1, P2 and P3 in Figure 5.7. Comparing the mean annual rainfall of the reanalyses with AWAP data, all three uncorrected reanalyses overestimate the mean annual rainfall for almost all grid points. However, R2 reanalysis has rainfall depths most similar to AWAP.

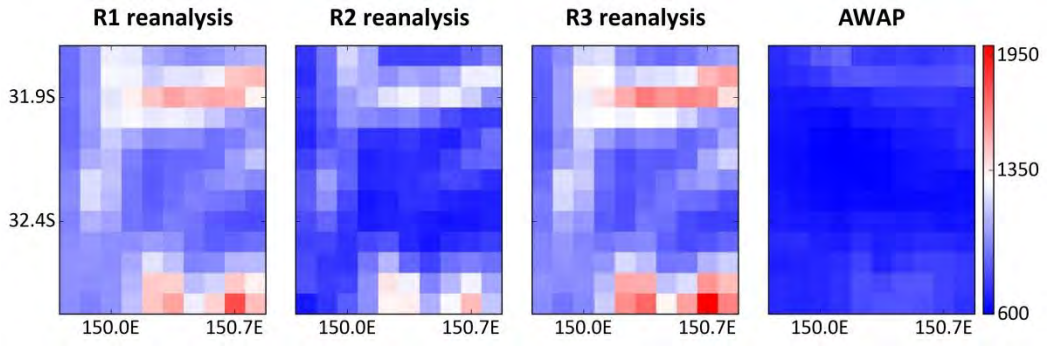

Figure 5.11 Spatial distribution of mean annual rainfall (mm) of NARCliM reanalysis data and AWAP.

The elevations of the study area are shown in Figure 5.12. The highest annual rainfall occurs in the south and north of the study area where the Blue Mountains and Liverpool Ranges are (see Figure 5.12b). McMahon (1964) found that there is a direct influence of topography on rainfall in the Hunter Valley. Hutchinson (1998a,b) also analysed this dependence of the rainfall with elevation using five spline models (which have different dependence with elevation) examined by Hutchinson (1995) and found that rainfall is highly correlated with elevation. A detailed analysis on this correlation will be presented in Chapter 8. However, as a preliminary result the relationship between NARCliM rainfall and elevation is shown in Figure 5.13. The positive trends shown in the scatter plots generated for the three reanalyses confirm that the high rainfall values are mostly associated with higher elevations. R2 shows the highest correlation (r=0.53) between rainfall and elevation.

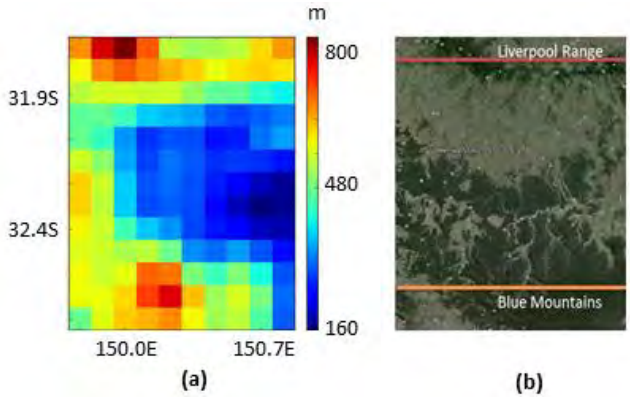

Figure 5.12 Merriwa field site: (a) Topography map of the area (as defined and used in NARCliM), (b) Google Earth aerial photo for the same region.

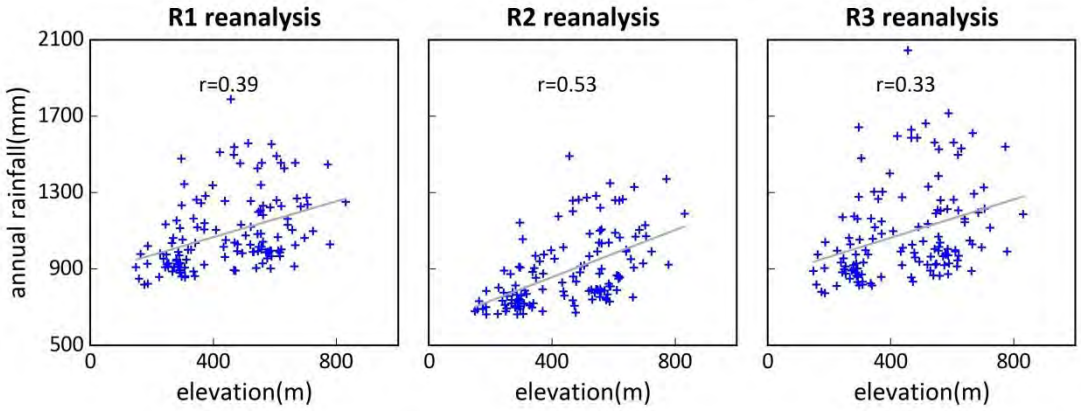

Figure 5.13 Scatter plots of annual rainfall vs elevation for each grid point in Figure 5.12a.

Figure 5.14 shows the spatial variation of the coefficient of variation (C_v) at daily, fortnightly, monthly and annual resolution.

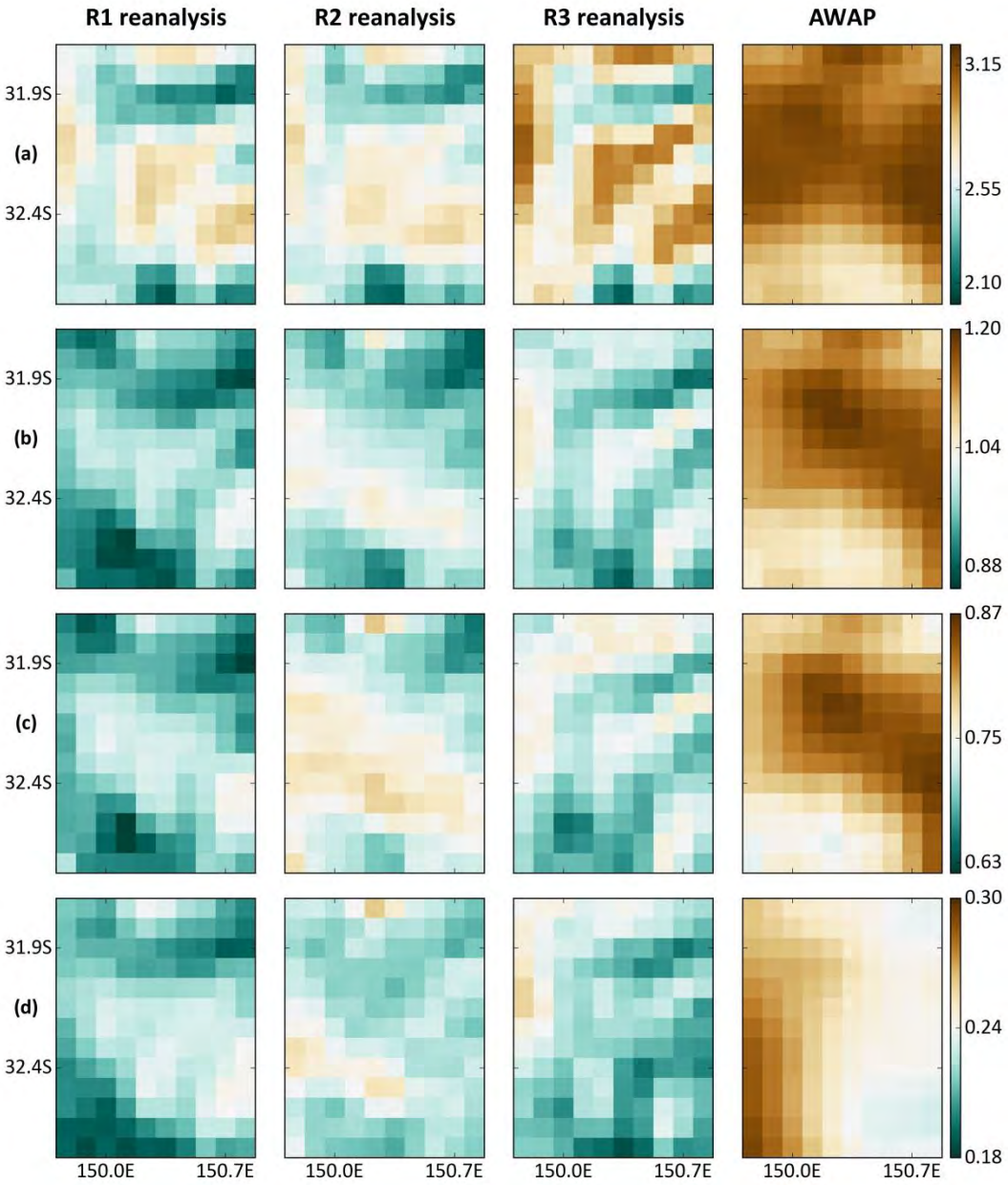

Figure 5.14 Spatial distribution of coefficient of variation C_v of rainfall for NARCliM reanalysis data and AWAP: (a) day, (b) fortnight, (c) month, and (d) annual.

Overall, the C_v ranging from 2 to 3.25 at the daily resolution shows high rainfall variability across the site for all reanalyses. Compared with the spatial variability of the mean (Figure 5.11), the spatial variation in C_v is relatively small and appears to be related to the spatial variation of the mean rainfall. The higher C_v values for the reanalyses and AWAP in the centre of Figure 5.14a show that rainfall is more variable in the centre, than the northern and southern regions where there are higher

elevations. For the longer resolutions, R1 and R2 reanalyses show a north-west to south-east band of high C_v through the centre of the study area which has a strong similarity with AWAP. However, for the annual resolution there seems to be no similarity in the spatial pattern of the reanalyses and AWAP. For R1 and R2 reanalysis, it appears that the rainfall variability is influenced by the topography of the study area, with lower C_v in the higher elevation regions.

The R3 reanalysis has higher daily rainfall variability than R1 and R2, but R2 has higher variability for other time resolutions. R3 also shows a different spatial pattern to R1 and R2 with a north-east to south-west banding that appears to be unrelated to the topography. Compared with AWAP, all reanalyses underestimated the C_v for all grid points of the site. R2 has the most similar C_v to AWAP, both the values and spatial pattern.

The spatial patterns of the lag-1 autocorrelation coefficient for the NARCliM and AWAP gridded data are shown by Figure 5.15. The general spatial patterns of R1, R2 and R3 are similar, with R3 being different at the annual resolution. R3 has significantly weaker autocorrelations than R1 and R2. When compared with AWAP R3 has similar magnitude autocorrelations, but has significantly higher autocorrelations at the annual resolution. While the spatial patterns of all the reanalyses are similar to each other (though the average values vary significantly between reanalyses) their patterns are completely different from the pattern of AWAP. Comparing the three reanalyses, at fortnightly and monthly resolutions, the lag-1 autocorrelations of R1 and R2 are overestimated to a greater extent than R3, with both R3 and AWAP having autocorrelations very close to zero. This result is consistent with the lag-1 autocorrelations shown in Figures 5.1 to 5.3. For the annual resolution, all three reanalyses overestimated the lag-1 autocorrelation of AWAP. In what is perhaps the most intriguing result the annual AWAP data shows a large area of negative lag-1 autocorrelations, which is not shown in any of the reanalyses. This result is probably marginally statistically significant because the 95% confidence limits for lag-1 annual analyses are about 0.25 to -0.25 (see the lag-1 95% confidence limits for the annual analyses in Figures 5.1 to 5.3), very similar to the observed result of -0.3.

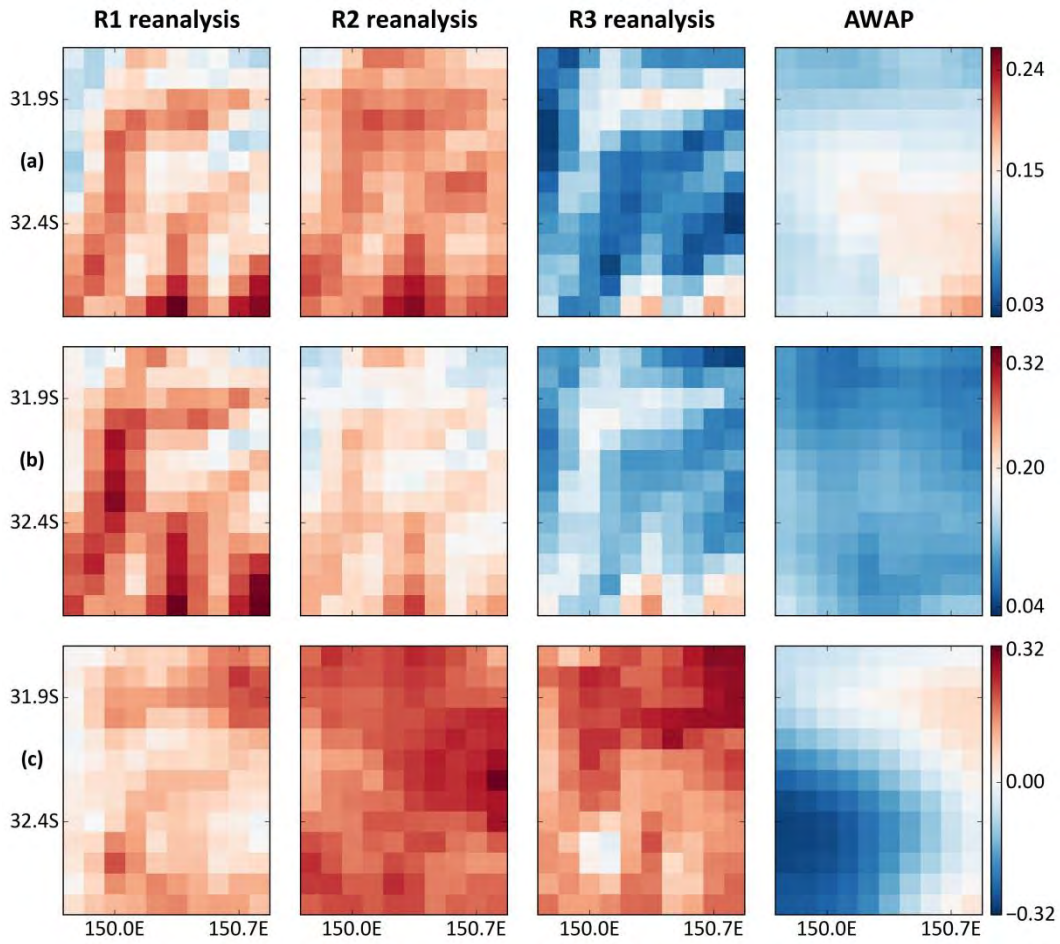

Figure 5.15 Spatial distribution of lag-1 correlation of rainfall for NARCliM reanalysis data and AWAP: (a) fortnight, (b) month, and (c) annual.

Overall, the spatial variation of mean rainfall for all NARCliM reanalyses' grid points in the site reveals that the mean annual rainfall is higher in the hilly areas in all three reanalyses and R1 and R3 produce higher rainfall than R2. The spatial variation in the coefficient of variation shows similar results for all three reanalyses. The spatial pattern of the coefficient of variation is similar for all reanalyses but is significantly different from that of AWAP. The pattern of the coefficient of variation for the reanalyses was similar to that for mean rainfall, which has a link with elevation. The relationship was that rainfall was less variable in hilly areas while flat areas show high rainfall variability. However, the rainfall variability is strongly influenced by the topography of the study area.

The spatially plotted lag-1 autocorrelation results show that for the fortnightly, monthly and annual time resolutions, the autocorrelation values are quite low. R1 and R2 reanalysis produce higher lag-1 autocorrelations compared to the R3 reanalysis. In summary, statistics calculated at the catchment scale show that the NARCliM reanalyses are not capable of reproducing the observed spatial pattern shown by AWAP. They also tend to overestimate both mean rainfall and lag-1 correlations while underestimating the coefficient of variation relative to AWAP. The ability of NARCliM reanalyses to reproduce the spatial pattern of observed rainfall statistics is a necessary but not sufficient requirement for hydrological studies, particularly catchment hydrology modelling.

5.2 Conclusions

The results show that the NARCliM reanalyses datasets do not reliably reproduce the correct spatial and temporal correlations for the Merriwa site. Cross correlating the NARCliM reanalyses against gauge and AWAP shows that the agreement between NARCliM reanalysis and observed rainfall is poor and suggests that the Regional Climate Model (RCM) reanalysis datasets do not produce the spatial distribution of rainfall correctly. The failure to reproduce the spatial distribution of rainfall may lead to biased and incorrect reservoir dynamics if these datasets are used as inputs to rainfall-runoff models. However, it should be noted that the data used in this chapter is uncorrected raw RCM simulations and an appropriate bias correction may improve the performance, though bias correction can also introduce other uncertainties and limitations (e.g. Parry et al., 2007; Randall et al., 2007; Stainforth et al., 2007; Koutsoyiannis et al., 2008; Kiem and Verdon-Kidd, 2011; Stephens et al., 2012). It should be noted that a comprehensive assessment of the bias corrected RCM data is presented in Chapter 9. A possible link between the statistics and topography at the catchment scale was found during this pilot study and this will be further discussed in following chapters to better understand the statistical characteristics of the orographic effect. Unlike previous work on orography, the rainfall effect does not appear to be simply a function of elevation.

Chapter 6
Testing the rainfall statistics of NARCliM uncorrected and bias-corrected reanalyses using AWAP data for the broader East Coast of Australia

6.1 Introduction

Chapter 5 presented a case study performed for a single site in the Upper Hunter region of NSW. However, knowing that the current GCMs poorly resolve the climate of the eastern coastal strip, there is a need to assess the performance of this finer resolution NARCliM dynamically downscaled data along the entire east coast. Chapter 5 also found that the NARCliM RCMs poorly simulate the rainfall at high elevation regions compared with low elevations. Therefore it is worthwhile assessing the rainfall simulated by NARCliM RCMs at various sites with different orography. Combining these objectives, this chapter aims to fulfil the second major objective of this thesis: Validation of the NARCliM data along the broader east coast at various sites with different orography. The analysis presented in this chapter extends that of Chapter 5, and was performed at four sites located along the NSW east coast: Williams River site, Richmond River site, Bega River site and the site of Sydney water supply system, referred as Sydney site in this thesis (see Chapter 3: Sites and Data for more details). The three NARCliM NCEP/NCAR uncorrected and bias corrected reanalysis (R1, R2 and R3 reanalyses) driven datasets (1950-2009) were used for the analyses.

Using the method explained in Section 4.2, the ability of reanalysis data to reproduce the observed rainfall probability distribution is first evaluated. Both the spatial and temporal distribution of the reanalysis rainfall were calculated and compared with AWAP at four grid points of each site. The selected grid points and elevations of each site are shown in Figures 6.1 to 6.4.

As in Chapter 5, the mean, coefficient of variation (C_v) and the lag-1 autocorrelation computed at each grid point of the reanalyses datasets were used to assess the spatial variability of the rainfall. The statistics of all three reanalyses datasets were calculated and then compared with AWAP data. There are several reasons for choosing AWAP as the primary observed dataset in this chapter; (1) The distribution of the rain gauge network is sparse in each site, so that it was impossible to find a rain gauge at each grid point, (2) As explained in the literature review, downscaled rainfall data can be validated against point scale and pixel scale observations. However, the validation of NARCliM gridded data against another gridded dataset eliminates the scale discrepancy between the datasets.

Later in this chapter, the ability of reanalyses to reproduce the rainfall autocorrelation was assessed by following the methodology explained in Section 4.4. The analysis was performed at the same grid points used for the probability distribution analysis.

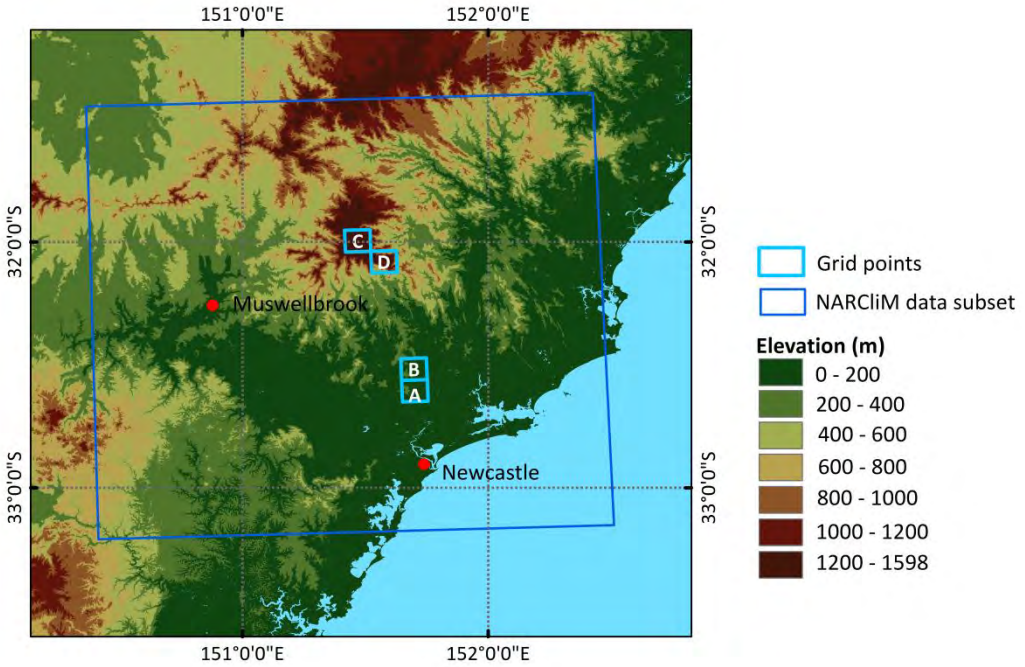

Figure 6.1 Map of the Williams River site with topography. The NARCliM data subset outlined is 20 x 20 pixels (10 km resolution). The grid points A - D are the NARCliM pixels used for comparison.

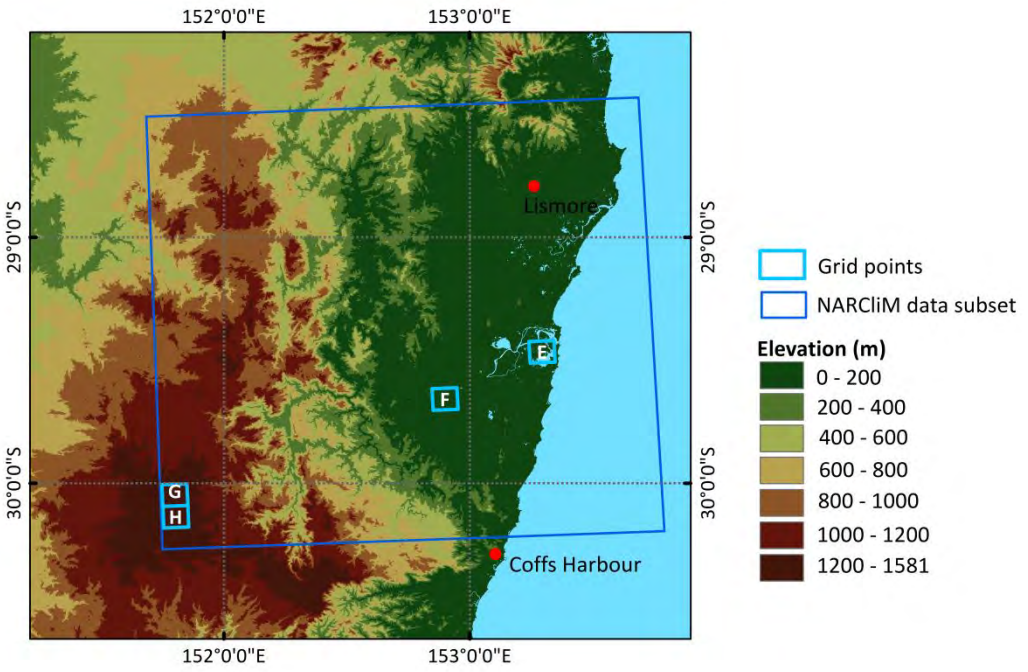

Figure 6.2 Map of the Richmond River site with topography. The NARCliM data subset outlined is 20 x 20 pixels (10 km resolution). The grid points E - H are the NARCliM pixels used for comparison.

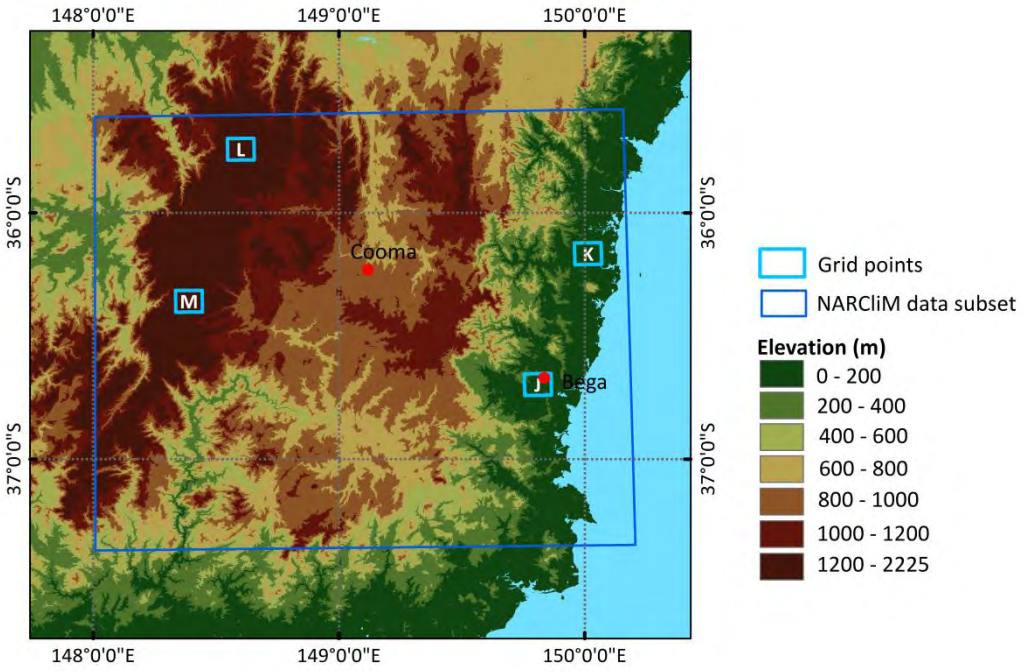

Figure 6.3 Map of the Bega River site with topography. The NARCliM data subset outlined is 20 x 20 pixels (10 km resolution). The grid points J - M are the NARCliM pixels used for comparison.

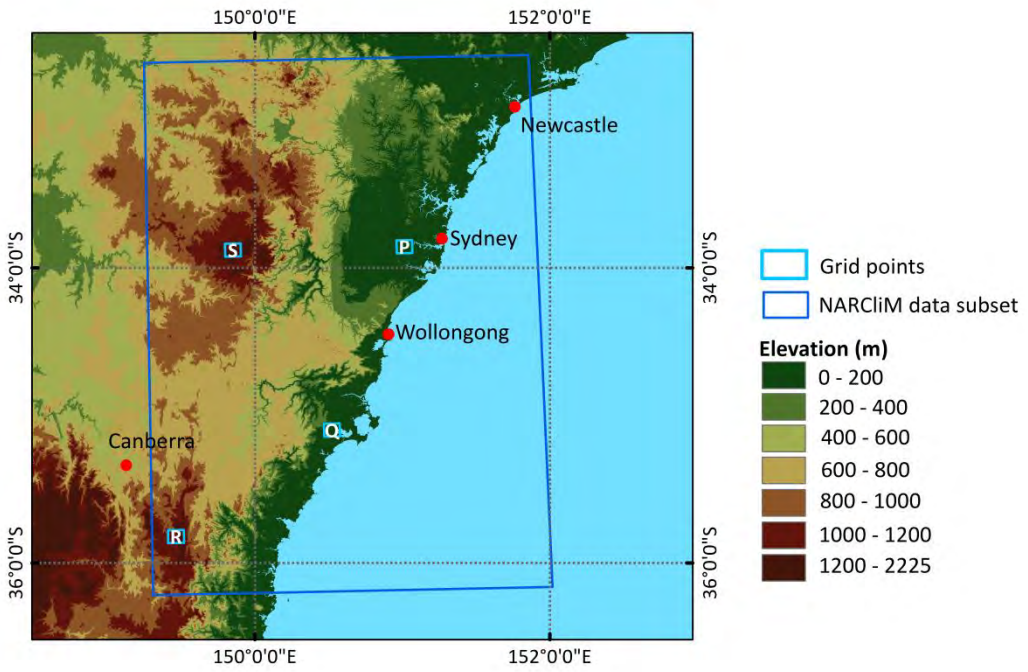

Figure 6.4 Map of the Sydney site with topography. The NARCliM data subset outlined is 41 x 25 pixels (10 km resolution). The grid points P - S are the NARCliM pixels used for comparison.

6.2 Probability distribution of the daily rainfall

This section assesses the ability of uncorrected and bias corrected NARCliM reanalyses data to reproduce the observed rainfall probability distributions. The cumulative probability distributions of the mean annual rainfall of uncorrected reanalyses and AWAP for all grid points of all four sites are shown in Figures 6.5a to 6.8a respectively. There is a general trend of uncorrected reanalyses to underestimate the mean annual rainfall probabilities of AWAP at each site, particularly the occurrence of greatest rainfall values. Further, the underestimation is higher in R1 and R3 than R2.

The cumulative probability distribution of the daily uncorrected and bias corrected NARCliM and AWAP rainfall data was calculated at the grid points chosen within all four sites. The elevations of grid points are listed in Table 6.1. The focus was on high and low elevation points in order to assess the performance of NARCliM data for different terrain conditions.

Table 6.1 Elevation of grid points

Study site	*Grid point*	*Elevation (m)*	*Elevation Category*	
			low	*high*
Williams River site	A	35.5	✓	
	B	86.7	✓	
	C	959.8		✓
	D	615.2		✓
Richmond River site	E	30.8	✓	
	F	85.6	✓	
	G	1097.6		✓
	H	1003.7		✓
Bega River site	J	122.5	✓	
	K	108.6	✓	
	L	1298.1		✓
	M	1506.0		✓
Sydney site	P	7.0	✓	
	Q	35.6	✓	
	R	1162.6		✓
	S	1024.25		✓

The CDFs are for the uncorrected reanalyses and AWAP at grid points A to D at the Williams River site, E to H at the Richmond River site, J to M at the Bega River site and P to Q at the Sydney site are shown in Figures 6.5b to 6.8b respectively.

At low elevation grid points of the Williams River site all three uncorrected reanalyses tend to underestimate the daily probability distribution, particularly the small rainfall events (0.2 to 7 mm). R2 is able to capture the probabilities of AWAP midsized to large events (rainfall greater than 7 mm) while R1 and R3 underestimate the CDF. These results are typical of all other low elevation grid points except for the grid points E, K and Q; At grid point E of the Richmond River site, midsized and large rainfall events of AWAP are captured by both R1 and R3 uncorrected reanalyses while R2 overestimating those probabilities slightly. At grid point K of Bega River site, R2 reanalysis is able to produce the entire rainfall distribution of AWAP with all the probabilities approximately correct. At grid point Q of Sydney site, R2 closely reproduces the entire rainfall distribution with a slight

underestimation. However, it is worth noting that all these three points are located very close to the eastern coast line where there is a high rainfall band in the mean annual rainfall plots of AWAP (see Figures 6.13a, 6.15a, 6.17a and 6.19a).

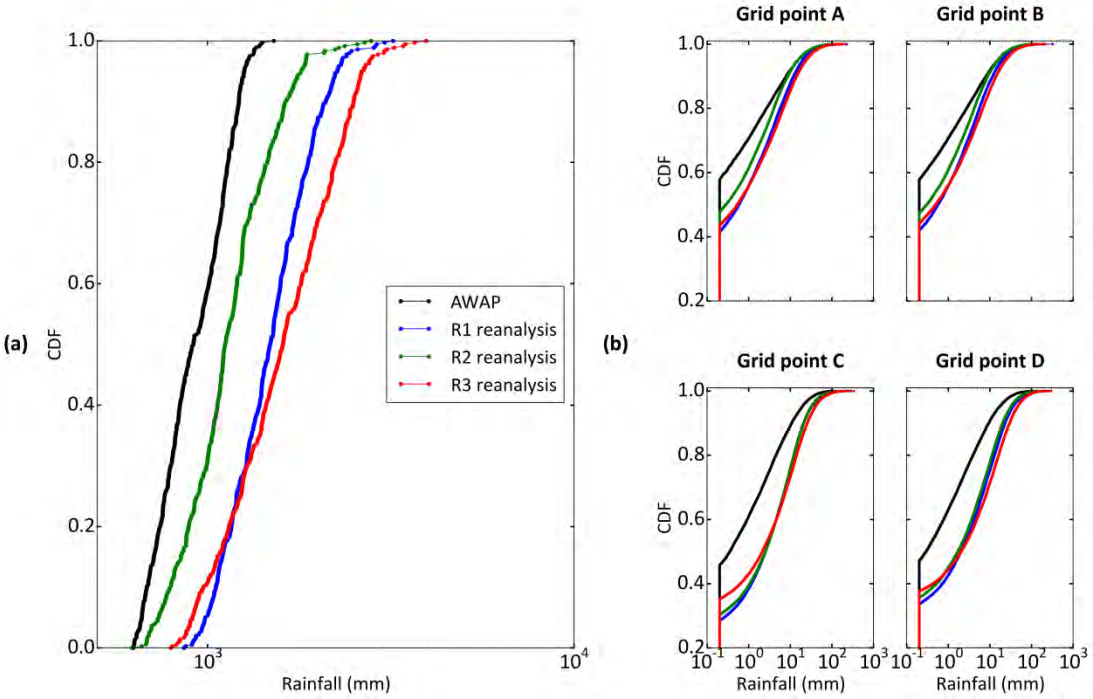

Figure 6.5 Cumulative probability distributions of (a) mean annual rainfall of uncorrected reanalyses and AWAP across the Williams River site and (b) daily rainfall at grid points A, B, C and D. Note that daily rainfall are in log scale and only values greater than 0.2 mm are plotted.

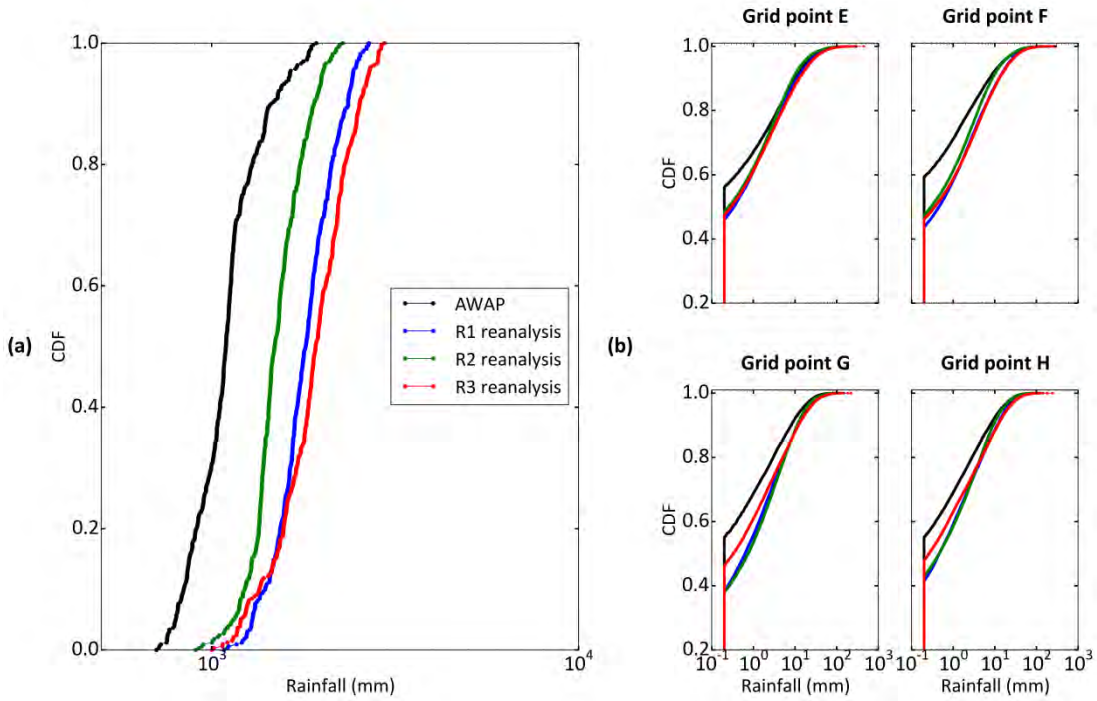

Figure 6.6 Cumulative probability distributions of (a) mean annual rainfall of uncorrected reanalyses and AWAP across the Richmond River site and (b) daily rainfall at grid points E, F, G and H. Note that daily rainfall are in log scale and only values greater than 0.2 mm are plotted.

At the high elevation grid points of all sites, all three uncorrected reanalyses underestimate the daily rainfall probabilities of AWAP for all rainfall events. Compared with R1 and R2, R3 reanalysis appears to better simulate AWAP rainfall probabilities, but cannot be considered as good as what was seen with R2 reanalysis at low elevation pixels. These results indicate that uncorrected NARCliM reanalyses are poor simulating the rainfall probability distributions at high elevation regions than low elevations. This can be attributed to the intrinsic difficulty of NARCliM RCMs to model the observed precipitation processes in topographically complex areas.

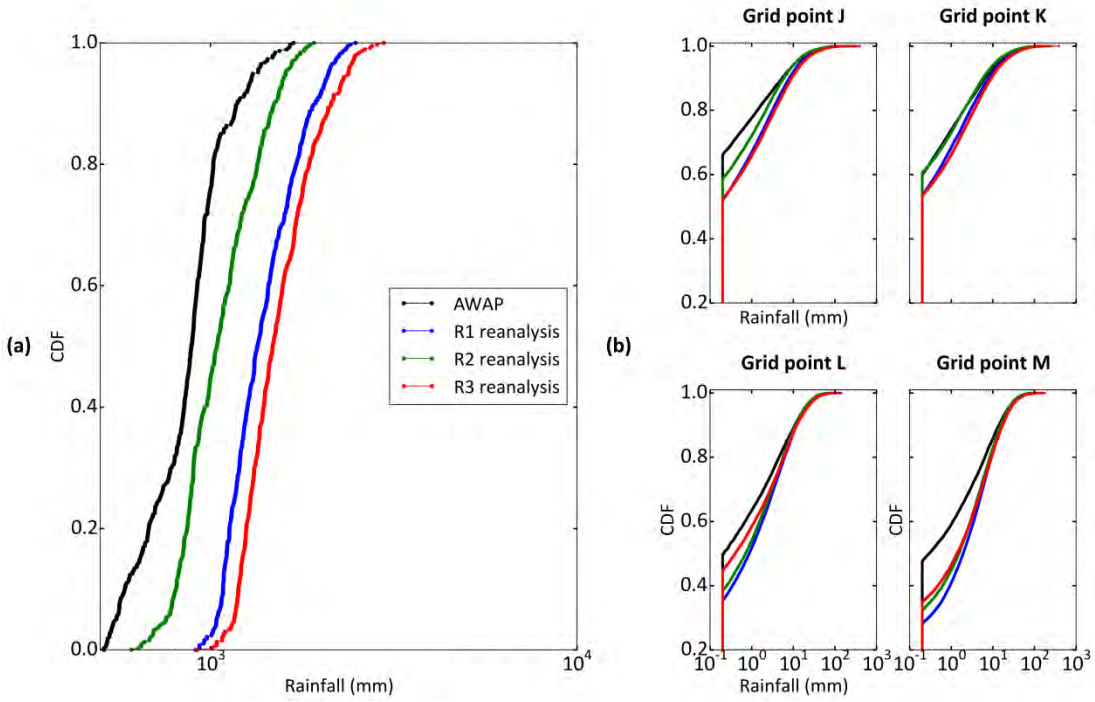

Figure 6.7 Cumulative probability distributions of (a) mean annual rainfall of uncorrected reanalyses and AWAP across the Bega River site and (b) daily rainfall at grid points J, K, L and M. Note that daily rainfall are in log scale and only values greater than 0.2 mm are plotted.

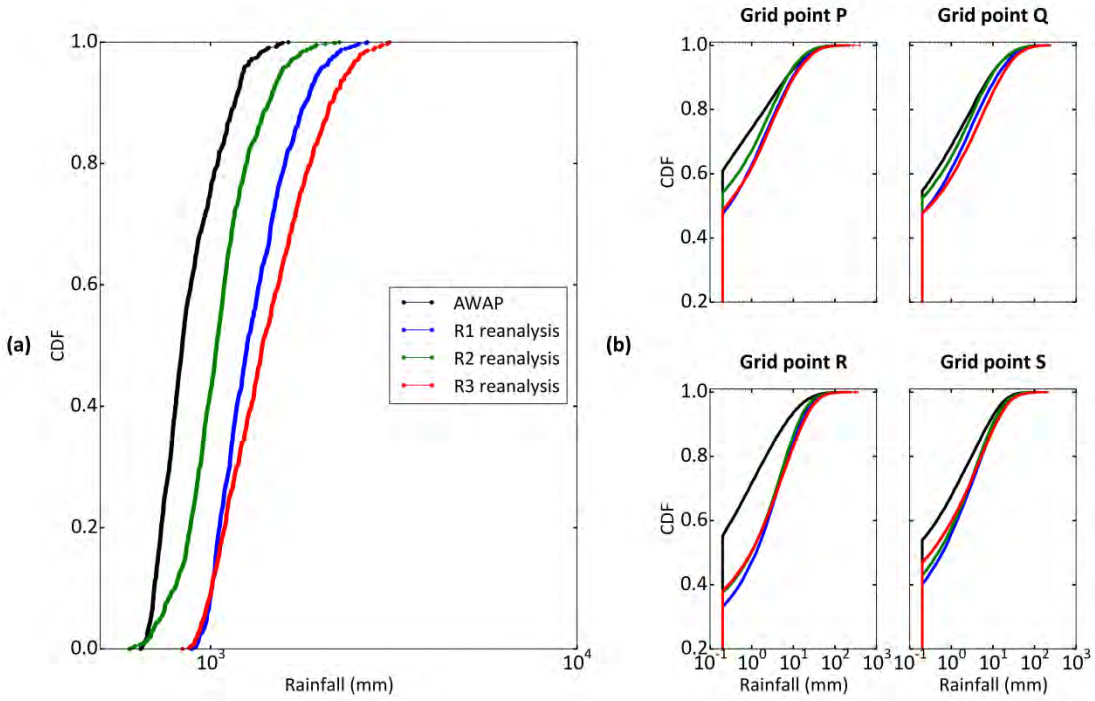

Figure 6.8 Cumulative probability distributions of (a) mean annual rainfall of uncorrected reanalyses and AWAP across the Sydney site and (b) daily rainfall at grid points P, Q, R and S. Note that daily rainfall are in log scale and only values greater than 0.2 mm are plotted.

The cumulative probability distributions of the mean annual rainfall of the bias corrected reanalyses and AWAP for all grid points of all four sites are shown in Figures 6.9a to 6.12a respectively. After the bias correction, all reanalyses tend to reproduce the CDF of AWAP while sharing almost 98% of AWAP's CDF. This is a good example, which shows the extent of improvement in the mean statistics of reanalyses after the bias correction. The bias corrected R2 reanalysis better captures the CDF of AWAP than R1 and R3. However, at Bega River and Sydney sites, R1 reanalysis also captures the CDF of AWAP as closely as R2 reanalysis.

The cumulative probability distributions of the daily rainfall of bias corrected reanalyses and AWAP at grid points A to D at the Williams River site, E to H at the Richmond River site, J to M at the Bega River site and P to Q at the Sydney site are shown in Figures 6.9b to 6.12b respectively. Note that these comparisons are for the daily rainfall but are typical of results for fortnightly to yearly averaged data as well. An analysis these longer timescale was done for the Williams River site and can be found in Appendix A.1 – Figures A.1 and A.2.

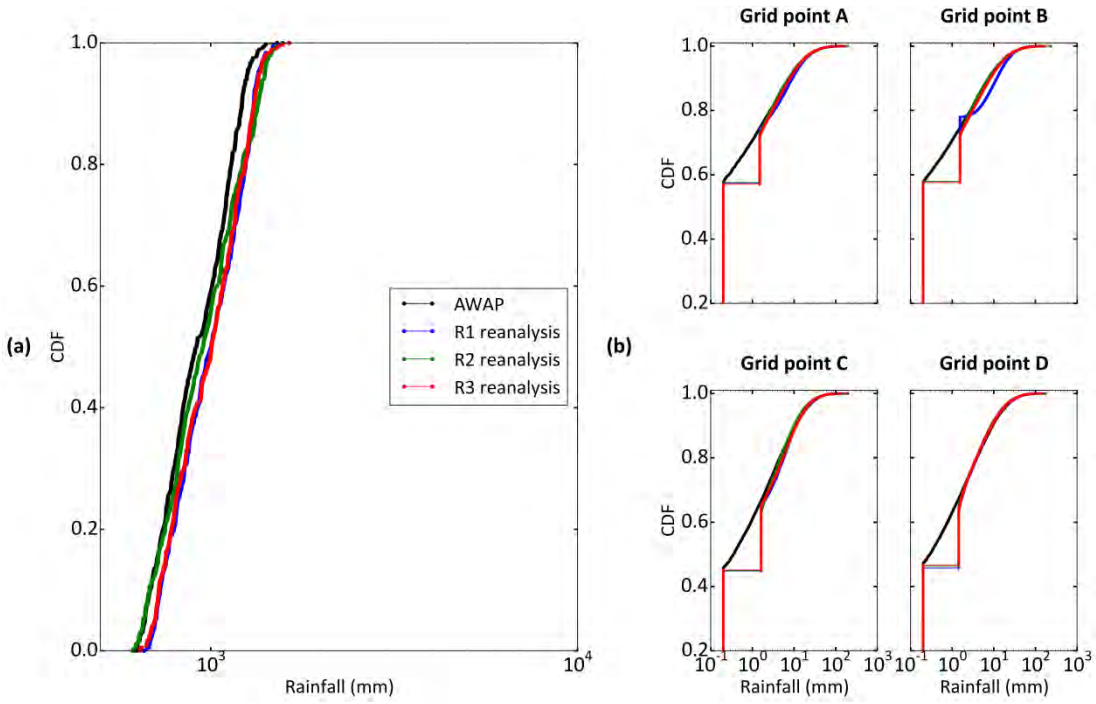

Figure 6.9 Cumulative probability distributions of (a) mean annual rainfall of bias corrected reanalyses and AWAP across the Williams River site and (b) daily rainfall at grid points A, B, C and D. Note that daily rainfall are in log scale and only values greater than 0.2 mm are plotted.

In general, there is a significant improvement of reanalyses after the bias correction, but it is clear that only a part of the CDF has been improved. The CDF of bias corrected rainfall at grid points A-D show that none of the NARCliM simulations capture the probabilities of light rainfall events (rainfall less than 1.5 mm) of AWAP, hence the bias correction method (i.e. a method which fit cumulative distribution function (CDF) of simulated data and observed data to gamma distributions, see Evans and Argüeso, 2014; Argüeso et al., 2013; Piani et al., 2010a,b) appears to be reliable only for rainfall events with rainfall greater than 1.5 to 2 mm. For these low-to-high rainfall events (rainfall greater than 1.5 mm), bias corrected R2 reanalyses tend to reproduce the rainfall probabilities of all four grid points at the Williams River site. R1 and R3 bias corrected reanalyses are also capable to reproduce the CDF of AWAP at high elevation grid points (C and D), but tend to slightly under or overestimate the CDF at low elevation grid points. Note that the sudden rise seen at 1.5 mm rainfall value (Figure 6.9b) in daily NARCliM CDF is an artefact which may have caused by the bias correction process, and is consistently seen for all the sites studied.

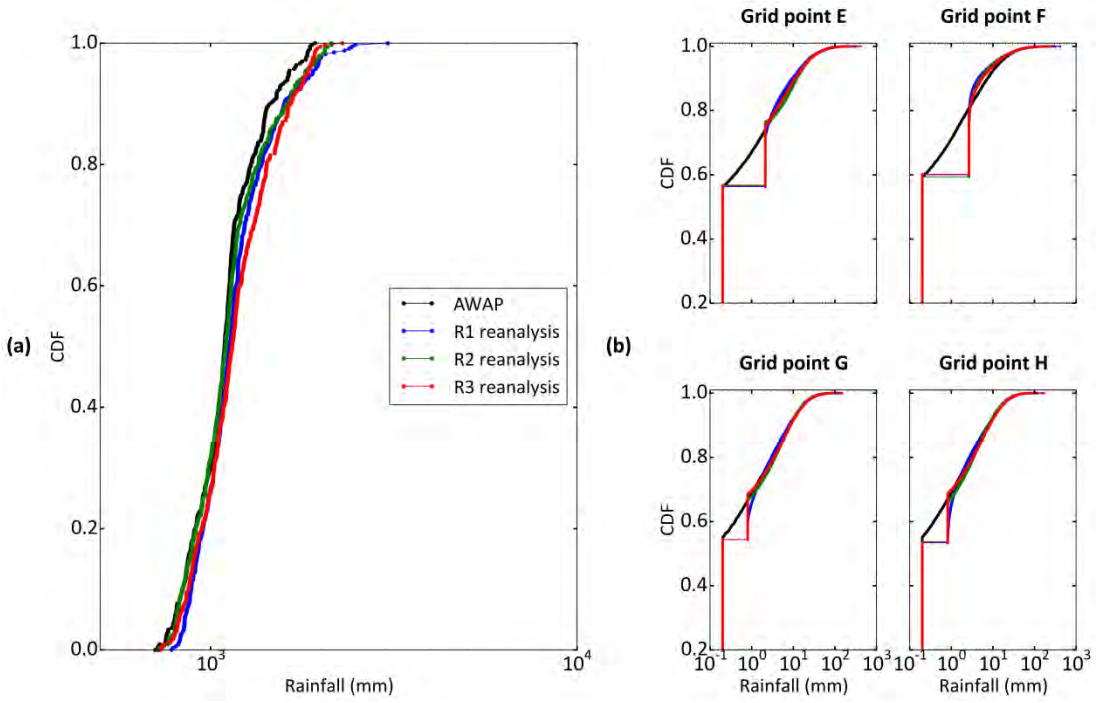

Figure 6.10 Cumulative probability distributions of (a) mean annual rainfall of bias corrected reanalyses and AWAP across the Richmond River site and (b) daily rainfall at grid points E, F, G and H. Note that daily rainfall are in log scale and only values greater than 0.2 mm are plotted.

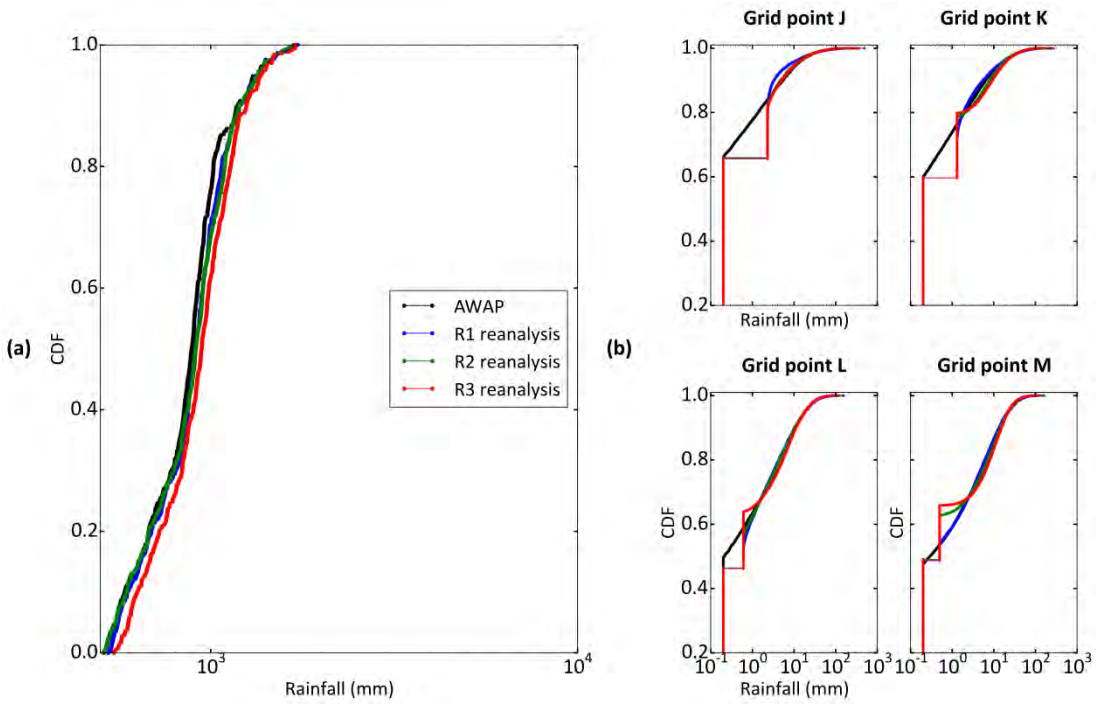

Figure 6.11 Cumulative probability distributions of (a) mean annual rainfall of bias corrected reanalyses and AWAP across the Bega River site and (b) daily rainfall at grid points J, K, L and M. Note that daily rainfall are in log scale and only values greater than 0.2 mm are plotted.

Comparing all sites, R2 bias corrected reanalysis best reproduces the probability distribution of low-to-high rainfall events of AWAP. As was seen at the Williams River site, R1 and R3 reanalyses tend to either under or overestimate the CDF of AWAP at low elevation grid points of Richmond and Bega River sites (grid points E and F at the Bega River site and J and K at the Bega River site). This suggests that the results are typical for other sites.

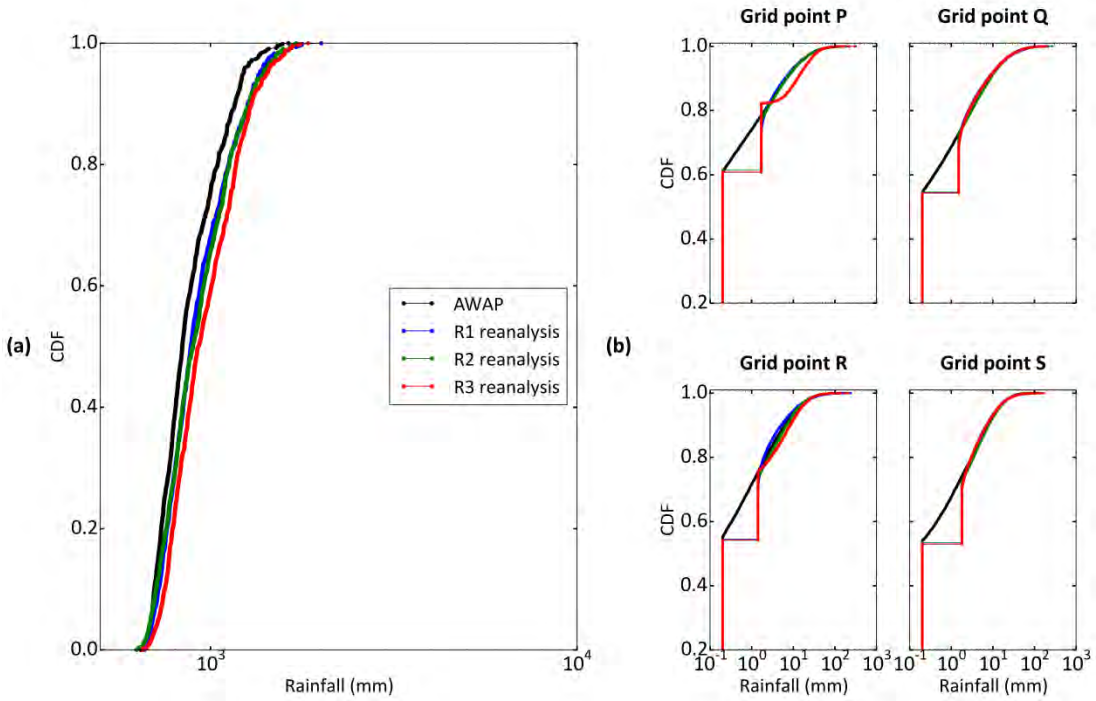

Figure 6.12 Cumulative probability distributions of (a) mean annual rainfall of bias corrected reanalyses and AWAP across the Sydney site and (b) daily rainfall at grid points P, Q, R and S. Note that daily rainfall are in log scale and only values greater than 0.2 mm are plotted.

Overall, the results suggest that bias corrected reanalyses are only reliable in reproducing the daily rainfall probabilities of rainfall events with rainfall greater than 1.5 mm. Within this range (rainfall greater than 1.5), bias corrected reanalyses are more capable to closely reproduce the CDF of AWAP at high elevation grid points than the uncorrected reanalyses.

6.3 Spatial Variability of the rainfall

6.3.1 Mean rainfall

The spatial distribution of the mean annual rainfall of uncorrected reanalyses and AWAP, the ratio of the mean of the uncorrected reanalyses and AWAP and the elevation of all grid points for the Williams River site is shown in Figure 6.13.

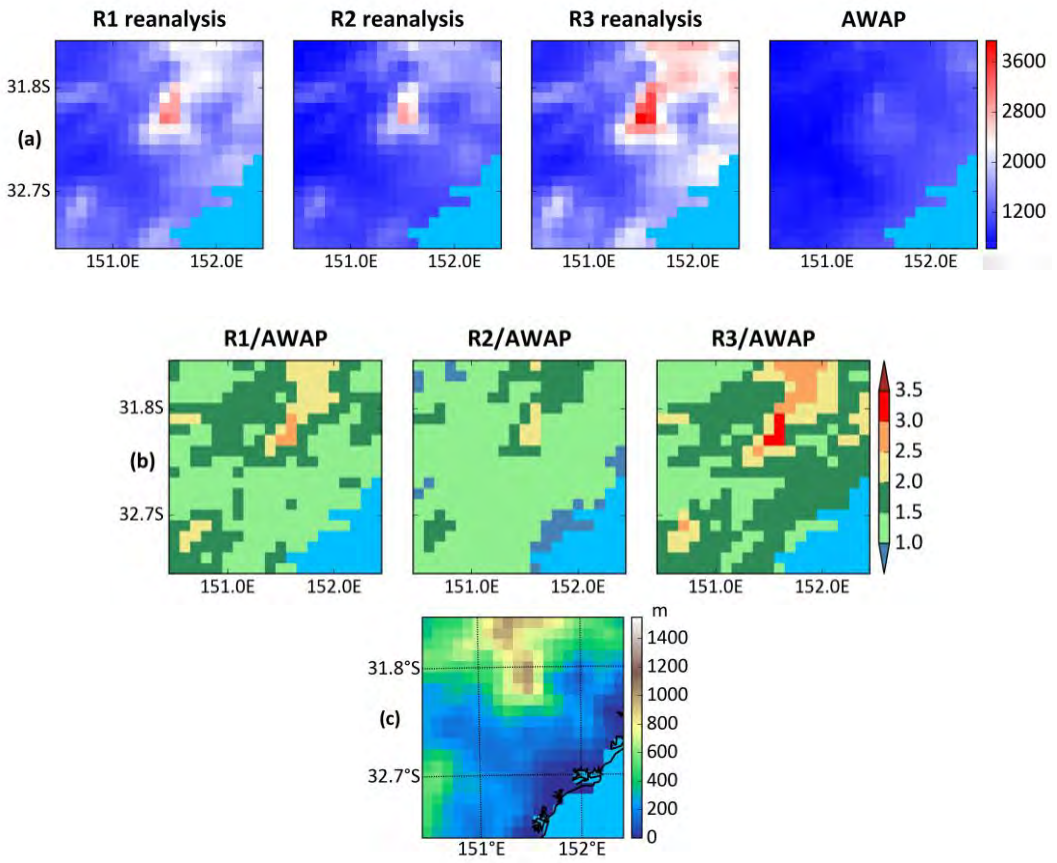

Figure 6.13 Spatial distribution of the mean annual rainfall – Williams River site (a) mean annual rainfall of uncorrected reanalyses and AWAP, (b) ratio of the mean annual rainfall of uncorrected reanalyses to AWAP and (c) topography map of the site (as defined and used by NARCliM).

The mean annual rainfall of AWAP at the Williams River site varies from 626-1,516 mm whereas the mean simulated by the uncorrected reanalyses lies in the range of 616-3,942 mm. This clearly shows that reanalyses simulations tend to overestimate the rainfall of AWAP, particularly the higher rainfall regions. This effect is more pronounced in R3 compared with R1 and R2. In general, the mean annual rainfall is

higher at high elevations than low elevations of Figure 6.13c in each dataset. As was seen at the Goulburn River site, the general spatial pattern of the mean rainfall of reanalyses is qualitatively similar for that of AWAP data.

Figure 6.13b shows the mean rainfall of NARCliM uncorrected reanalyses divided by AWAP. The ratio ranging from 0.5 to 3.5 for the Williams River site indicates that the mean rainfall of the NARCiM reanalyses tends to be greater than the mean of the AWAP rainfall. While there are slight discrepancies between the spatial patterns of AWAP and reanalysis datasets, all reanalyses, except R2, overestimate the mean annual rainfall of the AWAP across the site. As was found earlier, the overestimation of uncorrected R3 reanalysis is greater than R1 and R2. Compared with R1 and R3, uncorrected R2 reanalysis simulates the mean rainfall of AWAP well, with a ratio varying from 1 to 1.5 for more than 75% of the total grid points of the site.

The spatial distribution of the mean annual rainfall of bias corrected reanalyses and AWAP and the ratio of the mean of the bias corrected reanalyses and AWAP for the Williams River site is shown in Figure 6.14.

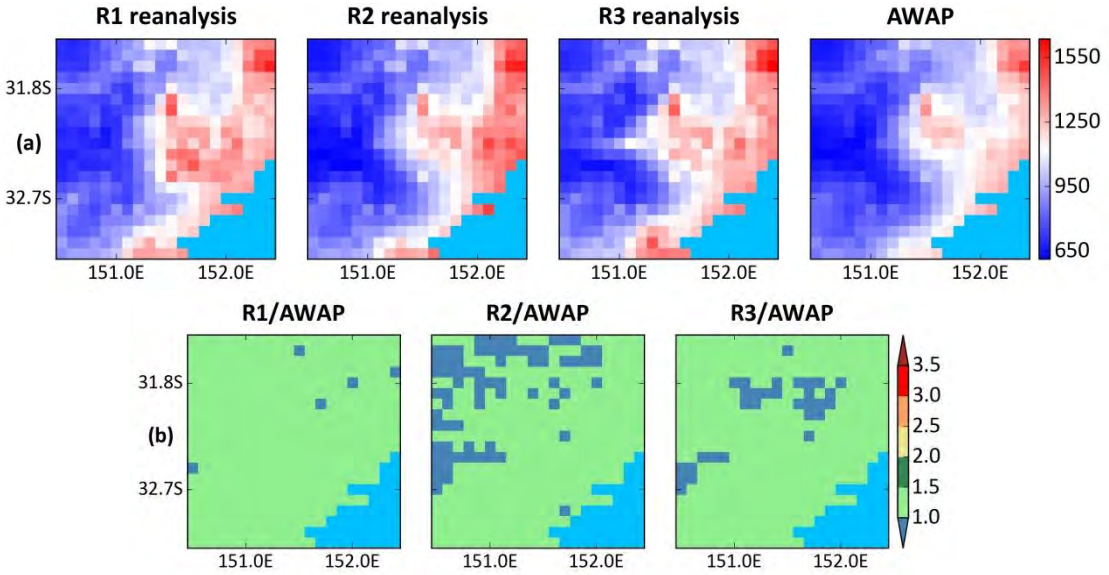

Figure 6.14 Spatial distribution of the mean rainfall – Williams River site (a) mean annual rainfall of bias corrected reanalyses and AWAP and (b) ratio of the mean annual rainfall of bias corrected reanalyses to AWAP.

Compared with Figure 6.13a, Figure 6.14a indicates that bias correction has improved the individual performance of each reanalysis dataset by reducing most of

the biases present in the mean of the uncorrected data. In particular, both the magnitude and spatial pattern of the mean annual rainfall of AWAP are better reproduced by the bias corrected reanalyses than uncorrected at each grid point across the site. This improvement in the rainfall magnitudes can clearly be seen in the plots of bias corrected reanalyses rainfall divided by AWAP shown in Figure 6.14b. Most of the ratios ranging from 0.5 to 1.5 suggest that all three reanalyses are able to closely reproduce the rainfall of AWAP with slightly over or underestimating the values. Of all three reanalyses, R1 tends to overestimate the AWAP rainfall more than R2 and R3, which have underestimated rainfall values mostly away from the coastline.

The spatial distribution of the mean annual rainfall of uncorrected reanalyses and AWAP, the ratio of the mean of the uncorrected reanalyses and AWAP and the elevation of all grid points for the Richmond River site is shown in Figure 6.15. In contrast to the Williams River site, reanalyses datasets for the Richmond River site have a spatial pattern which is different to AWAP while having a north-east south-west band of high rainfall through the centre of the site, particularly along the rain shadow of the Great Dividing Range where the elevation varies from medium to high.

The results in Figure 6.13a of the Williams River site showed that there is a positive relationship between the rainfall and elevation. In contrast, this positive relationship between the rainfall and elevation does not appear to be true for all the grid points of AWAP across the Richmond River site which is located in the north coast of NSW.

Rainfall of NARCliM uncorrected reanalyses divided by AWAP for the Richmond River site is shown in Figure 6.15b. The ratio ranging from 0.5 to 3.5 shows that there is a consistency in results between sites, with all the reanalyses are overestimating the rainfall of AWAP. As was seen at the Williams River site, R2 reanalysis appear to reproduce AWAP rainfall closely with ratios ranging from 1 to 1.5 for most of the low elevation grid points. It is also worthwhile to note that there is a slight underestimation of the rainfall along the coast which was also seen at the Williams River site.

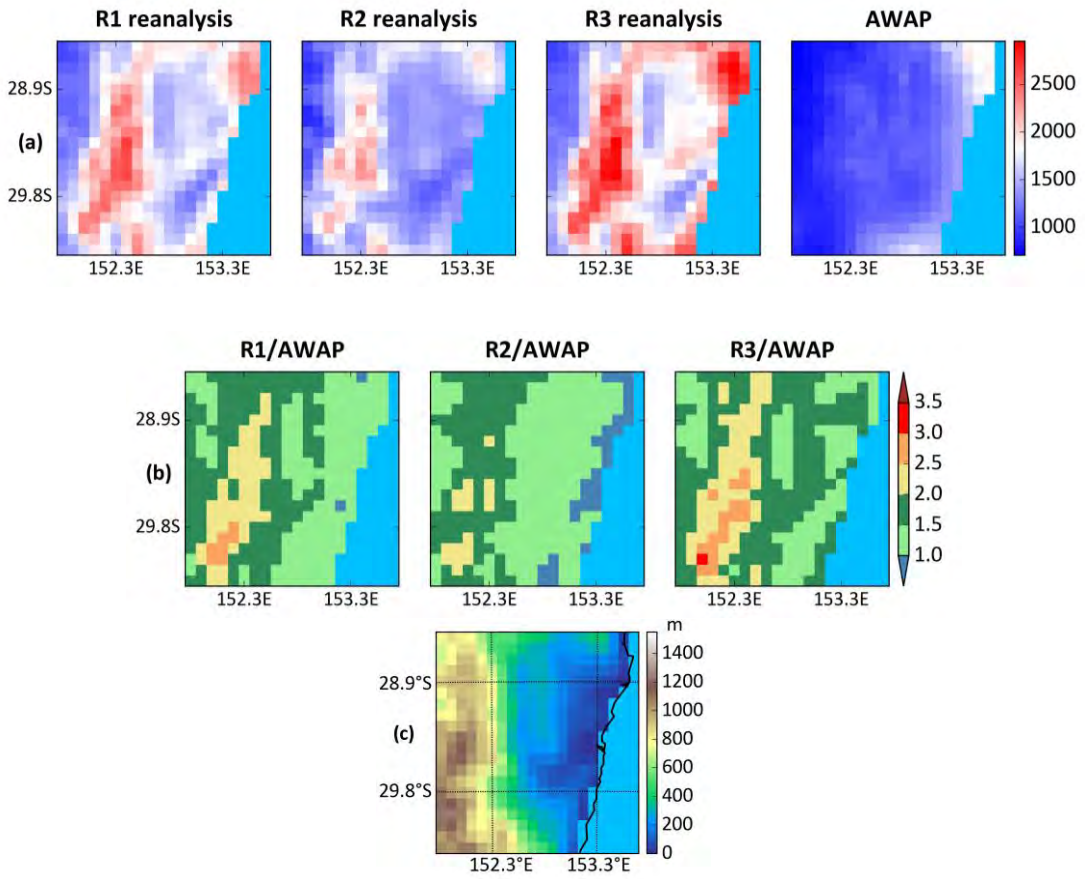

Figure 6.15 Spatial distribution of the mean rainfall – Richmond River site (a) mean annual rainfall of uncorrected reanalyses and AWAP, (b) ratio of the mean annual rainfall of uncorrected reanalyses to AWAP and (c) topography map of the site (as defined and used by NARCliM).

The spatial distribution of the mean annual rainfall of bias corrected reanalyses and AWAP and the ratio of the mean of the bias corrected reanalyses and AWAP for the Richmond River site is shown in Figure 6.16.

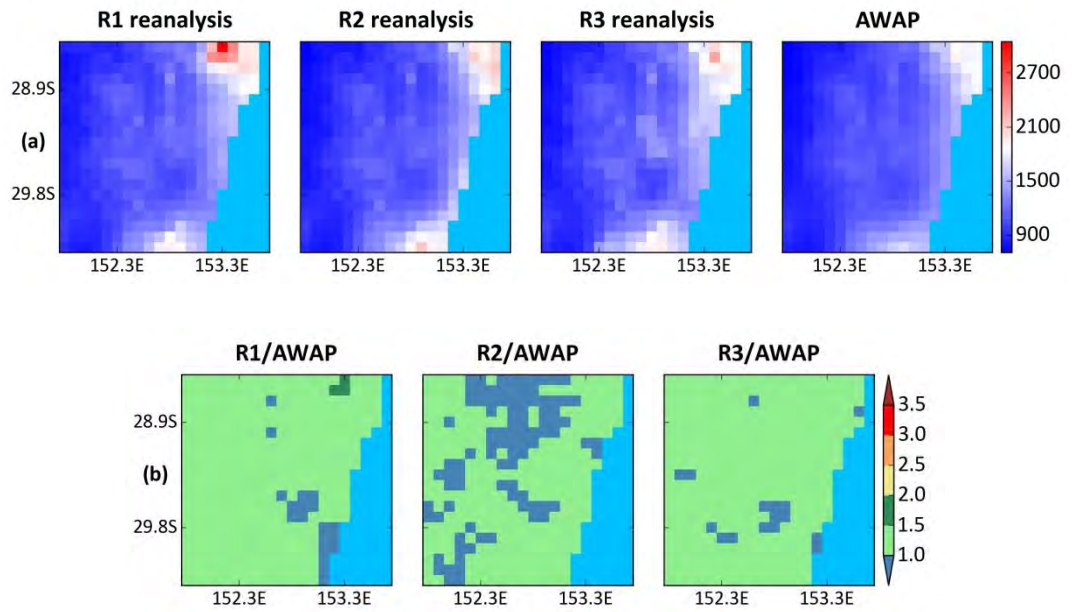

Figure 6.16 Spatial distribution of the mean rainfall – Richmond River site (a) mean annual rainfall of bias corrected reanalyses and AWAP and (b) ratio of the mean annual rainfall of bias corrected reanalyses to AWAP.

As was seen at the Williams River site, there is a significant improvement in the performance of reanalyses by reducing most of the biases present in the uncorrected data at the Richmond River site. Most significantly, the north-east south-west band of enormously high rainfall which was previously seen in the uncorrected reanalysis in Figure 6.15a has been removed after the bias correction. Therefore, this suggests that some of the significant biases which have being introduced in the initial design of NARCliM are most likely to be removed with the applied bias correction at some sites. Additionally, the ratio plots shown in Figure 6.16b suggest that R1 and R3 reanalyses tend to overestimate the rainfall more than R2. However, R1 appear to overestimate the mean rainfall of AWAP at three grid points located at medium to high elevations (400 to 300 m) in the north of the site even after the bias correction. Therefore, in contrast this suggests that NARCliM's bias correction method does not completely remove all the biases at a site, particularly some biases which are being introduced by the topography.

Similarly, the spatial distribution of the mean annual rainfall of uncorrected and bias corrected reanalyses, and AWAP, the ratio of the mean of the uncorrected and bias corrected reanalyses, and AWAP for the Bega River and Sydney sites are shown in Figures 6.17 to 6.20.

It should be noted that the sky blue grid points within the sites in Figures 6.18 and 6.20 are the large water bodies with undefined rainfalls. Because in the bias-correction process, grid points containing large water bodies at Bega River and Sydney sites were not calculated (i.e. the rainfall was undefined). There are three grid points at the Bega River sites and four grid points for the Sydney sites with undefined rainfall. This is in contrast to the uncorrected simulation where the rainfall for these pixels was simulated (Figures 6.17 and 6.19).

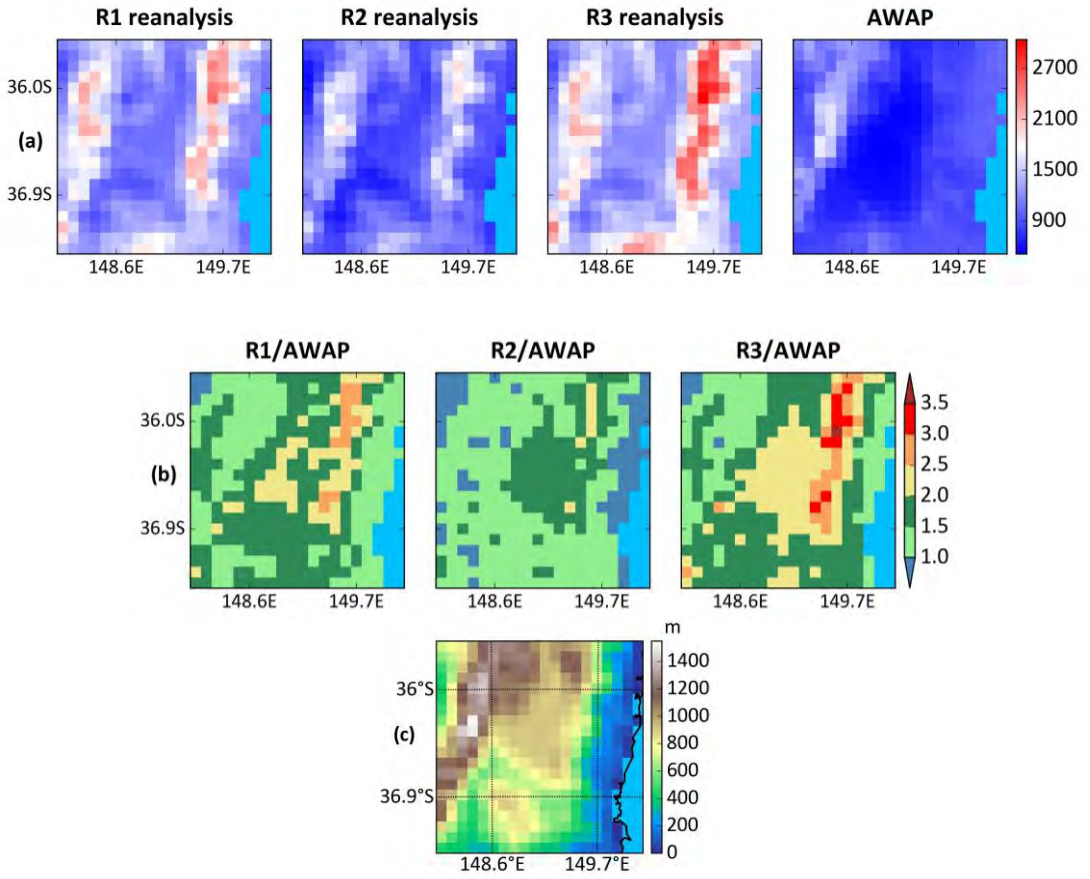

Figure 6.17 Spatial distribution of the mean rainfall – Bega River site (a) mean annual rainfall of uncorrected reanalyses and AWAP, (b) ratio of the mean annual rainfall of uncorrected reanalyses to AWAP and (c) topography map of the site (as defined and used by NARCliM).

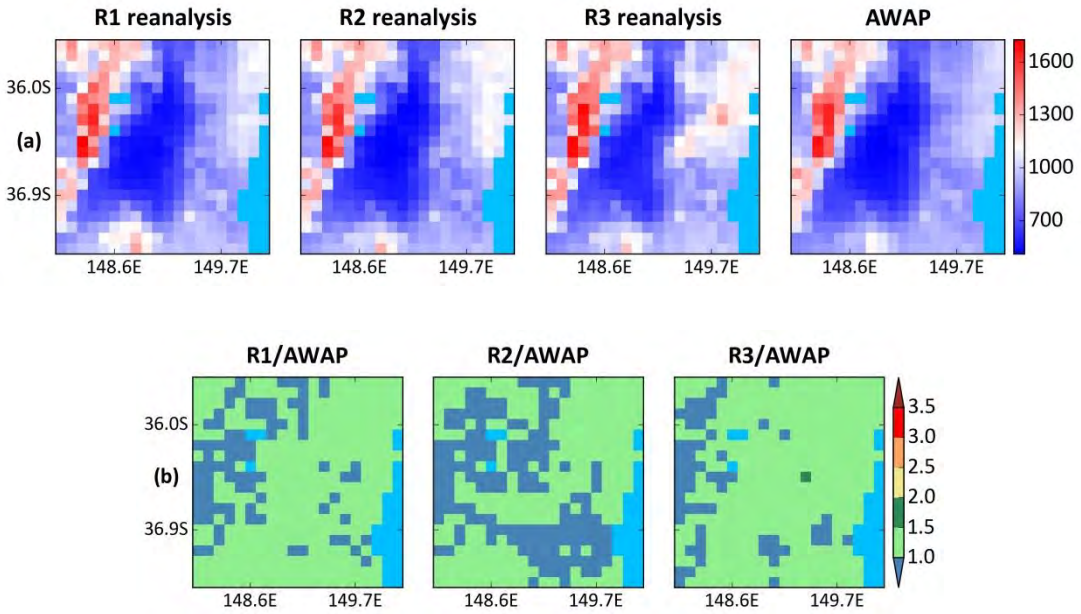

Figure 6.18 Spatial distribution of the mean rainfall – Bega River site (a) mean annual rainfall of bias corrected reanalyses and AWAP and (b) ratio of the mean annual rainfall of bias corrected reanalyses to AWAP.

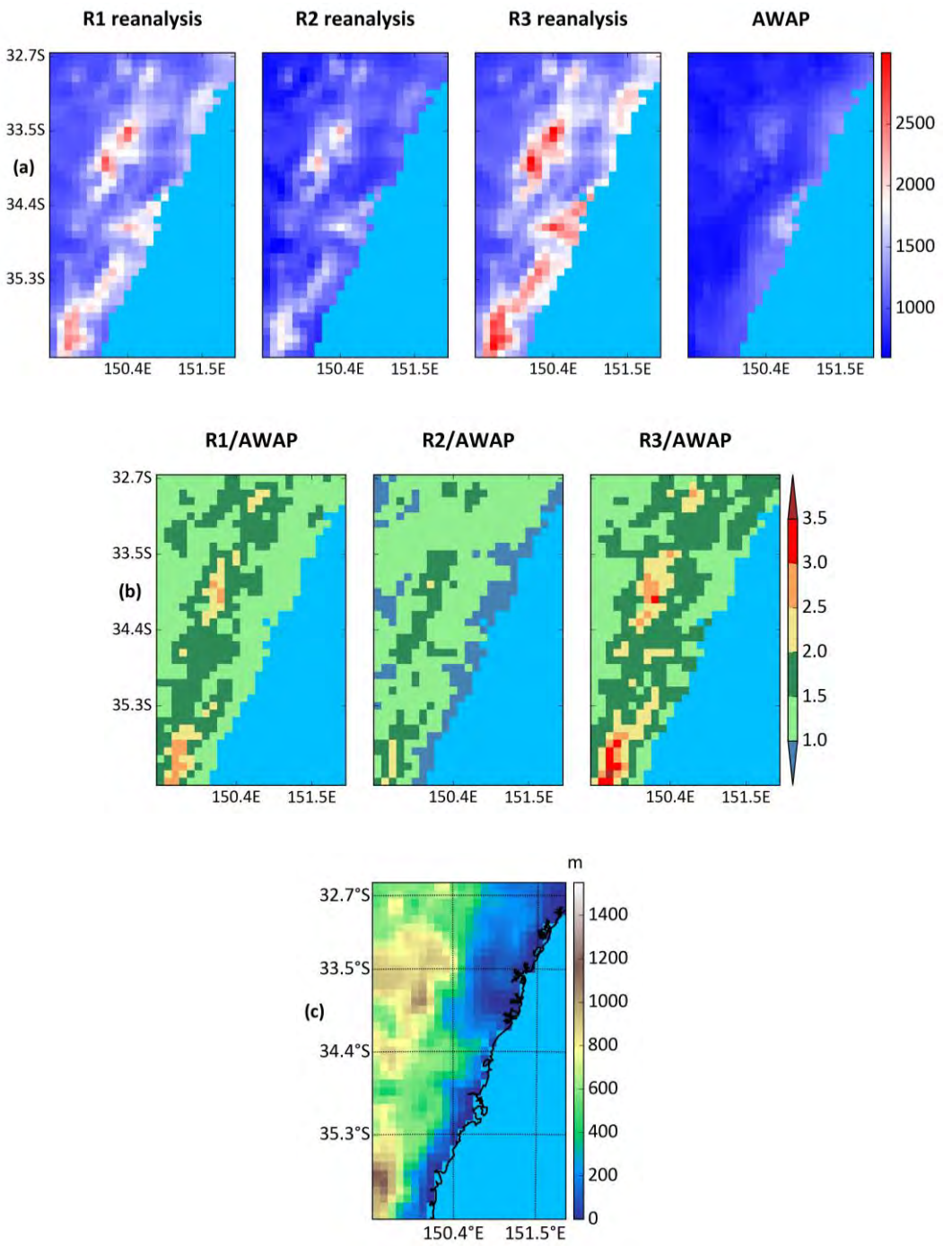

Figure 6.19 Spatial distribution of the mean rainfall – Sydney site (a) mean annual rainfall of uncorrected reanalyses and AWAP, (b) ratio of the mean annual rainfall of uncorrected reanalyses to AWAP and (c) topography map of the site (as defined and used by NARCliM).

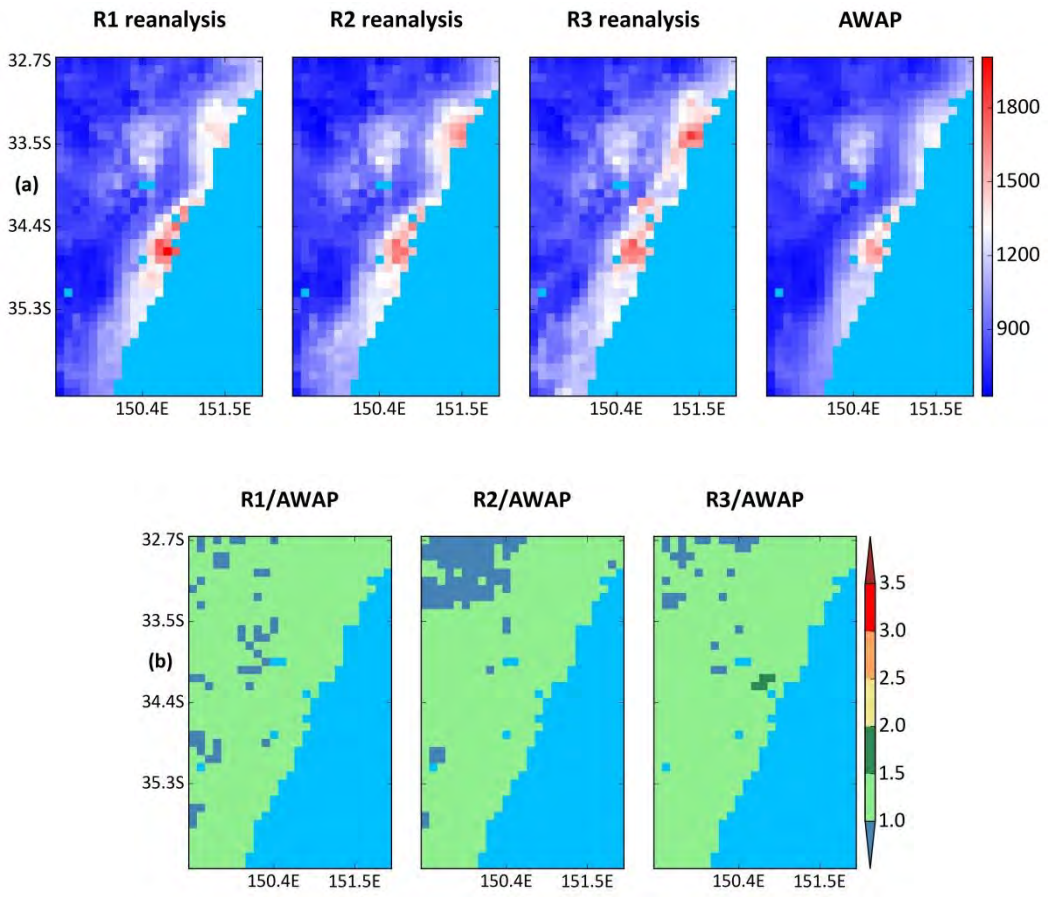

Figure 6.20 Spatial distribution of the mean rainfall – Sydney site (a) mean annual rainfall of bias corrected reanalyses and AWAP and (b) ratio of the mean annual rainfall of bias corrected reanalyses to AWAP.

As was seen at the Merriwa site in Chapter 5 and the Williams River site, there is a positive relationship between the AWAP rainfall and the elevation for all grid points of Bega River and Sydney sites. This suggests that the positive relationship between the rainfall and elevation is true for all sites, except for the Richmond River which is located at the northern part of the broader east coast. The ratio between the uncorrected reanalysis and AWAP rainfall ranging from 0.5 to 4.0 for Bega River and Sydney sites also shows similar trends of all reanalyses overestimating the AWAP rainfall, with uncorrected R2 reanalysis better simulating the rainfall of AWAP at all sites.

Overall, uncorrected R2 reanalysis has rainfall most similar to AWAP showing a ratio varying from 0.5 to 1.5 for over 60% of the grid points of each site. At low elevations of the Williams River, Richmond River and Sydney sites, the ratio of the mean rainfall of R2 and AWAP is close to 1, but still overestimates the rainfall at

higher elevations. In contrast, this effect of having ratios lower than 1.5 at low elevations cannot be seen in the Bega River site. Further, R2 uncorrected reanalysis tends to underestimate the AWAP rainfall for all sites mostly along the coast and at few other grid points inland.

Figures 6.18 and 6.20 generated using the bias corrected reanalyses indicate that there is a consistency between the performances of the bias corrected datasets between the sites. As was seen earlier, all bias corrected reanalyses are able to reproduce both the magnitude and the spatial pattern of AWAP of Bega River and Sydney sites. In particular, at the Bega River site, all reanalyses mirror the spatial pattern in AWAP mean rainfall. This is likely due to the use of AWAP data for the bias correction process (see Section 2.6.3 for more details on NARCliM bias correction). The ratio between bias corrected reanalyses and AWAP mean rainfall at Bega River and Sydney site also varies from 0.5 to 1.5, and suggests that reanalyses slightly under or overestimate the mean rainfall of AWAP at all sites. R1 and R3 reanalyses tends to overestimate the AWAP mean rainfall slightly more than R2 at all sites, except at Bega River where all three reanalyses have approximately equal tendency of either under or overestimating the means at grid points.

For all four sites, AWAP and reanalyses data show a band of high rainfall values along the coast to the coastal side of the escarpment which seems to be unrelated to the topography and appears to be consistent for each dataset. Further, this band can also be seen in the bias corrected reanalyses, particularly in R2 and R3 reanalyses along the coast of the Sydney site (Figure 6.20). This indicates how ocean interactions have influenced the mean rainfall distribution along the coastline of NSW. The extent of these influences on rainfall caused by the ocean will be further discussed in Chapter 8.

6.3.2 Coefficient of variation of the rainfall

The coefficient of variation (C_v, the ratio of standard deviation to mean) was also calculated for each grid point of all four sites at daily, fortnightly, monthly and annual time resolutions. The spatial distribution of the C_v of uncorrected reanalyses and AWAP for the Williams River site is shown by Figure 6.21.

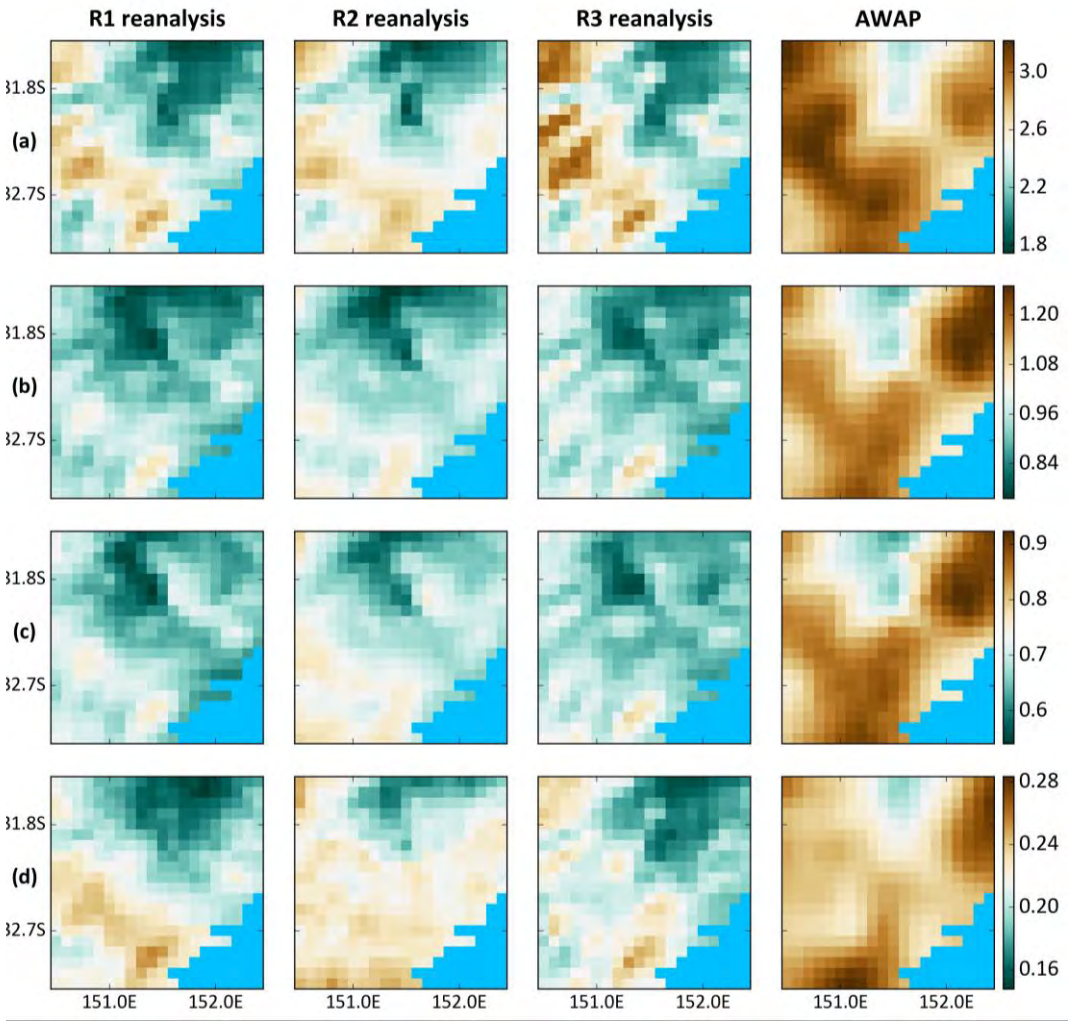

Figure 6.21 Spatial distribution of C_v of uncorrected rainfall - Williams River site: (a) day, (b) fortnight, (c) month and (d) annual.

The high C_v values ranging from 1.8 to 4 shown in Figure 6.21a indicate that the rainfall is highly variable at daily resolution compared with other longer time resolutions. As was seen at the Merriwa site in Section 5.1.3 the rainfall is less variable in high elevation areas while low elevations often have a high rainfall variability. Further, as for the mean annual rainfall, this variability measured by C_v

suggests that the rainfall variability is also influenced by the topography. However, the relationship between C_v of the rainfall and topography is negative, whereas the mean rainfall had a positive relationship with elevations. The C_v of reanalyses also follow a spatial pattern similar to AWAP, but tend to underestimate across the site.

Given that there is a tendency for NARCliM uncorrected reanalyses to underestimate the C_v of the AWAP rainfall, a quantitative assessment of the under or overestimation is needed. Therefore, the ratios of C_v of uncorrected reanalyses and AWAP was also calculated and shown by Figure 6.22.

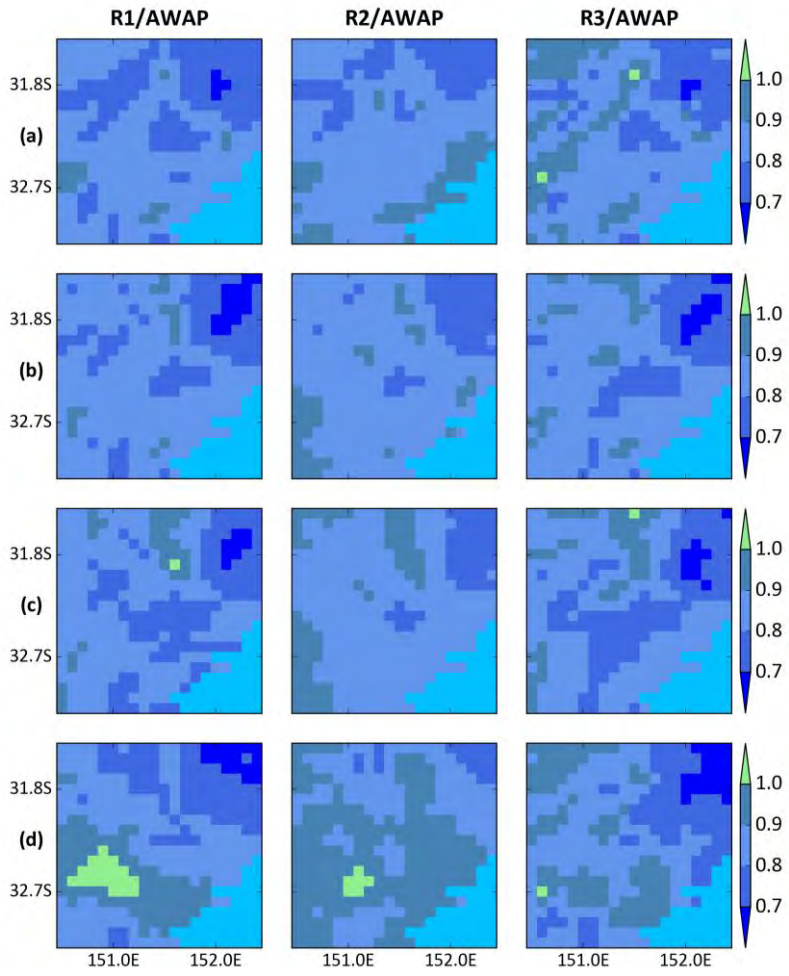

Figure 6.22 Ratio of C_v of uncorrected reanalyses to AWAP rainfall - Williams River site: (a) day, (b) fortnight, (c) month and (d) annual.

The ratios of C_v range from 0.6 to 1.1 across the site. This is a significant improvement in comparison with the mean annual rainfall, which had ratios varying

from 0.5 to 3.5 for the uncorrected reanalyses. The ratio of C_v ranging from 1 to 1.1 shows that the reanalyses tend to slightly overestimate the magnitudes. Compared with R1 and R3, R2 has closely simulated the C_v of the AWAP rainfall at the Williams River site.

The spatial distribution of the C_v of bias corrected reanalyses and AWAP for the Williams River site is shown by Figure 6.23.

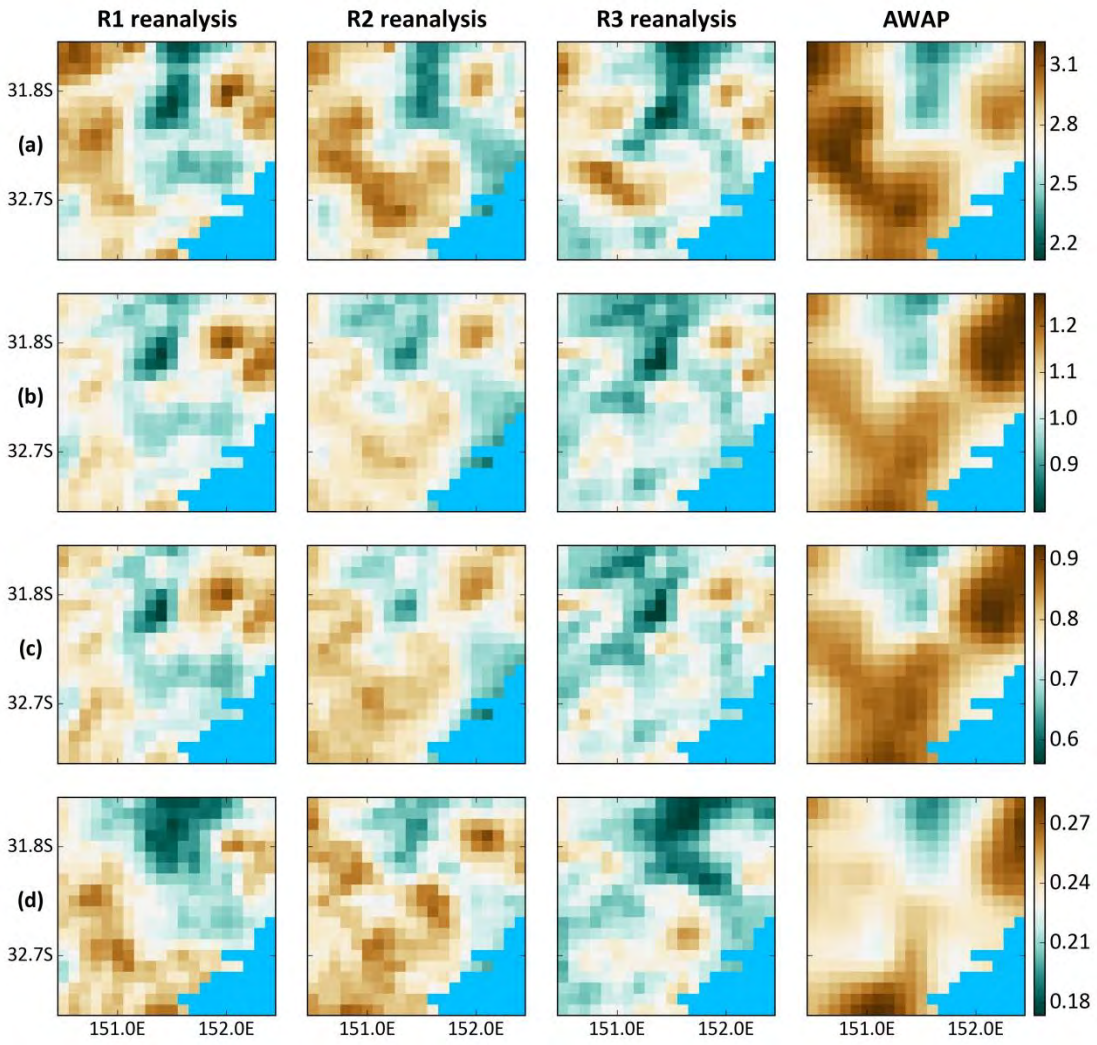

Figure 6.23 Spatial distribution of C_v of bias corrected reanalyses and AWAP rainfall - Williams River site: (a) day, (b) fortnight, (c) month and (d) annual.

Figure 6.23 indicates that most of the underestimated C_v values at individual grid points across the site have been corrected after the bias correction. The bias corrected R1 and R2 reanalyses tend to better produce both magnitude and the

spatial pattern in AWAP for all time resolutions than they did for uncorrected. In contrast, R3 reanalysis has the least improvement in capturing the C_v of AWAP.

The ratios for the C_v of bias corrected reanalyses and AWAP are shown by Figure 6.24. With bias correction, most of the underestimated C_v values of reanalyses have been corrected. In particular, this is clearly seen in R1 and R2 reanalyses which have ratios ranging from 0.8 to 1.1. Comparing number of grid points which have magnitudes of C_v close to AWAP (0.9 to 1.1), the bias corrected R2 appears to better reproduce the C_v of AWAP than R3 for all time resolutions.

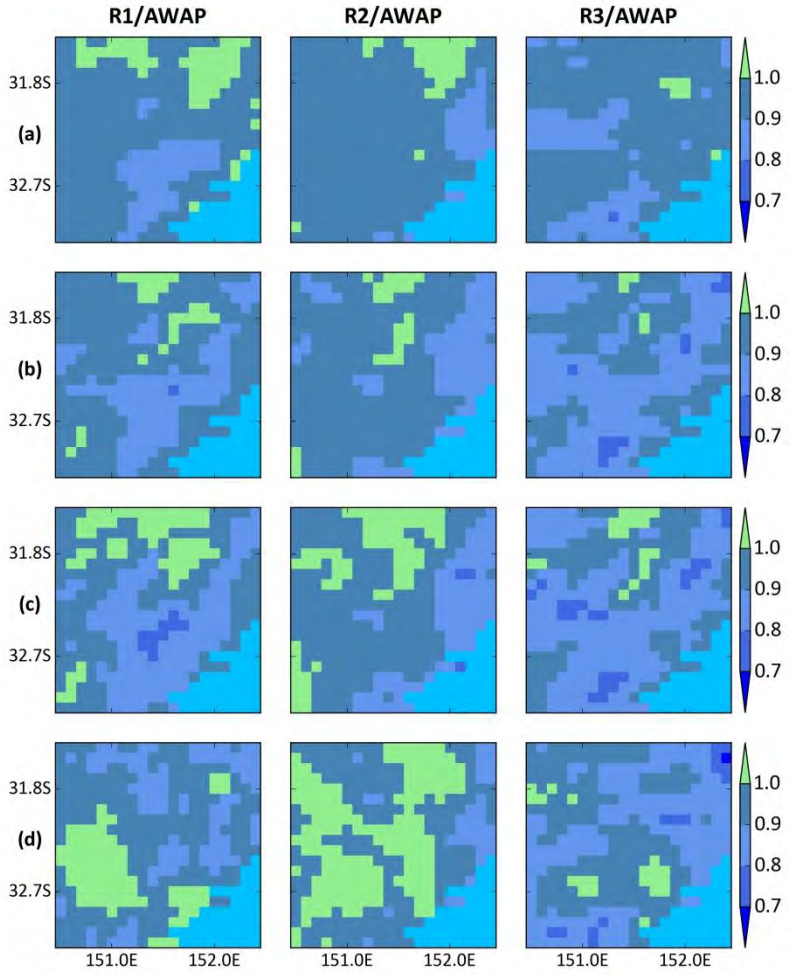

Figure 6.24 Ratio of C_v of bias corrected reanalyses to AWAP rainfall - Williams River site: (a) day, (b) fortnight, (c) month and (d) annual.

The spatial distribution of the C_v and the ratio of C_v of uncorrected reanalyses and AWAP for the Richmond River site are shown in Figures 6.25 and 6.26. The results are consistent with the Williams River site, all reanalyses tending to underestimate the C_v of AWAP at the Richmond River site for all time resolutions. Of all the

reanalyses, R3, particularly at the daily time resolution appears to most closely reproduce the C_v of AWAP.

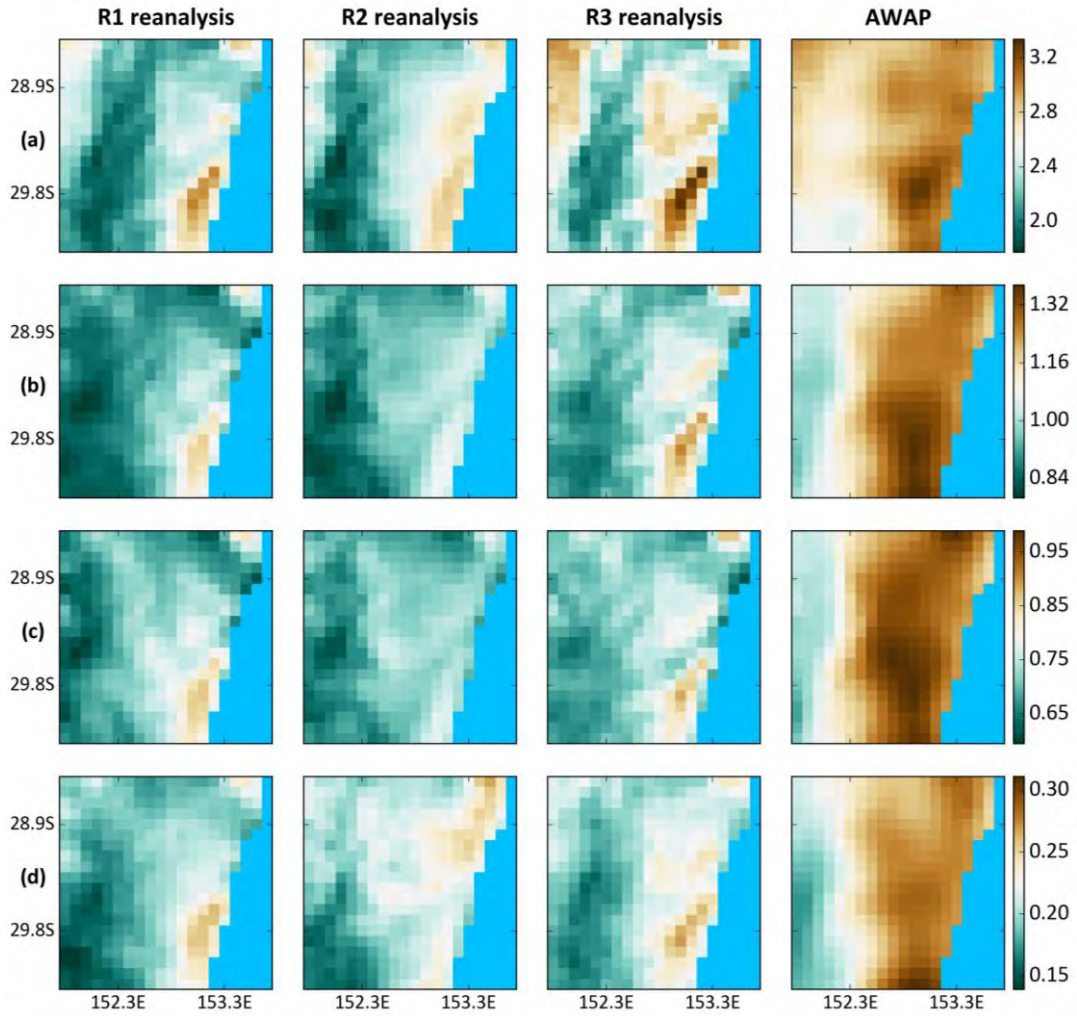

Figure 6.25 Spatial distribution of C_v of uncorrected reanalysis and AWAP rainfall - Richmond River site: (a) day, (b) fortnight, (c) month and (d) annual.

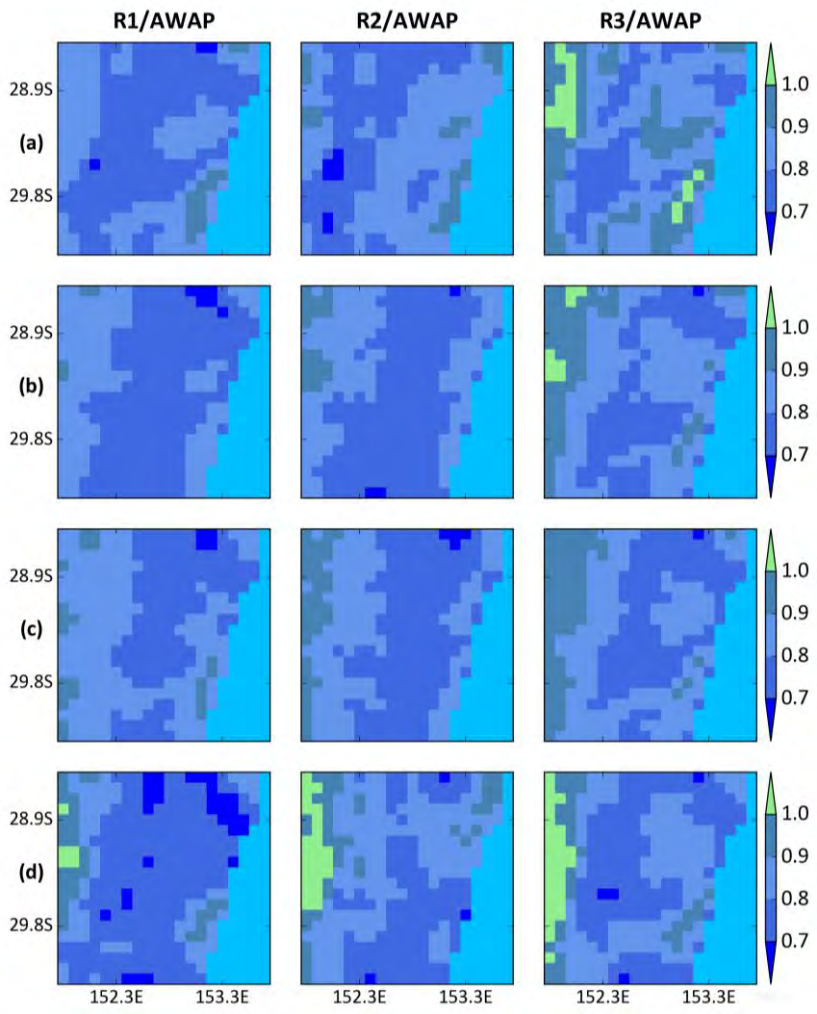

Figure 6.26 Ratio of C_v of uncorrected reanalyses to AWAP rainfall - Richmond River site: (a) day, (b) fortnight, (c) month and (d) annual.

The spatial distribution of the C_v and the ratio of C_v of bias corrected reanalyses to AWAP for the Richmond River site are shown in Figures 6.27 and 6.28. With the bias correction, R1 and R2 are improved. However, the improvement in capturing the C_v of AWAP is relatively less at the Richmond River site for all time resolutions relative to Williams River site. In particular, R1 reanalysis has a C_v close to AWAP at the low elevation grid points for all time resolutions, yet the overall spatial pattern in the C_v does not match with that of the AWAP. In contrast, R2 reanalysis appears to better capture the C_v of AWAP, particularly for high elevations, yet underestimates the C_v values at low elevations. This effect can clearly be seen for both fortnight and monthly time resolutions (Figures 6.28b and 6.28c).

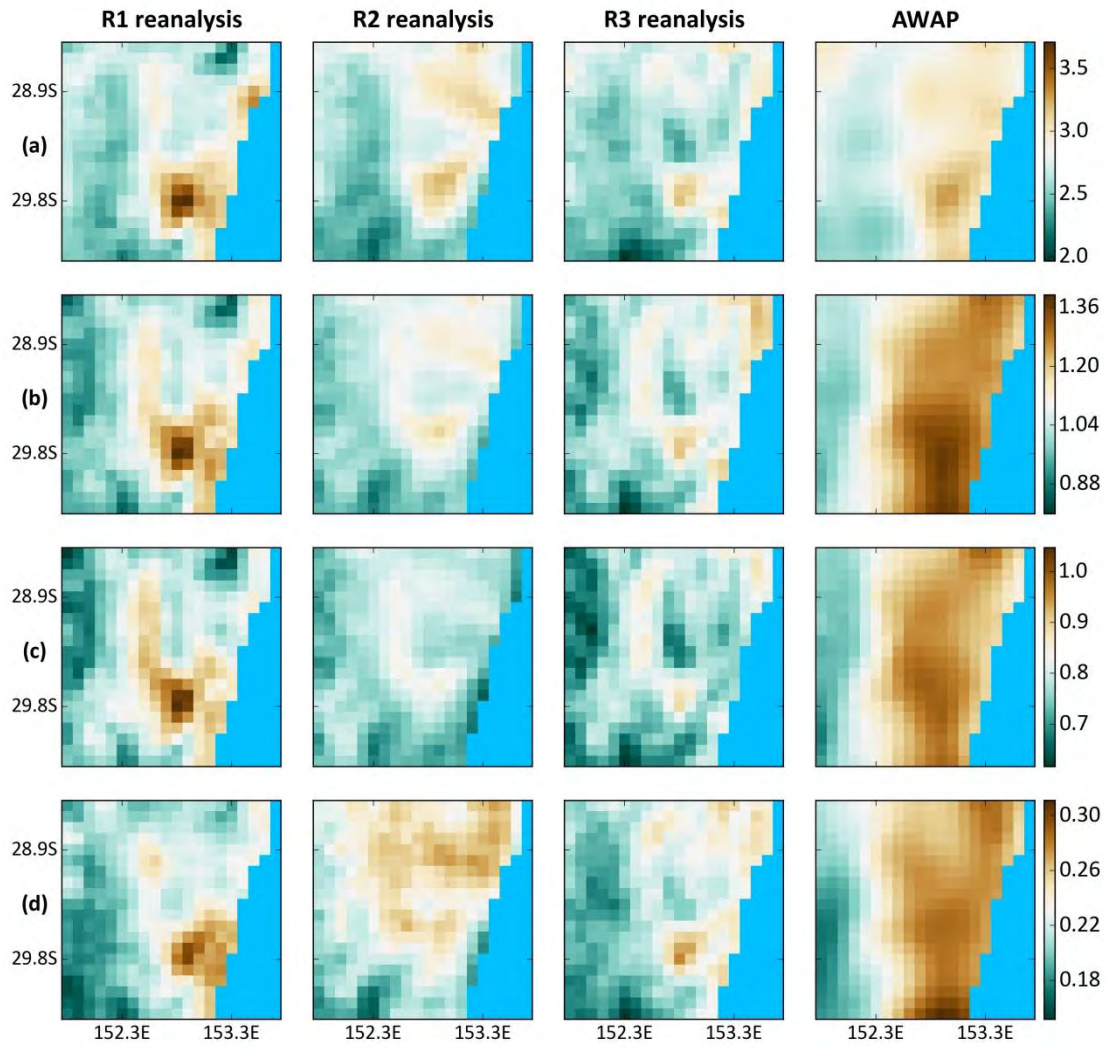

Figure 6.27 Spatial distribution of C_v of bias corrected reanalysis and AWAP rainfall - Richmond River site: (a) day, (b) fortnight, (c) month and (d) annual.

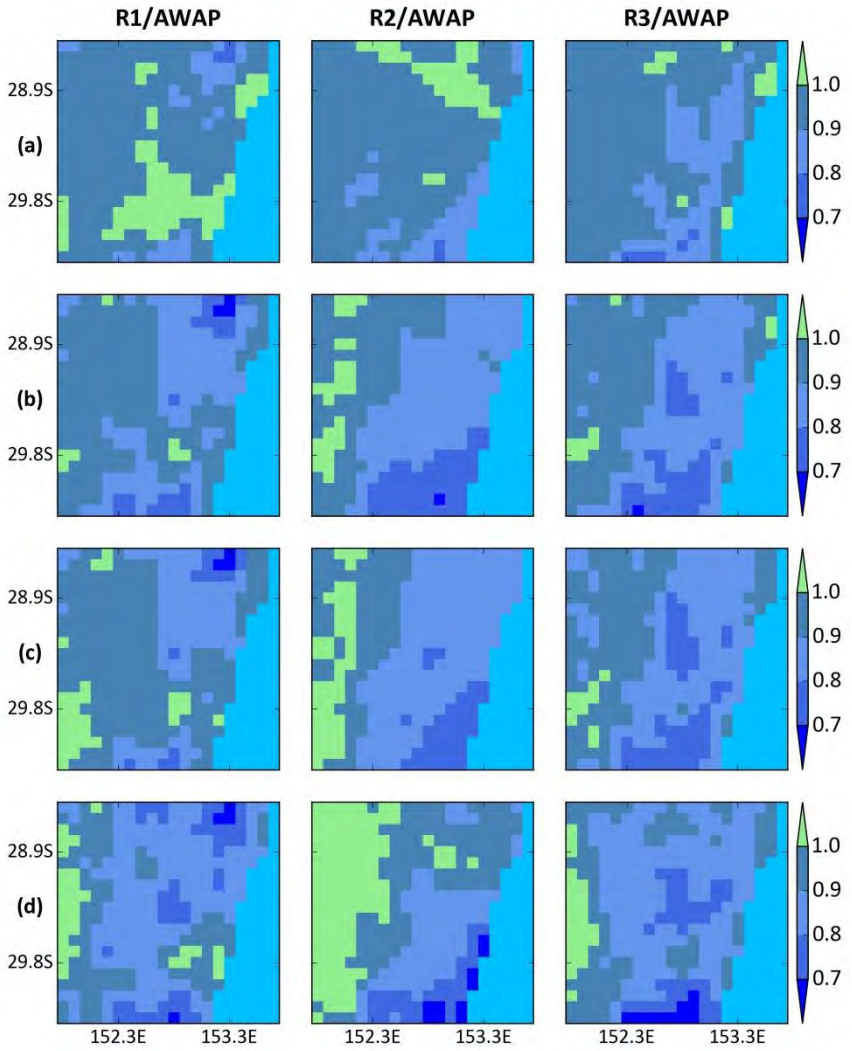

Figure 6.28 Ratio of C_v of bias corrected reanalyses to AWAP rainfall - Richmond River site: (a) day, (b) fortnight, (c) month and (d) annual.

The spatial distribution of the C_v and the ratio of C_v of uncorrected and bias corrected reanalyses, and AWAP for the Bega River and Sydney sites are shown by Figures 6.29 to 6.36 respectively.

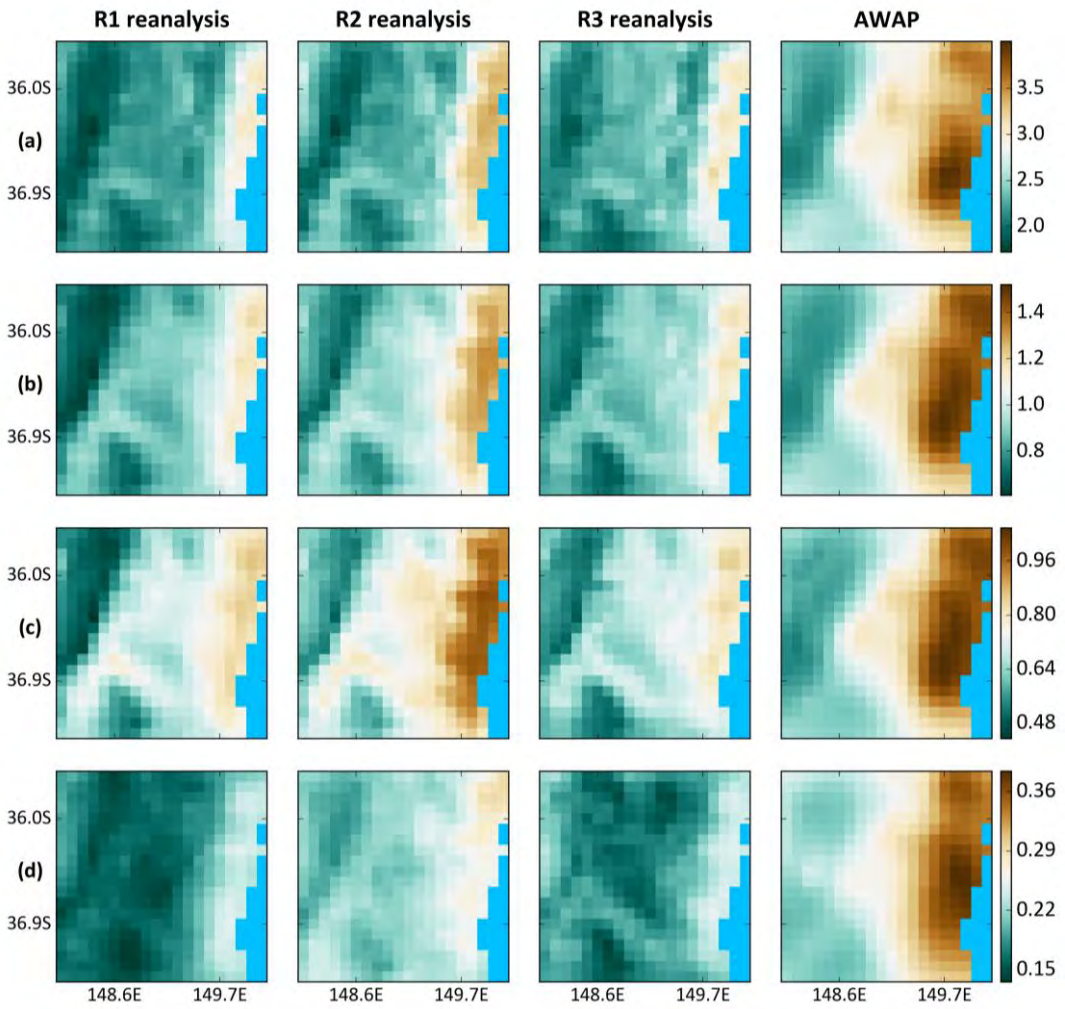

Figure 6.29 Spatial distribution of C_v of uncorrected reanalysis and AWAP rainfall - Bega River site: (a) day, (b) fortnight, (c) month and (d) annual.

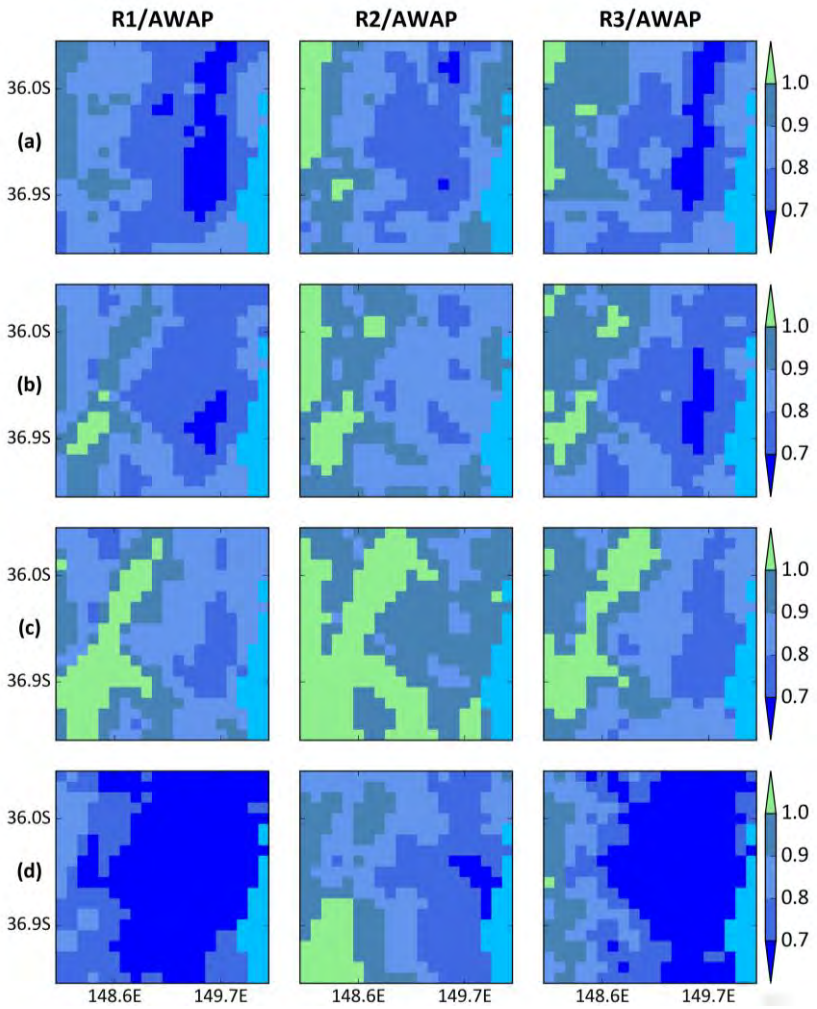

Figure 6.30 Ratio of C_v of uncorrected reanalyses to AWAP rainfall - Bega River site: (a) day, (b) fortnight, (c) month and (d) annual.

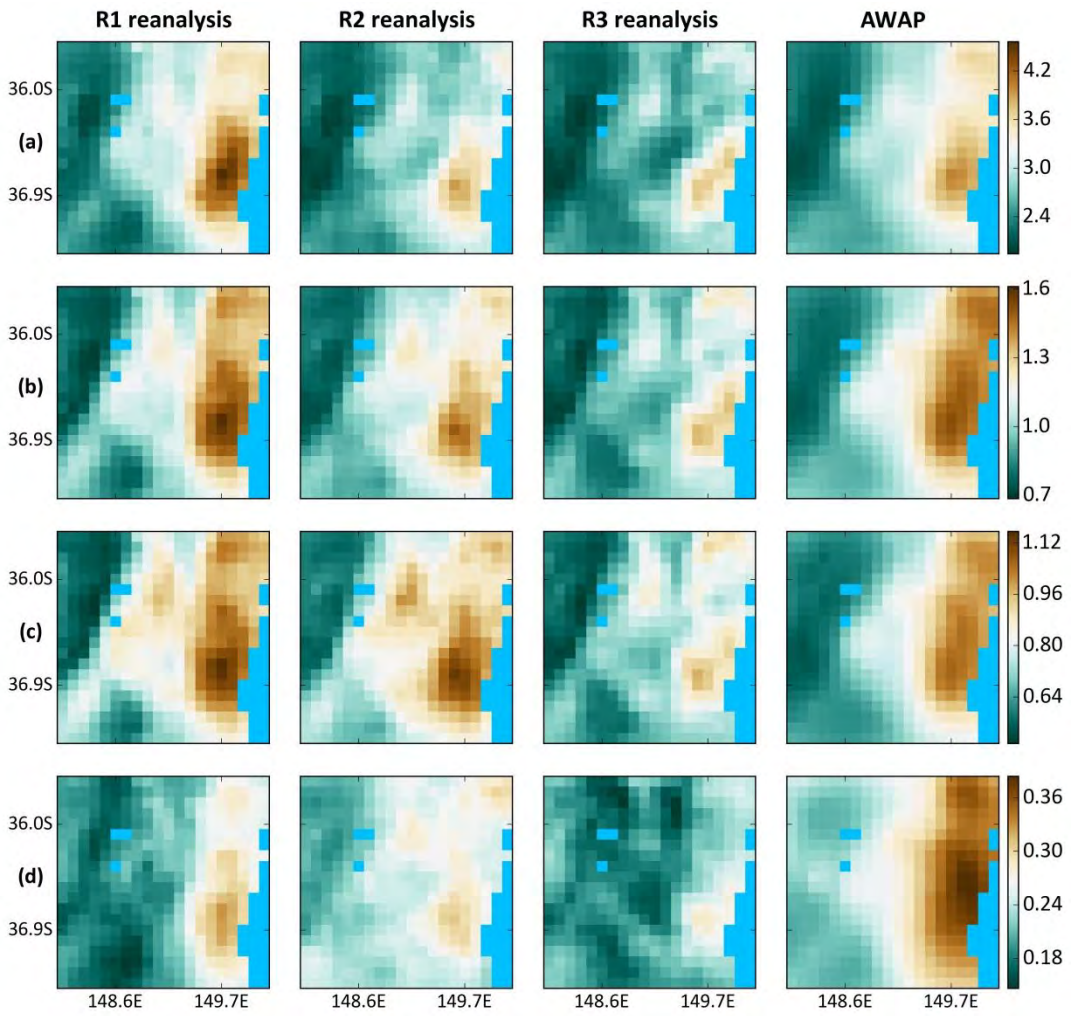

Figure 6.31 Spatial distribution of C_v of bias corrected reanalysis and AWAP rainfall - Bega River site: (a) day, (b) fortnight, (c) month and (d) annual.

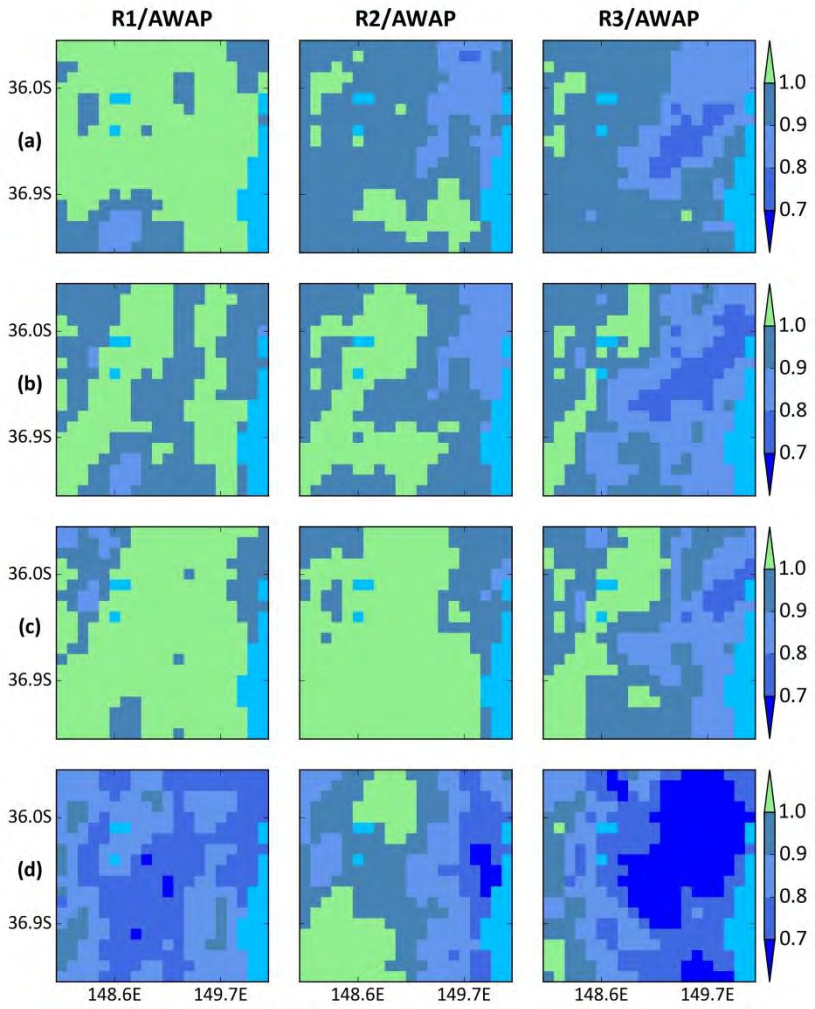

Figure 6.32 Ratio of C_v of bias corrected reanalyses to AWAP rainfall - Bega River site: (a) day, (b) fortnight, (c) month and (d) annual.

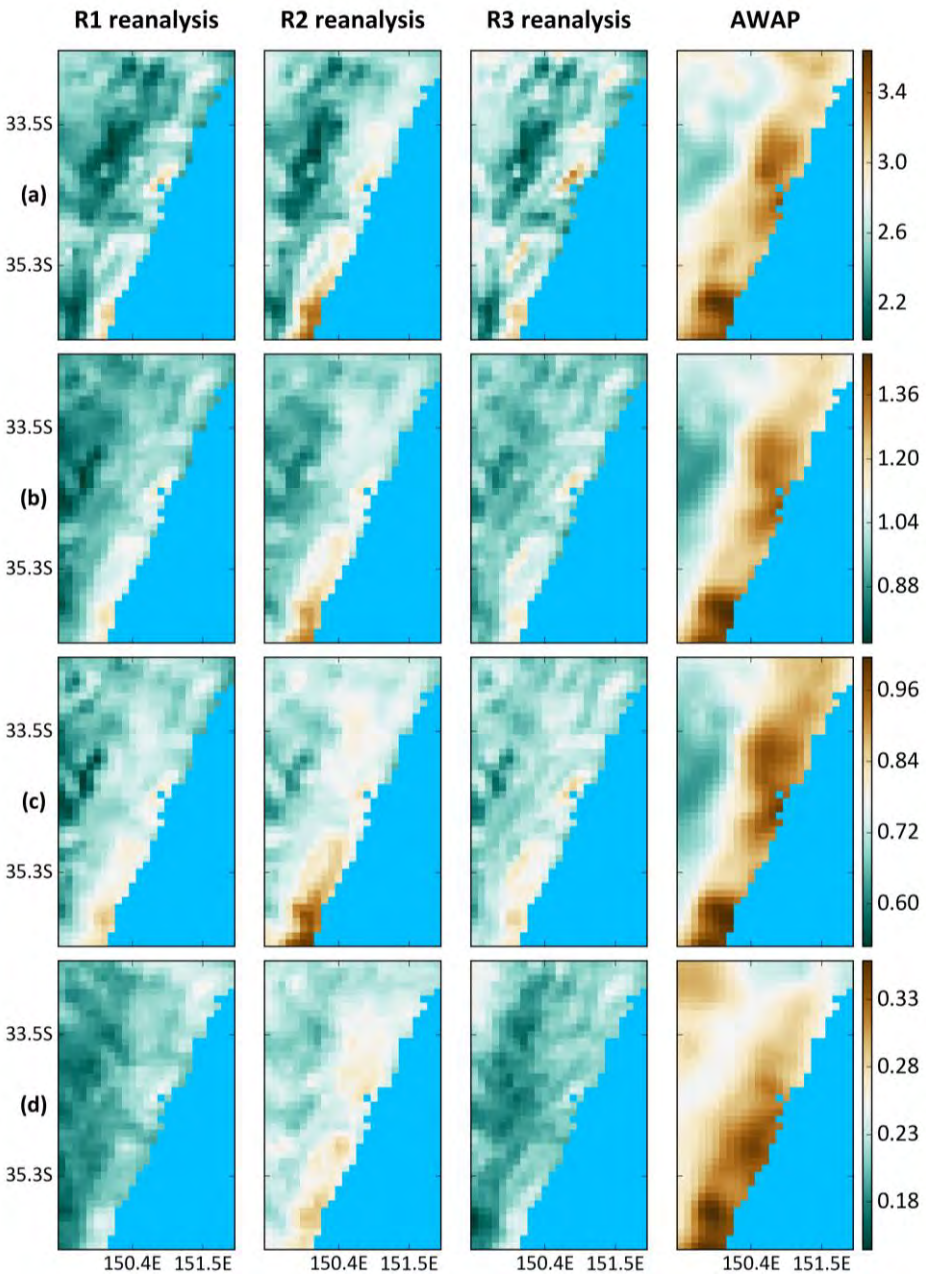

Figure 6.33 Spatial distribution of C_v of uncorrected reanalysis and AWAP rainfall - Sydney site: (a) day, (b) fortnight, (c) month and (d) annual.

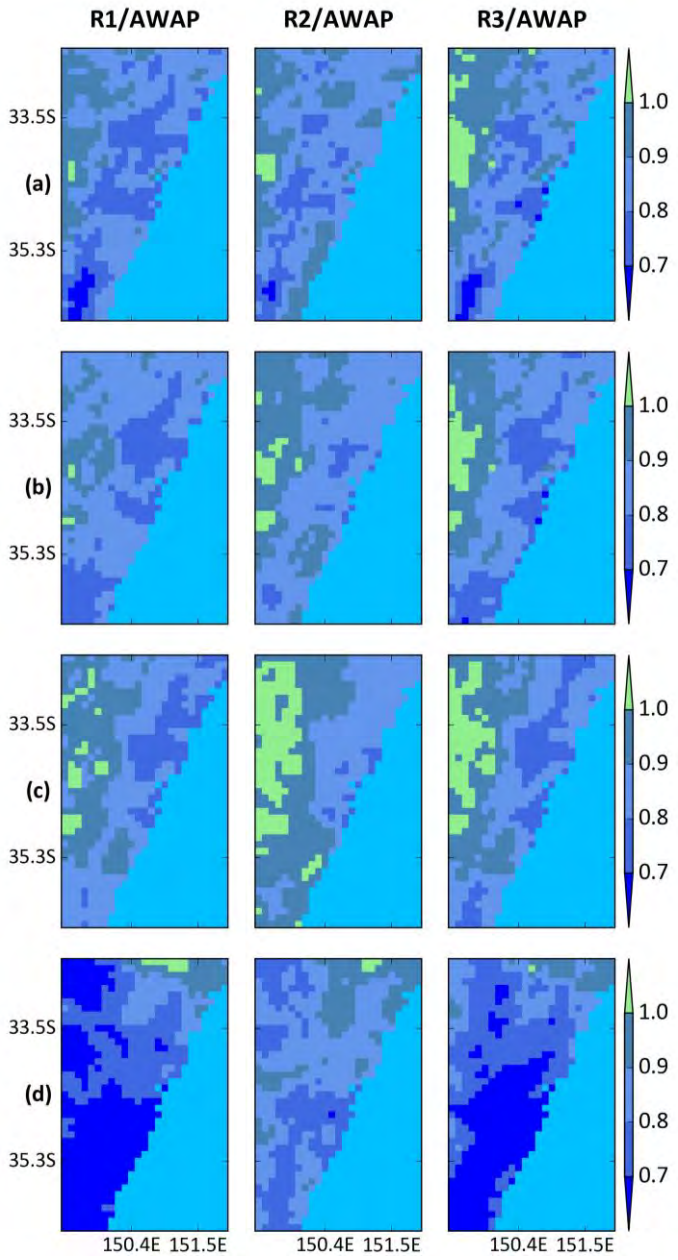

Figure 6.34 Ratio of C_v of uncorrected reanalyses to AWAP rainfall - Sydney site: (a) day, (b) fortnight, (c) month and (d) annual.

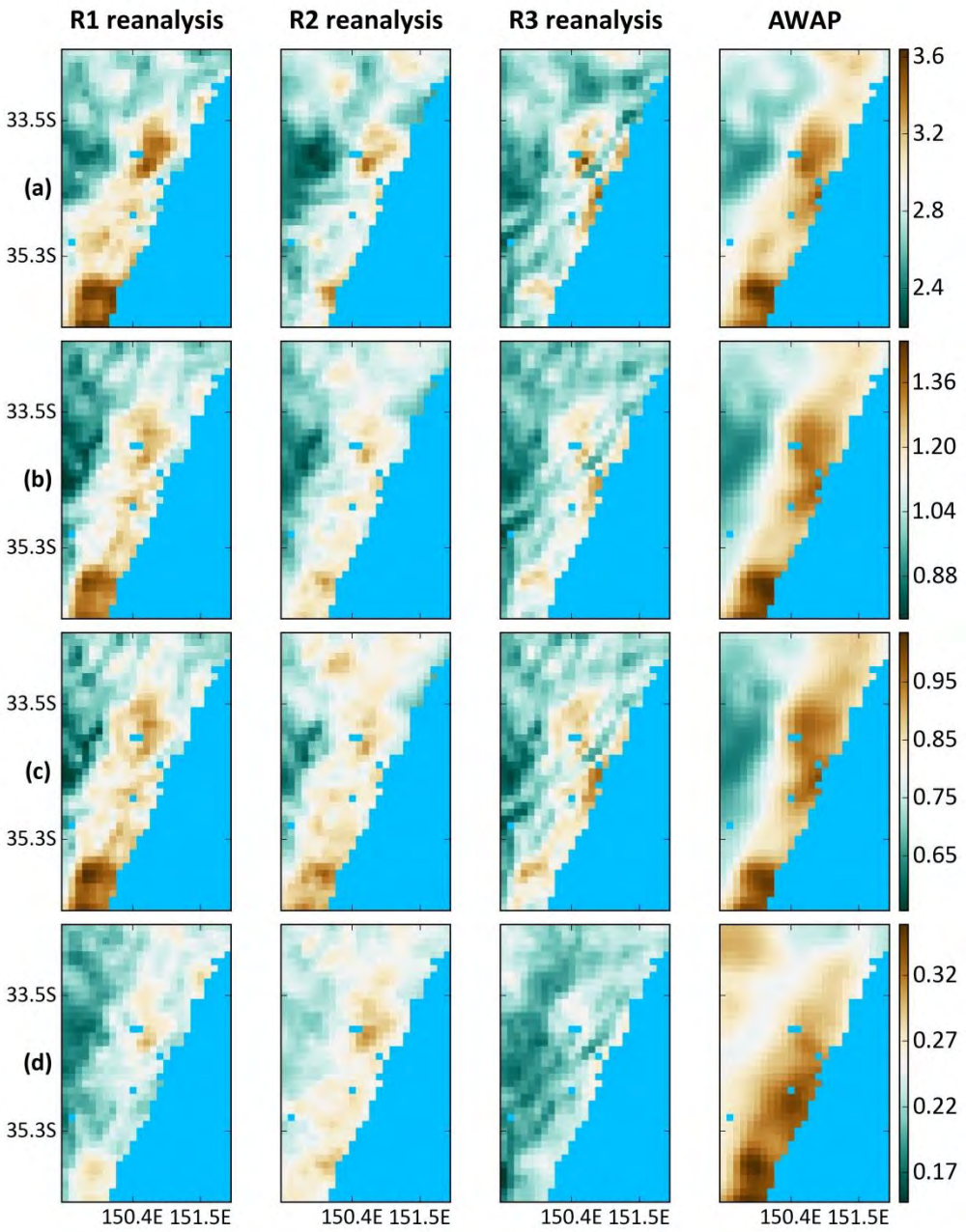

Figure 6.35 Spatial distribution of C_v of bias corrected reanalysis and AWAP rainfall - Sydney site: (a) day, (b) fortnight, (c) month and (d) annual.

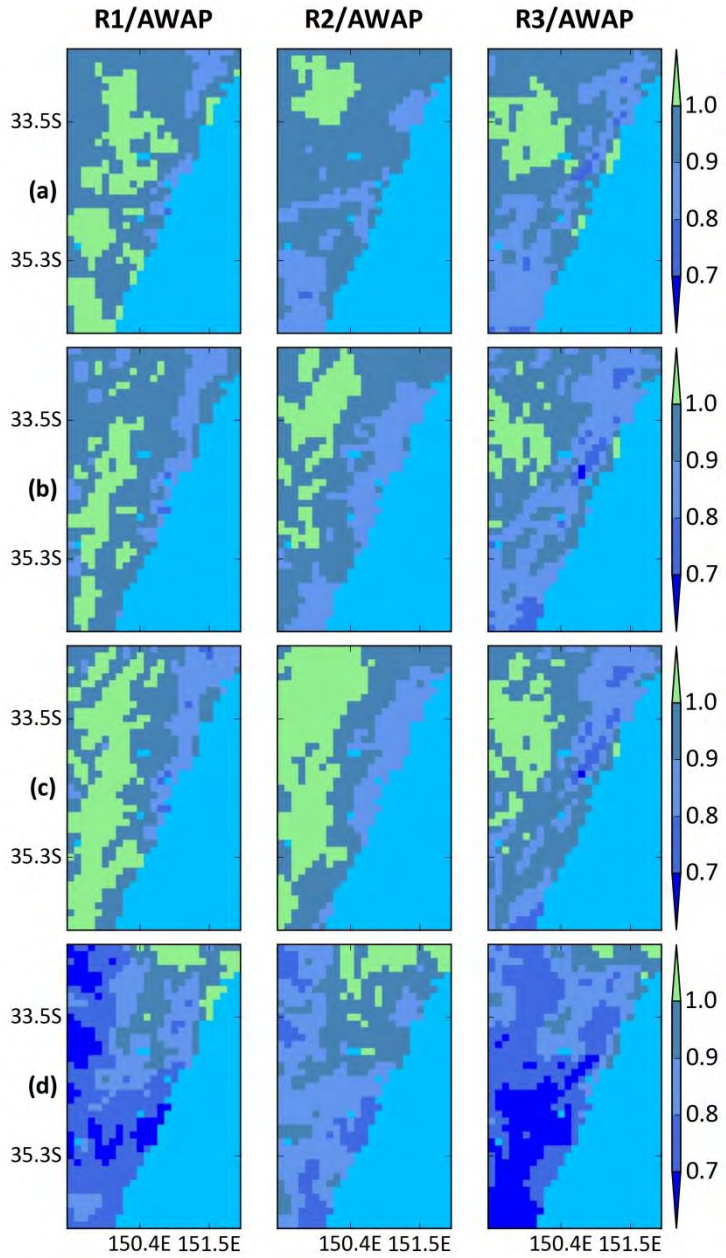

Figure 6.36 Ratio of C_v of bias corrected reanalyses to AWAP rainfall - Sydney site: (a) day, (b) fortnight, (c) month and (d) annual.

Comparing all sites, bias corrected rainfall fits AWAP rainfall better than uncorrected data for rainfall variability (i.e. coefficient of variation, C_v). However at the Richmond River site, R3 the uncorrected reanalysis simulates the C_v of AWAP better than the corrected while having some isolated overestimated values to the west along the Great Dividing Range. The R1 and R3 uncorrected reanalyses have spatial patterns most similar to each other for all sites. Compared with other two sites, Bega River site shows high rainfall variability for all datasets for all time resolutions.

For the Bega River and Sydney sites, R2 has the C_v values most similar to AWAP, particularly for the monthly resolution with varying C_v ratio from 0.9 to 1.1. However, compared with monthly there is a significant underestimation of the C_v for other three time resolutions, particularly for annual showing some large regions of low C_v values (C_v <0.7). This will likely have implications for low estimates of long term variability of reservoir volumes in Sydney and Bega sites because they are driven by the variability of the long term resolution of the dataset. This can clearly be seen in Bega River and Sydney sites. Overall, comparing all three reanalyses, it appears that R2 uncorrected reanalysis better simulates the C_v of AWAP than uncorrected R1 and R3.

With the bias correction, R1 and R2 reanalyses have more improved results than uncorrected reanalyses for all sites. The ratios between bias corrected reanalysis and AWAP ranging from 0.8 to 1.1 suggest that most of the underestimated C_v values of uncorrected reanalyses have been corrected with the applied bias correction for all sites. However, this improvement is most significant only for daily, fortnightly and monthly resolutions.

Comparing the results for different time resolutions there is a general tendency for sub-annual uncorrected data to overestimate the C_v but for the annual results to underestimate it. This is consistent with results that will be shown in Section 6.4 which show that the NARCliM reanalyses have a significantly higher annual autocorrelation than AWAP.

6.3.3 Lag-1 autocorrelation of the rainfall

The spatial distribution of the lag-1 correlation of the rainfall of uncorrected NARCliM reanalyses and AWAP for the Williams River site is shown in Figure 6.37. As in Chapter 5, daily autocorrelations were not used due to the large number of days with zero rainfall.

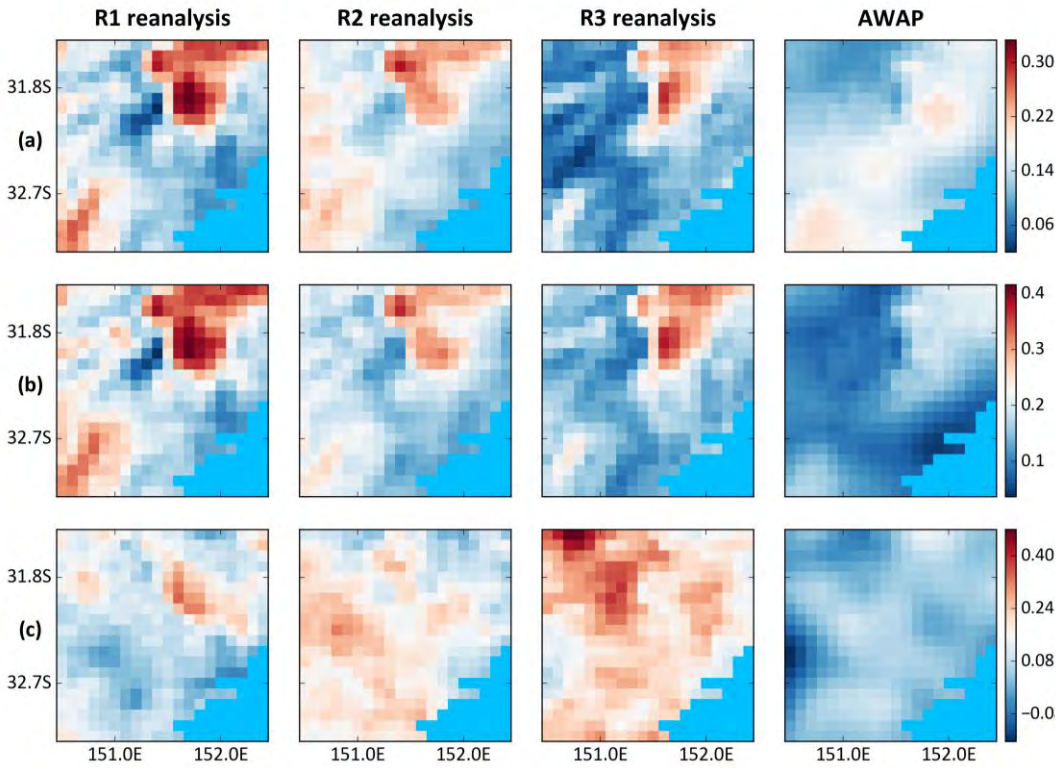

Figure 6.37 Spatial distribution of lag-1 correlation of uncorrected reanalysis and AWAP rainfall – Williams River site: (a) fortnight, (b) month and (c) annual.

The spatial patterns of lag-1 correlation of R1, R2 and R3 reanalyses are similar and mirror the mean annual rainfall pattern shown in Figure 6.13a for all time resolutions, except for the annual. In contrast to the lag-1 correlations of Merriwa site presented in Chapter 5, there is a similarity of the spatial pattern of reanalyses and AWAP at the monthly time resolution. As for the lag-1 autocorrelations shown in Figure 5.15 for the Merriwa site (in Chapter 5), the annual AWAP data again shows regions of negative lag-1 autocorrelations.

The magnitude of R3 appears to closely reproduce the lag-1 autocorrelations of monthly AWAP with some regions of under or overestimations. The overestimated regions are located at the high elevations while the underestimated regions are at low elevations. However, compared with R3, R1 and R2 had autocorrelations similar to each other for fortnightly and monthly resolutions across the site.

Figure 6.38 shows the ratio of the lag-1 correlation to AWAP (uncorrected NARCliM reanalyses divided by AWAP) for the Williams River site.

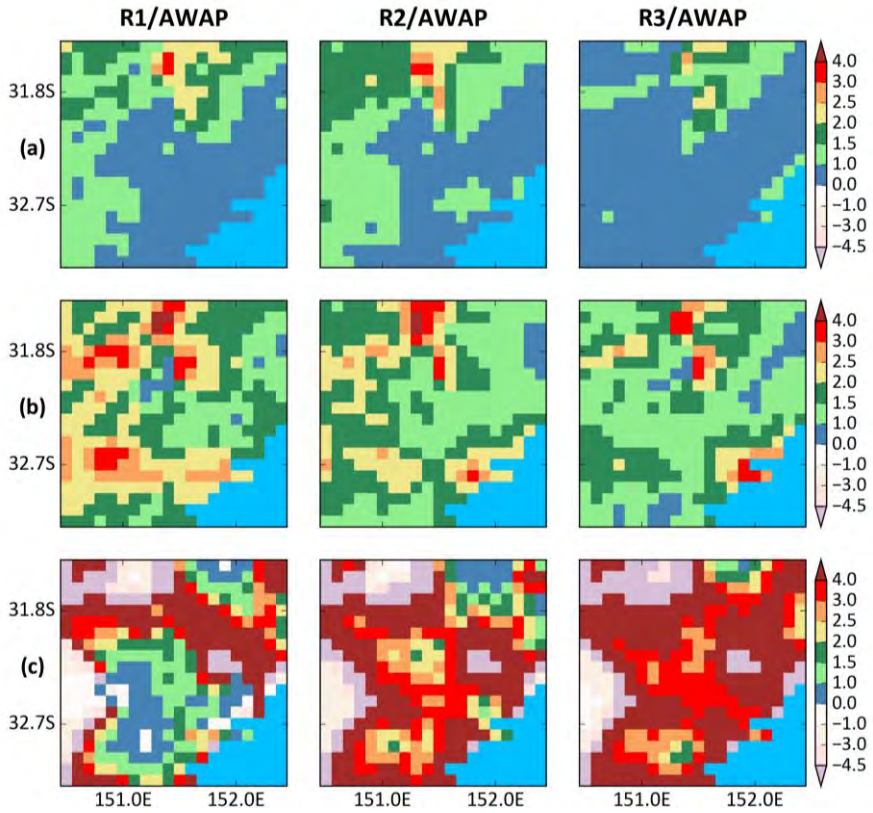

Figure 6.38 Ratio of the lag-1 correlation of uncorrected reanalyses and AWAP rainfall – Williams River site: (a) fortnight, (b) month and (c) annual.

As was for the mean, the ratio plots for the fortnightly time resolution show that reanalyses tend to underestimate the lag-1 correlations of AWAP (underestimated regions are shown in steel blue regions) at low elevations, while overestimating at high elevations with R1 and R2 overestimating more than R3. The annual ratio also does not reflect any close relationship with the elevation and show that reanalyses overestimate the lag-1 correlation of AWAP for most of the grid points. The negative lag-1 correlation region shown in annual AWAP data (shown in Figure

6.37) is clearly visible in the annual ratio plots. These negative regions have ratios ranging from 0 to -5.0 and are shown by a range of colours varying from white to light purple. Overall, compared with R1 and R2, R3 reanalysis closely reproduce the lag-1 correlations of fortnightly and monthly AWAP rainfall at the Williams River site, with most of the ratio values varying from 0 to 1.5.

The spatial distribution of the lag-1 correlation and the ratio of lag-1 correlation of bias corrected reanalysis and AWAP for the Williams River site is shown in Figures 6.39 and 6.40.

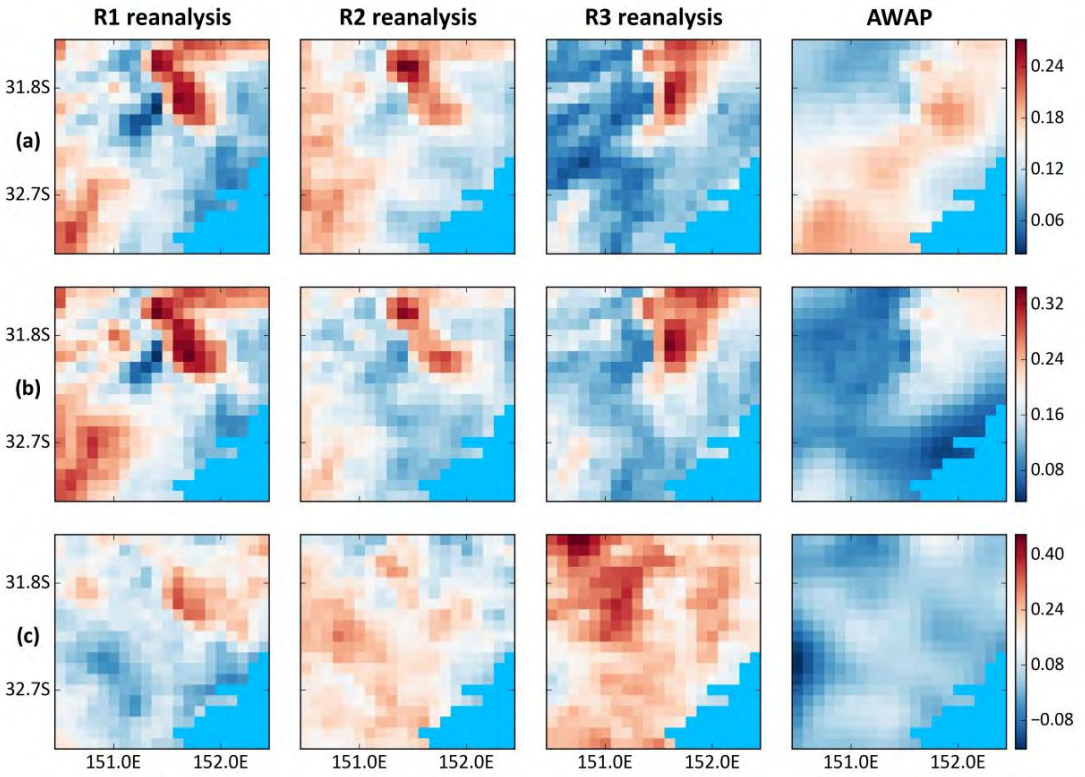

Figure 6.39 Spatial distribution of lag-1 correlation of bias corrected reanalysis and AWAP rainfall – Williams River site: (a) fortnight, (b) month and (c) annual.

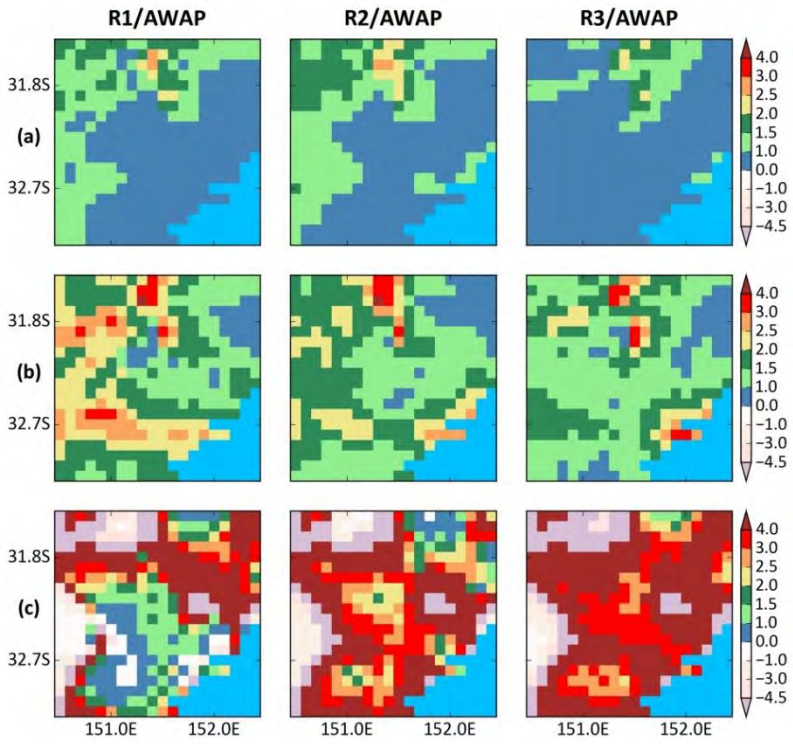

Figure 6.40 Ratio of the lag-1 correlation of bias corrected reanalyses and AWAP rainfall – Williams River site: (a) fortnight, (b) month and (c) annual.

There is only a slight improvement in the lag-1 correlation of the reanalyses rainfall after the bias correction. This is inconsistent to the improvement observed for the mean and C_v of the rainfall. Apart from the slight improvements of the magnitudes at some grid points, overall the spatial pattern and magnitude of the lag-1 correlation of reanalysis are almost unchanged. The ratio of lag-1 correlation of bias corrected reanalysis and AWAP is similar to the uncorrected rainfall. This suggests that even though the bias correction method applied by NARCliM tends to improve the distribution statistics such as mean and C_v of the rainfall (since bias correction modifies the probability distribution function), it does not change the time series characteristics of the rainfall, particularly lag-1 autocorrelations. This is because bias correction does not modify the temporal autocorrelations.

The spatial distribution of the lag-1 correlation and the ratio of lag-1 correlation of reanalyses to AWAP for the Richmond River site are shown in Figures 6.41 and 6.42 (uncorrected data) and Figures 6.43 and 6.44 (bias corrected data).

As was seen at the Williams River site, there is no significant improvement in the performance of the reanalysis in capturing the AWAP autocorrelations after the bias correction and the fit to AWAP is equally poor to that obtained for the Richmond River site.

Similarly, the spatial distribution of the lag-1 correlation and the ratio of lag-1 correlation of uncorrected and bias corrected reanalyses, to AWAP for the Bega River and Sydney sites are shown by Figures 6.45 to 6.52 respectively.

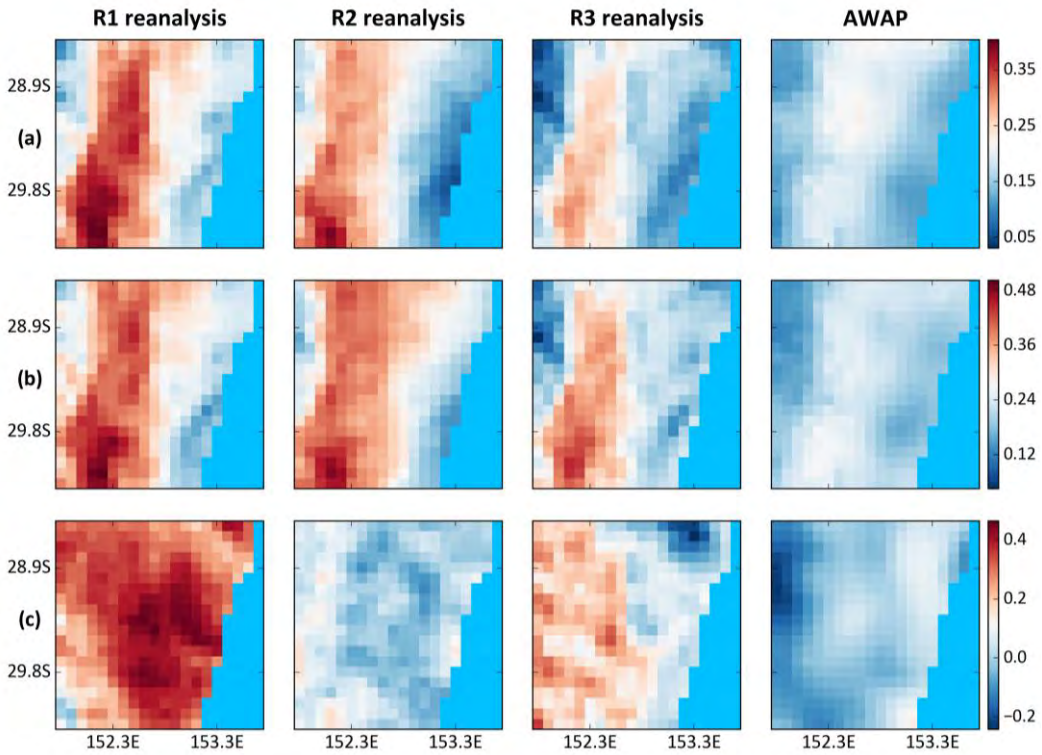

Figure 6.41 Spatial distribution of lag-1 correlation of uncorrected reanalysis and AWAP rainfall – Richmond River site: (a) fortnight, (b) month and (c) annual.

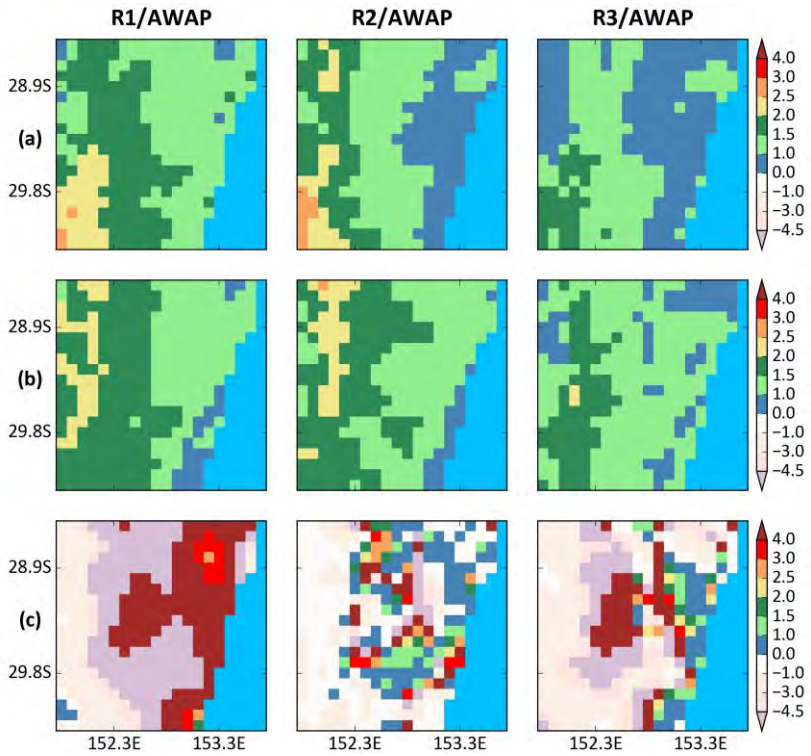

Figure 6.42 Ratio of the lag-1 correlation of uncorrected reanalyses and AWAP rainfall – Richmond River site: (a) fortnight, (b) month and (c) annual.

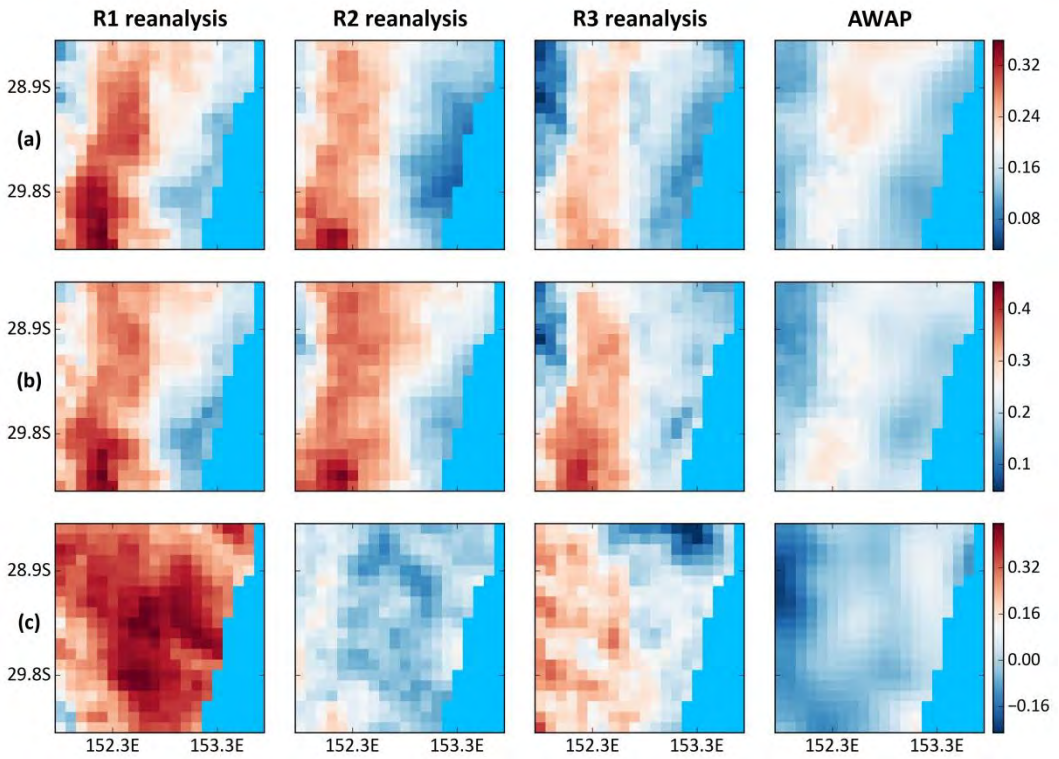

Figure 6.43 Spatial distribution of lag-1 correlation of bias corrected reanalysis and AWAP rainfall – Richmond River site: (a) fortnight, (b) month and (c) annual.

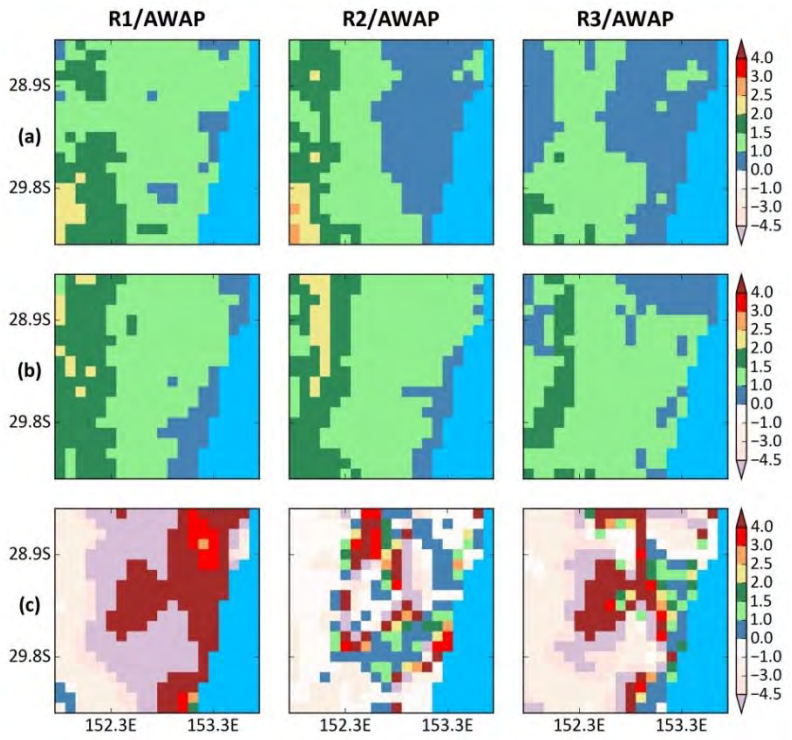

Figure 6.44 Ratio of the lag-1 correlation of bias corrected reanalyses and AWAP rainfall – Richmond River site: (a) fortnight, (b) month and (c) annual.

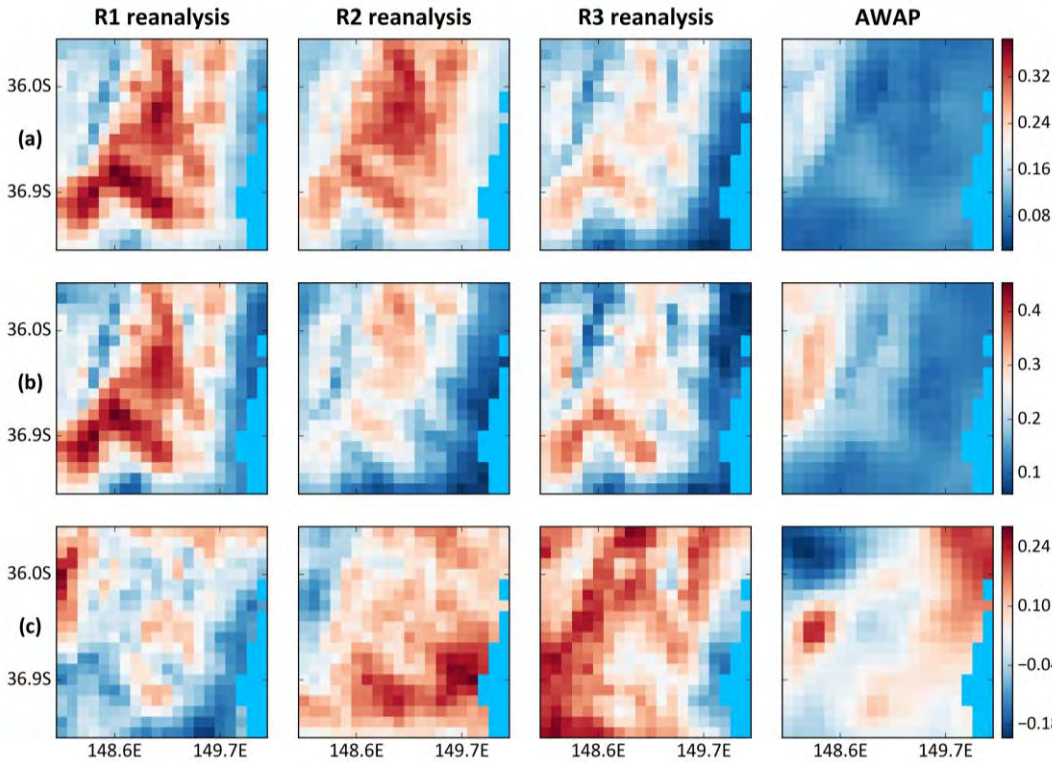

Figure 6.45 Spatial distribution of lag-1 correlation of uncorrected reanalysis and AWAP rainfall – Bega River site: (a) fortnight, (b) month and (c) annual.

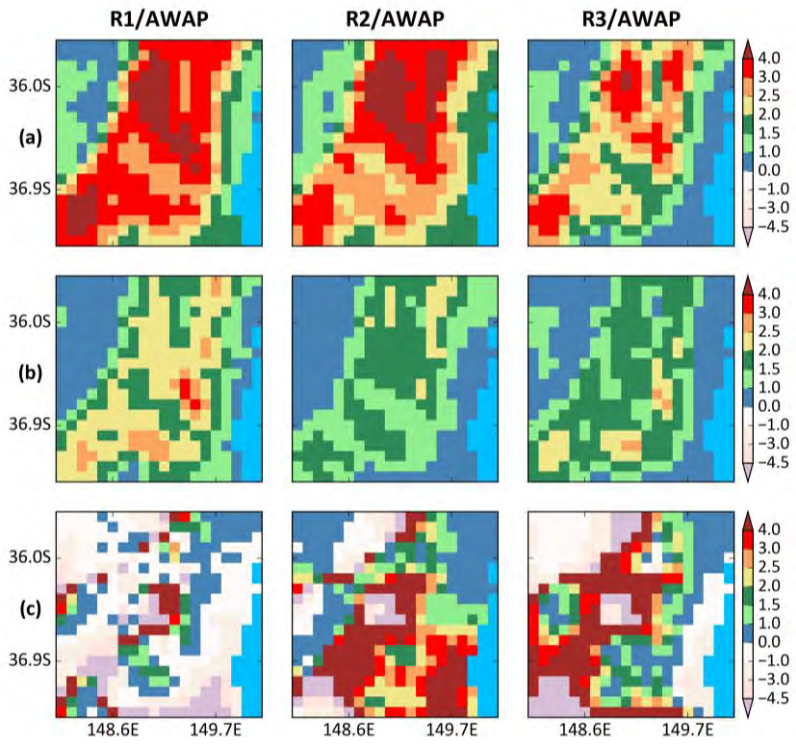

Figure 6.46 Ratio of the lag-1 correlation of uncorrected reanalyses and AWAP rainfall – Bega River site: (a) fortnight, (b) month and (c) annual.

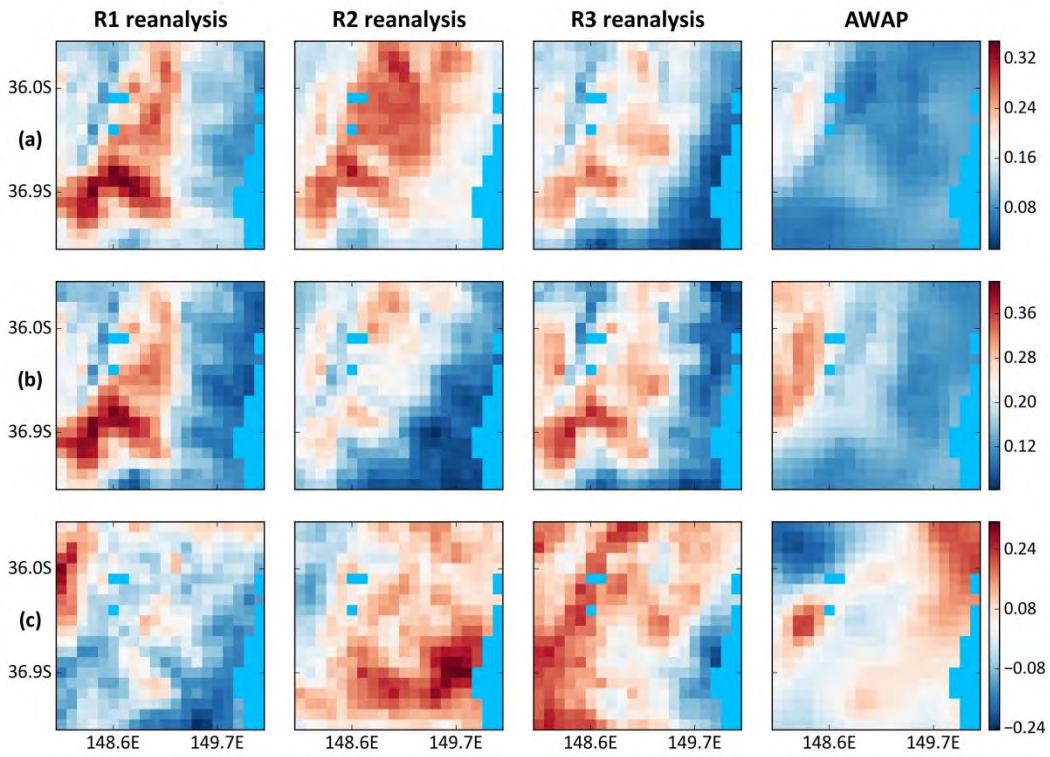

Figure 6.47 Spatial distribution of lag-1 correlation of bias corrected reanalysis and AWAP rainfall – Bega River site: (a) fortnight, (b) month and (c) annual.

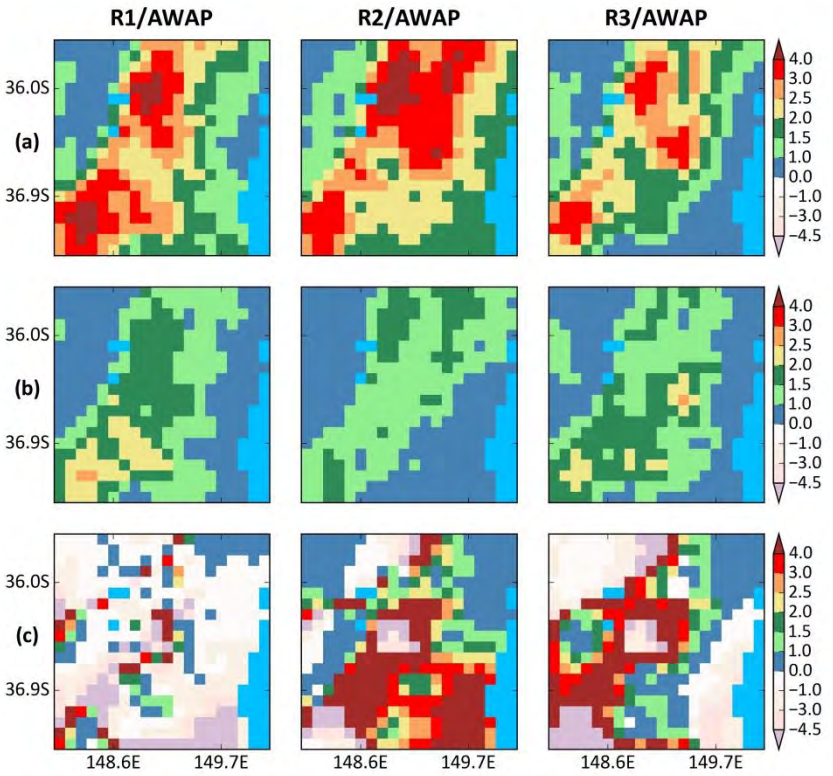

Figure 6.48 Ratio of the lag-1 correlation of bias corrected reanalyses and AWAP rainfall – Bega River site: (a) fortnight, (b) month and (c) annual.

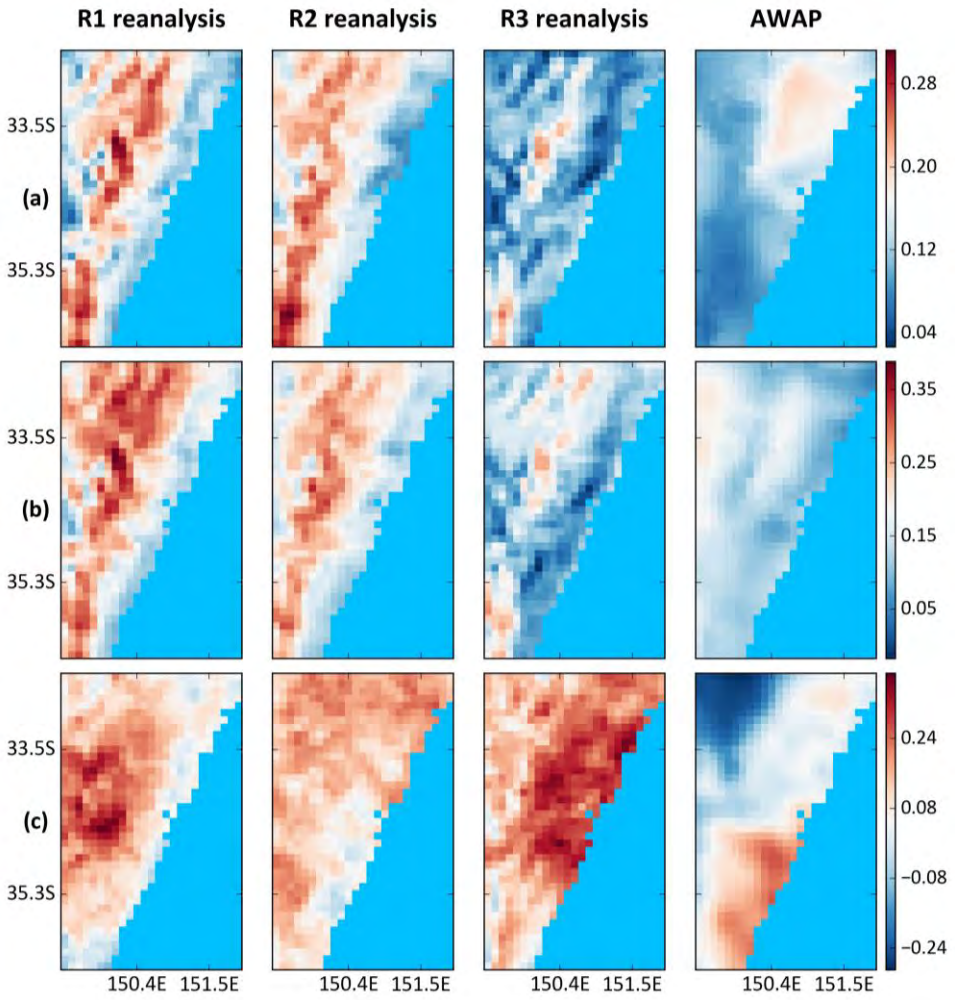

Figure 6.49 Spatial distribution of lag-1 correlation of uncorrected reanalysis and AWAP rainfall – Sydney site: (a) fortnight, (b) month and (c) annual.

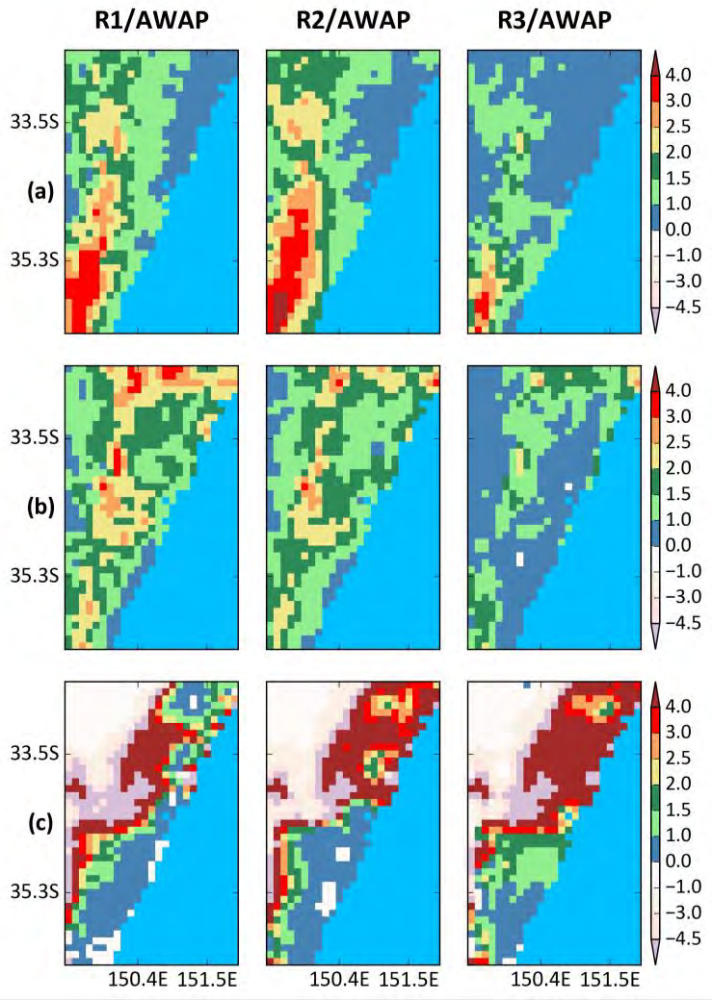

Figure 6.50 Ratio of the lag-1 correlation of uncorrected reanalyses and AWAP rainfall – Sydney site: (a) fortnight, (b) month and (c) annual.

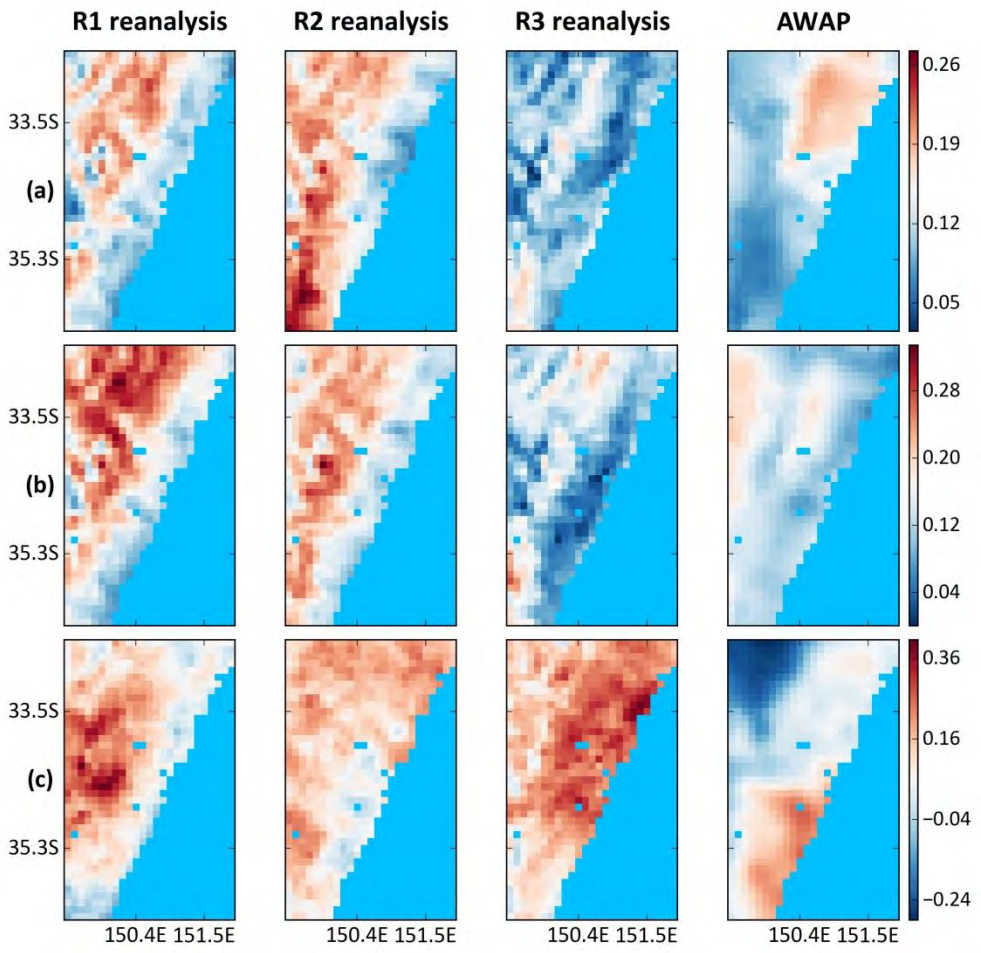

Figure 6.51 Spatial distribution of lag-1 correlation of bias corrected reanalysis and AWAP rainfall – Sydney site: (a) fortnight, (b) month and (c) annual.

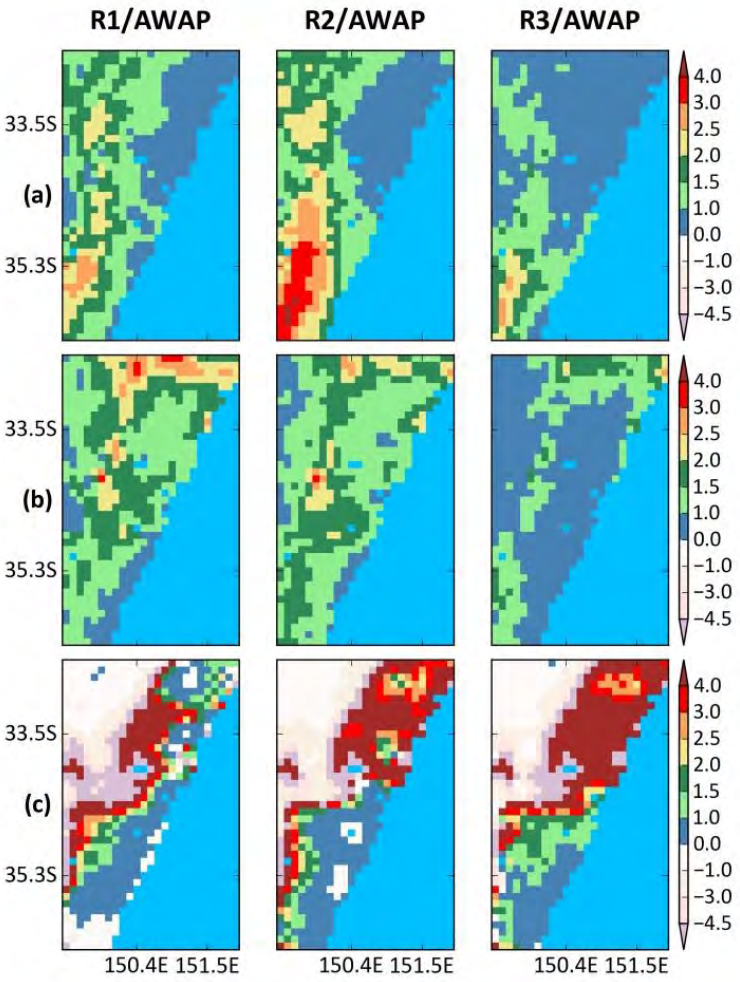

Figure 6.52 Ratio of the lag-1 correlation of bias corrected reanalyses and AWAP rainfall – Sydney site: (a) fortnight, (b) month and (c) annual.

As was seen for the coefficient of variation of the rainfall shown in Section 6.3.2, there is a consistency of the performance of three reanalyses datasets for all sites. The general spatial patterns of R1, R2 and R3 reanalyses are similar to each other for all sites except for Sydney. At Sydney the R3 reanalysis closely produces the lag-1 correlation of AWAP, while R1 and R2 significantly overestimate the magnitudes for fortnightly and monthly resolutions. There is a slight similarity of the spatial pattern of reanalyses and AWAP at fortnightly and monthly time resolutions for all sites except for the Williams River which has only the monthly pattern similar to AWAP. At annual resolution, all reanalyses poorly simulate the lag-1 correlation of AWAP for all sites. For all sites, there are regions of negative lag-1 autocorrelations (typically as low as -0.3 which is close to confidence limits, see for example Figure

6.54) in annual AWAP rainfall. This suggests that AWAP data might also have some issues of producing the correct autocorrelations and this will be further discussed later in Section 6.4.

The ratio plots show that all reanalyses (both uncorrected and corrected) tend to underestimate the lag-1 correlations of AWAP at low elevations of each site. At high elevation grid points, NARCliM reanalyses overestimated the lag-1 correlations of AWAP with R1 and R2 overestimating more than R3. This effect is more pronounced at the Bega River and Sydney sites showing the highest ratio ranging from 2.0 to 5.0. The general spatial pattern of the monthly ratio is similar to the pattern of fortnightly ratio for all sites, except for the Williams River and Sydney sites where there are no clear patterns related with elevation.

The bias corrected reanalysis results are similar to the uncorrected for all time resolutions and sites. Bias correction does not change the time series characteristics of the rainfall, particularly the lag-1 autocorrelations.

6.4 Autocorrelation Functions of the rainfall

The previous section examined only the lag-1 autocorrelation but was able to map the distribution in space for the sites. The results showed a poor fit irrespective of the site studied or the reanalyses used. In this section, the autocorrelation function for all lags is examined for a small number of locations (four grid points) in each site in an attempt to understand why this poor performance occurs.

The autocorrelations of uncorrected and bias corrected NARCliM and AWAP rainfall data at different lags were calculated at the grid points chosen within all four sites. The grid points are listed in Table 6.1. As for the autocorrelations results presented in Chapter 5, it should be noted that all the rainfall time series were transformed to have a zero skewness (i.e. so that the data are approximately Gaussian distributed) using the Box-Cox power transformation (See Section 4.4). The correlograms generated at grid points A, B, C and D of Williams River sites are shown in Figure 6.54. The spatial distribution of the Lambda (λ) used in the Box-Cox transformation (Equation 4.1) for the monthly rainfall is shown in Figure 6.53, and λ values for grid points A to D are shown in Table 6.2. The lambda plots show how close to Gaussian (λ=0) or log-Gaussian (λ=1) the rainfall probability distribution is.

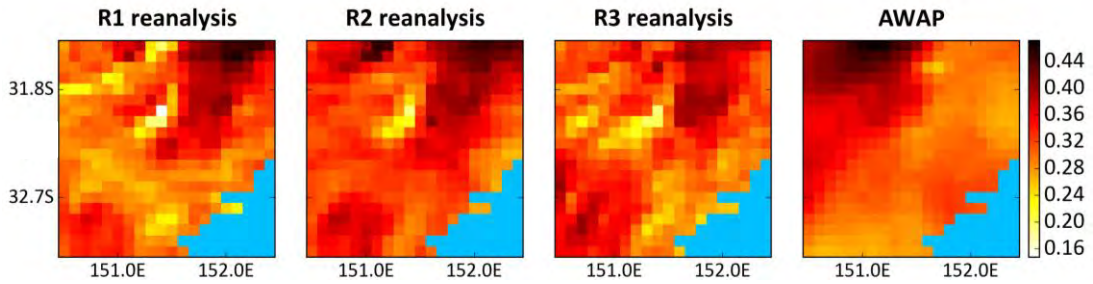

Figure 6.53 The spatial distribution of λ for the monthly rainfall at the Williams River site

As for the mean, C_v and lag-1 correlation, the spatial distribution of λ for the uncorrected reanalyses also mirrors the topography map of the Williams River site. Compared with AWAP, R1 and R3 reanalyses tend to have underestimated λ (for A to C grid points), while R2 reanalysis overestimate λ of AWAP for A, B and D grid points. This suggests that there is no general trend in reanalysis to either over or underestimate λ of AWAP.

Table 6.2 Lambda for the grid points of Williams River site

Grid point	*R1 reanalysis*	*R2 reanalysis*	*R3 reanalysis*	*AWAP*
A	0.31	0.33	0.30	0.32
B	0.28	0.33	0.30	0.31
C	0.27	0.32	0.31	0.34
D	0.38	0.41	0.40	0.30

The strong seasonal signals in autocorrelations of AWAP data in Figure 6.54 reflect that the rainfall is more strongly correlated to the next period (fortnight or month) at high elevation grid points than low elevations. However as for the Merriwa site, the autocorrelations of AWAP, particularly at lags greater than 1 are not significantly different from 0 (with correlations falling inside the 95% confidence limit) and have a consistent trend for all grid points of the Williams River site.

The correlograms of grid points A and B located in low elevations of Williams River site show that uncorrected NARCliM reanalyses data slightly overestimate the autocorrelations of AWAP for all three time resolutions with R3 producing some closer values than R1 and R2. The strength of autocorrelations of reanalyses is stronger than AWAP particularly at fortnightly and monthly resolutions showing some statistically significant autocorrelations. This effect of overestimation is more pronounced at grid points C and D which are located at the high elevations.

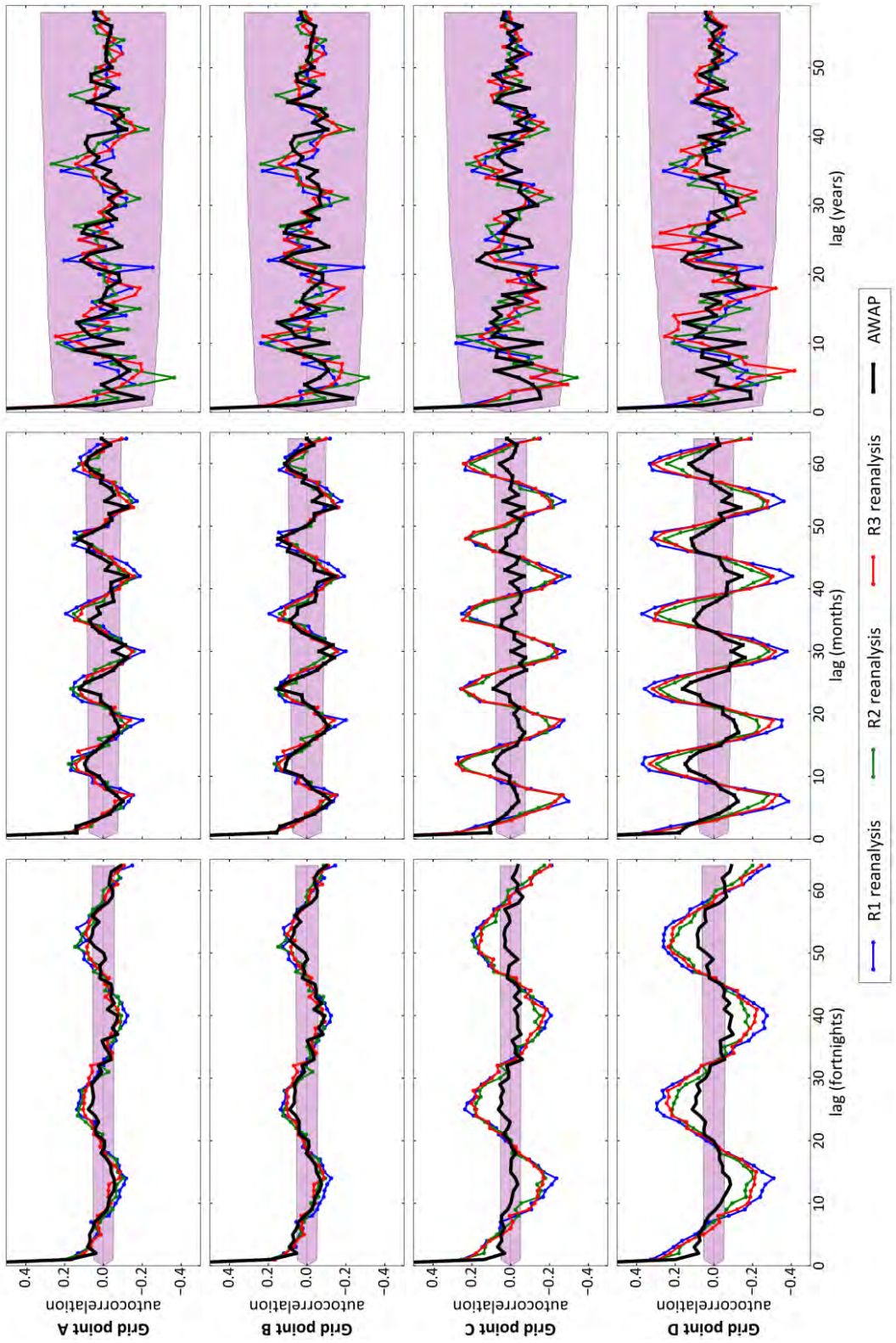

Figure 6.54 Correlograms of uncorrected reanalysis and AWAP at the Williams River site. Grid points A and B are low elevations, and C and D are high elevations. The shaded regions are the 95% confidence limits of the null hypothesis (i.e. correlations are not significantly different from 0).

The correlograms generated for the bias corrected reanalysis at grid points A, B, C and D of Williams River site are shown in Figure 6.55. In Section 6.3.3, it was found that the lag-1 correlation of reanalysis remained unchanged while generating similar magnitudes and seasonality as was with the uncorrected, after the bias correction. Likewise, Figure 6.54 (uncorrected rainfall) and Figure 6.55 (bias-corrected rainfall) are similar and indicate that bias correction does not significantly change the correlograms. This indicates that the reanalyses show no significant change in the autocorrelation at the Williams River site.

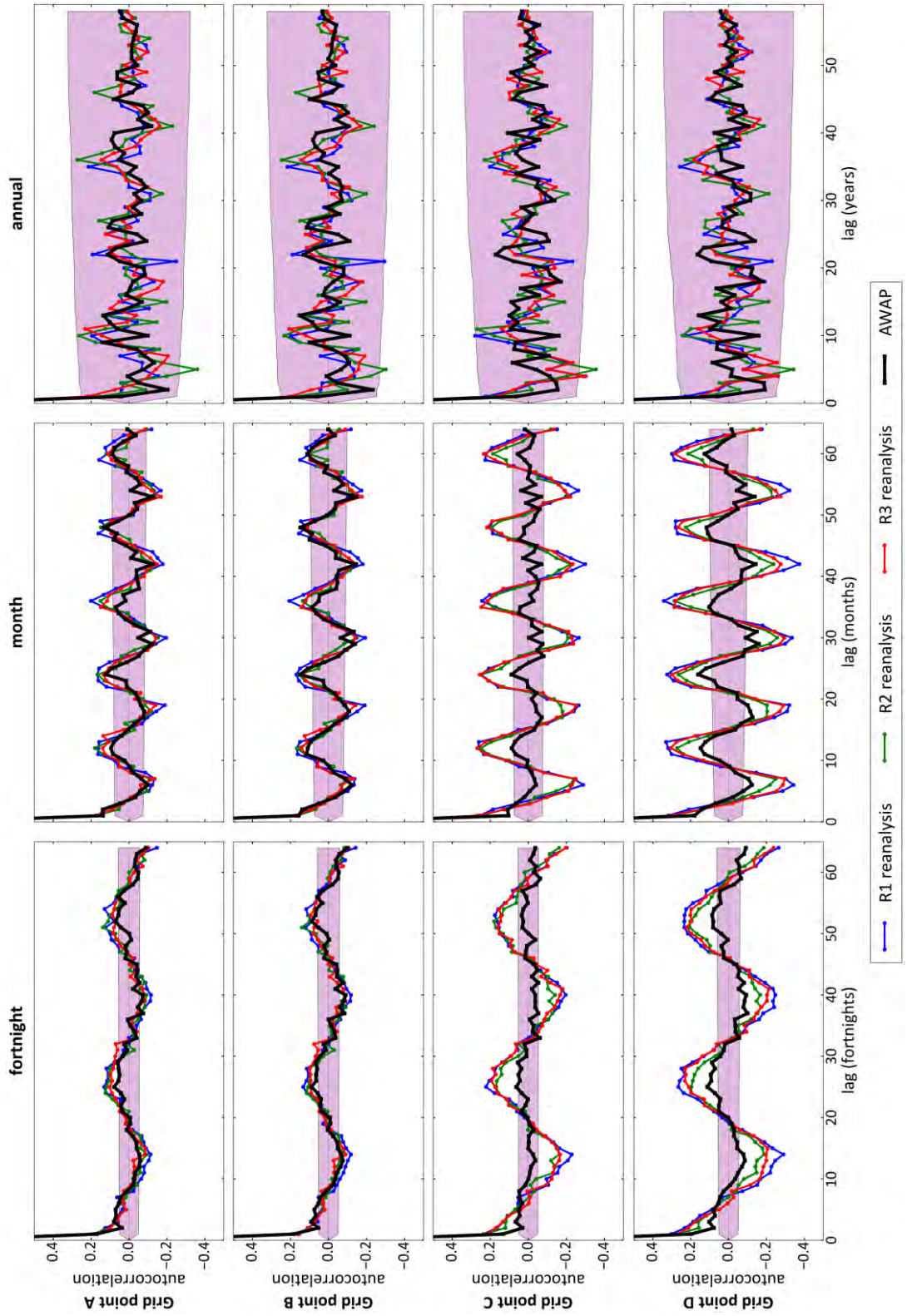

Figure 6.55 Correlograms of bias corrected reanalysis and AWAP at the Williams River site. Grid points A and B are low elevations, and C and D are high elevations. The shaded regions are the 95% confidence limits of the null hypothesis (i.e. correlations are not significantly different from 0).

The correlograms for the grid points of Richmond River site are shown in Figure 6.56. At Richmond River, the AWAP rainfall also shows significant autocorrelations (lying outside the 95% confidence limit) for all the grid points. Due to this high autocorrelations of AWAP, reanalyses tend to underestimate the autocorrelation of AWAP, particularly at low elevation grid points (E and F) and overestimate them at high elevation grid points (G and H). This underestimation of the AWAP correlation is contrast with the behaviour of the Williams River site.

The correlograms for the bias corrected reanalyses are shown in Figure 6.57. As before for the Williams River site, the correlograms are unchanged after the bias correction.

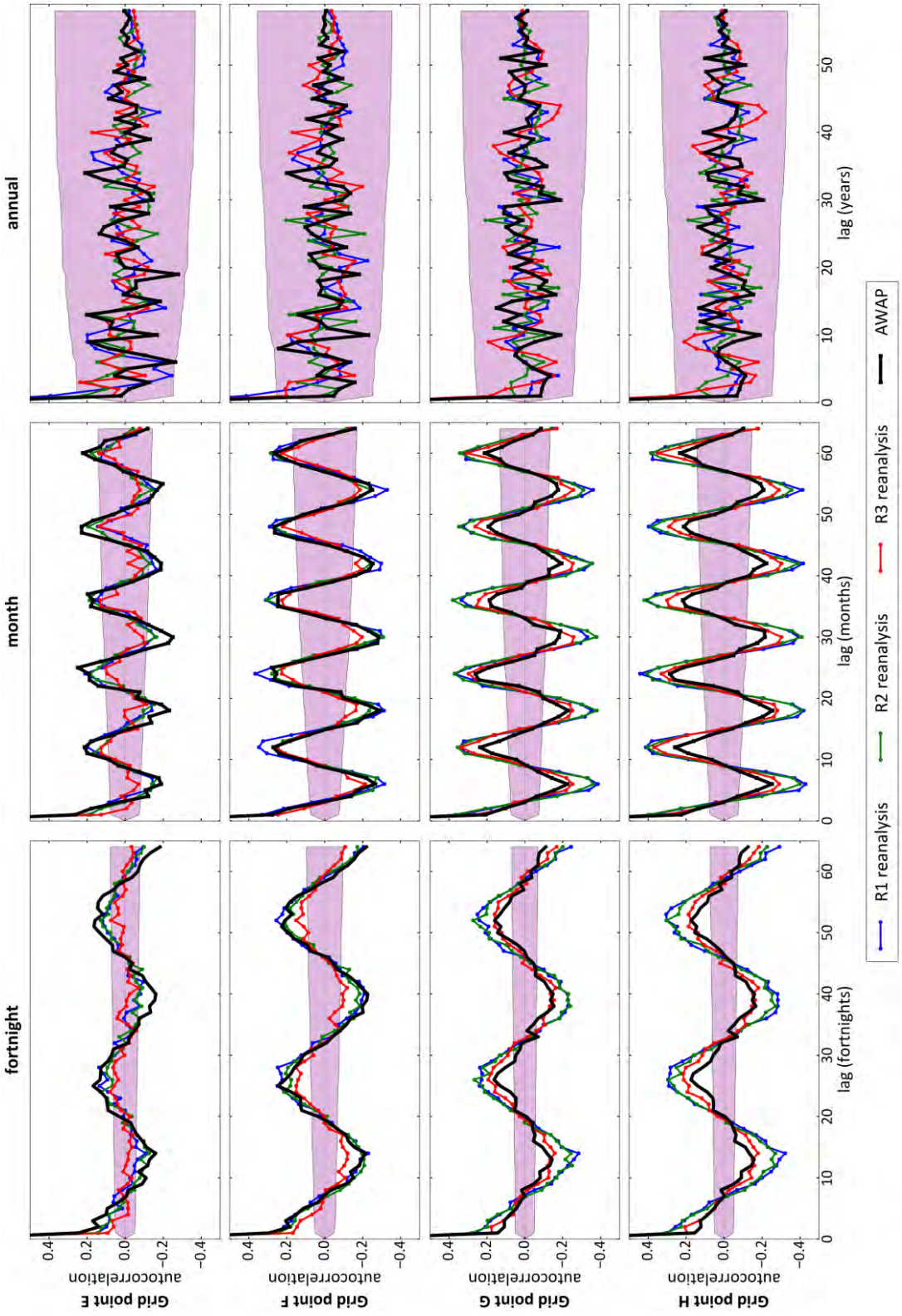

Figure 6.56 Correlograms of uncorrected reanalysis and AWAP at the Richmond River site. Grid points E and F are low elevations, and G and H are high elevations. The shaded regions are the 95% confidence limits of the null hypothesis (i.e. correlations are not significantly different from 0).

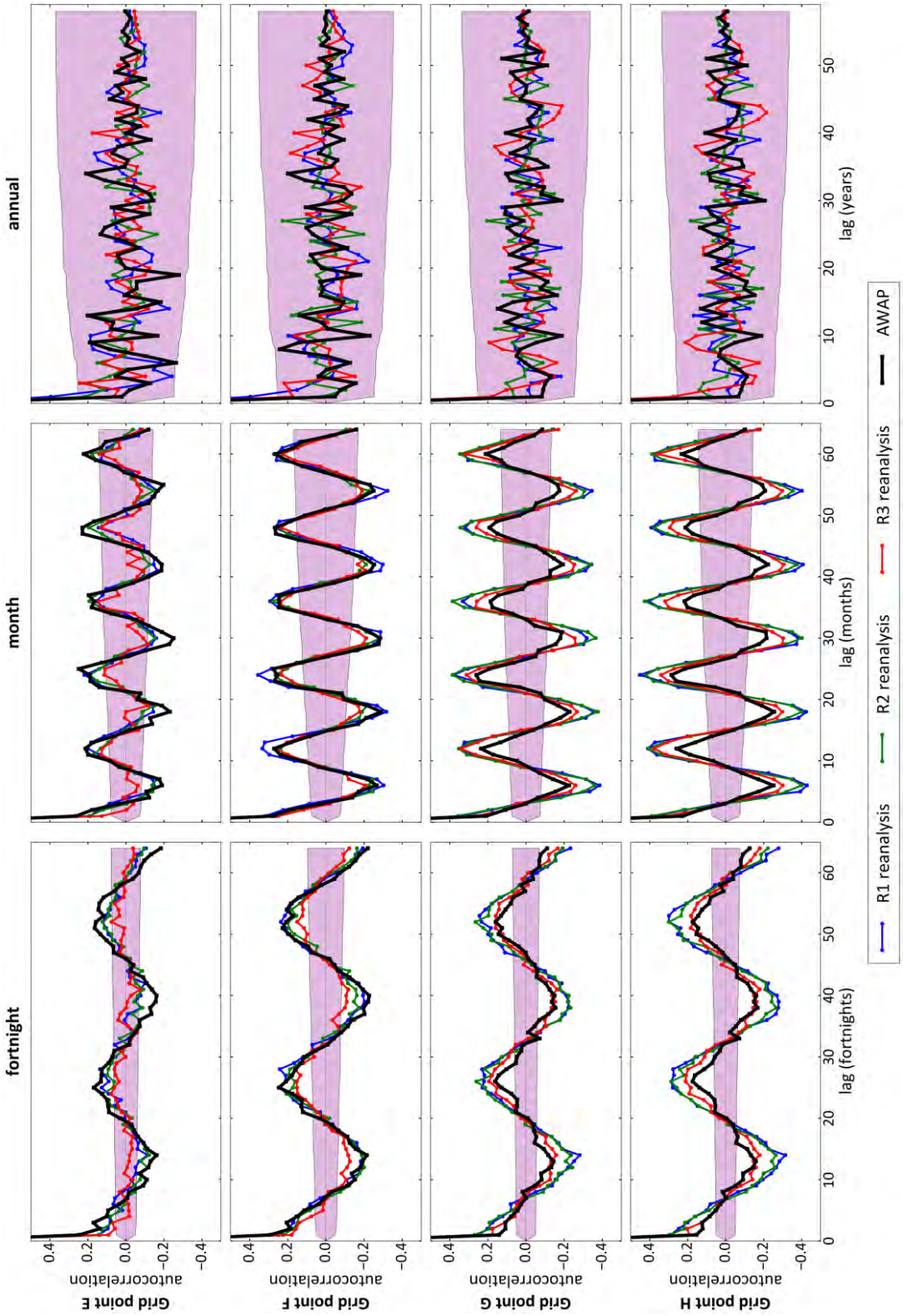

Figure 6.57 Correlograms of bias corrected reanalysis and AWAP at the Richmond River site. Grid points E and F are low elevations, and G and H are high elevations. The shaded regions are the 95% confidence limits of the null hypothesis (i.e. correlations are not significantly different from 0).

Figures 6.58 to 6.61 show correlograms of uncorrected and bias corrected reanalysis, and AWAP for the grid points of the Bega River and Sydney sites. For the Bega River site, NARCliM reanalysis data tend to overestimate the autocorrelations at low elevation grid points (J and K) and underestimate the autocorrelation of AWAP at the high elevation grid points (L and M).

For the Sydney site, reanalyses tend to overestimate the autocorrelations of AWAP rainfall at P, Q and R grid points. In particular at grid point R, reanalyses greatly overestimate autocorrelations of AWAP. In contrast to P, Q and R grid points, fortnightly autocorrelations are closely produced by reanalyses at the grid point S while underestimating the monthly AWAP autocorrelations.

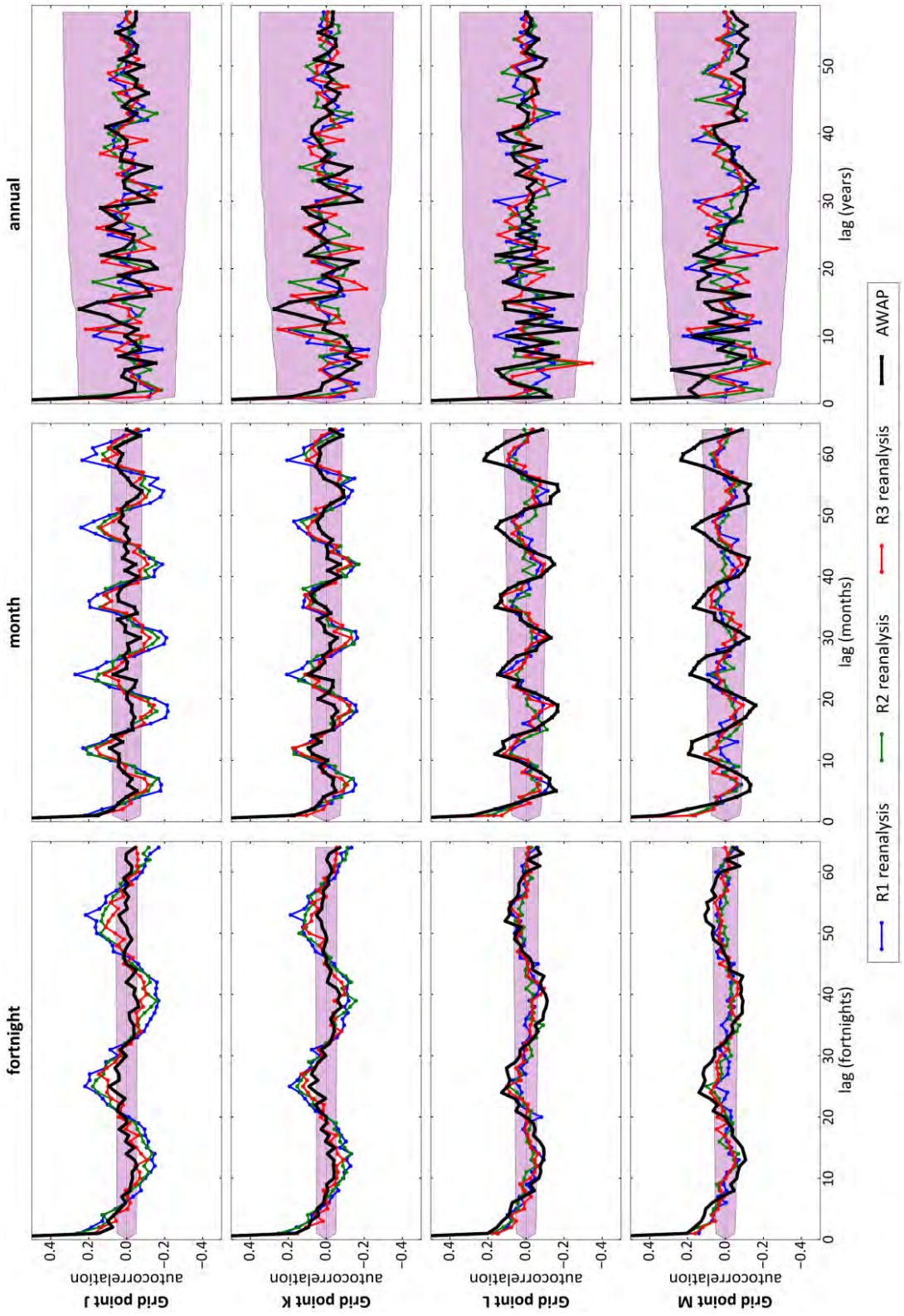

Figure 6.58 Correlograms of uncorrected reanalysis and AWAP at the Bega River site. Grid points J and K are low elevations, and L and M are high elevations. The shaded regions are the 95% confidence limits of the null hypothesis (i.e. the correlations are not significantly different from 0).

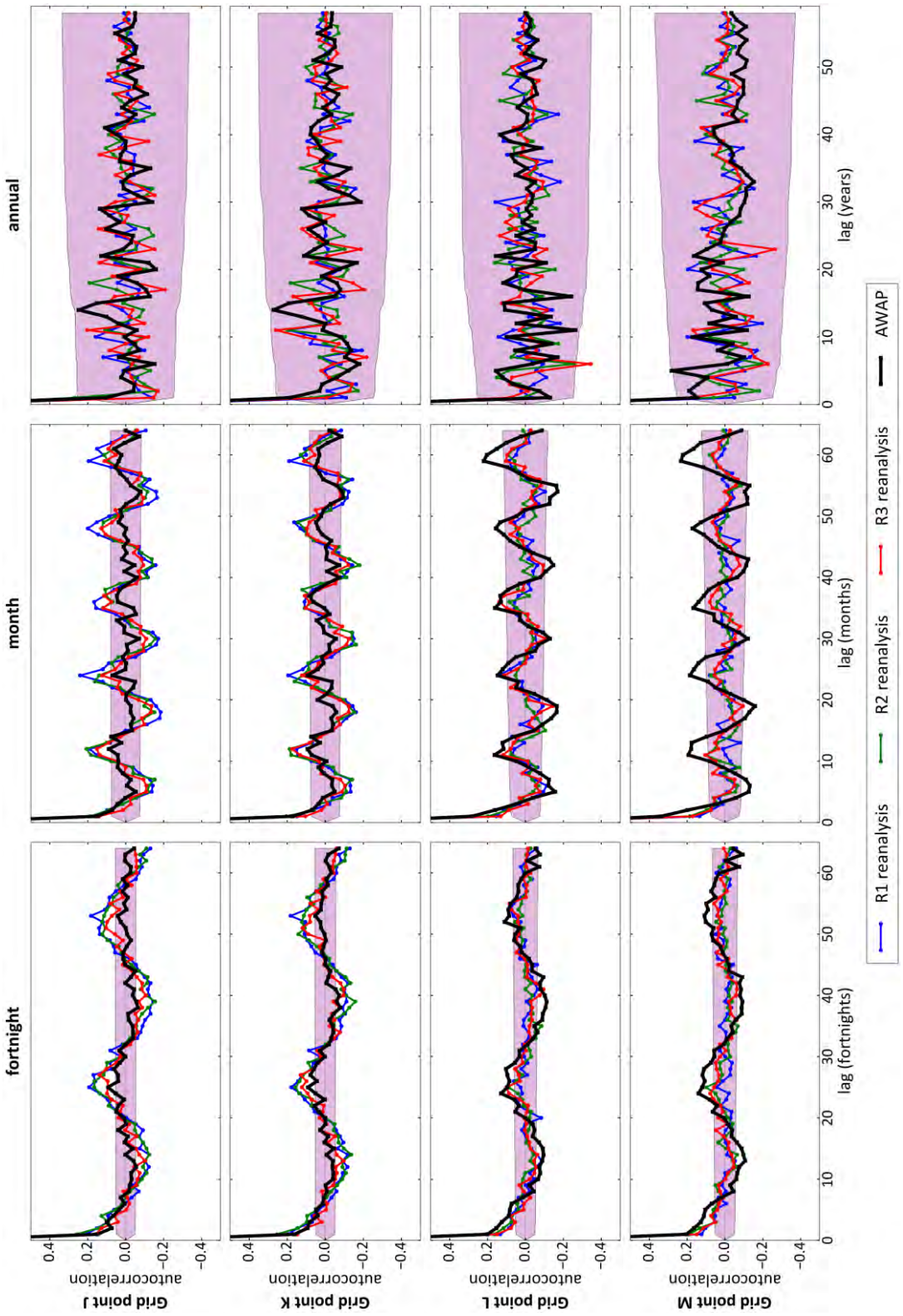

Figure 6.59 Correlograms of bias corrected reanalysis and AWAP at the Bega River site. Grid points J and K are low elevations, and L and M are high elevations. The shaded regions are the 95% confidence limits of the null hypothesis (i.e. the correlations are not significantly different from 0).

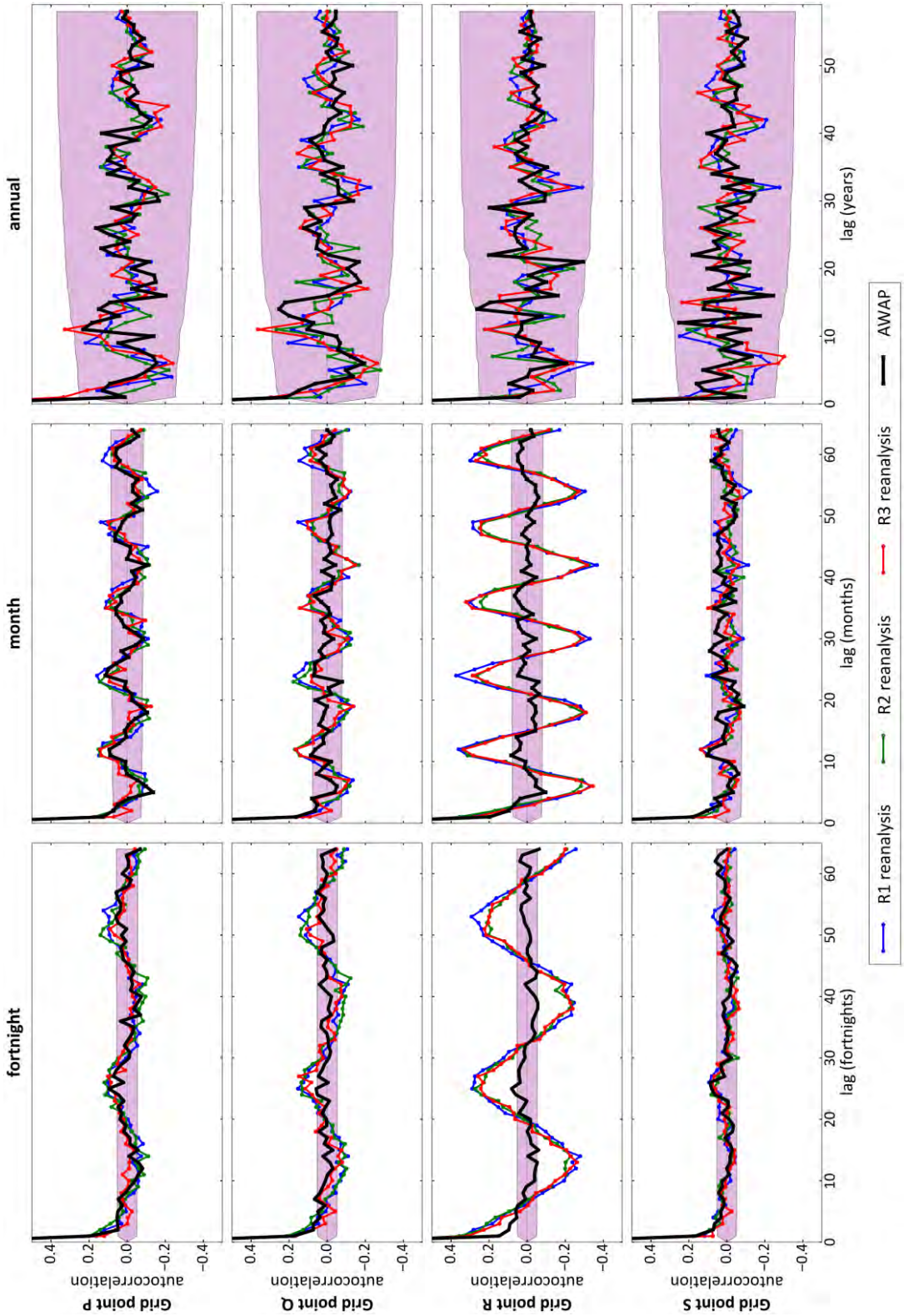

Figure 6.60 Correlograms of uncorrected reanalysis and AWAP at the Sydney site. Grid points P and Q are low elevations, and R and S are high elevations. The shaded regions are the 95% confidence limits of the null hypothesis (i.e. the correlations are not significantly different from 0).

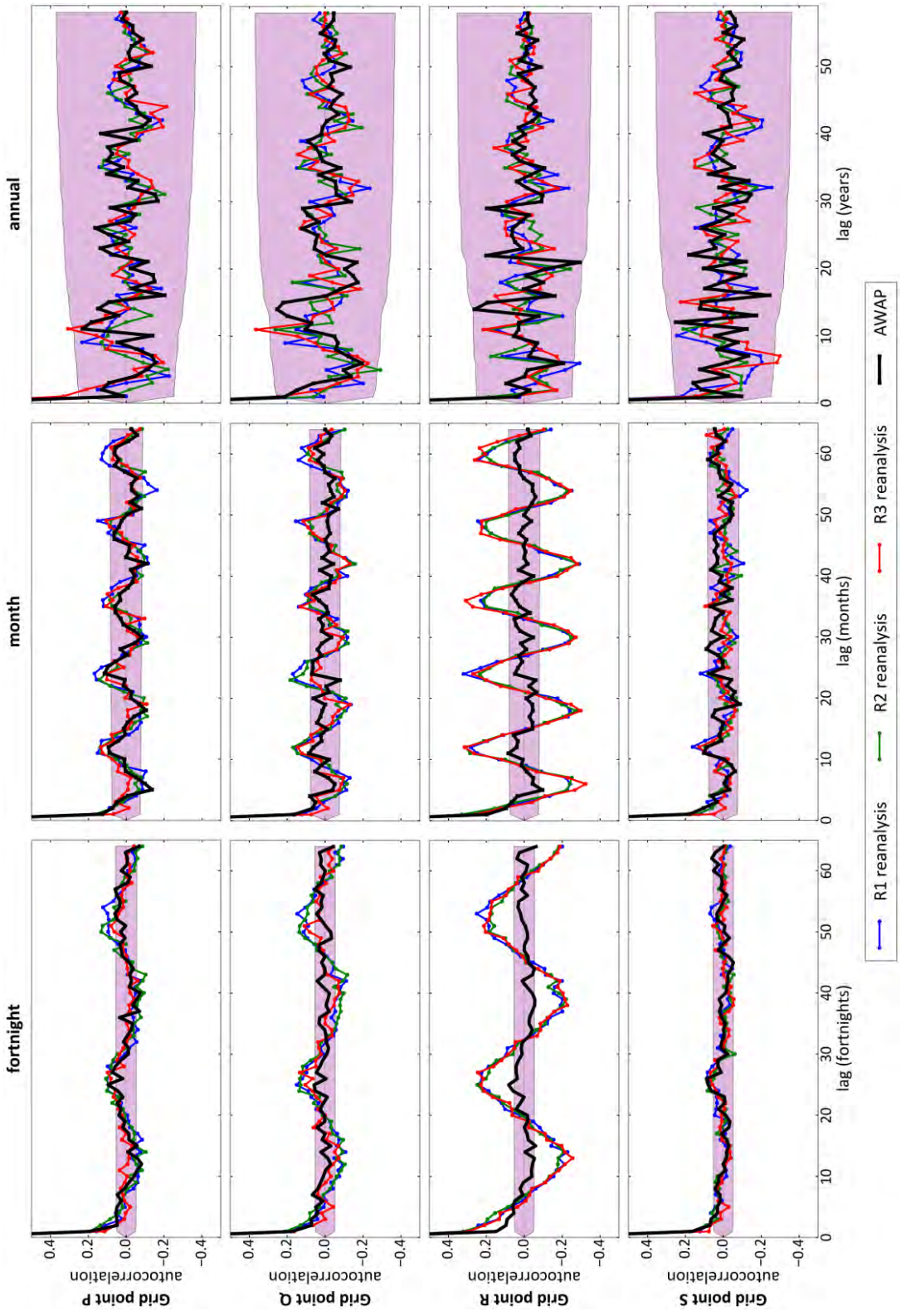

Figure 6.61 Correlograms of bias corrected reanalysis and AWAP at the Sydney site. Grid points P and Q are low elevations, and R and S are high elevations. The shaded regions are the 95% confidence limits of the null hypothesis (i.e. the correlations are not significantly different from 0).

Overall, the results of autocorrelation analysis suggest that the ability of reanalyses data to reproduce the observed autocorrelations is consistently poor and there is no consistency of either under or overestimating the observed magnitudes. The varying results at different sites located along the broader east coast indicate that the ability of NARCliM reanalyses to reproduce the autocorrelations of rainfall is not consistent between the sites with no trend from north to south. It appears to most strongly depend on the elevation of the site. Further, as explained earlier in chapter 5, it is also possible that the spatial averaging of elevation within the NARCliM pixels is affecting the results, particularly where rainfall volume is closely related to topography.

Furthermore, it should be noted that the method AWAP uses to interpolate data into the grid appears to neglect any autocorrelation in rainfall and therefore there may be artefacts in the generation of AWAP with respect to autocorrelations. The question raises here is whether this is an issue with AWAP, but not with the NARCliM data. In order to investigate the accuracy of autocorrelations of AWAP relative to rain gauges, autocorrelations analysis was again performed for two grid points with each have a rain gauge located within, and results are shown in Figure 6.62. Note that these two rain gauges, S1 and S2 (see Figure 3.10 and Table 3.6) were chosen as much as close to grid points R and S, while representing similar topographic conditions as of grid points R and S. The reason for using S1 and S22 is because there are no rain gauges in either R or S grid points.

Figure 6.62 shows that AWAP is able to reproduce the autocorrelations well for all the lags at grid point S2, while underestimating the autocorrelations at the rain gauge S22, particularly for lags 1 to 50. Therefore, this suggests that there are discrepancies in the performance of AWAP in reproducing the autocorrelations of rain gauges, and this requires more investigations in future. However, consistent with the results in Section 5.1.2.1, what is clear is that reanalyses have autocorrelations different to both rain gauges and AWAP at the Sydney site.

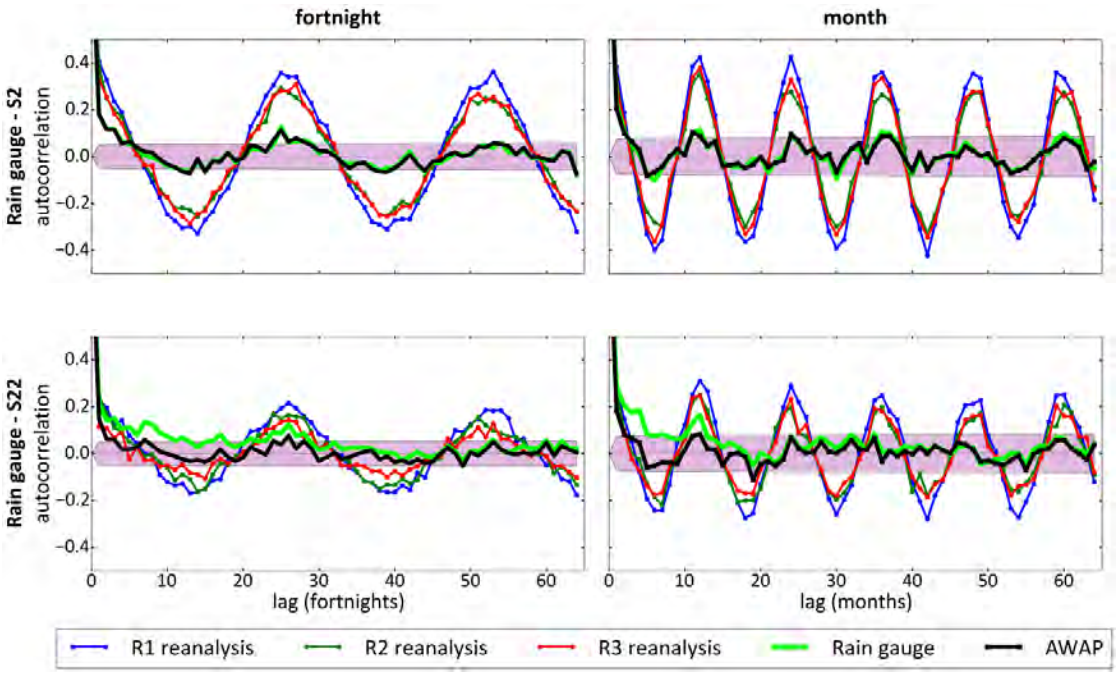

Figure 6.62 Correlograms of uncorrected reanalysis, AWAP and rain gauges at grid points S2 and S22.

However, all reanalyses data were able to reproduce the correct timing of the seasonal variability (i.e. the shape of the autocorrelation with time) present in the AWAP data for all sites even though the peaks of the seasonal cycles were under or overestimated. This result is consistent with the autocorrelations assessed at the Merriwa site in Chapter 5.

The bias corrected reanalyses produce similar results as the uncorrected data for all grid points at each site. Bias correction does not change the performance of reanalyses. Bias correction does not improve the time series statistics of rainfall.

6.5 Some insights on the seasonality

The autocorrelation analysis of both uncorrected and bias corrected datasets exhibits a seasonal signal. To see if there is any persistence in the seasonal anomalies, the fortnightly and monthly bias corrected rainfall time series were detrended, using the mean and standard deviation (see step 3 of Section 4.4), and then the autocorrelation analysis was repeated on the residual anomaly time series. Shown in Figure 6.63 are the correlograms of detrended rainfall of reanalyses and AWAP for the Williams River site.

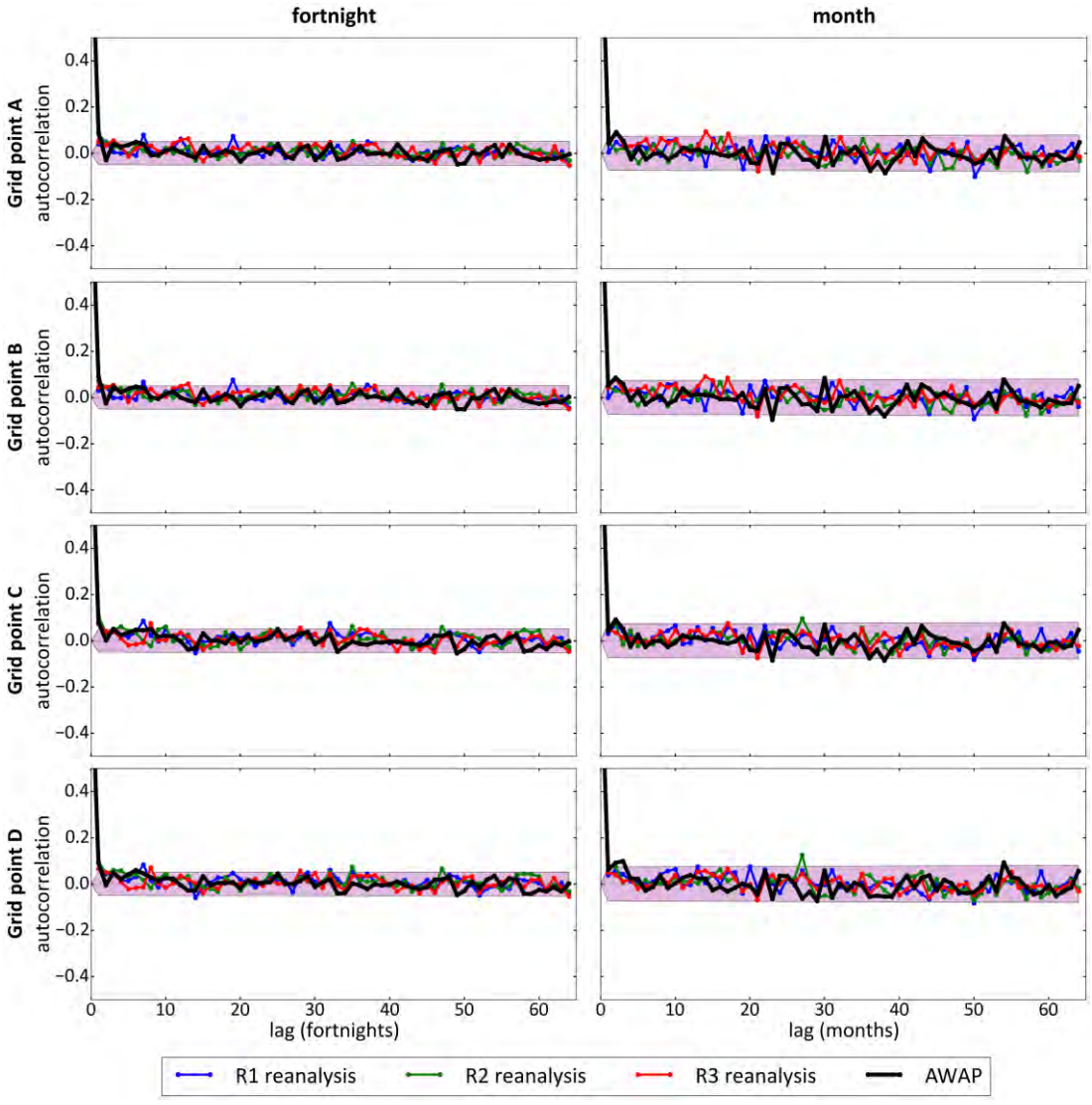

Figure 6.63 Correlograms of detrended NARCliM reanalysis and AWAP at Williams River site. Grid points A and B are low elevations, and C and D are high elevations. The shaded regions are the 95% confidence limits of the null hypothesis (i.e. the correlations are not significantly different from 0).

For the fortnight resolution, the bias corrected R1 reanalysis show some significant autocorrelations, particularly at lags 7 and 32 for all grid points except grid point C, and bias corrected R3 reanalysis also has significant correlations at lag 8 for high elevation grid points. None of these significant autocorrelations in reanalyses data have been replicated by AWAP. For the monthly resolution, AWAP show a statistically significant lag-1 correlation at all grid points, but this has only been reproduced by the bias corrected R3 reanalyses at low elevation grid points, and either R1 or R2 reanalysis at high elevation grid points. AWAP also shows three significant autocorrelations for 20 > lags > 50, yet none of them are replicated by the reanalyses. In contrast, there are significant autocorrelations either for R2 or R3 reanalyses for 10 > lags > 50 which cannot be seen in the AWAP dataset. These results suggest that there are discrepancies between the bias corrected reanalyses and AWAP datasets even though the seasonal signal was removed from the datasets. However, the reduction in the number of significant autocorrelations in the correlograms for the original and detrended data is consistent with a strong seasonal signal.

6.6 Summary and Conclusions

The following dot points summarise the results in this chapter.

- The uncorrected NARCliM reanalyses, particularly R1 and R3 do not reproduce the probability distribution of the observed rainfall correctly. The bias corrected reanalyses show improved reproduction, but it is clear that only a part of the daily probability distribution has been improved. Neither uncorrected nor bias corrected reanalyses data reproduce the light rainfall events.
- The uncorrected NARCliM reanalyses rainfall, particularly R1 and R3 often overestimate the mean rainfall of AWAP for the broader east coast.
- All uncorrected reanalyses underestimate the coefficient of variation of AWAP, in fact tend to underestimate the temporal variability of the rainfall. R2 reanalysis is most similar to the AWAP at lower elevations, but still overestimates the rainfall statistics at high elevations. In contrast, bias corrected reanalyses tends to reproduce the mean and C_v of rainfall better

than they did before when uncorrected. In particular, the improvement to capture the mean rainfall of AWAP is more significant than C_v of rainfall. The ability of uncorrected reanalyses data to reproduce the observed autocorrelations is consistently poor and there is no consistency of either under or overestimating the observed magnitudes. A preliminary analysis shows that AWAP tends to underestimate the autocorrelation of rain gauge rainfall at some grid points, yet the difference between autocorrelations of reanalyses and rain gauges is much higher than that between AWAP and rain gauges. All reanalyses are capable of reproducing the correct timing of the seasonal cycle of the observed data with R2 and R3 are closely producing the autocorrelations at some locations, yet this does not show a direct link with the terrain. The bias corrected reanalyses produce similar results as the uncorrected data for all grid points at each site. Therefore, the results show that bias correction does not improve the performance of reanalyses and is not designed to capture the autocorrelations of AWAP at all sites studied. The reduction in the number of significant autocorrelations in the correlograms for the original and detrended data is consistent with a strong seasonal signal.

- There is no north to south trend in either AWAP or NARCliM rainfall statistics in the broader east coast.
- The uncorrected NARCliM reanalyses are able to reproduce the spatial pattern of AWAP, but do not produce the magnitudes correctly. The ability of NARCliM reanalyses to reproduce the spatial pattern of observed rainfall statistics is necessary but not sufficient requirement for hydrological studies, particularly reservoir modelling. Since the NARCliM reanalyses data do not produce the long-term observed rainfall characteristics correctly, the reliability of the use of this data in rainfall-runoff models to generate estimates of runoff is uncertain.
- There is a tendency of the statistics such as mean, coefficient variation and lag-1 correlations calculated for NARCliM reanalyses data to be correlated to the terrain and the distance to the coast.

- The strong seasonal signal and differences of temporal correlations seen in NARCliM from north to south of the east coast, is not replicated either by AWAP or rain gauge data.
- Bias correction has no significant impact on the poor performance of NARCliM which does not correctly capture the temporal correlation of the AWAP rainfall.

Chapter 7
Testing the uncorrected and bias-corrected NARCliM reanalyses data using spatial correlation of the rainfall

7.1 Introduction

The spatial correlation of the rainfall is important when estimating the rainfall in hydrological and water availability analysis. When the rainfall is not uniform over a catchment, the spatial correlation between the subcatchments can be used to estimate the whole catchment rainfall total. Additionally, if the distribution of a rain gauge network is sparse or the available data at a specific location is not highly reliable, an existing spatial correlation of the rainfall can be useful to predict the rainfall. For example, if there are two rainfall stations which are separated by a distance less than a few kilometres, with one station having long continuous records, records of this particular rainfall station can be used for estimating the rainfall of the other. The reason behind this is if one station has a high rainfall, it is usually observed that the other station also experiences a high rainfall at the same time. However, this is not always true for some locations. Therefore, understanding of the existing correlations between rainfall stations in a catchment is beneficial, particularly when predicting the runoff for the water availability analysis in reservoir modelling.

This chapter focuses on testing the NARCliM gridded data based on the spatial correlation of the rainfall at the four sites along the east coast. As in the previous chapter, the analysis was performed at the Williams River, Richmond River, Bega River and Sydney sites, and 10 km resolution uncorrected and bias corrected NARCliM reanalyses data (1950-2010) were used. The analysis is in two parts: (1) Assessment of the spatial correlation of the daily rainfall and its variability at the site scale (for all grid points), and (2) Validation against the 10 km resolution AWAP and rain gauge data (for selected grid points where the rain gauges are).

As explained in Section 4.5 about the methodology, the spatial correlations between the daily rainfall of NARCliM grid points were first evaluated using the Pearson's correlation coefficient; correlation between all other grid points were calculated with

reference to two grid points located at high and and two grid points at low elevations for each site. The method is descriptively explained in Section 4.5. Then, results are compared with spatial correlation of AWAP which was calculated using the same method.

Later, spatial correlation of both NARCliM and AWAP gridded data are compared with the observed spatial correlations, calculated for the selected rain gauges within each site. Only grid points (NARCliM/AWAP) which have rain gauges inside were used for the comparison. The selected reference grid points/rain gauges and all other grid points/rain gauges used in the analysis are shown in Table 7.1 and Figures 7.1 to 7.4.

Table 7.1 Reference grid points selected at each site

Site name	*Total rain gauges used*	*Reference grid point/rain gauge ID*	*Elevation of the reference grid point (m)*	*Elevation range*
Williams River site	17	W17	595	high
		W4	24	low
Richmond River site	25	P20	938	high
		P9	2	low
Bega River site	25	Q12	1075	high
		Q3	10	low
Sydney site	29	S22	1225	high
		S8	10	low

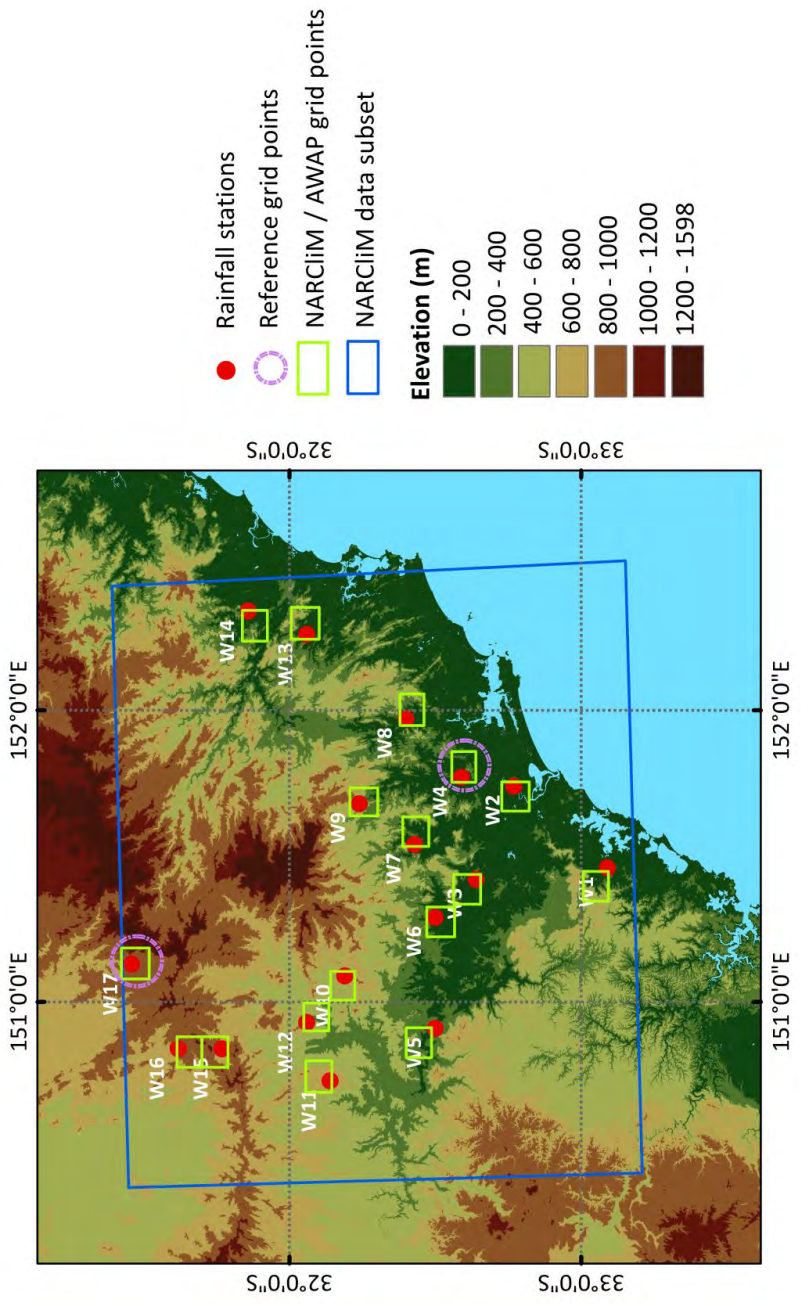

Figure 7.1 Map of the rain gauges and NARCliM/AWAP grid points selected at the Williams River site.

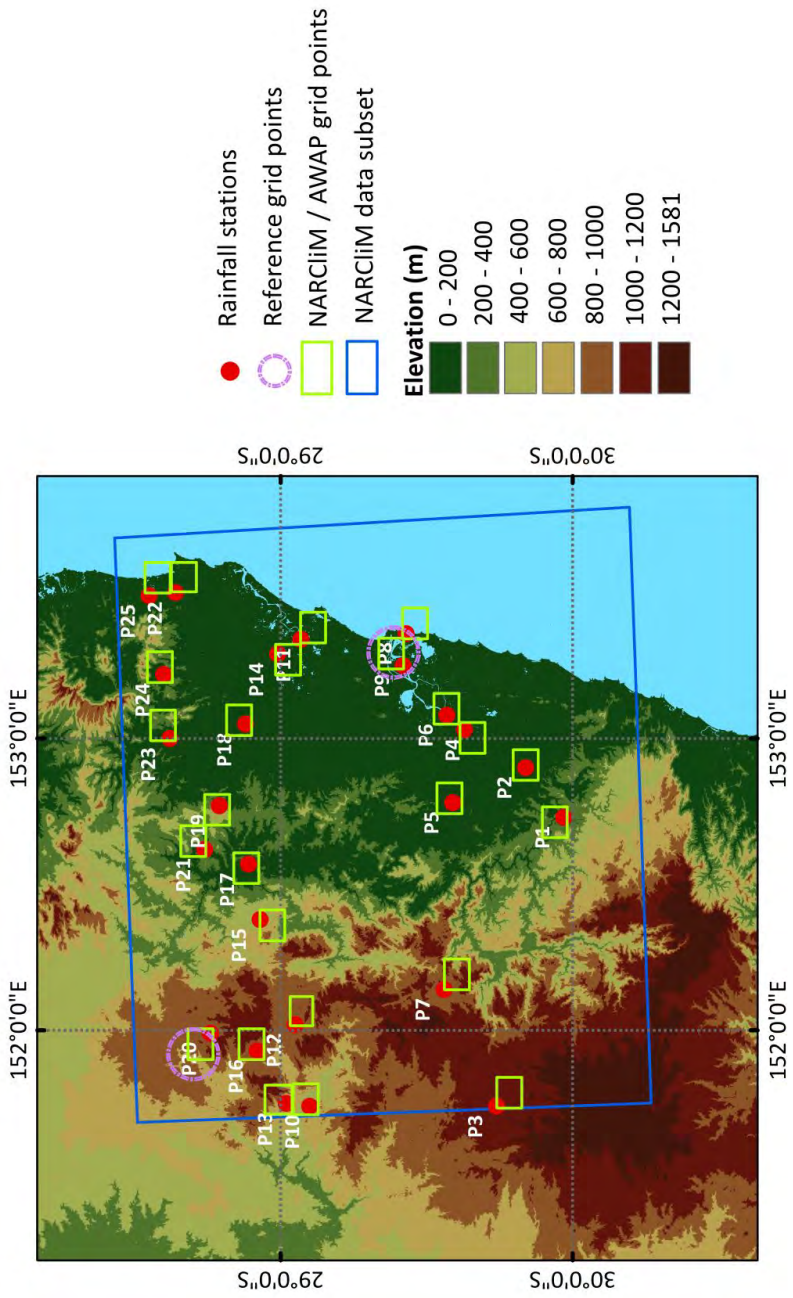

Figure 7.2 Map of the rain gauges and NARCliM/AWAP grid points selected at the Richmond River site.

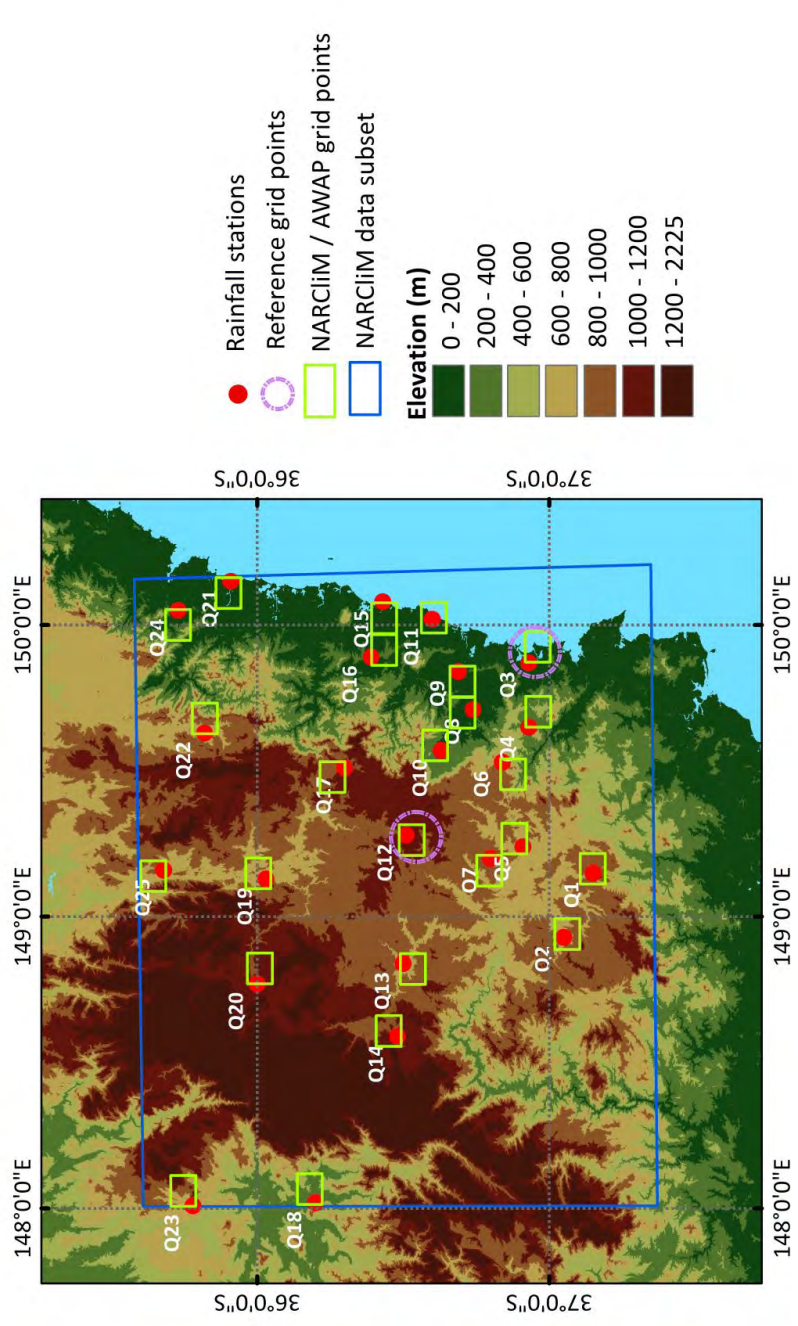

Figure 7.3 Map of the rain gauges and NARCliM/AWAP grid points selected at the Bega River site.

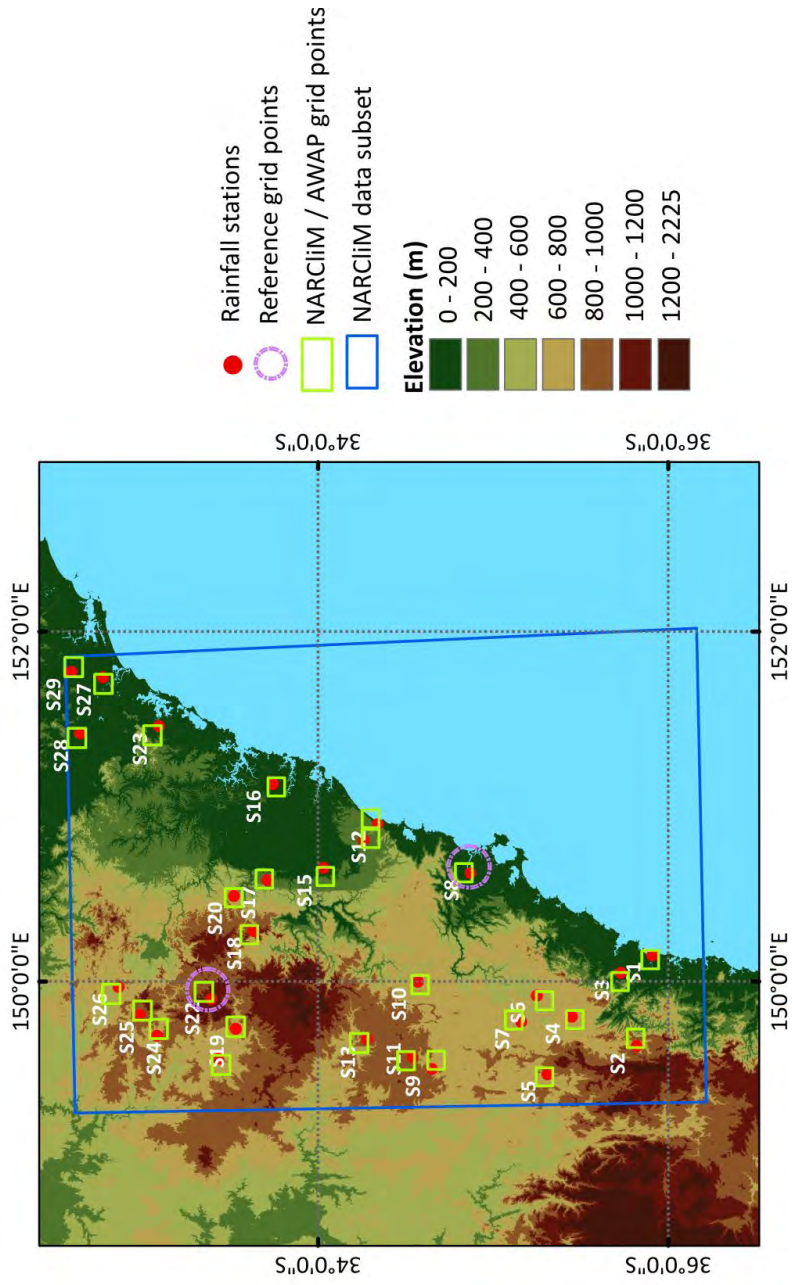

Figure 7.4 Map of the rain gauges and NARCliM/AWAP grid points selected at the Sydney site.

7.2 Spatial correlation of NARCliM reanalyses and AWAP rainfall

The spatial correlation of the rainfall between the high elevation grid point (W17) and all other grid points of the Williams River site are shown in Figure 7.5. All plots generated for the uncorrected reanalyses and AWAP data show that grid points which are close to the reference have higher correlations with the reference point than do farther away. However, as was seen with the other statistics (mean, C_v and lag-1 correlations in Section 6.3), the spatial correlations also appear to be related with the topography. The topography map of the Williams River site is shown in Figure 7.5b. High elevation grid points are more correlated to each other and appear to cluster together following the same spatial pattern of the elevation, suggesting that spatial correlation is not simply an effect of proximity, and is significantly influenced by both the topography and the distance between the points.

The general spatial pattern in correlations of all uncorrected reanalyses is qualitatively similar to that of the AWAP data. Relative to the reanalyses data, there is a smoothing in the spatial pattern of the correlations of AWAP data which seems likely to be related with the inherent interpolation artefacts of AWAP data. Some of these artefacts were previously discussed in Section 6.3. However, the general spatial pattern in the correlations of all three reanalyses data is similar to each other.

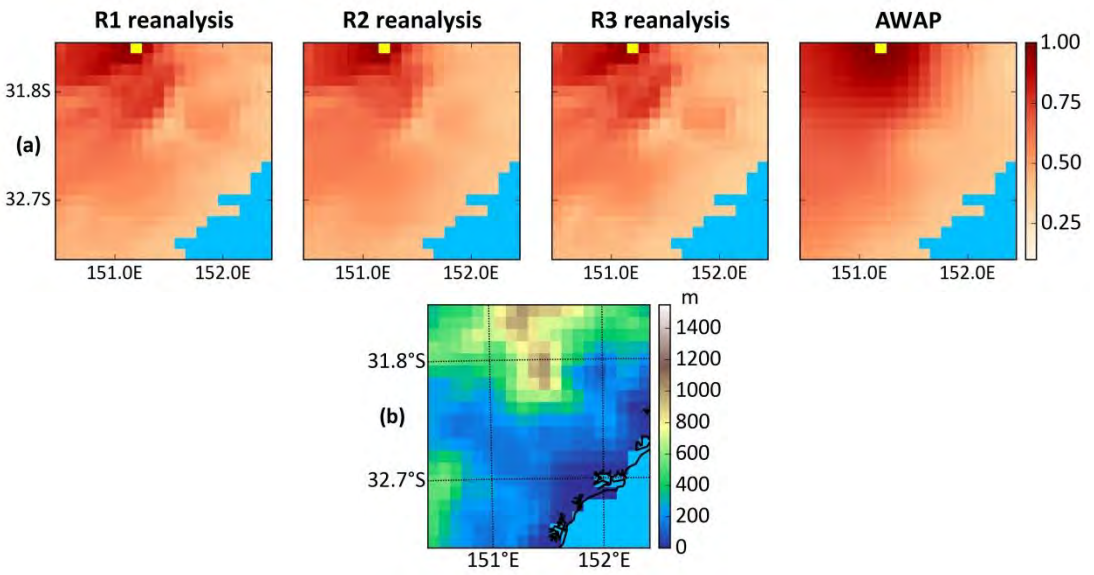

Figure 7.5 Spatial correlations for all grid points of uncorrected reanalysis and AWAP at the Williams River site: (a) spatial distribution of correlations between the reference grid point and all other grid points and (b) topography map of the site (as defined and used by NARCliM). The reference is W17 high elevation grid point (shown in yellow boxes).

The spatial correlation functions generated against the distance between the grid points (i.e. separation) are shown in Figure 7.6. As shown by Rodriguez-Iturbe and Mejia (1974), the spatial correlation function of each data set replicates an exponential decay function; the correlation gradually decreases with the increasing separation between the grid points. The different colour markers represent the elevation difference between the points (see Section 4.5, Methodology). The scatterplots indicate that all uncorrected reanalyses underestimate the spatial correlation function of AWAP, with R2 and R3 reanalyses underestimating the exponents of the fitted curve of AWAP more than R1. Compared with R1 and R2, the scatter in R3 reanalysis is very similar to AWAP for all separations.

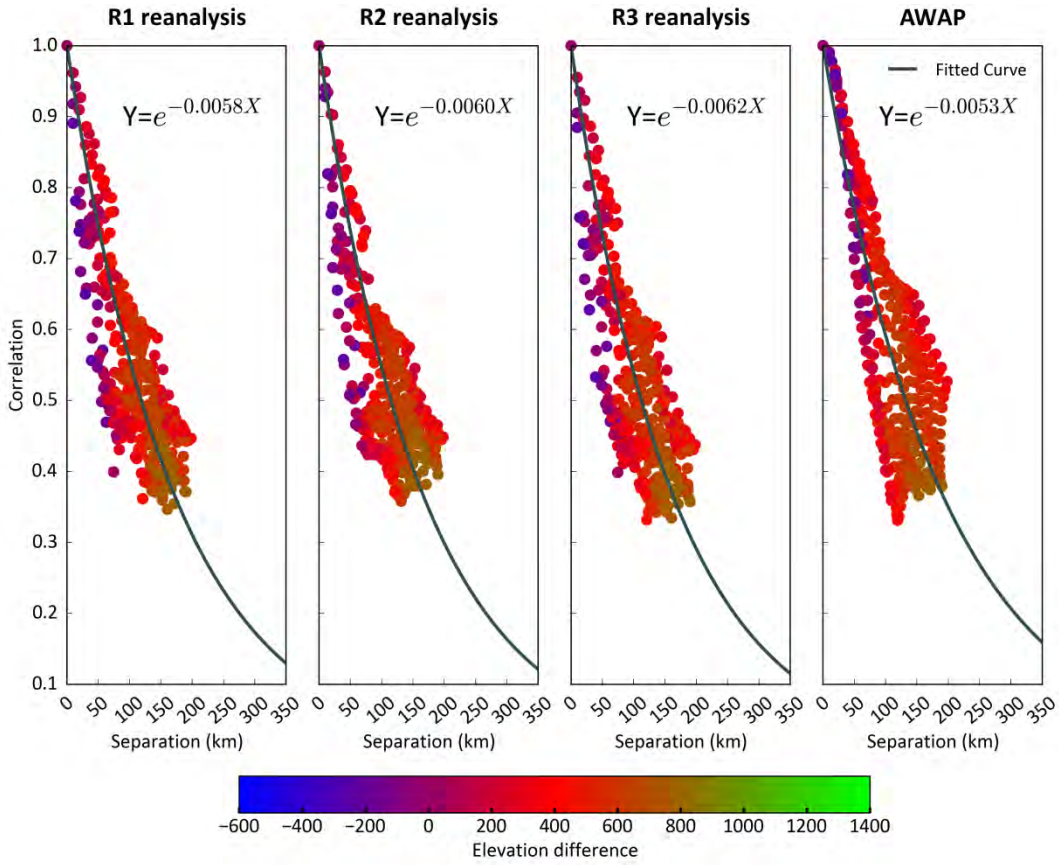

Figure 7.6 Spatial correlations function of the uncorrected reanalysis and AWAP at the Williams River site. The reference is W17 high elevation grid point.

The spatial correlation of the rainfall between the high elevation grid point (W17) and all other grid points of the Williams River site generated for the bias corrected reanalysis are shown in Figure 7.7. The corresponding spatial correlation functions are shown in Figure 7.8.

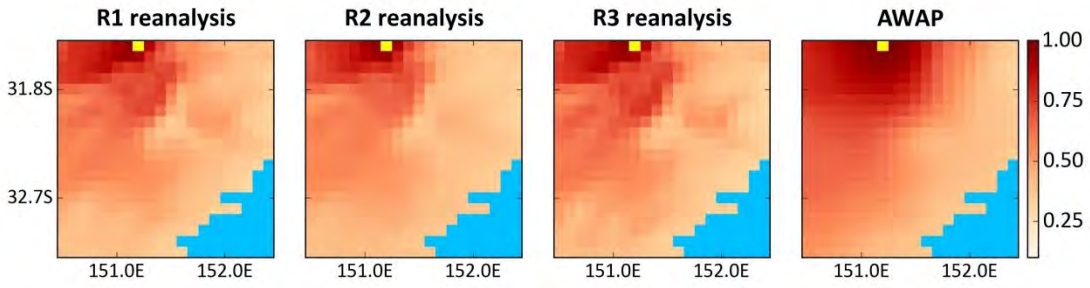

Figure 7.7 Spatial correlations for all grid points of bias corrected reanalysis and AWAP at the Williams River site. The reference is W17 high elevation grid point (shown in yellow boxes).

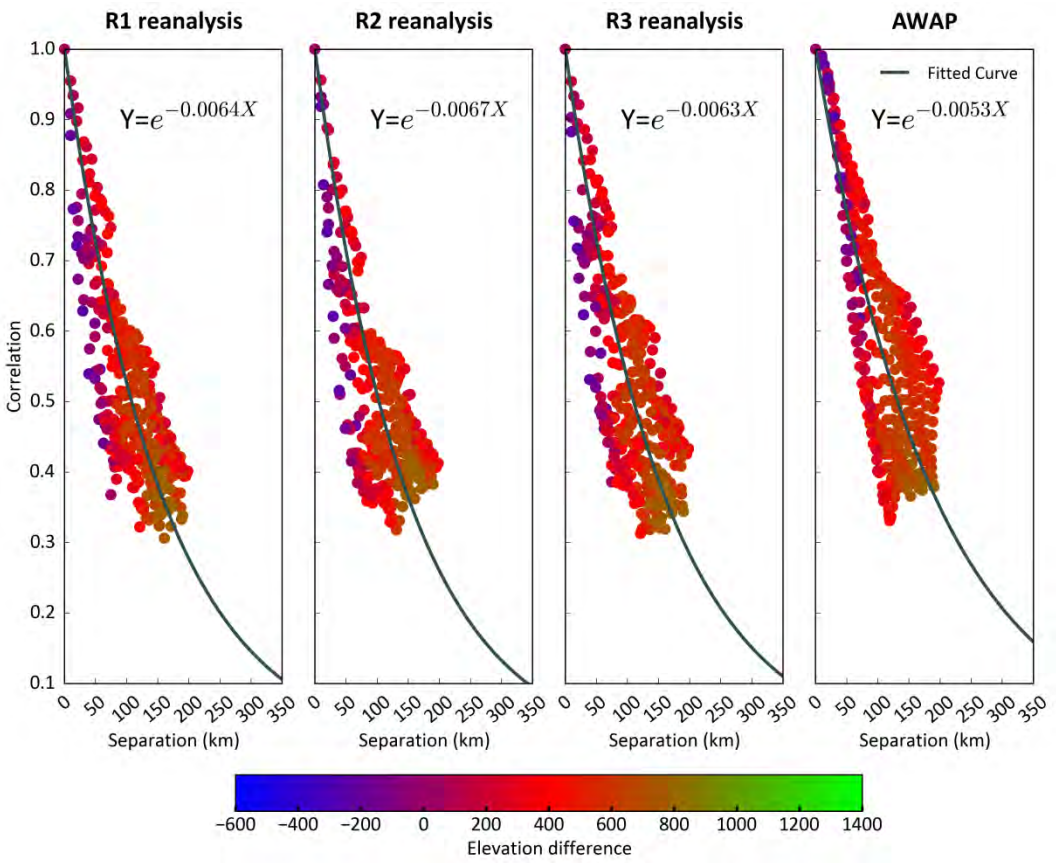

Figure 7.8 Spatial correlations function of the bias corrected reanalysis and AWAP at the Williams River site. The reference is W17 high elevation grid point.

The results indicate that the bias corrected reanalyses generate similar spatial patterns of correlations as the uncorrected data. Compared with AWAP, bias corrected R3 reanalyses appear to better reproduce the spatial pattern in the correlations of AWAP than R1 and R2 reanalyses. Figure 7.8 shows that all bias corrected reanalyses tend to underestimate the magnitudes of the spatial correlation of AWAP relative to the uncorrected. R1 and R2 reanalyses, have reduced exponents of -0.0064 and -0.0067 relative to the uncorrected data. Therefore, this suggests that bias correction has not improved the performance of reanalyses to reproduce the spatial correlation function of AWAP.

The spatial correlations of the daily rainfall of uncorrected reanalyses and AWAP between the low elevation grid point (W4) and all other grid points of the Williams River site are shown in Figure 7.9. The results show that grid points which are close to W4 have high correlations of the rainfall compared to the points which are located at long separations. Again the spatial pattern of correlations for all reanalyses mirrors

the topography, with low elevation points highly correlated to the other low elevation grid points. As explained previously, the occurrence of these high correlated grid points follow the same spatial pattern of the elevation, and appear to not be an effect from the proximity. Apart from the general trend, this effect is less pronounced in the AWAP data as AWAP shows a smoother correlation pattern.

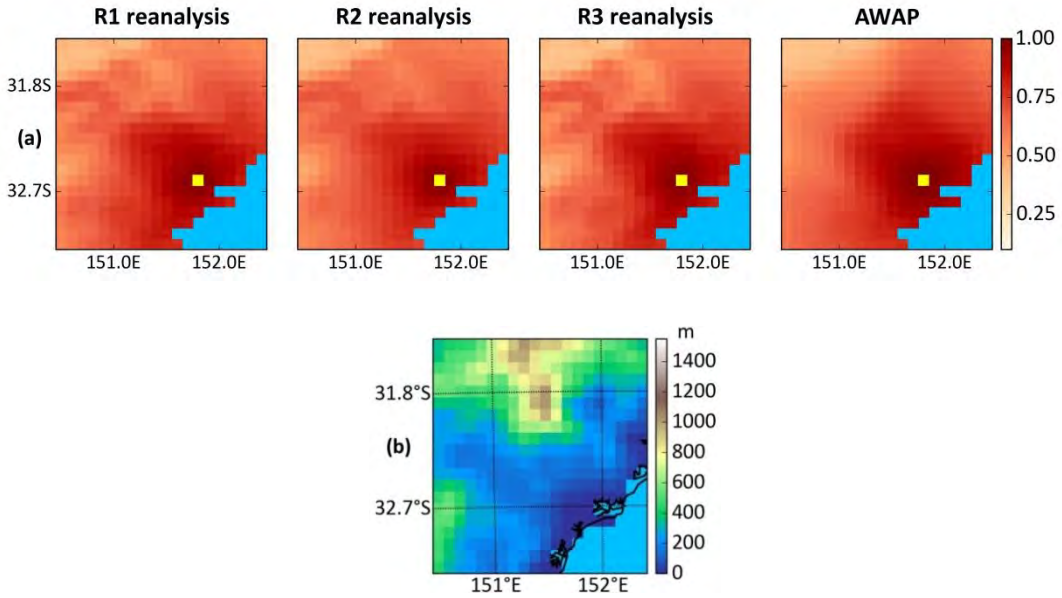

Figure 7.9 Spatial correlations for all grid points of uncorrected reanalysis and AWAP at the Williams River site: (a) spatial distribution of correlations between the grid points and (b) topography map of the site (as defined and used by NARCliM). The reference is W4 low elevation grid point (shown in yellow boxes).

The spatial correlation structure generated with reference to the low elevation grid point is shown in Figure 7.10. In contrast to the high elevation reference, all uncorrected reanalyses data simulate the spatial correlation function of AWAP well except for the few grid points separated by 100-150 km from the reference. However compared with Figure 7.6, there is less scatter in the correlation functions for all datasets for the low elevation point. It appears that there is a higher variability in the spatial correlation with reference to a high elevation point than to a low elevation reference.

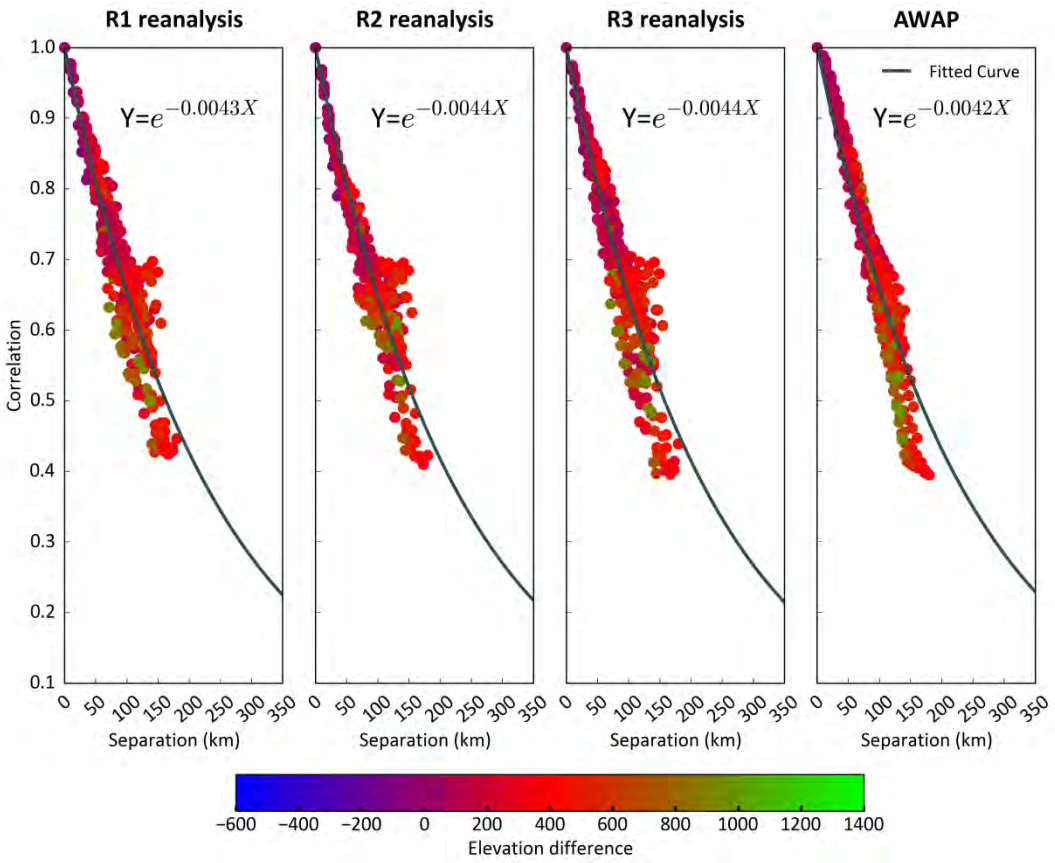

Figure 7.10 Spatial correlations function of the uncorrected reanalysis and AWAP at the Williams River site. The reference is W4 low elevation grid point.

The similar results generated for the bias corrected reanalysis and AWAP with reference to the low elevation grid point of the Williams River site is shown in Figures 7.11 and 7.12.

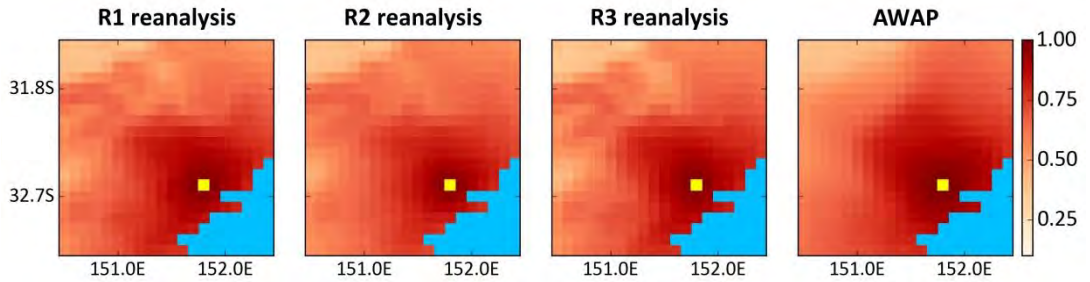

Figure 7.11 Spatial correlations for all grid points of bias corrected reanalysis and AWAP at the Williams River site. The reference is W4 low elevation grid point (shown in yellow boxes).

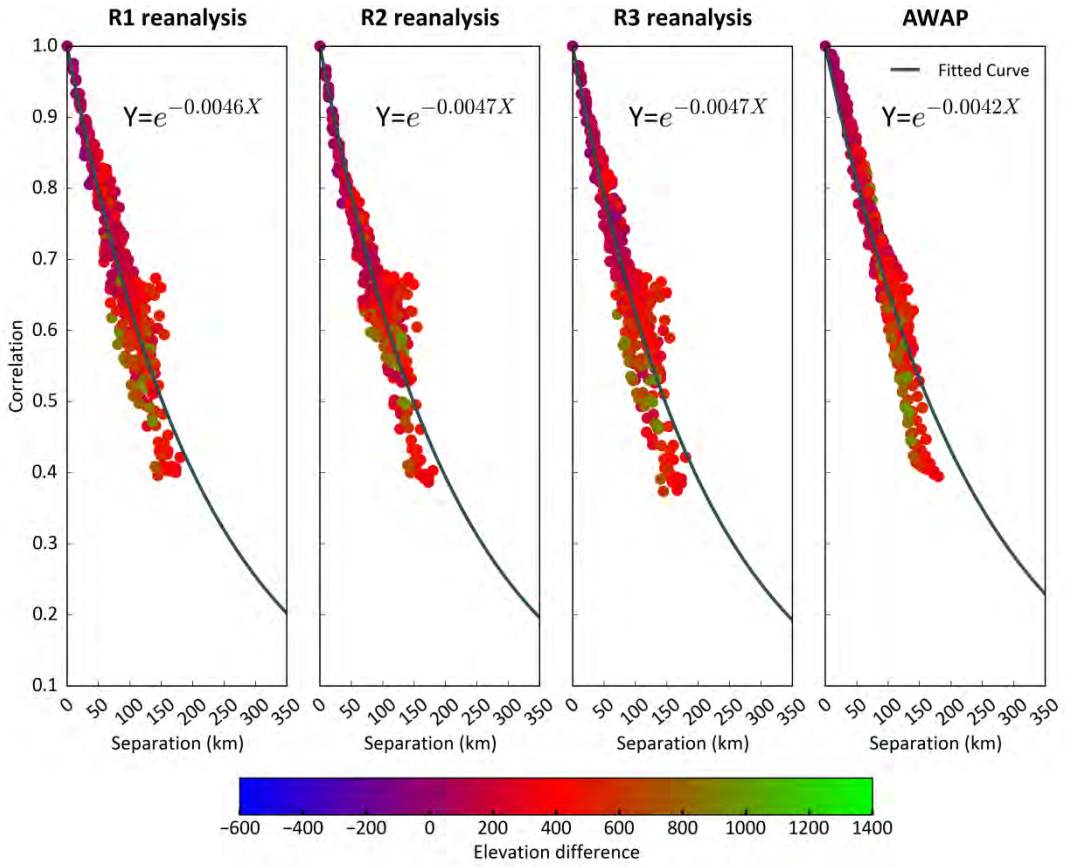

Figure 7.12 Spatial correlations function of the bias corrected reanalysis and AWAP at the Williams River site. The reference is W4 low elevation grid point.

Figures 7.11 and 7.12 are similar to Figures 7.9 and 7.10, suggesting that there is little difference in the performance of bias corrected reanalyses to capture the spatial correlation functions of AWAP for the low elevation reference. In contrast to the high elevation reference, all bias corrected reanalyses have a similar performance, with each underestimating AWAP autocorrelations by 10 to 12%.

Similarly, the spatial correlation plots of uncorrected reanalysis and AWAP generated with reference to high and low elevation grid points of the Richmond River site are shown in Figures 7.13 and 7.14 respectively. These results are similar to that of the Williams River site and hence, reflect that there is a consistency of the performance of the reanalyses and AWAP data between the sites.

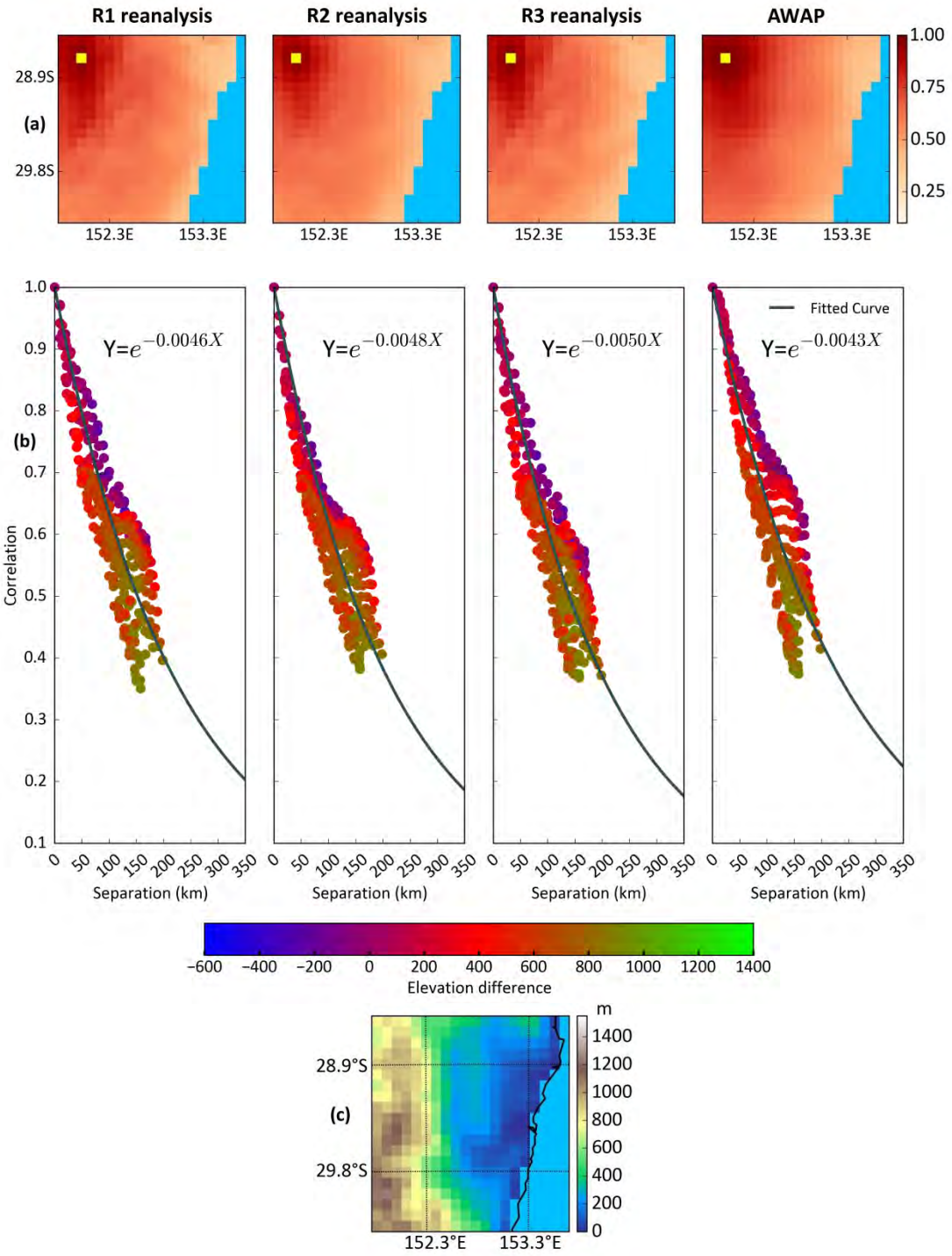

Figure 7.13 Spatial correlations for all grid points of uncorrected reanalysis and AWAP at the Richmond River site: (a) spatial distribution of correlations between the grid points, (b) spatial correlation vs separation and (c) topography map of the site (as defined and used by NARCliM). The reference is P20 high elevation grid point.

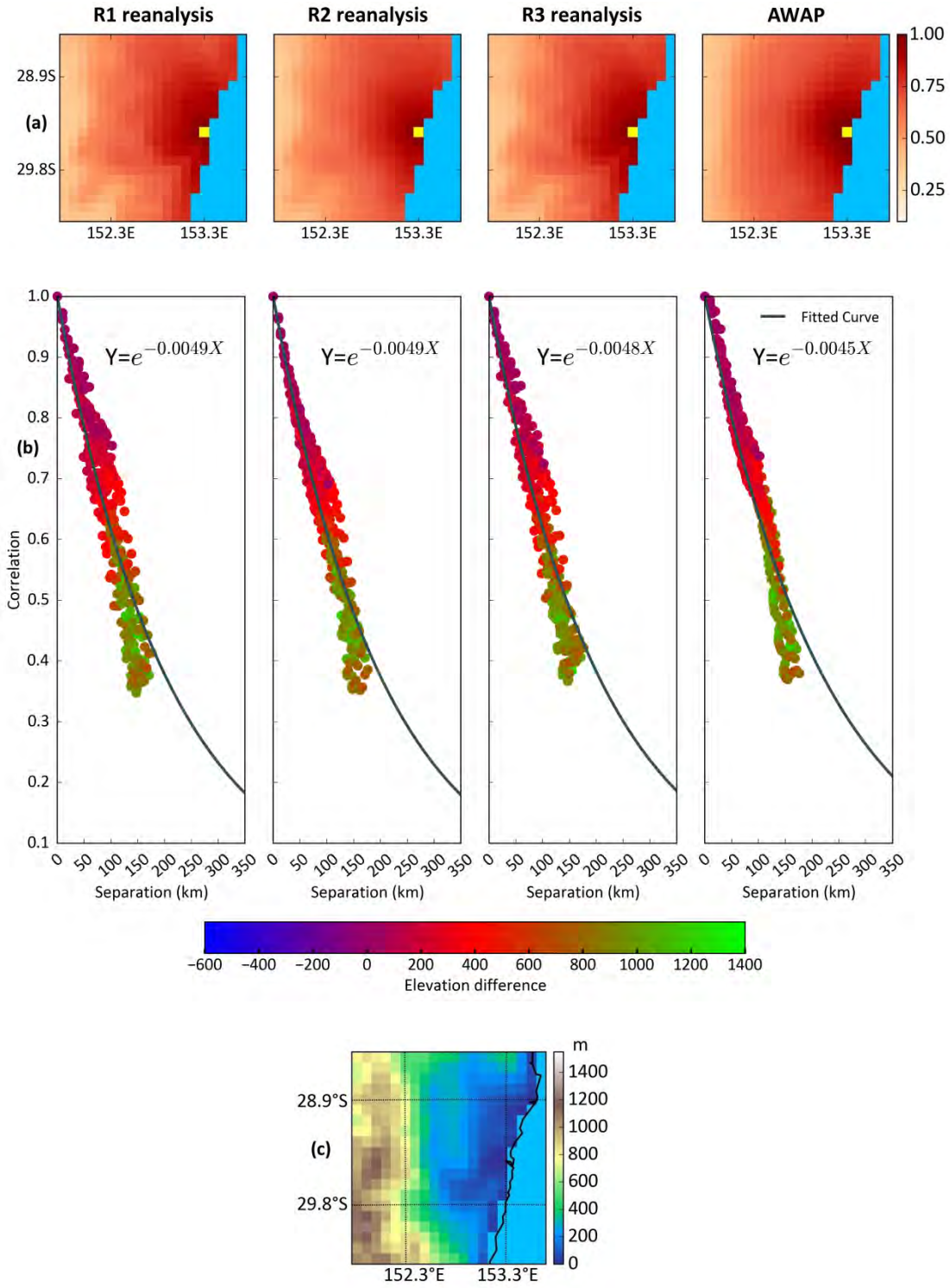

Figure 7.14 Spatial correlations for all grid points of uncorrected reanalysis and AWAP at the Richmond River site: (a) spatial distribution of correlations between the grid points, (b) spatial correlation vs separation and (c) topography map of the site (as defined and used by NARCliM). The reference is P9 low elevation grid point.

The spatial correlation plots generated for the bias corrected reanalysis and AWAP generated with reference to high and low elevation grid points of the Richmond River site are shown in Figures 7.15 and 7.16 respectively. At the high elevation reference of the Richmond River site, bias corrected R1 and R2 reanalyses tends to underestimate the AWAP spatial correlations 8 to 9% more than they did for the uncorrected. Comparing all three reanalyses, bias corrected R3 reanalysis better capture the spatial correlation functions of AWAP for both high and low elevation references.

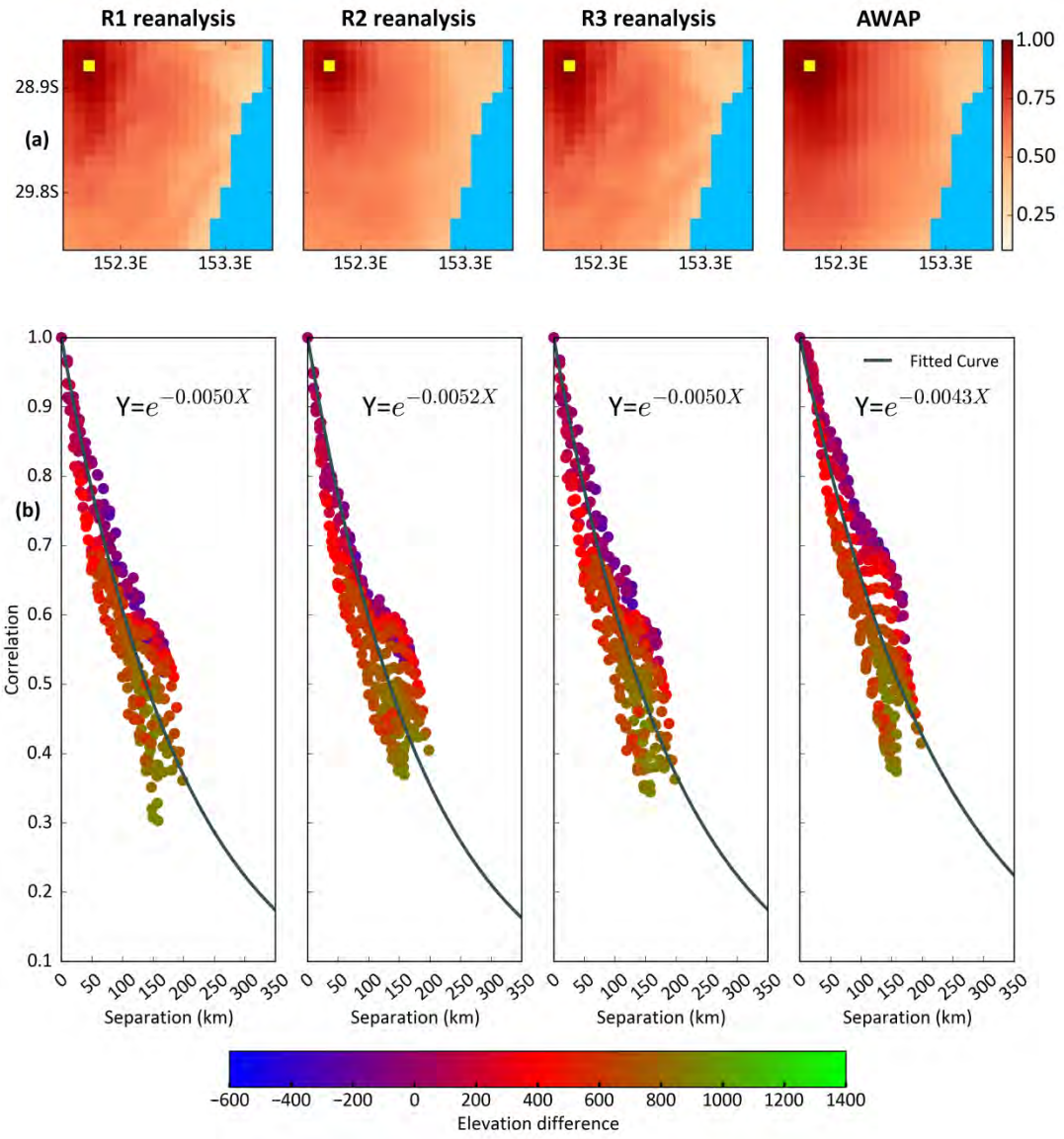

Figure 7.15 Spatial correlations for all grid points of bias corrected reanalysis and AWAP at the Richmond River site: (a) spatial distribution of correlations between the grid points and (b) spatial correlation vs separation. The reference is P20 high elevation grid point.

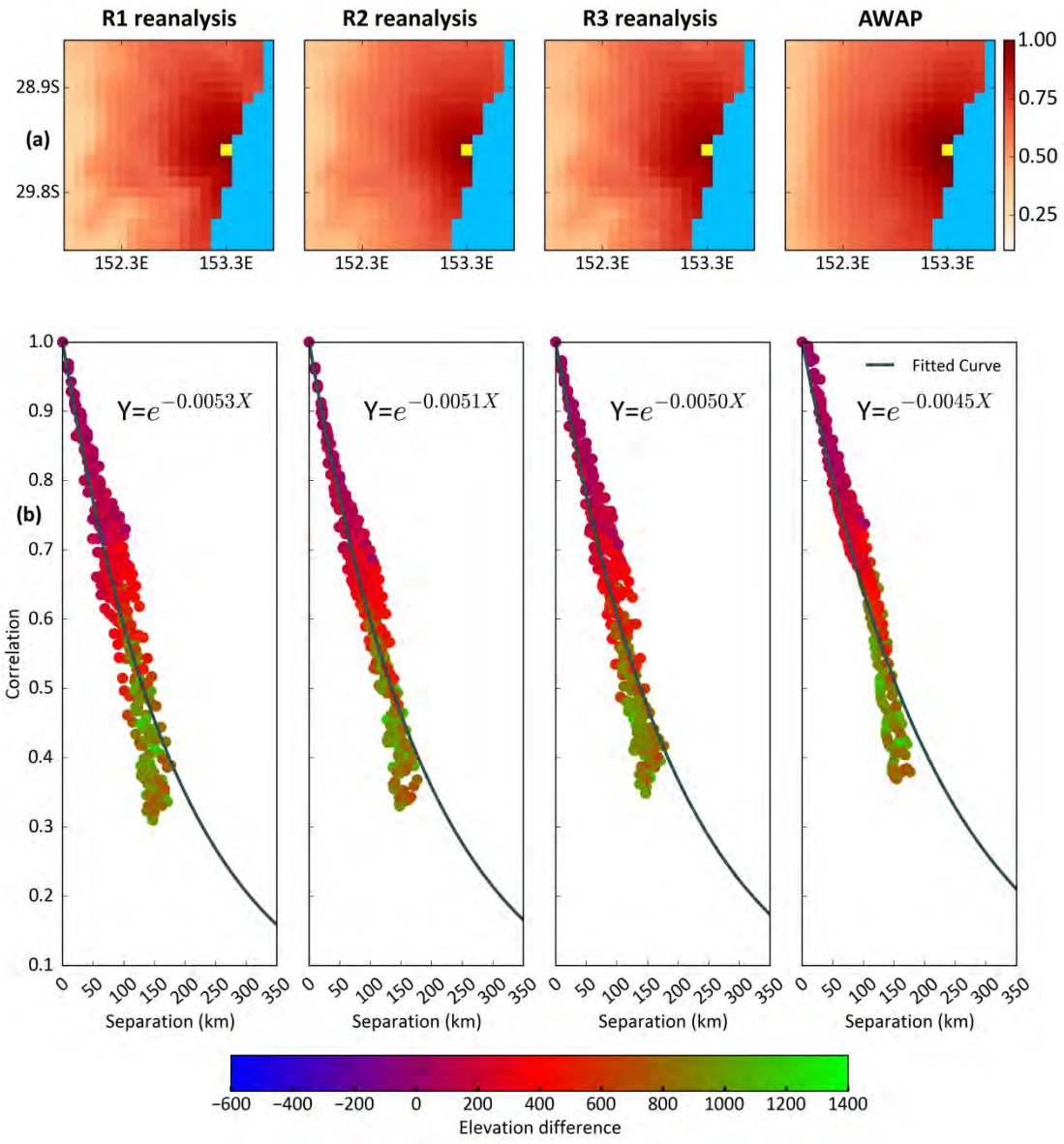

Figure 7.16 Spatial correlations for all grid points of bias corrected reanalysis and AWAP at the Richmond River site: (a) spatial distribution of correlations between the grid points and (b) spatial correlation vs separation. The reference is P9 low elevation grid point.

Figures 7.17 and 7.18 show the spatial correlation plots generated for the uncorrected reanalysis and AWAP at the Bega River site. According to the topography map shown in Figure 7.17c, there is a significant variation of the elevations at this site. The Australian Alps located from south-west to north are the highest elevations in the regions. This mountain range is well resolved in the spatial pattern of the correlation plots for all three reanalyses (Figure 7.17a) while mirroring the general spatial pattern of the topography across the site. This effect can also be seen in the spatial pattern of the AWAP, though not as distinctly as in the reanalyses

datasets. This suggests that the averaging smoothing effect of the topography in AWAP data is higher than that of the reanalysis at high-to-very high elevations (greater than 1200 m). However in the plots of spatial correlation functions, the reanalyses grid points located along the Australian Alps (shown in the blue markers in Figure 7.17b) appear to be less correlated with the reference point than that of AWAP's grid points, and have a significant downward shift from the fitted exponential curve, resulting up to 53% underestimation of the AWAP correlations. This might be attributed to the averaging of topography in AWAP data, and so with the daily rainfall time series.

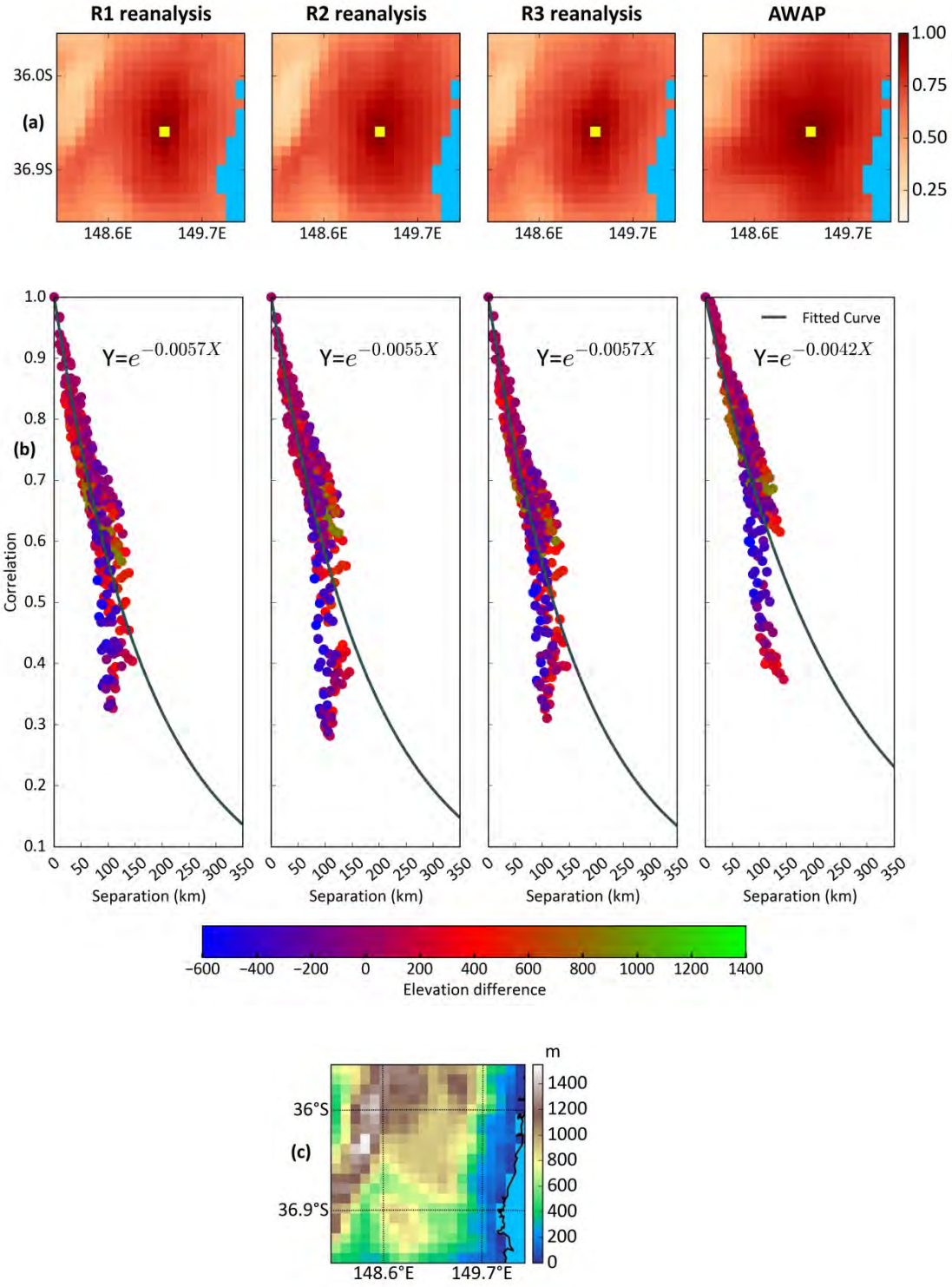

Figure 7.17 Spatial correlations for all grid points of uncorrected reanalysis and AWAP at the Bega River site: (a) spatial distribution of correlations between the grid points, (b) spatial correlation vs separation and (c) topography map of the site (as defined and used by NARCliM). The reference is Q12 high elevation grid point.

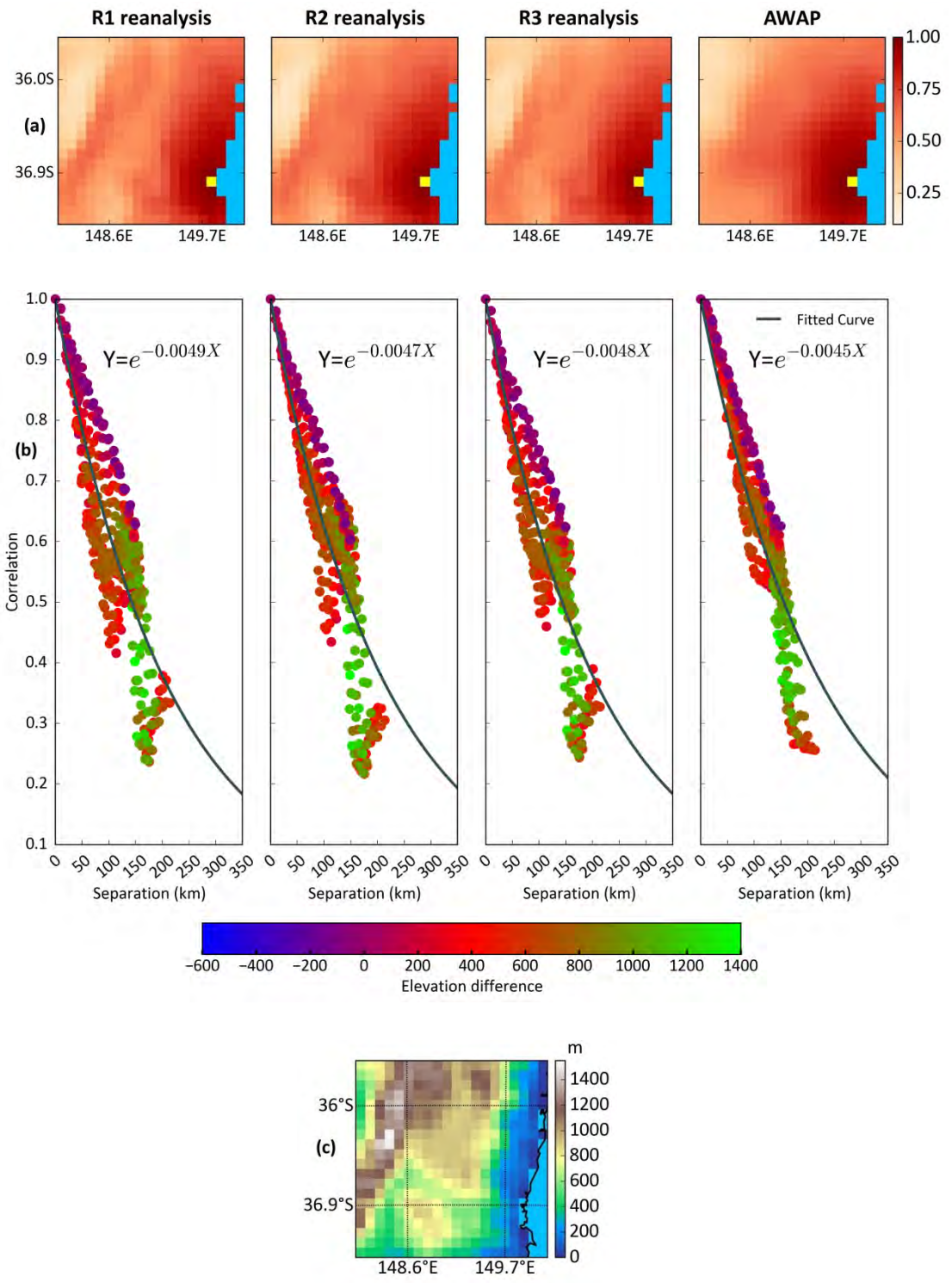

Figure 7.18 Spatial correlations for all grid points of uncorrected reanalysis and AWAP at the Bega River site: (a) spatial distribution of correlations between the grid points, (b) spatial correlation vs separation and (c) topography map of the site (as defined and used by NARCliM). The reference is Q3 low elevation grid point.

The corresponding plots generated for the bias corrected reanalyses and AWAP at low and high elevation references at the Bega River site are shown in Figures 7.19 and 7.20.

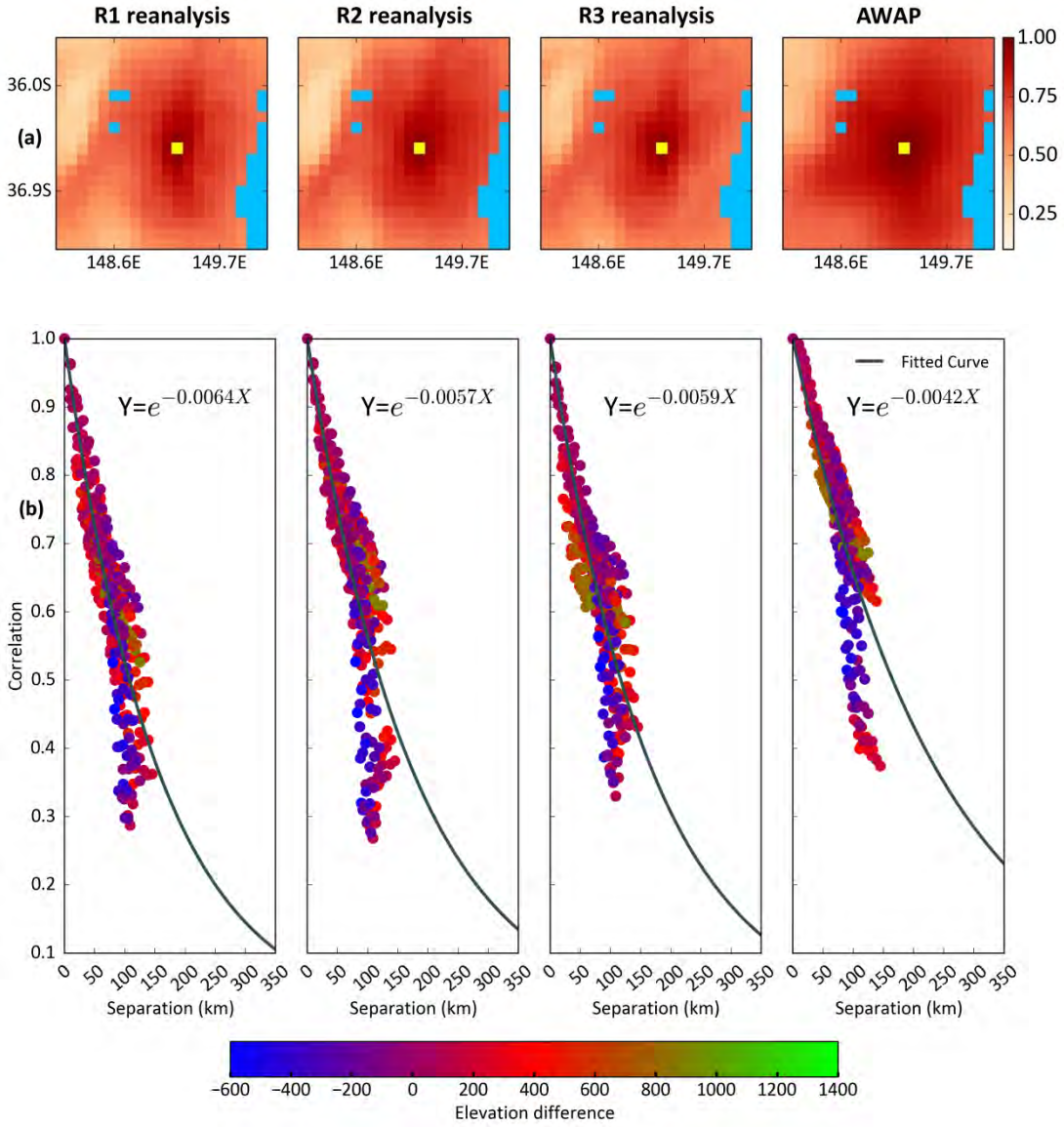

Figure 7.19 Spatial correlations for all grid points of bias corrected reanalysis and AWAP at the Bega River site: (a) spatial distribution of correlations between the grid points and (b) spatial correlation vs separation. The reference is Q12 high elevation grid point.

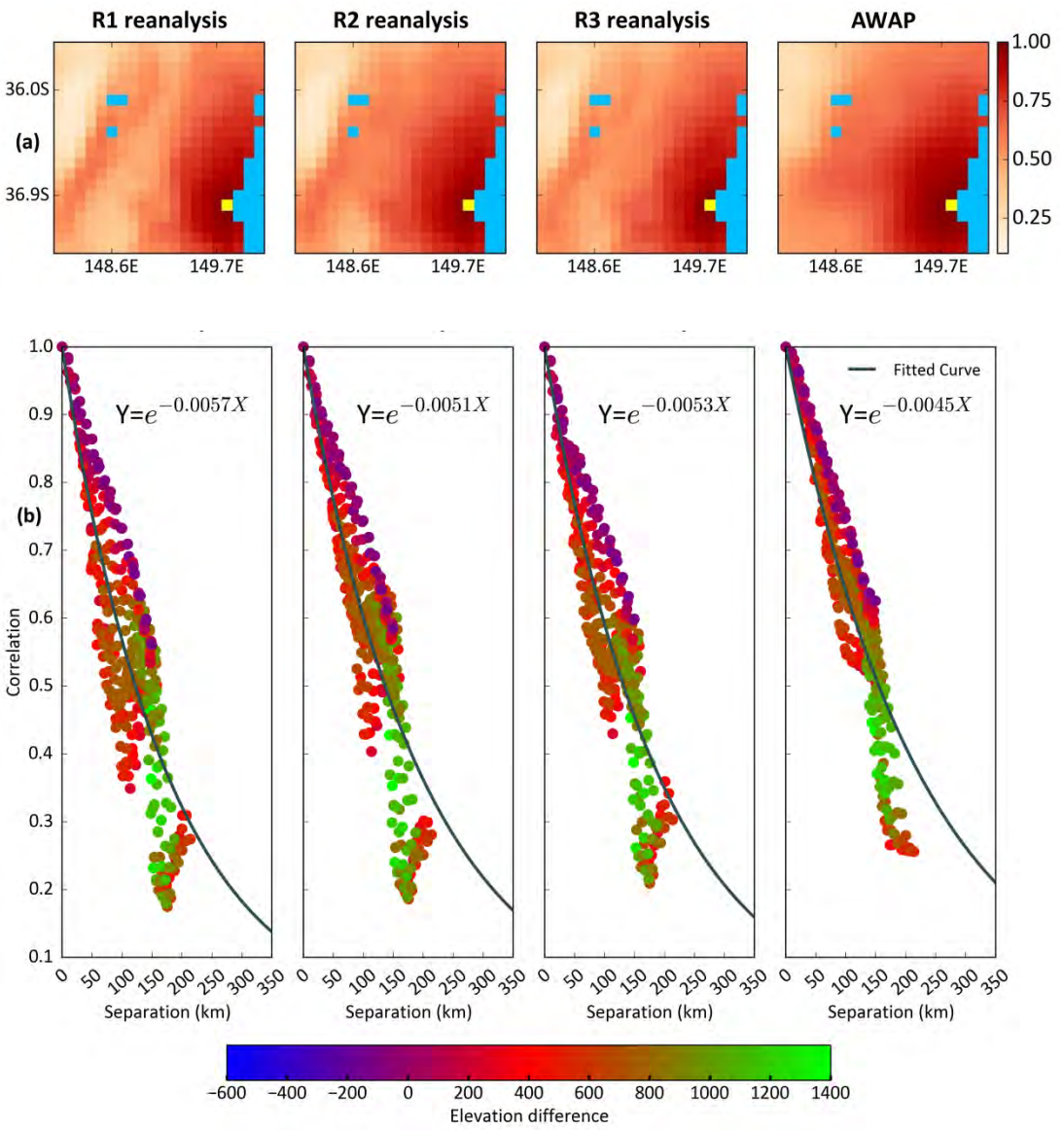

Figure 7.20 Spatial correlations for all grid points of bias corrected reanalysis and AWAP at the Bega River site: (a) spatial distribution of correlations between the grid points and (b) spatial correlation vs separation. The reference is Q3 low elevation grid point.

The spatial correlations calculated for the uncorrected reanalysis and AWAP with reference to the low and high elevation grid points (S8 and S22) at the Sydney site (Figures 7.21 and 7.22) also follow a similar spatial pattern to the topography map of the area. As was seen at the Richmond River site, all reanalyses datasets of Sydney site have a spatial correlation function similar to each other, but show some discrepancies compared with the spatial correlations of AWAP data, particularly for the correlations calculated with reference to the high elevation grid point. For example when the reference is a high elevation grid point, AWAP has more scatter

in the correlations than reanalyses for separations greater than 200 km. For the correlation functions generated at the low elevation point, all reanalyses data underestimate the correlations of AWAP for the large separations.

The results for the bias corrected reanalysis shown in Figures 7.23 and 7.24 are similar to the uncorrected reanalyses. All bias corrected reanalyses tend to underestimate the spatial correlation function of AWAP. However, this effect is not as significant as in the Bega River site. As for the Bega River site, R1 and R3 reanalyses has the highest underestimation of the spatial correlations of AWAP.

In general for all four sites, both uncorrected and bias corrected reanalyses underestimate the spatial correlation function, and this underestimation is more significant at Bega River (up to 53%) and Sydney (up to 42%) sites, though more typically the underestimation is 10-20%. Bias corrected R1 reanalysis appears better capture the spatial correlation of AWAP at Williams River and Richmond site, while R2 reanalysis perform better for the Bega River and Sydney sites. All three reanalyses tend to underestimate the magnitudes of spatial correlations of AWAP even after bias correction.

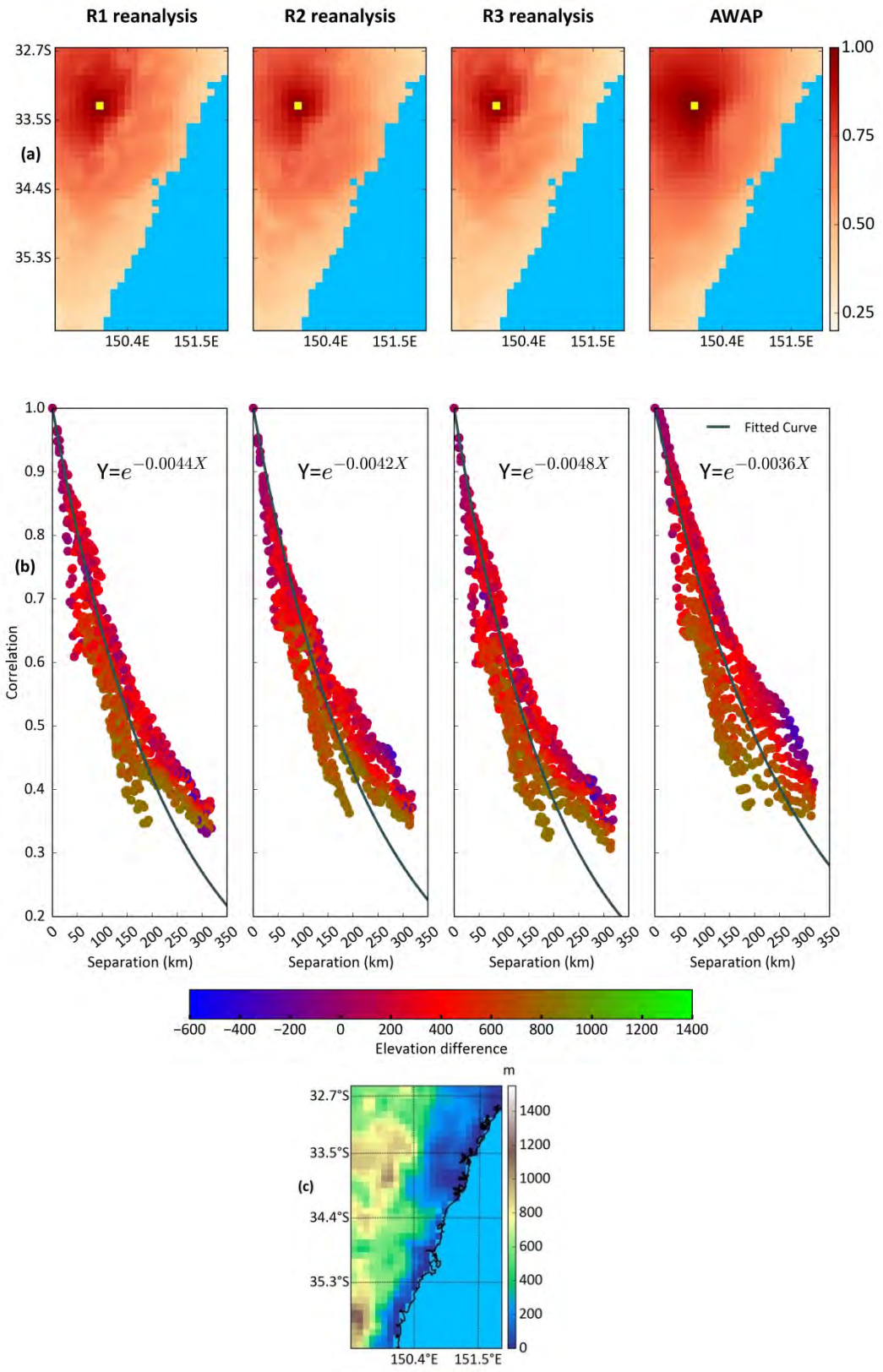

Figure 7.21 Spatial correlations for all grid points of uncorrected reanalysis and AWAP at the Sydney site: (a) spatial distribution of correlations between the grid points, (b) spatial correlation vs separation and (c) topography map of the site (as defined and used by NARCliM). The reference is S22 high elevation grid point.

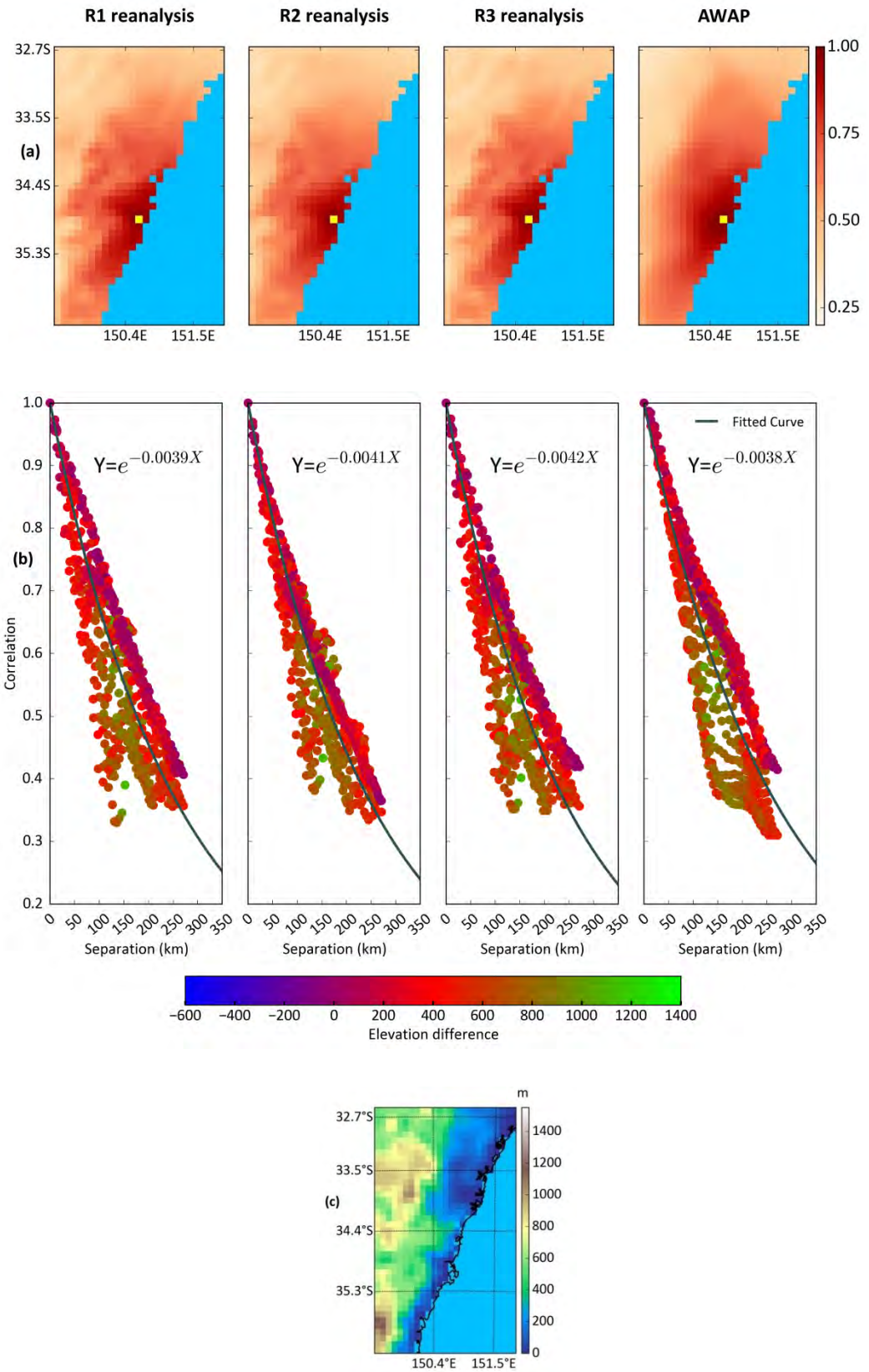

Figure 7.22 Spatial correlations for all grid points of uncorrected reanalysis and AWAP at the Sydney site: (a) spatial distribution of correlations between the grid points, (b) spatial correlation vs separation and (c) topography map of the site (as defined and used by NARCliM). The reference is S8 low elevation grid point.

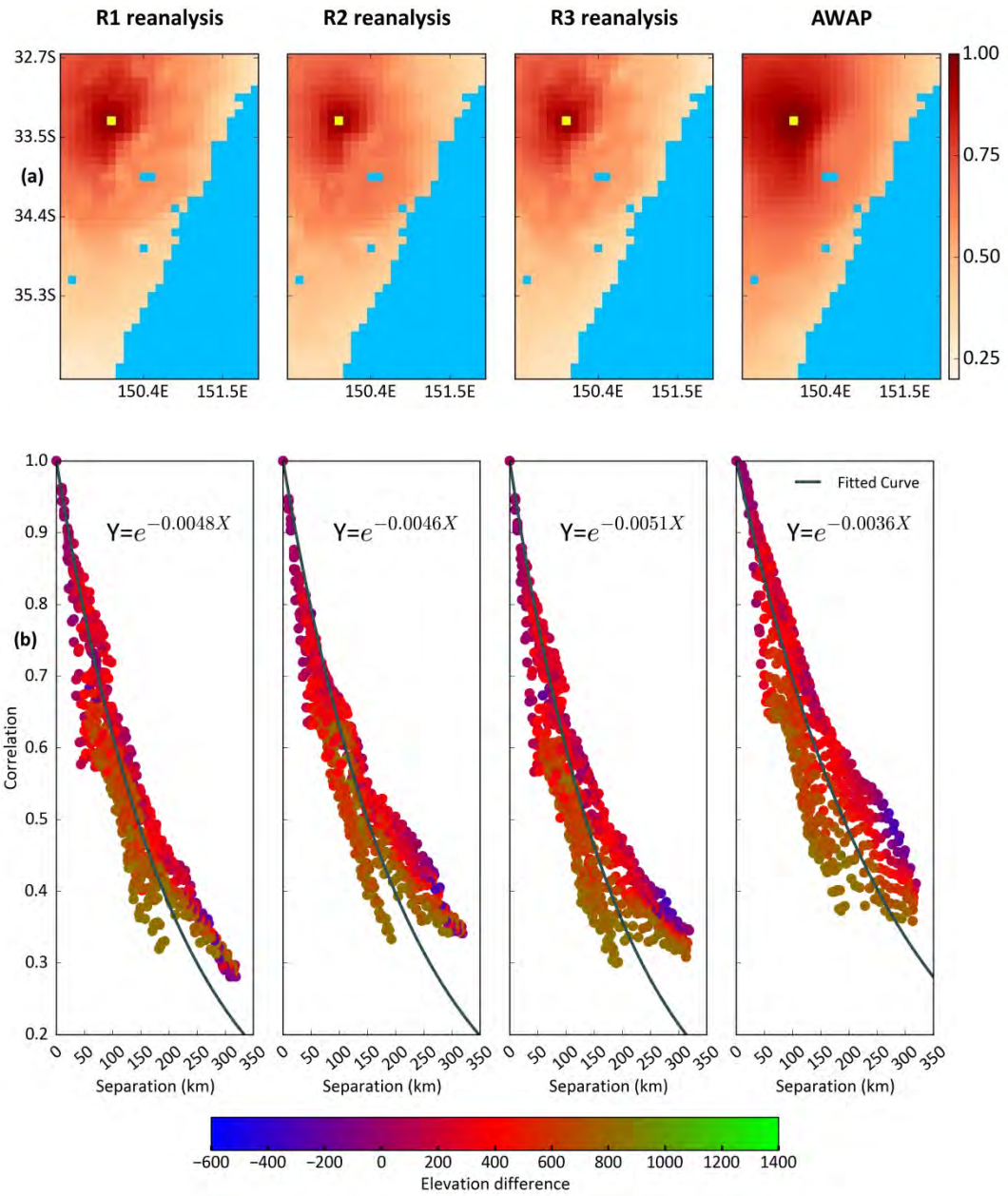

Figure 7.23 Spatial correlations for all grid points of bias corrected reanalysis and AWAP at the Sydney site: (a) spatial distribution of correlations between the grid points and (b) spatial correlation vs separation. The reference is S22 high elevation grid point.

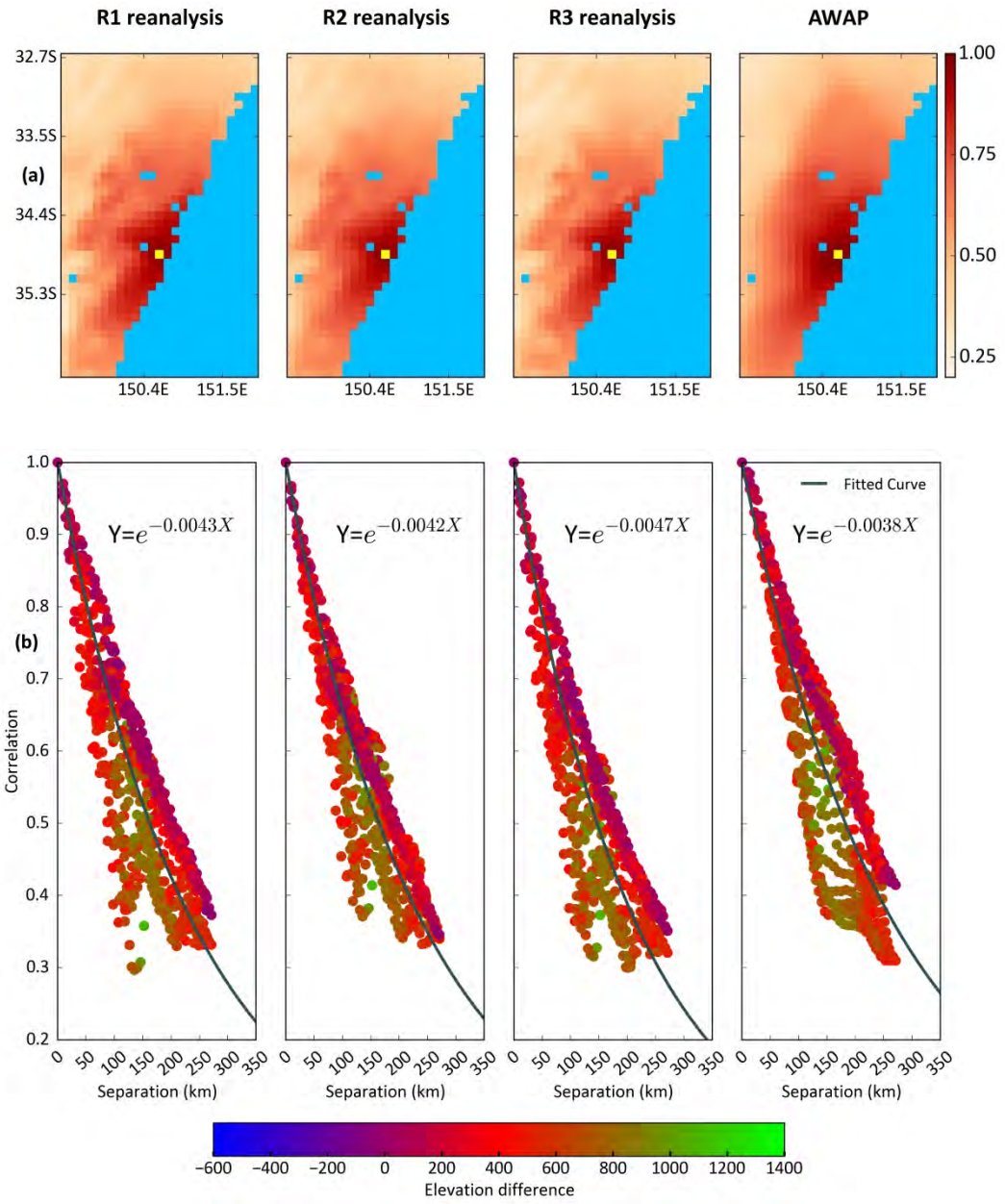

Figure 7.24 Spatial correlations for all grid points of bias corrected reanalysis and AWAP at the Sydney site: (a) spatial distribution of correlations between the grid points and (b) spatial correlation vs separation. The reference is S8 low elevation grid point.

Additionally for all sites, grid points which are close to the reference have high correlations than points farther away. Further, rainfall at high elevation points are more highly correlated to the rainfall of close by high elevation points and rainfall at low elevation points are more correlated to the close by low elevation points. However, this is only true for the 'close by' grid points (separated approximately by

500-1000 km) which have similar elevations as for the reference. For example, at the Bega River site, grid points located along the Australian Alps which have even higher elevations are less correlated with the high elevation reference point. Therefore, this suggests that rainfall is more correlated to the distance between the points (separation) than to the difference of the elevation of the two points. Figures 7.25 and 7.26 show the spatial correlation of the rainfall versus elevation difference for all grid points of the Bega River site with reference to the high, and low elevation grid point respectively. As for the figures, the rainfall of the nearby grid points are more correlated to the reference than the grid points further away, even if they have similar or different elevation differences. Therefore, this suggests that there is a relationship between the rainfall and the distance between the gauge locations or grid points, which appears to be is less synchronous with the elevation.

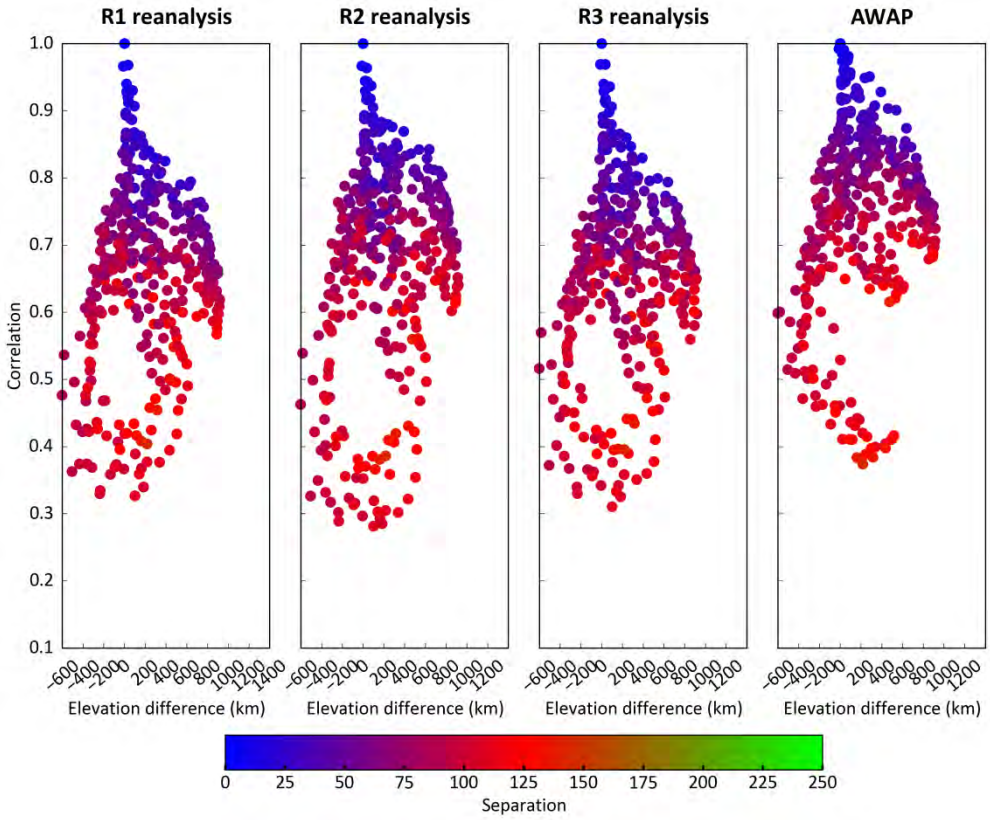

Figure 7.25 Elevation vs spatial correlation for all grid points of uncorrected reanalysis and AWAP at the Bega River site: The reference is Q12 high elevation grid point.

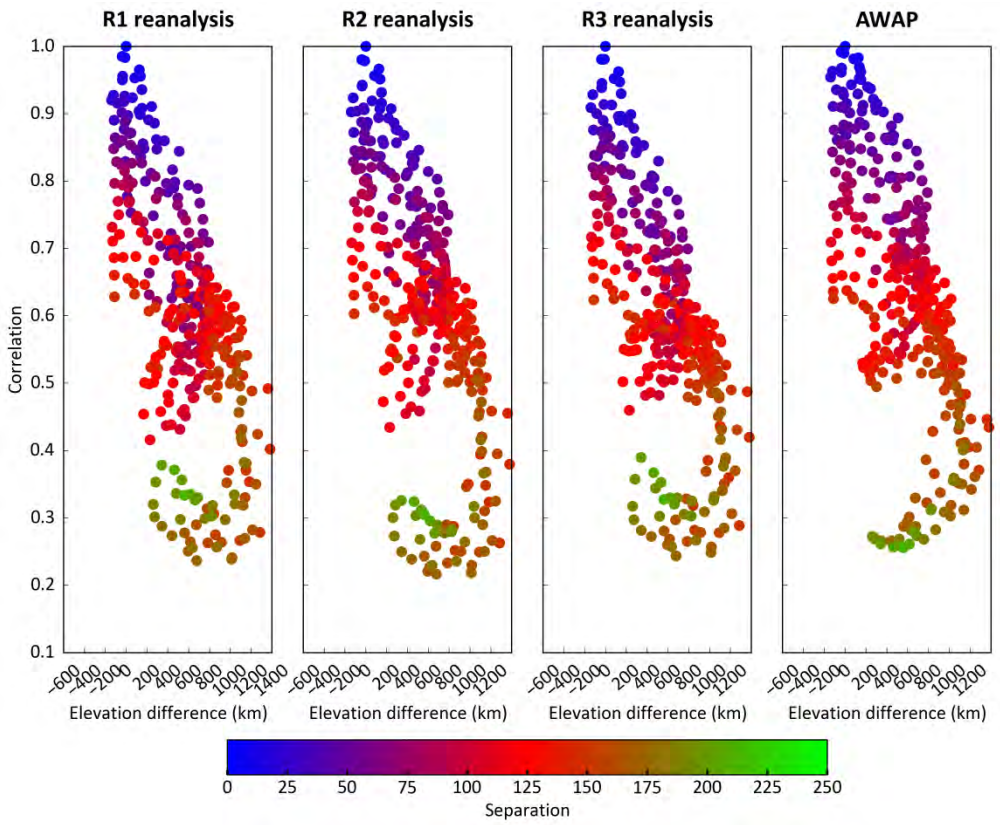

Figure 7.26 Elevation vs spatial correlation for all grid points of uncorrected reanalysis and AWAP at the Bega River site: The reference is Q3 low elevation grid point.

7.3 Testing the spatial correlation of NARCliM reanalyses and AWAP against rain gauge data

Spatial correlation functions between the rain gauges, uncorrected reanalyses grid points and AWAP grid points are shown in Figure 7.27. In this section, spatial correlations were calculated only for the grid points (reanalyses and AWAP) which included the rain gauges, while the spatial correlation functions shown in the previous section are for all grid points at a site. The left hand side subplots are the spatial correlation functions with reference to the high elevation grid points while the right hand side subplots are with reference to the low elevation points (Table 7.1) selected at each site. It should be noted that three rain gauges; rain gauge P15 of the Richmond River site and rain gauges S4 and S29 of the Sydney site were removed from the analyses since they have abnormally low correlations (between the reference and other gauges) compared with other surrounding rain gauges, thus available rainfall records of these gauges were judged as unreliable. No reasons for this abnormal result could be identified other than unusual topographic conditions.

The spatial correlation functions in Figure 7.27 show that both reanalyses and AWAP gridded datasets have correlations higher than that of the rain gauges, with approximately 20 to 30% overestimation of correlations relative to the raingauges for all the grid points used. However, both reanalyses and AWAP showed the same general trend of the spatial correlation function of rain gauges for all low and high elevation references, except for the high elevation reference (P20) of the Richmond River site. For the correlation functions generated for the high elevation grid points, all reanalyses slightly underestimate the correlations of AWAP, as was found in the previous section.

The results suggest that neither NARCliM reanalyses nor AWAP data correctly reproduce the spatial correlation function of the rain gauges for any of the sites. All reanalyses are able to reproduce the spatial correlations of AWAP rainfall with a slight underestimation. This suggest that the 10 km resolution reanalyses data are nearly equally capable of reproducing the spatial correlations of 5 km AWAP data, even though both datasets overestimate the observed spatial correlations of the raingauges. The discrepancies between the reanalyses are insignificant compared with differences between AWAP and rain gauge data.

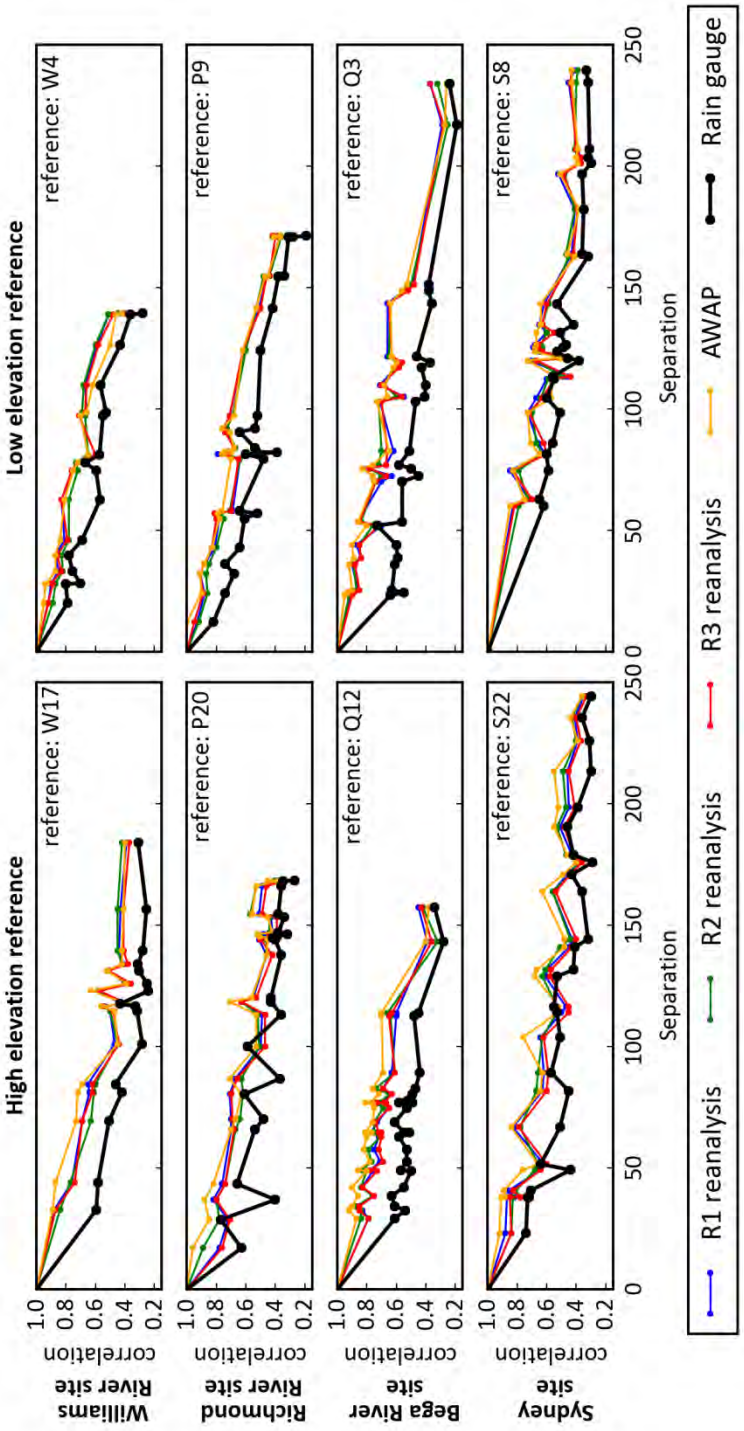

Figure 7.27 Spatial correlation between rain gauges (left: high elevation rain gauges as the reference and right: low elevation rain gauge as the reference). Note that reanalyses rainfalls are uncorrected.

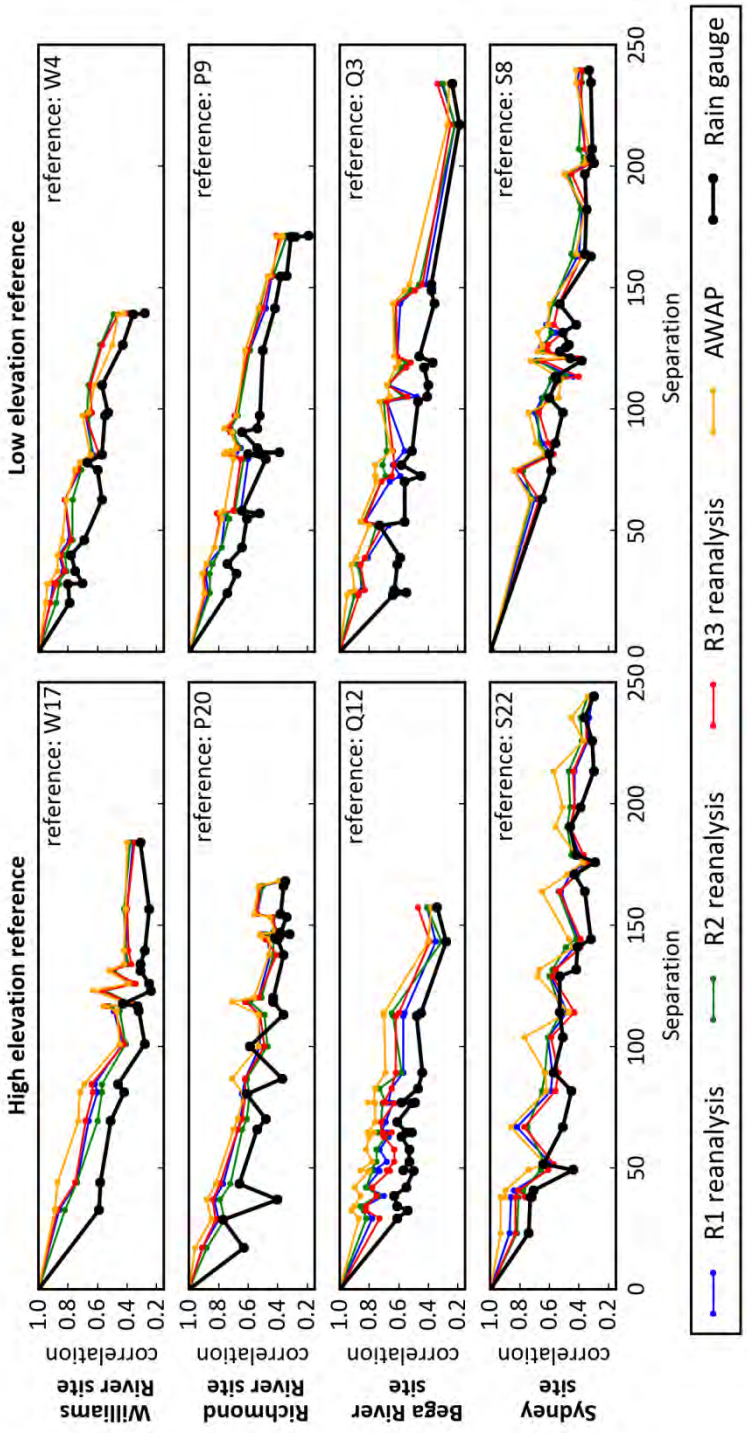

Figure 7.28 Spatial correlation between rain gauges (left: high elevation rain gauges as the reference and right: low elevation rain gauge as the reference). Note that reanalyses rainfalls are bias corrected.

The spatial correlation functions generated using the bias corrected reanalyses, AWAP and rain gauge data are shown in Figure 7.28. As found in the previous section, the differences between the uncorrected and bias corrected results are small.

Therefore, results suggest that bias correction does not change the performance of reanalyses to capture the spatial correlation of either AWAP or rain gauges.

7.4 Conclusions

The ability of NARCliM reanalyses data to reproduce the spatial variation of the autocorrelation of the AWAP and raingauge rainfall was assessed in this chapter. The analysis of the spatial variability of correlation showed that the spatial pattern of the correlation of the reanalyses rainfall is qualitatively similar to that of the AWAP data and is driven by the spatial pattern of the topography in combination with the distance between the rain gauges. Grid points (both reanalyses and AWAP) which are close to the reference have higher correlations than the far points, but this appears to be primarily because nearer grid points are at similar elevations. Rainfall at high elevation points are more correlated to the rainfall of the close by high elevation points and rainfall at low elevation points are more correlated to the close by low elevation points.

The spatial correlation trend of the rainfall for all datasets (gridded and point) approximately follow a single exponential function with distance. This exponential correlation function tends to have more scatter when a high elevation grid point is used as the reference. All reanalyses reproduce the overall spatial correlation trend of AWAP. This means that the decrease in correlation with distance is similar between the reanalyses and AWAP. The main discrepancy is that R1 and R3 tend to underestimate AWAP for large separations between the grid points for some site locations with correlations about 10 to 20% lower. Both reanalyses and AWAP gridded datasets have correlations higher than that of the rain gauges, with approximately 20 to 30% overestimation for all the grid points used.

The bias corrected reanalyses tend to underestimate AWAP more than the uncorrected data for all sites, with the performance of R1, R2 and R3 varying between sites. Therefore, bias correction slightly degrades the fit of the reanalyses to the AWAP spatial correlations. Finally, neither NARCliM nor AWAP reproduce the spatial correlations of the daily rainfall of rain gauges.

Chapter 8
East Coast Low impacts on the relationship between rainfall and elevation

8.1 Introduction

The spatial patterns of the rainfall, particularly at daily time resolution, are mostly related to the topography and some other factors, such as prevailing wind directions (Hutchinson, 1998a). As discussed in Section 5.1.3, Hutchinson (1998a,b) analysed this dependence of the rainfall with elevation using five spline models and found that the rainfall is highly correlated with the elevation.

The statistical testing results, particularly the mean annual rainfall patterns presented in Chapters 5 and 6 showed that there is a possible link between the rainfall and topography. This link was consistently seen in both NARCliM reanalyses and AWAP data for all sites except for the Richmond River site which had a negative relationship between the mean annual rainfall of AWAP and the topography. The analysis in this chapter does investigate the elevation dependency in AWAP, because Hutchinson's elevation dependent spline model was used for interpolation in generating AWAP. However, the elevation dependency in the NARCliM is investigated. Further both AWAP and reanalyses data showed a band of high rainfall values along the coast which seems to be unrelated to the topography and appears in all datasets. This indicates that the rainfall is not only related with the topography, but that there are also possible ocean interactions influencing the mean rainfall distribution along the coastline of NSW.

As explained earlier in Chapter 1, the research work presented in this thesis was carried out under the ESCCI- East Coast Lows (ECL) Project 5. Linking with the objectives of ECL Project 5, this chapter aims to fulfil the third major objective of this thesis: Study the existing relationship between the rainfall and topography, and assess the impacts of ECLs on this relationship.

Some preliminary results on the relationship between NARCliM rainfall and elevation were discussed for the Merriwa site in Chapter 5 and the other sites in Chapter 7. The positive trends shown in the scatter plots (Figure 5.13) generated for

the three reanalyses showed that the high rainfall values are mostly associated with high elevations. McMahon (1964) also found that there is a direct influence of topography on rainfall in the Hunter Valley. Incorporating findings of McMahon (1964) and the results in Chapters 5 and 7, the relationship between the rainfall and elevation is further investigated in this chapter, while trying to link whether there are any impacts from ECLs. The Williams River site located in the Hunter Region was selected for the analysis in this chapter. The three 10 km resolution NARCliM reanalyses datasets, 5 km resolution AWAP data and rain gauge data (see Table 3.4) available for the period of 1950-2009 at the Williams River site were used for the analysis.

8.2 Mean annual rainfall vs Elevation

Scatter plots of NARCliM mean annual rainfall vs elevation for all grid points of the Williams River site are shown in Figure 8.1. The 10 km resolution elevation data used by the NARCliM project was used as the elevation in this plot for both the NARCliM and AWAP data.

A summary of the linear regression analysis for the three reanalyses and AWAP data is shown in Table 8.1. The low correlations (r) reflect that there is a weak relationship between the rainfall and elevation for all datasets. The highest r^2 value of 0.20 for R2 reanalysis, indicates that only 20% of the total variation of the rainfall is explained by the linear relationship with elevation, while 80% of the variation remains unexplained. For AWAP, the correlation is negative and only 1% of the variation of the rainfall is explained by the linear relationship between the rainfall and elevation. Therefore, these results suggest that there is only a weak linear relationship between rainfall and elevation. However, statistically significant p-values (less0.05) for all three reanalyses indicate that results are different from the null hypothesis (i.e. no relationship of rainfall with elevation), so the relationship between rainfall and elevation, while weak, is statistically significant.

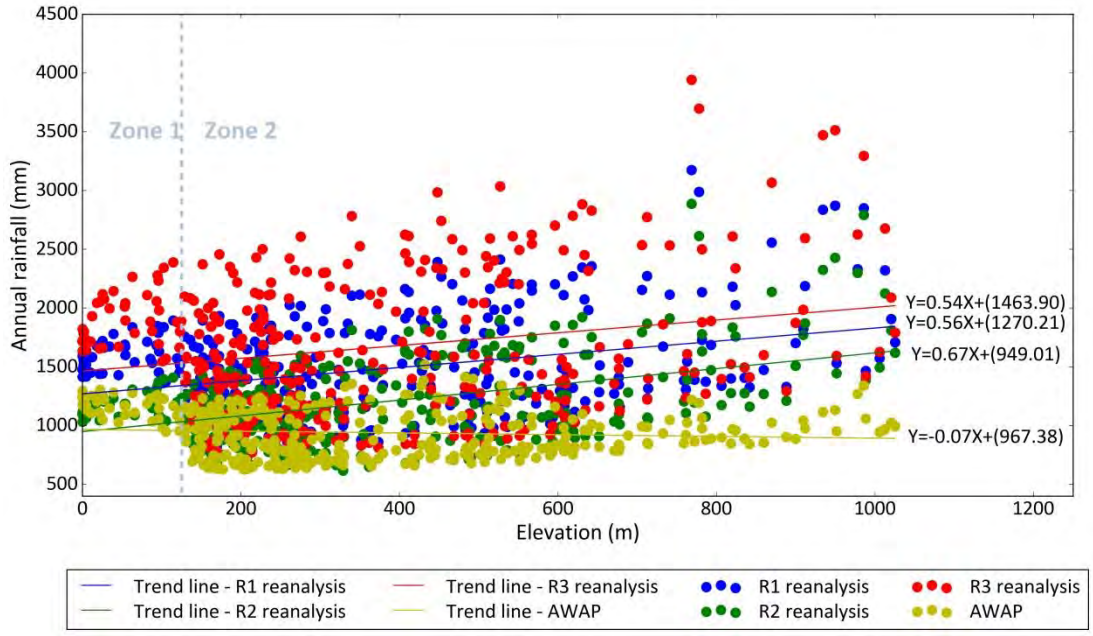

Figure 8.1 Scatter plots of NARCliM mean annual rainfall vs elevation for reanalyses and AWAP data. Zone 1 and Zone 2 are regions with two different trends.

Table 8.1 Summary of the regression analysis for all gridded datasets

Data	*Regression equation*	*Correlation (r)*	*R-squared (r^2)*	*p-value*
R1 reanalysis	Y=0.56X+1270.21	0.32	0.11	0.001
R2 reanalysis	Y=0.67X+949.01	0.45	0.20	7.99e-19
R3 reanalysis	Y=0.54X+1463.90	0.22	0.05	2.29e-05
AWAP	Y=-0.07X+967.38	-0.09	0.01	0.1

However by visually inspecting the linear trends in Figure 8.1, there are two different trends in rainfall; one for the grid points which have elevations less 125 m and the other is for the grid points where the elevation is greater than 125 m (shown as Zone 1 and 2 in Figure 8.1). Therefore, dividing the rainfall into two separate samples and assessing each separately may improve the understanding of the relationship between rainfall and elevation. The relationship between the elevation and gridded rainfall, and rain gauge data is compared in Figure 8.2. The same rain

gauges used in Section 7.2 (Table 3.4) were used in this plot. There are two differences between Figure 8.1 and Figure 8.2: (1) only grid points which included rain gauges were used for the comparison, and (2) elevation values were taken from the metadata file provided by BoM (i.e. NARCliM 10 km resolution elevation were replaced by the BoM gauge elevations). The results for the regression analysis are shown in Table 8.2.

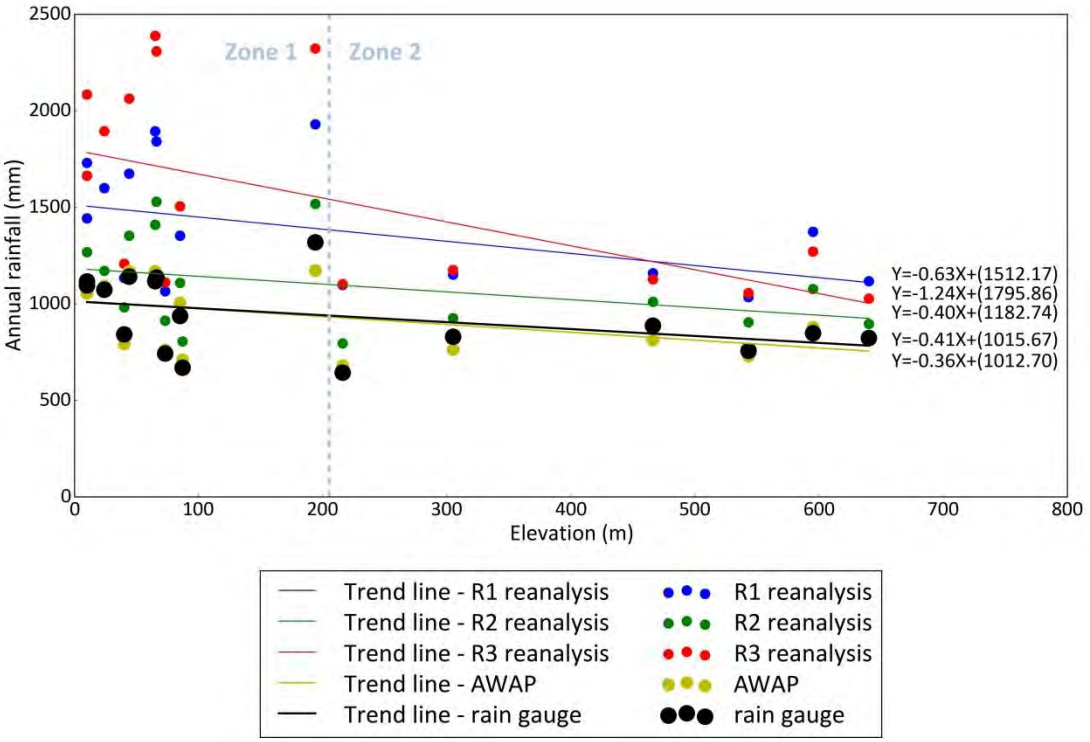

Figure 8.2 Scatter plots of mean annual rainfall vs elevation for reanalyses, AWAP and rain gauge data. Zone 1 and Zone 2 are the regions with two different trends. Note that Zones 1 and 2 are defined on a different distance threshold than in Figure 8.1.

Compared with Figure 8.1, all rainfall datasets show a weak (negative) relationship with elevation for all the rain gauges studied. In contrast, rainfall for all datasets is negatively correlated with elevation whereas in Figure 8.1, only AWAP has a negative correlation. However, as for Figure 8.1, rainfall trends in Figure 8.2 also indicate that there might be a possible relationship between rainfall and elevation, but it appears to exist differently as two regions on the actual ground; regions with elevations less 200 m and regions with elevation greater than 200 m (shown as Zone 1 and 2 in Figure 8.2). The two elevation regions and the rain gauges are shown in

Figure 8.3. In general, low elevation regions of the Williams River site are located along the coast while high elevation regions are generally located inland. This suggests that the elevation relationship may be influenced by the distance to the coast and subsequent exposure to ECLs.

Table 8.2 Summary of the regression analysis for rain gauges and corresponding reanalyses and AWAP grid points

Data	*Regression equation*	*Correlation (r)*	*R-squared (r^2)*	*p-value*
R1 reanalysis	Y=-0.63X+1512.17	-0.41	0.17	0.10
R2 reanalysis	Y=-0.40X+1182.74	-0.37	0.14	0.14
R3 reanalysis	Y=-1.24X+1795.86	-0.52	0.27	0.03
AWAP	Y=-0.41X+1015.67	-0.48	0.23	0.05
Rain gauges	Y=-0.36X+1012.70	-0.41	0.17	0.11

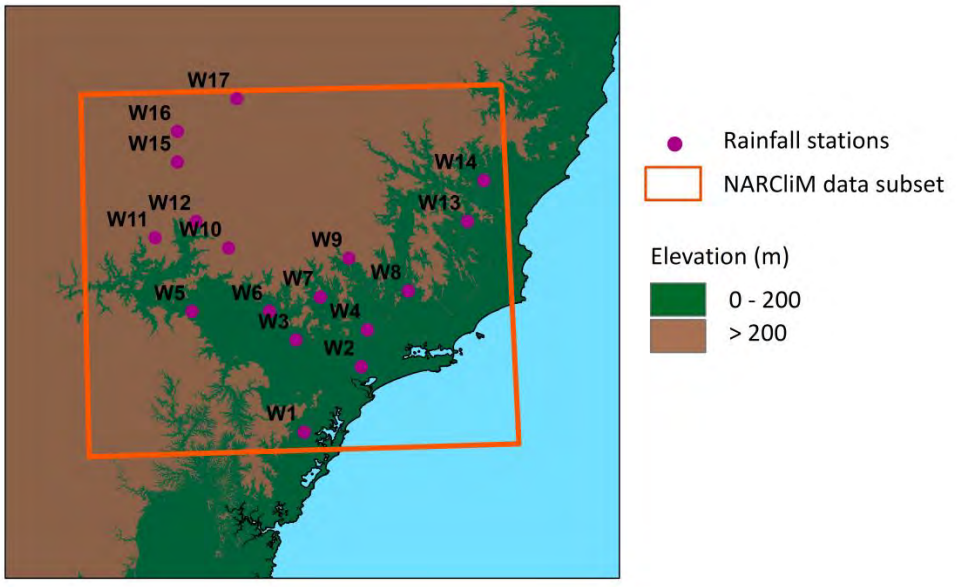

Figure 8.3 Topography map of the Williams River site. The elevation is classified into two groups: elevations less 200 m and elevations greater than 200.

8.3 Impacts from the East Coast Lows (ECL)

The rainfall statistics, particularly the mean annual rainfall, were identified as being related to the distance from the ocean in Chapter 6. This influence of distance (denoted 'impact distance') is often dependant on how far ocean interactions such as ECLs, are felt in a catchment. This section focuses on the influence and characterization of this impact distance from an ECL event.

The average daily rainfall calculated for all ECL events occurring from 1979-2001 is shown in Figure 8.4. The 5 km resolution raster dataset of ECL average rainfall was taken from Kiem et al. (2016) and only Easterly Trough Lows (ETL) averages are shown in this map. The reason for selecting ETLs is because these events are identified as to evolve mostly east of the Great Dividing Range and in a southerly direction (Browning and Goodwin, 2013) and have high impact on the east coast of the NSW.

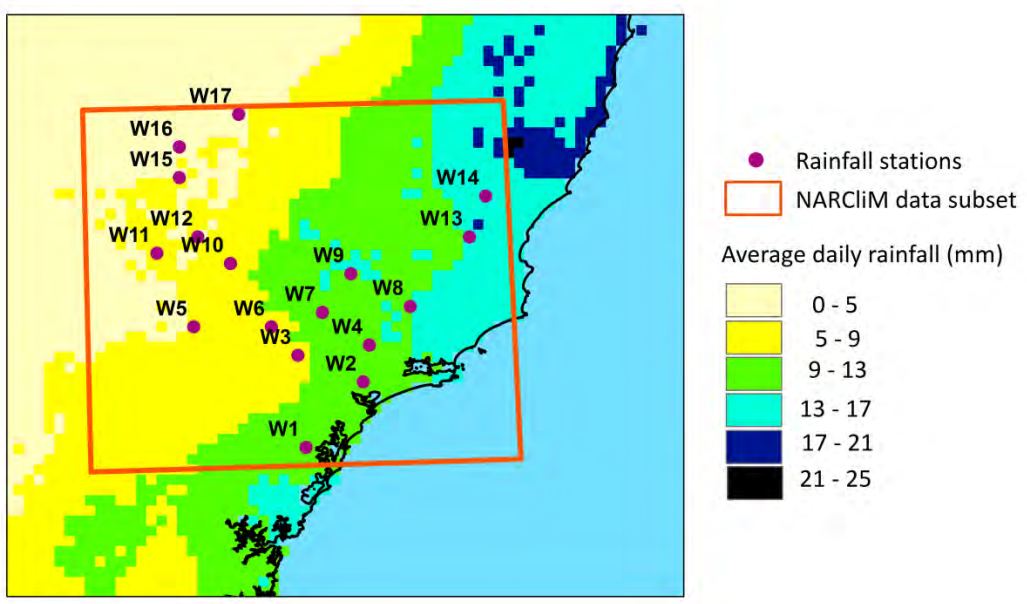

Figure 8.4 Average daily rainfall associated with ETL-ECLs at the Williams River site

Medium to high rainfall values ranging from 9 to 25 mm in Figure 8.4 indicate that the past ECL events have had the greatest influence on the coastal area, within 115 km from the coastline. Therefore compared with low ECL impact regions (the

yellow regions with average rainfall less than 9 mm), there is a significant increase of the mean annual rainfall, which is dominated by ECL events which occurred throughout the year in these regions. This may possibly explain the band of high rainfall values in AWAP data along the coast for all sites studied in Section 6.3.1. However, since there is a clear impact from ECLs on the rainfall, it is possible that at least a portion of the variation of the rainfall not explained by the relationship between rainfall and elevation could be explained by the ECL impacts.

8.4 A combined approach: ECL impacts on the relationship between the rainfall and elevation

The results in Section 8.2 suggested that studying the rainfall at the Williams River site as two elevation groups (taking two samples of rain gauges) might improve the understanding of the relationship between rainfall and elevation. The results in Section 8.3 showed that rainfall along the coastal area (the region with elevation less 200 m as shown by Figure 8.3) has been significantly impacted by ECLs, hence ECLs also play a major role when explaining the rainfall variation in this region.

By combining the results of Sections 8.2 and 8.3, the relationship between rainfall and elevation is assessed for two samples of rain gauges: (1) rain gauges inside the ECL impacted region (region with rainfall average greater than 9 mm), and (2) rain gauges outside the ECL impacted regions (region with rainfall average less 9 mm). The map of rain gauges divided by the ECL impacts is shown in Figure 8.5.

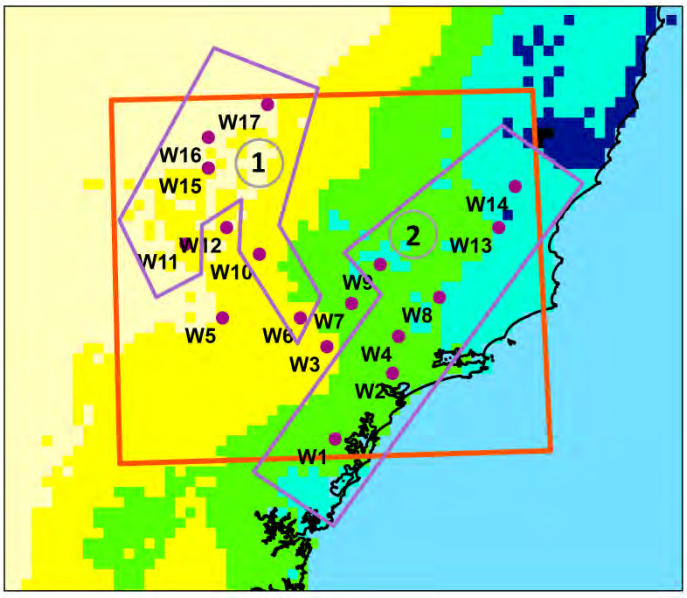

Figure 8.5 Map of rain gauges divided by the ECL impacts: (1) rain gauges inside the ECL impacted region, and (2) rain gauges outside the ECL impacted region.

The moisture-bearing winds often tend to amplify precipitation on windward slopes, and decrease it on leeward slopes (Smith, 1979; Daly et al., 1994). This decreasing of the precipitation is the rain shadow effect, and is common to this region due to the coastal escarpment and closeness to the ocean. Therefore, rain gauges W5, W7 and W12 located in rain shadow locations (see Figure 8.3) and were excluded from the analysis. Since the analysis is based on the ECL impacts, rain gauge W3 located on the boundary of the high and low ECL impacted region was also removed in the analysis. Thus, 13 rain gauges (out of 17) were used for this analysis.

8.5 Assessment of the rainfall in two regions

Scatter plots of the mean annual rainfall vs elevation for the rain gauges inside and outside the ECL impact regions are shown in Figure 8.6. Results for the regression analysis are shown in Tables 8.3 and 8.4.

Rain gauge data in the ECL impacted region show a very strong linear relationship with r^2 value of 0.91. This means that 91% of the variation of the rainfall is explained by the linear relationship between the rainfall and elevation. This is a

strong statistically significant linear relationship (p-value < 0.05), compared with three reanalyses datasets and AWAP.

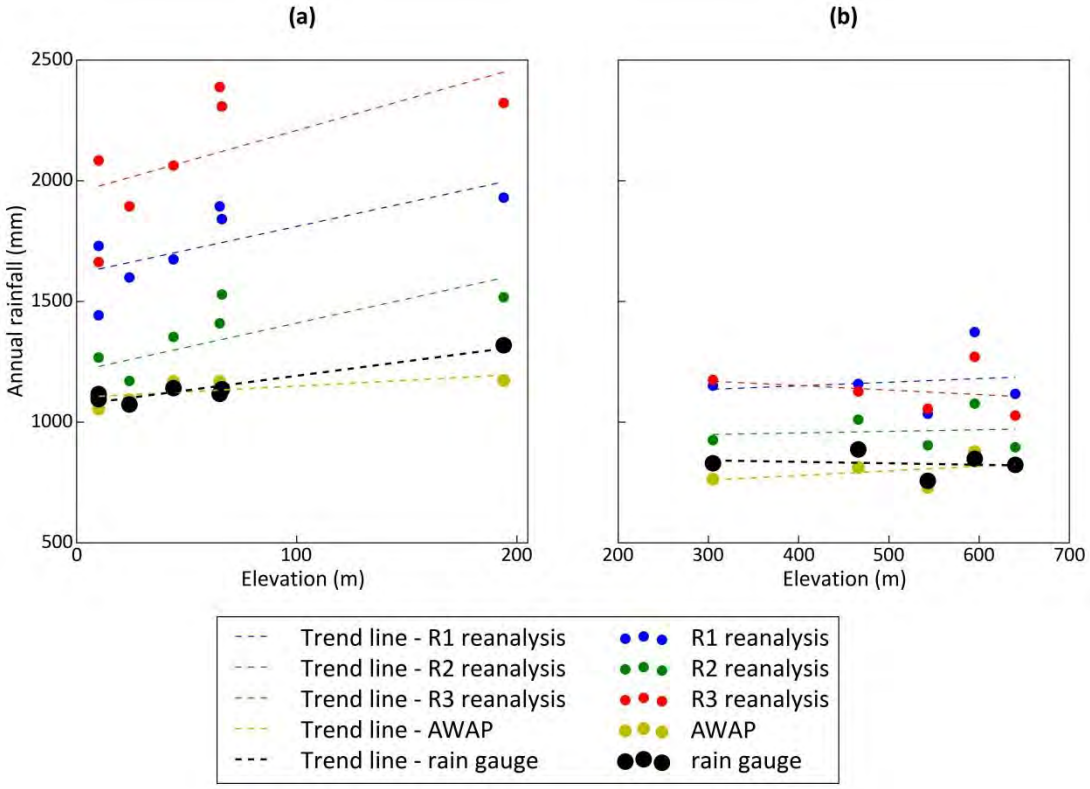

Figure 8.6 Scatter plots of the mean annual rainfall vs elevation for the rain gauges, reanalyses and AWAP data: (a) gauges/grid points inside the ECL impact region, (b) gauges/grid points outside the ECL impact region.

All three reanalyses and AWAP rainfall also produce a linear relationship with elevation, with R2 reanalyses being able to better reproduce the linear relationship shown in the gauge data, but the statistical significance of AWAP and R3 reanalysis has also been dropped (Table 8.3) due to the less data points. However, for R2 reanalysis, only 72% of the variation of the rainfall is explained by the relationship between rainfall and elevation.

Table 8.3 Summary of the regression analysis for rain gauges and corresponding reanalyses and AWAP grid points located inside the ECL impact region

Data	*Regression equation*	*Correlation (r)*	*R-squared (r^2)*	*p-value*
R1 reanalysis	Y=1.96X+(1614.14)	0.72	0.52	0.067
R2 reanalysis	Y=2.00X+(1210.31)	0.72	0.72	0.066
R3 reanalysis	Y=2.57X+(1951.50)	0.63	0.40	0.13
AWAP	Y=0.47X+(1101.93)	0.66	0.44	0.11
Rain gauges	Y=1.21X+(1071.32)	0.95	0.91	0.00093

Outside the ECL impact region, none of the rainfall datasets are able to produce a statistically significant relationship (all data have p-values greater than 0.05) between rainfall and elevation. This suggests that the relationship between the rainfall and elevation is less definitive for the regions which are away from the coast.

Table 8.4 Summary of the regression analysis for rain gauges and corresponding reanalyses and AWAP grid points located outside the ECL impact region

Data	*Regression equation*	*Correlation (r)*	*R-squared (r^2)*	*p-value*
R1 reanalysis	Y=0.15X+(1090.67)	0.16	0.02	0.80
R2 reanalysis	Y=0.07X+(928.57)	0.11	0.01	0.86
R3 reanalysis	Y=-0.19X+(1226.28)	-0.25	0.06	0.68
AWAP	Y=0.19X+(701.33)	0.45	0.20	0.45
Rain gauges	Y=-0.06X+(859.78)	-0.17	0.03	0.79

Using the limited number of rain gauge data available for the time period investigated (1950-2009), there are two major findings:

(1) There is a strong statistically significant linear relationship between the rainfall and the elevation at the Williams River site, but only for regions which are close to the ocean (up to an approximate distance of 100 km from the coast) and inside the ECL impacted region.

(2) The relationship between the rainfall and elevation is less definitive for the regions which are away from the coast (greater than 115 km) and outside the ECL impact region.

It should be noted that the statistical significance of the results may improve by increasing the number of rain gauges, though it was not possible at this particular site where rain gauges are sparsely distributed and there were only 17 gauges which had continuous rainfall records for the 60 year analysis period.

8.6 Conclusions

A combined approach of assessing the relationship between the rainfall and elevation, and impacts from ECLs on this relationship was investigated in this chapter. The results of the analysis suggest that there is a statistically significant positive linear relationship between the observed rainfall and the elevation at the regions which are close to the coastline of the Williams River site, where the ECL impacts are most dominant. When the distance from the coast increases, this relationship becomes weaker.

In general, the relationship between the rainfall and elevation is not consistent across a site and may depend on other factors such as wind direction and ocean interactions. However, it should be noted that this combined approach of the assessment of the relationship between rain gauge and elevation was performed as a preliminary case study and further investigations are warranted. A different site with a larger number of rain gauges may improve the results.

Section 2

Assessment of rainfall statistics of NARCliM GCM projections (1990-2009)

The results presented in Section 1 (Chapters 5-8) were for the downscaled NARCLIM reanalysis RCMs (1950-2009). The 60-year period reanalysis RCMs were produced during the first phase of the NARCliM project (Evans et al., 2014).

However, as explained in Chapter 3: Sites and Data, there are twelve different RCM simulations (produced with three RCM configurations: each driven by four GCMs (1990-2009)) and three reanalyses (1950-2009) covering the current day, 20 year epoch (1990-2009). The next four chapters (Chapter 9-12) assess the ability of these RCMs to reproduce the rainfall statistics of the observed rainfall at the Williams River, Richmond River, Bega River and Sydney sites. Here in Section 2 the main focus is on the performance of the GCM driven simulations for the shorter 1990-2009 period this is the period common to the GCM-RCM and reanalyses simulation data. To minimize the confusion between datasets, GCM driven simulations are referred by the name of the GCM, while reanalyses driven simulations are referred to as reanalysis. Further, to indicate which model configuration of WRF RCM is used, R1, R2 or R3 is used at the beginning of a name followed by a hyphen (for example, if an output RCM dataset is produced by downscaling the CCCMA3.1 GCM using the R1 configuration of WRF, the output RCM is called as R1-CCCMA3.1 or R1-CCCMA3.1 RCM). Collectively, all datasets are referred as RCMs.

The four statistical methods which were used to assess the 60 year reanalyses data are the same as was used in previous chapters. The statistical methods used were: (1) probability distribution of the rainfall, (2) spatial variability of the rainfall statistics, (3) temporal autocorrelation of the rainfall, and (4) spatial correlation of the rainfall.

The key focus of this section is to determine the performance of NARCliM simulations in capturing the observed rainfall statistics, focussing on the GCM-RCM performance because it is these models that are used for the future climate

projections. Knowing that the four GCMs have been downscaled using three RCM configurations, evaluation of the performance of each simulation is important to identify which models (i.e. either RCM or GCM) are dominant in driving the characteristics of the rainfall outputs.

As before, there are two types of rainfall data: uncorrected and bias corrected. First the statistical testing results for the uncorrected data are presented, and then these results are compared with the results for the bias corrected simulations.

Chapter 9
Testing NARCliM GCM simulations using the probability distribution of the rainfall

9.1 Introduction

This chapter evaluates the rainfall properties and how they are modified by the bias correction. The probability distributions of the uncorrected and bias corrected current day GCM projections (1990-2009) are assessed and results are compared against 10 km AWAP data. Additionally, a 20 year subset, 1990-2009, extracted from the 60 year reanalyses is also compared with GCM projections. The methods explained in Section 4.2 were used to calculate the rainfall probability distribution.

9.2 Probability distribution of the rainfall

The ability of NARCliM RCMs to reproduce the AWAP rainfall distribution is assessed in this section. The cumulative probability distributions (CDF) of the mean annual rainfall for the uncorrected NARCliM RCMs and AWAP for all grid points of the Williams River site are shown in Figure 9.1.

As shown in Figure 9.1, R1 and R3 configurations of CSIRO-Mk3.0, MIROC3.2 and ECHAM5 underestimate the probabilities of the mean annual rainfall of AWAP. The underestimation is least for R2-CSIRO-Mk3.0 and R2-MIROC3.2, while R2-ECHAM5 closely reproduced the CDF of AWAP, particularly for the mean rainfall less than 850 mm. In contrast, the CCCMA3.1 simulations overestimated the CDF of AWAP for all three RCMs. As was seen in Section 6.2, the reanalyses for 1950-2009 also underestimated the rainfall and had the largest underestimation of all the GCM simulations.

The CDFs generated for the bias corrected simulations, shown in Figure 9.2 indicate that most of the systematic biases in the mean annual rainfall in the uncorrected simulations are removed by the bias correction. All CSIRO-Mk3.0 RCM simulations reproduced approximately 95 to 98% of the CDF of AWAP after the bias correction, and were therefore the GCM-RCM combination most able to simulate the mean

rainfall probabilities of AWAP at the annual resolution. For R3, all GCM simulations satisfactorily reproduced the CDF of AWAP, with ECHAM5 slightly underestimating the probabilities of the greater rainfall values. In general for the rainfall greater than 850 mm, ECHAM5 underestimated the CDF of AWAP, and this can be seen for R1. Compared with GCM simulations, the reanalysis, in particular R1 and R3, tend to underestimate the CDF of AWAP significantly, showing that there are some biases still remaining in the datasets which are not corrected by the bias correction.

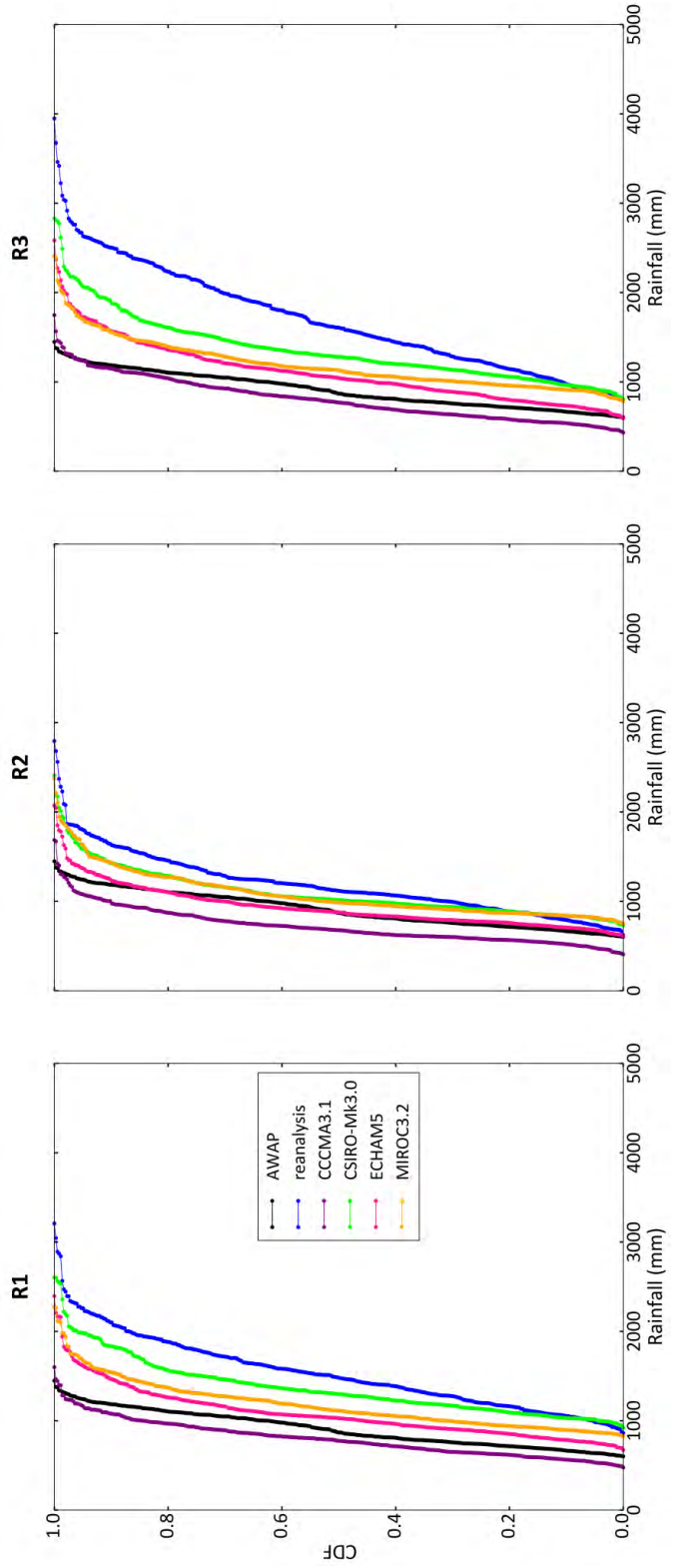

Figure 9.1 Cumulative probability distributions of mean annual rainfall of uncorrected NARCliM GCMs and AWAP across the Williams River site. R1, R2 and R3 (columns) are the three RCM configurations.

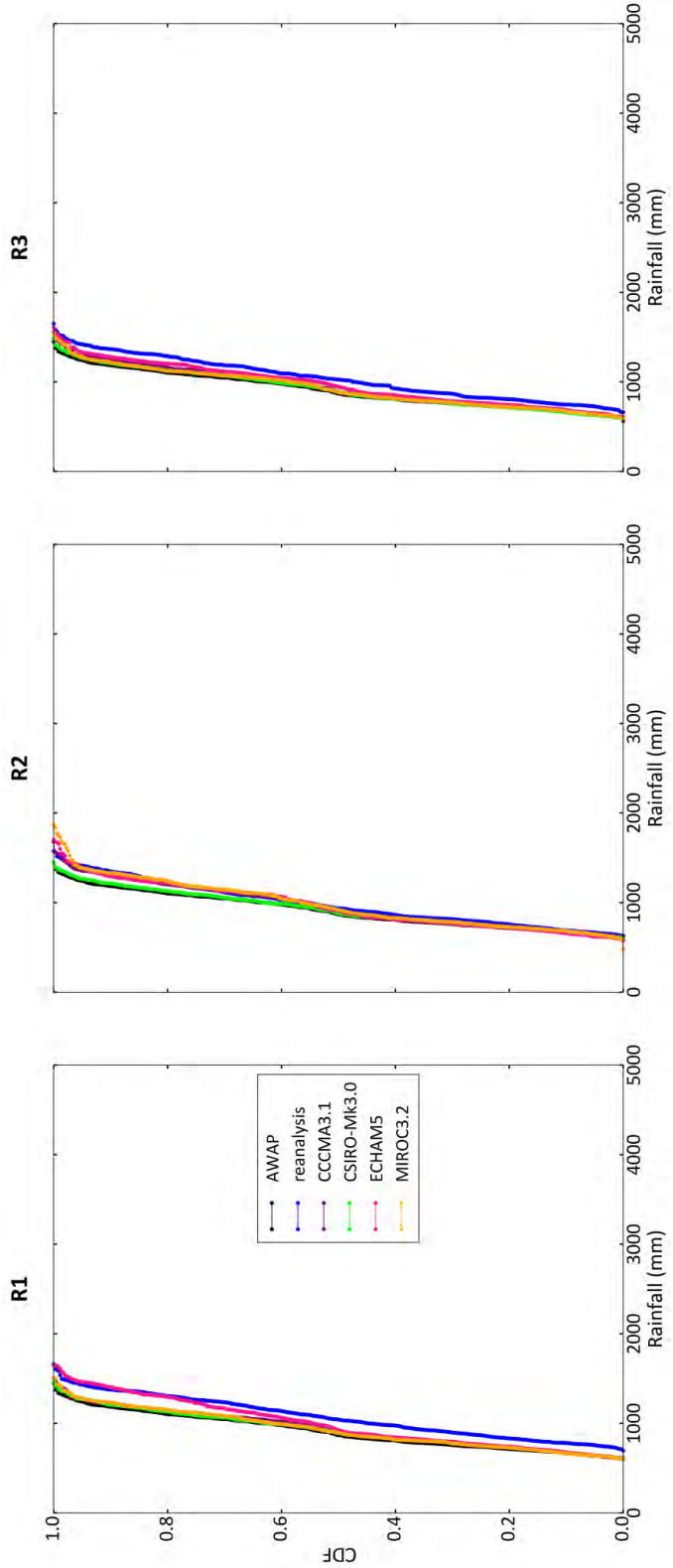

Figure 9.2 Cumulative probability distributions of mean annual rainfall of bias corrected NARCliM GCMs and AWAP across the Williams River site. R1, R2 and R3 (columns) are the three RCM configurations.

The cumulative probability distributions of the daily rainfall of the uncorrected NARCliM RCMs and AWAP at grid points A to D for the Williams River site are shown in Figure 9.3. For the low elevation grid points (A and B), both MIROC3.2 and ECHAM5 RCMs were able to reproduce the CDF of the daily rainfall of AWAP for all three configurations. R1 and R3 configuration reanalysis and CSIRO-Mk3.0 tend to underestimate the CDF of AWAP, while CCCMA3.1 overestimated it. However, all GCM simulations reproduced the CDF of AWAP for R2. For the high elevation grid point C, all GCMs except CCCMA3.1 underestimated the CDF of AWAP. R1-CCCMA3.1 was able to reproduce approximately 98% of the CDF of AWAP though R3-CCCMA3.1 overestimated the probabilities of the midsized rainfall (0.2 to 7 mm) events of AWAP. In contrast, at grid point D all GCM simulations overestimate the CDF of AWAP with R1 providing the best fit. However, this behaviour of R1 reanalysis is not consistent with the 60 years reanalyses (Figure 6.29), where all reanalyses underestimate the rainfall probabilities of AWAP.

The CDFs generated for the bias corrected simulations are shown in Figure 9.4. In general, there was a significant improvement for all simulations after the bias correction, but it is clear that only part of the CDF has been improved. The CDF of bias corrected rainfall at grid points A-D show that none of the NARCliM RCMs capture the probabilities of light rainfall events (rainfall less 1 mm) of AWAP, hence the bias correction method (see Section 2.6.3) appeared to be reliable only for moderate to high rainfall events with rainfall greater than 1.5-2 mm. For moderate rainfall events, R2 configuration bias corrected RCMs tended to reproduce the rainfall probabilities, but this can only be seen in the rainfall at low elevation points (A and B). For the high elevation grid points (C and D), all simulations have discrepancies, either under or overestimating the observed rainfall probabilities. Note that the sudden rises around the 1.5 mm rainfall value (Figure 9.4) in daily NARCliM CDFs are artefacts that seem to be a result of the bias correction process, and are consistently seen for all the sites studied.

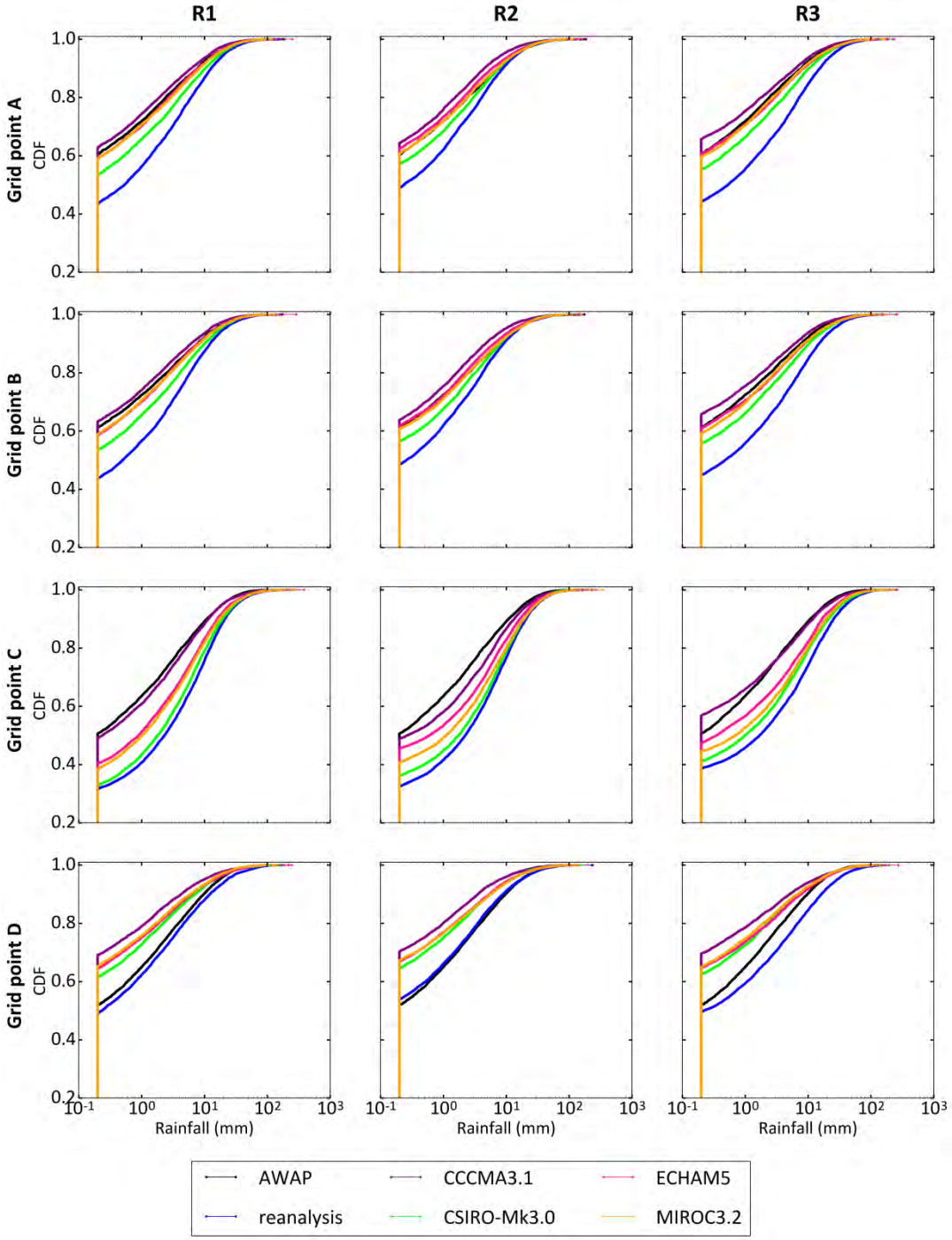

Figure 9.3 Cumulative probability distributions of daily rainfall of uncorrected NARCliM GCMs and AWAP at Grid point A, B, C and D of Williams River site. Note that daily rainfall is in log scale and only values greater than 0.2 mm are plotted. R1, R2 and R3 (columns) are the three RCM configurations. Points A and B are low elevation, C and D high elevation.

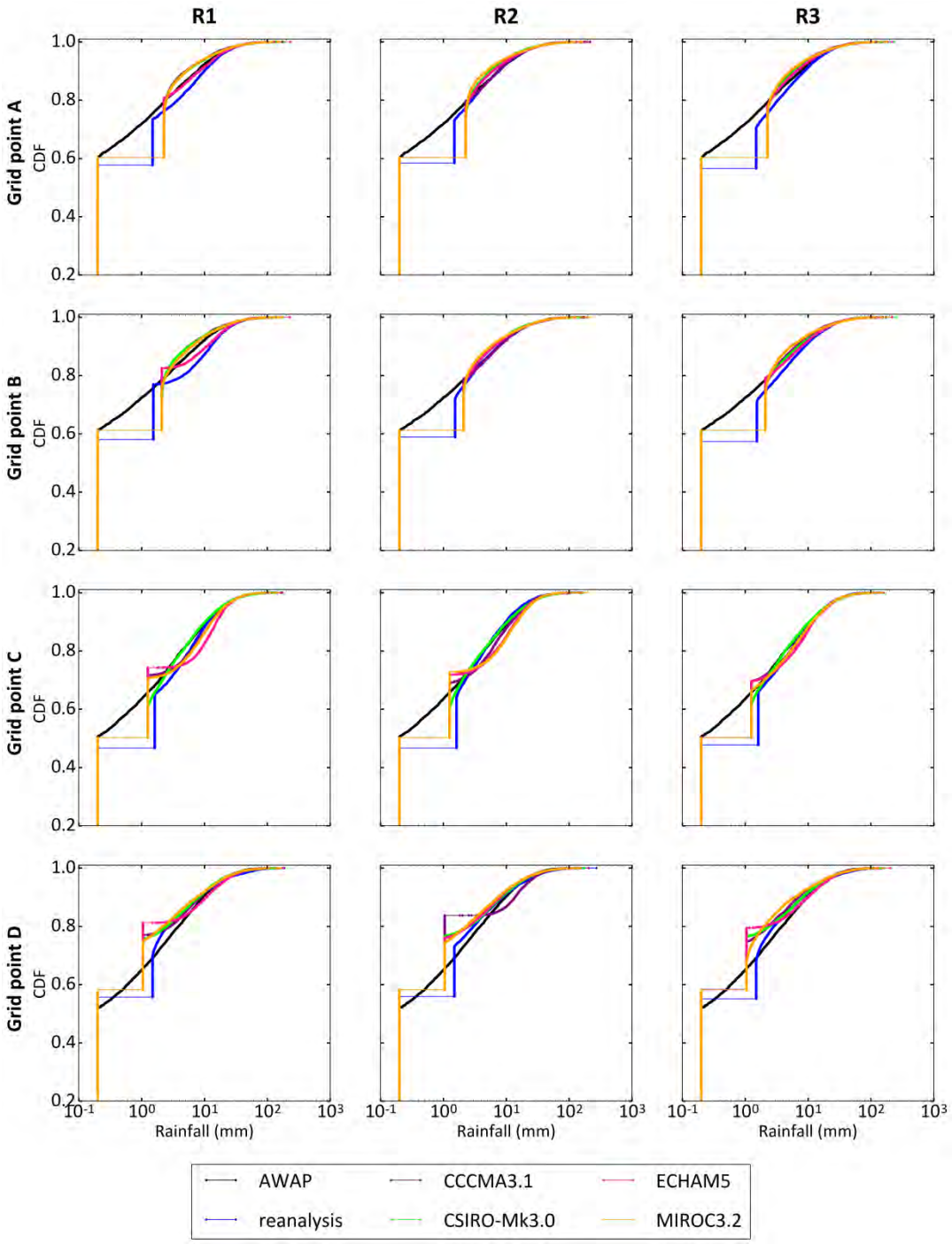

Figure 9.4 Cumulative probability distributions of daily rainfall of bias corrected NARCliM GCMs and AWAP at Grid point A, B, C and D of Williams River site. Note that daily rainfall is in log scale and only values greater than 0.2 mm are plotted. R1, R2 and R3 (columns) are the three RCM configurations. Points A and B are low elevation, C and D high elevation.

The cumulative probability distribution of the mean annual rainfall of uncorrected NARCliM simulations and AWAP for all grid points of Bega River site is shown in Figure 9.5. The Bega River site is an interesting example, because it has the highest

elevation of all the sites and most of the rainfall is controlled by the orography. Since GCM-RCMs often tend to underestimate the rainfall at mountainous regions, a significant underestimation of AWAP can be expected. This can clearly be seen in Figure 9.5, where the CDF of AWAP, particularly for the mean rainfall greater than 800 mm is highly underestimated by the GCM-RCM simulations. For the rainfall less than 800 mm, all GCM-RCM combinations, except CCCMA3.1, systematically underestimate the rainfall probabilities of AWAP. The R1-CCCMA3.1 reproduced the CDF of AWAP for the mean rainfall less than 800 mm, yet underestimated the largest rainfall occurrences. The CDFs of all the bias corrected GCM-RCMs (Figure 9.6) indicate that most of the biases have been removed after the bias correction and the improvements are consistent with the results of the Williams River site. These results are typical for the other two sites; Richmond River and Sydney and, are therefore not discussed under this section (see Appendix A.2 – Figures A.3 to A.10 for full details).

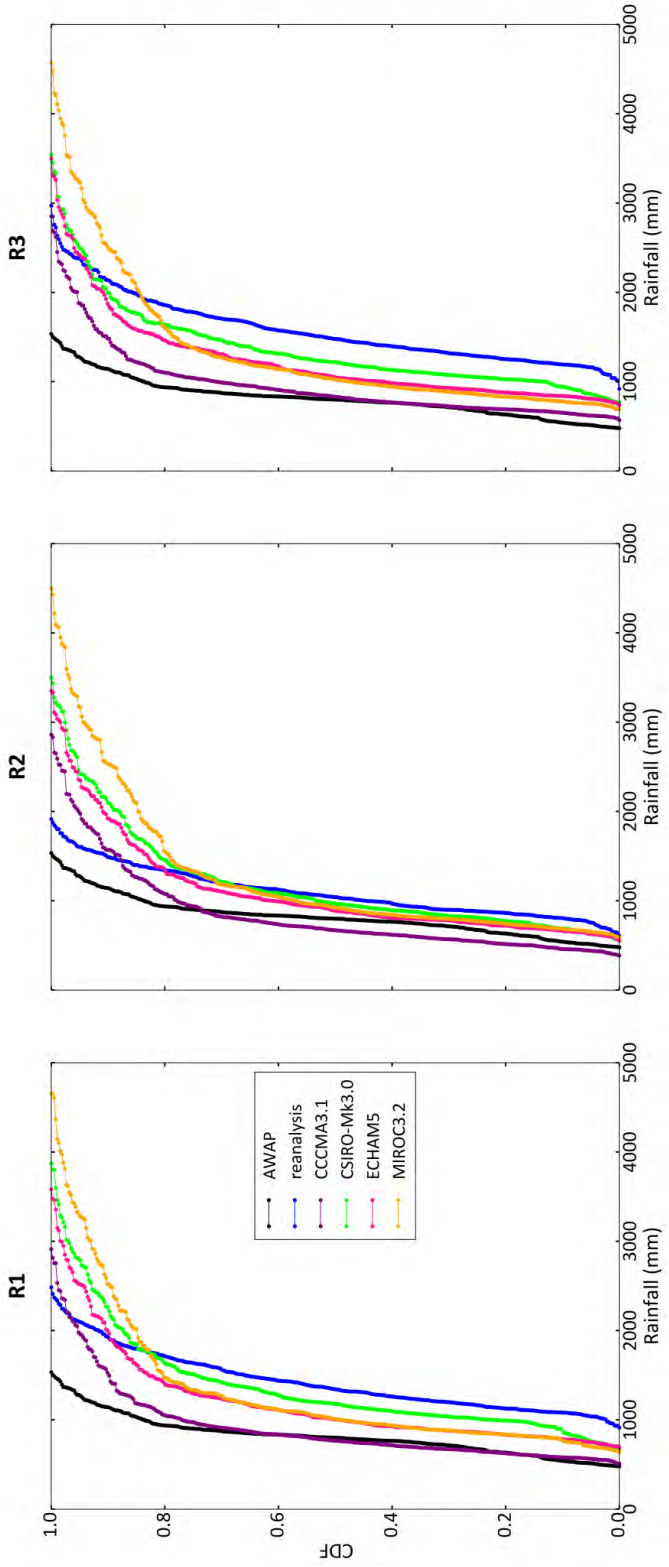

Figure 9.5 Cumulative probability distributions of mean annual rainfall of uncorrected NARCliM GCMs and AWAP across the Bega River site. R1, R2 and R3 (columns) are the three RCM configurations.

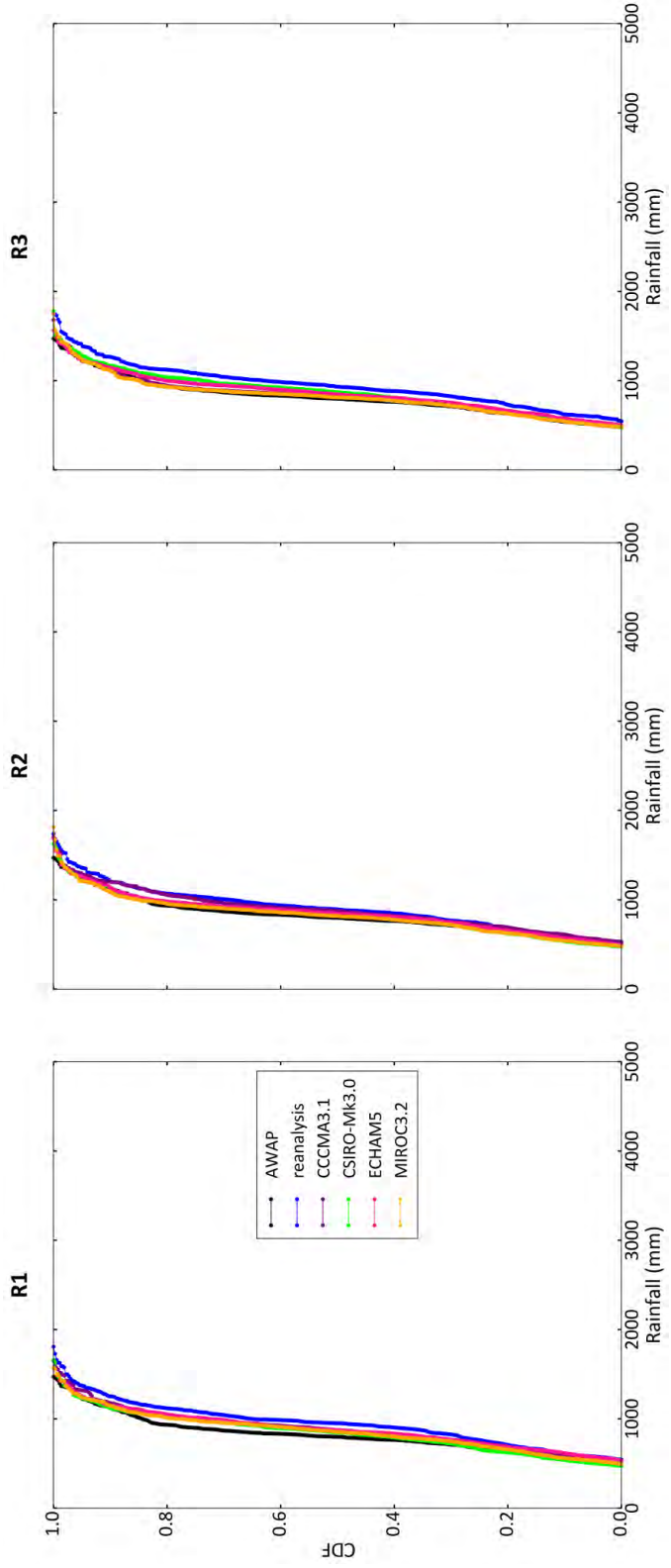

Figure 9.6 Cumulative probability distributions of mean annual rainfall of bias corrected NARCliM GCMs and AWAP across the Bega River site. R1, R2 and R3 (columns) are the three RCM configurations.

The cumulative probability distributions of the daily rainfall of uncorrected NARCliM simulations and AWAP at grid points J to M at the Bega River site are shown in Figure 9.7. There is a general trend at the Bega River site that all GCM-RCM combinations closely reproduce or slightly overestimate the daily rainfall probabilities of AWAP at low elevation grid points and, greatly underestimate all rainfall probabilities of AWAP at the high elevation points. All reanalyses simulations, except R2 at grid point K underestimate the daily rainfall probabilities of AWAP at all grid points for all rainfall intensities. The CDFs generated with bias corrected simulations (shown in Figure 9.8) also have similar trends to the Williams River sites.

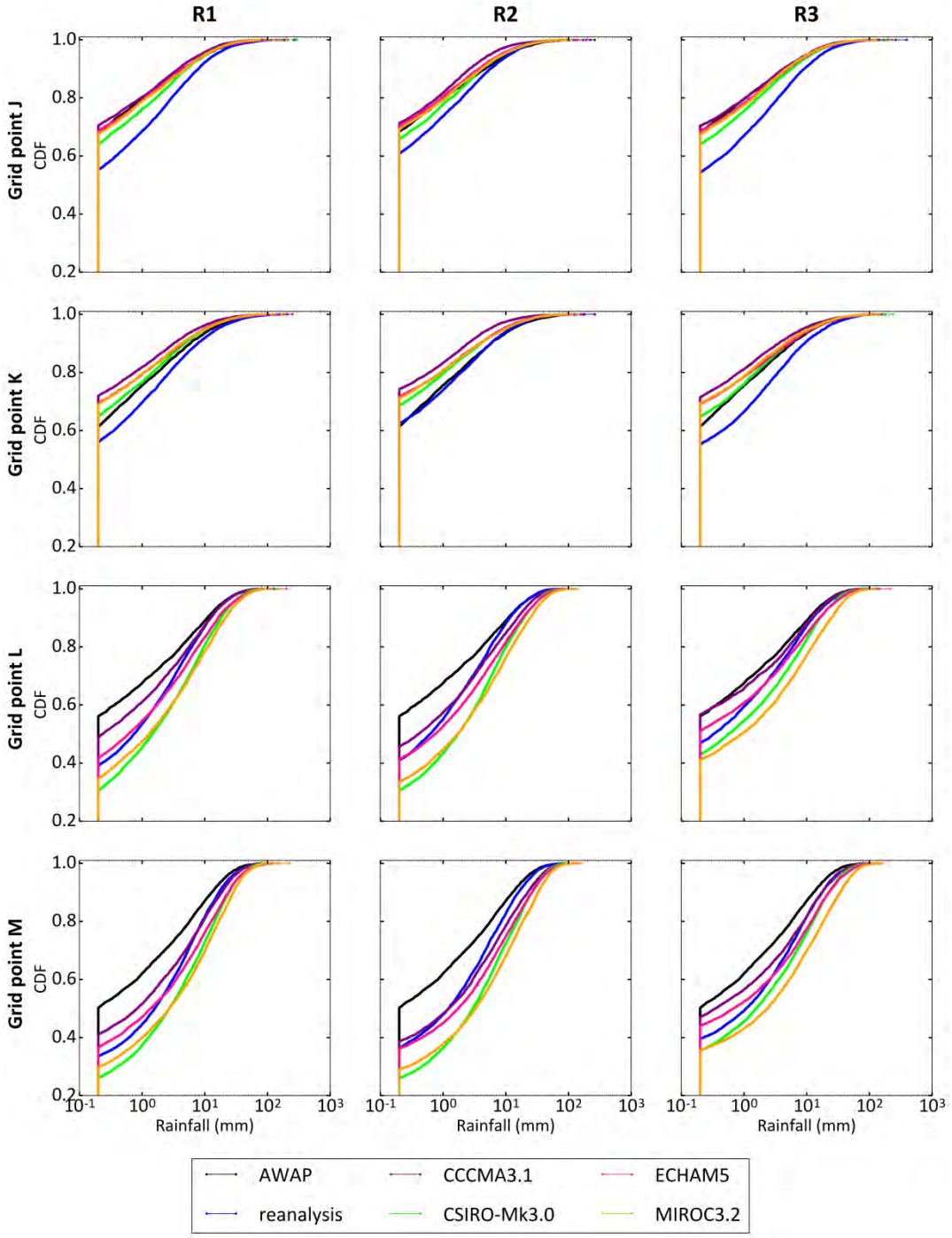

Figure 9.7 Cumulative probability distributions of daily rainfall of uncorrected NARCliM GCMs and AWAP at Grid point J, K, L and M of Bega River site. Note that daily rainfall is in log scale and only values greater than 0.2 mm are plotted.

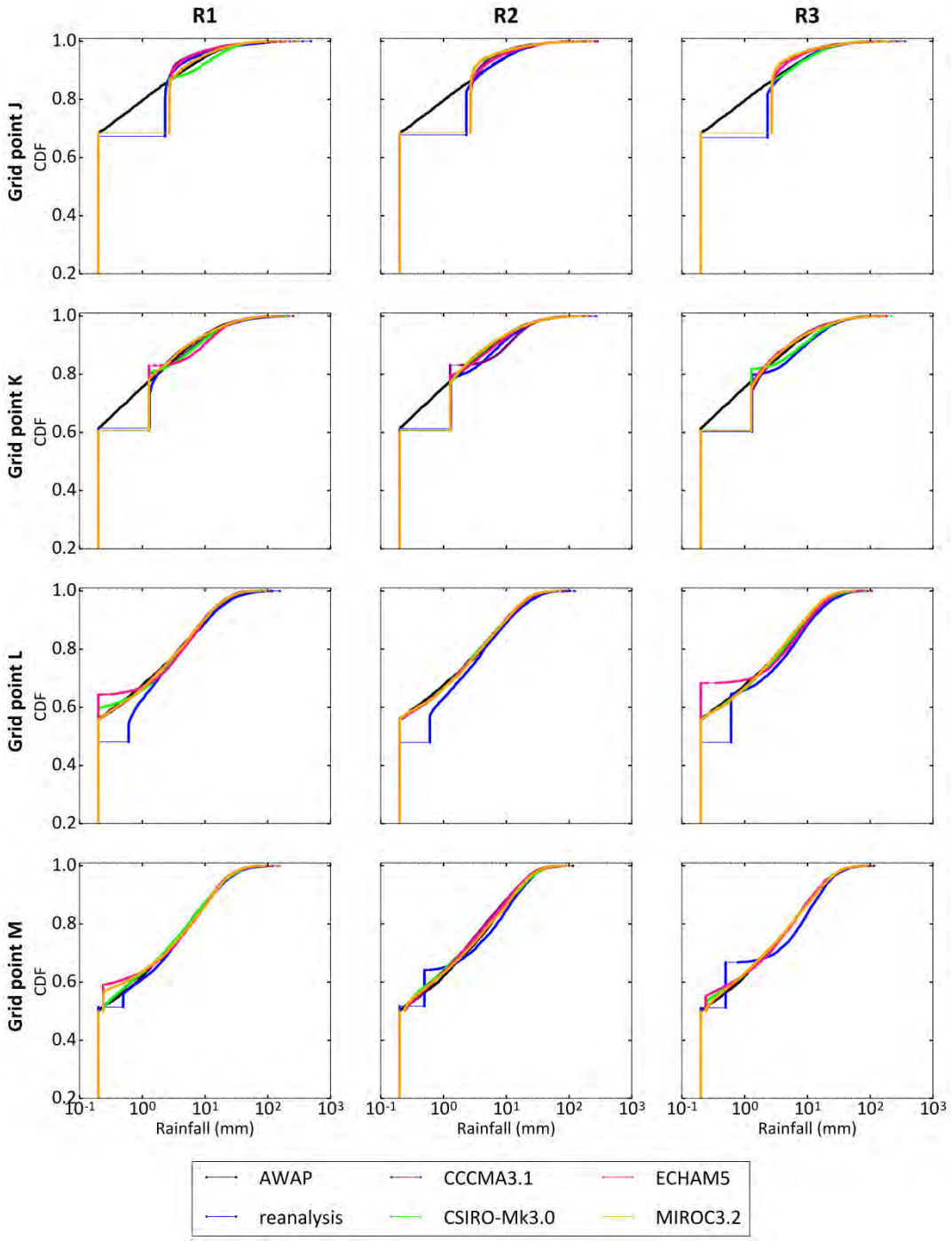

Figure 9.8 Cumulative probability distributions of daily rainfall of bias corrected NARCliM GCMs and AWAP at Grid point J, K, L and M of Bega River site. Note that daily rainfall is in log scale and only values greater than 0.2 mm are plotted.

9.3 Conclusions

The ability of NARCliM GCM-RCM combinations to reproduce the AWAP rainfall distribution for 1990-2009 was assessed in this chapter. CSIRO-Mk3.0, ECHAM5 and MIROC3.2 RCMs underestimated the mean rainfall probabilities across the sites, while CCCMA3.1 overestimated all probabilities. Reanalysis and CSIRO-Mk3.0 tended to underestimate the daily rainfall probabilities at almost all the grid points, while ECHAM5 and MIROC3.2 RCMs closely reproduced the daily rainfall probabilities at low elevations. At high elevations, CCCMA3.1 most closely reproduced the observed rainfall probabilities for all sites. Results for the bias corrected data suggest that most of the systematic biases in the mean annual rainfall of the uncorrected simulations had been removed by the bias correction. Compared with other GCM-RCMs, the improvement in the CSIRO-Mk3.0 was quite significant. There was a significant improvement in the daily rainfall time series of RCM simulations after bias correction, however, it should be noted that only that portion of the rainfall time series with rainfall on a day being greater than 1 mm had been improved.

Chapter 10
Testing the spatial variability of the NARCliM downscaled GCM uncorrected and bias-corrected rainfall

10.1 Introduction

The spatial variability of the reanalyses rainfall for 1950-2009 was assessed in Sections 5.1.3 and 6.3. Similarly, the spatial variability of the mean, coefficient of variation, standard deviation and lag-1 autocorrelation of the uncorrected and bias corrected current day GCM-RCM data and reanalysis projections for 1990-2009 is assessed in this chapter. Extending the analysis in Chapter 9 these data are compared with observed statistics of the 10 km resolution AWAP data for 1990-2009. The methods explained in Section 4.3 were used to calculate the spatial variability of the statistics at each site.

10.2 Spatial variability of the rainfall statistics

10.2.1 Mean rainfall

Mean annual uncorrected rainfall for all RCM simulations and AWAP for the Williams River site is shown in Figure 10.1. All simulations were able to reproduce the spatial pattern in the mean rainfall of AWAP. CCCMA3.1 was the best at reproducing both the magnitude and the spatial pattern of the mean rainfall of AWAP, though there is a slight underestimation of the rainfall at some grid points. All other GCM-RCM simulations overestimated the mean rainfall of AWAP for the Williams River site. CSIRO-Mk3.0 and reanalysis had the highest overestimation. In particular, this overestimation is most significant at higher elevations.

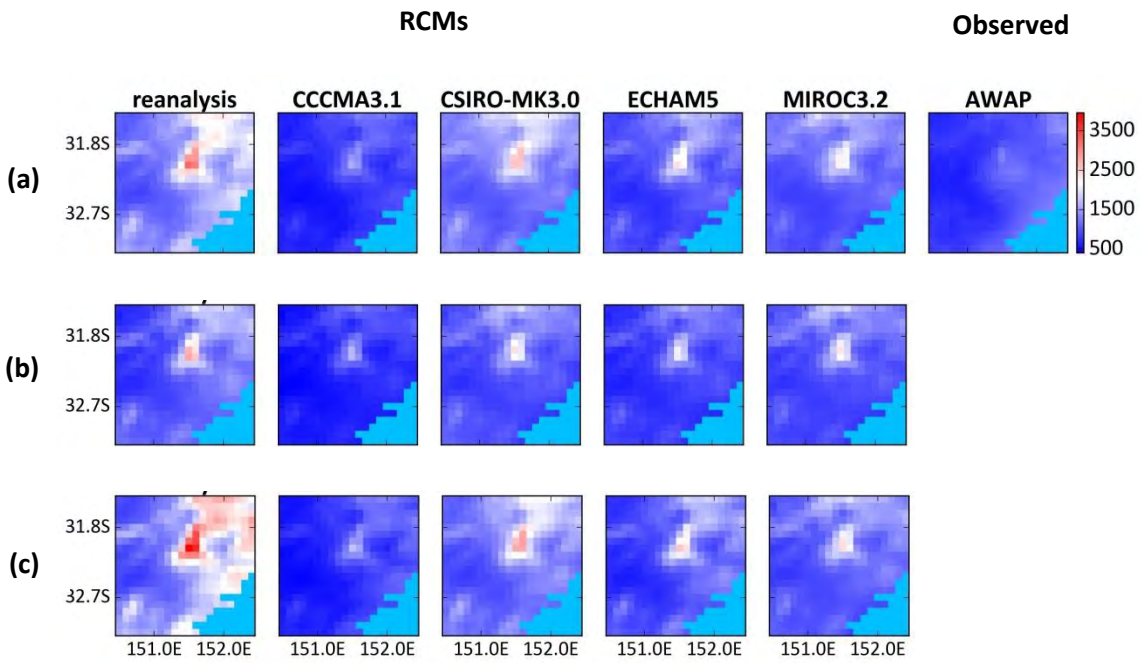

Figure 10.1 Spatial distribution of the mean annual rainfall (1990-2009) for the Williams River site. The plots are for the uncorrected simulations of (a) R1, (b) R2, and (c) R3, and AWAP.

Overall, the ability of RCMs to reproduce the AWAP mean rainfall at the Williams River site can be summarized as follows. It should be noted that only the best WRF RCM model configuration is shown in brackets.

CCCMA3.1 (R2) **> ECHAM5** (R2) **> MIROC3.2** (R2) **> CSIRO-Mk3.0** (R2) **> reanalysis** (R2)

Comparing the three configurations, R2 is better able to simulate the mean rainfall of AWAP than R1 and R3 for all RCMs. The overestimation of rainfall in R3 reanalysis is greater than R1 and R2. This result is consistent with the mean rainfall results for the 60-year reanalysis simulations discussed in Chapters 5 and 6.

A comparison between the mean annual rainfall of AWAP and the bias corrected RCMs for the Williams River site is shown in Figure 10.2. The figure indicates that bias correction has improved the models performance by reducing most of the biases present in the uncorrected data. For example, the mean annual rainfall is reduced to below 1900 mm for all RCMs, from what was previously 4,000 mm (Figure 10.1).

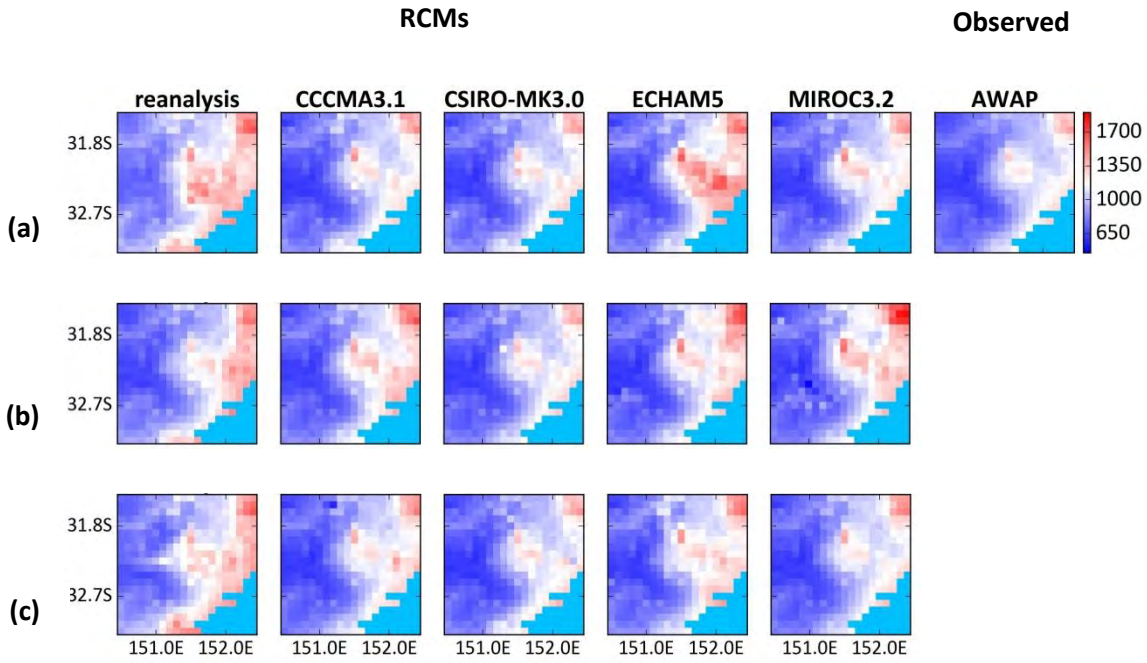

Figure 10.2 Spatial distribution of the mean annual rainfall (1990-2009) of the Williams River site: The plots are for the bias corrected simulations of (a) R1, (b) R2, and (c) R3, and AWAP. Note the colour scale is different to Figure 10.1.

Compared with all other models, CSIRO-Mk3.0 (all RCMs) show a larger improvement after the bias correction and appear to be the closest to simulating both the magnitude and the spatial pattern of the mean annual rainfall of AWAP. All three reanalyses, R2-MIROC3.2 and R1- and R2-ECHAM5 overestimate the mean rainfall, particularly along the coast. The ability of R1- and R3-CCCMA3.1 is also improved in simulating the mean rainfall of AWAP, as in the CSIRO-Mk3.0 after the bias correction.

The relative performance of the bias corrected RCMs is:

CSIRO-Mk3.0 (R1, R2 and R3)> **CCCMA3.1** (R1 and R3)**> ECHAM5 (**R3)**≈ MIROC3.2** (R1 and R3)> **reanalysis** (R2)

The spatial distribution of the mean rainfall of the uncorrected RCMs of Richmond River site is shown in Figure 10.3.

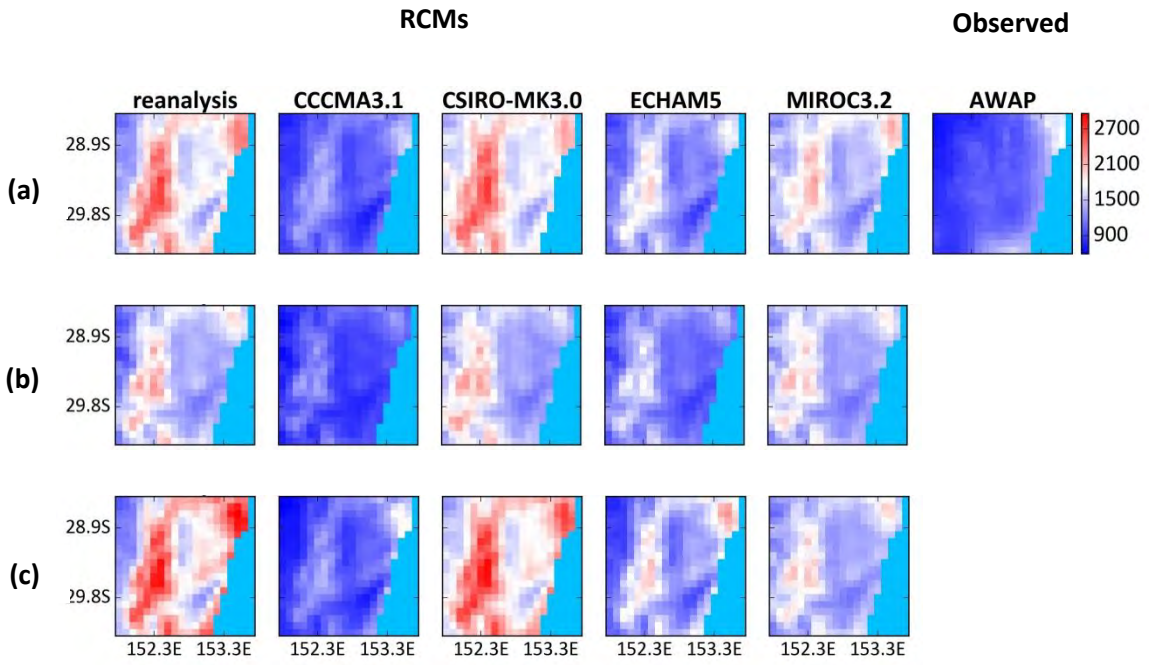

Figure 10.3 Spatial distribution of the mean annual rainfall (1990-2009) of the Richmond River site: The plots are for the uncorrected simulations of (a) R1, (b) R2, and (c) R3, and AWAP.

Of all uncorrected simulations of Richmond River site, CCCMA3.1 RCM is better able to simulate the mean rainfall of AWAP than the others. As was found for the Williams River site, both reanalyses and CSIRO-Mk3.0 poorly match the mean rainfall of AWAP, overestimating the rainfall from north to south across the centre of the site. The relative performance of the uncorrected RCM simulations at the Richmond River site is:

CCCMA3.1 (R2) **> ECHAM5** (R2) **> MIROC3.2** (R2) **> CSIRO-Mk3.0** (R2) **> reanalysis** (R2)

As discussed in Section 6.3.1 there is a north-south band of high rainfall values in all uncorrected reanalyses RCM simulations. This is due to the biases in the RCMs which overestimate the precipitation caused by orography, generating too much precipitation in the mountains (see Section 6.3.1). Argüeso et al. (2013) also studied this effect and suggested that NARCliM model outputs often amplify the orographic blocking of fronts coming from the ocean, leading to an underestimation of rainfall

inland. The bias corrected mean annual rainfall of all RCMs shown in Figure 10.4 indicates that most of these systematic errors have been removed by the bias correction.

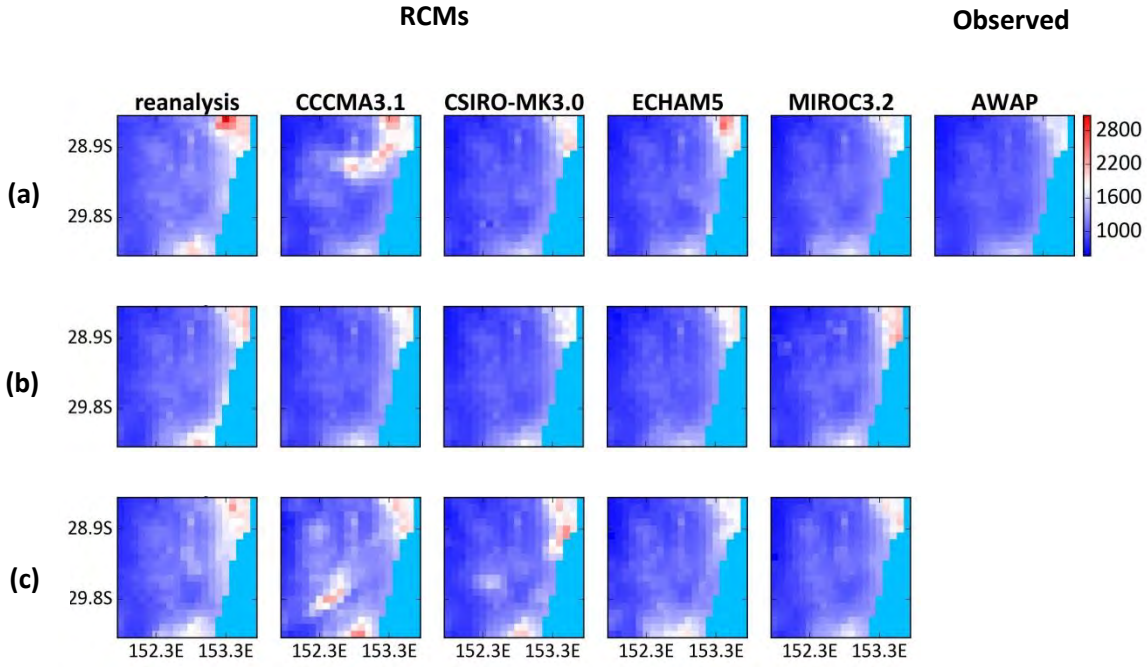

Figure 10.4 Spatial distribution of the mean annual rainfall (1990-2009) of the Richmond River site: The plots are for the bias corrected simulations of (a) R1, (b) R2, and (c) R3, and AWAP. Note the colour scale is different to Figure 10.3.

The relative performance of the bias corrected RCM simulations at the Richmond River site is:

CSIRO-Mk3.0 (R2)> **CCCMA3.1** (R2)**> ECHAM5 (**R2 and R3)**≈ MIROC3.2** (R1)> **reanalysis** (R2)

All uncorrected R2 RCMs better capture the mean rainfall of AWAP than R1 and R3. Therefore from this point onwards, only the uncorrected R2 RCMs are shown for the remaining two sites (Bega River and Sydney, see Appendix A.3 – Figures A.11 to A.12 for more details). In contrast, there is no consistency about which bias corrected simulation is best. Therefore, all fifteen simulations are shown.

The spatial distribution of the mean rainfall of the uncorrected R2 RCMs and bias corrected R1, R2 and R3 simulations for the Bega River site are shown in Figure 10.5 and 10.6.

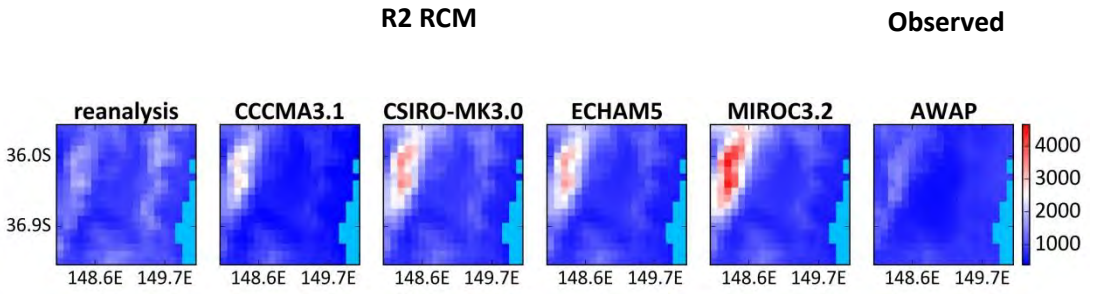

Figure 10.5 Spatial distribution of the mean annual rainfall (1990-2009) of the Bega River site: The plots are for the uncorrected simulations of R2 and AWAP.

The relative performance of the uncorrected RCMs at the Bega River site is:

CCCMA3.1 (R2) **> ECHAM5** (R2) **> MIROC3.2** (R2) **> reanalysis** (R2)

> CSIRO-Mk3.0 (R2)

All RCMs, but particularly MIROC3.2, ECHAM5 and CSIRO-Mk3.0, tend to overestimate the mean annual rainfall at high elevations for Bega River. These results suggest that uncorrected MIROC3.2, ECHAM5 and CSIRO-Mk3.0 RCMs have larger errors at high elevations, particularly along the Australian Alps for the Bega River site. This is consistent with Chubb et al. (2016) who suggested that AWAP provides poor estimates of rainfall on the Australian Alps. They suggested that AWAP rainfalls at high elevations were about 50% too low after comparing AWAP with raingauges.

After bias correction, all RCMs shown in Figure 10.6 appear to perform equally well, capturing the mean rainfall of AWAP at the Bega River site with minor discrepancies between each other. All RCMs overestimate the rainfall slightly along the coast and the high elevations regions, particularly along the Australian Alps. This overestimation is greatest for the reanalysis.

Note that the sky blue grid points are large water bodies with undefined rainfall. As mentioned in Section 6.3.1, these can only be seen in the bias corrected plots.

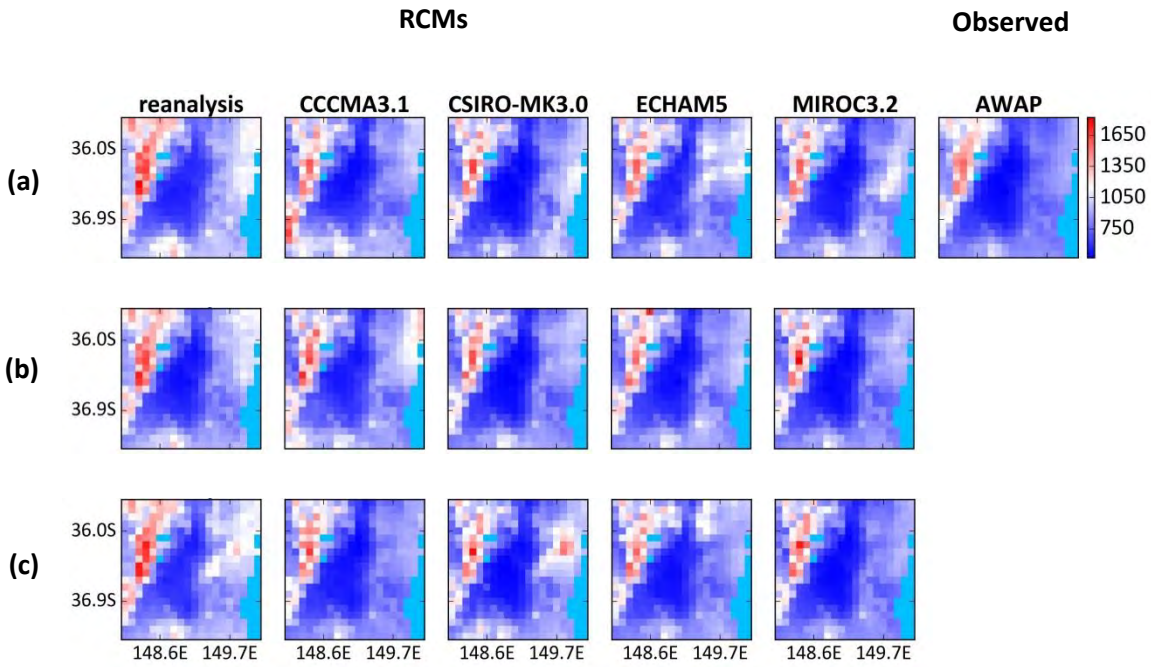

Figure 10.6 Spatial distribution of the mean annual rainfall (1990-2009) of the Bega River site: The plots are for the bias corrected simulations of (a) R1, (b) R2, and (c) R3, and AWAP. Note the colour scale is different to Figure 10.5.

The relative performance of the bias corrected RCMs at the Bega River site is:

CCCMA3.1 (R3) **≈ ECHAM5** (R3) **≈ MIROC3.2** (R2) **≈ CSIRO-Mk3.0** (R2) **> reanalysis** (R2)

The spatial distribution of the mean rainfall of the uncorrected R2 RCMs and bias corrected R1, R2 and R3 RCMs of Sydney River site are shown in Figures 10.7 and 10.8 respectively. All uncorrected RCMs overestimate the rainfall at high elevations of the Bega River and Sydney sites.

The relative performance of the uncorrected RCMs at the Sydney site is:

CCCMA3.1 (R2) **> ECHAM5** (R2) **> MIROC3.2** (R2) **> CSIRO-Mk3.0** (R2) **> reanalysis** (R2)

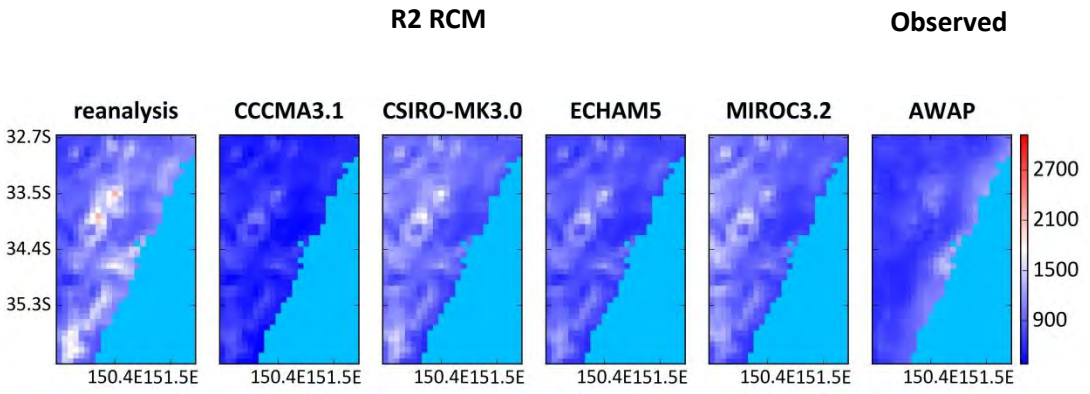

Figure 10.7 Spatial distribution of the mean annual rainfall (1990-2009) of the Sydney site: The plots are for the uncorrected simulations of R2 and AWAP.

As was seen at the Bega River site, all RCMs for the Sydney site (shown in Figure 10.8), except reanalyses, appear to perform equally well after the bias correction, capturing the mean rainfall of AWAP at the Sydney site. Consistent with the mean annual rainfall at Williams River, Richmond River and Bega River sites, all of the bias corrected reanalyses for Sydney overestimate the rainfall along the coast.

The relative performance of the bias corrected RCMs at Sydney site is:

CCMA3.1 (R2) ≈ **ECHAM5** (R3) ≈ **MIROC3.2** (R2) ≈ **CSIRO-Mk3.0** (R2) > **reanalysis** (R3)

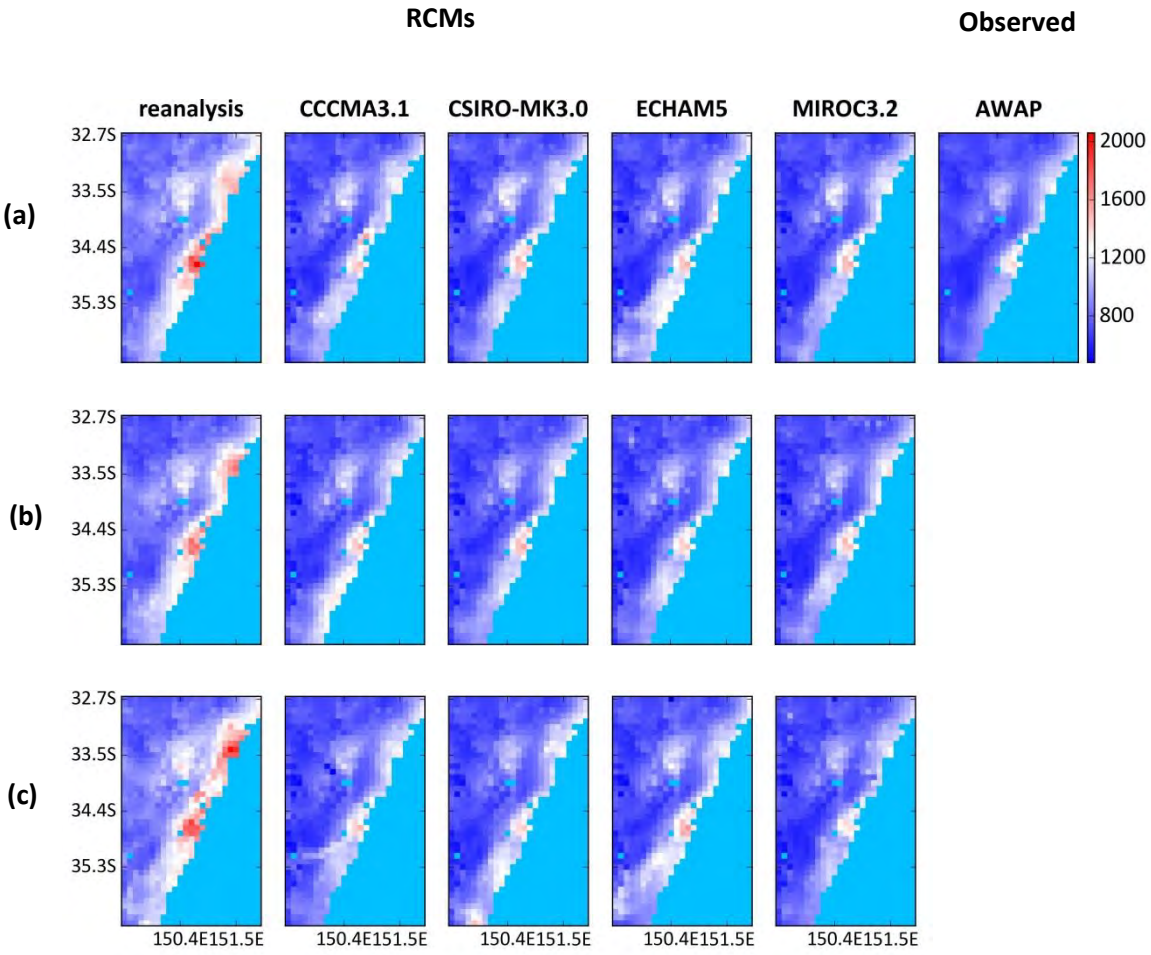

Figure 10.8 Spatial distribution of the mean annual rainfall (1990-2009) of the Sydney site: The plots are for the bias corrected simulations of (a) R1, (b) R2, and (c) R3, and AWAP. Note the colour scale is different to Figure 10.7.

10.2.2 Standard deviation of the rainfall

The results of the standard deviation of rainfall for all RCMs (uncorrected and bias corrected) are shown in this section. This section focuses on the changes in the standard deviation of the rainfall after the bias correction.

While comparing the underlying RCM configurations, differences between RCM performance at different time resolutions (i.e. differences between the aggregated rainfalls; daily, fortnightly, monthly and annually) are assessed. The results of the Sydney site are only presented in this section. Since there is an overlap between the boundary of the Sydney site, and Williams River and Bega River sites, the Sydney site is used as a representative of all three sites together in this section.

The standard deviation of rainfall for the uncorrected RCMs compared with AWAP is shown in Figures 10.9 to 10.11.

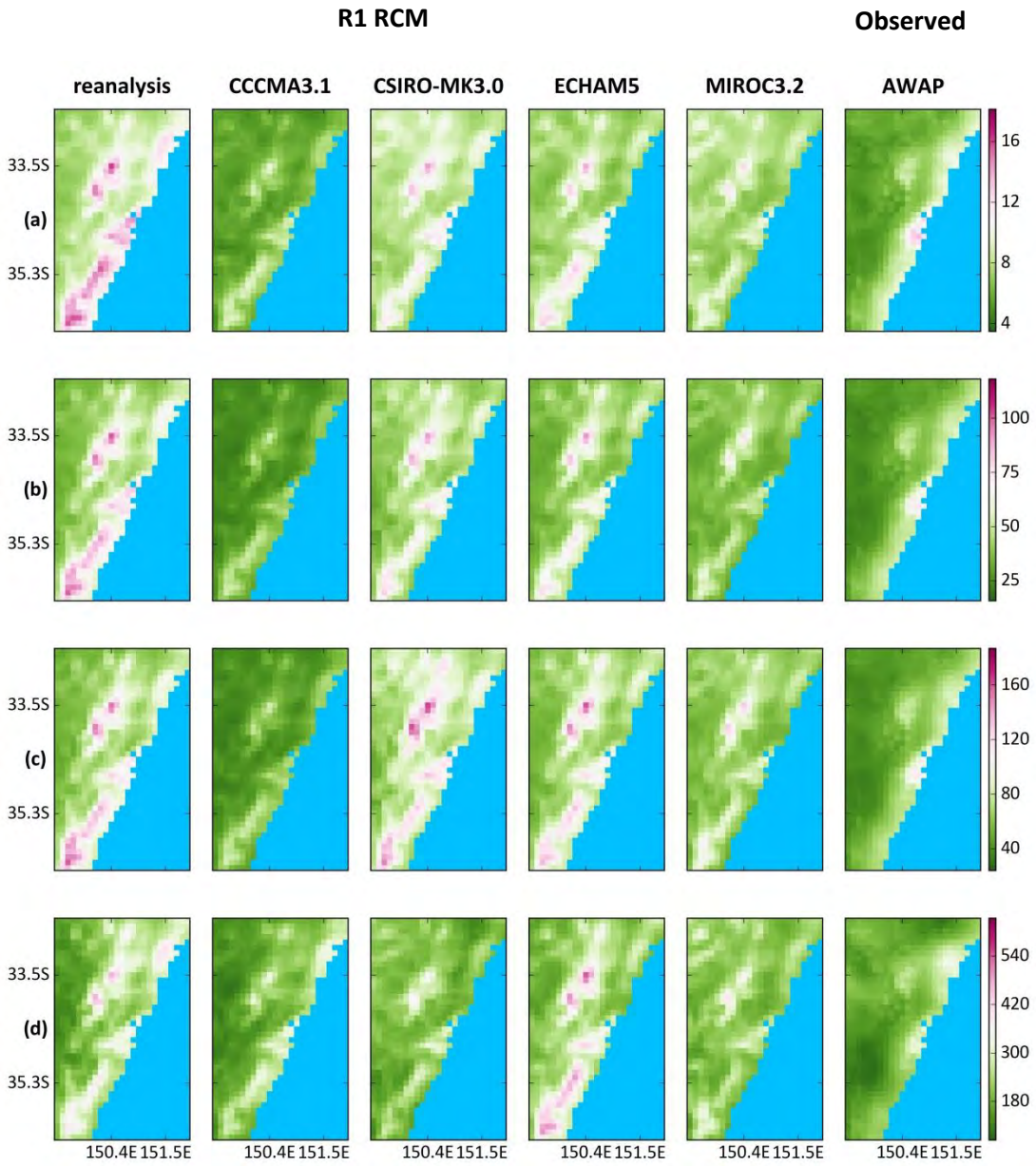

Figure 10.9 Spatial distribution of the standard deviation of the rainfall (1990-2009) of the Sydney site: The plots are for the uncorrected simulations of R1 and AWAP. Time resolutions are; (a) daily, (b) fortnightly, (c) monthly, and (d) annual.

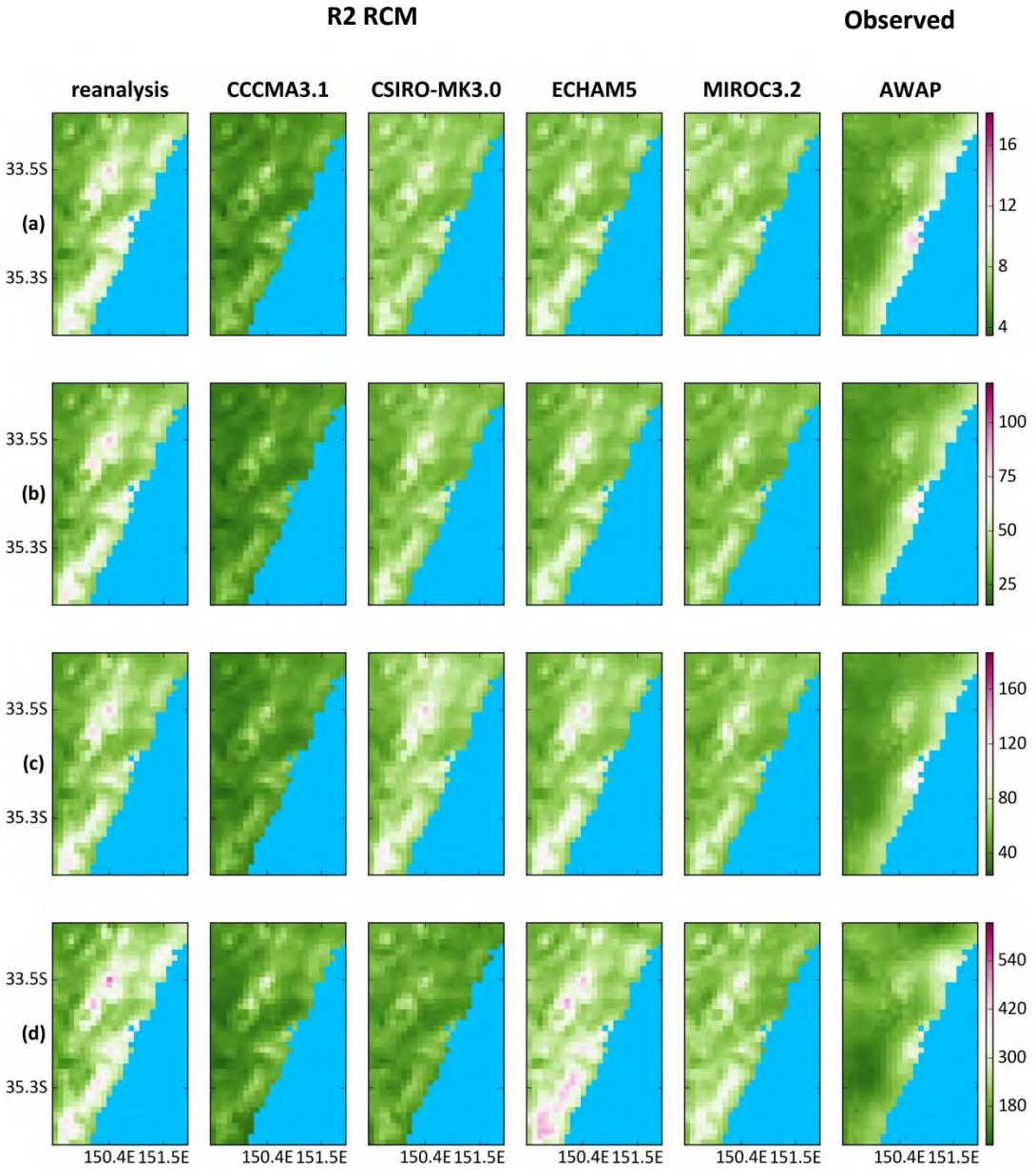

Figure 10.10 Spatial distribution of the standard deviation of the rainfall (1990-2009) of the Sydney site: The plots are for the uncorrected simulations of R2 and AWAP. Time resolutions are; (a) daily, (b) fortnightly, (c) monthly, and (d) annual.

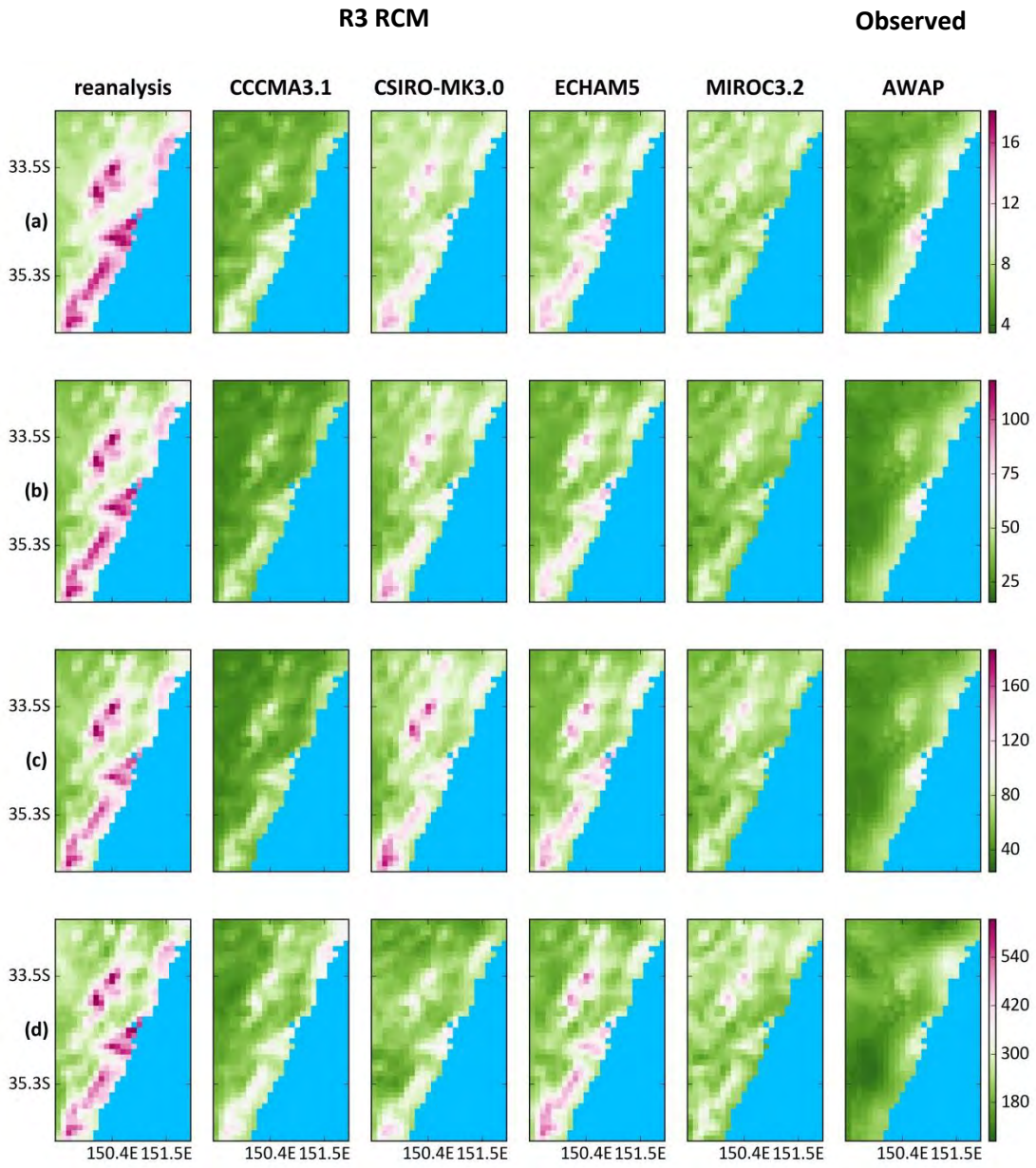

Figure 10.11 Spatial distribution of the standard deviation of the rainfall (1990-2009) of the Sydney site: The plots are for the uncorrected simulations of R3 and AWAP. Time resolutions are; (a) daily, (b) fortnightly, (c) monthly, and (d) annual.

R1- and R3-CCCMA3.1 most closely reproduce the standard deviation of AWAP while R2-CCCMA3.1 tends to underestimate the standard deviation. All other RCMs (GCM and reanalysis) simulations slightly overestimate. This overestimation is greatest at high elevations (at Blue Mountains) and along the coast. R3 reanalysis

has the highest overestimation. The R2 RCMs best reproduces the spatial pattern in the standard deviation of AWAP. Simulations of R3 and R1 tend to overestimate the standard deviation, particularly R3, for the low elevation coastal regions.

The relative performance for the standard deviation for the uncorrected RCMs at Sydney is (the best RCM configurations are shown in brackets):

CCCMA3.1 (R1 and R3) **> MIROC3.2** (R2) **> ECHAM5** (R2) **≈ CSIRO-Mk3.0** (R2) > **reanalysis** (R2)

The standard deviation of the bias corrected RCM simulations for R1, R2 and R3 compared with AWAP are shown in Figures 10.12 to 10.14. Note that the sky blue grid points within the site are large water bodies with undefined rainfall (see Section 6.3.1). As was seen with the mean, the ability of all RCMs to reproduce the standard deviation of AWAP has been improved by the bias correction. All R2 RCMs show the best results in reproducing the standard deviation of AWAP.

The relative performance for the standard deviation for the bias corrected RCMs is:

MIROC3.2 (R2) > **CCCMA3.1** (R2) **> CSIRO-Mk3.0** (R2) **≈ ECHAM5** (R2) > **reanalysis** (R2)

While the overall performance of the standard deviation of the RCM simulated rainfall has been significantly improved by the bias correction, it is worth noting that there are some erroneous grid points (to the west of the site) with very low standard deviation values which may have caused by the bias correction process. These grid points have very low standard deviation values, even lower than the surrounding grid points.

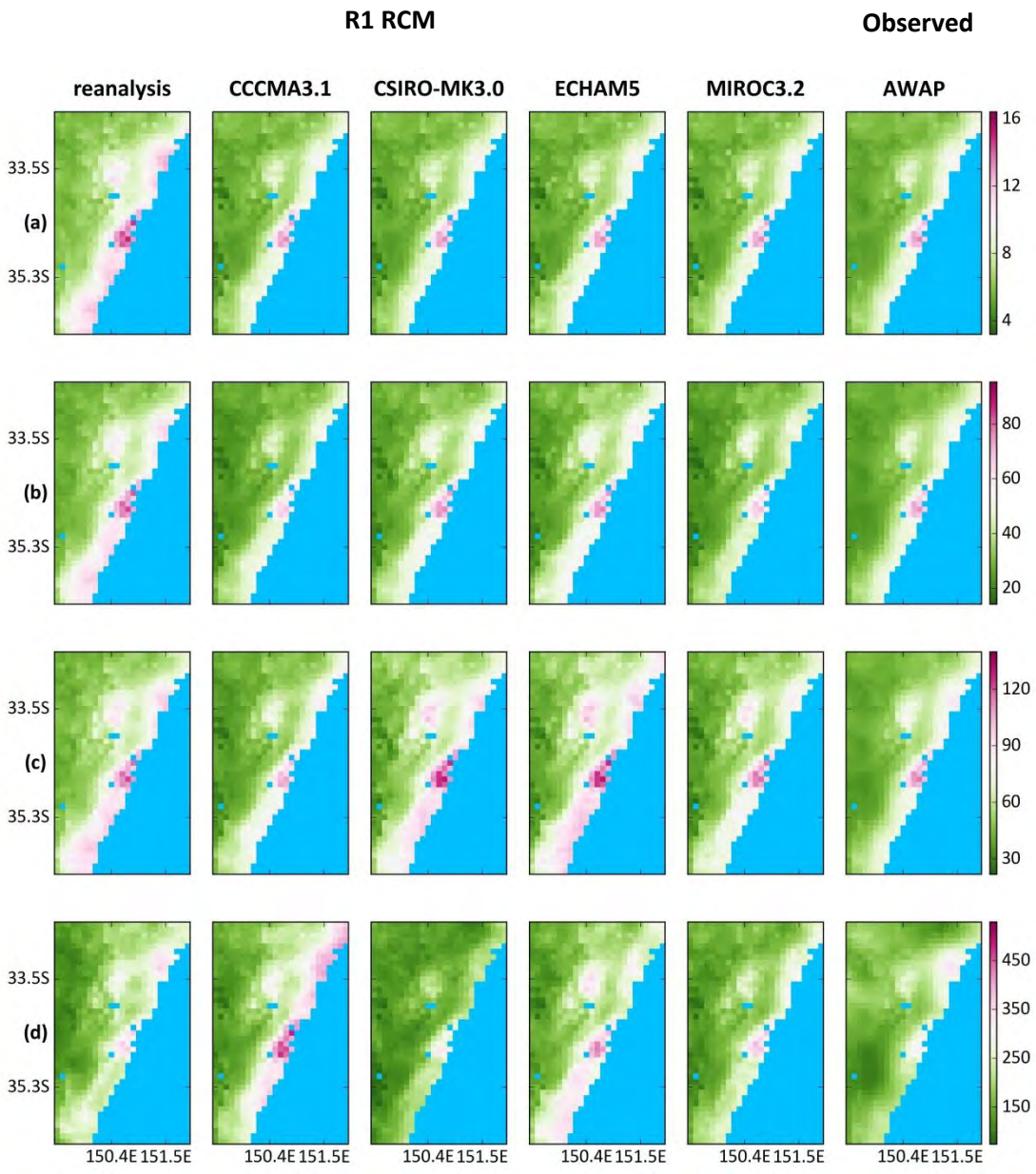

Figure 10.12 Spatial distribution of the standard deviation of the rainfall (1990-2009) of the Sydney site: The plots are for the bias corrected simulations of R1 and AWAP. Time resolutions are; (a) daily, (b) fortnightly, (c) monthly, and (d) annual.

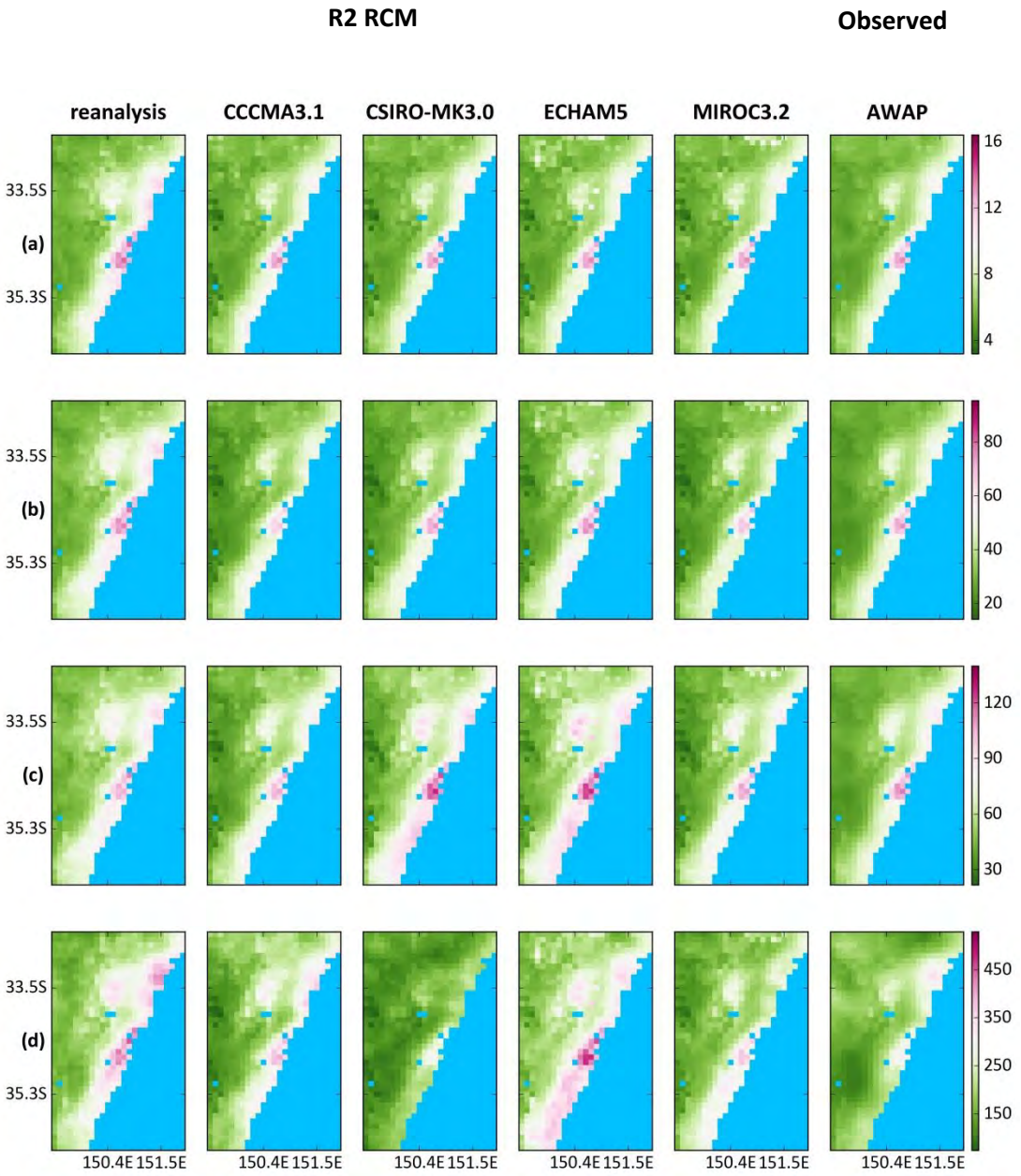

Figure 10.13 Spatial distribution of the standard deviation of the rainfall (1990-2009) of the Sydney site: The plots are for the bias corrected simulations of R2 and AWAP. Time resolutions are; (a) daily, (b) fortnightly, (c) monthly, and (d) annual.

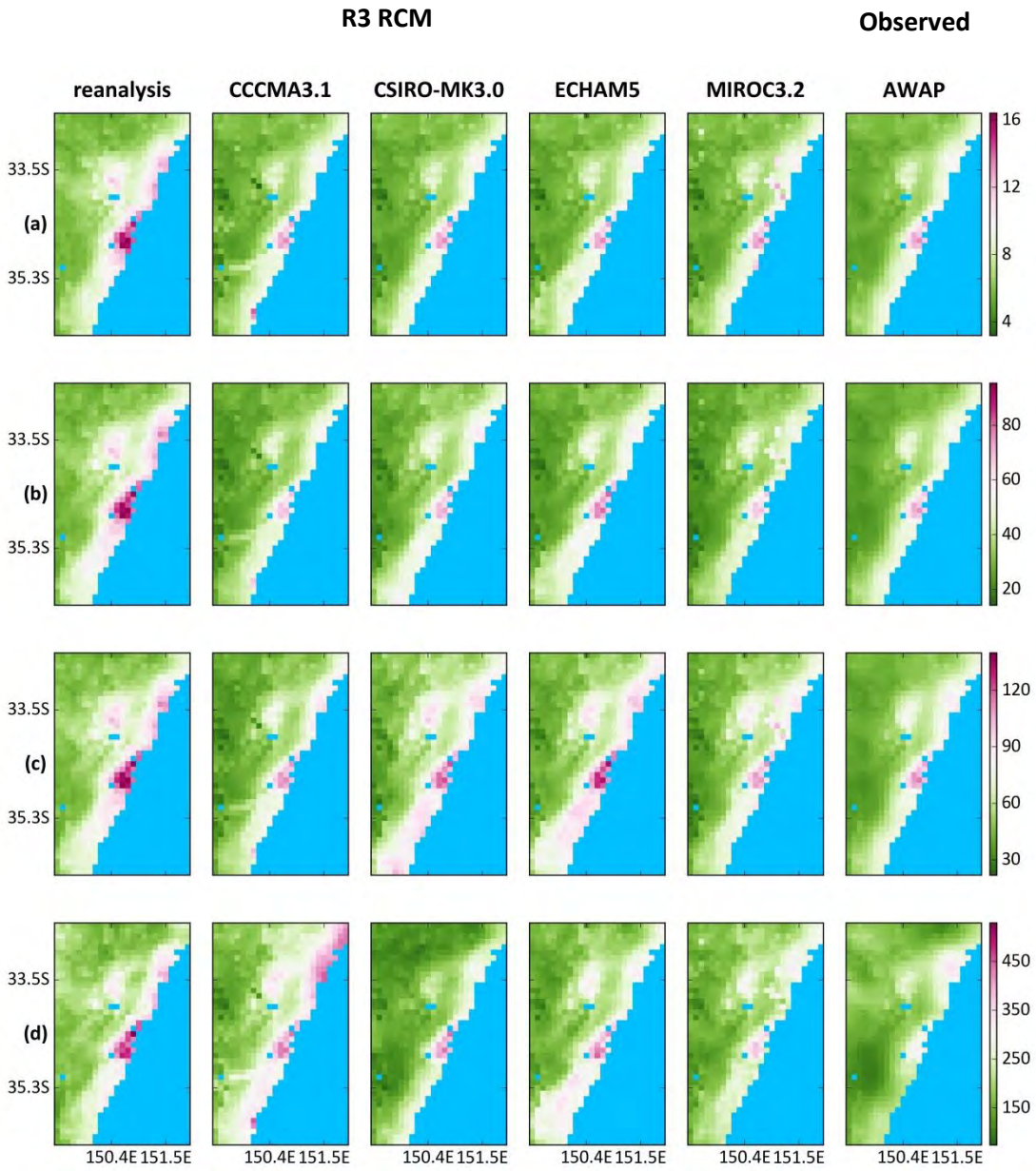

Figure 10.14 Spatial distribution of the standard deviation of the rainfall (1990-2009) of the Sydney site: The plots are for the bias corrected simulations of R3 and AWAP. Time resolutions are; (a) daily, (b) fortnightly, (c) monthly, and (d) annual.

Overall, the results presented for both uncorrected and bias corrected simulations at different time resolutions (daily, fortnightly, monthly and annual) suggest that the differences in the fits to AWAP between time resolutions are small, and the relative performance of all the models is similar across the time resolutions.

10.2.3 Coefficient of variation of the rainfall

The spatial variability of the coefficient of variation (the ratio of standard deviation to mean) for the uncorrected and bias corrected RCM simulated rainfall is assessed in this section. The results shown in Section 6.3.2 suggested that reanalyses simulations tend to underestimate the rainfall variability of AWAP. This section compares the coefficient of variation (C_v) for all RCMs against AWAP. Since the relative performance of RCMs is consistent across the sites, only the results for the Richmond River and the Sydney sites are shown (see Appendix A.4 – Figures A.13 to A.24 for the results of the Williams River and Bega River sites)

The C_v of uncorrected RCMs for R1, R2 and R3 compared with AWAP for the Richmond River site is shown in Figures 10.15 to 10.17. As was seen in the mean and standard deviation of the rainfall in Sections 10.2.1 and 10.2.2, all GCM-RCM combinations, except CSIRO-Mk3.0, best simulate the C_v of AWAP using R2.

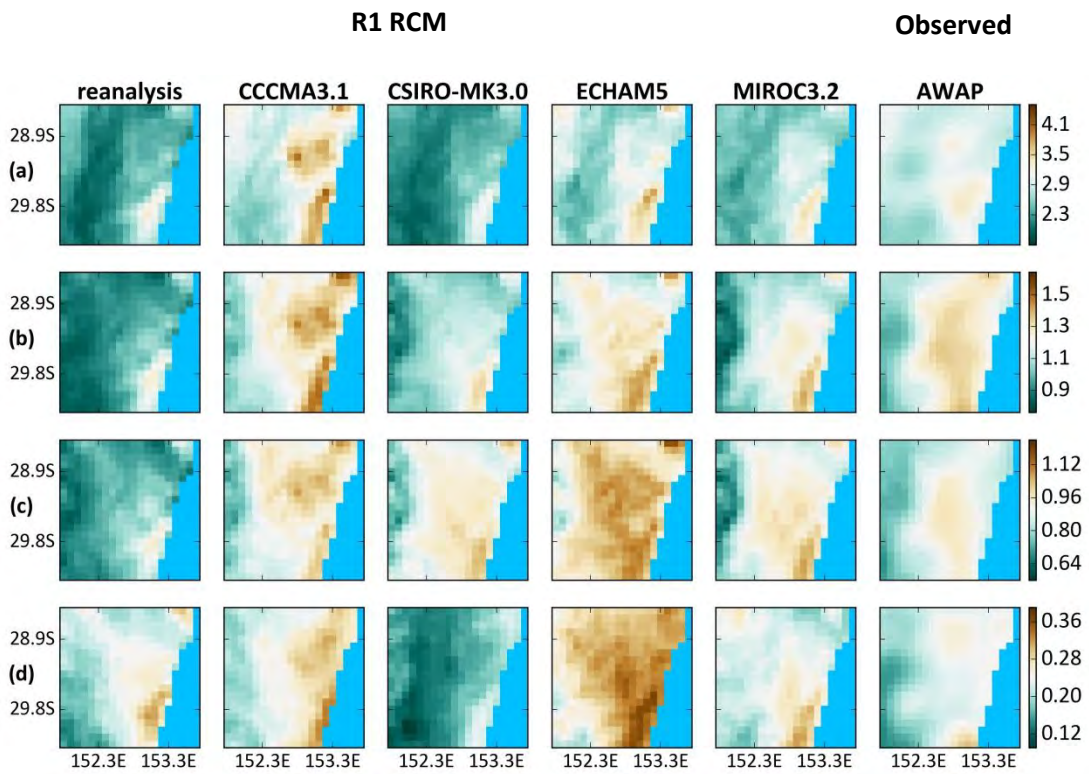

Figure 10.15 Spatial distribution of the coefficient variation of the rainfall (1990-2009) of the Richmond River site: The plots are for the uncorrected simulations of R1 and AWAP. Time resolutions are; (a) daily, (b) fortnightly, (c) monthly, and (d) annual.

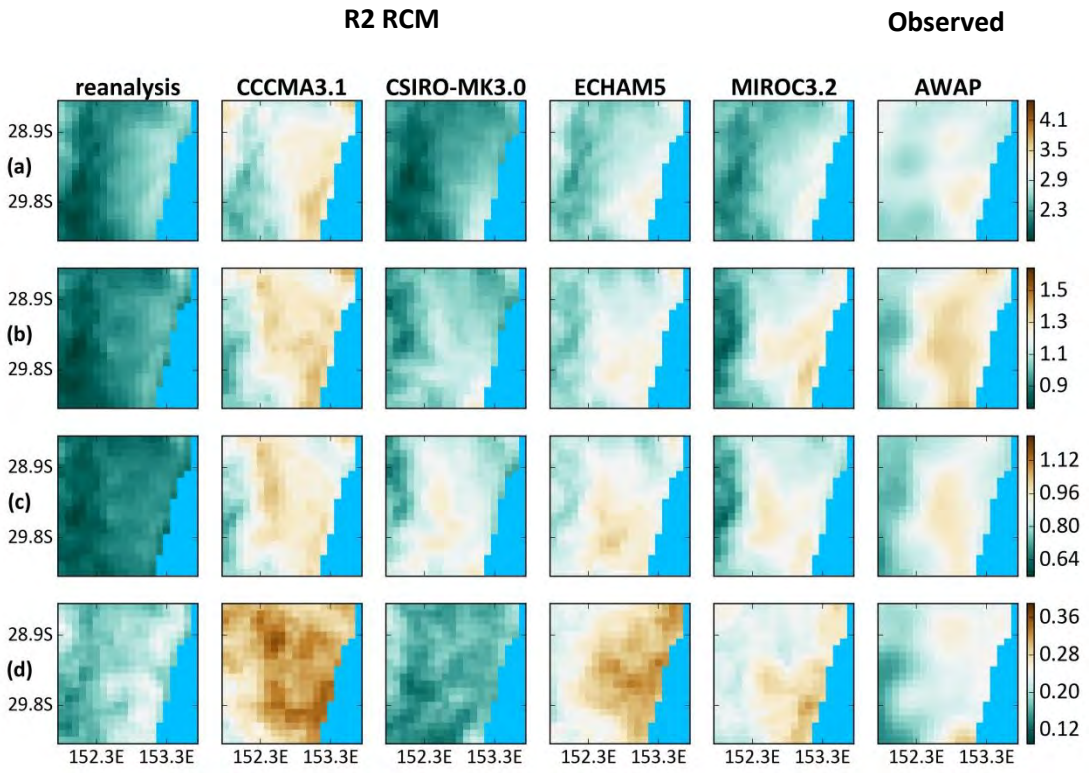

Figure 10.16 Spatial distribution of the oefficient variation of the rainfall (1990-2009) of the Richmond River site: The plots are for the uncorrected simulations of R2 and AWAP. Time resolutions are; (a) daily, (b) fortnightly, (c) monthly, and (d) annual.

The uncorrected CCCMA3.1 and ECHAM5 RCMs overestimate the C_v of AWAP, with R3-CCCMA3.1 and R3-ECHAM5 overestimating more than R1 and R2. Due to this overestimation, the uncorrected CCCMA3.1 fails to reproduce the C_v of rainfall, even though it was identified as the best uncorrected model simulation for capturing the mean annual rainfall at all sites in the previous section. The R2-MIROC3.2 best simulates the C_v of AWAP at fortnightly and monthly resolutions, but with slight underestimation at high elevation regions. R3-CSIRO-Mk3.0 closely simulates the C_v of AWAP at monthly and annual time resolutions. The reanalyses, R1- and R2-CSIRO-Mk3.0 underestimate the C_v of AWAP for most time resolutions.

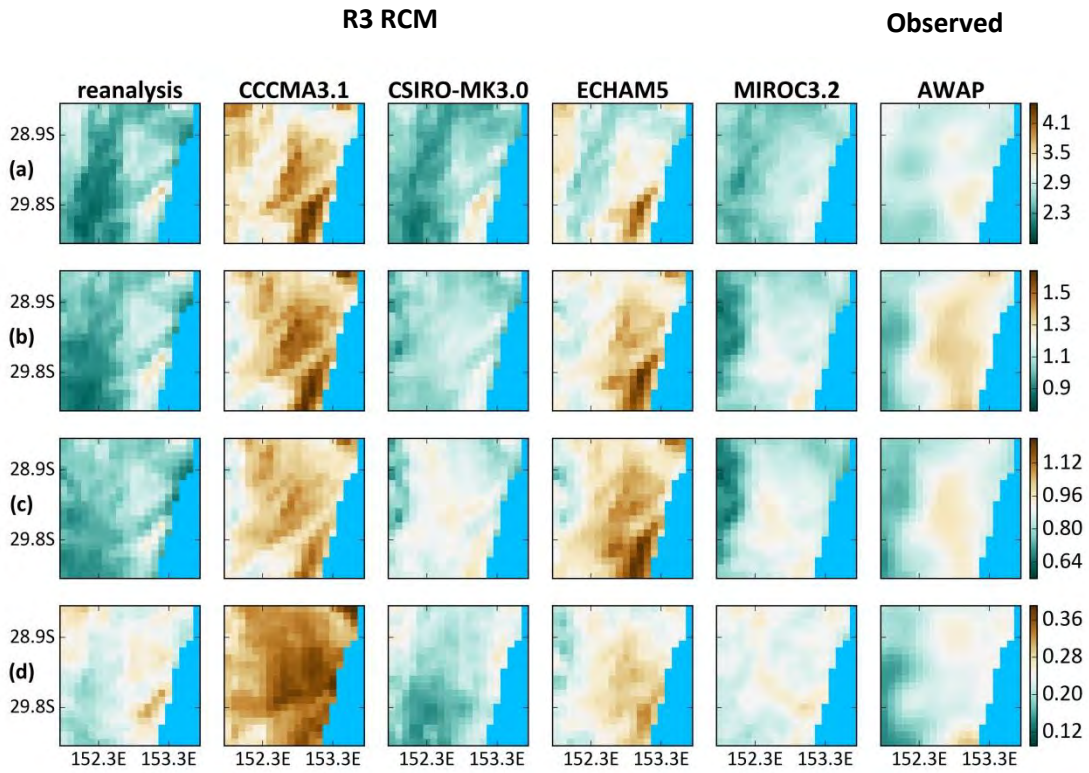

Figure 10.17 Spatial distribution of the coefficient variation of the rainfall (1990-2009) of the Richmond River site: The plots are for the uncorrected simulations of R3 and AWAP. Time resolutions are; (a) daily, (b) fortnightly, (c) monthly, and (d) annual.

The relative performance for the C_v for the uncorrected RCMs is (the best RCM configurations are shown in brackets):

MIROC3.2 (R2) > **ECHAM5** (R2) >**CCCMA3.1** (R2) >**CSIRO-Mk3.0** (R3) > **reanalysis** (R2)

The C_v of the bias corrected RCM simulations for R1, R2 and R3 compared with AWAP is shown in Figures 10.18 to 10.20.

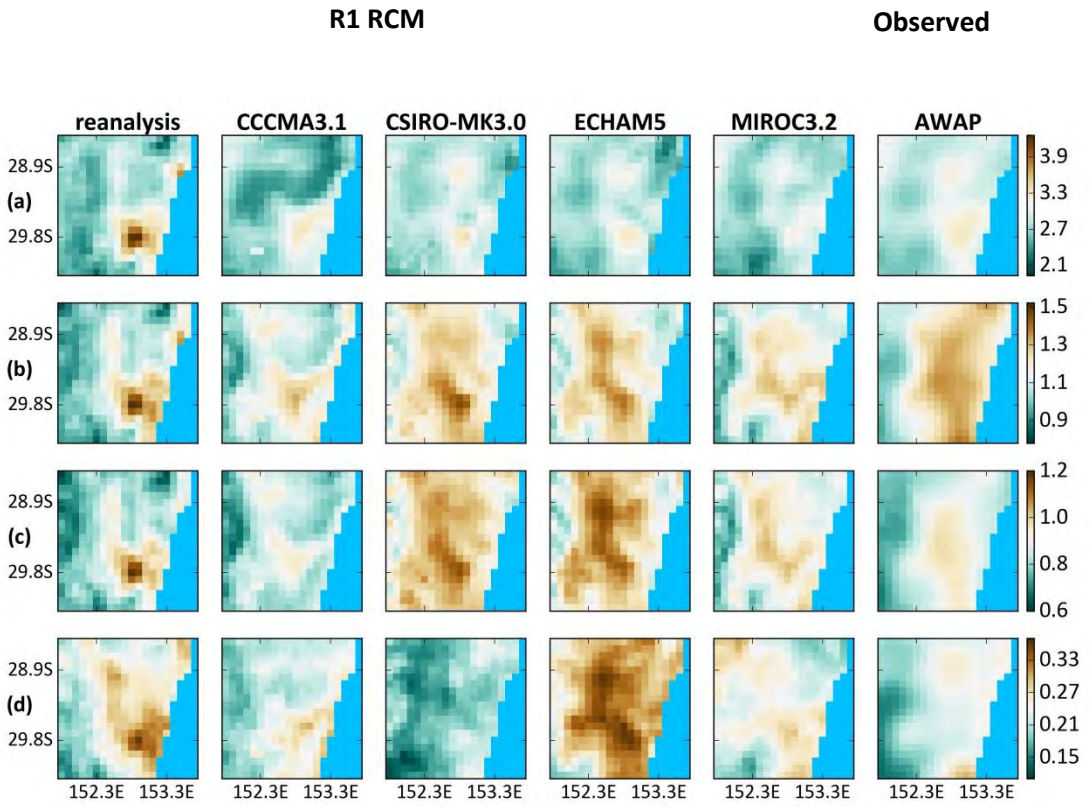

Figure 10.18 Spatial distribution of the coefficient of variation of the rainfall (1990-2009) of the Richmond River site: The plots are for the bias corrected simulations of R1 and AWAP. Time resolutions are; (a) daily, (b) fortnightly, (c) monthly, and (d) annual.

With the bias correction, most of the errors of CCCMA3.1 and ECHAM5 have been corrected. Reanalyses data, particularly the R3 reanalysis also show some significant improvement in reproducing the C_v of AWAP. Similarly, the performance of R1 and R3-MIROC3.2 has been improved by the bias correction. An improvement in the simulation of the C_v using bias-correction is seen for almost all RCMs for all configurations. Overall, this suggests that bias correction has improved the performance of the simulations at the RCM configuration level (i.e. R1, R2 and R3) and in particular R1 and R3 have been significantly improved. The best improvements occur for the daily resolution (the resolution at which the bias correction is performed) with relatively poorer improvement at the longer time resolutions.

The ability to capture the C_v of AWAP in the bias corrected RCMs is (the best model configurations are shown in brackets):

MIROC3.2 (R1 and R3)> **ECHAM5** (R3)> **CCCMA3.1** (R1)> **CSIRO-Mk3.0** (R3) > **reanalysis** (R3)

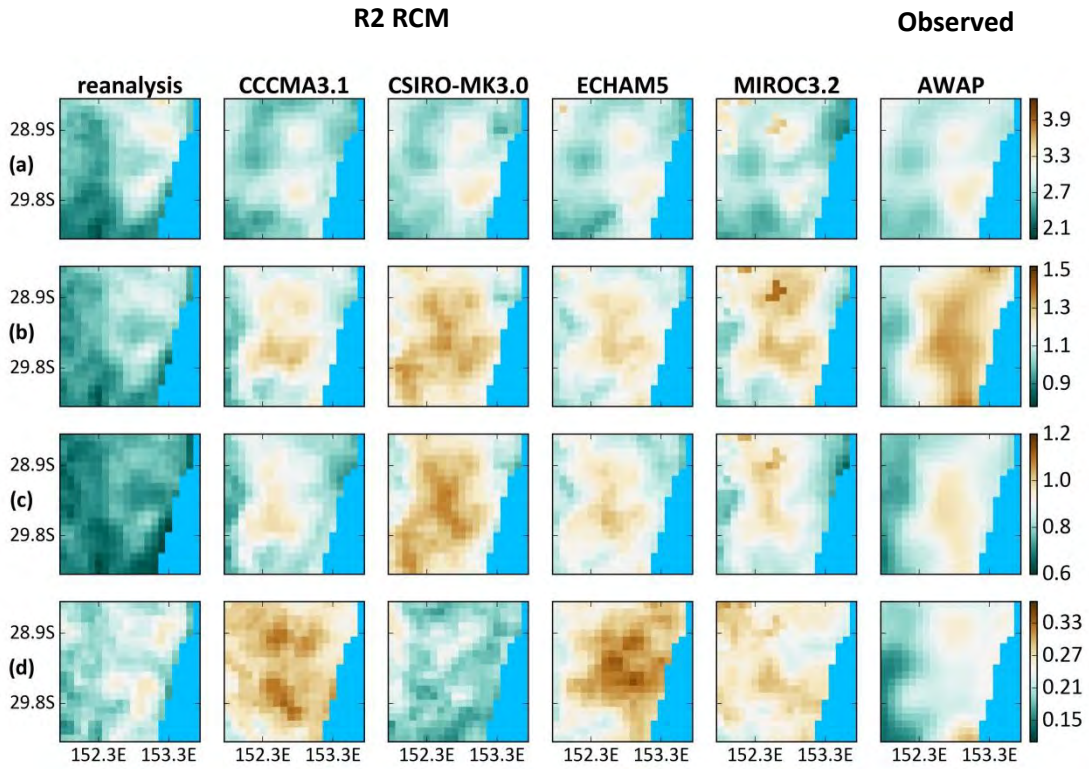

Figure 10.19 Spatial distribution of the coefficient variation of the rainfall (1990-2009) of the Richmond River site: The plots are for the bias corrected simulations of R2 and AWAP. Time resolutions are; (a) daily, (b) fortnightly, (c) monthly, and (d) annual.

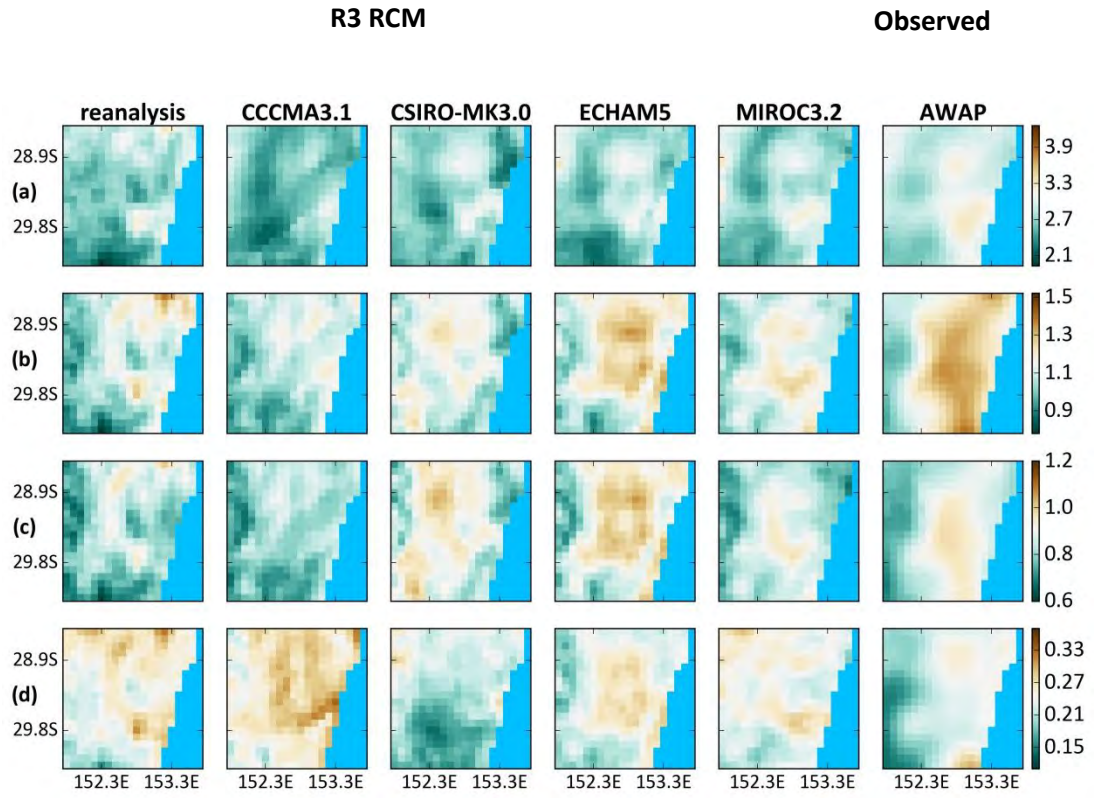

Figure 10.20 Spatial distribution of the coefficient variation of the rainfall (1990-2009) of the Richmond River site: The plots are for the bias corrected simulations of R3 and AWAP. Time resolutions are; (a) daily, (b) fortnightly, (c) monthly, and (d) annual.

The C_v of uncorrected RCMs compared with AWAP at the Sydney site is shown in Figures 10.21 to 10.23. As was seen at the Richmond River site, MIROC3.2 appears to closely simulate the C_v of AWAP at the Sydney site while slightly underestimating the C_v along the Great Dividing Range. Overall, all R2 RCMs, except reanalysis and ECHAM5 appear to closely reproduce the spatial pattern of the C_v but significantly underestimates the magnitude by as much as 30%. The overall performance of the individual models is consistent with Richmond River site and can be summarized as follows.

MIROC3.2 (R2) > **ECHAM5** (R3) > **CCCMA3.1** (R2) >**CSIRO-Mk3.0** (R3) >**reanalysis** (R2)

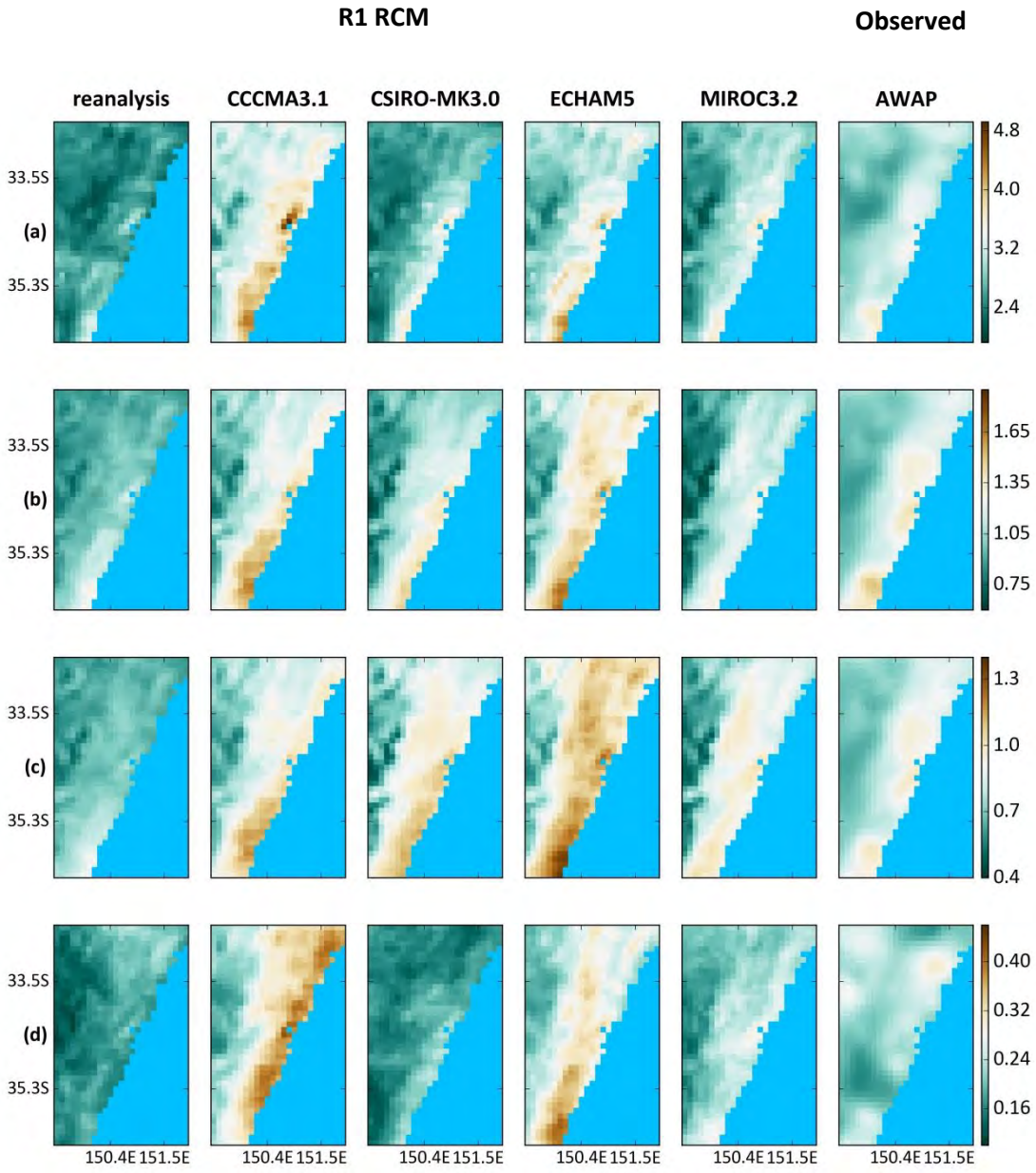

Figure 10.21 Spatial distribution of the coefficient variation of the rainfall (1990-2009) of the Sydney site: The plots are for the uncorrected simulations of R1 and AWAP. Time resolutions are; (a) daily, (b) fortnightly, (c) monthly, and (d) annual.

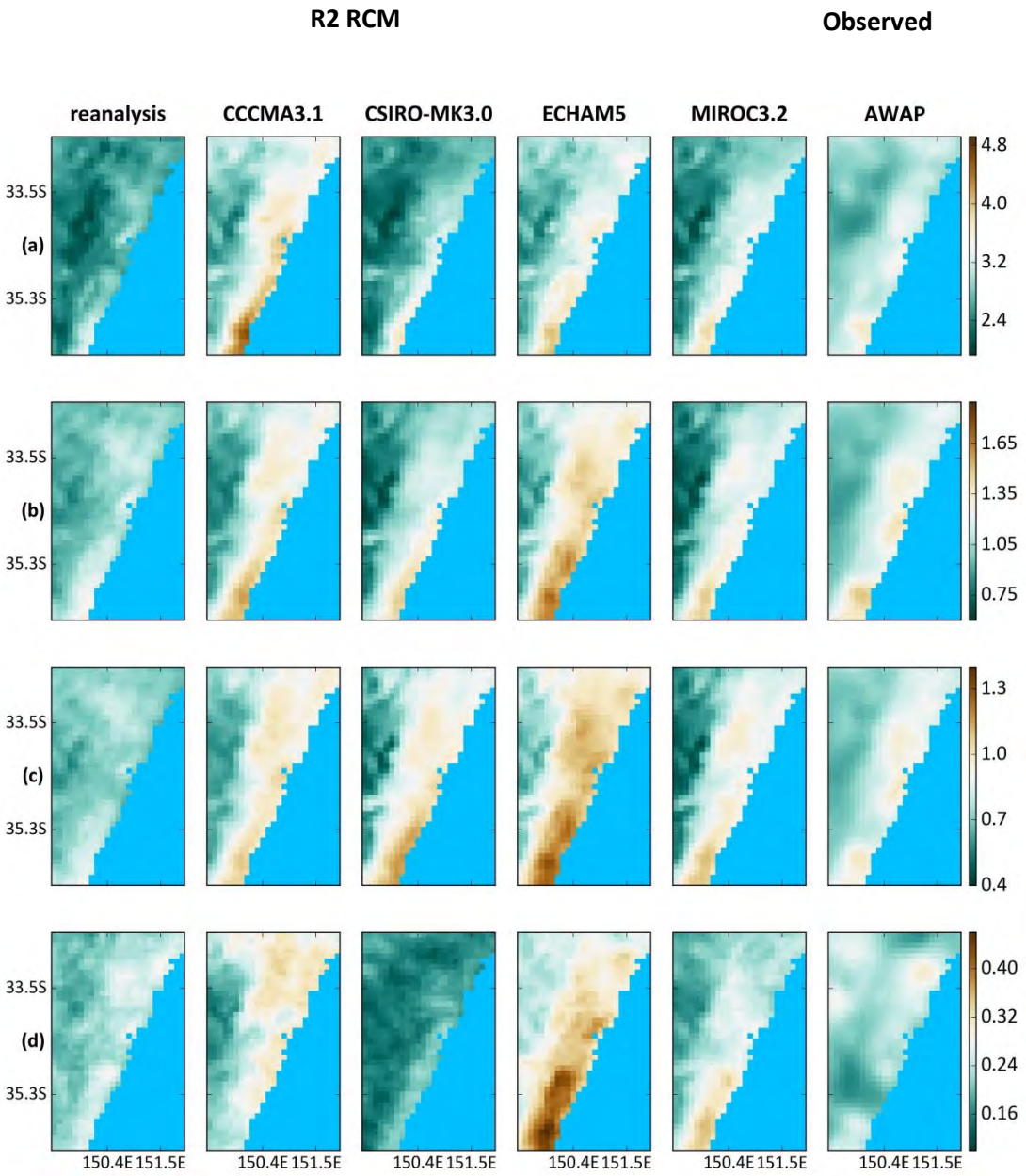

Figure 10.22 Spatial distribution of the coefficient variation of the rainfall (1990-2009) of the Sydney site: The plots are for the uncorrected simulations of R2 and AWAP. Time resolutions are; (a) daily, (b) fortnightly, (c) monthly, and (d) annual.

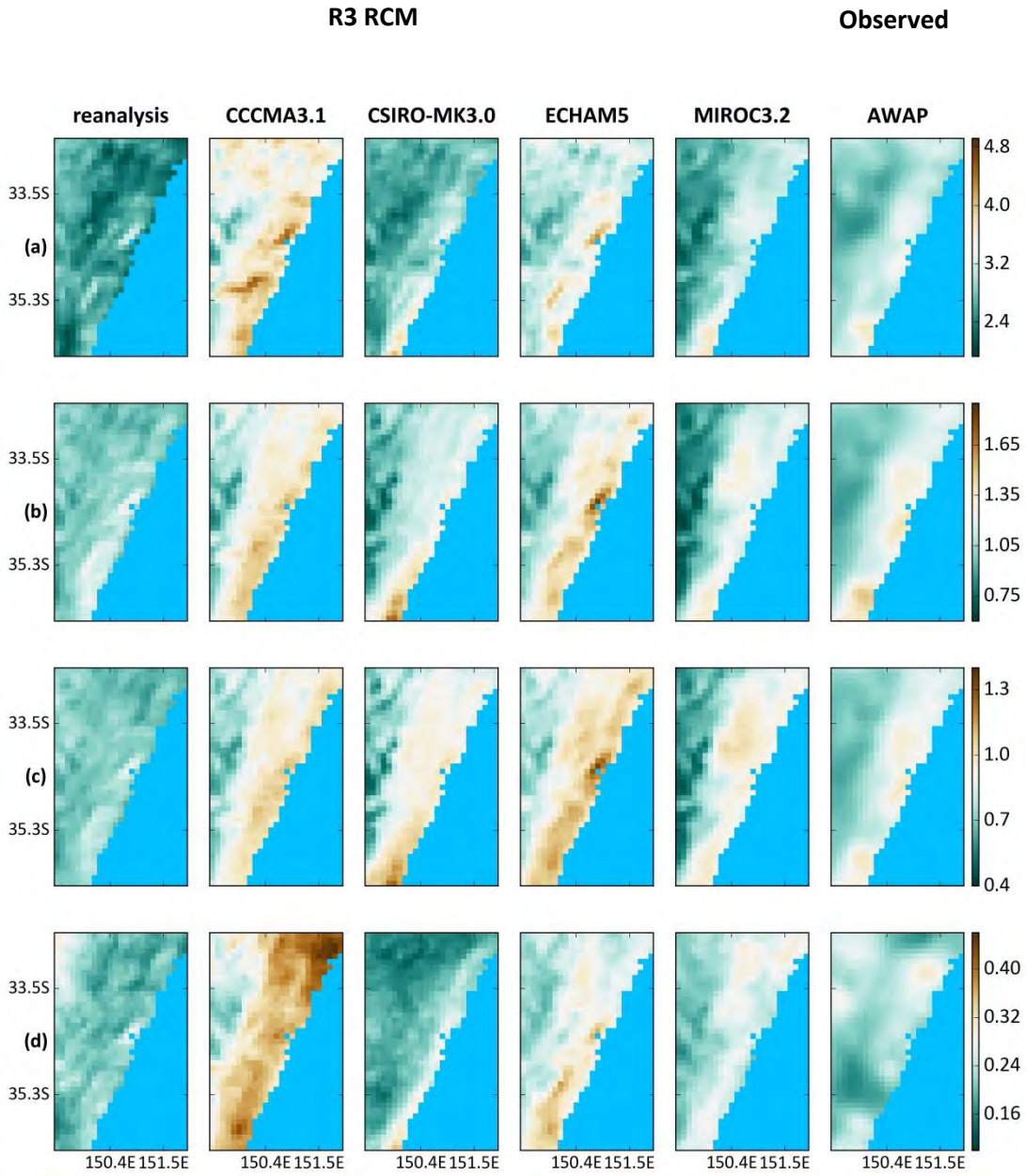

Figure 10.23 Spatial distribution of the coefficient variation of the rainfall (1990-2009) of the Sydney site: The plots are for the uncorrected simulations of R3 and AWAP. Time resolutions are; (a) daily, (b) fortnightly, (c) monthly, and (d) annual.

The C_v of the bias corrected RCMs compared with AWAP are shown in Figures 10.24 to 10.26. The performance of reanalysis, CCCMA3.1 and ECHAM5 has been improved after the bias correction which is consistent with the results at the Richmond River site. Note that the sky blue grid points within the site are large water bodies with undefined rainfall (see Section 6.3.1).

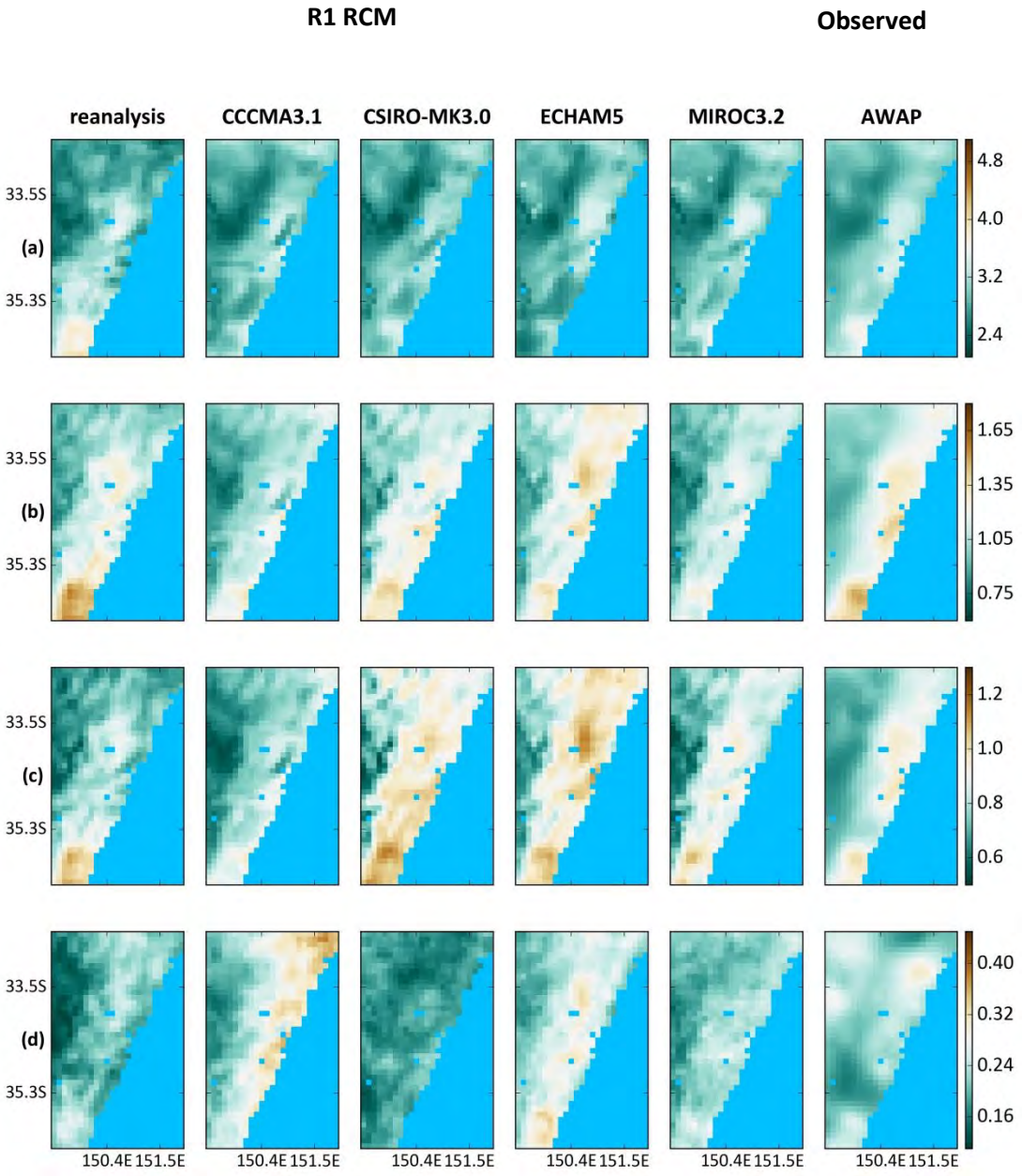

Figure 10.24 Spatial distribution of the coefficient variation of the rainfall (1990-2009) of the Sydney site: The plots are for the bias corrected simulations of R1 and AWAP. Time resolutions are; (a) daily, (b) fortnightly, (c) monthly, and (d) annual.

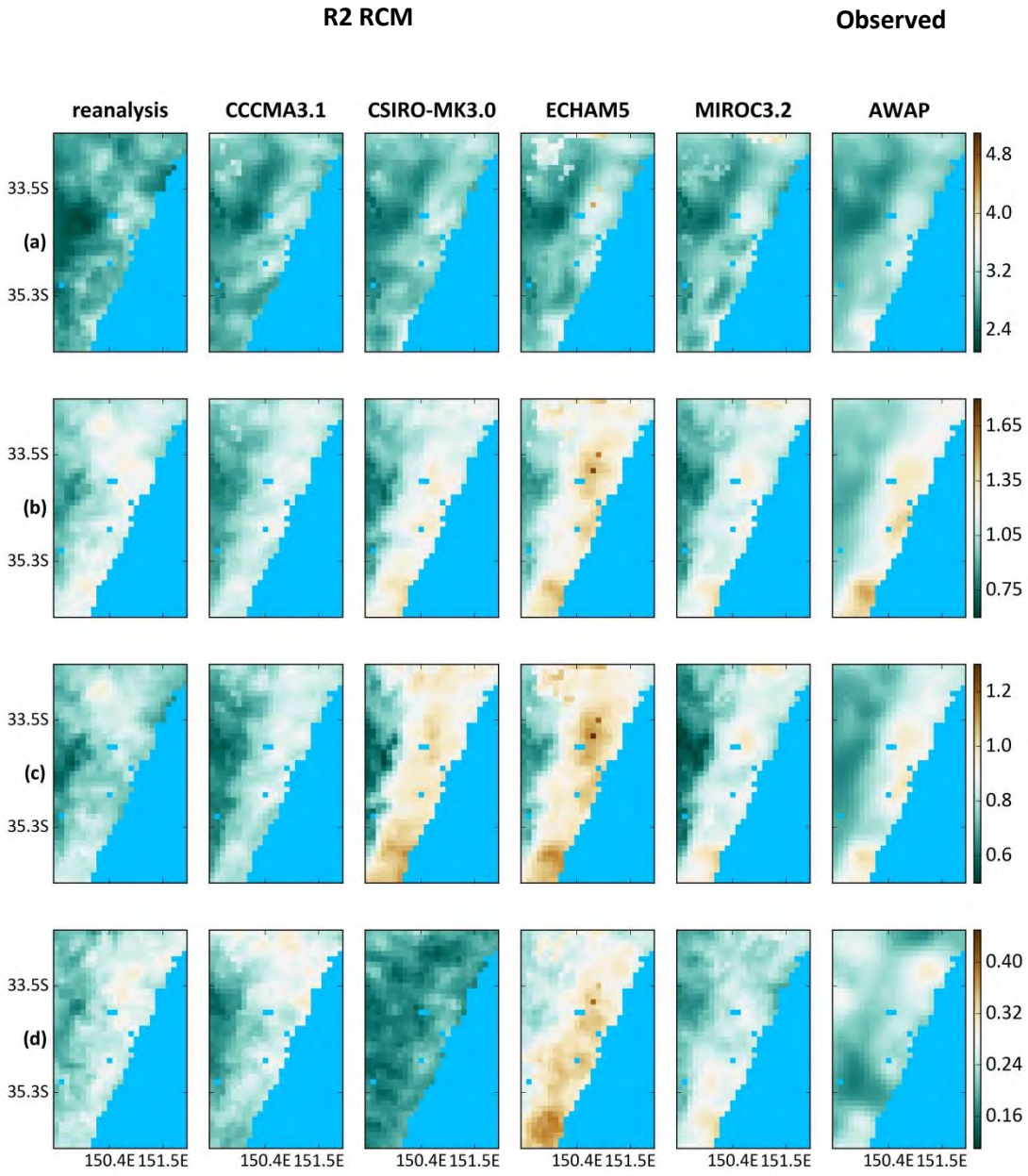

Figure 10.25 Spatial distribution of the coefficient variation of the rainfall (1990-2009) of the Sydney site: The plots are for the bias corrected simulations of R2 and AWAP. Time resolutions are; (a) daily, (b) fortnightly, (c) monthly, and (d) annual.

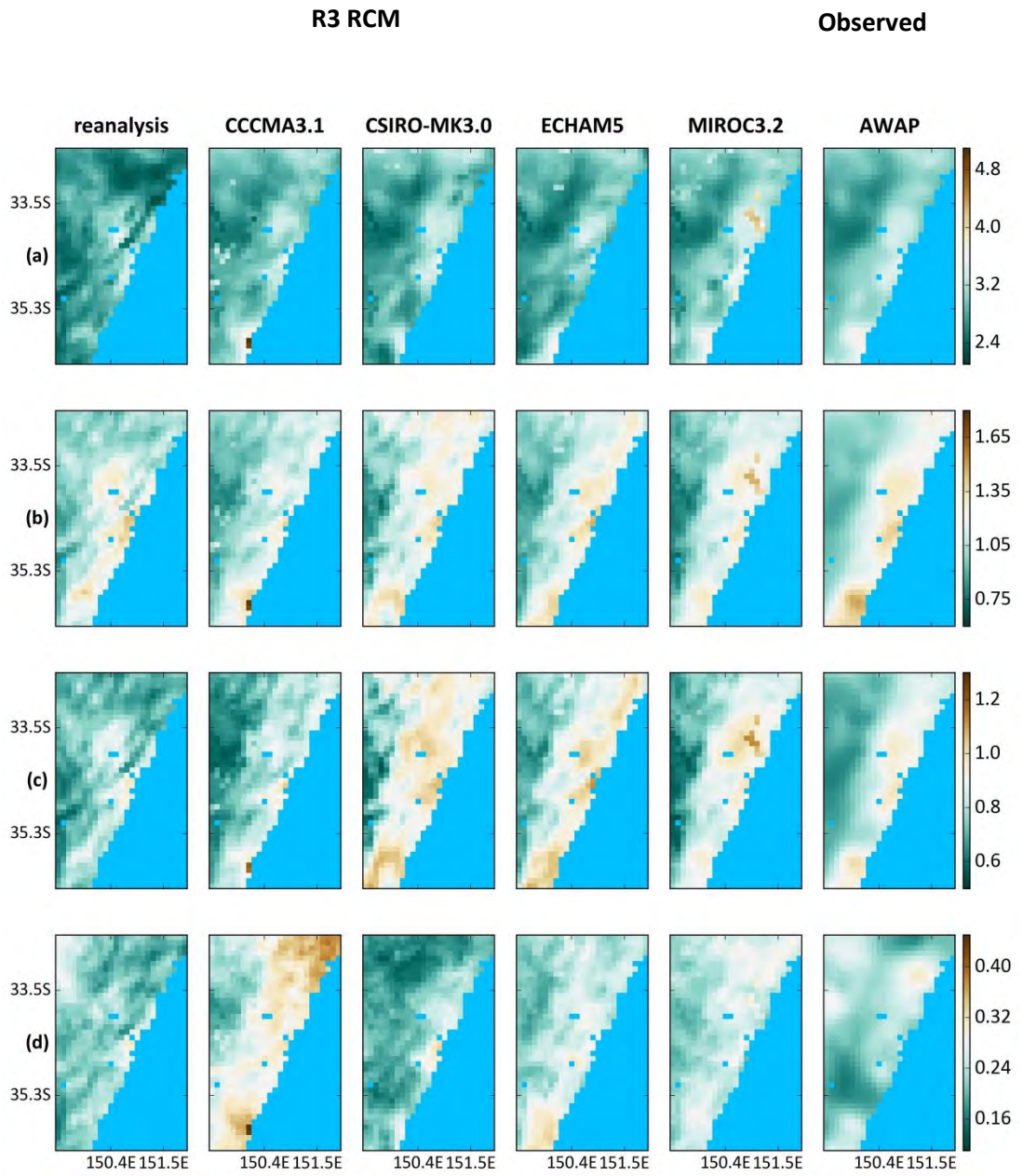

Figure 10.26 Spatial distribution of the coefficient variation of the rainfall (1990-2009) of the Sydney site: The plots are for the bias corrected simulations of R3 and AWAP. Time resolutions are; (a) daily, (b) fortnightly, (c) monthly, and (d) annual.

The relative performance for C_v for the bias corrected RCMs is (the best RCM configurations are shown in brackets):

MIROC3.2 (R2)> **ECHAM5** (R3)> **CCCMA3.1** (R1)> **CSIRO-Mk3.0** (R3) **> reanalysis** (R3)

The results for the Sydney site also suggest that the performance of R1 and R3 RCMs, which performed poorly for the uncorrected rainfall, have been improved the most by the bias correction.

10.2.4 Lag-1 autocorrelation of the rainfall

This section assesses the performance of RCMs to reproduce the lag-1 autocorrelation of AWAP. As in Section 10.2.3, only results for the Richmond River and Sydney sites are shown (see Appendix A.5 – Figures A.25 to A.36 for the results of Williams River and Bega River sites).

The spatial distribution of lag-1 autocorrelation of the uncorrected RCMs compared with AWAP at the Richmond River site is shown in Figures 10.27 to 10.29. Of all simulations, the uncorrected CCCMA3.1 closely reproduces the lag-1 correlation of AWAP for all three configurations. R3-CCCMA3.1 tends to better simulate the lag-1 autocorrelation for all three time resolutions, yet the spatial pattern in the annual autocorrelation of AWAP is not well simulated; particularly the negative lag-1 autocorrelations regions of AWAP are not well matched by CCCMA3.1.

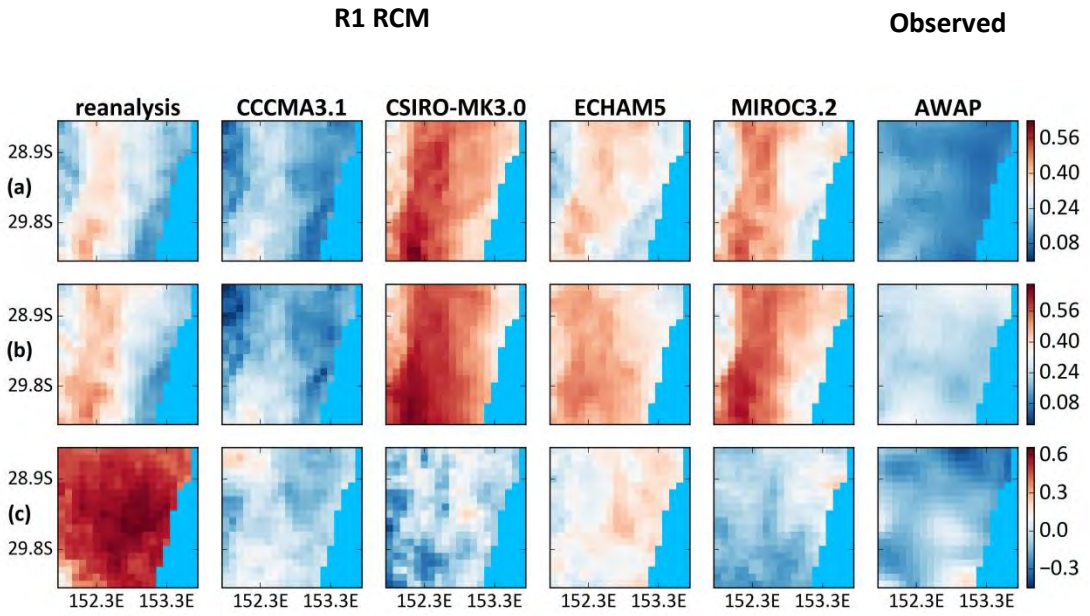

Figure 10.27 Spatial distribution of the lag-1 correlation of the rainfall (1990-2009) of the Richmond River site: The plots are for the uncorrected simulations of R1 and AWAP. Time resolutions are; (a) fortnightly, (b) monthly, and (c) annual.

The uncorrected R1 and R2 configuration CSIRO-Mk3.0, ECHAM5 and MIROC3.2 largely overestimate the lag-1 correlation of AWAP, particularly at fortnightly and monthly resolutions, while having a minimum overestimation for the R3 configuration. Only R3-CCCMA3.1 and R3-CSIRO-Mk3.0 appear to reproduce the lag-1 autocorrelation at the annual resolution. As was seen in Section 6.3.3 for 1950-2009, R1 and R2 reanalyses do not reproduce the spatial pattern of AWAP and for most locations overestimate the lag-1 autocorrelation everywhere.

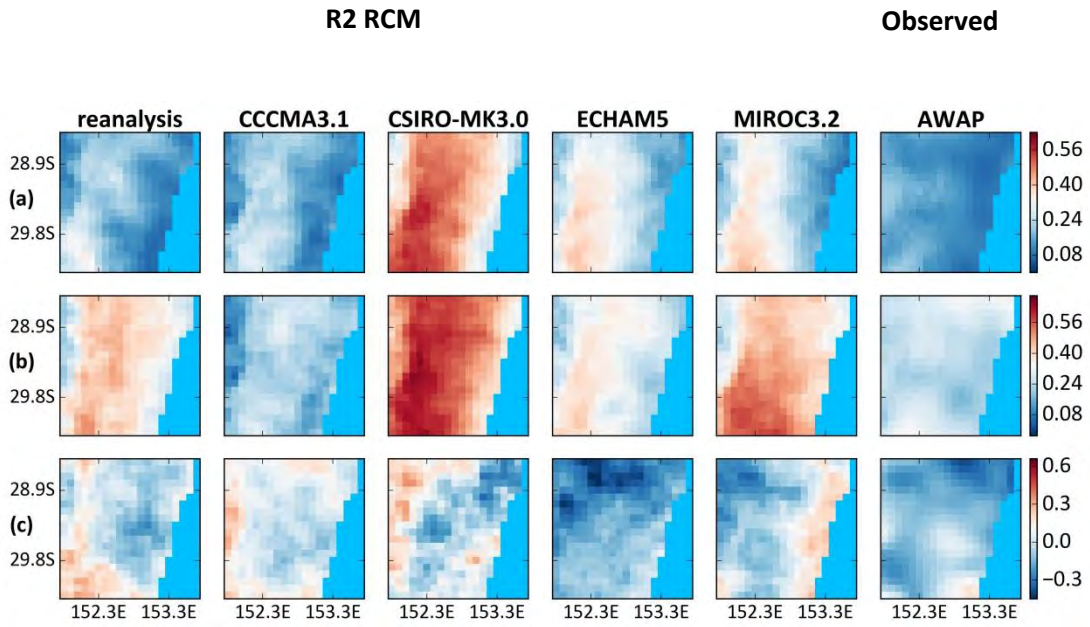

Figure 10.28 Spatial distribution of the lag-1 correlation of the rainfall (1990-2009) of the Richmond River site: The plots are for the uncorrected simulations of R2 and AWAP. Time resolutions are; (a) fortnightly, (b) monthly, and (c) annual.

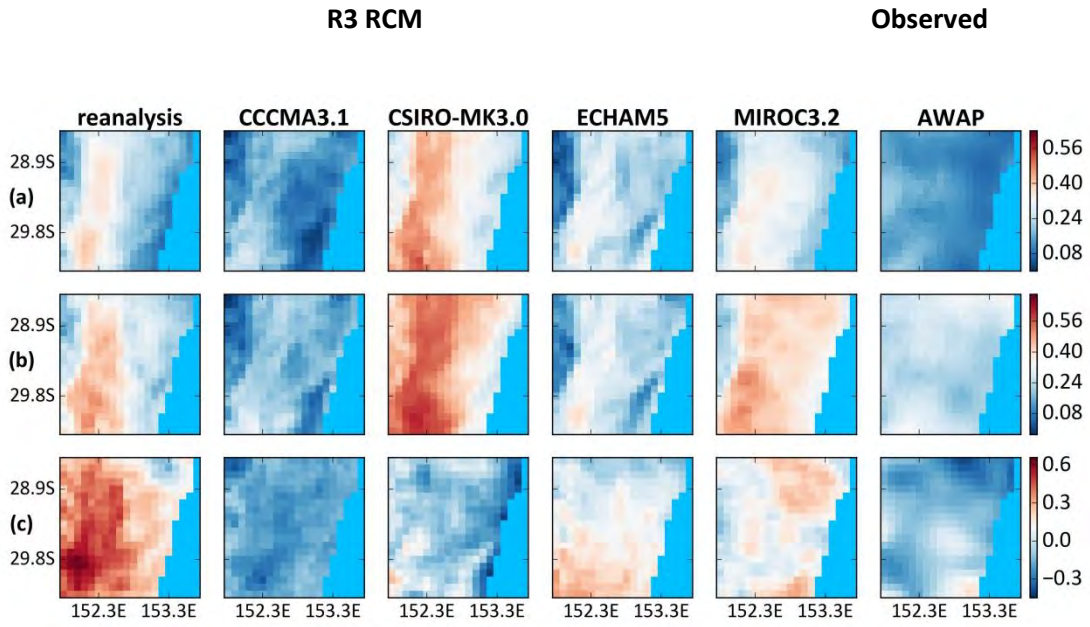

Figure 10.29 Spatial distribution of the lag-1 correlation of the rainfall (1990-2009) of the Richmond River site: The plots are for the uncorrected simulations of R3 and AWAP. Time resolutions are; (a) fortnightly, (b) monthly, and (c) annual.

The relatiuve performance for the lag-1 correlation for the uncorrected RCMs is (the best model configurations are shown in brackets):

CCCMA3.1 (R3) > **ECHAM5** (R3) **> reanalysis** (R3) **> MIROC3.2** (R3)

> CSIRO-Mk3.0 (R3)

Lag-1 correlations of the bias corrected RCMs compared with AWAP are shown in Figures 10.30 to 10.32. The spatial pattern in the lag-1 correlation of the bias corrected R3-CCCMA3.1 better match with AWAP, but only for the month and annual resolutions. The bias corrected CCCMA3.1 shows highly overestimated correlations compared with the uncorrected, particularly for the fortnightly resolution, but the reason for this drastic change in the autocorrelation is not known. Except for the slight improvement of R3-CCCMA3.1, all simulations remain unchanged after the bias correction. This suggests that the bias correction does not improve the time series characteristics of the rainfall, particularly lag-1 autocorrelations. Therefore, the ability to reproduce the lag-1 correlation of AWAP in the bias corrected RCMs is unchanged by bias correction.

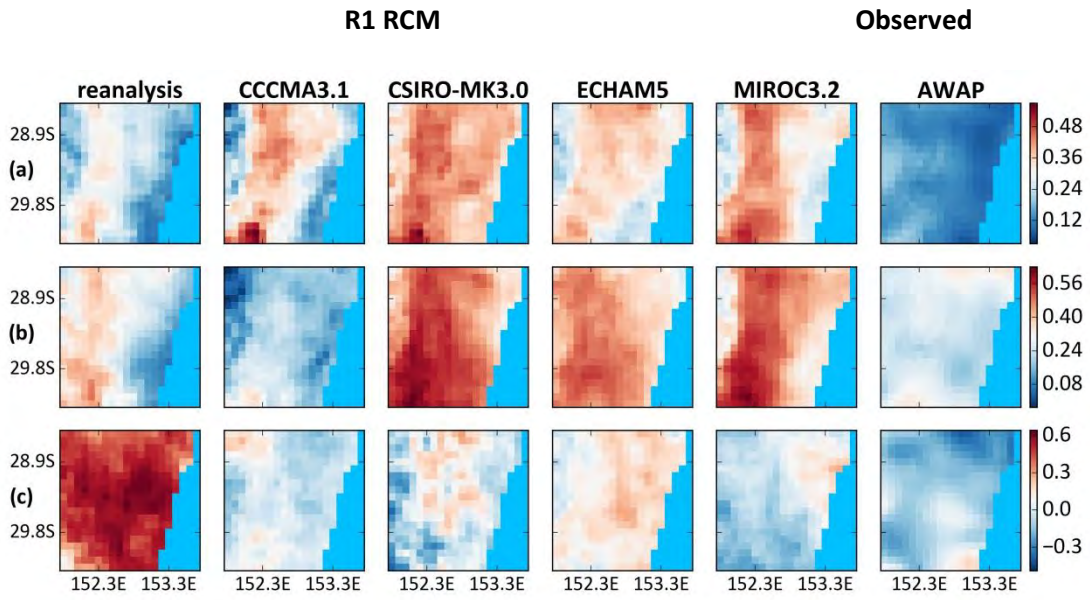

Figure 10.30 Spatial distribution of the lag-1 correlation of the rainfall (1990-2009) of the Richmond River site: The plots are for the bias corrected simulations of R1 and AWAP. Time resolutions are; (a) fortnightly, (b) monthly, and (c) annual.

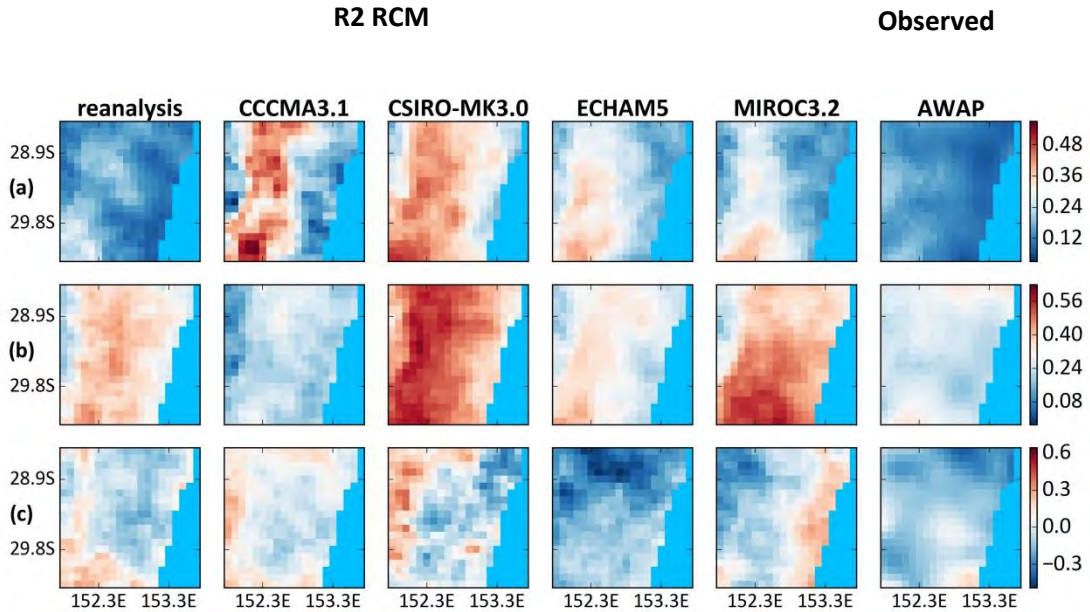

Figure 10.31 Spatial distribution of the lag-1 correlation of the rainfall (1990-2009) of the Richmond River site: The plots are for the bias corrected simulations of R2 and AWAP. Time resolutions are; (a) fortnightly, (b) monthly, and (c) annual.

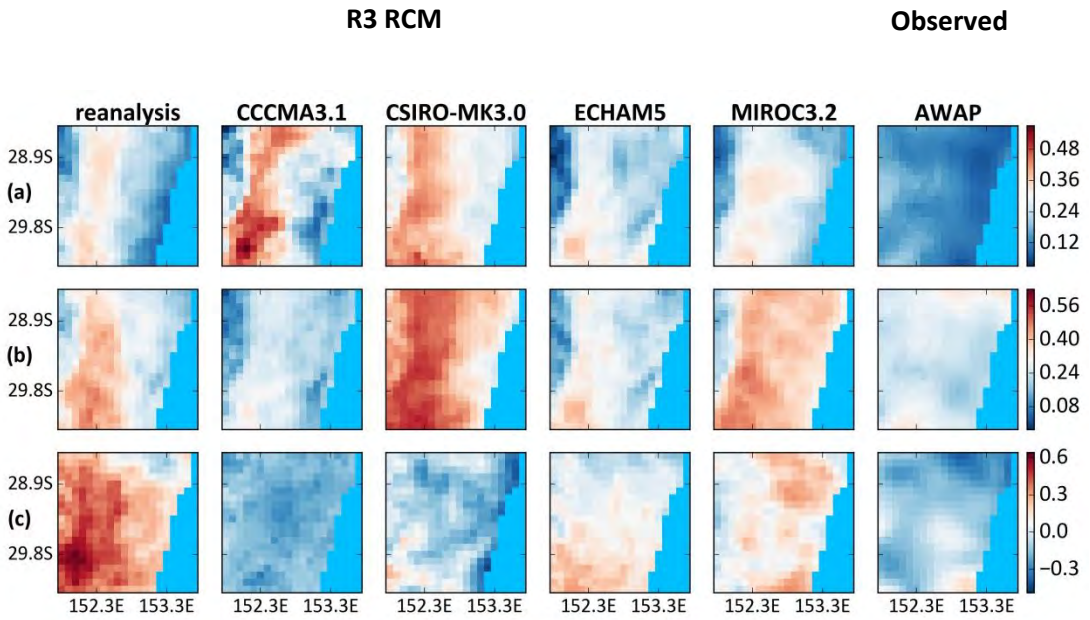

Figure 10.32 Spatial distribution of the lag-1 correlation of the rainfall (1990-2009) of the Richmond River site: The plots are for the bias corrected simulations of R3 and AWAP. Time resolutions are; (a) fortnightly, (b) monthly, and (c) annual.

The spatial distribution of lag-1 autocorrelations of the uncorrected RCMs compared with AWAP for Sydney site are shown in Figures 10.33 to 10.35.

At the fortnightly and monthly resolutions, reanalysis and CCCMA3.1 reproduce the lag-1 correlation of AWAP at the Sydney site. This improvement of the performance of reanalyses data, particularly R3 reanalysis is consistent with the results for Sydney site shown in Section 6.3.3.

The relative performance for the lag-1 correlation for the uncorrected RCMs is (the best model configurations are shown in brackets):

CCCMA3.1 (R3) > **reanalysis** (R3) **> ECHAM5** (R3) **> MIROC3.2** (R3)

> CSIRO-Mk3.0 (R3)

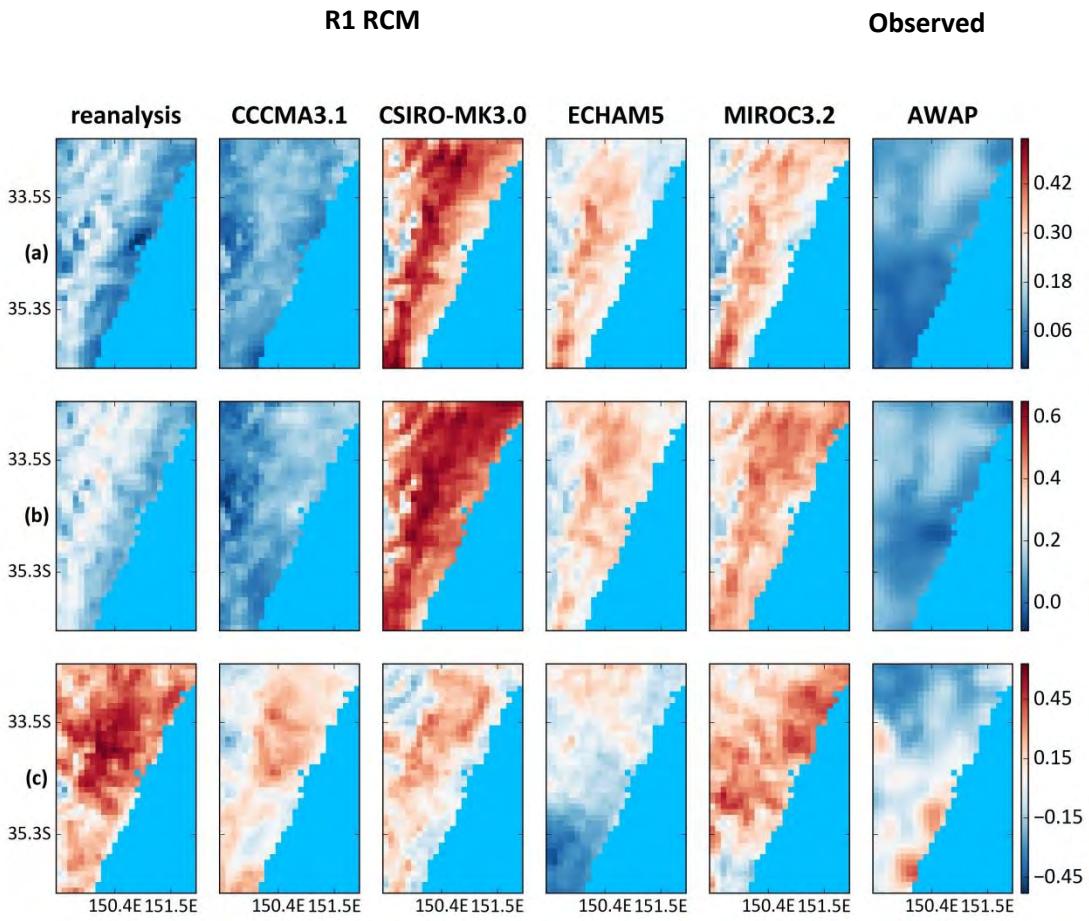

Figure 10.33 Spatial distribution of the lag-1 correlation of the rainfall (1990-2009) of the Sydney site: The plots are for the uncorrected simulations of R1 and AWAP. Time resolutions are; (a) fortnightly, (b) monthly, and (c) annual.

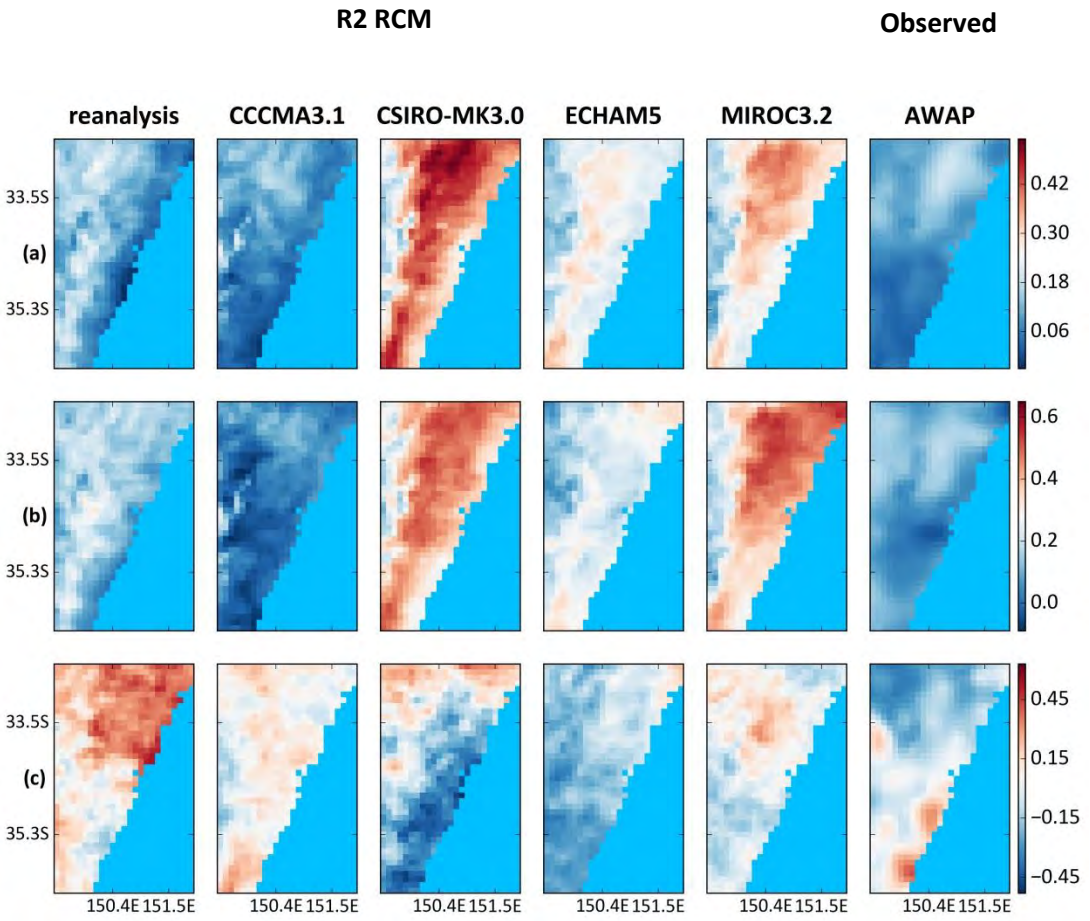

Figure 10.34 Spatial distribution of the lag-1 correlation of the rainfall (1990-2009) of the Sydney site: The plots are for the uncorrected simulations of R2 and AWAP. Time resolutions are; (a) fortnightly, (b) monthly, and (c) annual.

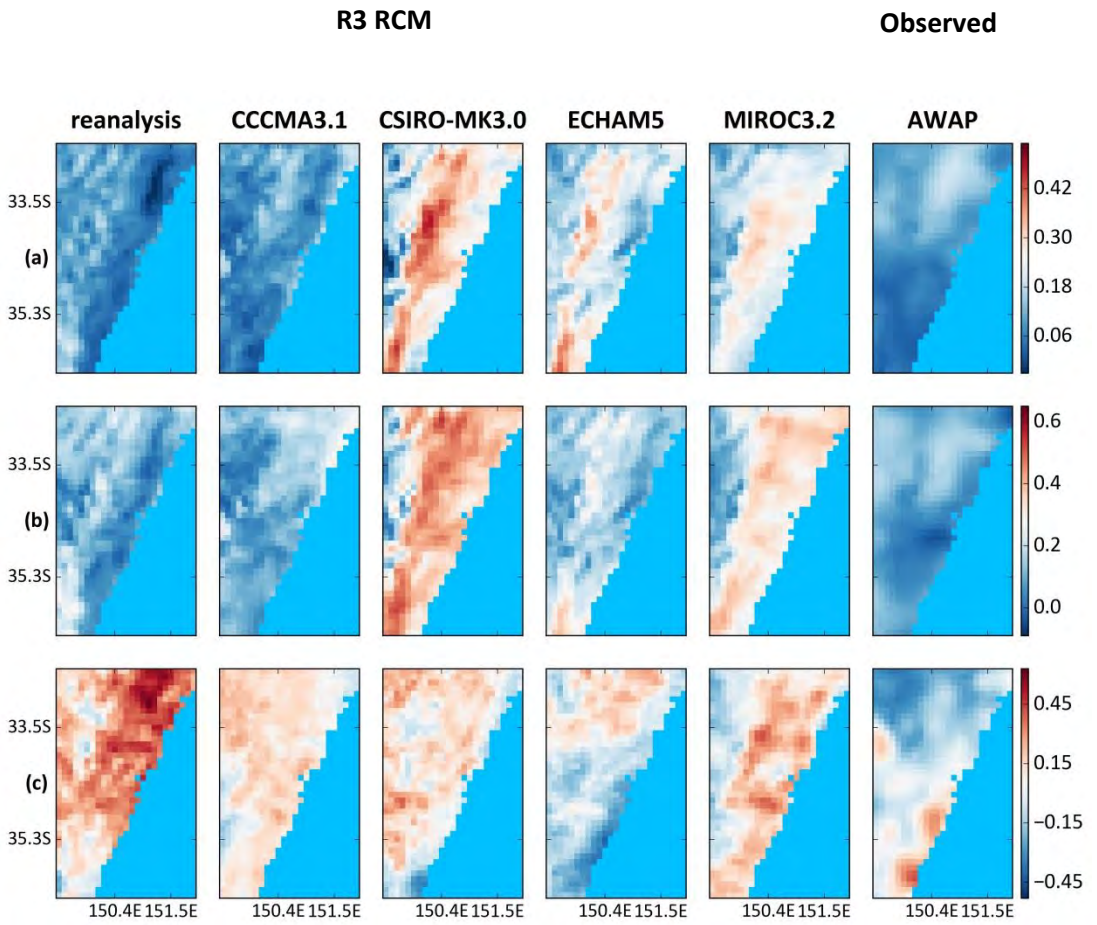

Figure 10.35 Spatial distribution of the lag-1 correlation of the rainfall (1990-2009) of the Sydney site: The plots are for the uncorrected simulations of R3 and AWAP. Time resolutions are; (a) fortnightly, (b) monthly, and (c) annual.

The lag-1 correlation of the bias corrected RCMs compared with AWAP are shown in Figures 10.36 to 10.38. Compared with uncorrected simulations, there is no significant improvement of the ability of bias corrected simulations of capturing lag-1 auto correlations of AWAP data. Model performance remains unchanged after bias correction.

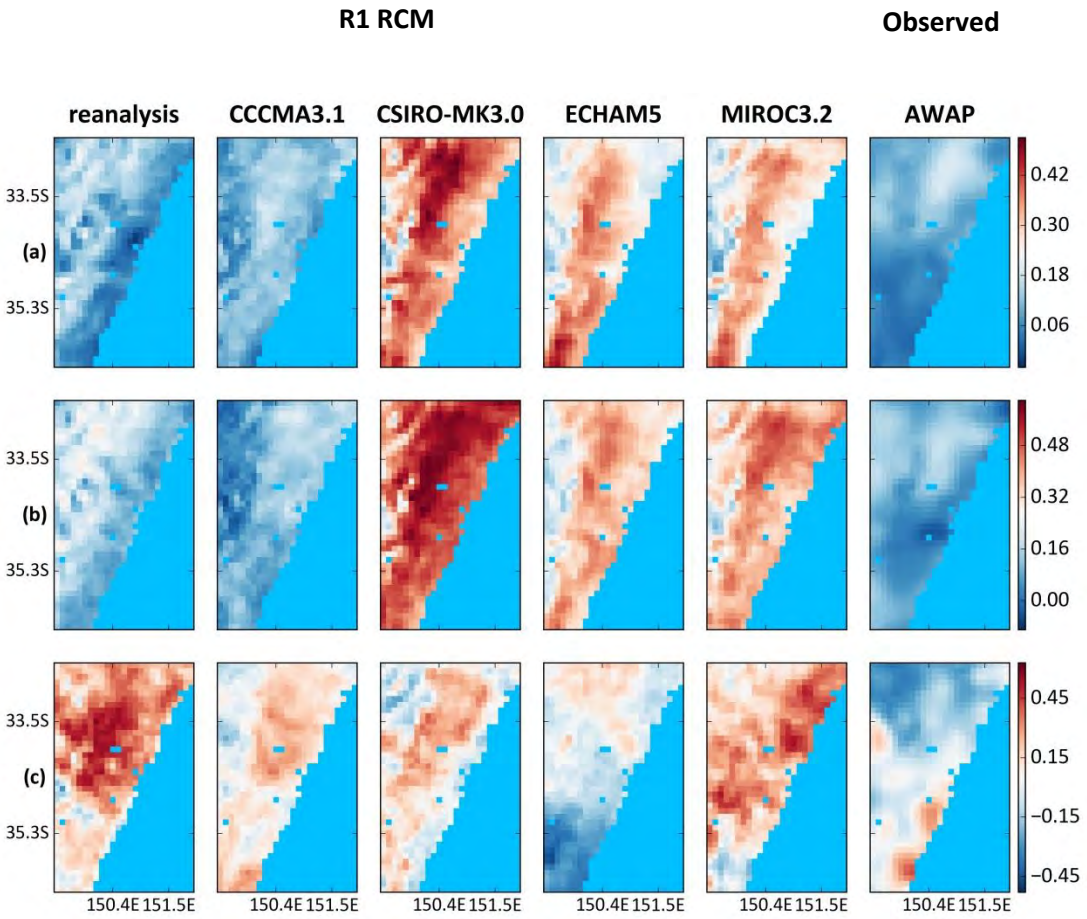

Figure 10.36 Spatial distribution of the lag-1 correlation of the rainfall (1990-2009) of the Sydney site: The plots are for the bias corrected simulations of R1 and AWAP. Time resolutions are; (a) fortnightly, (b) monthly, and (c) annual.

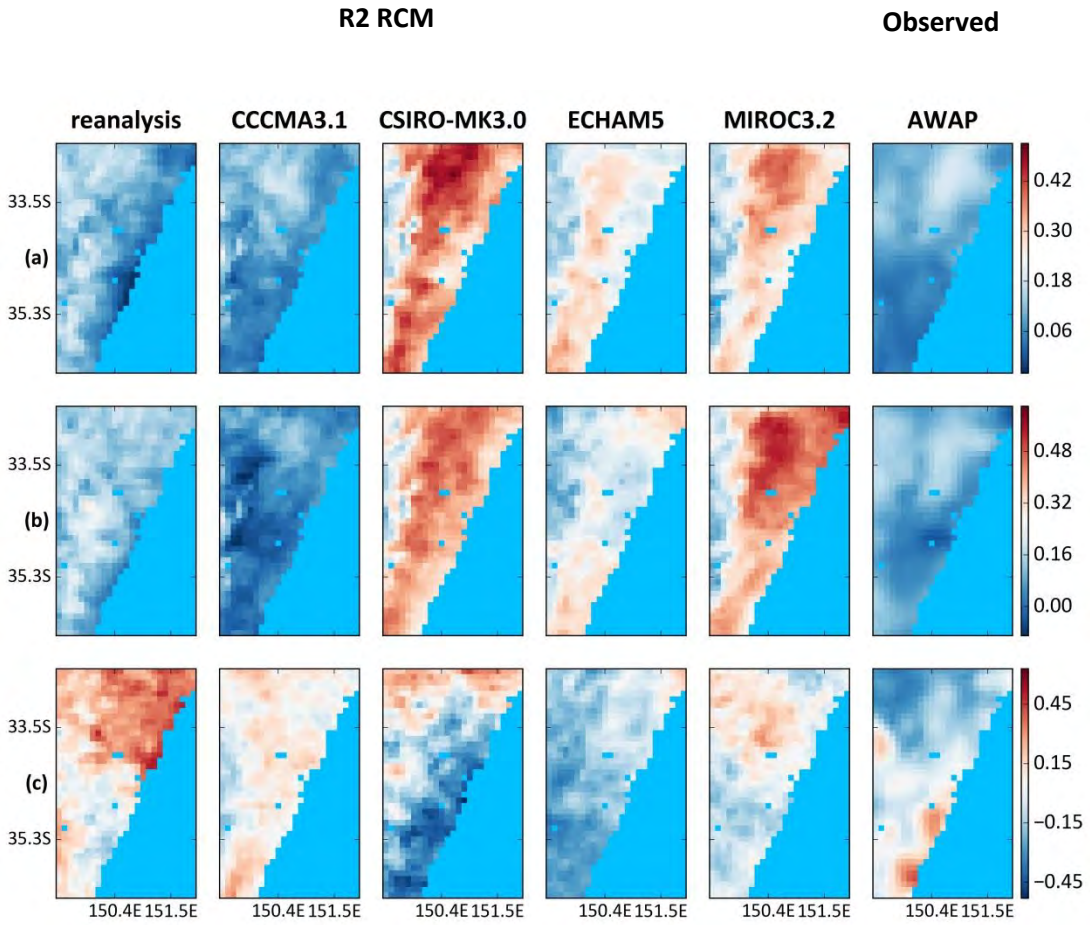

Figure 10.37 Spatial distribution of the lag-1 correlation of the rainfall (1990-2009) of the Sydney site: The plots are for the bias corrected simulations of R2 and AWAP. Time resolutions are; (a) fortnightly, (b) monthly, and (c) annual.

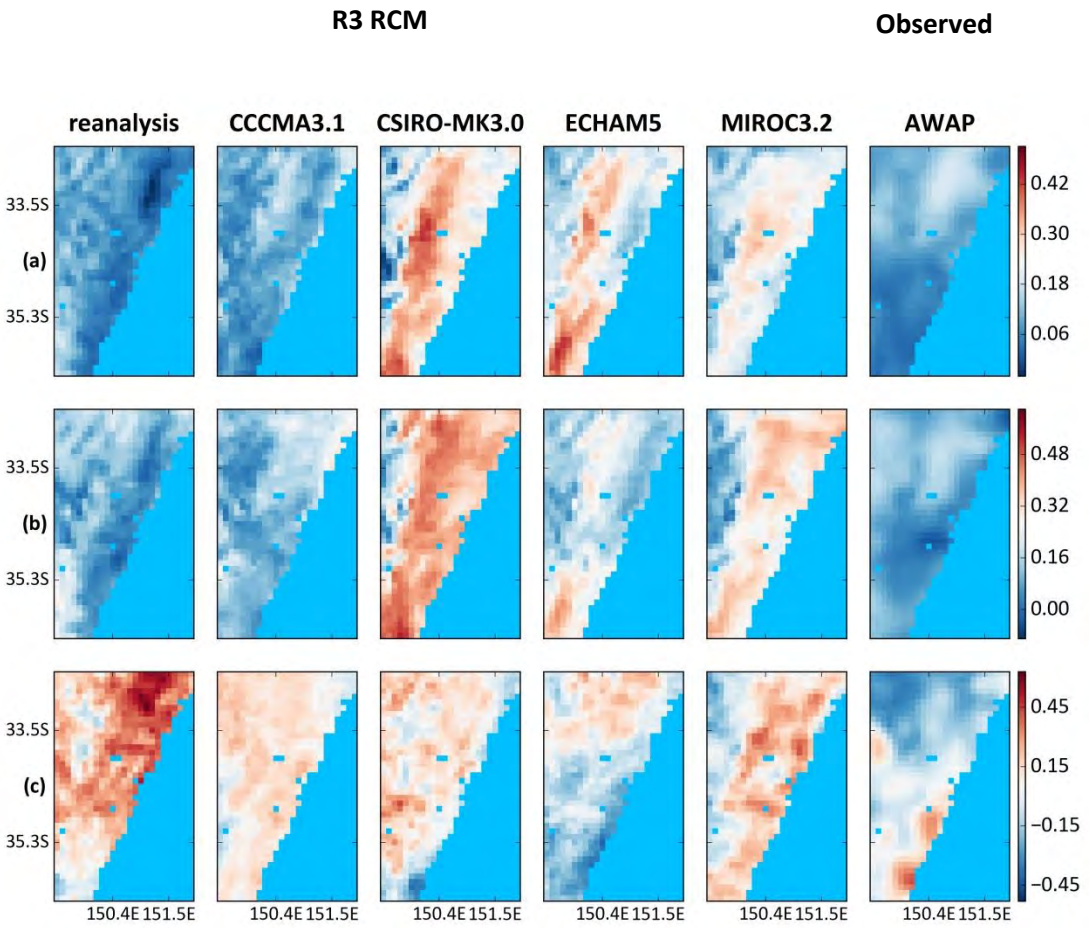

Figure 10.38 Spatial distribution of the lag-1 correlation of the rainfall (1990-2009) of the Sydney site: The plots are for the bias corrected simulations of R3 and AWAP. Time resolutions are; (a) fortnightly, (b) monthly, and (c) annual.

10.3 Conclusions

The uncorrected CCCMA3.1 RCMs appears to be the best at reproducing the mean, standard deviation and the lag-1 correlation of rainfall of AWAP, while all other simulations show discrepancies with AWAP for all sites. The overestimation of standard deviation in CSIRO-Mk3.0 and reanalysis RCMs is higher than others. MIROC3.2 better simulates the coefficient of variation of AWAP for all time resolutions. The uncorrected CCCMA3.1 is poor at reproducing the C_v of rainfall, even though it was the best at reproducing the mean, standard deviation and lag-1 correlation at all sites. Comparing the three configurations of the WRF model, R2 RCMs are best at reproducing the mean, standard deviation and coefficient of variation of AWAP rainfall. In contrast, the uncorrected R3 RCMs best reproduce the lag-1 correlations of AWAP.

The bias correction has improved the GCM-RCM model performance, particularly for the mean and standard deviation of rainfall, by removing most of the biases present in the uncorrected data. This is expected as the bias correction adjusts the daily rainfall probability distribution, but it should be noted this doesn't guarantee better performance for the weekly, monthly and yearly statistics. The performance of the CSIRO-Mk3.0 RCM has been significantly improved after the bias correction, particularly the bias corrected CSIRO-Mk3.0 RCM appears to be the best at reproducing the mean rainfall of AWAP. The overall the ability of the RCMs to reproduce the standard deviation of AWAP has been significantly improved by the bias correction. The differences between the performance of RCMs to reproduce the coefficient of variation and lag-1 correlation of AWAP remains almost unchanged after the bias correction, with slight improvements between outputs from different RCM model configurations. The performance of the R1 and R3 configurations has been the most improved by the bias correction but this is due to them being the worst performers for the uncorrected data.

Chapter 11
Testing NARCliM GCM simulations using temporal correlation of the rainfall

11.1 Introduction

The temporal correlation (i.e. autocorrelation) of NARCliM GCM projections (1990-2009) is assessed in this chapter. The simulations used in Chapters 9 and 10 are used for the assessment and results are compared with autocorrelation of AWAP. The methods explained in Sections 4.4 were used to calculate the autocorrelations of each dataset.

11.2 Autocorrelation of the rainfall

The autocorrelation of reanalyses RCMs for 1950-2009 was assessed in Section 6.4. This section extends the analysis in Section 6.4 for all available NARCliM the GCM simulations and compares them with the 20 year reanalysis (1990-2009) done in Chapters 9 and 10. Hereafter all NARCliM GCMs and 20 year reanalysis simulations for 1990-2009 are collectively referred as NARCliM RCMs. The autocorrelation of NARCliM and AWAP rainfall for 1990-2009 for different lags were calculated at the grid points chosen at all four sites (see Table 6.1 and Figures 6.1 to 6.4). As in Chapter 9, the difference in the performance of the uncorrected GCM simulations is first examined and then they are compared with the bias corrected simulations.

The correlograms generated for uncorrected NARCliM projections and AWAP at grid points A, B, C and D in the Williams River site are shown in Figure 11.1. Since all RCMs have a similar trend with similar peaks from the annual seasonal cycle only the results for monthly resolution are shown.

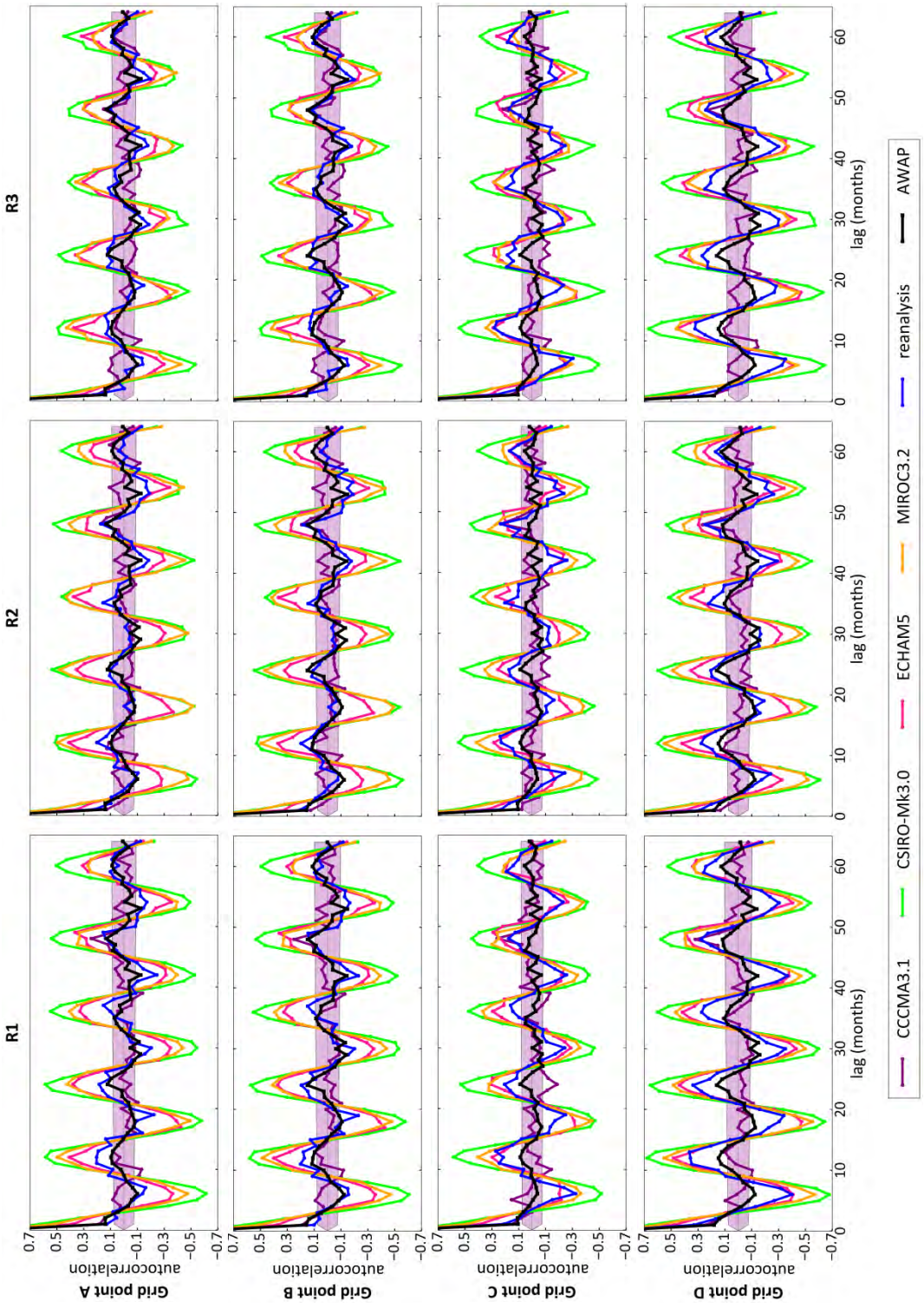

Figure 11.1 Correlograms of monthly uncorrected NARCliM RCMs and AWAP (1990-2009) at the Williams River site. R1, R2 and R3 (columns) are three RCM configurations. Grid points A and B are low elevations, and C and D are high elevations. The shaded regions are the 95% confidence limits of the null hypothesis (i.e. the correlations are not significantly different from 0).

All RCMs, except CCCMA3.1 greatly overestimate the monthly autocorrelations and seasonality of the AWAP rainfall for all four grid points of the Williams River site. CSIROMk-3.0 has the highest overestimation compared with MIROC3.2 and ECHAM5 RCMs. As was discussed in Section 6.4, the autocorrelation of the monthly AWAP data does not have many 95% significant autocorrelation values for the Williams River site. However for all grid points, the timing of the minimum and maximum autocorrelations for the CSIRO-Mk3.0, MIROC3.2 and ECHAM5 models is similar to that of AWAP. In contrast, the CCCMA3.1 RCMs, particularly at low elevation grid points (A and B) appear to have similar magnitudes of autocorrelations of AWAP, but does not produce the correct timing of the seasonal signal with peaks at different lags compared with AWAP. The autocorrelations of the 20 year reanalysis data (1990-2009) produced similar results as for the full 1950-2009 dataset. However, compared with CCCMA3.1, reanalysis appears to reproduce the timing of the seasonal cycle better than the other GCMs while slightly overestimating the magnitudes, particularly for high elevation points (C and D). Comparing the RCM configurations, there is no significant difference in the performance of the simulations, though ECHAM5 tends to overestimate the AWAP correlations more in the R2 configuration.

The correlograms of bias corrected RCMs at the Williams River site are shown in Figure 11.2. Figure 11.1 (uncorrected rainfall) and Figure 11.2 (bias-corrected rainfall) are almost identical and there is no significant change in model performance.

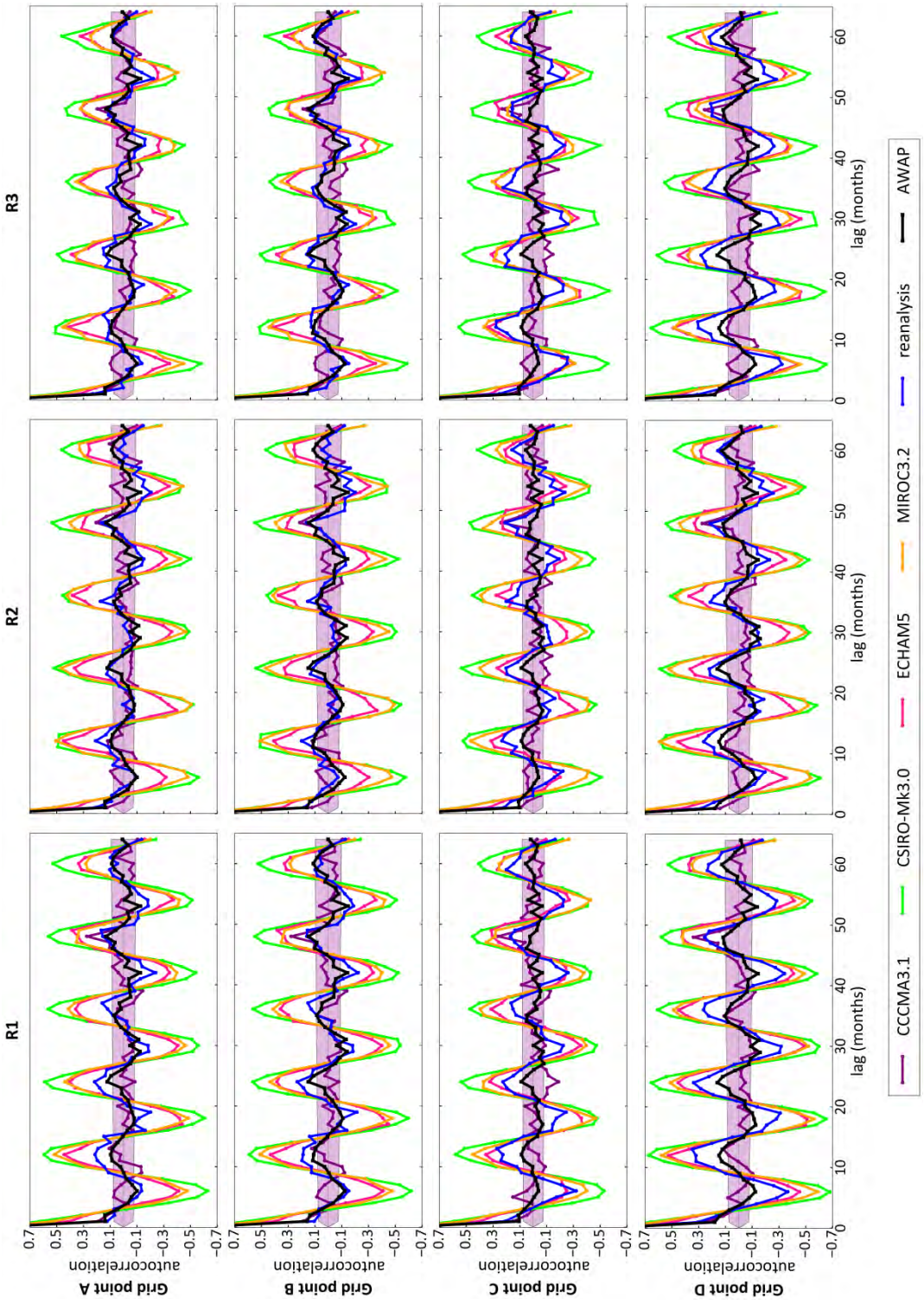

Figure 11.2 Correlograms of monthly bias corrected NARCliM RCMs and AWAP (1990-2009) at the Williams River site. R1, R2 and R3 (columns) are three RCM configurations. Grid points A and B are low elevations, and C and D are high elevations. The shaded regions are the 95% confidence limits of the null hypothesis (i.e. the correlations are not significantly different from 0).

The correlograms generated for uncorrected NARCliM RCMs and AWAP at grid points E, F, G and H of Richmond River sites are shown in Figure 11.3. At all grid points, CSIRO-Mk3.0, MIROC3.2 and ECHAM5 RCMs overestimate the monthly autocorrelations of the AWAP rainfall, while reproducing the correct timing of the seasonal cycle. As was seen at the Williams River site, CCCMA3.1 tends to underestimate the autocorrelations of AWAP rainfall at all four grid points of Richmond River site. In contrast, reanalyses RCMs, particularly at E and F low elevation grid points slightly underestimate the autocorrelations of AWAP. However, the autocorrelations of AWAP appear to be significant (lying outside the 95% confidence limit) for all grid points of the Richmond River site, therefore, this underestimation for the reanalysis is a result of this relative change in AWAP autocorrelations. A similar behaviour was noticed in Section 6.4 for both 60 year AWAP and reanalyses rainfall. This changed behaviour in AWAP (i.e. having significant autocorrelations) at the Richmond River site was previously attributed to the uncertainties of AWAP data in this region and the slightly stronger seasonality of the climate on the north coast due to the rtopical influence (see Section 6.4). Further, compared with Williams River site, the performance of the individual NARCliM RCMs is similar for the Richmond site and this suggests that the main difference is in AWAP rainfall rather than the GCM-RCM performance. At grid point E, all R3 NARCliM RCMs, except reanalysis and CCCMA3.1 tend to have autocorrelations close to AWAP, while the magnitudes are overestimated slightly. This effect was not seen any other grid point of the site and therefore, appears to be simulation specific.

The correlograms of bias corrected RCMs at the Richmond River site are shown in Figure 11.4. As was seen at the Williams River site, there is no change in the autocorrelations after the bias correction.

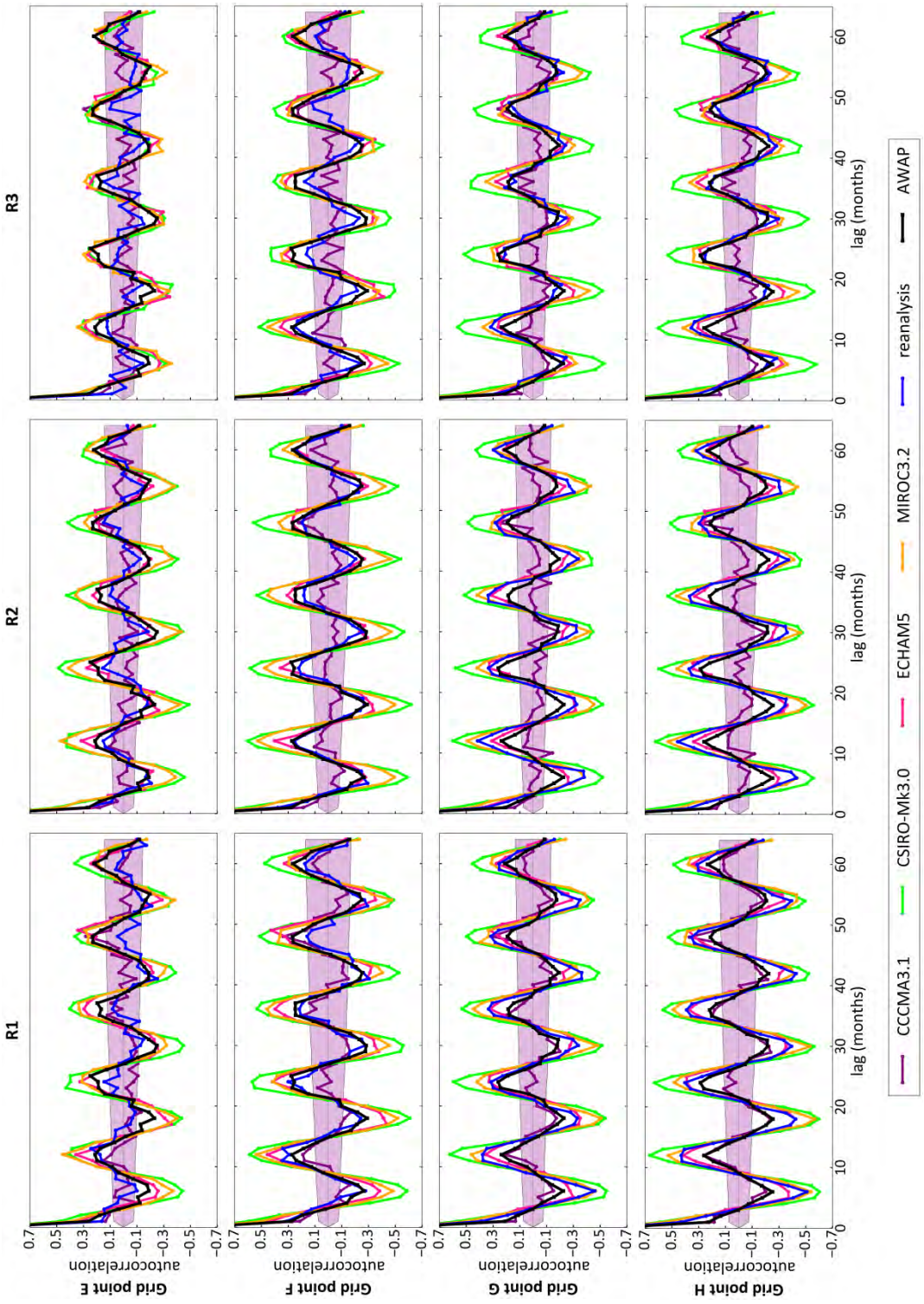

Figure 11.3 Correlograms of monthly uncorrected NARCliM RCMs and AWAP (1990-2009) at the Richmond River site. R1, R2 and R3 (columns) are three RCM configurations. Grid points E and F are low elevations, and G and H are high elevations. The shaded regions are the 95% confidence limits of the null hypothesis (i.e. the correlations are not significantly different from 0).

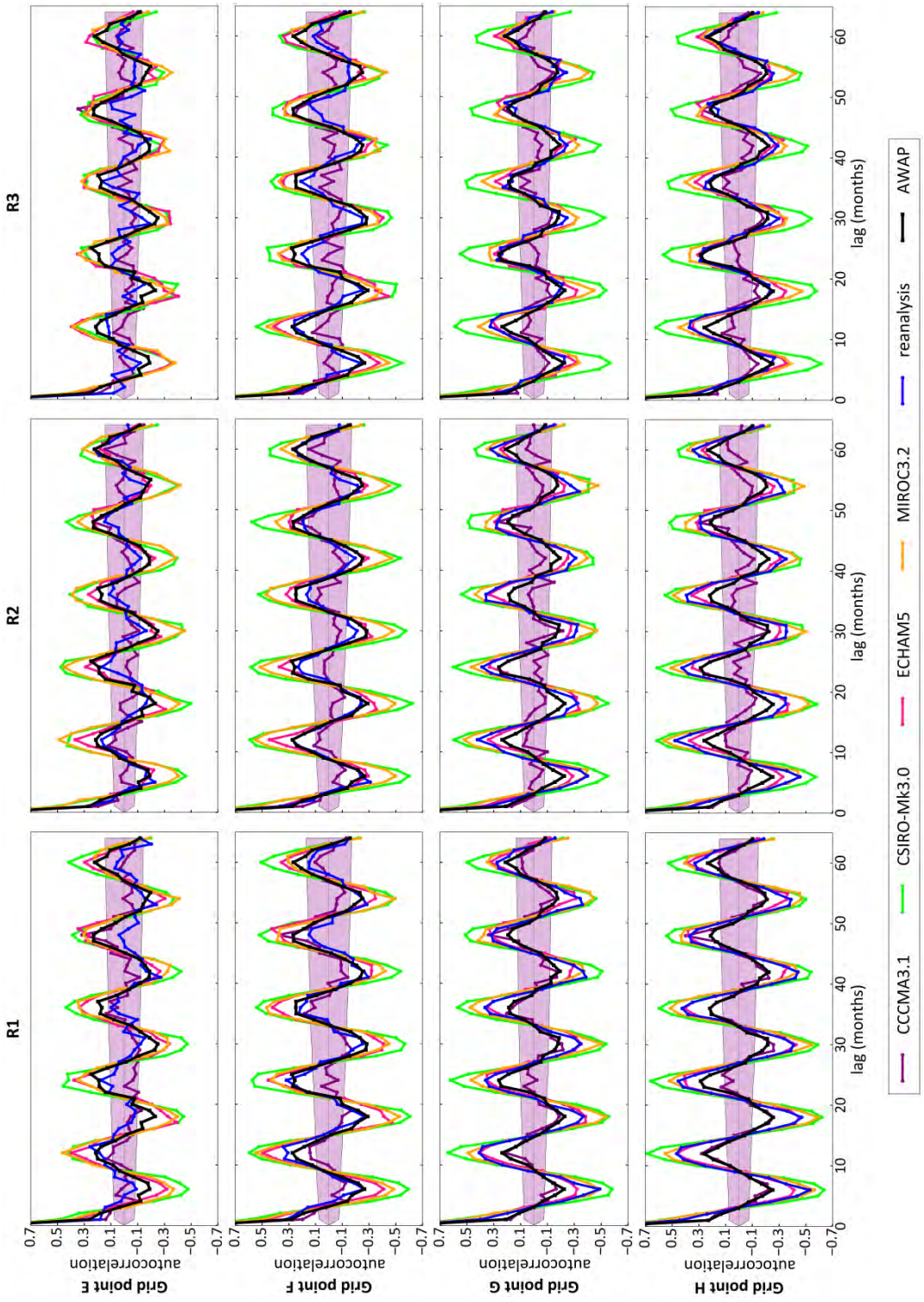

Figure 11.4 Correlograms of monthly bias corrected NARCliM RCMs and AWAP (1990-2009) at the Richmond River site. R1, R2 and R3 (columns) are three RCM configurations. Grid points E and F are low elevations, and G and H are high elevations. The shaded regions are the 95% confidence limits of the null hypothesis (i.e. the correlations are not significantly different from 0).

The correlograms for the uncorrected NARCliM RCMs and AWAP at grid points J, K, L and M of the Bega River site are shown in Figure 11.5. The figure indicates that all RCMs overestimate the autocorrelation of AWAP, while reproducing the timing of the minimum and maximum autocorrelations of AWAP at the low elevation points, but at high elevation points (L and M), located along the Australian Alps with elevation greater than 1298 m (See Figure 6.3 and Table 6.1), CCCMA3.1 tends to largely overestimate the AWAP autocorrelations for all three RCM configurations. This overestimation by CCCMA3.1 is in contrast to the other sites. A similar effect was also seen in the spatial variability of the lag-1 autocorrelations at the Bega River site (see Appendix A.5 – Figures A.31 to A.33).

Further at these two high elevation grid points (L and M), all GCMs except CCCMA3.1 produce relatively lower autocorrelations compared with other study sites (particularly at Grid Point L). This suggests that, given the effect is only seen for the high elevation points, the NARCliM RCMs also have some intrinsic difficulties in capturing autocorrelations, particularly when the site topography is complex with mountains.

The correlograms of bias corrected RCMs for Bega River site are shown in Figure 11.6. Again, bias correction makes only a small difference in the results.

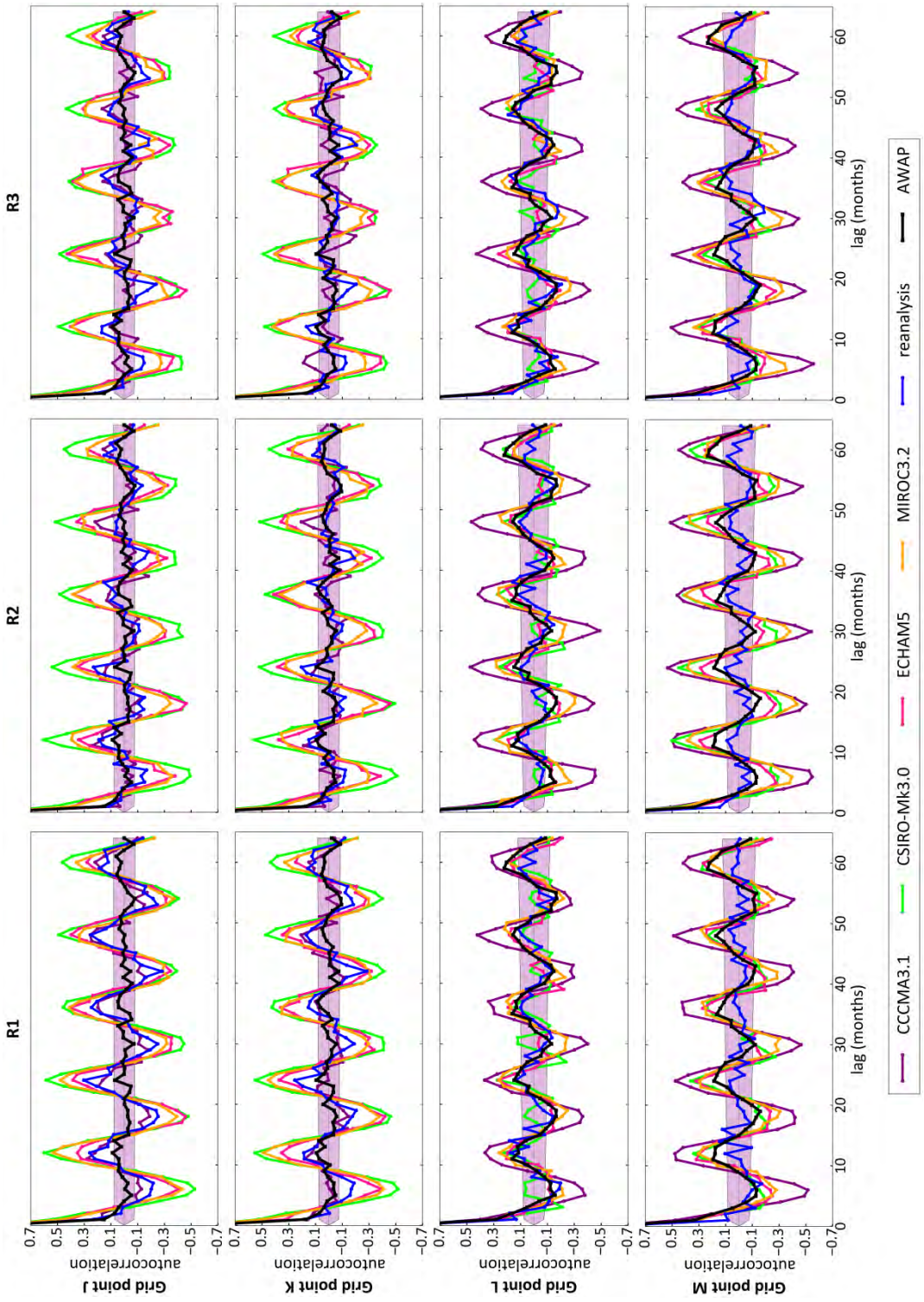

Figure 11.5 Correlograms of monthly uncorrected NARCliM RCMs and AWAP (1990-2009) at the Bega River site. R1, R2 and R3 (columns) are three RCM configurations. Grid points J and K are low elevations, and L and M are high elevations. The shaded regions are the 95% confidence limits of the null hypothesis (i.e. the correlations are not significantly different from 0).

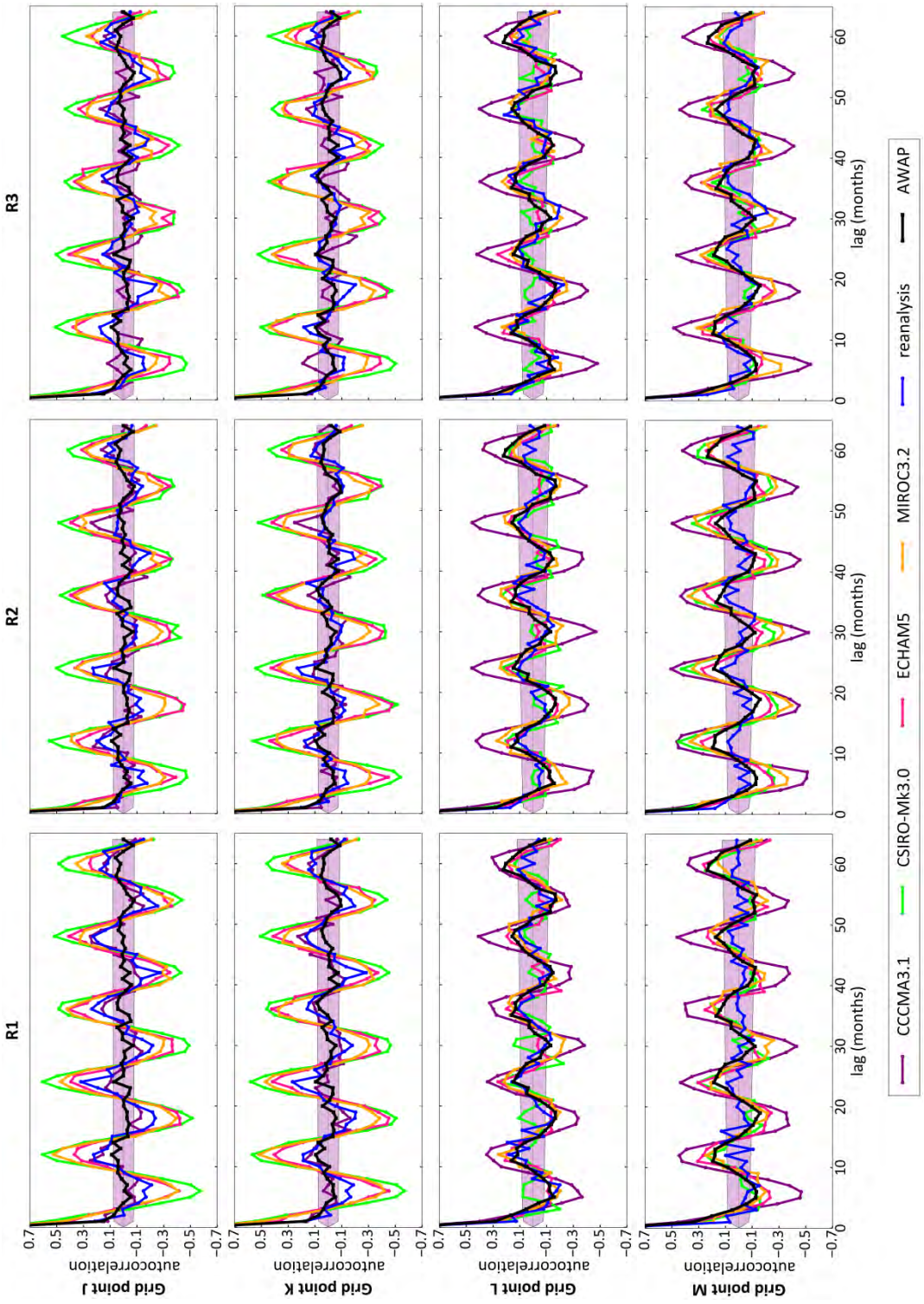

Figure 11.6 Correlograms of monthly bias corrected NARCliM RCMs and AWAP (1990-2009) at the Bega River site. R1, R2 and R3 (columns) are three RCM configurations. Grid points J and K are low elevations, and L and M are high elevations. The shaded regions are the 95% confidence limits of the null hypothesis (i.e. the correlations are not significantly different from 0).

The correlograms generated for uncorrected NARCliM RCMs and AWAP at grid points P, Q, R and S of Sydney sites are shown in Figure 11.7. The performance of RCMs is similar for P, Q and R grid points at Sydney site. CSIRO-Mk3.0, MIROC3.2 and ECHAM5 RCMs overestimate the monthly autocorrelations of the AWAP rainfall, while reproducing the correct timing of the seasonal cycle.

Grid point S, located at the Blue Mountains range (the highest mountain range in the site) is different to the other 3 grid points for the Sydney site, as all RCMs have small magnitudes for autocorrelations and are close to the monthly AWAP autocorrelations. Because these results appeared anomalous the analysis was repeated for few adjacent grid points also, and the results remain unchanged. A similar effect was also found at the L and M high elevation grid points of the Bega River site. Additionally, this result is consistent with Figure 6.59, which had a similar effect in correlograms at the same grid point (S) for the 60 year period reanalyses datasets. Therefore, this suggests that there are some uncertainties associated either with AWAP or NARCliM RCMs or perhaps both types of gridded datasets, and they poorly represent the actual rainfall at this location.

The correlograms generated for the bias corrected simulations (shown in Figure 11.8) also produce similar results, again showing that bias correction does not change the autocorrelation of the rainfall.

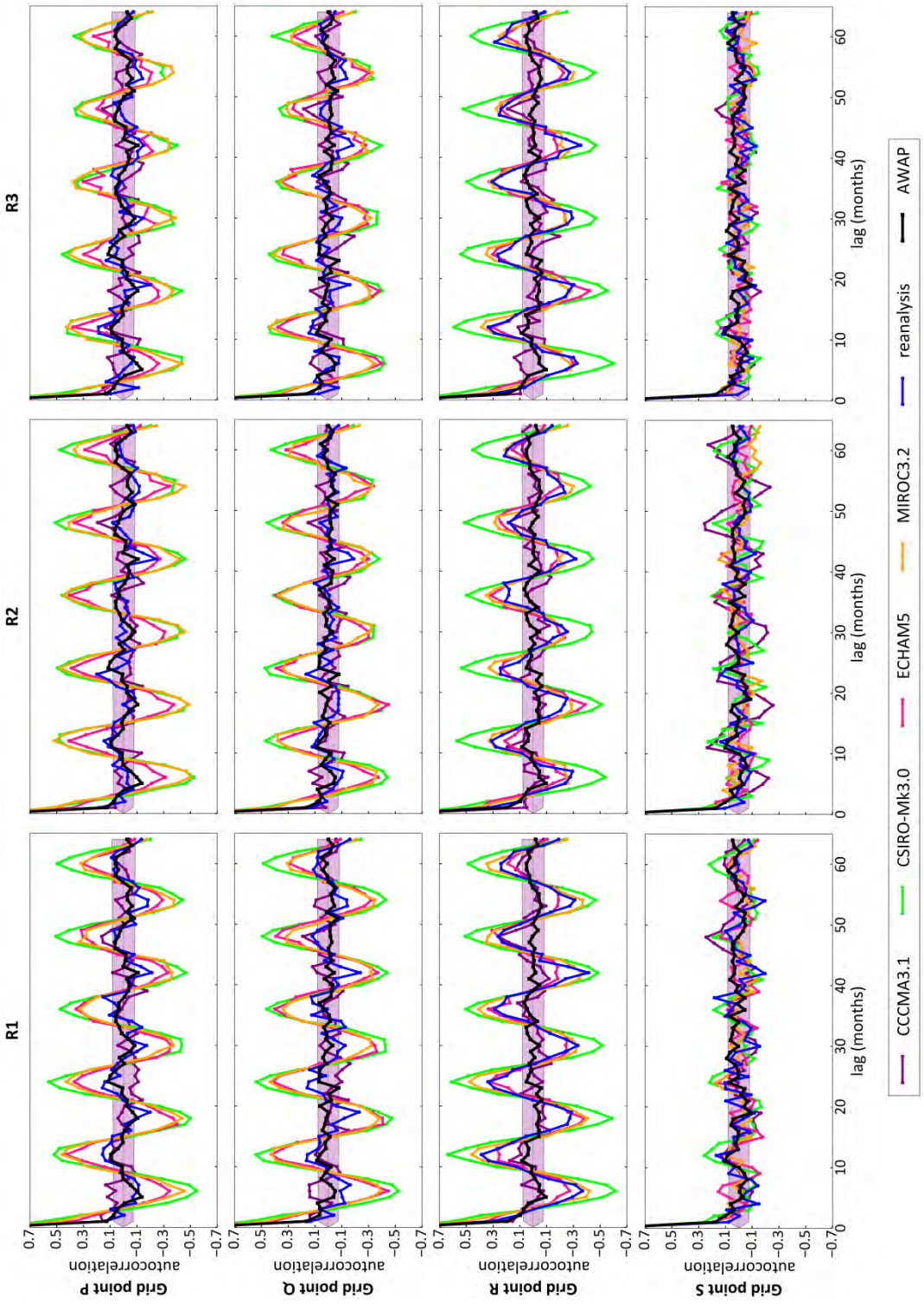

Figure 11.7 Correlograms of monthly uncorrected NARCliM RCMs and AWAP (1990-2009) at the Sydney site. R1, R2 and R3 (columns) are three RCM configurations. Grid points P and Q are low elevations, and R and S are high elevations. The shaded regions are the 95% confidence limits of the null hypothesis (i.e. the correlations are not significantly different from 0).

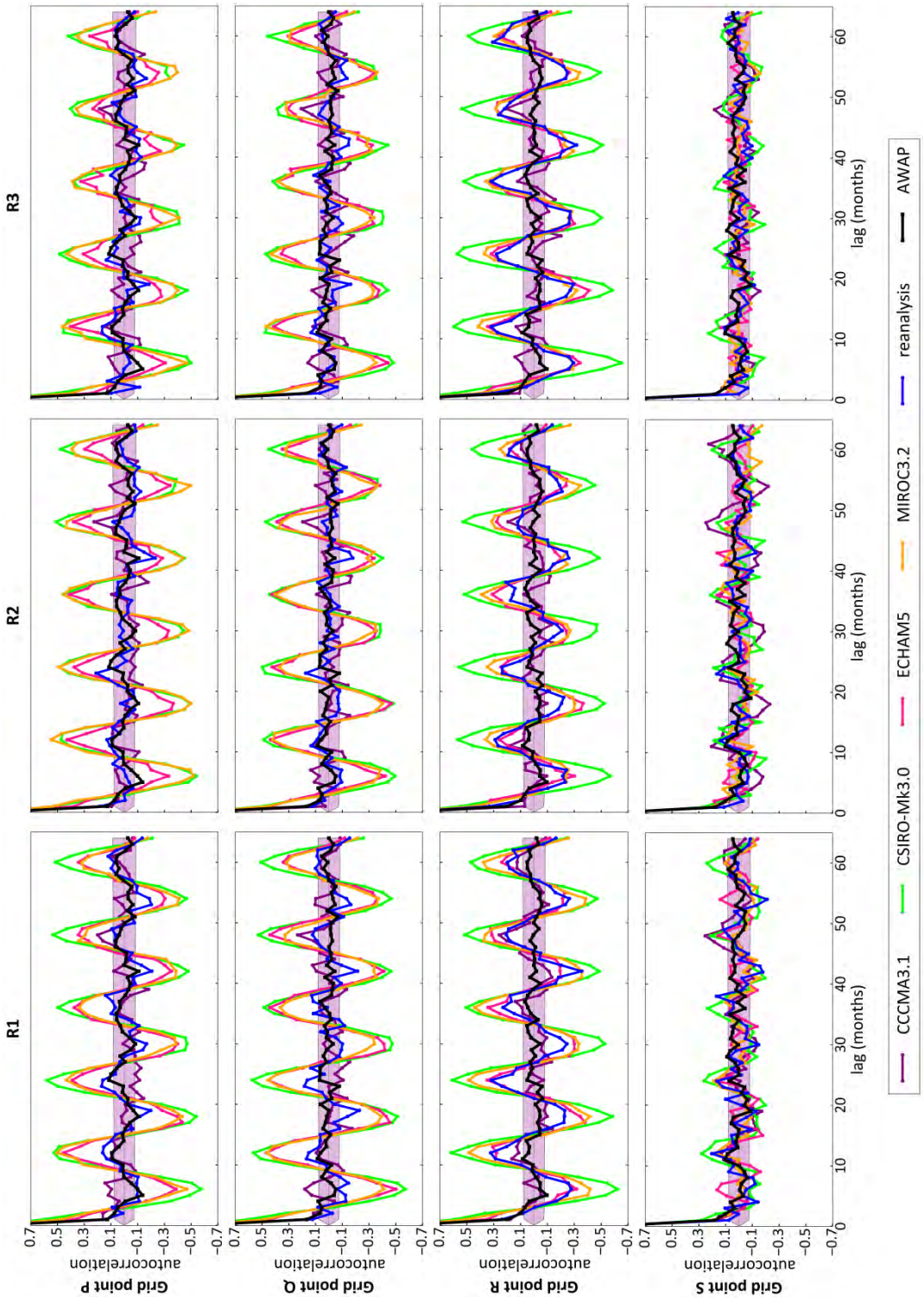

Figure 11.8 Correlograms of monthly bias corrected NARCliM RCMs and AWAP (1990-2009) at the Sydney site. R1, R2 and R3 (columns) are three RCM configurations. Grid points P and Q are low elevations, and R and S are high elevations. The shaded regions are the 95% confidence limits of the null hypothesis (i.e. the correlations are not significantly different from 0).

11.3 Conclusions

The results for the autocorrelation analysis show that all GCM simulations, except CCCMA3.1 highly overestimate the monthly autocorrelations of the AWAP rainfall for all sites. The CSIROMk-3.0 model simulation has the highest overestimation compared with ECHAM5 and MIROC3.2. The CCCMA3.1 simulations, particularly for low elevation grid points appear to have similar magnitudes of autocorrelations of AWAP, yet can neither produce the correct timing nor the phase of the seasonal signal. Therefore, CCCMA3.1 is less able to reproduce the autocorrelations of AWAP. The correlograms of bias corrected simulations look very similar to the uncorrected correlograms so that there is no significant change in autocorrelation after bias correction.

Chapter 12
Testing NARCliM GCM simulations using spatial correlation of the rainfall

12.1 Introduction

In this chapter, the spatial correlation (r) of the rainfall from the NARCliM GCM projections (1990-2009) is assessed against AWAP. Following the methodology explained in Section 4.5, the analysis was performed for the same NARCliM (uncorrected and bias corrected) and AWAP datasets used in Chapter 9-11. Similar to Chapter 9-11, NARCliM datasets (GCMs/reanalysis) are collectively referred as NARCliM RCMs. The grid points shown in Table 7.1 and Figures 7.1 to 7.4 were used as the references when calculating the spatial correlations. Additionally, spatial correlation of the daily rainfall of all the gridded datasets are tested against that of rain gauge data at selected grid points. The rain gauges selected for the analysis at different sites are listed in Tables 3.4 to 3.7.

12.2 Spatial correlation of the daily rainfall

12.2.1 Williams River site

The spatial correlation of the uncorrected NARCliM RCMs between the high elevation grid point (W17) and all other grid points of the Williams River site are shown in Figure 12.1. In general, reanalysis (1990-2009) and CCCMA3.1 RCMs have spatial patterns of correlations most similar to each other and their spatial patterns look approximately similar to that of AWAP. The spatial pattern in correlations for AWAP follows the topography of the Williams River site and this effect is similar to the results shown in Figure 7.5 for 60 year 1950-2009 AWAP rainfall. CSIRO-Mk3.0, ECHAM5 and MIROC3.2 RCMs have similar spatial patterns, but have higher correlations than AWAP or the reanalyses, particularly at the west of the site. Since the spatial pattern tends to follow the general trend of topography, part of this similarity in the spatial pattern of CSIRO-Mk3.0, ECHAM5 and MIROC3.2 RCMs is because, according to Evans et al. (2014), all RCMs use the

same elevation data. The said the R1 reanalysis, R2- and R3-CCCMA3.1 and R1- and R3-CSIRO-Mk3.0 are better able to reproduce the spatial pattern in AWAP than the other RCMs. In particular, this good performance of CCCMA3.1 is consistent with its performance for the other statistics discussed in Chapter 9-11. As previously discussed in Section 7.2, there is a smoother spatial pattern in AWAP data compared with the RCM simulations.

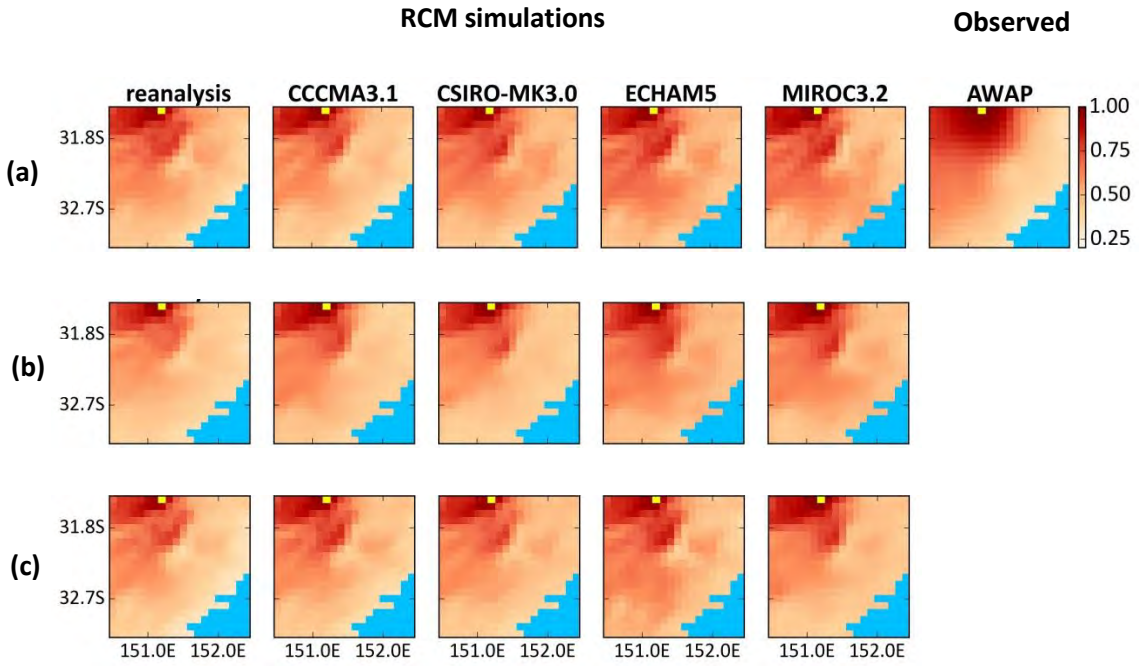

Figure 12.1 Spatial correlations of daily rainfall between the reference grid point and all other grid points in the Williams River site. The plots are for the uncorrected simulations of (a) R1, (b) R2, and (c) R3 RCMs, and AWAP. The reference is W17, a high elevation grid point (shown in yellow boxes).

The spatial correlation functions for the uncorrected R1 RCMs, corresponding to Figure 12.1a are shown in Figure 12.2. The trends shown in spatial variability plots can be more clearly seen in the spatial correlation functions. The figure indicates that R1-CCCMA3.1 and R1 reanalysis closely reproduce the exponential correlation structure of AWAP, with R1-CSIRO-Mk3.0, R1-ECHAM5 and R1-MIROC3.2 overestimating the exponent of the fitted curve of AWAP (6%, 11% and 11% respectively) for large spatial separations. Similarly, spatial correlation functions for uncorrected R2 and R3 RCMs, corresponding to Figures 12.1b and 12.1c are shown in Figures 12.3 and 12.4 respectively. All R3 RCMs, with the exception of R3-

ECHAM5, underestimate the correlations of AWAP for almost all separations. However, for high elevation grid points (i.e. points which have elevations higher than the reference, are shown in a range of purple to blue colours), all RCMs underestimate the correlations of AWAP. This may be due to the averaging of the topography in NARCliM elevation data. In particular, if this averaging effect is high at high peaks, the resulting lower, averaged, elevations at these grid points may lead to low spatial correlations as the spatial correlation follow the trends in topography.

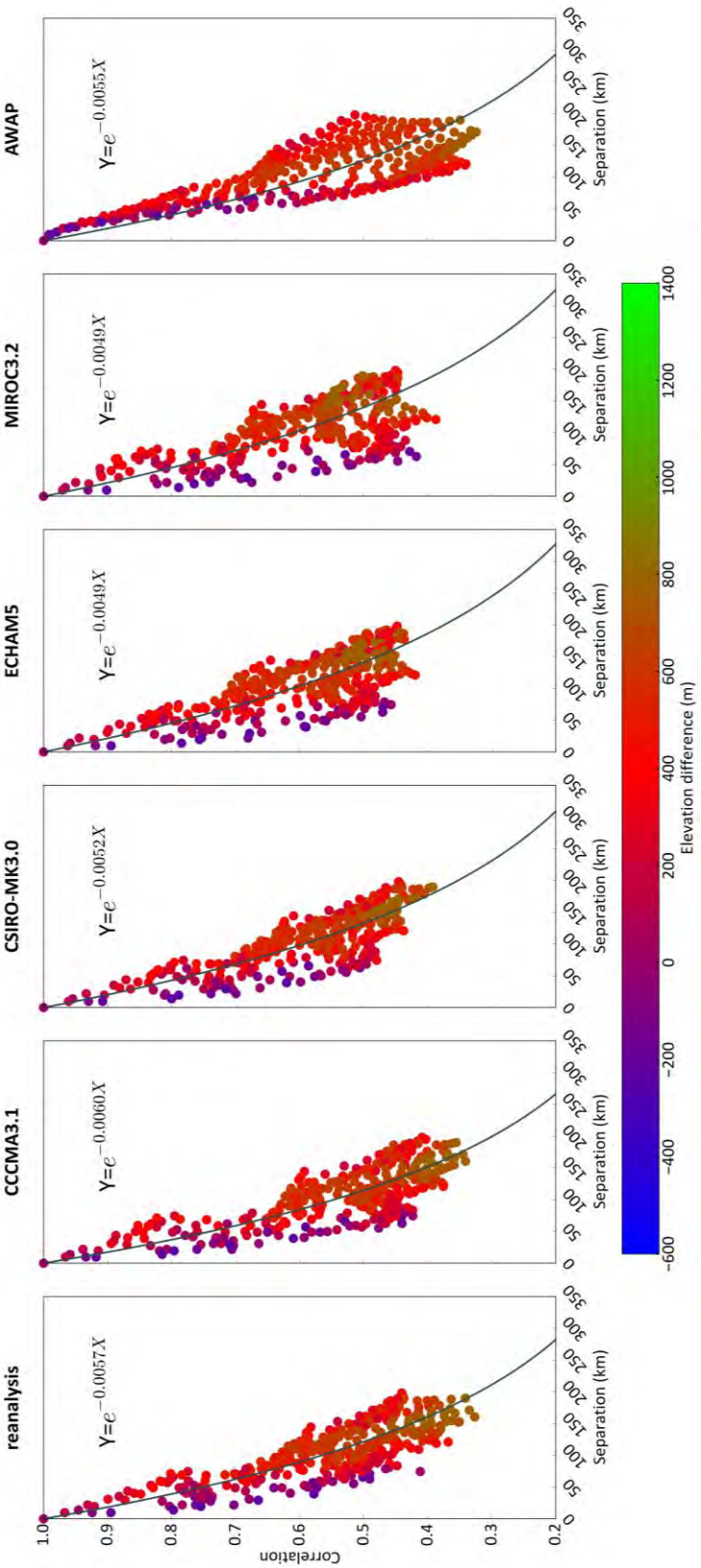

Figure 12.2 Spatial correlations function (1990-2009) of the Williams River site. The reference is W17 high elevation grid point. The plots are for the uncorrected GCM simulations of R1 RCM and AWAP.

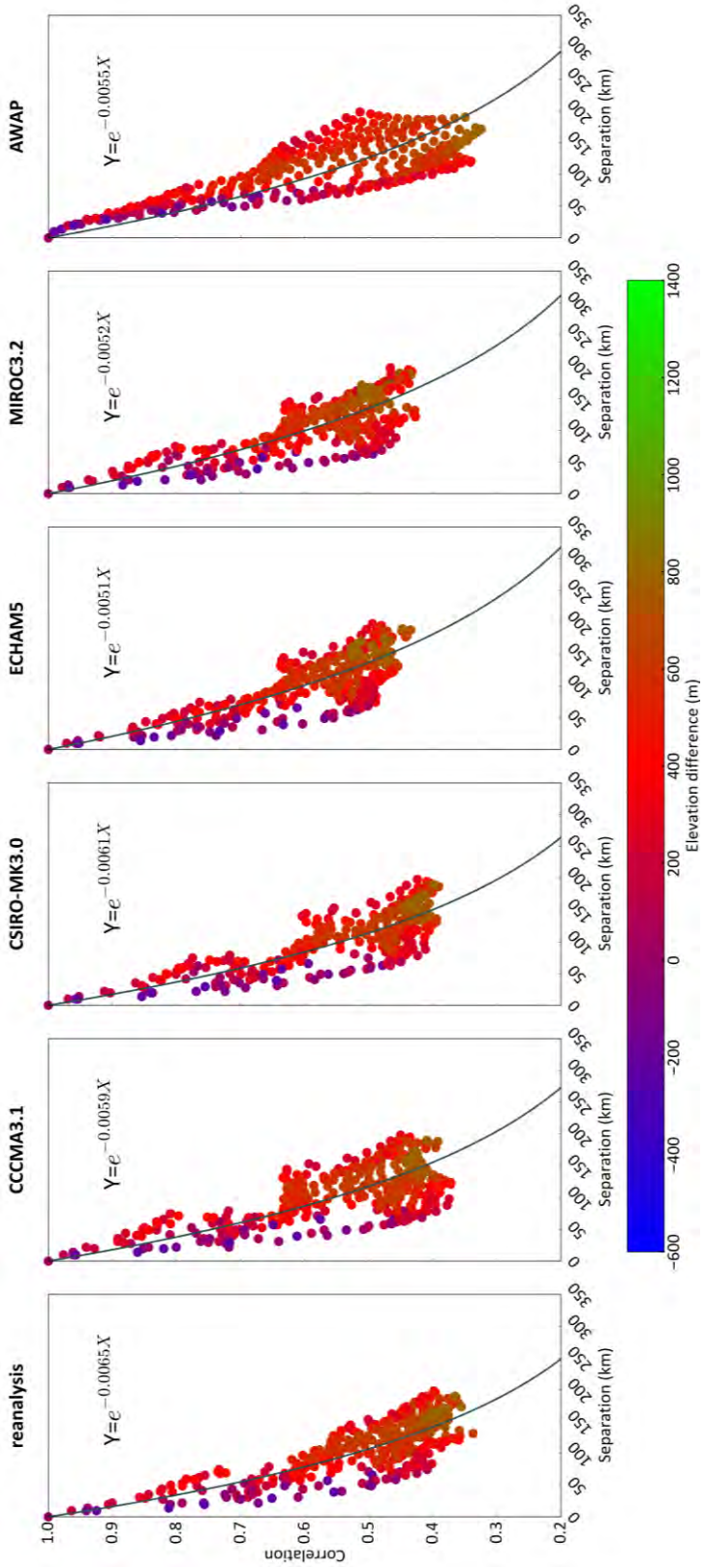

Figure 12.3 Spatial correlations function (1990-2009) of the Williams River site. The reference is W17 high elevation grid point. The plots are for the uncorrected GCM simulations of R2 RCM and AWAP.

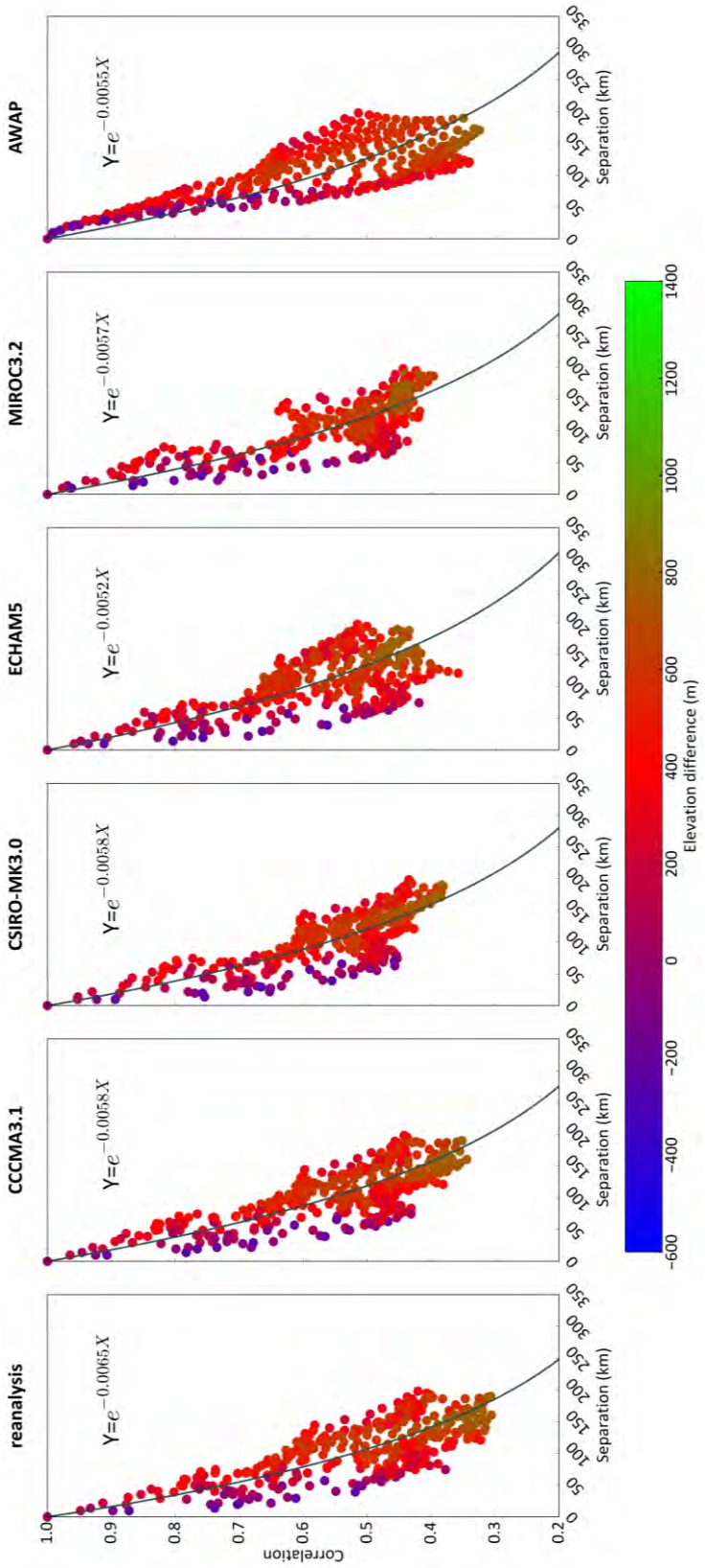

Figure 12.4 Spatial correlations function (1990-2009) of the Williams River site. The reference is W17 high elevation grid point. The plots are for the uncorrected GCM simulations of R3 RCM and AWAP.

Figure 12.5 shows the spatial correlation calculated for the bias corrected NARCliM daily RCMs. Comparing Figure 12.1 and Figure 12.5, there is a consistency in the results for all RCMs, suggesting that the bias-correction has not changed the spatial variability of the correlations. The exception is CSIRO-Mk3.0. In the CSIRO-Mk3.0 RCMs, most of the overestimated correlations which initially occurred in the west of the site have been corrected with the bias correction and therefore, the bias-corrected results appear to have a more similar spatial pattern to CCCMA3.1 and reanalysis.

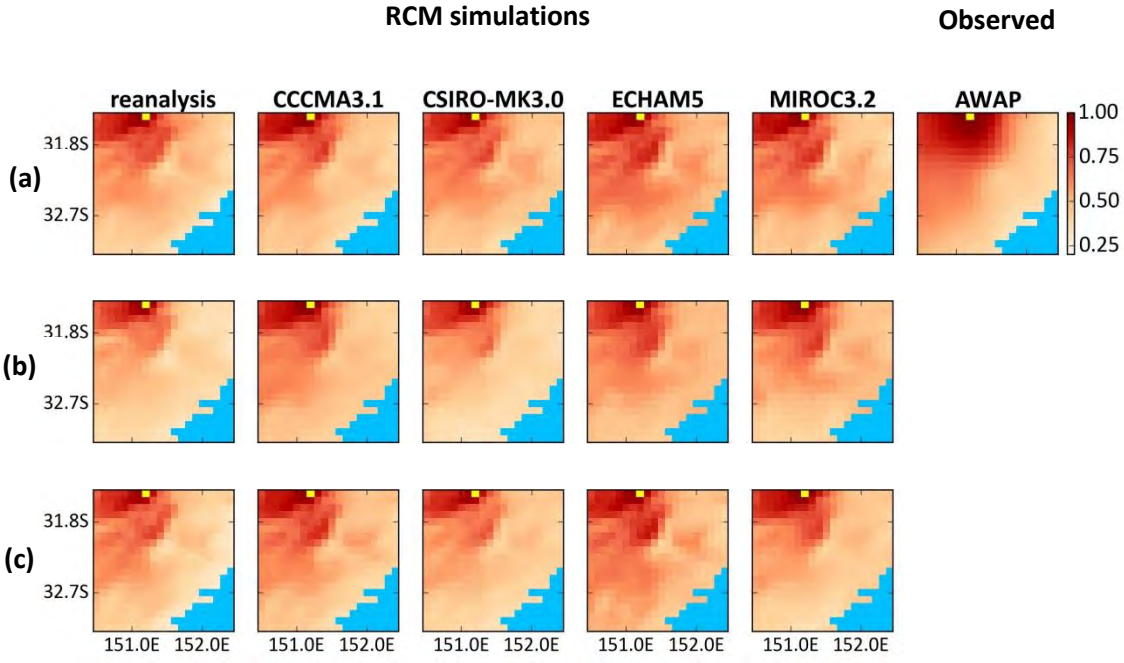

Figure 12.5 Spatial correlations of daily rainfall between the reference grid point and all other grid points in the Williams River site. The plots are for the bias corrected simulations of (a) R1, (b) R2, and (c) R3 RCMs, and AWAP. The reference is W17, a high elevation grid point (shown in yellow boxes).

The spatial correlation functions for bias corrected R1, R2 and R3 RCMs corresponding to Figure 12.5 are shown in Figures 12.6 to 12.8. In general, the ability to reproduce the spatial correlation function of AWAP has only been improved in MIROC3.2 and CSIRO-Mk3.0 RCMs, by correcting most of the overestimated correlations. The reanalysis and CCMA3.1 RCMs appear to remain same as uncorrected, with R1 and R3 better capturing the correlations of AWAP. Similarly, spatial correlation function of ECHAM5 RCMs also remain almost unchanged after the bias correction with overestimating spatial correlations of AWAP as it did before for uncorrected.

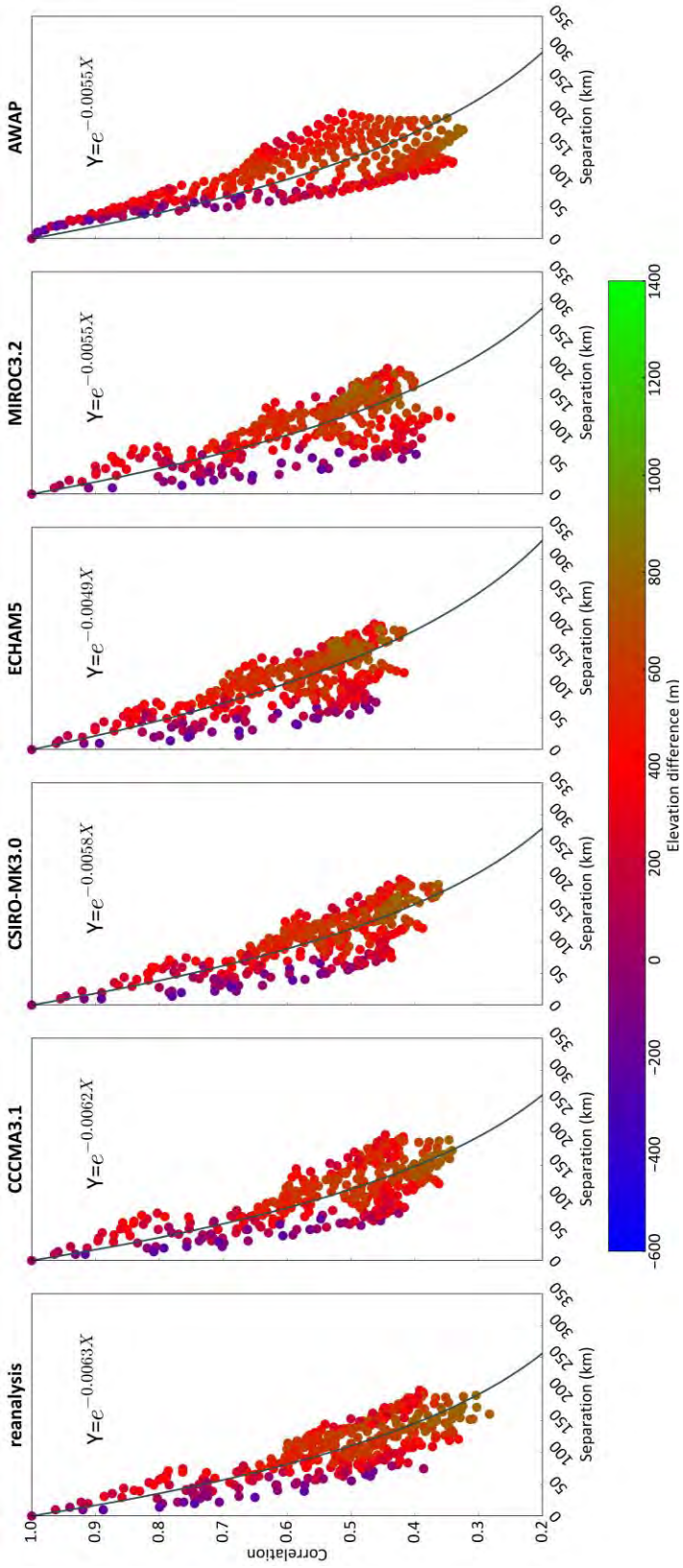

Figure 12.6 Spatial correlations function (1990-2009) of the Williams River site. The reference is W17 high elevation grid point. The plots are for the bias corrected GCM simulations of R1 RCM and AWAP.

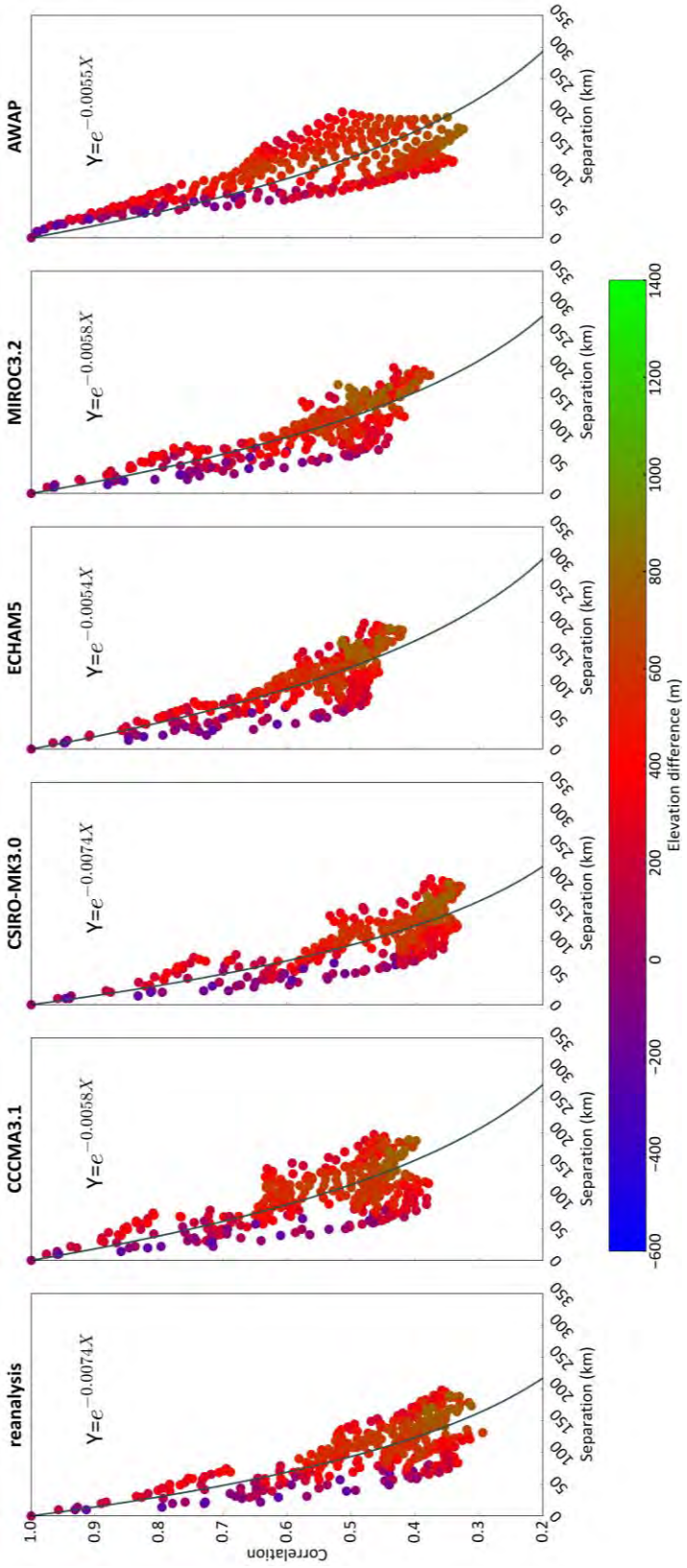

Figure 12.7 Spatial correlations function (1990-2009) of the Williams River site. The reference is W17 high elevation grid point. The plots are for the bias corrected GCM simulations of R2 RCM and AWAP.

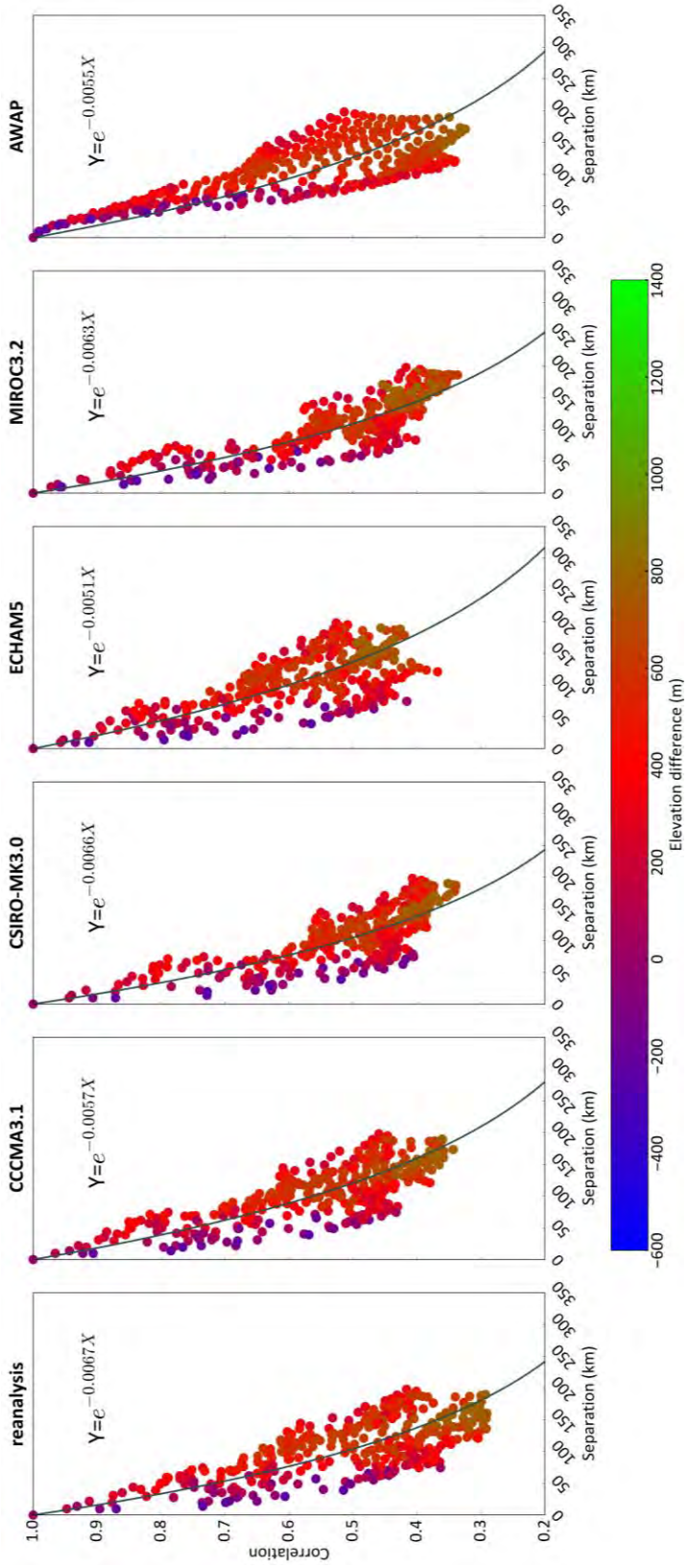

Figure 12.8 Spatial correlations function (1990-2009) of the Williams River site. The reference is W17 high elevation grid point. The plots are for the bias corrected GCM simulations of R3 RCM and AWAP.

The spatial correlation of the uncorrected NARCliM GCM simulations between the low elevation grid point (W4) and all other grid points in the Williams River site are shown in Figure 12.9. The figure indicates that all RCM simulations have similar spatial patterns, but fail to replicate the smoother spatial pattern of AWAP. Of all simulations, MIROC3.2 and ECHAM5 overestimate the correlations of AWAP, particularly at grid points far from the reference. Reanalysis (1990-2009), particularly the R1, best reproduces the spatial pattern of AWAP.

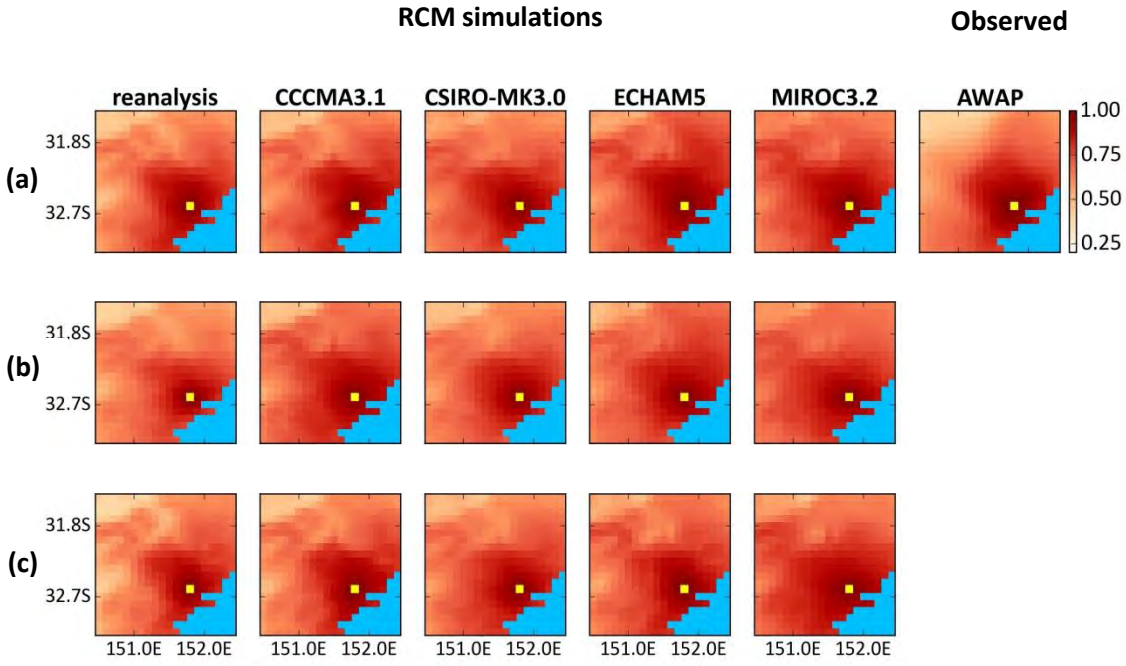

Figure 12.9 Spatial correlations of daily rainfall between the reference grid point and all other grid points in the Williams River site. The plots are for the uncorrected simulations of (a) R1, (b) R2, and (c) R3 RCMs, and AWAP. The reference is W4, a low elevation grid point (shown in yellow boxes).

The spatial correlation functions for uncorrected R1, R2 and R3 RCMs corresponding to Figure 12.9 are shown in Figures 12.10 to 12.12. In contrast to the high elevation reference, only reanalysis and CCCMA3.1 RCMs closely reproduce the spatial correlation function of AWAP. All other RCMs have overestimated correlations for all grid points of the sites. However, compared with the high elevation reference, there is a less scatter around the mean trend of the correlations for all datasets including AWAP.

Further, the general trend of RCMs having a similar spatial correlation pattern as the topography (Figure 12.9) is consistent for both cases (i.e. studying spatial correlation with respect to low and high elevation references). Therefore, this suggests that RCM performance is independent from the elevation of the reference grid point (i.e. we cannot conclude that the observed spatial correlations are better captured for high elevation grid points and vice versa). The R3 RCMs are best able to capture the spatial correlations of AWAP.

At the Williams River site, rainfall for the close by low elevation grid points are more correlated to the low elevation reference and high elevation points close by are more correlated to the high elevation reference. As explained in Section 7.2 for the 60 year reanalyses, the spatial correlation of rainfall appear to be not simply an effect of proximity, and is significantly influenced by the combination distance between the points and differences in elevation.

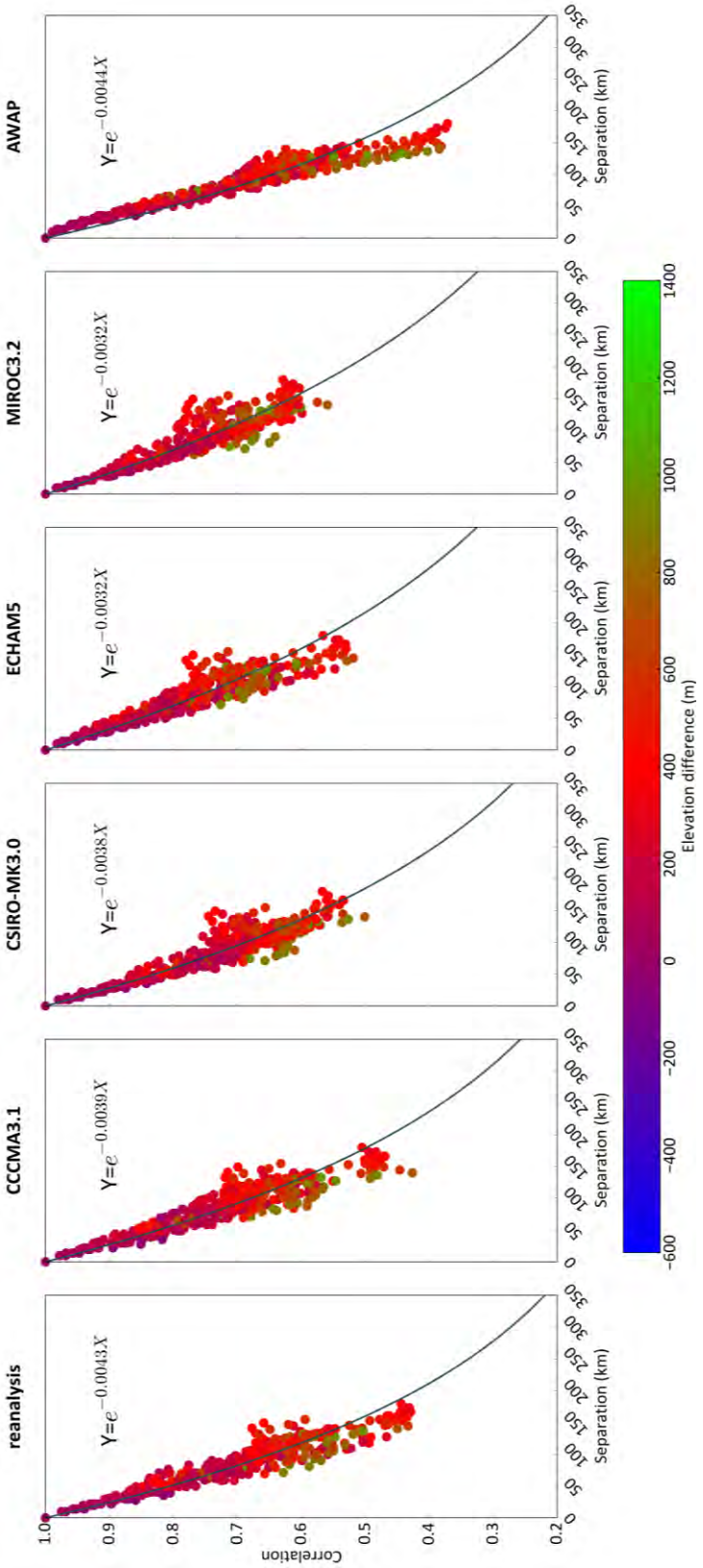

Figure 12.10 Spatial correlations function (1990-2009) of the Williams River site. The reference is W4 low elevation grid point. The plots are for the uncorrected GCM simulations of R1 RCM and AWAP.

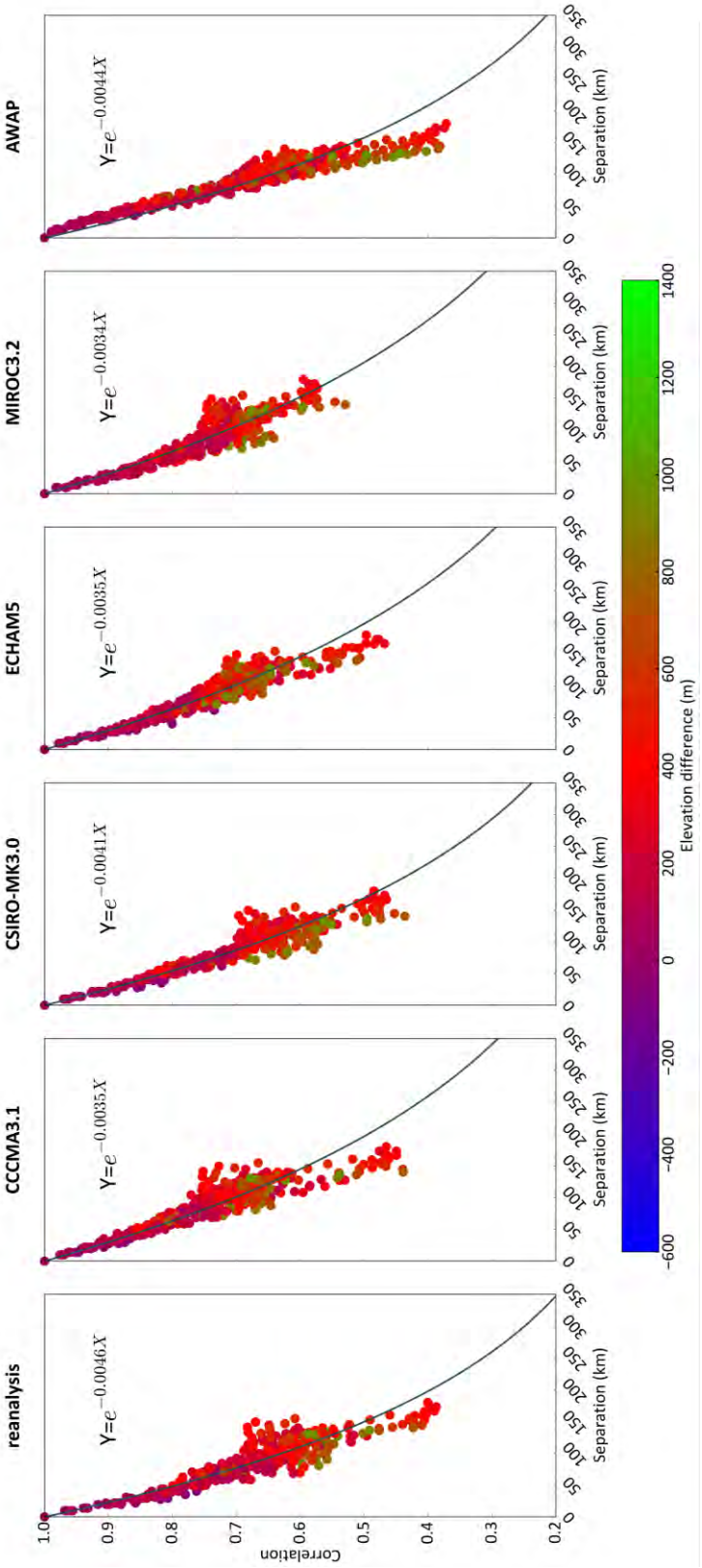

Figure 12.11 Spatial correlations function (1990-2009) of the Williams River site. The reference is W4 low elevation grid point. The plots are for the uncorrected GCM simulations of R2 RCM and AWAP.

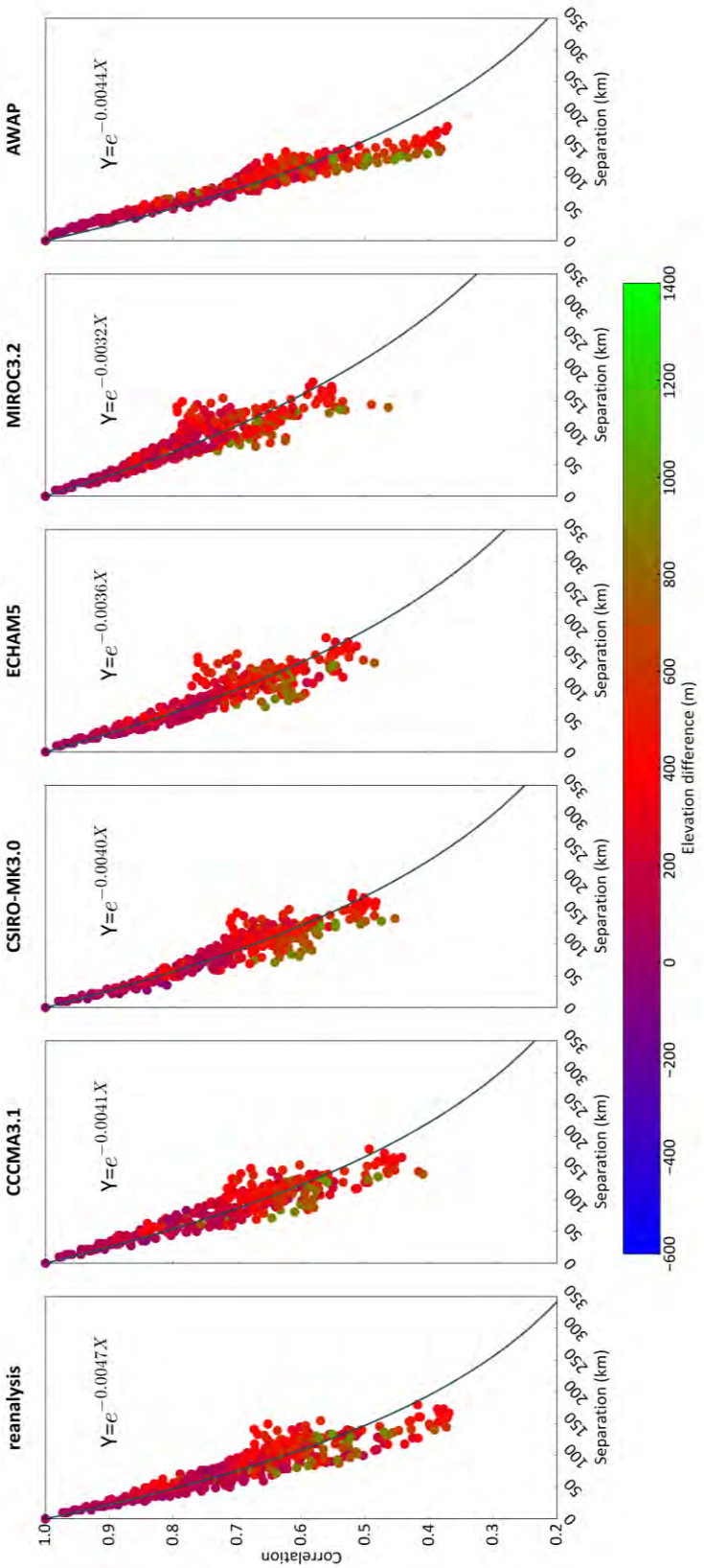

Figure 12.12 Spatial correlations function (1990-2009) of the Williams River site. The reference is W4 low elevation grid point. The plots are for the uncorrected GCM simulations of R3 RCM and AWAP.

Figure 12.13 shows the spatial correlation calculated for the bias corrected NARCliM daily RCMs using the low elevation point as the reference. There is a clear improvement in the CSIRO-Mk3.0 simulations after the bias correction as CSIRO-Mk3.0 has a similar spatial pattern to AWAP after the bias correction. Apart from this, results remain unchanged for the rest of the RCMs.

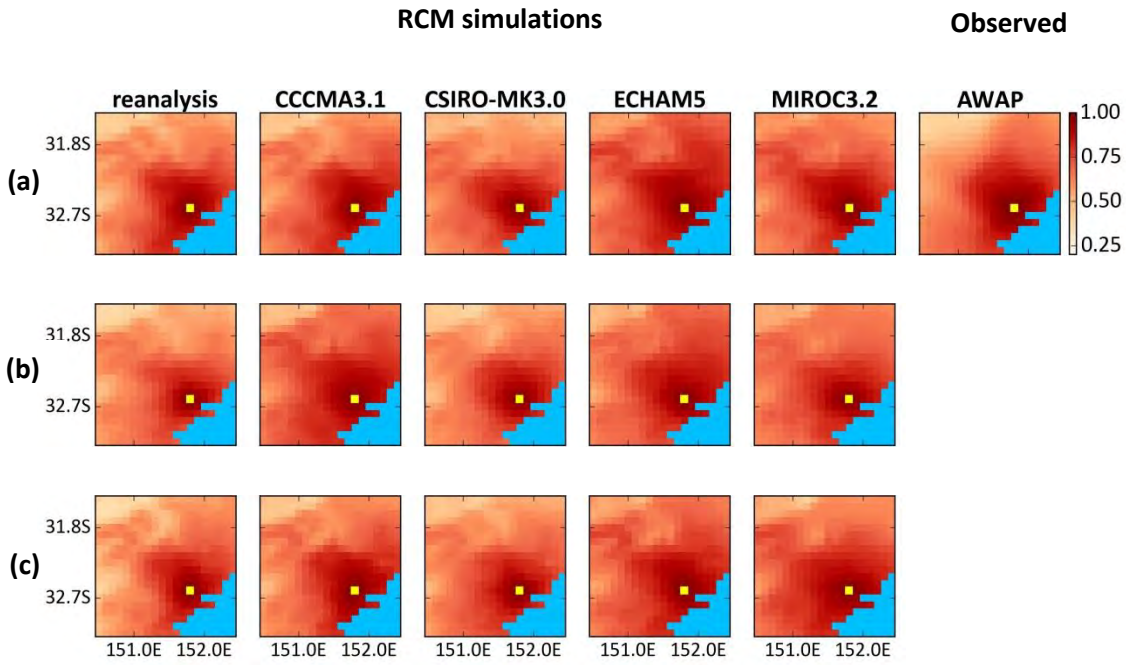

Figure 12.13 Spatial correlations of daily rainfall between the reference grid point and all other grid points in the Williams River site. The plots are for the bias corrected simulations of (a) R1, (b) R2, and (c) R3 RCMs, and AWAP. The reference is W4, a low elevation grid point (shown in yellow boxes).

The spatial correlation functions for bias corrected R1, R2 and R3 configuration simulations corresponding to Figure 12.13 are shown in Figures 12.14 to 12.16. As was seen in the results for the high elevation reference, the ability to reproduce the spatial correlation function of AWAP has been slightly improved in all RCMs, by correcting most of the overestimated correlations across the site. After the bias correction, CSIRO-Mk3.0 RCMs produce a similar spatial correlation function as for the reanalysis and this can clearly be seen in R1 and R3- CSIRO-Mk3.0 RCMs. However, all RCMs tend to perform well for the R3 configuration, but have a different pattern of improvement in the spatial correlations compared with the high elevation case.

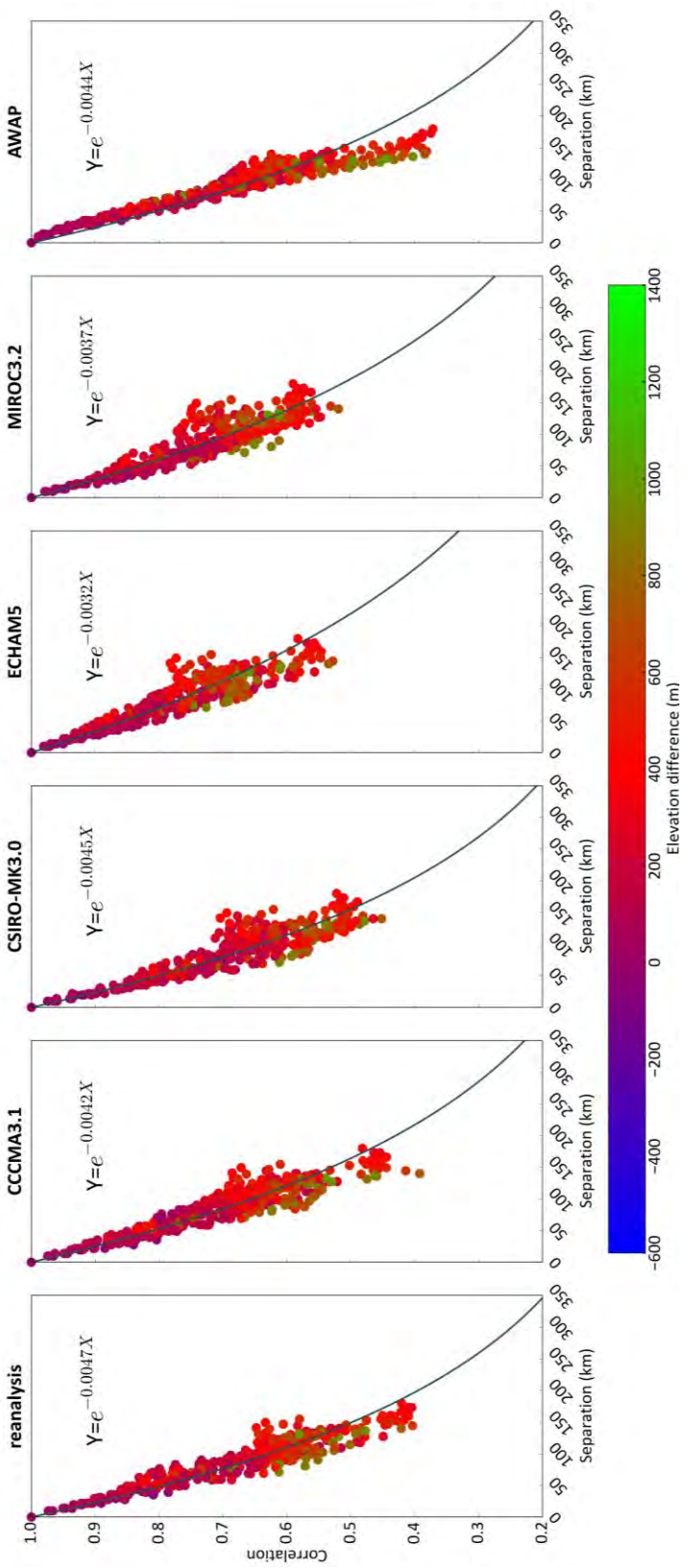

Figure 12.14 Spatial correlations function (1990-2009) of the Williams River site. The reference is W4 low elevation grid point. The plots are for the bias corrected GCM simulations of R1 RCM and AWAP.

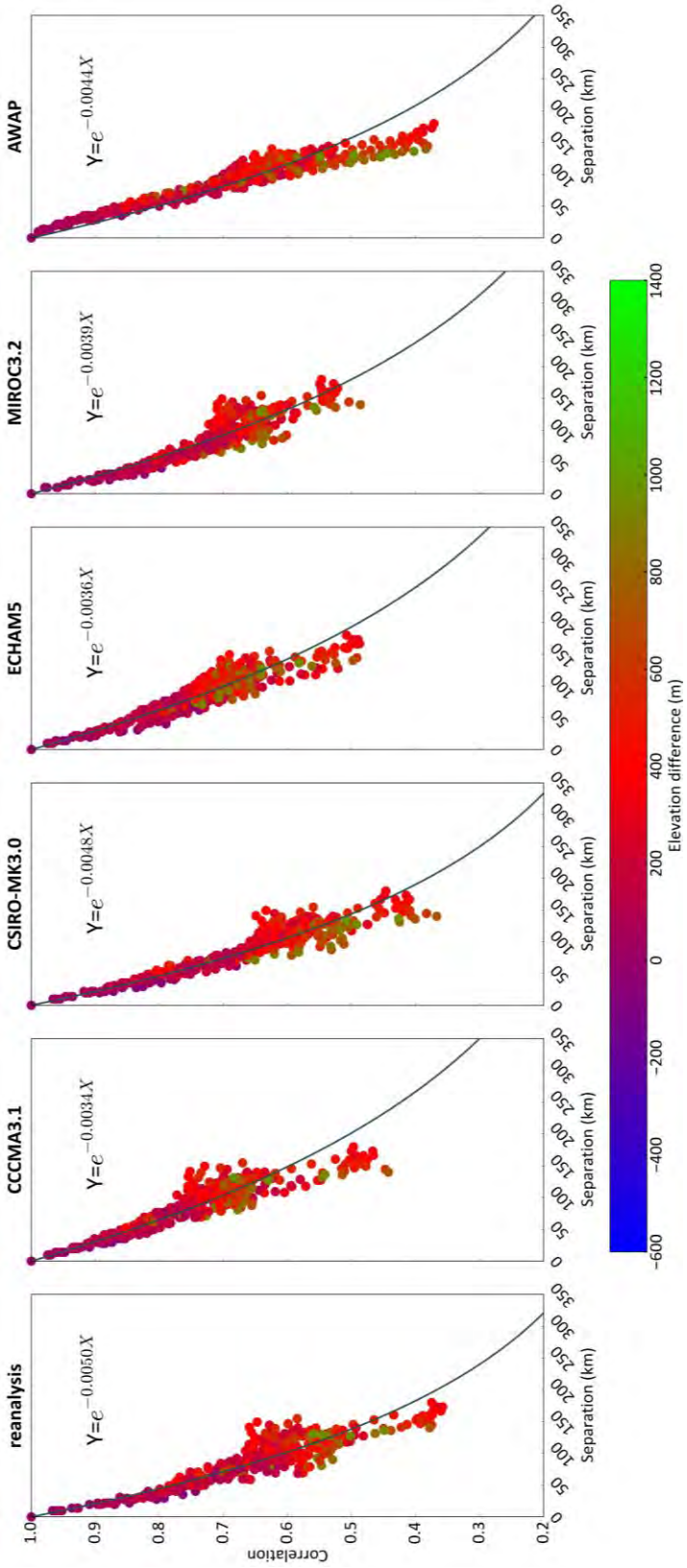

Figure 12.15 Spatial correlations function (1990-2009) of the Williams River site. The reference is W4 low elevation grid point. The plots are for the bias corrected GCM simulations of R2 RCM and AWAP.

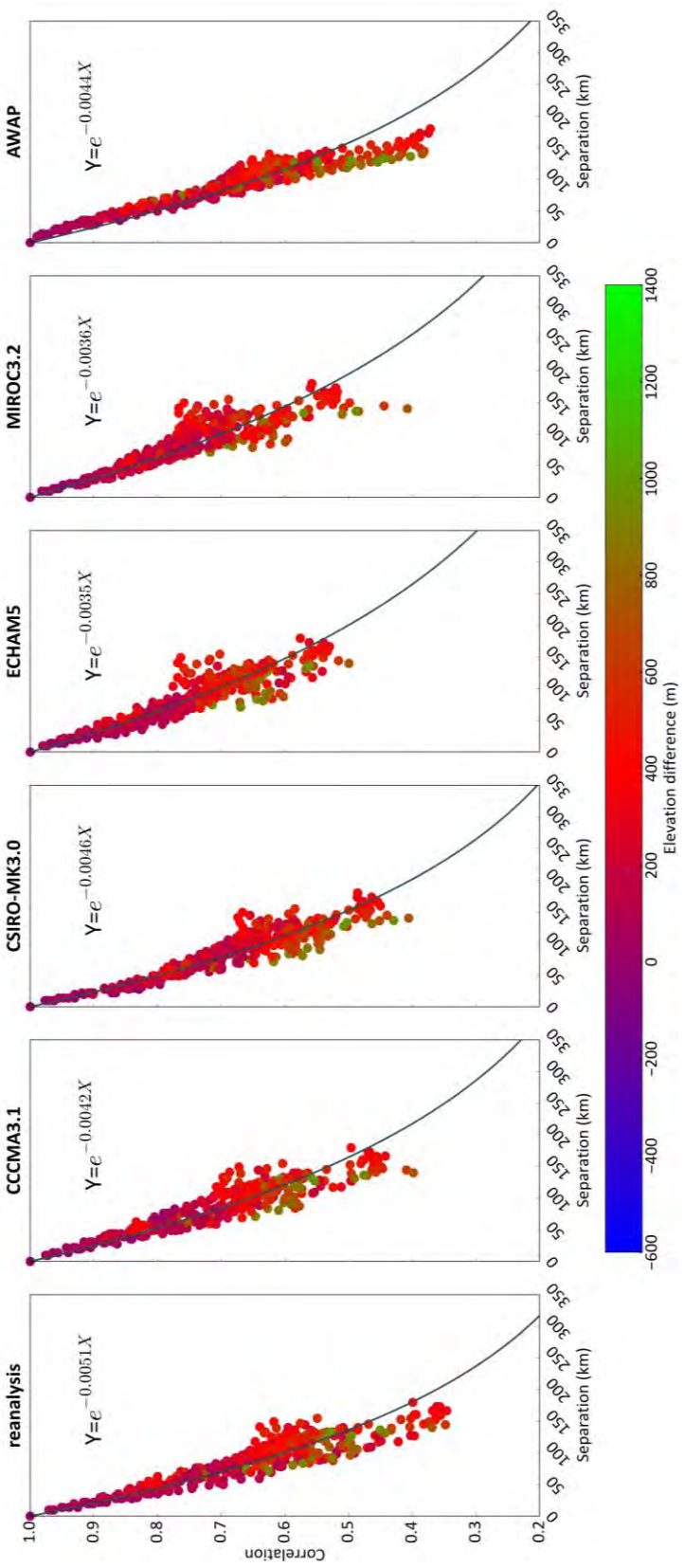

Figure 12.16 Spatial correlations function (1990-2009) of the Williams River site. The reference is W4 low elevation grid point. The plots are for the bias corrected GCM simulations of R3 RCM and AWAP.

12.2.2 Richmond River site

The Richmond River site spatial correlation for the uncorrected NARCliM RCMs between the high elevation grid point (P20) and all other grid points of the site are shown in Figure 12.17. As was the case for the Williams River site, all RCM simulations reproduce the spatial pattern of spatial correlation of AWAP which itself approximately follows the topography of the Richmond River site (see Figure 7.13c). However, in contrast to the Williams River site, all R3 configuration RCMs (including ECHAM5, MIROC3.2 and CSIRO-Mk3.0), closely reproduce both the spatial pattern and magnitudes of correlations of AWAP. This suggests that the ability of the NARCliM RCMs to capture the AWAP spatial correlation varies between sites. Compared with other simulations, MIROC3.2 tends to slightly overestimate (10%) the spatial correlation of AWAP and this overestimation is greatest at low elevations.

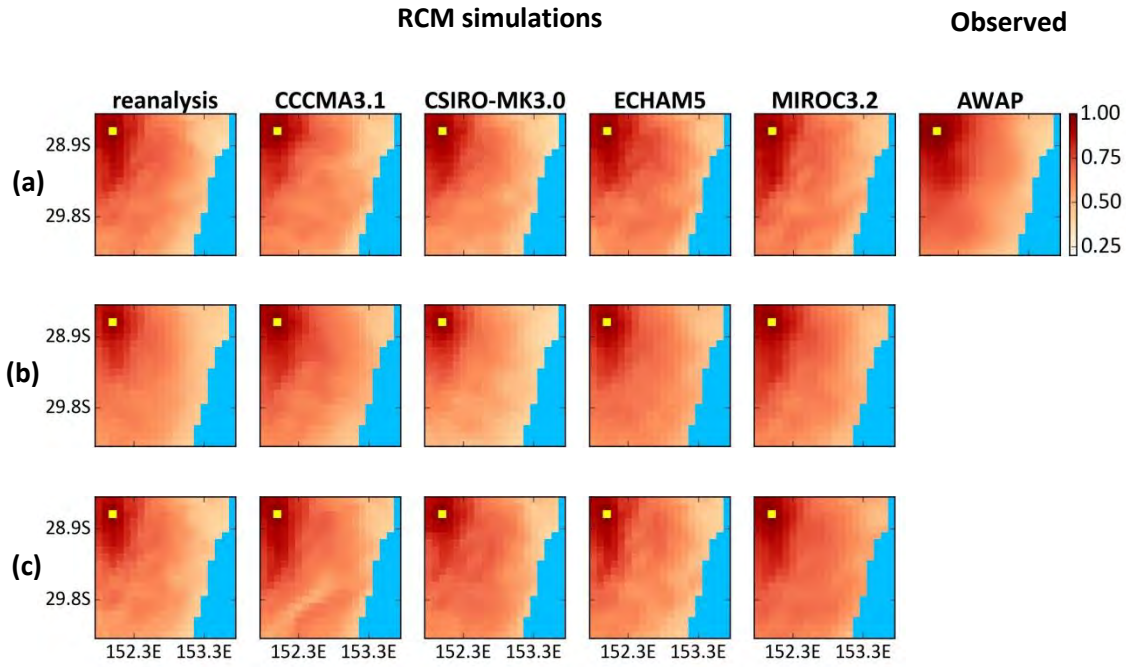

Figure 12.17 Spatial correlations of daily rainfall between the reference grid point and all other grid points in the Richmond River site. The plots are for the uncorrected simulations of (a) R1, (b) R2, and (c) R3 RCMs, and AWAP. The reference is P20, a high elevation grid point (shown in yellow boxes).

The spatial correlation functions for uncorrected R1, R2 and R3 configuration RCMs corresponding to Figure 12.17 are shown in Figures 12.18 to 12.20. The uncorrected

R1-ECHAM5, R1- and R2-MIROC3.2 and R3-CSIRO-Mk3.0 RCMs reproduce the spatial correlation function of AWAP. In particular, the improvement in the performance of ECHAM5 and CSIRO-Mk3.0 is significant as they were found to be the poorest performer at the Williams site. The reanalysis and CCCMA 3.1 are also able to reproduce the spatial correlation function of AWAP, and tend to perform better for R1 for reanalysis, and R2 and R3 for CCCMA3.1. With the exception of MIROC3.2 and reanalysis, all uncorrected R3 configuration RCMs reproduce the spatial correlation of AWAP.

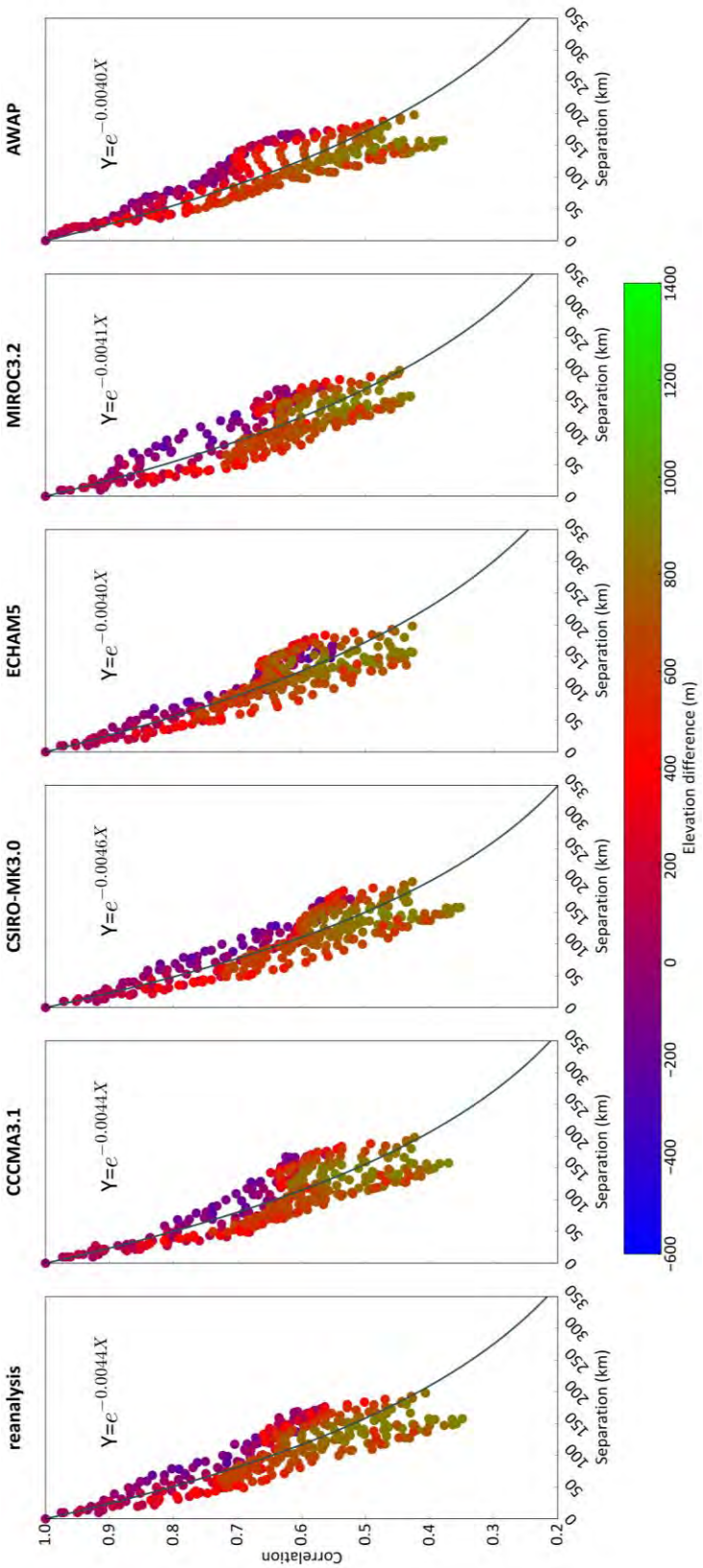

Figure 12.18 Spatial correlations function (1990-2009) of the Richmond River site. The reference is P20 high elevation grid point. The plots are for the uncorrected GCM simulations of R1 RCM and AWAP.

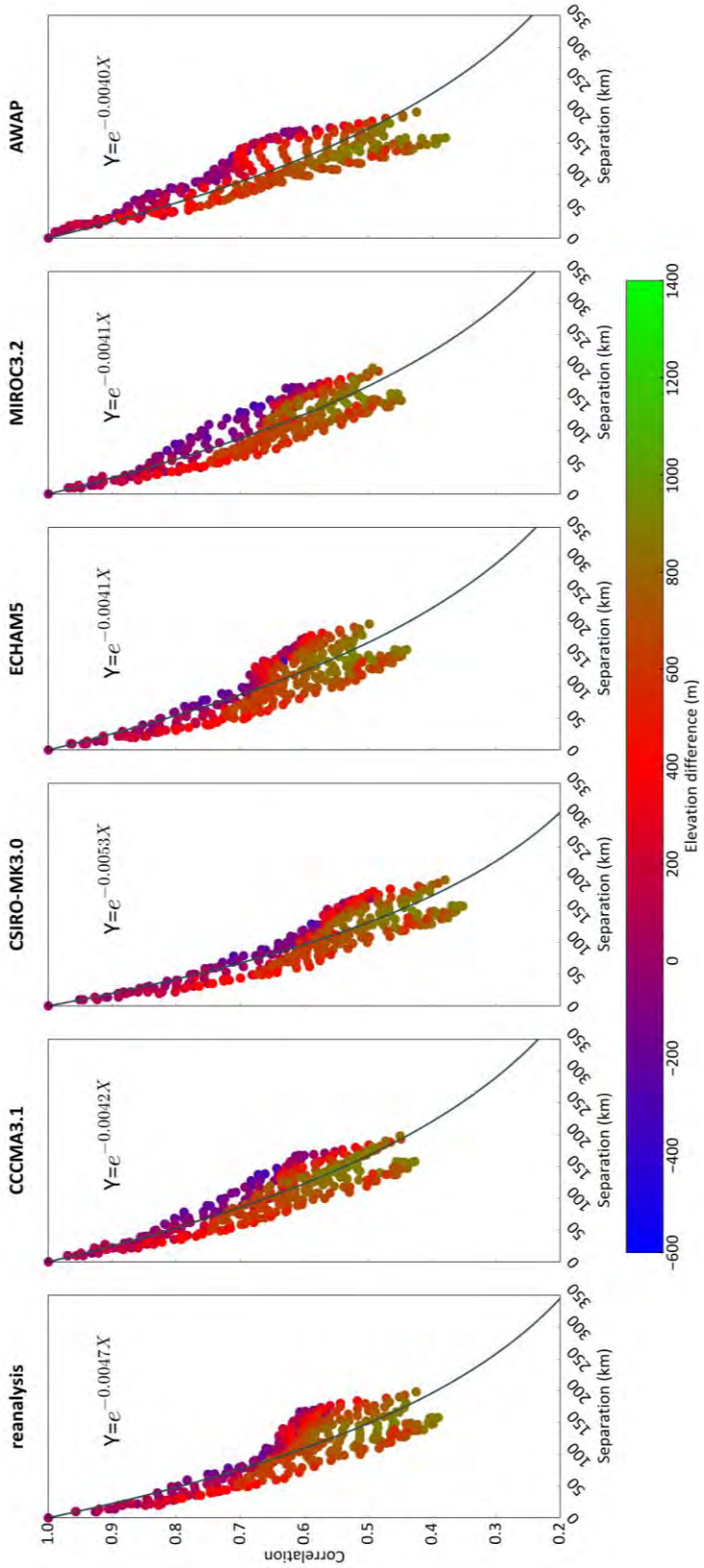

Figure 12.19 Spatial correlations function (1990-2009) of the Richmond River site. The reference is P20 high elevation grid point. The plots are for the uncorrected GCM simulations of R2 RCM and AWAP.

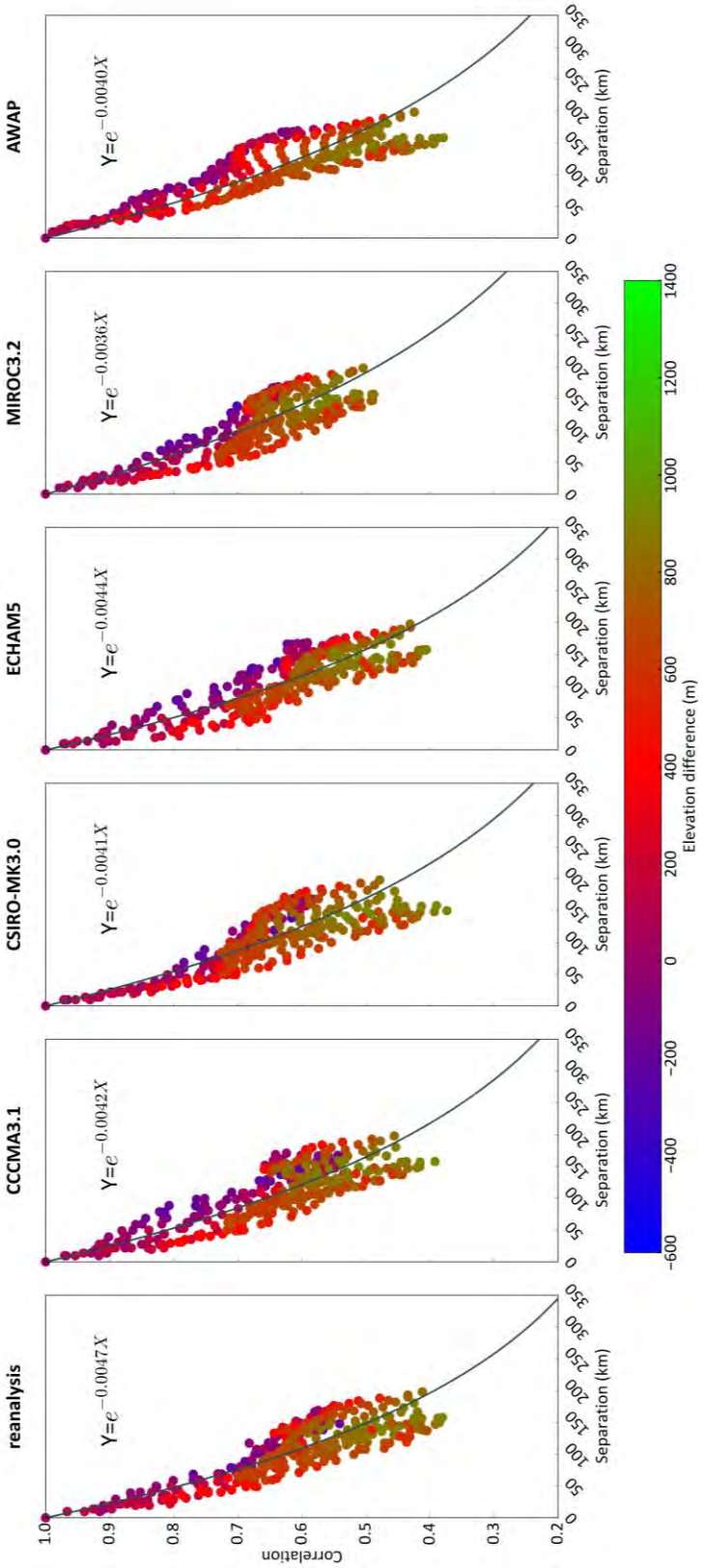

Figure 12.20 Spatial correlations function (1990-2009) of the Richmond River site. The reference is P20 high elevation grid point. The plots are for the uncorrected GCM simulations of R3 RCM and AWAP.

Figures 12.21 to 12.24, show the spatial correlation and corresponding spatial correlation functions for the bias corrected NARCliM daily simulations calculated for the high elevation reference.

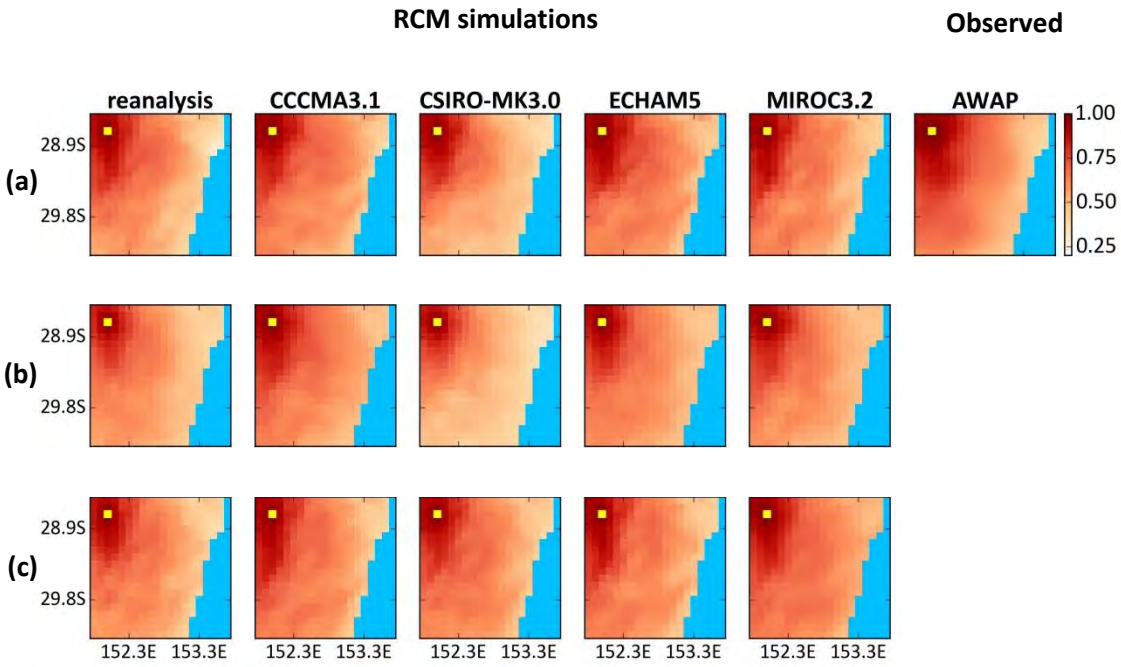

Figure 12.21 Spatial correlations of daily rainfall between the reference grid point and all other grid points in the Richmond River site. The plots are for the bias corrected simulations of (a) R1, (b) R2, and (c) R3 RCMs, and AWAP. The reference is P20, a high elevation grid point (shown in yellow boxes).

Compared with Figure 12.17, there is only a small change in the performance of the NARCliM RCMs after the bias correction; the underestimated correlations have been corrected at only a few points. Overall, after bias correction the model improvement is insignificant at the Richmond River site. However, after the bias correction R2 reanalysis and R2-CSIRO-Mk3.0 in Figure 12.22a tend to underestimate the spatial correlation function of AWAP for large spatial separations.

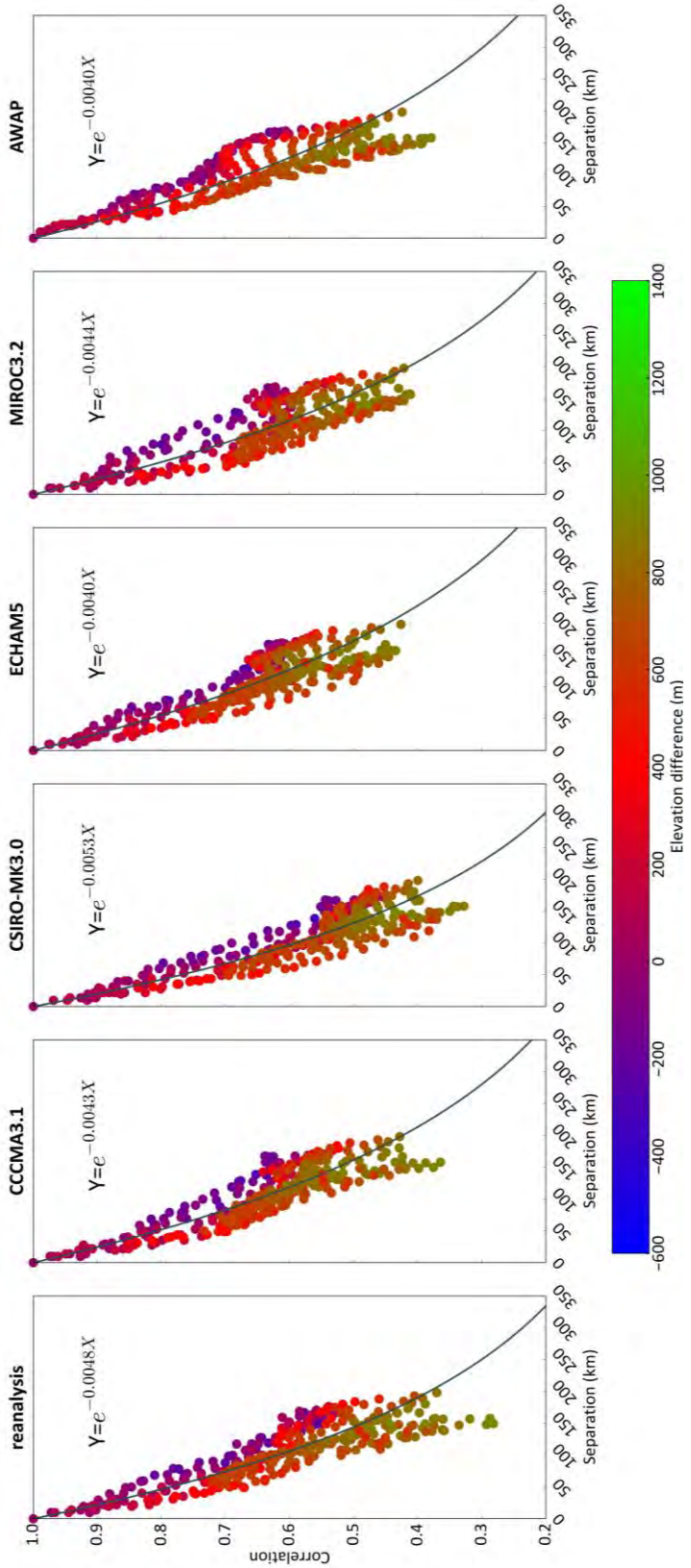

Figure 12.22 Spatial correlations function (1990-2009) of the Richmond River site. The reference is P20 high elevation grid point. The plots are for the bias corrected GCM simulations of R1 RCM and AWAP.

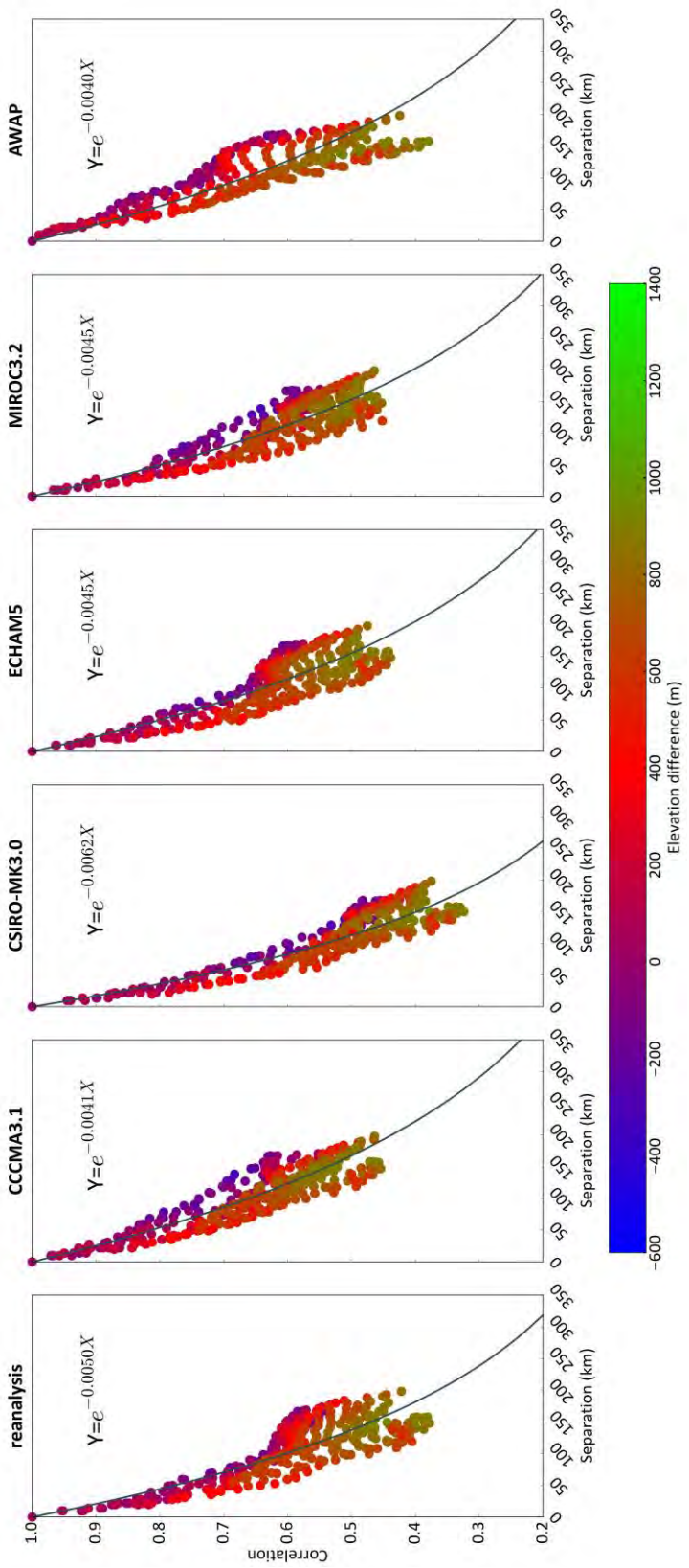

Figure 12.23 Spatial correlations function (1990-2009) of the Richmond River site. The reference is P20 high elevation grid point. The plots are for the bias corrected GCM simulations of R2 RCM and AWAP.

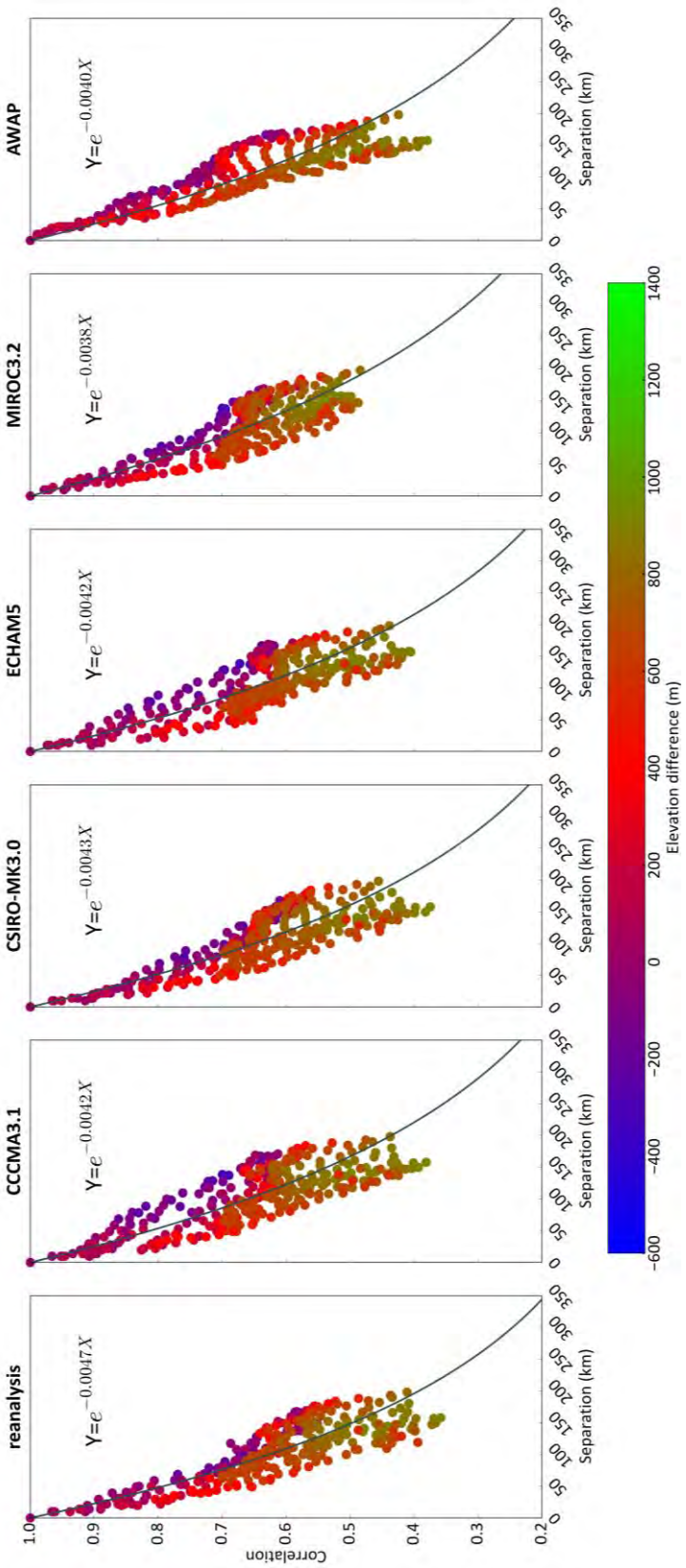

Figure 12.24 Spatial correlations function (1990-2009) of the Richmond River site. The reference is P20 high elevation grid point. The plots are for the bias corrected GCM simulations of R3 RCM and AWAP.

The spatial correlation of the uncorrected NARCliM RCMs for the low elevation grid point (P9) in the Richmond River site are shown in Figure 12.25.

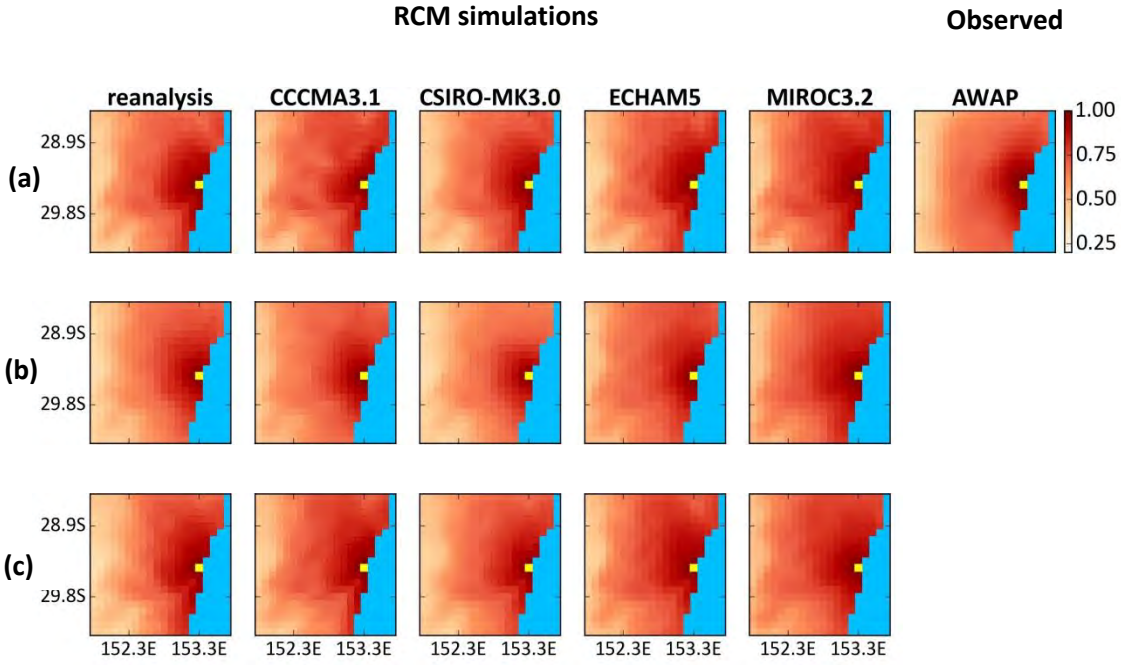

Figure 12.25 Spatial correlations of daily rainfall between the reference grid point and all other grid points in the Richmond River site. The plots are for the uncorrected simulations of (a) R1, (b) R2, and (c) R3 RCMs, and AWAP. The reference is P9, a low elevation grid point (shown in yellow boxes).

Of all simulations, R1 reanalysis, R1-CSIRO-Mk3.0 and R1-ECHAM5 tend to better reproduce the spatial distribution of the AWAP at low elevation reference. All three configurations of MIROC3.2, and R1 and R3 configurations of CCCMA3.1 appear to overestimate the magnitude of the spatial correlations, particularly at low elevation grid points close to the reference point.

Figures 12.26 to 12.28 show the spatial correlation functions corresponding to Figure 12.25. Comparing the spatial correlation functions of all RCMs reanalysis, CSIRO and ECHAM5 all produce similar spatial correlation functions and they all reproduce the spatial correlation function of AWAP. Compared to the results at the high elevation reference the R1 and R3 model configuration reanalysis, CSIRO-Mk3.0 reproduce the overall spatial correlation function of AWAP better than R2, and again the mean trend of the spatial correlation functions for all datasets have less scatter around the fitted exponential function compared with high elevation case.

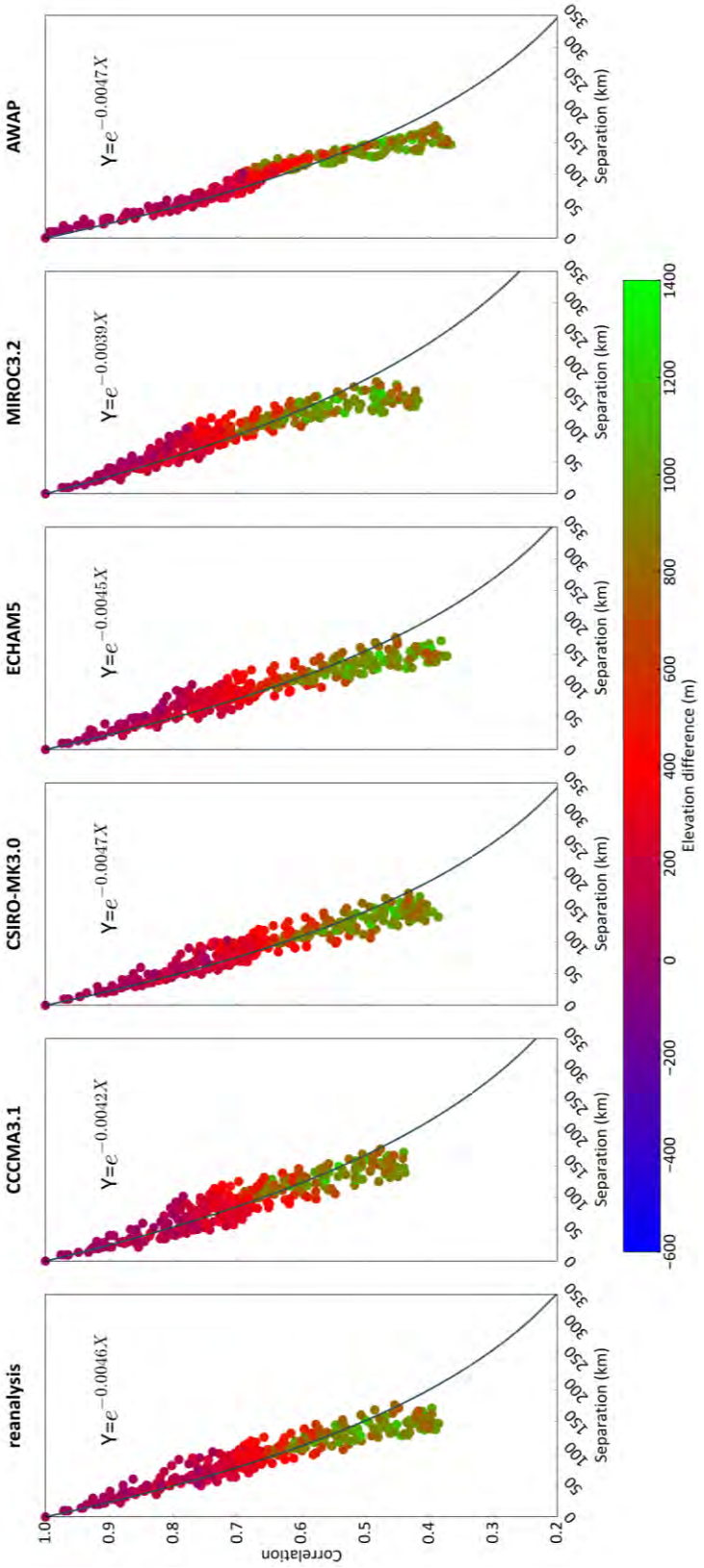

Figure 12.26 Spatial correlations function (1990-2009) of the Richmond River site. The reference is P9 low elevation grid point. The plots are for the uncorrected GCM simulations of R1 RCM and AWAP.

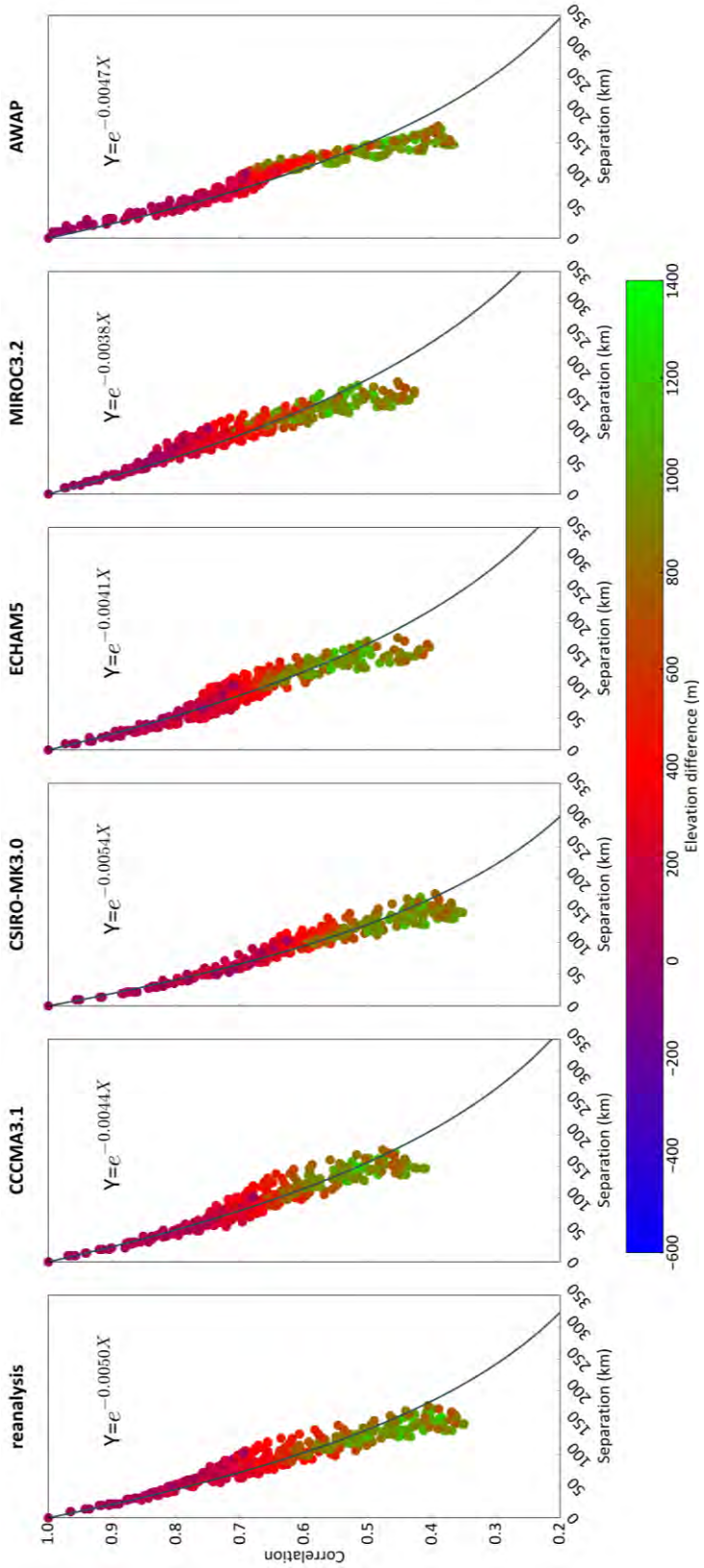

Figure 12.27 Spatial correlations function (1990-2009) of the Richmond River site. The reference is P9 low elevation grid point. The plots are for the uncorrected GCM simulations of R2 RCM and AWAP.

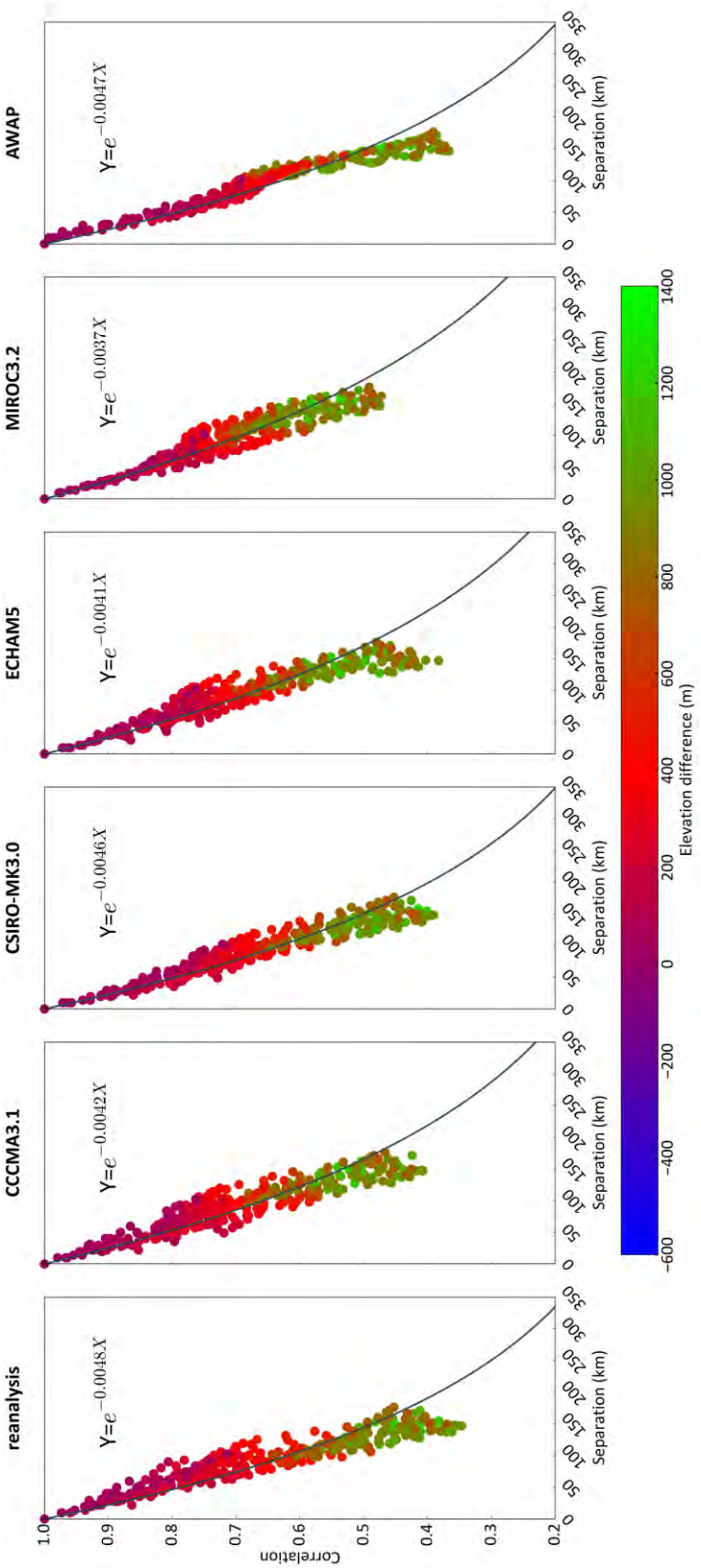

Figure 12.28 Spatial correlations function (1990-2009) of the Richmond River site. The reference is P9 low elevation grid point. The plots are for the uncorrected GCM simulations of R3 RCM and AWAP.

Figures 12.29 to 12.32, show spatial correlation plots and corresponding spatial correlation functions for the bias corrected NARCliM daily simulations calculated at the low elevation reference of the Richmond River site. After bias correction, reanalysis and CSIRO-Mk3.0 tend to slightly underestimate the AWAP spatial correlations, particularly along the boundary of the escarpment of the Richmond site (see Figure 7.13c). There is a slight improvement in results of MIROC3.2, CCCMA3.1 and ECHAM5 model simulations, particularly for R1 simulations. The R1 configuration simulations, with the exception of CSIRO-Mk3.0, appear to perform well after the bias correction.

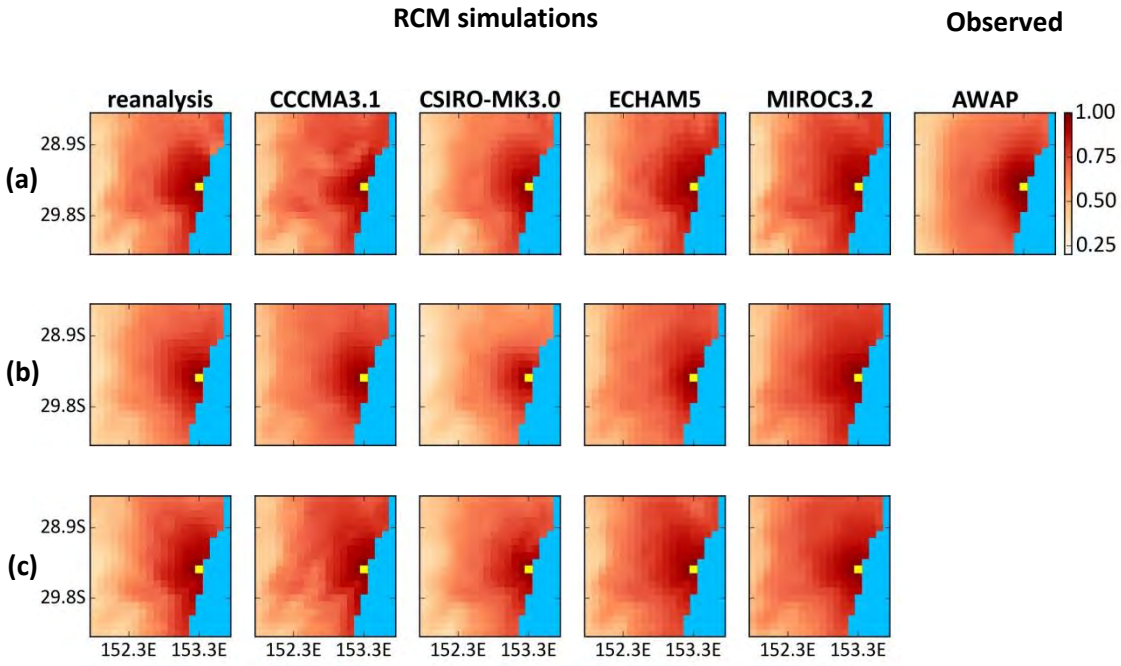

Figure 12.29 Spatial correlations of daily rainfall between the reference grid point and all other grid points in the Richmond River site. The plots are for the bias corrected simulations of (a) R1, (b) R2, and (c) R3 RCMs, and AWAP. The reference is P9, a low elevation grid point (shown in yellow boxes).

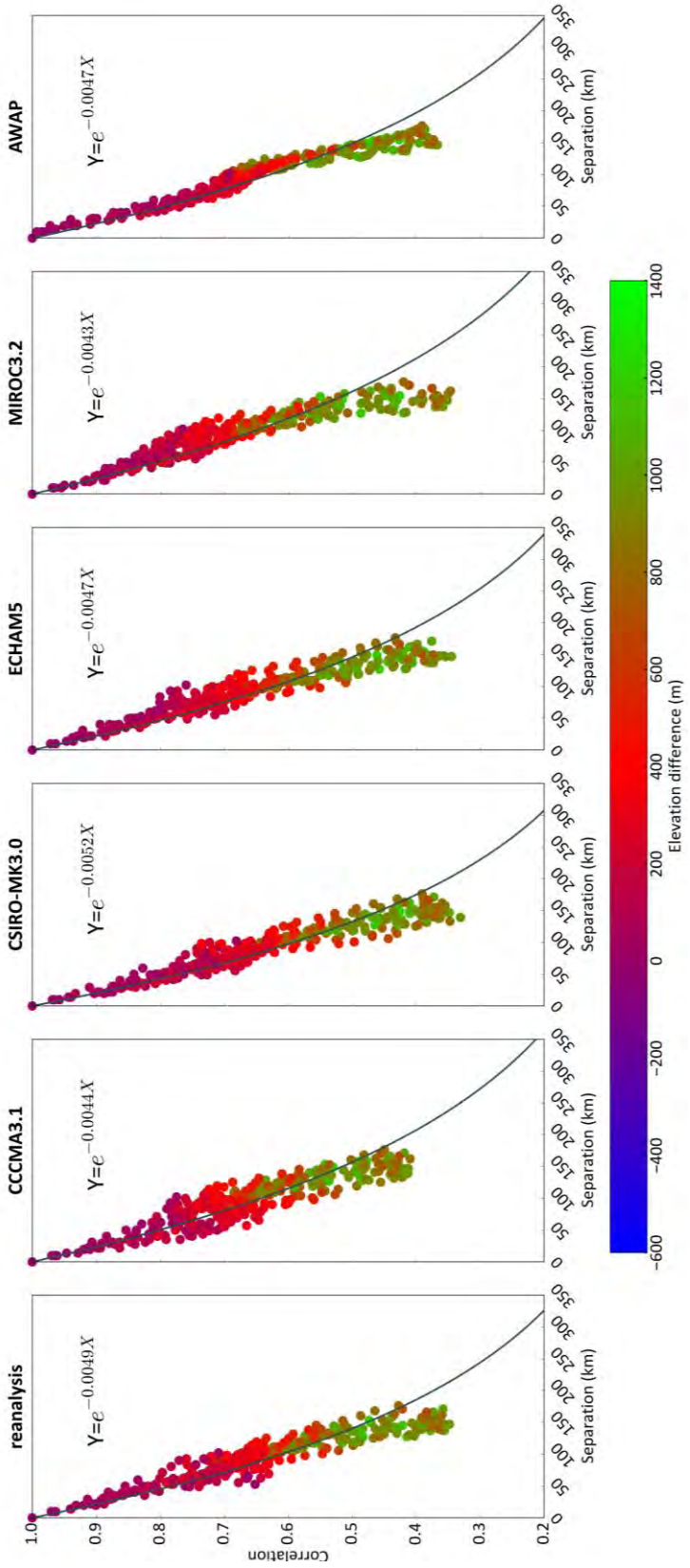

Figure 12.30 Spatial correlations function (1990-2009) of the Richmond River site. The reference is P9 low elevation grid point. The plots are for the bias corrected GCM simulations of R1 RCM and AWAP.

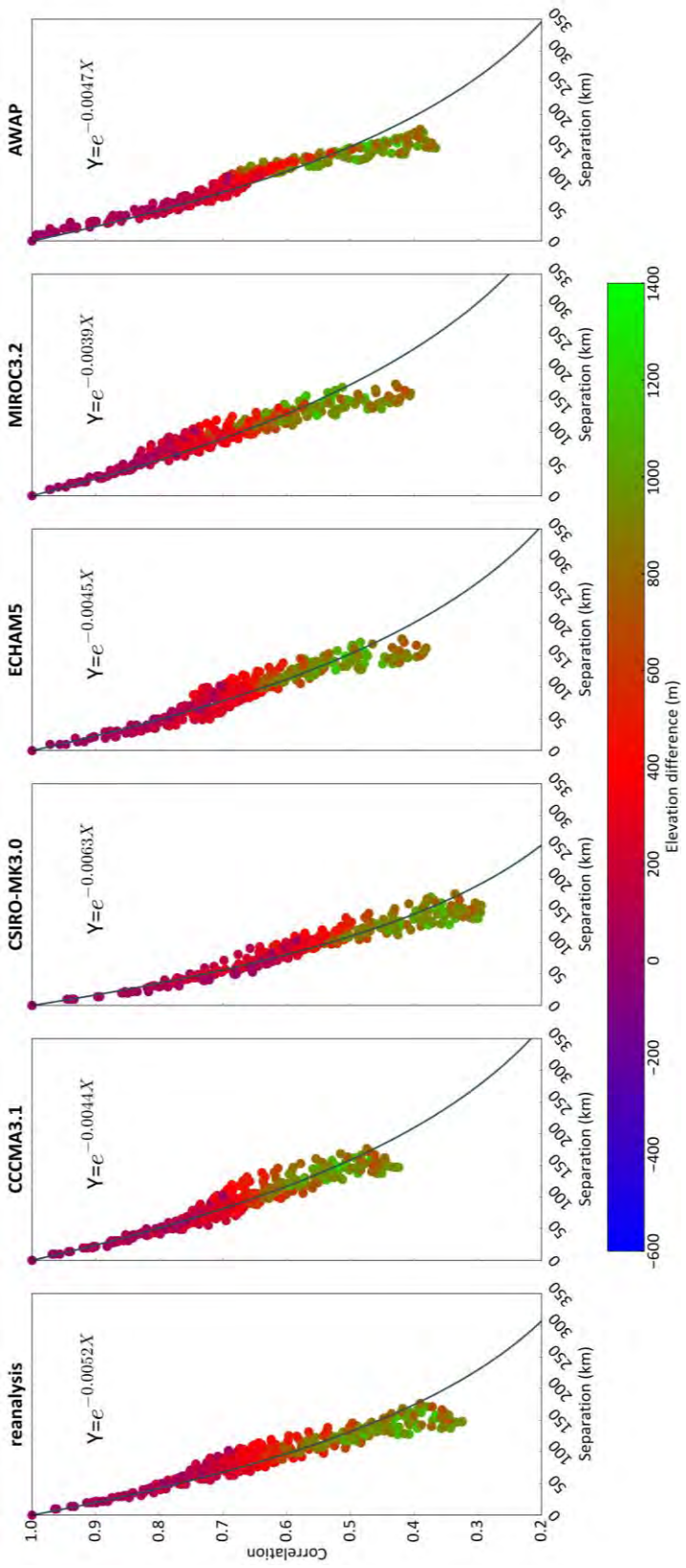

Figure 12.31 Spatial correlations function (1990-2009) of the Richmond River site. The reference is P9 low elevation grid point. The plots are for the bias corrected GCM simulations of R2 RCM and AWAP.

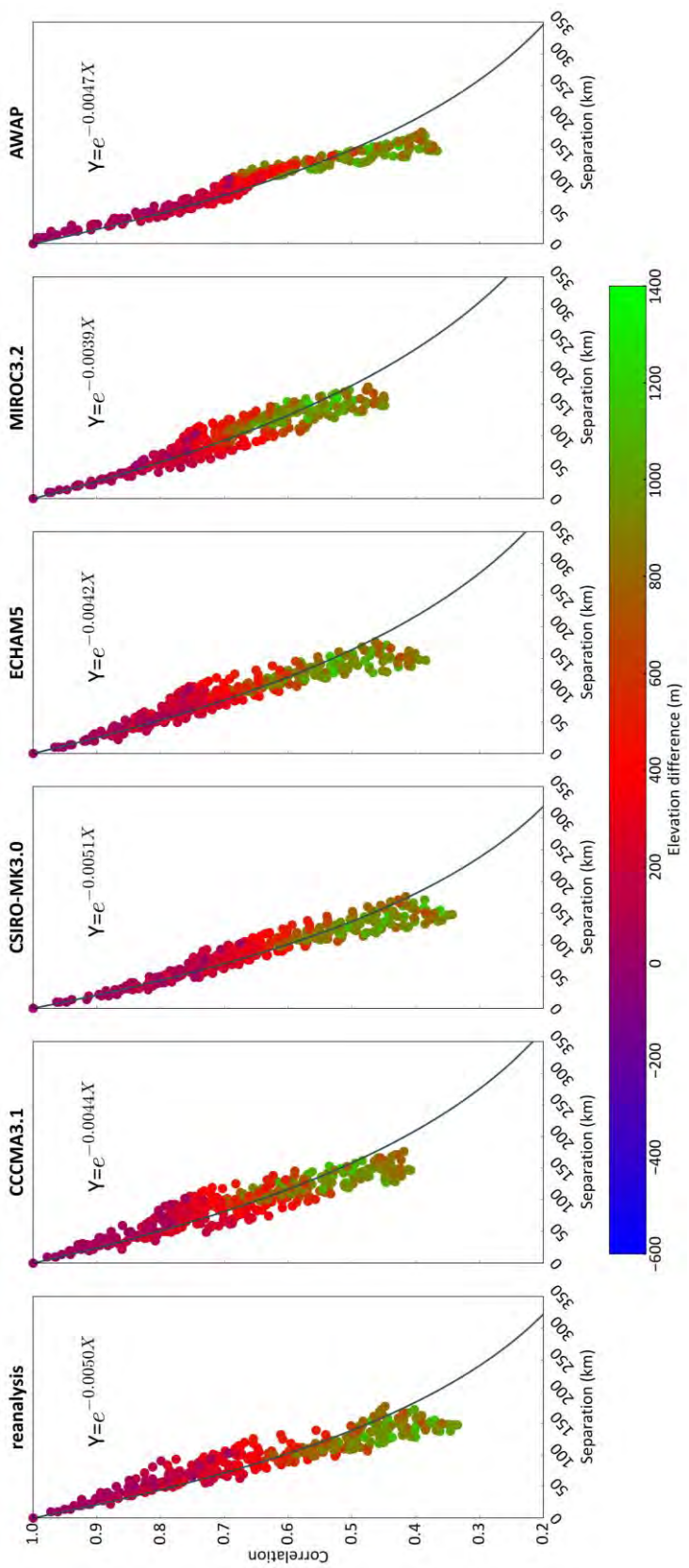

Figure 12.32 Spatial correlations function (1990-2009) of the Richmond River site. The reference is P9 low elevation grid point. The plots are for the bias corrected GCM simulations of R3 RCM and AWAP.

12.2.3 Summary of the spatial correlation analysis

The results show that uncorrected reanalysis is best able to reproduce the spatial correlations of AWAP and tends to perform consistently well between the sites. R1 reanalysis performs better than either R2 or R3. CSIRO-Mk3.0 appears to better reproduce the spatial correlation of AWAP than the other GCMs for all sites, but does not perform as well as the reanalysis. The R3 and R1 RCMs consistently perform better than R2 for both Williams and Richmond River sites, and this suggests that there are subtle and consistent differences between the outputs of the underlying RCM used in the downscaling. ECHAM5 and CCCMA3.1 RCMs better capture the AWAP spatial correlations than MIROC3.2. However, the performance of these models is dependent on the site rainfall and topography. Of all simulations, MIROC3.2 is less able to reproduce the spatial correlations of AWAP for all sites. However, the exception is the Bega River site (see Appendix A.6 – Figures A.37 to A.52). At the Bega River site, reanalysis, ECHAM5 and MIROC3.2 are able to reproduce the spatial correlation pattern and spatial correlation function of AWAP, while CSIRO-Mk3.0 and CCCMA3.1 underestimate the AWAP correlations across the site. However, apart from a few discrepancies, there is a consistency of relative model performance.

Results of the Bega River and Sydney sites are not discussed under this section but brioadly follow the Williams and Richmond River trends (see Appendix A.6 - Figures A.37 to A.68). At the Sydney site, reanalysis, CCCMA3.1 and CSIRO-Mk3.0 uncorrected RCMs are best able to reproduce the spatial correlation of AWAP than the other RCMs.

The scatter of the spatial correlation functions around the fitted exponential functions to all NARCliM RCMs is higher than that of the AWAP for Williams, Richmond and Bega River sites. This suggests that there is high variability in the correlations of NARCliM simulations compared with AWAP. The reduced scatter in AWAP may be due to the smoothing seen in the spatial variability plots for all sites and it is reasonable to suggest that it is an interpolation artefact as discussed in Section 7.2.

Overall, though the spatial correlation function of AWAP is correctly captured by all NARCliM RCMs for all the sites, there are some discrepancies of the trend of the

spatial correlation functions of individual NARCliM RCMs, particularly for the correlations calculated with reference to the high elevation grid points. Further this appears to depend on the individual site characteristics. For example when the reference is a high elevation grid point, AWAP has more scattered correlations than reanalyses for separations greater than 200 km at the Sydney site and this is different to other sites.

The results generated for the bias corrected RCMs at Richmond River and Sydney sites also indicate that bias correction mostly improves the performance of each RCM, but the improvement is small. However, this is an expected result, because the spatial correlations presented in this chapter were calculated using the daily rainfall of RCM simulations and bias correction is not designed to adjust spatial correlations (see Section 9.2). Compared with all sites, the lowest spatial correlation of AWAP daily rainfall is for the Richmond River site.

As for the 60 year reanalyses, rainfall for the 20 year RCMs is also more correlated to the distance between the points (separation) than to the difference of the elevation of the two points.

12.3 Testing the spatial correlation of NARCliM GCM simulations rain gauge data

Spatial correlation functions between the rain gauges, NARCliM RCM grid points and, AWAP grid points for Williams River, Richmond River, Bega River and Sydney sites are shown in Figures 12.33 to 12.36. The figures also compare the spatial correlations of uncorrected and bias corrected RCMs. Spatial correlations were calculated only for the grid points (reanalyses, GCMs and AWAP) where the rain gauges are, while the spatial correlation functions shown in the previous section are for all grid points at a site. Note that only the R3 configurations simulations are shown in the figures, as it was identified as the best performing RCM configuration in the previous section. The spatial correlation functions of the Williams River site shown in Figure 12.33 reflect that all NARCliM uncorrected RCMs and AWAP have correlations 20-30% higher than that of the rain gauges. This difference between rain gauge and gridded datasets (NARCliM RCMs and AWAP) is unlikely to be because of the spatial averaging of the rainfall within a pixel.

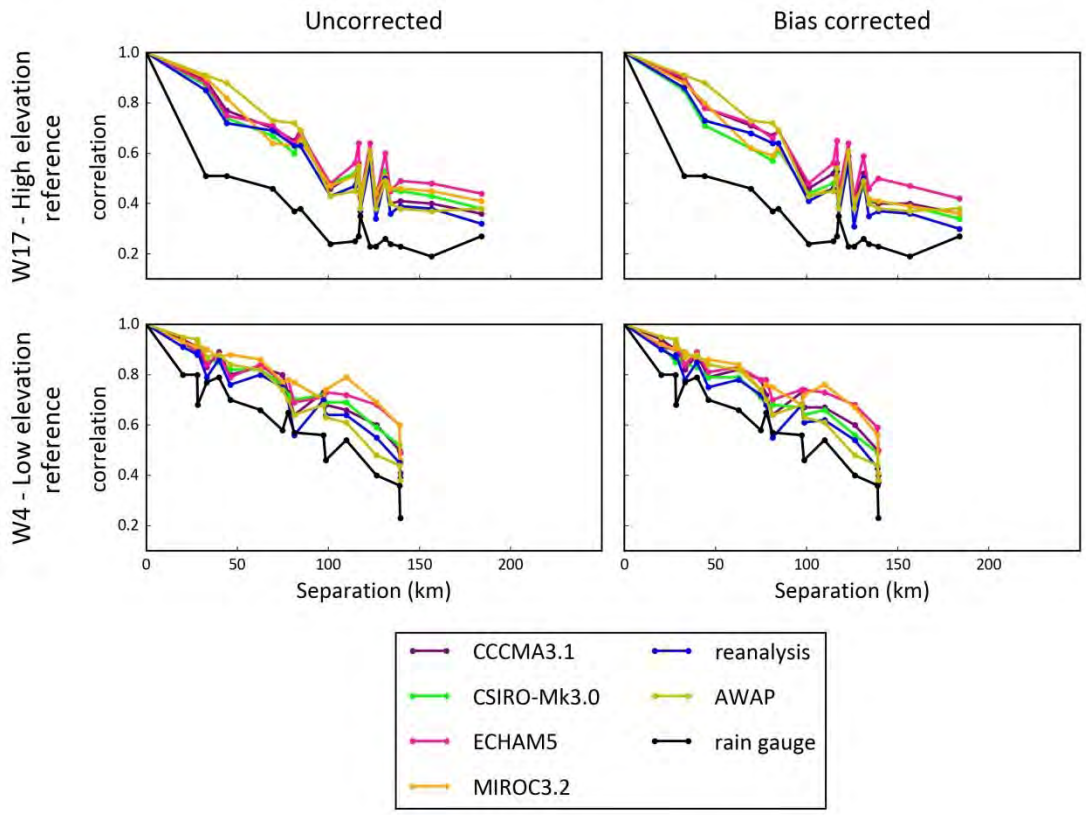

Figure 12.33 Spatial correlation between rain gauges at Williams River site. Left plots are for the uncorrected NARCliM simulations and right are for the bias corrected simulations.

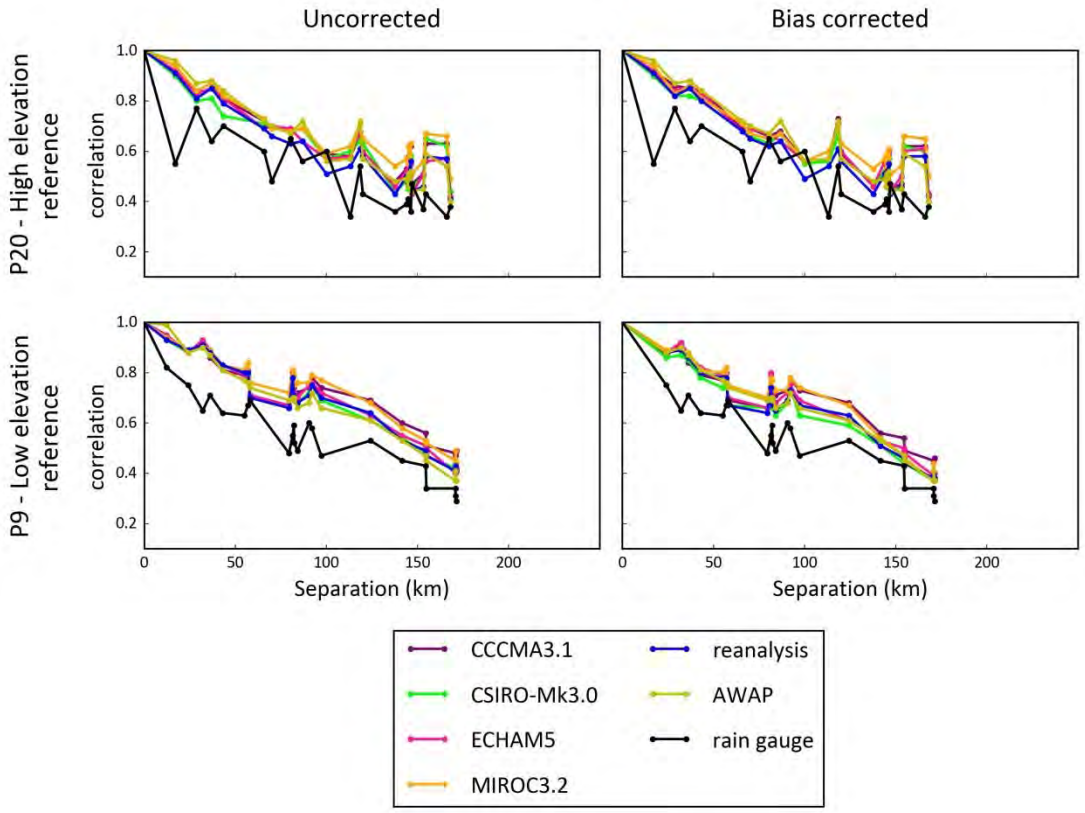

Figure 12.34 Spatial correlation between rain gauges at Richmond River site. Left plots are for the uncorrected NARCliM simulations and right are for the bias corrected simulations.

As was seen in the Section 7.3, the reanalyses have the lowest overestimation of the spatial correlation of rain gauges, while MIROC3.2 most overestimates the rain gauge correlation, except W17 high elevation reference at the Williams River site. Reanalysis and CSIRO-Mk3.0 RCMs have spatial correlations similar to AWAP for almost all references. This highlights that NARCliM RCMs, particularly reanalysis and CSIRO-Mk3.0 perform as well as AWAP for generating the spatial correlation of the rainfall. However, while the spatial correlation functions of reanalysis and CSIRO-Mk3.0 and AWAP look similar to each other, they all fail to reproduce the spatial correlation function of the rain gauge network. While reanalysis and CSIRO-Mk3.0 consistently perform as well as AWAP, ECHAM5 and CCCMA3.1 show varying ability to reproduce the spatial correlation of daily rainfall at different sites. For example, at the Williams and Bega River sites, the spatial correlation function of CCCMA3.1 is very similar to that of AWAP, but appear to overestimate the

correlation of AWAP at the Richmond River and Sydney sites. At the high elevation reference of the Sydney site, there is a slightly different trend in the spatial correlation of rain gauges compared with all other gridded datasets (RCMs and AWAP). The reason for this is not known but may be related with the lower variability in the topography in this particular site. Comparing the plots for uncorrected and bias corrected RCMs at each site, there is no significant difference between spatial correlation functions of all the simulations. Therefore, this suggests that the impact of bias correction is minimal.

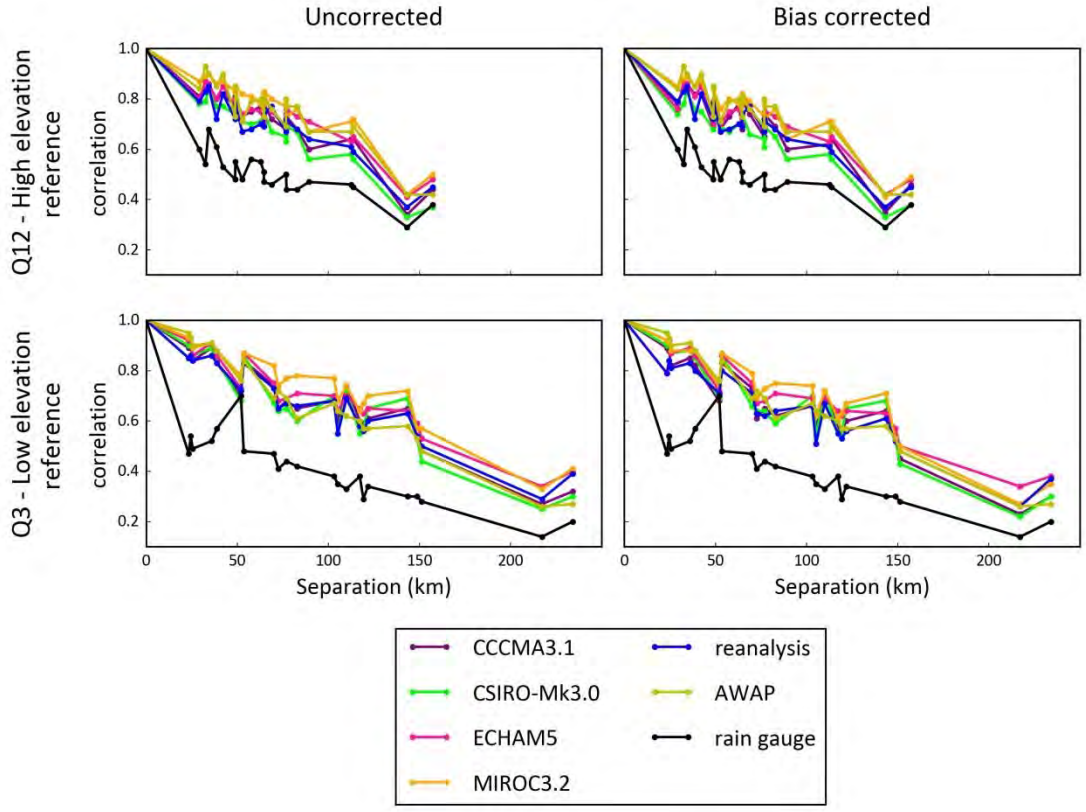

Figure 12.35 Spatial correlation between rain gauges at Bega River site. Left plots are for the uncorrected NARCliM simulations and right are for the bias corrected simulations.

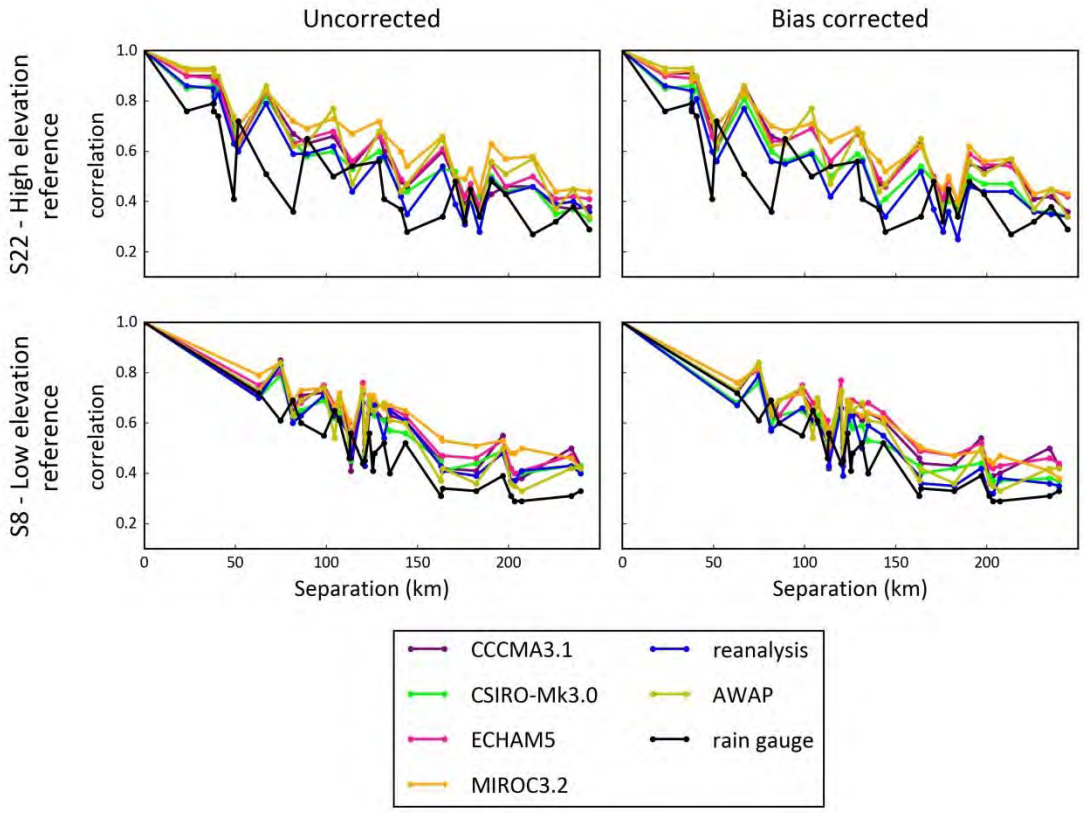

Figure 12.36 Spatial correlation between rain gauges at Sydney River site. Left plots are for the uncorrected NARCliM simulations and right are for the bias corrected simulations.

12.4 Conclusions

The results suggest that reanalysis is best at reproducing the AWAP spatial correlations. Of the GCMs, the uncorrected CCCMA3.1 and CSIRO-Mk3.0 perform similarly to reanalysis at all sites. However, which model (either CCCMA or CSIRO-Mk3.0) performs better varies depending on the site topography and the general hydrology. Though the exponential structure of the spatial correlation function of AWAP is closely captured by NARCliM RCMs, there are some discrepancies in the scatter of the spatial correlation functions of individual NARCliM RCM simulations at some reference grid points.

After the bias correction, the ability to capture the AWAP spatial correlation in all RCM simulations is only slightly changed. The difference in the performance between NARCliM RCMs, rain gauge and AWAP for the high elevation reference is

very similar to that for the low elevation reference at all sites, therefore, model performance appears to be independent of the elevation of the reference grid point.

Of the three RCM model configurations, R3 configuration simulations better reproduce the spatial correlations of AWAP rainfall than R1 and R2. This suggests that apart from having possible discrepancies between the individual RCMs, there are differences between the outputs depending on the underlying RCM configurations which were used in the downscaling process.

All NARCliM RCM and AWAP gridded datasets have correlations higher than that of rain gauges, with approximately 20-30% overestimation for all the grid points used. Subject to this consistent overestimation NARCliM RCMs and AWAP preserve the general trend of the spatial correlation function of rain gauge at all reference grid points of all sites. Reanalysis and CSIRO-Mk3.0 have spatial correlation functions similar to AWAP, but they all overestimate the magnitudes of the spatial correlation of gauge.

Chapter 13
NARCliM future climate projections for the East Coast of Australia

13.1 Introduction

Projections of climate change are essential for long term sustainable natural resources planning and urban water resources planning. In general, the rainfall change projections are available regionally and their reliability can be different from one region to another. In particular, there is a higher level of uncertainty associated with projections of rainfall change along the east coast of Australia than some other regions (Grose et al., 2015), due to the influence of a number of different weather phenomena including fronts, subtropical cyclones, ECLs and thunderstorms which drive the climate of this region.

This chapter aims to assess the future change of rainfall along the broader east coast of Australia, using the 10 km resolution NARCliM regional projections. As explained in Section 2.6.3 in the Literature review, the four GCMs used by NARCliM are CCCMA3.1, MIROC3.2, ECHAM5 and CSIRO-Mk3.0 (Evans et al., 2014).

The results in Section 10.2 showed that bias corrected NARCliM GCMs were capable of reproducing the observed mean and coefficient of variation (C_v) of the rainfall better than uncorrected RCMs. In contrast, both uncorrected and bias corrected NARCliM GCMs, particularly CSIRO-Mk3.0, ECHAM5 and MIROC3.2 were not capable of reproducing the lag-1 autocorrelation and spatial correlations of the observed rainfall. Therefore, when assessing the future rainfall change, the mean and coefficient of variation (C_v) of the rainfall are the statistics that are more likely to be correctly represented in future projections of NARCliM. Using this argument, the future rainfall change was primarily assessed using two statistics; mean and C_v of the rainfall.

The change in the mean annual rainfall and the C_v for mean monthly rainfall are presented. The NARCliM RCMs were best at reproducing the observed C_v (AWAP) at fortnightly and monthly time resolutions. Therefore, the aggregated monthly

rainfall time series were used in the analysis. The change of the rainfall was assessed from 2009 to 2079 using NARCliM's current (1990-2009, referred to as 2000) and far future (2060-2079, referred to as 2070) bias corrected projections. The analysis was performed at the same four sites of the broader east coast: Williams River, Richmond River, Bega River and Sydney sites.

Additionally, a preliminary analysis on the future change of autocorrelations and spatial correlation relative to the current climate was also evaluated. Note that this analysis was performed only at the Williams River site, and the GCM simulations used are bias corrected.

13.2 Changes in mean annual rainfall

Figure 13.1 shows the percentage change in the mean annual rainfall simulated by GCMs for 2070 relative to 2000 at the Williams River site. The mean annual rainfall of the Williams River site is predicted to change by -14% to 51% by 2070. The Williams River site is projected to have significant increases in rainfall using CCCMA3.1 and MIROC3.2 GCMs while using CSIRO-Mk3.0 a decrease is projected. In contrast, ECHAM5 projects a combination of increases and decreases.

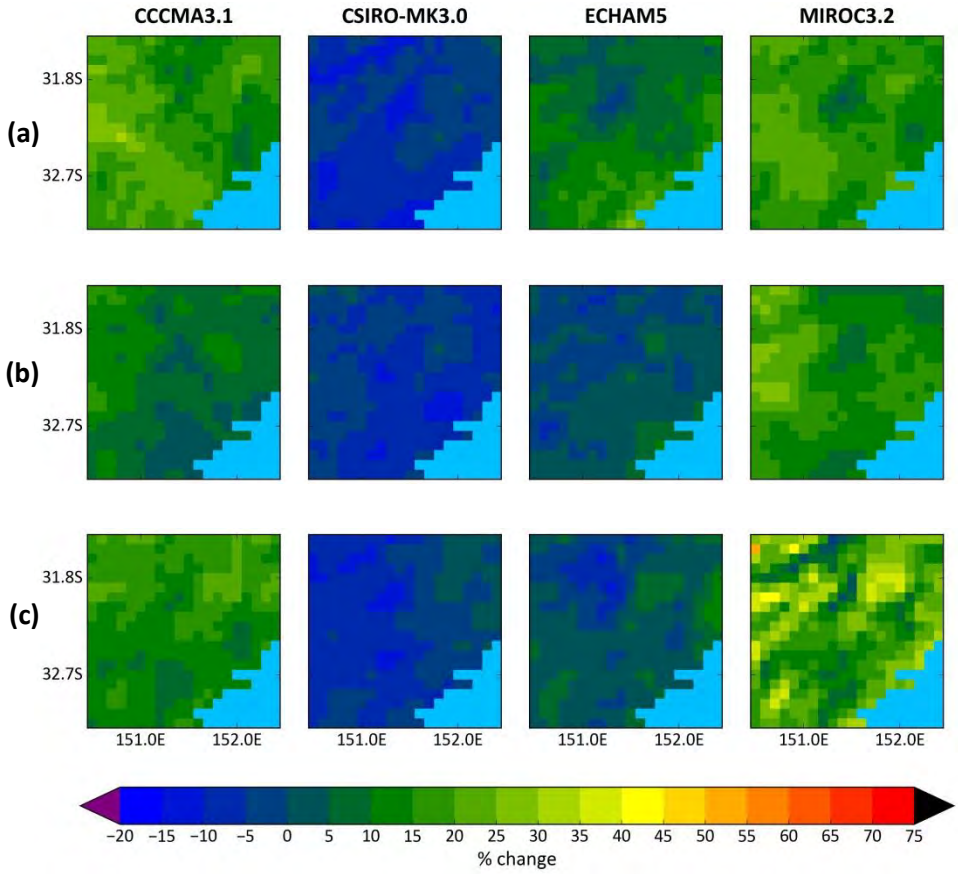

Figure 13.1 Percent change in mean annual rainfall for 2070 relative to 2000 at the Williams River site. (a) R1, (b) R2, and (c) R3 RCM.

There are slight differences between the results of the same GCM depending on its underlying RCM model configuration. For example, R1-ECHAM5 projects up to 25% increase in the rainfall in the Williams River site while R2- and R3-ECHAM5 show a change in rainfall from -15-10%. These discrepancies in the consistency of the individual GCMs can also be seen in the projections of CCCMA3.1 and MIROC3.2, though they tend to project increased rainfall; R2- CCCMA3.1 projects up to 5% decrease in the rainfall while R3-MIROC3.2 changes by -5 to 50%. However, CSIRO-Mk3.0 projects a decrease in the rainfall for all three model configurations for almost all grid points (except 5% increase in the rainfall shown for R3-CSIRO-Mk3.0 at few grid points located to the east) of the Williams River site.

Figure 13.2 shows the percentage change in the mean annual rainfall simulated by GCMs for 2070 relative to 2000 at the Richmond River site. Compared with Williams River site, there is a similarity in the GCM projections with CCCMA3.1 and MIROC3.2 GCMs projecting an increase of rainfall, with CSIRO-Mk3.0 projecting a decrease. However, R3-MIROC3.2 projects significant increases in the rainfall mostly along the Great Dividing Range (up to 55%) and along the northern coast (up to 70% from Byron Bay to Coffs Harbour) of the Richmond River site.

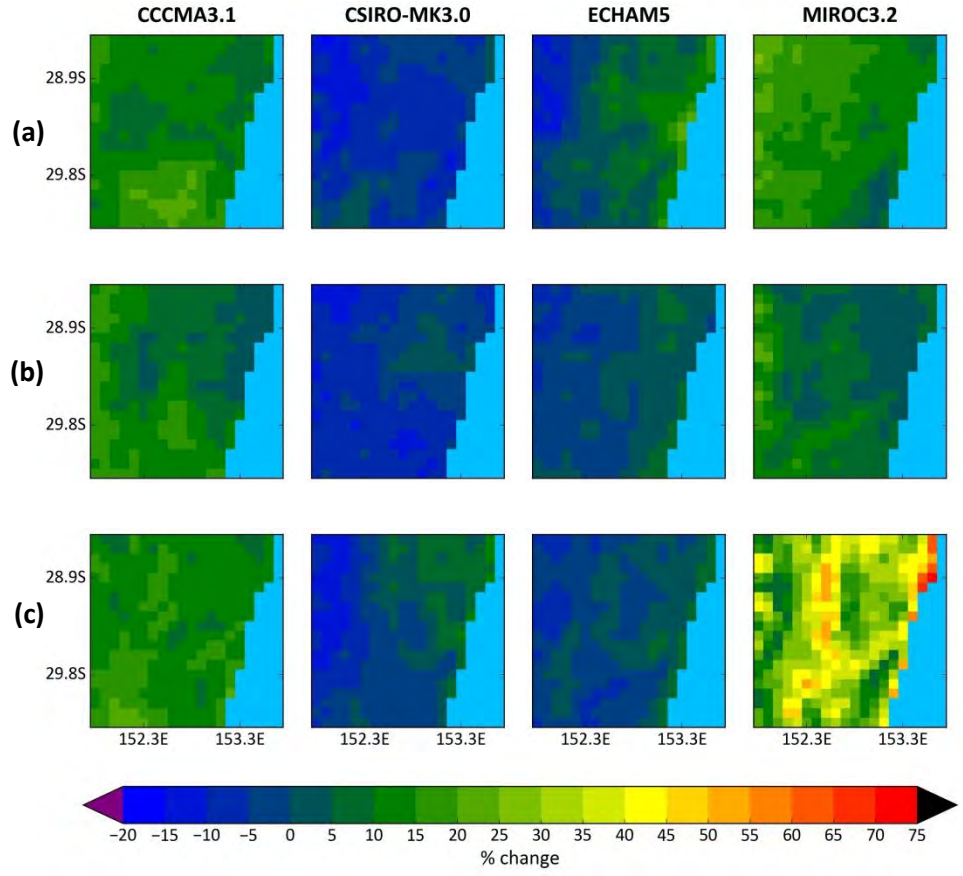

Figure 13.2 Percent change in mean annual rainfall for 2070 relative to 2000 at the Richmond River site. (a) R1, (b) R2, and (c) R3 RCM.

The percentage change in the mean annual rainfall simulated by GCMs for 2070 relative to 2000 at the Bega River site is shown in Figure 13.3. The Bega River site is projected to experience decreases of the rainfall by 2070 relative to 2000. R2-CSIRO-Mk3.0, R3-CSIRO-Mk3.0 and R3-CCCMA3.1 all project decreases in the rainfall for most of the site, while all other GCMs, except R1-CCCMA3.1 and R2-ECHAM projecting a decrease only in mountainous regions (Australian Alps)

located from north to south-west across the centre of the site. The 30% decrease in the rainfall (shown in purple) projected by R3-MIROC3.2 along the Australian Alps is significantly different to the other projections.

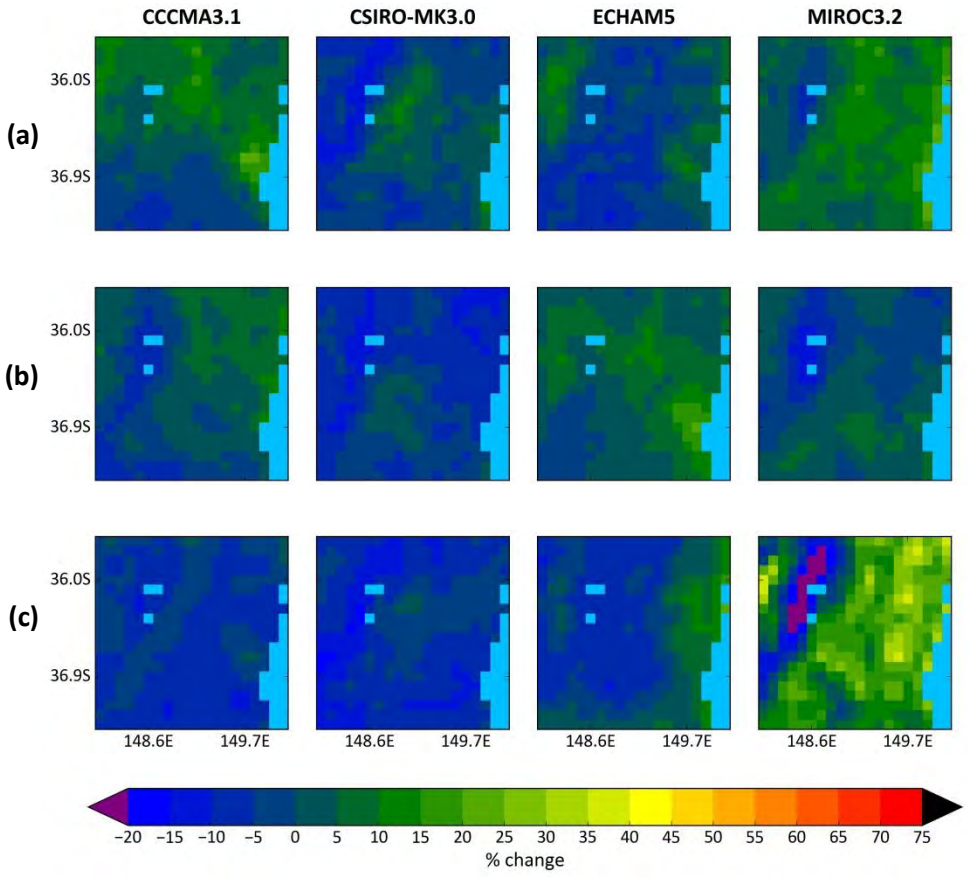

Figure 13.3 Percent change in mean annual rainfall for 2070 relative to 2000 at the Bega River site. (a) R1, (b) R2, and (c) R3 RCM.

CCCMA3.1 (R1 and R2), ECHAM5 (all configurations) and MIROC3.2 (R1 and R3) all project an increase of the rainfall (up to a maximum of 40%) particularly along the coast.

Figure 13.4 shows the mean rainfall projections for the Sydney site. Similar to the Williams River site, the rainfall of the Sydney site is also likely to vary from -14% to 54% and tends to follow similar trends to the other sites in the change of the rainfall; CSIRO-Mk3.0 (all three RCM configurations) mostly projects decreases of the mean annual rainfall while CCCMA3.1 (R1 and R2) and MIROC3.2 (R1 and R3) project

increases. All GCMs, except CSIRO-Mk3.0 project an increase of the rainfall along the south coast of NSW (from central coast to Narooma).

Overall, the assessment performed at all four sites reveals that -19% to 54% (averages of maximums for all sites) projected change in the mean annual rainfall can be expected across the broader east coast by 2070. Particularly, the increase in mean annual rainfall along the coastline (Sydney, central coast and Illawarra) is consistent with Ji et al. (2013). CSIRO-Mk3.0 generally projects decreases of the rainfall for all sites, while CCCMA3.1 and MIROC3.2 project increases. The ECHAM5 GCM also tends to project more decreases than increases.

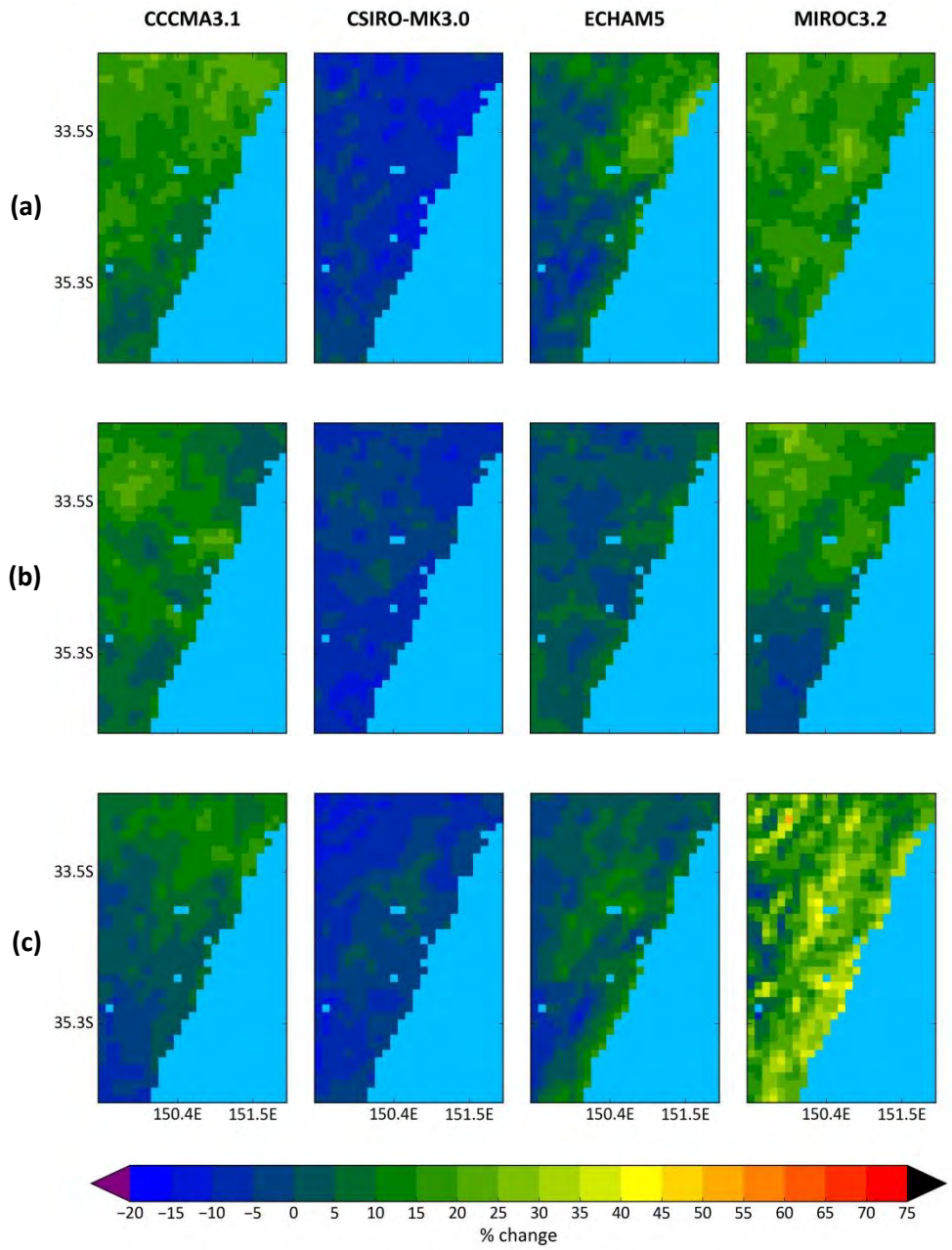

Figure 13.4 Percent change in mean annual rainfall for 2070 relative to 2000 at the Sydney site. (a) R1, (b) R2, and (c) R3 RCM.

13.3 Changes in the rainfall variability (C_v)

Projected changes in the temporal rainfall variability at the monthly time resolution are investigated in this section. The change in the C_v of rainfall for 2070 relative to 2000 at the Williams River site is shown in Figure 13.5. The figure indicates that the monthly rainfall C_v is likely to vary from -17% to 38% by 2070 in this region. According to the results of CSIRO-Mk3.0 and ECHAM5 GCMs, the Williams River

site is projected to have an increased rainfall C_v across the entire site. The increase in the projected rainfall C_v (0 to 30%) is more significant in CSIRO-Mk3.0 than ECHAM5. The MIROC3.2 GCM (all RCM configurations) projects both decreases and increases in the rainfall variability, varying across the site, with more decreases at grid points which are located in the north-east of the site. The R2-CCCMA3.1 projects decreased rainfall C_v across most of the site, while R1- CCCMA3.1 and R3-CCCMA3.1 project increased C_v across most of the site.

Noticeably, the decreasing trend in rainfall shown in Figure 13.1 seems to be accompanied with an increase in rainfall C_v and the decreases in C_v (the purple regions in Figure 13.5) only occur in areas of increasing rainfall.

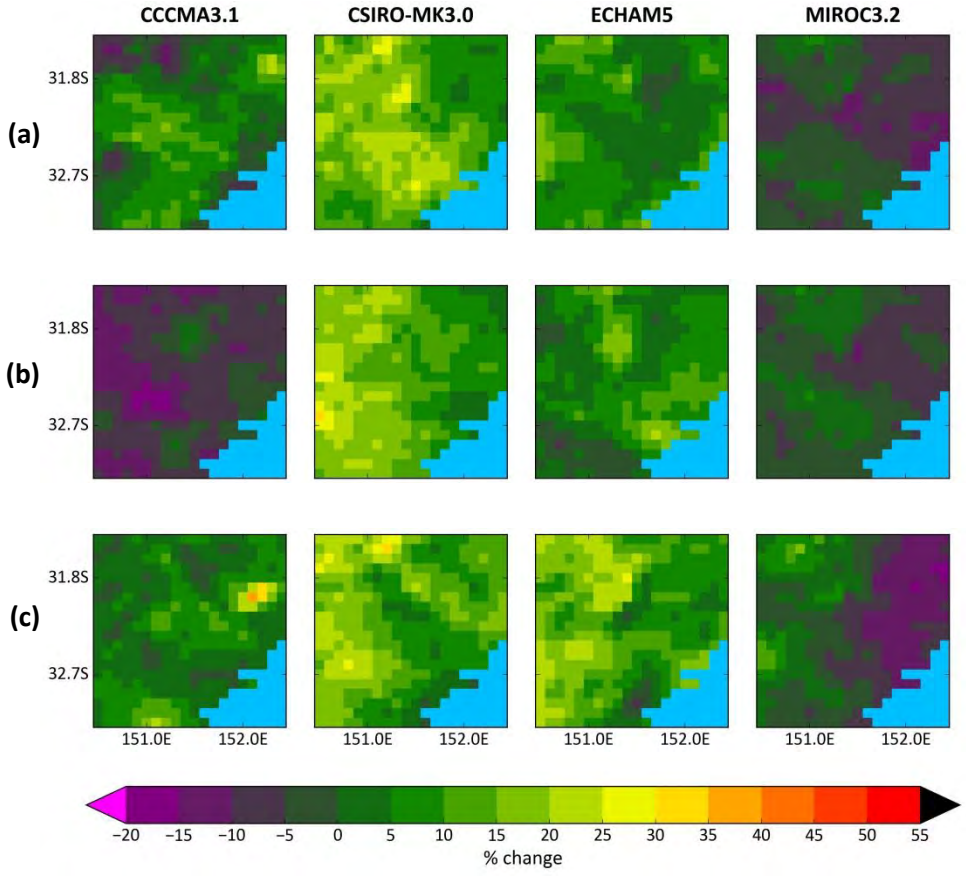

Figure 13.5 Percent change in C_v for 2070 relative to 2000 at the Williams River site. (a) R1, (b) R2, and (c) R3 RCM.

The change in the C_v of rainfall for 2070 relative to 2000 at the Richmond River site is shown in Figure 13.6. As for the Williams River site, the Richmond River site is projected to have significant increases in the rainfall C_v by all three configurations of CSIRO-Mk3.0 and ECHAM5 GCMs, while MIROC3.2 and CCCMA3.1 (R1 and R2) generally project more decreases than increases. In contrast to the results for the Williams River site, ECHAM5 projects greater increases in magnitudes (0 to 30%) across the site than CSIRO-Mk3.0. As for the Williams River catchment, regions with reduced rainfall C_v have a higher mean rainfall and vice versa.

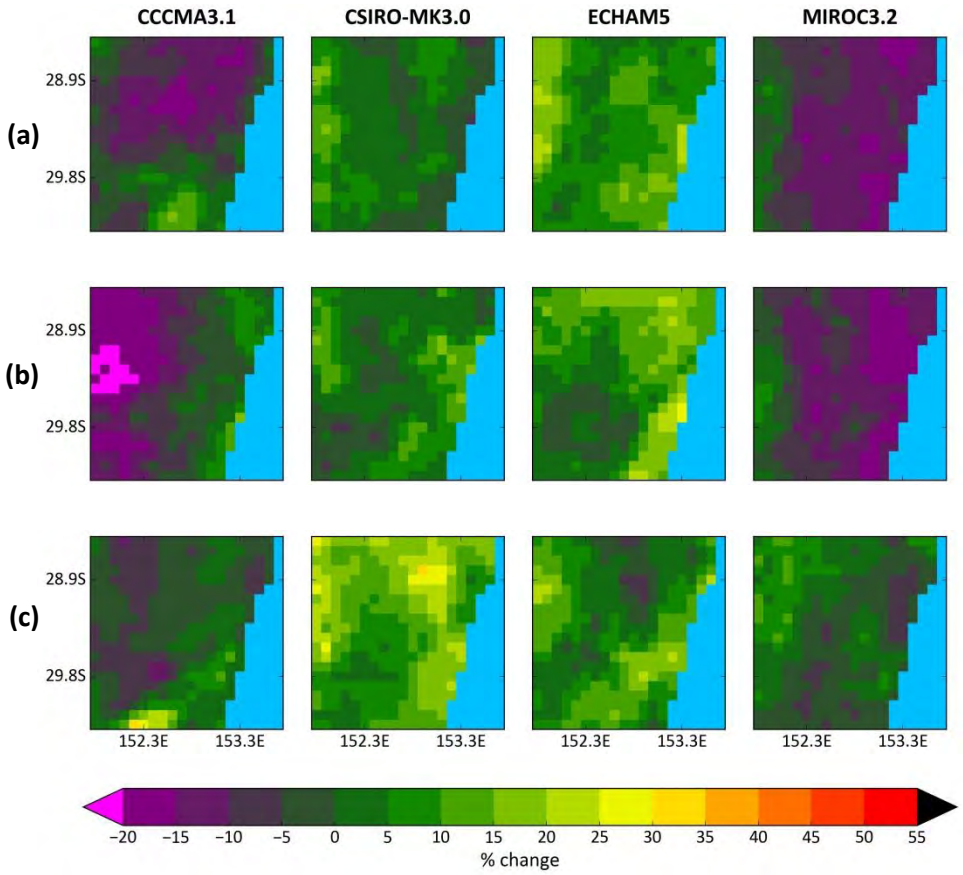

Figure 13.6 Percent change in C_v for 2070 relative to 2000 at the Richmond River site. (a) R1, (b) R2, and (c) R3 RCM.

Figure 13.7 shows the rainfall variability trends for the Bega River site. The projected changes in C_v varying from -19% to 54% indicate that Bega River site will experience increases in the rainfall C_v by 2070 across the site (i.e. individual GCMs have more grid points with increased C_v) in contrast with the Williams and Richmond River sites. R1- and R3-ECHAM5 project a considerable increase in the

rainfall C_v with R3-ECHAM5 projecting up to a 54% increase. Additionally, there is a significant decrease in the rainfall C_v for the Australian Alps which is projected only by the three RCM configurations of MIROC3.2. In the Australian Alps regions, these reductions in rainfall C_v are also accompanied by a reduction in mean annual rainfall.

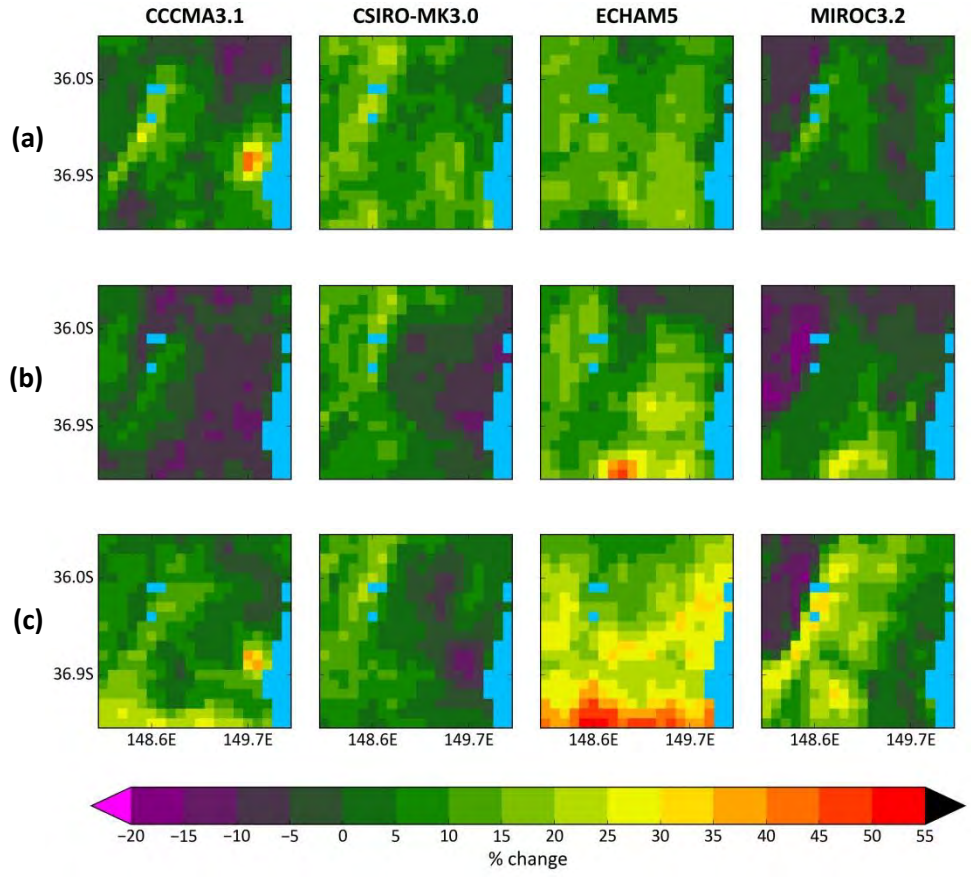

Figure 13.7 Percent change in C_v for 2070 relative to 2000 at the Bega River site. (a) R1, (b) R2, and (c) R3 RCM.

Figure 13.8 shows the rainfall C_v trends for the Sydney site. As for the Williams River site, the rainfall C_v of the Sydney site is also likely to vary from -18% to 37%, with CSIRO-Mk3.0 (all three RCM configurations) mostly projecting increases of the monthly rainfall C_v and CCCMA3.1 (R1 and R2) and MIROC3.2 (all configurations) projecting decreases.

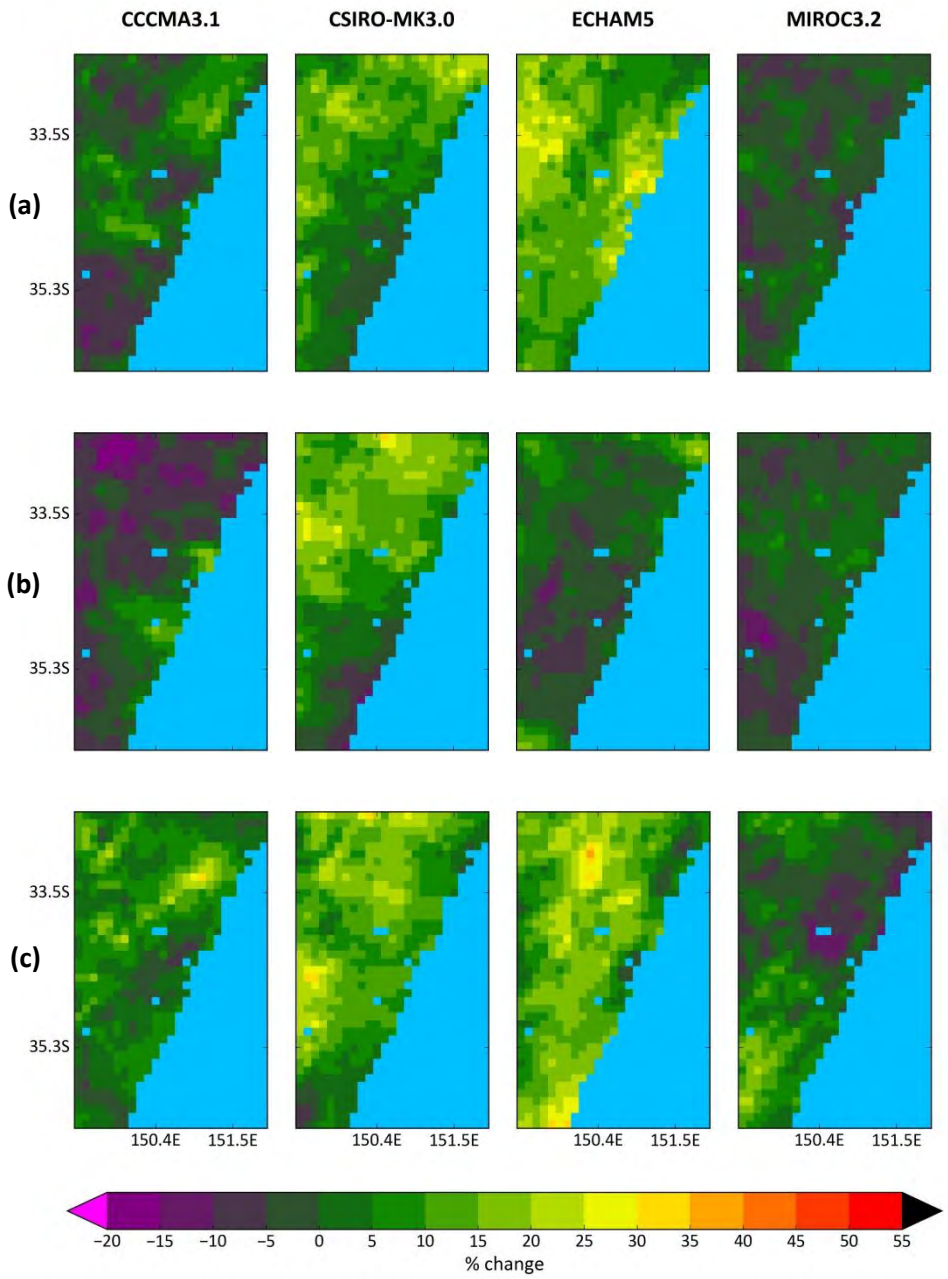

Figure 13.8 Percent change in C_v for 2070 relative to 2000 at the Sydney site. (a) R1, (b) R2, and (c) R3 RCM.

The overall conclusions from the four sites are that in general, the occurrence of an increased or decreased in coefficient of variation does not have any consistent spatial pattern between the site as well as GCMs. As was the case for the mean rainfall, there is no general trend that the rainfall variability with distance from the coast, because at the Williams River site the coefficient of variation of the CSIRO-Mk3.0 GCM increases more inland than at the coast while this trend is inverted for the

Sydney site. Moreover, the negative correlation of rainfall coefficient of variation with mean rainfall seen at the other sites is less clear at the Sydney site.

13.4 Changes in autocorrelation and spatial correlation of rainfall

13.4.1 Autocorrelation

The change in the lag-1 correlation of monthly rainfall for 2070 relative to 2000 at the Williams River site is shown in Figure 13.9. As for the CSIRO-Mk3.0 and MIROC3.2 GCMs, the monthly lag-1 correlation is likely to vary from -40% to 40% by 2070 for most of the region.

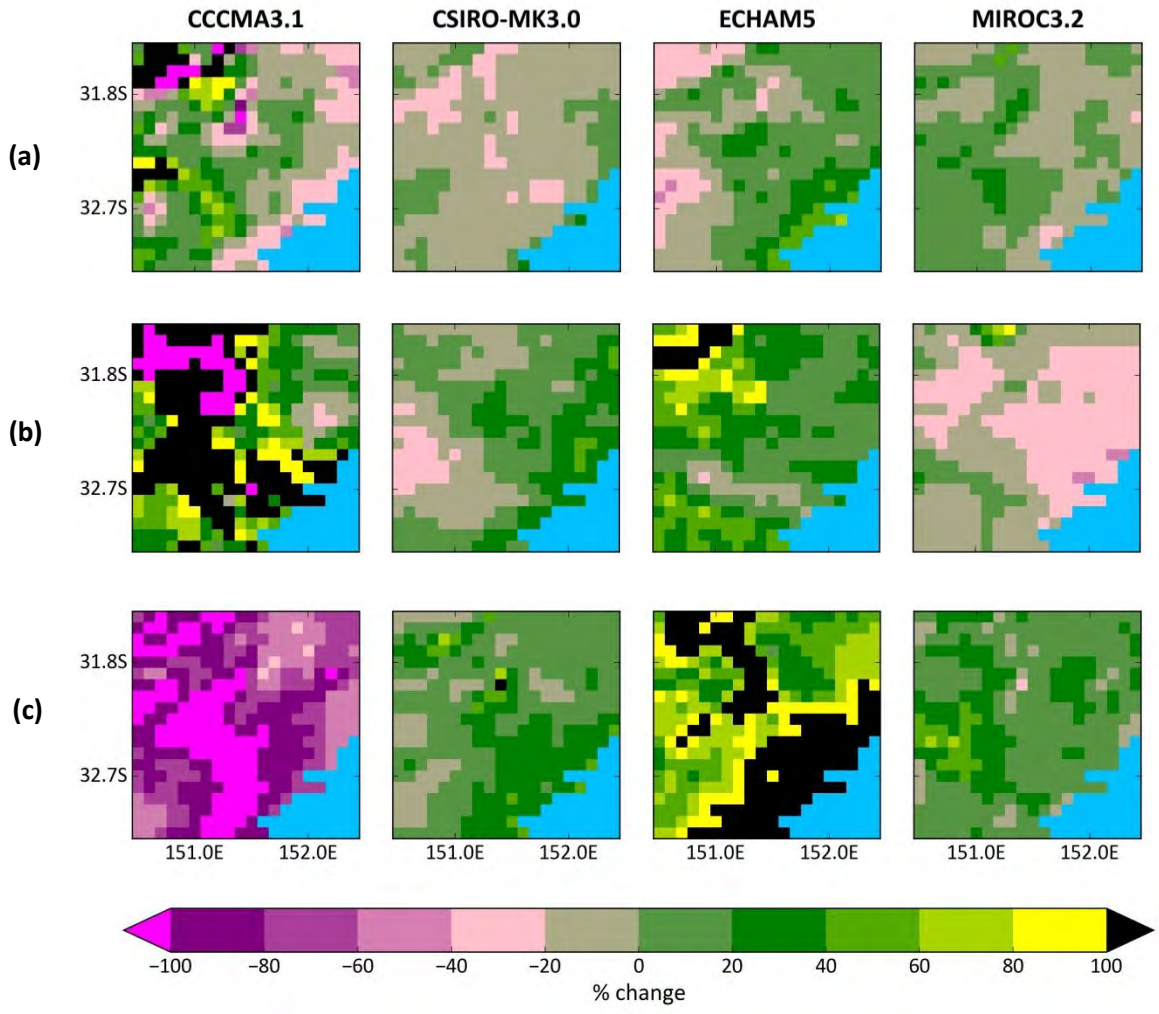

Figure 13.9 Percent change in lag-1 correlation (monthly) for 2070 relative to 2000 at the Williams River site. (a) R1, (b) R2, and (c) R3 RCM.

CSIRO-Mk3.0 and MIROC3.2 GCMs, R1-ECHAM5 all show similar results. R2- and R3-ECHAM5 have increases of up to 100% for some regions in the site. In contrast, results for CCCMA3.1 indicate that monthly lag-1 correlation at the Williams River site is likely to vary from -100% to 100%, with R3 projecting more decreases than R1 and R2.

However, this changing nature of either largely increasing or decreasing the magnitudes of lag-1 correlation of CCCMA3.1 can consistently be seen in Figure 13.10, which shows the autocorrelations calculated for up to 60 lags for the monthly rainfall of CCCMA3.1 RCM for current (2000) and future (2070) periods at a single grid point (grid point A, see Figure 4.1) at the Williams River site.

Similarly, monthly autocorrelations for CSIRO-Mk3.0, ECHAM5 and MIROC3.2 GCMs are shown in Figures 13.11 to 13.13. As for the lag-1 correlations, the difference between the autocorrelations (1< lags < 60) for current and future periods is small for CSIRO-Mk3.0 and MIROC3.2 GCMs. ECHAM5 projects more increases than decreases for the future.

However in all cases the changes in the autocorrelation are small.

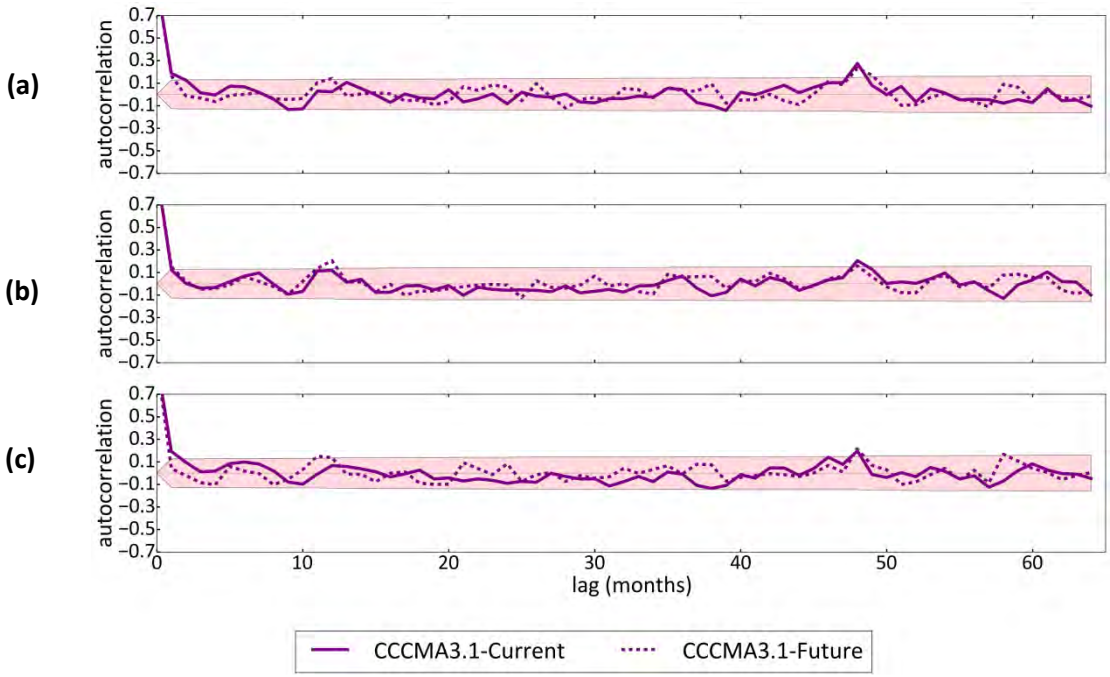

Figure 13.10 Monthly autocorrelations for the CCCMA3.1 GCM for current (2000) and future (2070) periods at grid point A - Williams River site. (a) R1, (b) R2, and (c) R3 RCM.

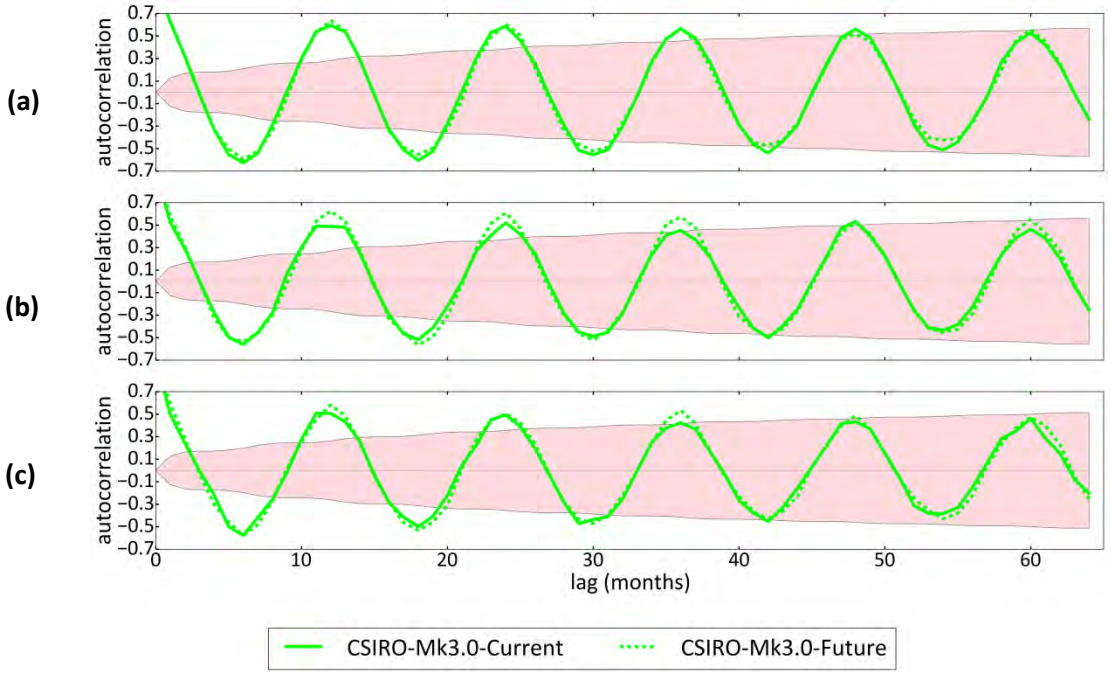

Figure 13.11 Monthly autocorrelations for the CSIRO-Mk3.0 GCM for current (2000) and future (2070) periods at grid point A - Williams River site. (a) R1, (b) R2, and (c) R3 RCM.

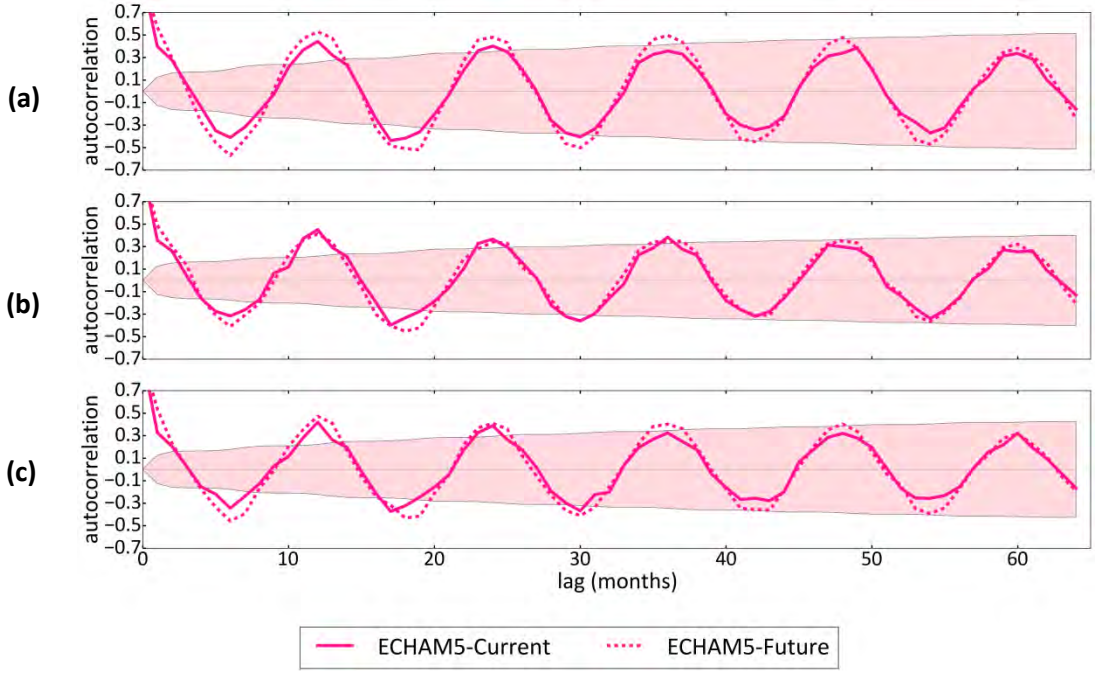

Figure 13.12 Monthly autocorrelations for the ECHAM5 GCM for current (2000) and future (2070) periods at grid point A - Williams River site. (a) R1, (b) R2, and (c) R3 RCM.

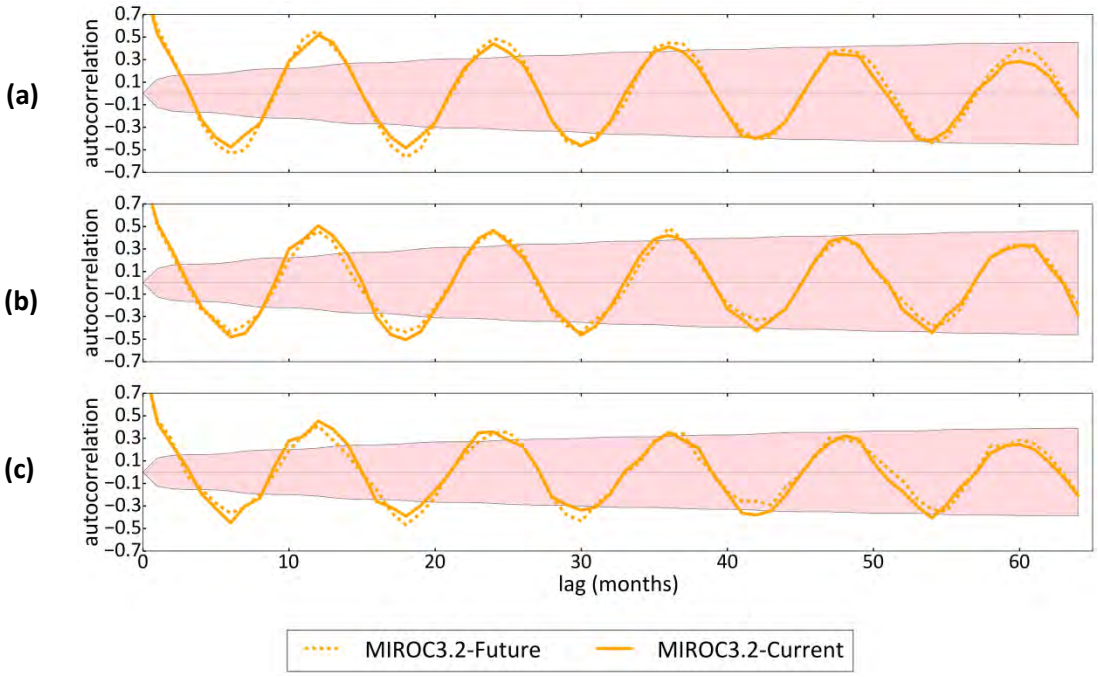

Figure 13.13 Monthly autocorrelations for the MIROC3.2 GCM for current (2000) and future (2070) periods at grid point A - Williams River site. (a) R1, (b) R2, and (c) R3 RCM.

13.4.2 Spatial correlation

Spatial correlations functions for current (2000) and future (2070) periods for R1-CCCMA3.1, R1-CSIRO-Mk3.0, R1-ECHAM5 and R1-ECHAM5 for the high elevation reference of Williams River site (see Table 4.2 and Figure 4.5) are shown in Figure 13.14. Similarly, the results for the R2 and R3 GCMs are shown in Figure 13.15 and Figure 13.16 respectively.

Figures 13.14 to 13.16 indicate that all GCMs, except R1-CSIRO-Mk3.0, R3-CCCMA3.1 and R3-ECHAM5 tend to produce slight increases in the spatial correlation of the rainfall by 2070. However compared with general trends in the exponential fitted curves, the difference between the spatial correlations for current and future time periods are small for all GCMs and they mostly remain unchanged. Therefore, as for the autocorrelations (for $1 < \text{lags} < 60$), there is no significant change in the spatial correlation of the rainfall by 2070.

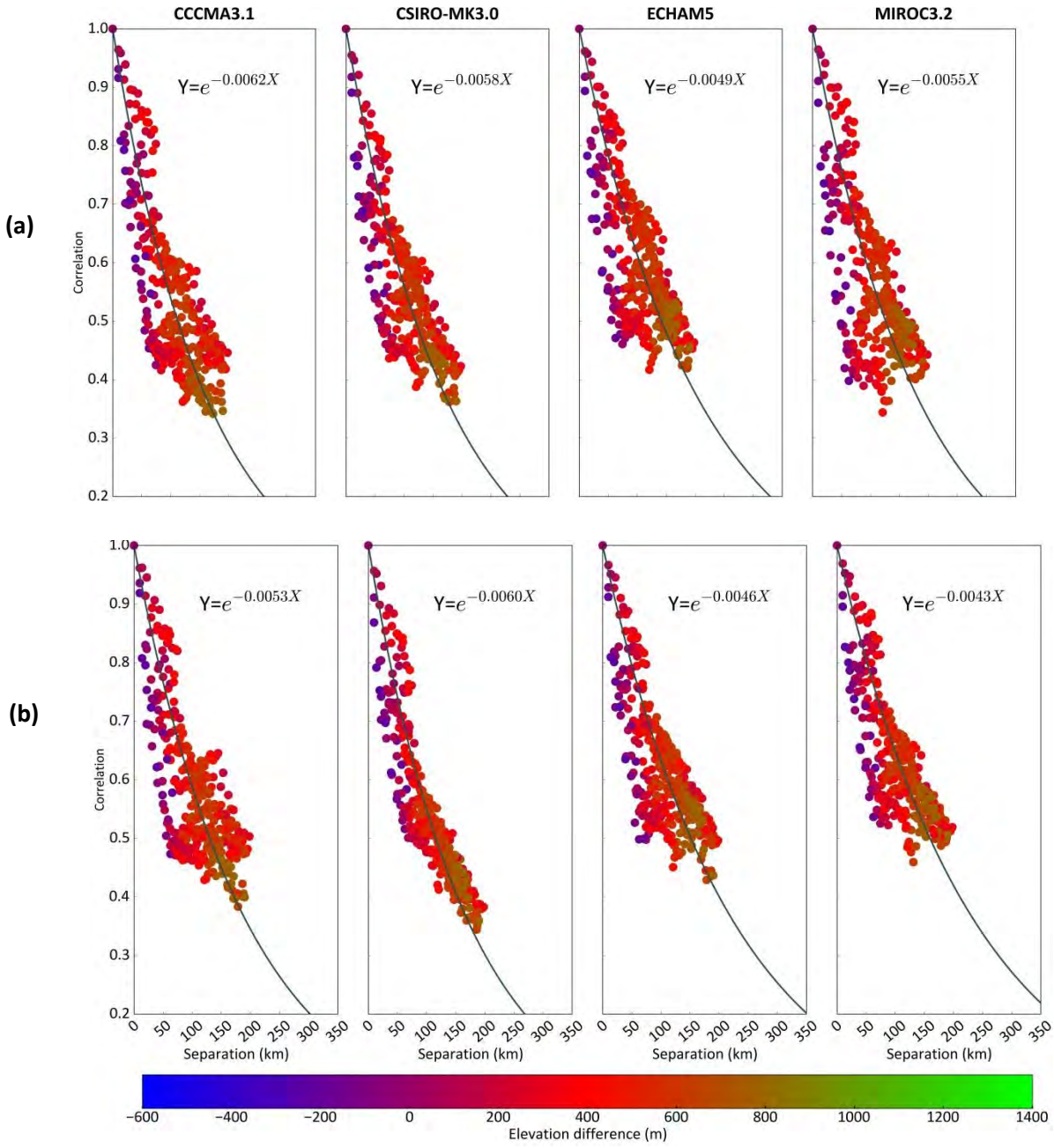

Figure 13.14 Spatial correlations function for current (2000) and future (2070) periods for the Williams River site. The reference is W17 high elevation grid point. The plots are for the bias corrected GCM simulations of R1 RCM. (a) Current and (b) future.

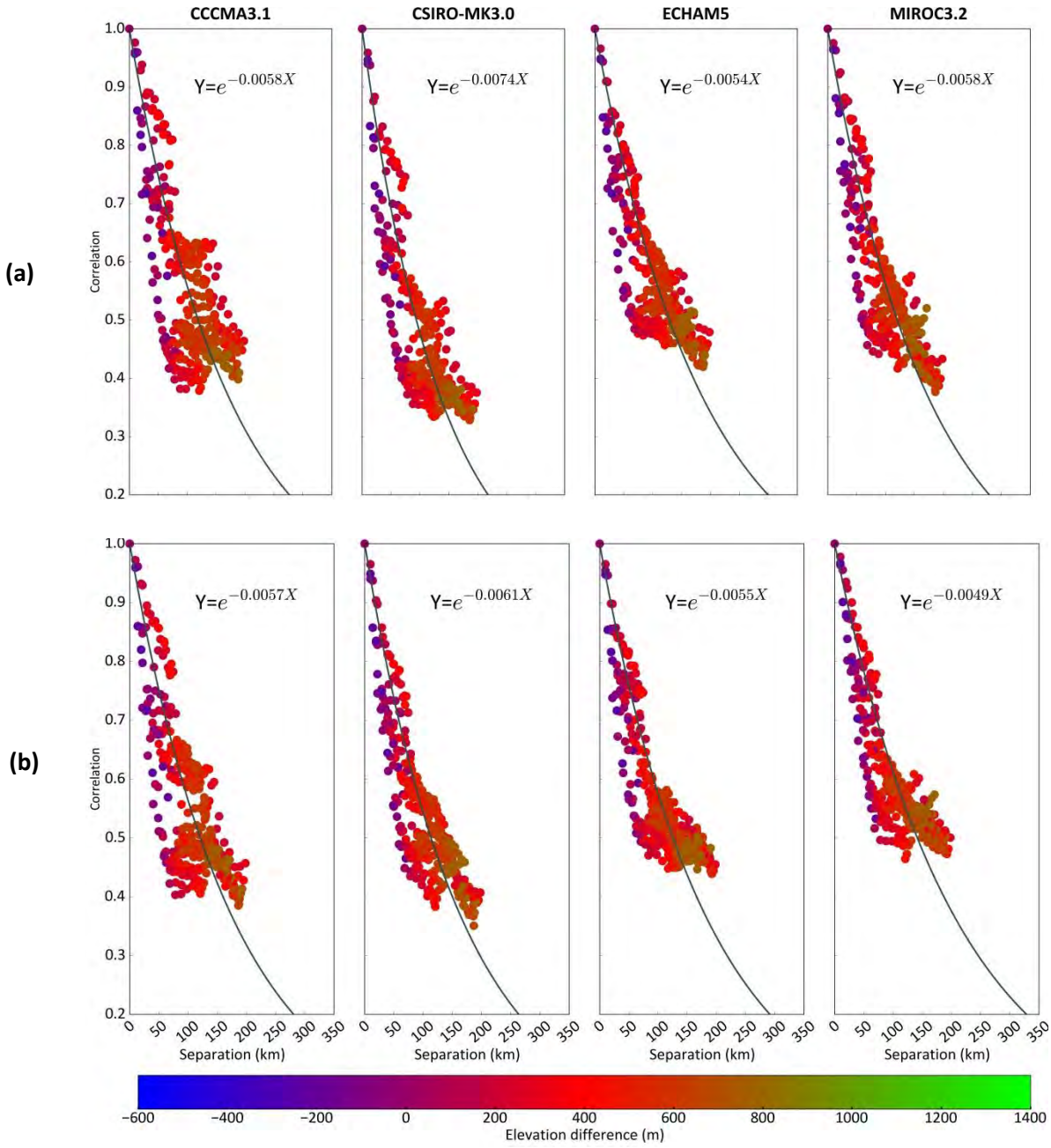

Figure 13.15 Spatial correlations function for current (2000) and future (2070) periods for the Williams River site. The reference is W17 high elevation grid point. The plots are for the bias corrected GCM simulations of R2 RCM. (a) Current and (b) future.

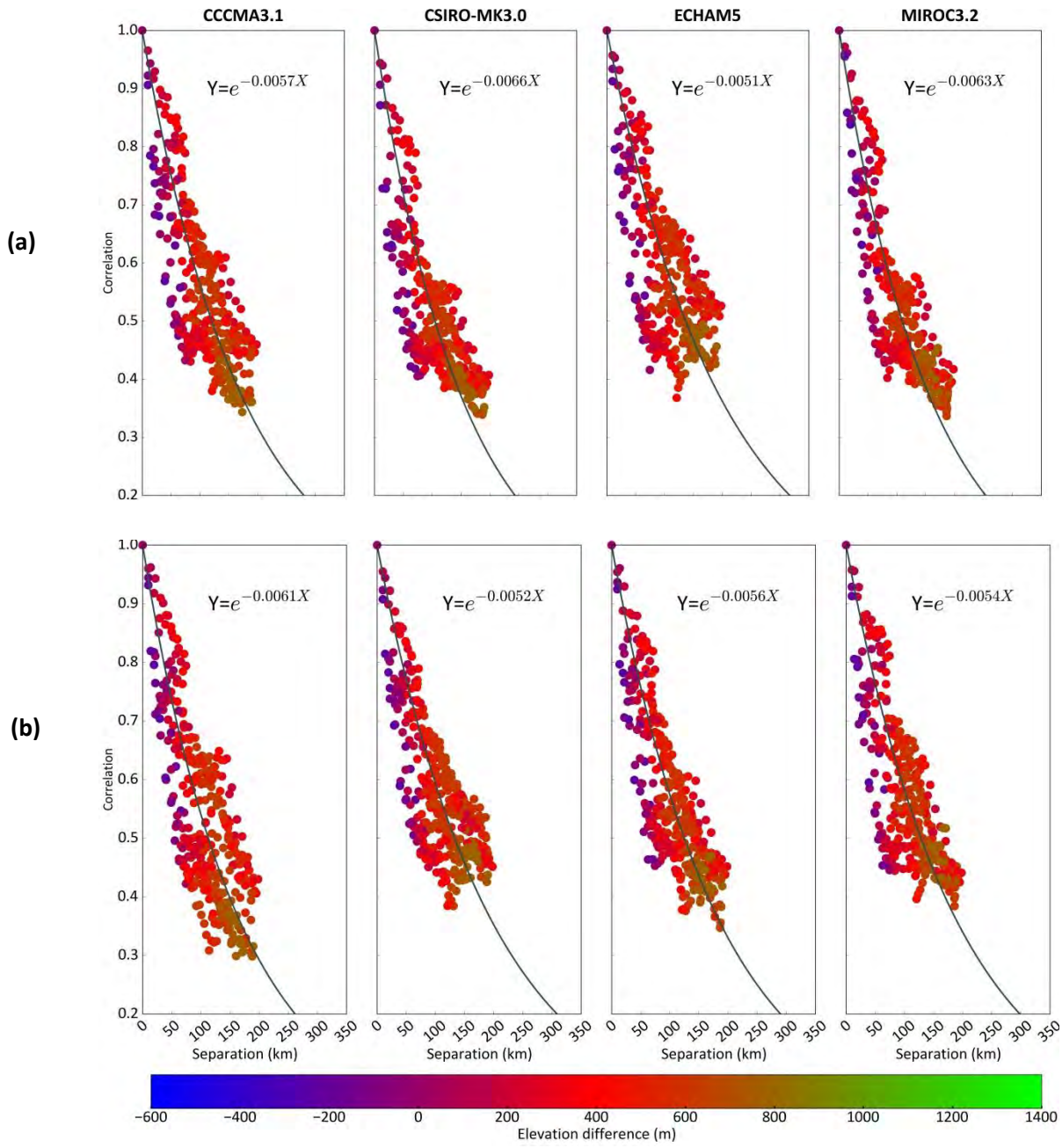

Figure 13.16 Spatial correlations function for current (2000) and future (2070) periods for the Williams River site. The reference is W17 high elevation grid point. The plots are for the bias corrected GCM simulations of R3 RCM. (a) Current and (b) future.

13.5 Conclusions

Overall, the assessment performed at all four sites reveals that -19% to 54% (averages of maximums and minimums for all sites) projected change in the mean rainfall can be expected across the broader east coast by 2070. These results match with the future rainfall projections by other organizations such as CSIRO and BOM (CSIRO and BoM, 2007). The lowest change for an individual site, -30% is for the Bega River site, while the highest 70% is for the Richmond River site. The rainfall is most likely to decrease in the future at the Bega River site at which has the most contrasting topography relative to other sites. CSIRO-Mk3.0 generally projects decreases of the rainfall for all sites, while CCCMA3.1 and MIROC3.2 project increases. The ECHAM5 GCM also tends to project more decreases than increases for the far future. All GCMs, except CSIRO-Mk3.0 project precipitation increases along the coast and this suggests that coastal regions will experience more rainfall in the future than the present-day.

The change in the monthly rainfall coefficient of variation (C_v) was also assessed. The results suggest that there will be -19% to 40% (averages of maximums and minimums for all sites) change in the monthly rainfall C_v across the coastal sites by 2070. CSIRO-Mk3.0 and ECAHM5 tend to project increases of the rainfall C_v across the sites, while CCCMA3.1 and MIROC3.2 projecting either increases or decreases. In contrast to the changes in the mean annual rainfall, there is no general trend that the rainfall C_v is to increase along the coast more than inland. However, there is a general trend that regions with reduced rainfall C_v have a higher mean rainfall and vice versa for all sites, except for Sydney.

The change in the lag-1 correlation of the rainfall was also evaluated, but only for the Williams River site. The results suggest that monthly lag-1 correlation is likely to vary from -40% to 40% by 2070 for most of the region but there is non systematic trend. A preliminary investigation based on autocorrelations (for lags greater than 1) and spatial correlation of the rainfall reveal that difference between the correlations for current and future simulations is small and therefore, the correlations will likely remain almost unchanged by 2070.

Section 3

Overall NARCliM assessment

This section presents key insights, conclusions and recommendations of the results in Section 1 and Section 2.

The key focus of this section is to compare the ability of NARCliM RCM rainfall (reanalysis and GCMs driven) to reproduce the observed statistics of the rainfall, particularly those are important for hydrology predictions and reservoir performance along the east coast of NSW for two different epochs: 1990-2009(20 years) and 1950-2009 (60 years). A detailed comparison between the model performances reveals insights on the suitability and limitations of these RCMs for use in hydrologic applications. Additionally comparing the results generated for the uncorrected and bias corrected RCMs, the differences caused by the bias correction are also investigated.

The section comprises of two chapters: (1) Chapter 14: synthesis on the performance of NARCliM RCM data, and (2) Chapter 15: conclusions.

Chapter 14
Synthesis

14.1 Introduction

The ability of NARCliM RCM simulations to capture observed rainfall statistics was evaluated using different statistical methods and approaches, focusing on the use of these datasets in water security applications, particularly the use of these datasets to estimate the runoff at a catchment, throughout this thesis. The results showed that there are discrepancies between the performances of NARCliM RCMs showing that some RCMs perform best at capturing one type of statistic such as probability distribution of the rainfall while others are better able to capture a different statistic of the observed rainfall. Therefore, this chapter summarises the differences between RCM performances in capturing the observed rainfall statistics. Additionally, to assess the overall performance of NARCliM along the broader east coast a cross-comparison between the sites is also presented.

14.2 Assessment of NARCliM RCMs current projections

Section 1 of this thesis compared the performance of the three reanalysis RCMs for the 60 year (1950-2009) epoch, while Section 2 compared the performance of all NARCliM GCM projections, including the three reanalysis, for the 20 year (1950-2009) epoch. The most capable NARCliM RCMs which best reproduce the observed rain gauge and AWAP statistics at four east coast sites are summarised and shown in Tables 14.1 to 14.7.

14.2.1 Probability distribution of the rainfall

The ability of NARCliM RCMs to reproduce the cumulative probability distribution of the mean annual rainfall of AWAP for all the grid points at a site was also evaluated. The NARCliM RCMs which closely capture the CDF of the mean rainfall of AWAP at each site are shown in Table 14.1. The spatial variability of the mean annual rainfall at each site is summarised in Section 14.2.2.1.

Table 14.1 The most capable NARCliM RCMs to capture the cumulative probability distribution of the mean annual rainfall of AWAP

	Williams River site	Richmond River site	Bega River site	Sydney Site
60 year epoch	R2 reanalysis	R2 reanalysis	R2 reanalysis	R2 reanalysis
	1-R2 reanalysis 25% -U	1-R2 reanalysis 25% -U	1-R2 reanalysis 25% -U	1-R2 reanalysis 25% -U
	2-R1 reanalysis 40% -U	2-R1 reanalysis 40% -U	2-R1 reanalysis 40% -U	2-R1 reanalysis 40% -U
	3-R3 reanalysis 50% -U	3-R3 reanalysis 50% U	3-R3 reanalysis 50% -U	3-R3 reanalysis 50% -U
20 year epoch	R2-ECHAM5	R3-CCCMA3.1	R1-CCCMA3.1	R2-ECHAM5
	1- ECHAM5 0-5% U	1-CCCMA3.1 0-5% - O	1-CCCMA3.1 0-5% - O	1- ECHAM5 0-5% U
	2-CCCMA3.1 20% - O	2- ECHAM5 20% U	2- ECHAM5 20% U	2-CCCMA3.1 20% - O
	3- CSIROMk-3.0 20% - U	3- CSIROMk-3.0 40% - U	3- CSIROMk-3.0 40% - U	3- CSIROMk-3.0 20% - U
	4-MIROC3.2 20% -U	3-MIROC3.2 40% -U	3-MIROC3.2 40% -U	4-MIROC3.2 20% -U
	5- reanalysis 30% - U	3- reanalysis 40% - U	3- reanalysis 40% - U	5- reanalysis 30% - U
60 year epoch: bias corrected	All reanalyses	All reanalyses	All reanalyses	All reanalyses
	All reanalyses with 0-10% -U	All reanalyses with 0-10% -U	All reanalyses with 0-10% -U	All reanalyses with 0-10% -U
20 year epoch: bias corrected	R3 CSIRO-Mk3.0	R1-CSIRO-Mk3.0	R2-MIROC3.2 and R2-CSIRO-Mk3.0	R2-MIROC3.2
	All RCMs with 5%-U/O	All RCMs with 5%-U/O	All RCMs with 5%-U/O	All RCMs with 5%-U/O

The numbers 1 to 5 followed by the RCM name indicate the rank of model performance. U and O indicate an under or overestimation of CDF of annual rainfall compared with AWAP.

The results suggest that there is a general trend of all uncorrected reanalyses for the 60 year epoch to underestimate the probabilities (by 25 to 50%) of the mean annual rainfall of AWAP at each site, particularly for the greatest rainfall values. R2 reanalysis tends to closely reproduce the CDF of AWAP for all the sites.

For the 20 year epoch, the uncorrected R2-ECHAM5 for the Williams River and Sydney sites and R1- and R3-CCCMA3.1 for the Bega and Richmond River sites tended to closely reproduce the CDF of mean annual rainfall, particularly for the occurrence of mean rainfall less than 850 mm of AWAP. R1- and R3-CSIRO-Mk3.0 and MIROC3.2 generally underestimated the probabilities (up to 20%) of the mean annual rainfall of AWAP. Compared with R1 and R3, the underestimation was less for R2-CSIRO-Mk3.0 and R2-MIROC3.2. In contrast, CCCMA3.1 RCMs tended to overestimate the CDF (10 to 5%) of AWAP for all three configurations at all the sites. The underestimation in the uncorrected 20 year reanalysis was slightly worse than the GCMs, suggesting that uncorrected GCM simulations better reproduced the mean CDF of AWAP than the uncorrected reanalysis for the 20 year time period for all sites.

After the bias correction, all RCMs for both the 20 and 60 year epoch tended to closely reproduce the CDF of AWAP overlapping almost 95 to 98% of AWAP's CDF. This shows the extent of improvement in the mean statistics of NARCliM RCMs after the bias correction.

NARCliM RCMs' ability to reproduce the AWAP daily rainfall probability distributions for single grid points was evaluated for all four sites. The NARCliM RCMs which most closely reproduced the AWAP daily probability distribution at each site are shown in Table 14.2. As explained in Section 6.2, the uncorrected and bias corrected reanalyses are only reliable for the midsize to large rainfall events (rainfall greater than 1.5 mm) so the comparison in Table 14.2 was constrained to that particular range.

Table 14.2 The most capable NARCliM RCMs to capture the AWAP daily probability distributions (results are only for the midsized to large rainfall events)

	Elevation	Williams River site	Richmond River site	Bega River site	Sydney Site
60 year epoch	low	R2 reanalysis	R2 reanalysis	R2 reanalysis	R2 reanalysis
		1-R2 reanalysis 10% -O 2-R1 reanalysis 30% -O 3-R3 reanalysis 30% -O	1-R2 reanalysis 10% -O 2-R1 reanalysis 30% -O 3-R3 reanalysis 30% -O	1-R2 reanalysis 10% -O 2-R1 reanalysis 30% -O 3-R3 reanalysis 30% -O	1-R2 reanalysis 10% -O 2-R1 reanalysis 20% -O 3-R3 reanalysis 20% -O
	high	None	None	None	None
		All reanalyses 30% or more -U	All reanalyses 30% or more -U	All reanalyses 30% or more -U	All reanalyses 30% or more -U
20 year epoch	low	R2-ECHAM5 and R2-MIROC	R2-CCCMA3.1	R2-CSIRO-Mk3.0 and R2-ECAHM	R2-CSIRO-Mk3.0, ECHAM5 and MIROC3.2
		1- ECHAM5 0-5% U 2-MIROC3.2 5% -U 3-CCCMA3.1 10% - O 4- CSIROMk-3.0 25% - U 5- reanalysis 40% - U	1-CCCMA3.1 5% - O 2- ECHAM5 0-10% U/O 3-MIROC3.2 10-15% -U 4- CSIROMk-3.0 25% - U 5- reanalysis 40% - U	1- ECHAM5 0-5% U 2-CSIROMk-3.0 5-10% - U/O 3-MIROC3.2 5-10% -O 4-CCCMA3.1 10-20% - O 5- reanalysis 20-30% - U	1-CSIROMk-3.0 5-10% - U/O 2- ECHAM5 5-10% O 3-MIROC3.2 5-15% -O 4-CCCMA3.1 5-20% - O 5- reanalysis 20-30% - U
	high	R2 reanalysis	R2-CCCMA3.1	none	R3-CCCMA3.1
		1- reanalysis 5-30% - U 2- ECHAM5 0-40% U/O 3- CSIROMk-3.0 40% - U/O 4- CCCMA3.1 5 -40%- U/O 5- MIROC3.2 10-40% -U/O	1-CCCMA3.1 5% - O/U 2- ECHAM5 0-10% U/O 3-MIROC3.2 10-15% -U 4- CSIROMk-3.0 25% - U 5- reanalysis 40% - U	All GCMs 10-40%-U	1-CCCMA3.1 5% - U 2- ECHAM5 10-20% U 3-MIROC3.2 20-30% -U 4- CSIROMk-3.0 30-40% - U 5- reanalysis 40% - U
60 year epoch: bias corrected	low	R2 reanalysis	R2 reanalysis	R2 reanalysis	R2 reanalysis
		R2 reanalysis closely reproduces, and R1 and R3 reanalyses 0-10% -U/O	R2 reanalysis closely reproduces, and R1 and R3 reanalyses 0-10% -U/O	R2 reanalysis closely reproduces, and R1 and R3 reanalyse 0-10% -U/O	R2 reanalysis closely reproduces, and R1 and R3 reanalyses 0-10% -U/O
	high	R2 reanalysis	R2 reanalysis	R2 reanalysis	R2 reanalysis
		ditto as low elevation	ditto as low elevation	ditto as low elevation	ditto as low elevation
20 year epoch: bias corrected	low	R2 all simulations	R2 all simulations	R2 all simulations	R2 all simulations
		All RCMs with 5%-U/O	All RCMs with 5%-U/O	All RCMs with 5%-U/O	All RCMs with 5%-U/O
	high	R2 reanalysis	R2 all simulations	R2 all simulations	R2 all simulations
		All RCMs with 5%-U/O	All RCMs with 5%-U/O	All RCMs with 5%-U/O	All RCMs with 5%-U/O

The numbers 1 to 5 followed by the RCM name indicate the rank of model performance. U and O indicate an under or overestimation of CDF of annual rainfall compared with AWAP.

For low elevation grid points, all uncorrected reanalyses for 60 year epoch tended to underestimate the daily probability distribution of AWAP, particularly the midsized rainfall events (0.1 to 7 mm). R2 reanalysis was better able to capture the probabilities of AWAP midsized to large events (rainfall greater than 7 mm) than R1 and R3 reanalyses. At high elevation grid points, all three uncorrected reanalyses underestimated (30% or more) the daily rainfall probabilities of AWAP for all rainfall events. Therefore, none of the uncorrected reanalyses captured the daily rainfall probability distributions of AWAP at high elevations. There was no difference in the RCM performance between the sites.

For the 20 year epoch, uncorrected GCMs (R2-CSIRO-Mk3.0, R2-MIROC, R2-ECAM and R2-CCCMA3.1) tended to better capture the daily probabilities of the AWAP at low elevations than uncorrected R2 reanalysis. However, which RCM performed best along the broader east coast appears to be different for each site. At high elevations of Richmond River and Sydney sites, R2- and R3-CCCMA3.1 respectively appear to be the best RCMs and closely reproduced AWAP rainfall probabilities. At high elevations in the Williams River site, R2-reanalysis performed better than the GCMs. At the Bega site none of the RCMs captured the AWAP daily probabilities (underestimate up to 40%).

The bias corrected R2 reanalysis for the 60 year epoch tended to best capture the probabilities of midsized-to-high rainfall events of AWAP at all sites. Of bias the corrected RCMs for the 20 year epoch, all R2 RCMs reproduced the probabilities of low-to-high rainfall events (rainfall greater than 1.5 mm) of AWAP for all the grid points along the east coast, with small discripancies in the RCM performance. As mentioned earlier the probabilities of the light rainfall events (rainfall less than 1.5 mm) are not captured by any of the RCMs (neither for 20 nor 60 year epochs), because only a part of the daily probability function has been improved, and also there are artefacts caused by the bias correction.

Overall, the results suggest that the ability of NARCliM RCMs to capture the rainfall probabilities have been significantly improved with the bias correction. In particular, most of the systematic biases in the mean annual rainfall of uncorrected simulations have been removed as expected, by the bias correction. Compared with other RCMs, improvement in the CSIRO-Mk3.0 is most significant and this will be further

discussed in Section 14.2.2.1. With respect to the daily rainfall distributions, it is clear that daily probability distribution of midsized-to-high rainfall events of NARCliM RCMs' has only been improved while probability distribution of light rainfall events remains erroneous even after the bias correction. The improvement of the probability distribution after bias correction was true for all time resolutions from daily to annual, even the bias correction was only performed on the daily data.

14.2.2 Spatial variability of the rainfall statistics

In order to investigate the ability of NARCliM RCMs to reproduce the observed statistics, three types of statistics were calculated for every gridded rainfall series at each site along the east coast and tested against the AWAP rainfall. As catchments consist of multiple grid points, evaluation of the spatial variability and correlation between grid points using different statistics is important in determining the impact of rainfall averaging over a catchment. The statistics used were mean, coefficient of variation and lag-1 correlation of the rainfall.

14.2.2.1 Mean rainfall

The NARCliM RCMs which best reproduced the mean annual rainfall of AWAP at each site is shown in Table 14.3.

The uncorrected reanalyses for the 60 year epoch tended to overestimate the mean rainfall at all sites. In general, uncorrected reanalysis closely reproduced the mean rainfall (over or underestimation varies from 0 to 50%) of AWAP at low elevation grid points, but tended to overestimate, sometimes by more a factor of 2, the rainfall at higher elevations. A typical result was for the Merriwa site (not shown in Table 14.3, see Section 5.1.3) where uncorrected R2 reanalysis overestimated the AWAP rainfall by 250% while the overestimations by the uncorrected R1 and R3 reanalyses were 300 and 400% respectively. The spatial patterns of the mean annual rainfall for all reanalyses were similar to the spatial patterns from AWAP for all sites, except for the Richmond River site where the spatial pattern of mean annual rainfall did not follow the topography. Of all three reanalyses, R2 reanalysis had rainfall most similar to AWAP showing a ratio between the means varying from 0.5 to 1.5 for

over 60% of the grid points of each site. The remaining 40% of grid points have the greatest overestimated values varying from 1.5 to 2.5.

Table 14.3 The most capable NARCliM RCMs to capture the AWAP mean rainfall

	Williams River site	Richmond River site	Bega River site	Sydney Site
60 year epoch	R2 reanalysis	R2 reanalysis	R2 reanalysis	R2 reanalysis
	1-R2 reanalysis 0-250% -O, 50%-U	1-R2 reanalysis 0-250% -O, 50%-U	1-R2 reanalysis 0-250% -O, 50%-U	1-R2 reanalysis 0-250% -O, 50%-U
	2-R1 reanalysis 0-300% -O	2-R1 reanalysis 0-300% -O	2-R1 reanalysis 0-300% -O	2-R1 reanalysis 0-300% -O
	3-R3 reanalysis 0-400% -O	3-R3 reanalysis 0-400% -O	3-R3 reanalysis 0-400% -O	3-R3 reanalysis 0-400% -O
20 year epoch	R2-CCCMA3.1	R2-CCCMA3.1	R2-CCCMA3.1	R2-CCCMA3.1
	1-CCCMA3.1 50% - O/U	1-CCCMA3.1 50% - O/U	1-CCCMA3.1 50% - O/U	1-CCCMA3.1 50% - O/U
	2- ECHAM5 0-100% O	2- ECHAM5 0-100% O	2- ECHAM5 0-100% O	2- ECHAM5 0-100% O
	3-MIROC3.2 150% -O	3-MIROC3.2 150% -O	3-MIROC3.2 150% -O	3-MIROC3.2 150% -O
	4- CSIROMk-3.0 300% - O	4- CSIROMk-3.0 300% - O	4- reanalysis 300% - O	4- CSIROMk-3.0 300% - O
	5- reanalysis 400% - O	5- reanalysis 400% - O	5- CSIROMk-3.0 400% - O	5- reanalysis 400% - O
60 year epoch: bias corrected	All reanalyses	R2 and R3 reanalysis	All reanalyses	R1 and R2 reanalysis
	All reanalyses 0-50% O/U	R2 and R3 reanalyses 0-50% O/U R1 reanalysis 0-100%- O, 50%-U	All reanalyses 0-50% O/U	R1 and R2 reanalyses 0-50% O/U R3 reanalysis 0-100%- O, 50%-U
20 year epoch: bias corrected	CSIRO-Mk3.0 (R1,R2 and R3)	R2-CSIRO-Mk3.0	All GCMs (All RCMs except reanalysis)	All GCMs (All RCMs except reanalysis)
	1-CSIRO-Mk3.0 50% - O/U 2-All other RCMs 0-100% O	1-CSIRO-Mk3.0 50% - O/U 2-All other RCMs 0-100% O	1. All RCMs 0-50% O/U, except reanalysis (100% O)	1. All RCMs 0-50% O/U, except reanalysis (200% O)

The numbers 1 to 5 followed by the RCM name indicate the rank of model performance. U and O indicate an under or overestimation of mean annual rainfall compared with AWAP.

For the 20 year epoch, the uncorrected R2-CCCMA3.1 was the best RCM at reproducing both magnitude and the spatial pattern in mean rainfall of AWAP, though there was a slight underestimation of the rainfall at some grid points of the sites studied. All other RCMs overestimated the mean rainfall of AWAP. The overestimation in the CSIRO-Mk3.0 and reanalysis RCMs was relatively higher (0 to 400%) than other RCMs, and in particular, this effect was more significant at higher elevations.

As expected, all bias corrected reanalysis for the 60 year epoch better reproduced the mean annual rainfall of AWAP at all sites than the uncorrected. In particular, all uncorrected reanalyses mirror the spatial pattern in AWAP mean rainfall. The ratio between bias corrected reanalyses and AWAP mean rainfall generally varied from 0.5 to 1.5, and suggested that reanalyses slightly under or overestimated (up to 50%) the mean rainfall of AWAP at all sites. There was a significant improvement in R1 and R3 reanalyses after the bias corrections, sometimes simulating similar magnitudes as R2 reanalysis. Of bias corrected RCMs for the 20 year epoch, CSIRO-Mk3.0 RCMs tended to better capture the mean rainfall of AWAP than other RCMs for the Williams and Richmond River sites. At Bega River and Sydney sites, all RCMs, except reanalyses closely reproduced the AWAP mean, while over or underestimating the mean up to 50%. With respect to the CDFs generated for the mean rainfall (see Table 14.1 in Section 14.2.1) at a site of the bias corrected datasets, this over or underestimation was 0 to 10% for all the sites studied.

14.2.2.2 Coefficient of variation of rainfall

The NARCliM RCMs which best captured the C_v of rainfall of AWAP at each site are shown in Table 14.4.

The uncorrected reanalyses for the 60 year epoch tended to underestimate (20 to 30%) the C_v of the AWAP rainfall, thus underestimated the actual rainfall variability at a site. The ratios of C_v of reanalysis to AWAP varying from 0.6 to 1.1 for all sites suggesting that in addition to underestimations, there is a slight overestimation of C_v of AWAP at some grid points at all sites. In particular, this overestimation (up to 10%) was quite significant at the Bega River and Sydney sites. R2 and R3 reanalyses tended to better capture the magnitude and the spatial pattern of C_v of AWAP for all sites. The exception was Merriwa where the spatial patterns of the uncorrected

reanalyses were different from AWAP. Note that results for the Merriwa site are not shown in Table 14.4 as it was used as a pilot study where all analyses used only the uncorrected 60 years reanalyses datasets. However, the general underestimation of the magnitudes C_v of AWAP was similar to the other four sites (see Section 5.1.3).

Table 14.4 The most capable NARCliM RCMs to capture the AWAP coefficient of variation of rainfall

	Williams River site	Richmond River site	Bega River site	Sydney Site
60 year epoch	R2 reanalysis	R3 reanalysis	R2 reanalysis	R3 reanalysis
	1-R2 reanalysis 0-30% -U	1-R3 reanalysis 0-30% -U	1-R2 reanalysis 0-20% -U, 10%-O	1-R3 reanalysis 0-30% -U, 10%-O
	2-R1 reanalysis 0-40% -U, 10%-O	2-R1 reanalysis 0-40% -U	2-R1 reanalysis 0-30% -U, 10%-O	2-R1 reanalysis 0-30% -U, 10%-O
	3-R3 reanalysis 0-40% -U, 10%-O	3-R2 reanalysis 0-40% -U	3-R3 reanalysis 0-30% -U, 10%-O	3-R2 reanalysis 0-30% -U, 10%-O
20 year epoch	R2-MIROC3.2	R2-MIROC3.2	R2-MIROC3.2	R2-MIROC3.2
	1- MIROC3.2 20% -O	1- MIROC3.2 20% -O	1- MIROC3.2 20% -O	1- MIROC3.2 20% -O
	2- ECHAM5 0-40% O	2- ECHAM5 0-30% O	2- ECHAM5 0-30% O	2- ECHAM5 0-20% O
	3- CCCMA3.1 40% - O	3- CCCMA3.1 40% - O	3- CCCMA3.1 40% - O	3- CCCMA3.1 40% - O
	4- CSIROMk-3.0 40% - O, 10%-U	4- CSIROMk-3.0 40% - O, 10%-U	4- CSIROMk-3.0 40% - O, 10%-U	4- CSIROMk-3.0 40% - O, 10%-U
	5- reanalysis 40% - U	5- reanalysis 40% - U	5- reanalysis 40% - U	5- reanalysis 40% - U
60 year epoch: bias corrected	R2 reanalysis	R2 reanalysis	R2 reanalysis	R2 reanalysis
	1-R2 reanalysis 0-30% -U, 10% O	1-R2 reanalysis 0-30% -U	1-R2 reanalysis 0-20% -U, 10%-O	1-R2 reanalysis 0-20% -U, 10%-O
	2-R1 reanalysis 0-30% -U, 10%-O	2-R3 reanalysis 0-30% -U, 10%-O	2-R1 reanalysis 0-20% -U, 10%-O	2-R1 reanalysis 0-30% -U, 10%-O
	3-R3 reanalysis 0-30% -U, 10%-O	3-R1 reanalysis 0-40% -U, 10%-O	3-R3 reanalysis 0-30% -U, 10%-O	3-R3 reanalysis 0-40% -U, 10%-O
20 year epoch: bias corrected	R1 and R3-MIROC3.2	R1 and R3-MIROC3.2	R3- MIROC3.2	R2-MIROC3.2
	1- MIROC3.2 20% -O	1- MIROC3.2 20% -O	1- MIROC3.2 20% -O	1- MIROC3.2 20% -O
	2- ECHAM5 0-20% O	2- ECHAM5 0-20% O	2- ECHAM5 0-20% O	2- ECHAM5 0-20% O
	3- CCCMA3.1 20% - O	3- CCCMA3.1 20% - O	3- CCCMA3.1 20% - O	3- CCCMA3.1 20% - O
	4- CSIROMk-3.0 20% - O	4- CSIROMk-3.0 20% - O	4- CSIROMk-3.0 20% - O	4- CSIROMk-3.0 20% - O
	5- reanalysis 20% - U	5- reanalysis 30% - U	5- reanalysis 30% - U	5- reanalysis 30% - U

The numbers 1 to 5 followed by the RCM name indicate the rank of model performance. U and O indicate an under or overestimation of C_v compared with AWAP.

All the uncorrected GCMs, except CSIRO-Mk3.0 tended to overestimate the C_v for all sites for the 20 year epoch, and this was in contrast to the reanalysis. The uncorrected R2-MIROC3.2 for the 20 year epoch more closely captured the C_v of AWAP rainfall than other RCMs particularly for the fortnightly and monthly resolutions, overestimating the magnitudes (varying from 0 to 20%) for all sites.

As expected, after the bias correction, the reanalyses tended to better capture the C_v of AWAP than the uncorrected for the 60 year epoch. In particular, there is a clear improvement in R2 and R3 reanalyses which had ratios of reanalysis to AWAP ranging from 0.8 to 1.1. Comparing the number of grid points which have magnitudes of C_v close to AWAP (with ratio ranging from 0.9 to 1.1), the bias corrected R2 better reproduced the C_v of AWAP than R1 and R3 for all time resolutions. Of bias corrected RCMs for the 20 year epoch, all RCMs tended to produce improved results compared with the uncorrected. MIROC3.2 was the exception, yet it remained the best at capturing the C_v of AWAP for most of the grid points at a site. However R1 and R3-MIROC3.2 tended to perform better than R2 after the bias correction for all sites.

14.2.2.3 Lag-1 correlation of rainfall

This section compares the lag-1 correlation of NARCliM RCMs relative to AWAP. The lag-1 correlation of the rainfall was not calculated for the daily resolution due to the large number of zero rainfalls.

The NARCliM RCMs which best captured the lag-1 correlations of AWAP at each site are shown in Table 14.5.

The uncorrected reanalyses for the 60 year epoch poorly reproduced the lag-1 autocorrelations of fortnightly and monthly AWAP. There were some overestimated regions (up to 300%) located at the high elevations while there were some underestimated regions (up to 100%) at low elevations. There was a similarity in the spatial pattern of reanalyses and AWAP at fortnightly and monthly time resolutions for all sites except for the Williams River which had only the monthly pattern being similar to AWAP.

The uncorrected R3-CCCMA3.1 for the 20 year epoch tended to better simulate the lag-1 autocorrelation (with 10 to 40% over or underestimation) for all three time

resolutions than the other RCMs, yet the spatial pattern in the annual lag-1 autocorrelation of AWAP was poorly simulated. In particular the negative lag-1 autocorrelations regions shown in the annual AWAP were not well matched with that of CCCMA3.1. Compared with the uncorrected reanalysis for the 60 year epoch, there was a reduction in the extent of the overestimation (80%) of lag-1 correlation for the 20 year epoch, which was due to the lesser number of data points used.

The bias corrected RCMs produced very similar results to the uncorrected data for all time resolutions and sites. This suggests that the bias correction does not improve lag-1 autocorrelations except for the slight improvement of R3-CCCMA3.1 for the 20 year period. Therefore, the ability to capture the lag-1 correlation of AWAP in the bias corrected RCMs was equal to that of the uncorrected.

Table 14.5 The most capable NARCliM RCMs to capture the AWAP lag-1 correlation of rainfall

	Williams River site	Richmond River site	Bega River site	Sydney Site
60 year epoch	R3 reanalysis	R3 reanalysis	R3 reanalysis	R3 reanalysis
	1-R3 reanalysis 0-300% -O, 100%-U	1-R3 reanalysis 0-200% -O, 100%-U	1-R3 reanalysis 0-300% -O, 100%-U	1-R3 reanalysis 0-200% -O, 100%-U
	2-R2 reanalysis 0-400% -O, 100%-U	2-R1 reanalysis 0-250% -O, 100%-U	2-R2 reanalysis 0-250% -O, 100%-U	2-R2 reanalysis 0-300% -O, 100%-U
	3-R1 reanalysis 0-400% -O, 100%-U	3-R2 reanalysis 0-300% -O, 100%-U	3-R1 reanalysis 0-350% -O, 100%-U	3-R1 reanalysis 0-350% -O, 100%-U
20 year epoch	R3-CCCMA3.1	R3-CCCMA3.1	R3-CCCMA3.1	R3-CCCMA3.1
	1-CCCMA3.1 10-40% - O/U	1-CCCMA3.1 10-40% - O/U	1-CCCMA3.1 10-40% - O/U	1-CCCMA3.1 10-40% - O/U
	2- ECHAM5 0-50% O	2- reanalysis 0-50% O/U	2- reanalysis 0-50% O/U	2- reanalysis 0-50% O/U
	3- reanalysis 80% - O	3- ECHAM580% - O	3- ECHAM580% - O	3- ECHAM580% - O
	4- MIROC3.2 80% -O	4- MIROC3.2 80% -O	4- MIROC3.2 80% -O	4- MIROC3.2 80% -O
	5- CSIROMk-3.0 80-100% - O	5- CSIROMk-3.0 80-100% - O	5- CSIROMk-3.0 80-100% - O	5- CSIROMk-3.0 80-100% - O
60 year epoch: bias corrected	R3 reanalysis	R3 reanalysis	R3 reanalysis	R3 reanalysis
	ditto as uncorrected	ditto as uncorrected	ditto as uncorrected	ditto as uncorrected
20 year epoch: bias corrected	R3-CCCMA3.1	R3-CCCMA3.1	R3-CCCMA3.1	R3-CCCMA3.1
	1-CCCMA3.1 10-20% - O/U	1-CCCMA3.1 10-20% - O/U	1-CCCMA3.1 10-20% - O/U	1-CCCMA3.1 10-20% - O/U
	2-All other models are same as uncorrected.	2-All other models are same as uncorrected.	2-All other models are same as uncorrected.	2-All other models are same as uncorrected.

The numbers 1 to 5 followed by the RCM name indicate the rank of model performance. U and O indicate an under or overestimation of monthly lag-1 autocorrelations compared with AWAP. The detailed results are maximums of R1, R2 and R3RCMs.

14.2.2.4 Standard deviation of the rainfall

In addition to the mean, C_v and lag-1 correlation, the ability of the 20 year epoch NARCliM RCMs to capture the standard deviation of the rainfall was assessed, but the analysis was only performed at the Sydney site. The results showed that uncorrected R2-CCCMA3.1 tended to underestimate (20 to 30%) the standard deviation of AWAP, while all of the other uncorrected RCMs slightly overestimated (about 15 to 25%). However, R1 and R3-CCCMA3.1 uncorrected RCMs reproduced the standard deviation of AWAP better than R2. The bias corrected MIROC3.2 tend to reproduce the standard deviation better than the other RCMs and the overall performance of the standard deviation of the RCM simulated rainfall was significantly imporved by the bias correction.

14.2.2.5 Relationship between spatial variability of statistics and elevation

The NARCliM RCMs (20 and 60 year epochs) were better able to reproduce the rainfall distribution statistics such as mean and C_v. The bias corrected RCMs tended to produce more reliable results than uncorrected when capturing the mean and C_v of AWAP rainfall. However, there was no significant improvement in the lag-1 correlations of uncorrected RCMs after the bias correction. This showed that bias correction does not improve the time series characteristics of the NARCliM RCMs.

The statistics such as mean, C_v and lag-1 correlations calculated for NARCliM RCMs tended to be highly correlated to the elevation and the distance to the coast. The results shown in Figure 5.13 and a preliminary evaluation on the relationship between the mean rainfall and elevation (Chapter 8) suggested that there was a statistically significant positive linear relationship (r^2=0.91 and p= 0.001) between the observed rainfall and the elevation for the regions which were close to the coastline, where the ECL impacts were most dominant. Further from the coast, this relationship became weaker. This analysis was performed only at the Williams River site using the 60 year reanalyses rainfall, AWAP and rain gauge datasets. Compared with AWAP, and R1 and R3 reanalyses, R2 reanalysis was better at replicating the linear relationship between the gauged rainfall and elevation at the Williams River site.

14.2.3 Temporal autocorrelation of the rainfall

The autocorrelations of NARCliM RCMs at selected grid points of the Williams River, Richmond River, Bega River and Sydney sites were evaluated against AWAP data at three different resolutions: fortnightly, monthly and annual. The NARCliM RCMs which best captured the AWAP autocorrelations at each site are shown in Table 14.6. Note that this section presents the results for autocorrelations up to 50 lags, while Section 14.2.2.3 presented only the lag-1 correlation of the rainfall.

The results of the autocorrelation analyses showed that not all NARCliM RCMs were able to successfully reproduce the seasonality present in the observed rainfall, though most of them were able to capture the correct timing of the seasonal cycle for all time resolutions and epochs irrespective of the spatial location. Capturing the seasonal cycle is of much interest in Australia, where significant seasonal shifts in predominant patterns and distributions of rainfall and temperature occur.

Compared with the AWAP autocorrelations, the uncorrected R1 and R2 reanalyses for 60 year epoch often overestimated the strength of the autocorrelation at each lag while the R3 reanalysis tended to better reproduce the AWAP autocorrelations while still slightly overestimating the magnitudes for all sites, except for the Richmond River site (where R3 reanalysis underestimated autocorrelations up to 50% at low elevations). However for the high elevation grid points of the Williams River site, all reanalyses tended to greatly overestimate the magnitudes of the autocorrelations of AWAP, while there was no consistency in the autocorrelation results at the high elevation grid points for Sydney (see Table 14.6).

Table 14.6 The most capable NARCliM RCMs to capture the AWAP autocorrelations

	Elevation	Williams River site	Richmond River site	Bega River site	Sydney Site
60 year epoch uncorrected	low	R3 reanalysis	R1 reanalysis	R3 reanalysis	R3 reanalysis
		1-R3 reanalysis 10-40% - O 2-R2 reanalysis 50-80% - O 3-R1 reanalysis 50-100% - O	1-R1 reanalysis 10-15% - O/U 2-R2 reanalysis 10-20% - U 3-R3 reanalysis 10-50% - U	1-R3 reanalysis 10-40% - O 2-R2 reanalysis 30-80% - O 3-R1 reanalysis 30-100% - O	1-R3 reanalysis 10-40% - O 2-R2 reanalysis 20-50% - O 3-R1 reanalysis 30-60% - O
	high	None	R3 reanalysis	R3 reanalysis	None
		1-R3 reanalysis 100% - O 2-R2 reanalysis 125% - O 3-R1 reanalysis 50-150% - O	1-R3 reanalysis 10-50% - O 2-R2 reanalysis 80-100% - O 3-R1 reanalysis 80-100% - O	1-R3 reanalysis 10-50% - U 2- R1 reanalysis 20-80% - U 3- R2 reanalysis 20-100% - U	Results are not consistent. All reanalyses underestimate autocorrelations for one grid point while overestimating the values for the other.
20 year epoch uncorrected	low	R2 reanalysis	R2 reanalysis	R3 reanalysis	R3 reanalysis and R3-CCCMA3.1
		1-R2 reanalysis 10-40% - O 2-CCCMA3.1 10-50% - O/U 3-ECHAM5 200% - O 4-MIROC3.2 200-400% -O 5-CSIROMk-3.0 400% - O	1-R2 reanalysis 10-20% - U 2-CCCMA3.1 10-50% - U 3-ECHAM5 50-100% - O 4-MIROC3.2 200-400% -O 5-CSIROMk-3.0 400% - O	1-R3 reanalysis 10-40% - O 2-CCCMA3.1 10-50% - U 3-ECHAM5 100-200% - O 4-MIROC3.2 100-200% -O 5-CSIROMk-3.0 200-400% - O	1-R3 reanalysis 10-40% - O 2-CCCMA3.1 10-50% - U 3-ECHAM5 100-200% - O 4-MIROC3.2 100-200% -O 5-CSIROMk-3.0 200-400% - O
	high	None	R3 reanalysis	R3 reanalysis and R3-ECHAM5	None
		1-R2 reanalysis 125% - O 2-CCCMA3.1 10-50% - O/U 3-ECHAM5 200%-300% - O 4-MIROC3.2 200-500% -O 5-CSIROMk-3.0 500% - O	1- R2 reanalysis 80-100% - O 2-CCCMA3.1 80-100% - U 3-ECHAM5 80-100% - O 4-MIROC3.2 200-400% -O 5-CSIROMk-3.0 200-400% - O	1-R3 reanalysis 10-50% - U 2-ECHAM5 10-50% - O/U 3-MIROC3.2 100-200% -O 4-CSIROMk-3.0 100-200% - O 5-CCCMA3.1 400% - O	Results are not consistent for the two grid points.
60 year epoch bias corrected	low	R3 reanalysis	R1 reanalysis	R3 reanalysis	R3 reanalysis
		ditto uncorrected	ditto uncorrected	ditto uncorrected	ditto uncorrected
	high	None	R3 reanalysis	R3 reanalysis	None
		ditto uncorrected	ditto uncorrected	ditto uncorrected	ditto uncorrected
20 year epoch: bias corrected	low	R2 reanalysis	R2 reanalysis	R3 reanalysis	R3 reanalysis and R3-CCCMA3.1
		ditto uncorrected	ditto uncorrected	ditto uncorrected	ditto uncorrected
	high	None	R3 reanalysis	R3 reanalysis and R3ECHAM5	None
		ditto uncorrected	ditto uncorrected	ditto uncorrected	ditto uncorrected

The numbers 1 to 5 followed by the RCM name indicate the rank of model performance. U and O indicate an under or overestimation of the monthly autocorrelation of the 6th (6 months) lag compared with AWAP.

For all RCMs for the current 20 year epoch, the uncorrected R2 and R3 reanalyses performed better in capturing the spatial pattern of the autocorrelations of AWAP than the GCMs, yet tended to overestimate the magnitudes. Of the GCMs, CSIRO-Mk3.0, MIRO3.2 and ECHAM5 overestimated the magnitudes (up to 500%) of autocorrelations of AWAP. In contrast CCCMA3.1 had similar magnitudes of autocorrelations of AWAP, particularly the R3-CCCMA3.1 at the Sydney site, but did not produce the correct timing of the seasonal signal with peaks at different lags compared with AWAP.

The bias corrected reanalyses for 60 year epoch produced similar results was the uncorrected, except for some small improvements in magnitudes for some grid points at each site. Similarly, bias corrected GCM rainfall for the 20 year epoch also had similar autocorrelations to the uncorrected rainfall. This suggests that bias correction does not change the autocorrelation performance of RCMs (20 year and 60 year epoch) relative to AWAP for all sites studied. The results showed that bias correction did not improve the time series statistics of rainfall, particularly autocorrelations even though bias correction improved the distribution statistics of the rainfall.

The autocorrelation analysis for both uncorrected and bias corrected datasets exhibited a seasonal signal. Further investigations of anomaly time series after the seasonal detrending revealed that the reduction in the number of significant autocorrelations in the correlograms for the original and detrended data was consistent with a strong seasonal signal.

Overall, the overestimated autocorrelations (stronger persistence) of the uncorrected and bias corrected NARCliM RCMs suggests that if they are used in reservoir analysis, they would tend to predict longer durations for wet and dry periods, and hence likely over-predict the spillage from dams (i.e. wet periods) and the duration of periods of near empty reservoirs (i.e. dry periods). This overestimation was greater at high elevation grid points, particularly at Williams River and Sydney sites where none of the reanalyses reproduce the AWAP autocorrelations.

As mentioned in Section 14.2.2, it is possible that the spatial averaging of elevation within the NARCliM pixels was affecting the results, particularly where rainfall volume is closely related to topography. This effect was more pronounced at high

elevation regions such as Australian Alps at the Bega River site and Blue Mountains at the Sydney site.

14.2.4 Spatial correlation of the rainfall

NARCliM RCMs' ability to reproduce the spatial correlations of the daily AWAP and rain gauge rainfall was evaluated at four sites along the east coast. The spatial correlation of NARCliM daily time series calculated between one grid point and all other grid points across a site was compared with that of AWAP. The results were presented as spatial variability plots (spatial patterns) as well as the scatter plots of correlation vs distance between two points (spatial correlation function). Using the fitted exponential curves, the best NARCliM RCMs which captured the spatial correlation of AWAP at each site were identified and are shown in Table 14.7.

In general, all uncorrected reanalyses for the 60 year epoch were able to reproduce the spatial correlations of AWAP, although R1 and R3 reanalyses tended to underestimate the spatial correlations for the long distanced grid points (large separations) where there is a high elevation difference between the grid points. Bega River and Sydney sites are examples of this behaviour. Compared with spatial correlations of rain gauges, both the uncorrected reanalyses and AWAP gridded datasets had correlations higher than that of the rain gauges, with approximately 20 to 30% overestimation for all the grid points used (see Section 7.3).

Of the uncorrected RCMs for the 20 year epoch, uncorrected GCM simulations performed better than reanalysis at some sites such as Bega River and Sydney. The uncorrected R1- and R3-ECHAM5, MIROC3.2 and CSIRO-MK3.0 RCMs tended to better simulate the AWAP spatial correlation function than CCCMA3.1. However due to discrepancies in the performance of RCMs, which GCM and which RCM configuration (R1, R2 or R3) performed better was site specific. Though the general trends in the spatial correlation function of AWAP is closely captured by NARCliM RCMs, there are significant discrepancies in the scatter of the spatial correlation functions. In particular, for all datasets (AWAP and NARCliM RCMs), there is less scatter in the correlation functions when correlations was calculated using a low elevation point as the reference.

Table 14.7 The most capable NARCliM RCMs to capture the AWAP spatial correlation of rainfall

	Elevation	Williams River site	Richmond River site	Bega River site	Sydney Site
60 year epoch uncorrected	low	R1 reanalyses	R3 reanalysis	R2 reanalysis	R1 reanalysis
		1-R1reanalysis 2% - U 2-R2 reanalysis 5% - U 3-R3 reanalysis 5% - U	1-R3reanalysis 7% - U 2-R1 reanalysis 9% - U 3-R2 reanalysis 9% - U	1-R2 reanalysis 4% - U 2-R3 reanalysis 7% - U 3-R1 reanalysis 9% - U	1-R1 reanalysis 3% - U 2-R2 reanalysis 8% - U 3-R3 reanalysis 11% - U
	high	R1 reanalysis	R1 reanalysis	R2 reanalysis	R2 reanalysis
		1-R1 reanalysis 9% - U 2-R2 reanalysis 13% - U 3-R3 reanalysis 17% - U	1-R1 reanalysis 7% - U 2-R2 reanalysis 12% - U 3-R3 reanalysis 16% - U	1-R2 reanalysis 30% - U 2-R3 reanalysis 36% - U 3-R1 reanalysis 36% - U	1-R2 reanalysis 17% - U 2-R1reanalysis 22% - U 3-R3 reanalysis 33% - U
20 year epoch uncorrected	low	R1 reanalysis	R1 CSIRO-Mk3.0	R2 and R3 reanalyses	R3-CSIRO-Mk3.0
		1-Reanalysis 2% - O 2- CCCMA3.7% - O 3- CSIROMk-3.0 7% - O 4- MIROC3.2 18% - O 5- ECHAM5 23% -O	1-CSIROMk-3.0 0% 2-Reanalysis 2% - U/O 3- ECHAM5 4% - O 4- CCCMA3.1 6% - O 5- MIROC3.2 17% - O	1-Reanalysis 2% - U 2- CCCMA3.4% - U 3- CSIROMk-3.0 4% - U 4- MIROC3.2 8% - O 5- ECHAM5 8% -O	1- CSIROMk-3.0 2%-O 2- CCCMA3.1 5% - O 3-Reanalysis 5% - U 4- ECHAM5 15% -O 5- MIROC3.2 20% - O
	high	R1 reanalysis and R3-MIROC3.2	R1-ECHAM5	R3-MIROC3.2	R1 CSIRO-Mk3.0
		1-Reanalysis 4% - U 2- MIROC3.2 4% - U 3- CCCMA3.1 6% - U 4- ECHAM5 6% -O 5-CSIROMk-3.0 6% - U	1- ECHAM5 0% 2- MIROC3.2 2.5% - U 3-CSIROMk-3.0 2.5% - U 4- CCCMA3.1 5% - U 5-Reanalysis 10% - U	1- MIROC3.2 12% - U 2- ECHAM5 19%- U 3-Reanalysis 26% - U 4- CCCMA3.1 40% - U 5-CSIROMk-3.0 52% - U	1-CSIROMk-3.0 3% - U 2- ECHAM5 5%- O 3- MIROC3.2 8% -O 4- CCCMA3.1 8% - U 5-Reanalysis 16% - U
60 year epoch bias corrected	low	R1 reanalysis	R3 reanalysis	R2 reanalyses	R2 reanalysis
		1-R1 reanalysis 10% - U 2-R2 reanalysis 12% - U 3-R3 reanalysis 12% - U	1-R3reanalysis 11% - U 2-R2 reanalysis 13% - U 3-R1 reanalysis 18% - U	1-R2 reanalysis 13% - U 2-R3 reanalysis 17% - U 3-R1 reanalysis 27% - U	1-R2reanalysis 11% - U 2-R1 reanalysis 13% - U 3-R3 reanalysis 24% - U
	high	R3 reanalysis	R1 and R3 reanalyses	R2 reanalysis	R2 reanalysis
		1-R3reanalysis 19% - U 2-R1 reanalysis 20% - U 3-R2 reanalysis 26% - U	1-R1reanalysis 16% - U 2-R3 reanalysis 16% - U 3-R2 reanalysis 20% - U	1-R2reanalysis 36% - U 2-R3 reanalysis 40% - U 3-R1 reanalysis 53% - U	1-R2 reanalysis 28% - U 2-R1 reanalysis 33% - U 3-R3 reanalysis 42% - U
20 year epoch: bias corrected	low	R1-CSIRO-Mk3.0	R1-ECHAM5	R2 MIROC3.2	R3-CSIRO-Mk3.0
		1- CSIROMk-3.0 2% - U 2- CCCMA3. 5% - O 3-Reanalysis 7% - U 4- MIROC3.2 11% - O 5- ECHAM5 18% -O	1- ECHAM5 0% 2-Reanalysis 4% - U 3- CCCMA3.1 6% - O 4- CSIROMk-3.0 9% -U 5- MIROC3.2 9% - O	1- MIROC3.2 0% 2- ECHAM5 4%- O 3-Reanalysis 8% - U 4- CCCMA3.1 8% - U 5-CSIROMk-3.0 8% - U	1- CSIROMk-3.0 0% 2- CCCMA3. 2% - O 3-Reanalysis 2% - O/U 4- ECHAM5 12% -O 5- MIROC3.2 20% - O
	high	R1-MIROC3.2	R1-ECHAM5	R2-ECHAM5	R3-ECHAM5 and R2-MIROC3.2
		1- MIROC3.2 0% 2 - ECHAM5 2% -O 3- CCCMA3.1 6% - U 4- CSIROMk-3.0 6% - U 5- Reanalysis 15% - U	1- ECHAM5 0% 2- CCCMA3. 2 5% - U 3- MIROC3.2 5% - O 4-CSIROMk-3.0 7.5% - U 5-Reanalysis 20% - U	1- ECHAM5 24%- U 2- MIROC3.2 21% - U 3- CCCMA3.1 36% - U 4-Reanalysis 38% - U 5-CSIROMk-3.0 57% - U	1- ECHAM5 0% 2- MIROC3.2 0% 3- CCCMA3.1 3% - U 4-CSIROMk-3.0 5% - U 5-Reanalysis 27% - U

The numbers 1 to 5 followed by the RCM name indicate the rank of model performance. U and O indicate an under or overestimation of the exponent of the fitted curve relative to AWAP.

The bias corrected reanalyses for the 60 year epoch produced similar results to the uncorrected, with only some small differences in performance. However compared with the spatial correlation of rain gauges (shown in Figure 7.28), all three bias corrected reanalyses datasets had better results than AWAP. The bias corrected 20 year epoch RCMs had similar performance to the uncorrected.

It appears that the spatial variability of the spatial correlation of uncorrected and bias corrected rainfall for all sites was more influenced by the distance than the difference of the elevation between the points.

14.3 Uncertainty of NARCliM Rainfall Simulations

Uncertainties of climate outputs arise due to various contributing factors. For instance, the uncertainties of downscaled rainfall simulations are mainly due to the uncertainties associated with the underlying GCMs and RCM configurations. This section outlines uncertainties of NARCliM RCMs that have been introduced due to the use of different GCM and RCM combinations. The NARCliM bias corrected simulations for the current epoch (1990-2009) of the Williams River site were used in this analysis and only the key results and conclusions are shown below.

In order to quantify the uncertainties of each simulation, percentiles of monthly rainfall data were used throughout the analysis. This approach is somewhat similar to the method used in Woldemeskel et al (2012) which estimated the GCM/RCM model uncertainty based on the Square Root Error Variance of the median percentile (50^{th}). However, in contrast to Woldemeskel et al (2012), the standard deviation of the median percentile (50^{th}) was used in this thesis.

14.3.1 Percentile plots

The percentile plots for monthly NARCliM rainfall for all four GCMs and three RCMs at grid points A and C (see Figure 6.1) of the Williams River Catchment are shown in Figure 14.1. There is a clear variability of rainfall at different percentiles. In particular for percentiles greater than 50, this variability is significant across the simulations.

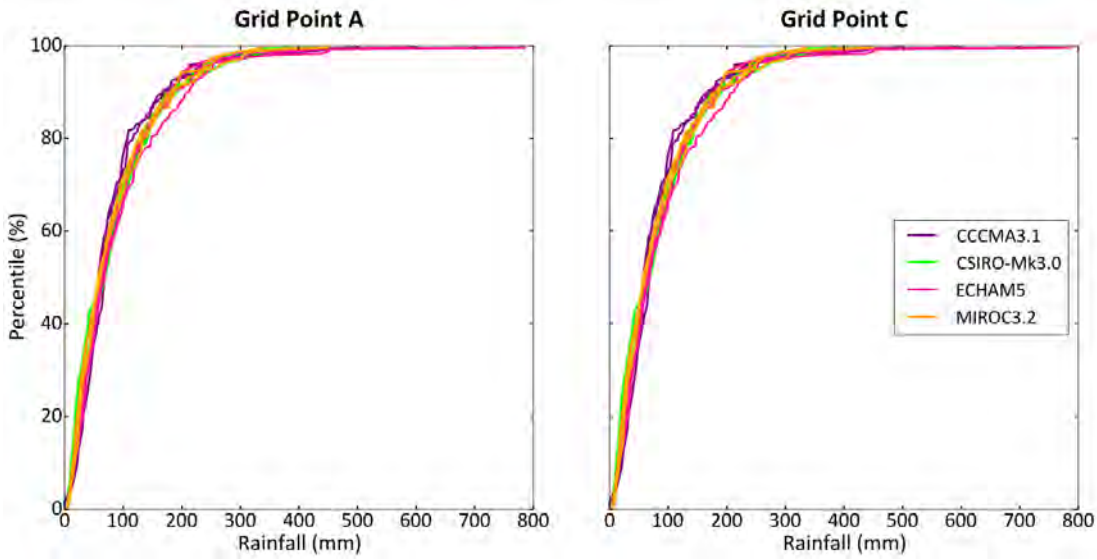

Figure 14.1 Percentile plots of rainfall for 1990-2009 at grid points A and C of Williams River site. Each colour shows different GCMs and consists of three precipitation values (For three RCM runs).

The variability between all twelve simulations (four GCMs: CCCMA3.1, CSIRO-Mk3.0, ECHAM5 and MIROC3.2, and three RCMs: R1, R2 and R3) for the 50th percentile of monthly rainfall at grid point A and C is shown in Figure 14.2 and Figure 14.3.

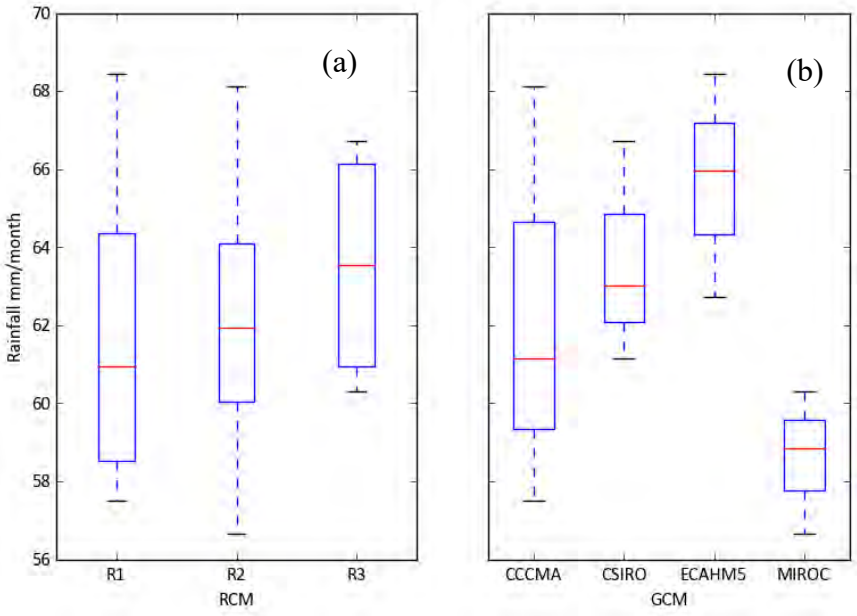

Figure 14.2 Variability of GCMs and RCMs for the 50th percentile for rainfall for 1990-2009 at grid point A of Williams River site: (a) model variability for three RCMs and (b) variability for four GCMs. Whiskers show range from minimum to maximum values.

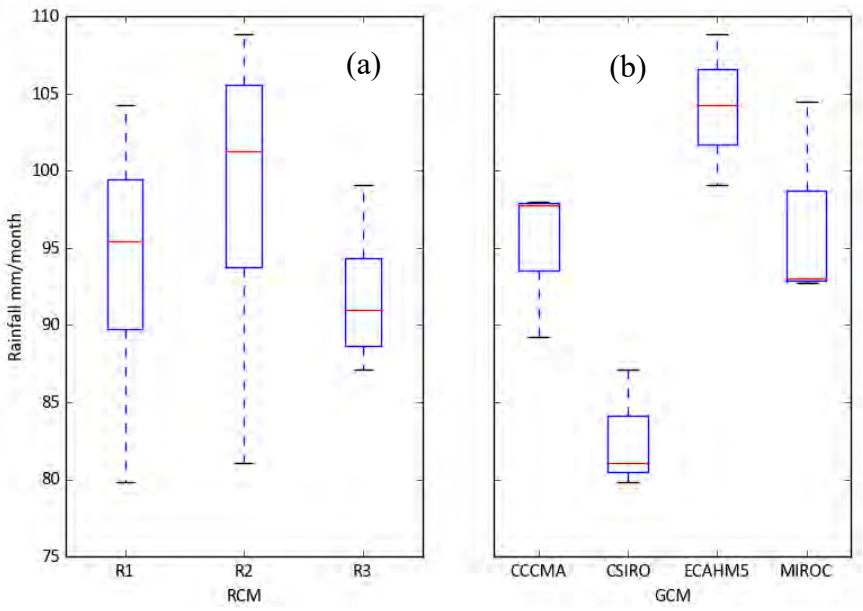

Figure 14.3 Variability of GCMs and RCMs for the 50th percentile for rainfall for 1990-2009 at grid point C of Williams River site: (a) model variability for three RCMs and (b) variability for four GCMs. Whiskers show range from minimum to maximum values.

As shown by Figure 14.2a and 14.3a, at both low (A) and high (C) elevation grid points, GCMs downscaled with R1 and R2 RCMs have a greater variability of the rainfall relative to R3. In contrast, a greater variability of the 50th rainfall percentile can also be seen for CCCMA GCM across three RCMs (Figure 14.2b and 14.3b), particularly at the lower elevation. Despite these slight differences, the overall range shows that variability across GCMs is higher than that across RCM runs. Therefore, this suggests that uncertainties of NARCliM model simulations are predominantly driven by the underlying GCMs, not by the RCMs.

14.3.2 Calculation of uncertainty

Uncertainty in climate simulations can be evaluated by analysing the consistency between different projections. As stated in Woldemeskel et al (2012), “Standard deviation at a specific percentile can be used as a measure of uncertainty”, as it calculates the variability between equally possible climate projections of multiple RCM/GCM combinations.

The uncertainty of NARCliM simulations was calculated as three values: (1) uncertainty across GCMs, (2) uncertainty across RCMs and (3) total uncertainty:

square root of (1) and (2). For instance, Figure 14.4 and Figure 14.5 show the standard deviation of the 50th percentile of uncorrected and bias corrected monthly rainfall (1990-2009) at all 400 grid points of Williams River site. As was in previous chapters, the purpose of calculating uncertainties of both uncorrected and bias corrected simulations was to study any possible increases or decreases of the uncertainty caused by the applied bias correction method. Further, as summarized in section 14.2.1, CSIRO-MK3.0 GCM and R2 RCM have been shown to better reproduce the observed PDFs of rainfall, therefore only the results based on CSIRO-Mk3.0 GCM and R2 RCM are shown in Figure 14.4 and Figure 14.5.

The three values plotted in each figure can be summerized as follows.

1. **GCM** uncertainty: standard deviation of the median percentile of rainfall of the four GCMs downscaled using RCM2- this is the variability of all GCMs for a single RCM configuration – The GCM/RCMs used were R2-CCCMA, R2-CSIRO, R2-ECHAM and R2-MIROC
2. **RCM** uncertainty: standard deviation of the median percentile of rainfall of the three RCMs using CSIRO GCM - this is the variability of all RCMs for a single GCM – The GCM/RCMs used were R1-CSIRO, R2-CSIRO and R3-CSIRO
3. **Total** uncertainty = $((\text{GCM uncertainty})^2 + (\text{RCM uncertainty})^2)^{1/2}$

As expected, Figure 14.4 shows that total uncertainty of uncorrected rainfall is higher than that of the bias corrected simulations (Figure 14.5). Similar to other statistics calculated in previous chapters, the spatial distribution of the standard deviation shows that uncertainty of GCMs mirrors the topography of the site, with greater uncertainty at higher elevations. The results also indicate that uncertainties of both GCM and RCM simulations have approximately similar or slightly different impacts on the total uncertainty of the uncorrected rainfall.

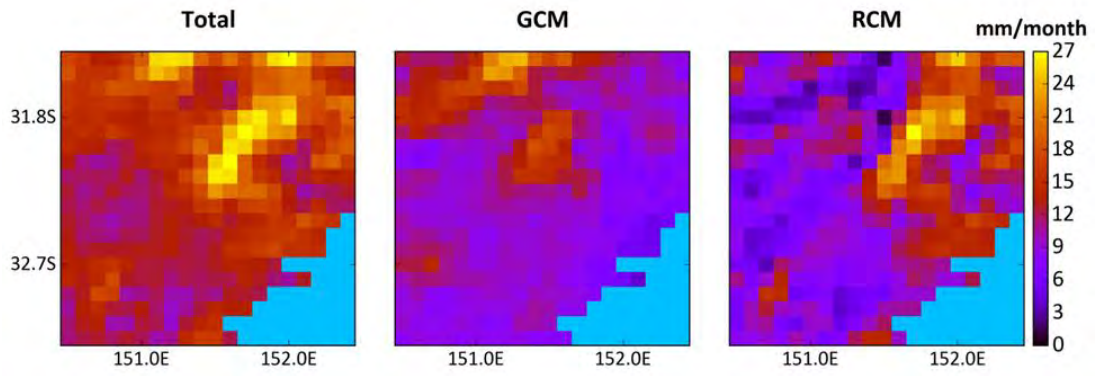

Figure 14.4 Maps of standard deviation values of 50th percentile for total, GCM, RCM and Total uncertainty for uncorrected rainfall for 1990-2009 of Williams River site. The standard deviation values are shown for CSIRO-Mk3.0 GCM and R2 RCM.

In contrast, results for the bias corrected rainfall (Figure 14.5) indicate that GCM uncertainty is the main contributor to the total uncertainty at all grid points showing higher uncertainty than RCMs, although this uncertainty is low across the whole catchment which is expected. This result is consistent with the results of whisker plots shown in Figure 14.2 and 14.3.

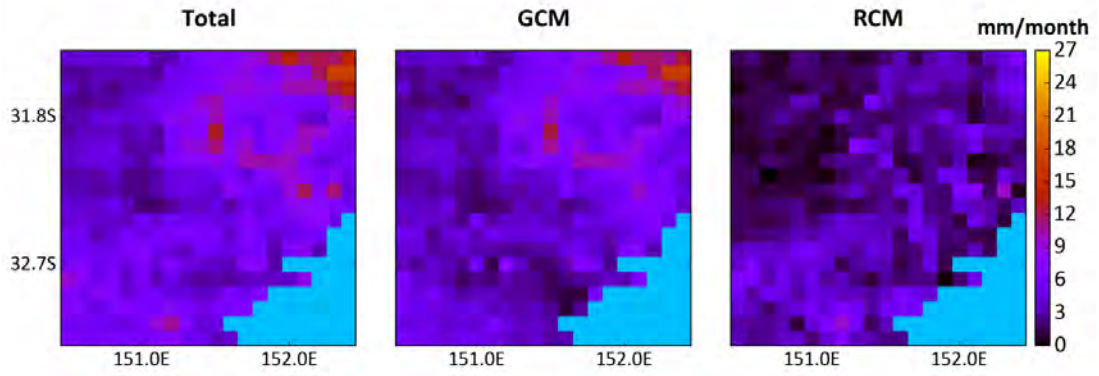

Figure 14.5 Maps of standard deviation values of 50th percentile for total, GCM and RCM uncertainty for bias corrected rainfall for 1990-2009 of Williams River site. The standard deviation values are shown for CSIRO-Mk3.0 GCM and R2 RCM.

The spatial distribution of coefficient of variation of the median percentile of rainfall for the Williams River site for current (1990-2009) and two future epochs (2020-2040 and 2060-2080) are shown in Figures 14.6 to 14.8. The results indicate that uncertainty is greater in future NARCliM projections, with far future (2060-2080) epoch showing greatest uncertainty compared with current and the near future epoch (2020-2040). Similar to the standard deviation, spatial distribution of uncertainty

calculated using coefficient of variation plots also show that GCM uncertainty follows the topography of the site, although the trend is not as pronounced.

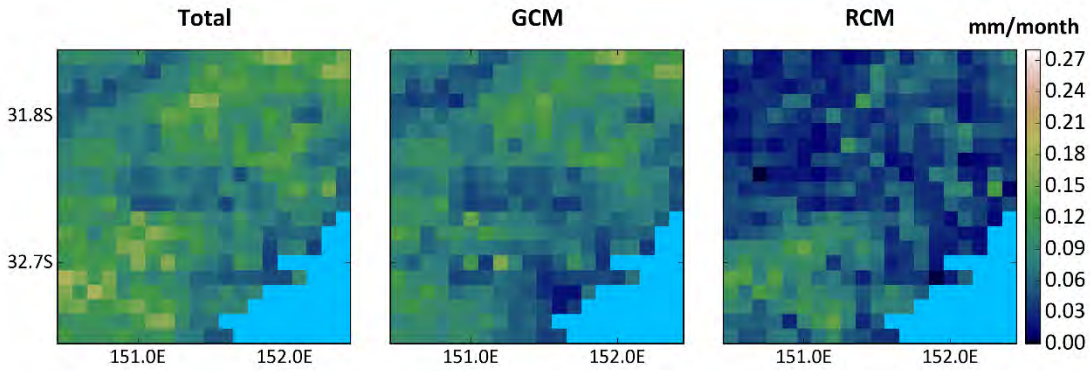

Figure 14.6 Maps of coefficient of variation values of 50th percentile for total, GCM and RCM uncertainty for bias corrected rainfall for 1990-2009 of Williams River site. The standard deviation values are shown for CSIRO-Mk3.0 GCM and R2 RCM.

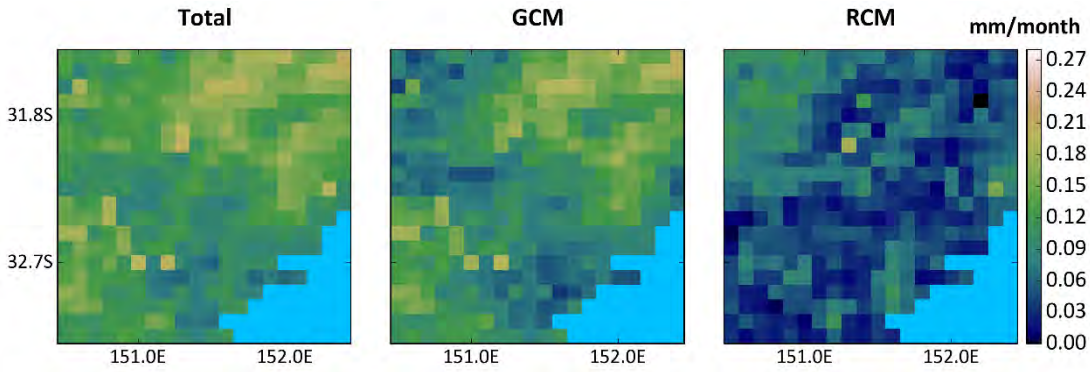

Figure 14.7 Maps of coefficient of variation values of 50th percentile for total, GCM and RCM uncertainty for bias corrected rainfall for 2020-2040 of Williams River site. The standard deviation values are shown for CSIRO-Mk3.0 GCM and R2 RCM.

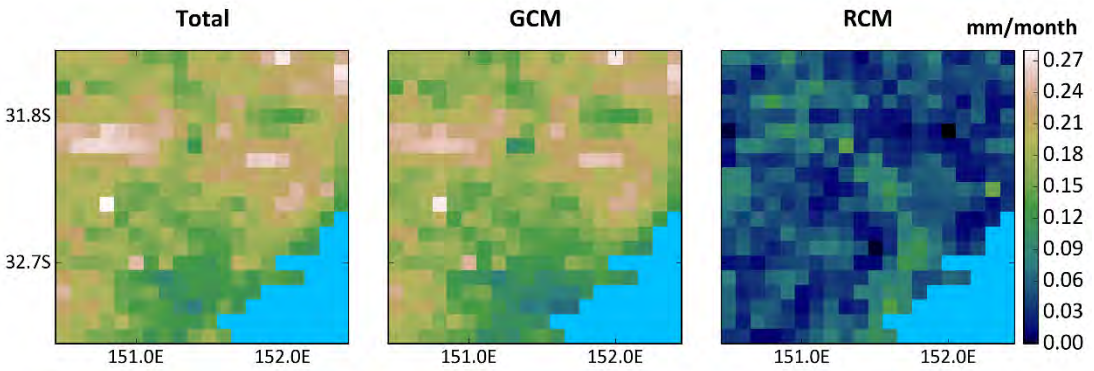

Figure 14.8 Maps of coefficient of variation values of 50th percentile for total, GCM and RCM uncertainty for bias corrected rainfall for 2060-2080 of Williams River site. The standard deviation values are shown for CSIRO-Mk3.0 GCM and R2 RCM.

Overall, the results show that GCM uncertainty is the main contributing factor for the total uncertainty of NARCliM bias corrected simulations. As expected the bias correction used in the NARCliM design clearly reduces the total, GCM and RCM uncertainties of NARCliM uncorrected simulations. Further, the uncertainty of NARCliM future projections appears to be higher than that of the current projection. In addition, similar to the other statistics, NARCliM model uncertainty also follows the topography of the site.

14.4 Assessment of NARCliM RCMs future projections

The future change of rainfall for 2070 relative to 2000 was assessed for the four east coast sites using the bias corrected NARCliM GCM projections, and is shown in Table 14.8.

The results reveal that -19% to 54% (averages of maximums and minimums of R1, R2 and R3 GCMs for all sites) projected change in the mean rainfall is predicted across the broader east coast by 2070. The lowest change for an individual site, -30% was for the Bega River, while the highest (70%) was for the Richmond River site. There was a general trend that CCCMA3.1 and MIROC3.2 GCMs projected an increase in the mean rainfall while CSIRO-mk3.0 and ECHAM5 projected a decrease for 2070 for all sites. For all sites the MIROC3.2 RCMs projected larger increases (up to 70%) than CSIRO-Mk3.0.

Table 14.8 Percent change in mean and C_v of rainfall for 2070 relative to 2000

	GCMs	Williams River site	Richmond River site	Bega River site	Sydney Site
Percent change in mean annual rainfall	CCCMA3.1	-5 to 40	-5 to 30	-20 to 30	-10 to 30
	CSIRO-Mk3.0	-20 to 5	-20 to 5	-20 to 5	-20 to 5
	ECHAM5	-20 to 10	-15 to 10	-30 to 20	-15 to 10
	MIROC3.2	-15to 50	0 to 75	-25 to 45	-15 to 50
Percent change in C_v of monthly rainfall	CCCMA3.1	-25 to 30	-25 to 30	-20 to 45	-20 to 35
	CSIRO-Mk3.0	-5 to 35	-10 to 25	-15 to 30	-15 to 35
	ECHAM5	-10 to 25	-5 to 30	-10 to 55	-15 to40
	MIROC3.2	-25 to 10	-20 to 10	-25 to 30	-20 to 30

The results are maximum and minimum values of all GCMs (R1, R2 and R3) for a particular GCM at a site.

Further, the models suggest that there will be a -19% to 40% (averages of maximums and minimums for all sites) change in the monthly rainfall variability across the coastal sites by 2070. CSIRO-Mk3.0 and ECHAM5 tend to project increases of the rainfall variability (up to 40%) across the sites, while CCCMA3.1 and MIROC3.2 project either increases or decreases (percent change varying from -25 to 45%). There is a general trend that regions with reduced rainfall variability have a higher mean rainfall and vice versa for all sites, except for Sydney.

Chapter 15
Conclusions

15.1 Introduction

The primary objective of this thesis was to evaluate the ability of NARCliM downscaled RCM data to generate the correct statistical representation of current day hydrology. Both the uncorrected and bias corrected data was used in each analysis to compare the performance of the datasets with and without bias correction. As a specific objective, the similarities and differences between the performance of NARCliM RCM data to capture the temporal and spatial statistics of observed rainfall was investigated at four study sites, from north to south along the east coast of NSW, and with different orography, exposure to the coastal weather systems and ECL occurrence.

The secondary objective was to assess the impacts of orography on rainfall and its potential impact on hydrology and water security. Most of the water supply catchments along the east coast are subjected to orographic rainfall due to closeness of the Great Divide to the coast. Therefore, the relationship between the rainfall and elevation was explored and inferences drawn about potential impact on hydrology and water security.

The third objective was to determine any future changes in NARCliM rainfall properties compared with current day rainfall statistics. This final chapter summarises how these objectives were achieved, the major findings and conclusions and future research directions.

15.2 Statistical testing of NARCliM rainfall

The past studies on the evaluation of NARCliM in the literature review showed that 10 km resolution NARCliM RCMs were able to successfully reproduce the daily statistics such as mean, bias in minimum and maximum precipitation and probability distributions of the rainfall when compared to AWAP observations. The results here support these findings in past studies, the results of the evaluation of the probability

distribution functions suggest there is a general trend of all uncorrected RCMs to underestimate the mean annual probability distribution of AWAP at a site, particularly the occurrence of greatest rainfall values. However, as was expected, this behaviour has been significantly improved with the bias correction and as a result, NARCliM RCMs tend to reproduce almost 98% of AWAP's CDF. This shows the extent of improvement in the mean statistics of NARCliM RCMs after the bias correction. Compared with other RCMs, improvement in the CSIRO-Mk3.0 to capture the CDF of mean annual rainfall of AWAP is quite significant. An important caveat is that the bias correction used daily AWAP data and many of the statistical conmparisons here also used AWAP, so improved performance for those specific statistics is not surprising.

The ability of NARCliM RCMs to capture the daily rainfall probabilities was also assessed. As for the results, R2 RCMs are better able to capture the daily rainfall CDF of AWAP than R1 and R3, though the probabilities of the light rainfall events (rainfall less 1.5 mm) are captured by none of the uncorrected RCMs (neither for 20 (1990-2009) nor 60 year (1950-2009) epochs). For the midsized to high rainfall events, the uncorrected R2 reanalysis for the period 1950-2009 closely captures the daily rainfall distribution at low elevations at the sites studied. For the 20 year epoch, uncorrected R2-GCMs tend to better capture the daily probabilities of AWAP at low elevations than reanalysis. At high elevations, all uncorrected RCMs, struggle to reproduce the daily rainfall distributions of AWAP for both 60 and 20 year epochs. Compared with the uncorrected, there is a significant improvement in the RCM performance after the bias correction, though datasets are only reliable for the rainfall events greater than 1.5 mm due to the artefacts caused by the bias correction method. However, since none of NARCliM RCMs (neither uncorrected nor bias corrected) simulate the entire daily rainfall distribution of AWAP, the reliability of using this data in rainfall-runoff models to generate estimates of runoff is questionable.

The results for the analysis of the spatial variability of temporal rainfall statistics show that NARCliM RCMs are able to capture the mean and standard deviation of the rainfall. While uncorrected RCMs tend to largely overestimate these statistics, as expected bias corrected RCMs better capture these statistics at the catchment scale. Of all RCMs for the 20 year epoch, the bias corrected CSIRO-Mk3.0 RCMs are able

to best capture the mean rainfall, while bias corrected MIROC3.2 captures the standard deviation of rainfall of AWAP. While these two models performed best, all other RCMs show some discrepancies compared with AWAP at all sites. Therefore, the results suggest that not all NARCliM RCMs are equally able to capture a particular statistic. The bias corrected MIROC3.2 RCMs were able to closely capture the coefficient of variation (C_v) of AWAP which determines the temporal variability of rainfall at a particular grid point, yet the ability of capturing the C_v was not as good for the mean and standard deviation of the rainfall. Further with respect to reproducing the C_v of AWAP, there is only a slight difference between bias corrected uncorrected RCMs. Further, it appears that the spatial variability of the rainfall (both uncorrected and bias corrected) has been influenced by the topography and the spatial patterns in all statistics are well simulated by NARCliM RCMs.

The ability of NARCliM RCMs to capture the lag-1 autocorrelation of the rainfall was also studied. In contrast to the CDF, mean, standard deviation and C_v, the ability of NARCliM RCMs to capture lag-1 correlation of AWAP is poor, with either under or overestimation of the magnitudes of AWAP autocorrelations. Both uncorrected and bias corrected R3-CCCMA3.1 for the 20 year epoch, produce similar results closely reproducing both the magnitude and spatial pattern of lag-1 autocorrelation of AWAP for fortnightly and monthly resolutions. The spatial pattern in the annual lag-1 autocorrelation of AWAP is not well simulated. In particular there are regions negative lag-1 autocorrelations in AWAP that are not well matched by CCCMA3.1. The similarity between the uncorrected and bias corrected results of lag-1 autocorrelations shows that bias correction does not improve the time series statistics of rainfall, particularly the lag-1 autocorrelations though they are capable to correct the systematic biases in distribution statistics such as CDF, mean, C_v and standard deviation of rainfall.

There are strong seasonal autocorrelations in the NARCliM data that are not observed in AWP or rain gauge data. The autocorrelation analyses showed that all NARCliM RCMs are unable to successfully reproduce the seasonal variability present in the observed rainfall at each time resolution for each time epoch irrespective of the spatial location. For the 20 year epoch, all GCMs, except CCCMA3.1 greatly overestimate the autocorrelations of the AWAP rainfall for all sites. The bias corrected R3-CCCMA3.1 RCM, particularly at low elevation grid

points appear to have similar magnitudes of autocorrelations of AWAP, yet does not produce the correct timing or the phase of the seasonal signal. For the 60 year epoch, R3 reanalysis tend to closely reproduce autocorrelations trends with time, yet overestimates the magnitudes. The overly strong seasonal signal in the NARCliM data is consistent with the number of significant autocorrelations in the detrended correlograms. As was seen for the lag-1 correlations, the correlograms of bias corrected RCMs look almost similar to the uncorrected correlograms and indicate that there is no significant improvement in model performances, with respect to the autocorrelations, after the bias correction. These results indicate that the significant deviations in the autocorrelation were not improved by the bias corrections.

Compared with the time series statistics such as temporal autocorrelations, NARCliM RCM data are better at reproducing the spatial correlation of AWAP rainfall. The analysis on the spatial correlation shows that R1 and R2 reanalyses produce similar spatial correlations as AWAP for all separations for all sites along the east coast. Compared with spatial correlations of rain gauges, both uncorrected reanalyses and AWAP gridded datasets have correlations higher than that of the rain gauges, with approximately 20-30% overestimation for all the grid points used. For the uncorrected RCMs for the 20 year epoch, R1- and R3-ECHAM5, MIROC3.2 and CSIRO-MK3.0 RCMs sometimes perform better than reanalysis at some sites. However, which model (ECHAM5, MIROC3.2 or CSIRO-MK3.0) and which configuration (R1, R2 or R3) performs better varies depending on the site topography and general climate properties. Though the exponential structure of the spatial correlation function of AWAP is closely captured by NARCliM RCMs, there are some discrepancies in the scatter of the spatial correlation functions of individual NARCliM RCM simulations. The bias corrected RCMs produce similar results as for the uncorrected, while having some small differences in the performance. Since both gridded datasets (bias corrected NARCliM RCMs and AWAP) overestimate the observed spatial correlations, usage of these datasets to estimate the rainfall, particularly the water availability in reservoir simulations in a catchment where there is no sufficient ground observations, may produce erroneous estimates with an over predicted actual water availability. As was seen for the other statistics, it appears that the spatial variability of the spatial correlation of rainfall also has been influenced by the topography.

15.3 Relationship between rainfall and the orography

It was found that the spatial variability of the rainfall statistics has a link to the topography. There are two types of rainfall and elevation relationships found in this study.

The first type is that there is a poor relationship between the mean rainfall and elevation which seems to be inconsistent across a catchment, with only 20% of the total variation of the mean rainfall explained by the linear relationship with elevation, while 80% of the variation remains unexplained. A combined approach of further assessing the relationship between the mean rainfall and elevation, and impacts from ECLs on this relationship suggest that there is a statistically significant positive linear relationship (r^2=0.91 and p= 0.001) between the mean rainfall and the elevation, but only for the regions which are close to the coastline of the Williams River site, where the ECL impacts are dominant. As the distance from the coast increases this relationship becomes weaker. However, it should be noted that this combined approach of the assessment of the relationship between mean annual rainfall and elevation was performed only as a preliminary case study, therefore further investigations are needed.

The second type is the relationship of the correlation of the rainfall with distance, and with elevation differences from a reference gauge. This means that even if two rain gauges have exactly similar mean rainfall, rainfall at one rain gauge can have a low correlation to the other because they are some distance away, or they have different elevations.

15.4 Performance of the NARCliM RCMs at various sites

The statistical tests performed at five study sites chosen along the east coast of Australia show that there is no north to south trend in either AWAP or NARCliM rainfall statistics along the broader east coast. Further, no specific recommendations can be made of a best GCM-RCM combination that performs best for any given site, due to the discrepancies between RCMs depending on the elevation, site hydrology, distance to the ocean, varying impacts from climatic phenomenon such as ECLs etc. There was a clear indication that NARCliM RCMs poorly simulate the rainfall

statistics at high elevation regions along the east coast, and this might be related to the averaging of the topography in NARCliM elevation data within a grid point. Note that most of the comparisons of the mean rainfall were against AWAP and there is emerging evidence that AWAP is poor for higher elevations. In particular, if this averaging effect is high at high elevations, the resulting lowered averaged elevations at these grid points may lead to low magnitudes of statistics as the rainfall statistics follow the trends in topography. Further, the rainfall in the Alpine region is less correlated with the other regions of the east coast and this was seen in both AWAP and NARCliM RCMs. Therefore, this suggests that both NARCliM and AWAP may not produce the rainfall at the Alpine region, where there is a distinct climate with snow occuring compared to other regions on the eastern seaboard.

15.5 Final remarks on NARCliM current rainfall projections

Overall, statistical testing performed along the east coast suggest that bias corrected NARCliM RCMs are able to capture the daily AWAP rainfall probabilities only for the midsized to large rainfall events, therefore fail to simulate the entire cumulative probability distribution of the daily rainfall at single grid points. The bias corrected NARCliM RCMs are able to reproduce both the magnitudes and spatial pattern in distribution statistics such as mean, standard deviation and C_v. The uncorrected R2 RCMs for both reanalysis and GCMs tend to perform better in capturing the distribution statistics of rainfall. This suggests that there are differences between the outputs depending on the underlying RCM configurations which were used in the downscaling process. Therefore, it appears that the internal dynamics of the RCMs plays a major role in driving the deterministic details of the rainfall time series. The spatial correlation function of AWAP rainfall is well captured by both uncorrected and bias corrected NARCliM RCMs. In contrast, the ability of both uncorrected and bias corrected NARCliM RCMs to reproduce the time series statistics such as autocorrelations of the rainfall is poor, and strongly overestimate the magnitudes of autocorrelations of AWAP. The similar correlograms for the uncorrected and bias corrected RCMs suggest that the bias correction does not influence the time series statistics, particularly the autocorrelations.

Since the NARCliM RCMs do not reproduce some of the statistics such as daily rainfall probabilities and time series statistics autocorrelations of the rain gauge and AWAP data which are important for the reservoir simulations at a site this raises unanswered questions about whether the NARCliM reanalysis datasets are sufficiently reliable to be used for reservoir analysis, particularly when generating estimates of runoff. In general, rainfall-runoff models are used to generate the daily runoff yield required for reservoir analysis and are typically calibrated using observed raingauge data at daily resolution. Therefore, this analysis suggests that NARCliM rainfall data cannot be used to drive a rainfall-runoff model calibrated to observed data and further, it is unlikely to generate correct estimates of runoff even if rainfall-runoff models are calibrated to NARCliM rainfall, particularly if the site average errors in NARCliM are greater than the site average errors in raingauge and AWAP data. It is important to note that the uncertainties associated with gauge and AWAP data cannot be neglected, particularly for possible interpolation errors in AWAP (e.g. Chubb et al., 2016), there is no simple way of assessing how accurately each dataset captures the rainfall in ungauged areas (Tozer et al., 2012).

Assessments of uncertainties of NARCiM simulations reveal that both GCM and RCM models that were used in the downscaling process contribute to the total uncertainty of NARCliM outputs. In particular, GCM uncertainty appears to be the main contributing factor for the total uncertainty of NARCliM bias corrected simulations. The reason of this is bias correction reduces all types of uncertainties including GCM, RCM and total uncertainties, however, the reduction of uncertainty in RCMs appears to be greater than that is of GCMs. As a result, uncertainties of RCMs have minimal impact on the total uncertainty of the simulations relative to the GCMs. Therefore, total uncertainty of bias corrected simulations tends to be mostly governed by the uncertainty of GCMs. In addition, uncertainity of NARCliM future projections appears to be higher than that of the current projection. Similar to the other statistics, NARCliM model uncertainity also follow the topography of the site, particularly this can clearly seen in uncertainity of GCMs than RCMs.

15.6 NARCliM future projections

Overall, the assessment performed at all four sites reveals that -19% to 54% (averages of maximums and minimums for all sites) projected change in the mean rainfall can be expected across the broader east coast by 2070. The lowest change for an individual site (-30%) is for the Bega River site, while the highest (70%) is for the Richmond River site. The rainfall is most likely to decrease by far future at the Bega River site, and this may be due to the relatively topography compared with the other sites. CSIRO-Mk3.0 and ECHAM5 GCMs generally project decreases of the rainfall for all sites, while CCCMA3.1 and MIROC3.2 project increases. All GCMs, except CSIRO-Mk3.0 project precipitation increases along the coast and this suggests that coastal regions will experience more rainfall in the future than the present-day.

The change in the monthly rainfall variability was also assessed. The results suggest that there will be -19% to 40% (averages of maximums and minimums for all sites) change in the monthly rainfall variability across the coastal sites by 2070. CSIRO-Mk3.0 and ECHAM5 tend to project increases of the rainfall variability across the sites, while CCCMA3.1 and MIROC3.2 project either increases or decreases.

In contrast to the changes in the mean annual rainfall, there is no general trend that the rainfall variability is to increase along the coast more than inland. There is a general trend that regions with reduced rainfall variability have a higher mean rainfall and vice versa for all sites, except for Sydney. This behaviour is consistent with the standard deviation of the rainfall remaining the same as the mean rainfall increases, which in turn is consistent with the rate of occurrence of rain days increasing but with the rain on each rainy day remaining unchanged. This is being studied in a parallel PhD project (Chowdhury, 2016).

15.7 Future work

The high-resolution RCMs can be evaluated using different approaches. As the primary objective, the ability of NARCliM RCMs to reproduce the current observed rainfall statistics which are important for reservoir modelling and water availability analysis was assessed in this thesis. However, this evaluation can be extended in several ways.

In the calculation of statistics, four time resolutions; daily, fortnights, months and annual were used in this thesis. The major motivation to use these different time resolutions is that reservoirs of different capacities respond to rainfall differently; small reservoirs respond to daily variations in rainfall while large reservoirs respond to rainfall variations over weeks or months. However, previous authors have evaluated the statistics of RCMs on seasonal basis. Therefore, the evaluation of the statistics based on the seasons could also reveal more insights on how these RCMs perform at different climate seasons.

Additionally, as a direct application on the reservoir simulation, the ability of NARCliM RCMs to generate the observed runoff could be evaluated. This assessment could be preceded by generating runoffs using a rainfall runoff model calibrated for the observed rainfall such as AWAP, and comparing the outputs against the historical runoff data.

Since this study focuses on the hydrologic validity of RCM simulations, the potential uses and limitations of these RCM datasets could be evaluated in many ways. For example, these datasets can be used to model the potential evapotranspiration, and then outputs can be compared against actual values.

Appendix A

The statistical testing performed at different sites showed that the rainfall properties show similar trends for all site studied. Therefore, when the difference is small between the sites, results for only two or more selected sites that highlight the differences were only presented in the text in previous chapters. This section presents the results for the sites that were not discussed in detail in previous sections.

A.1 Chapter 6 - Section 6.2

Cumulative probability distributions for the uncorrected and bias-corrected fortnightly to yearly averaged rainfall for the Williams River site are presented in Figures A.1 and A.2.

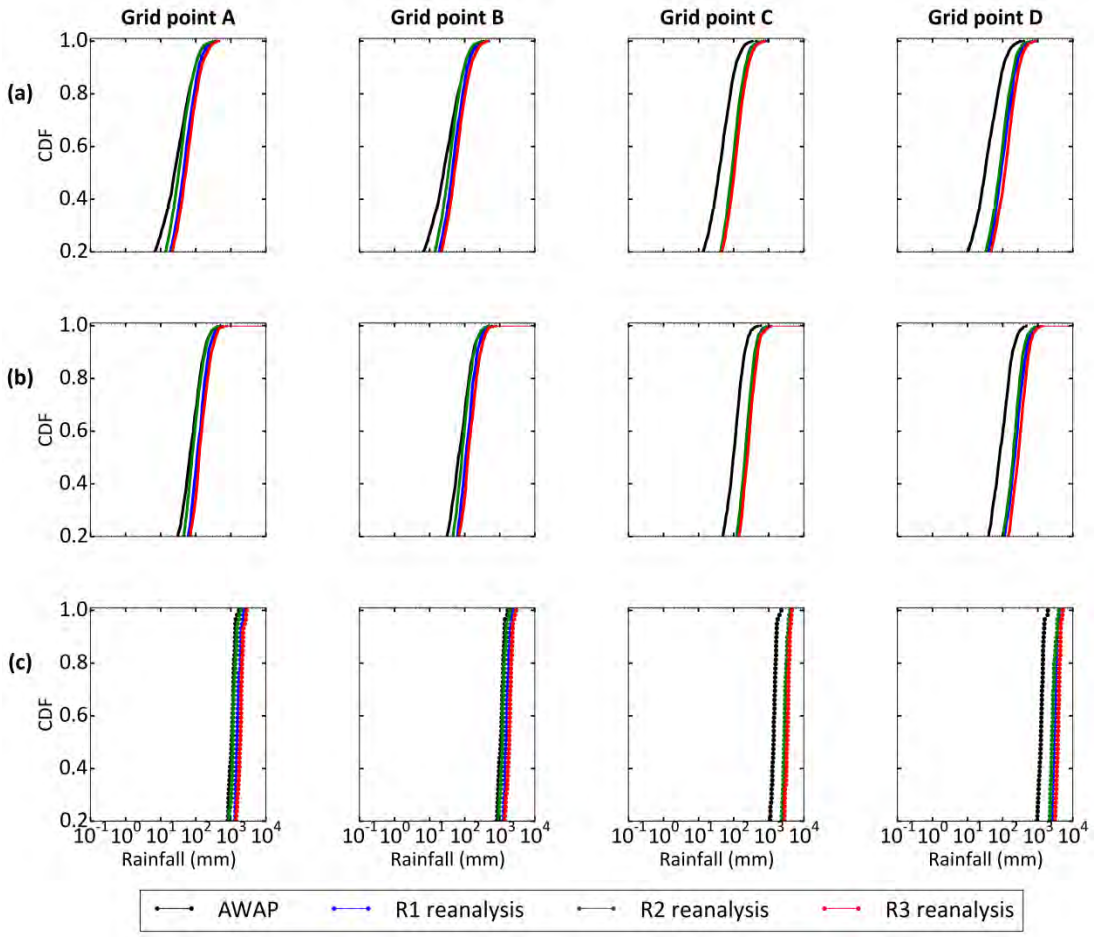

Figure A. 15.1 Cumulative probability distributions of uncorrected reanalyses and AWAP across the Williams River site for (a) fortnightly, (b) monthly and (c) annual resolutions at grid points A, B, C and D. Note that daily rainfall are in log scale and only values greater than 0.2 mm are plotted.

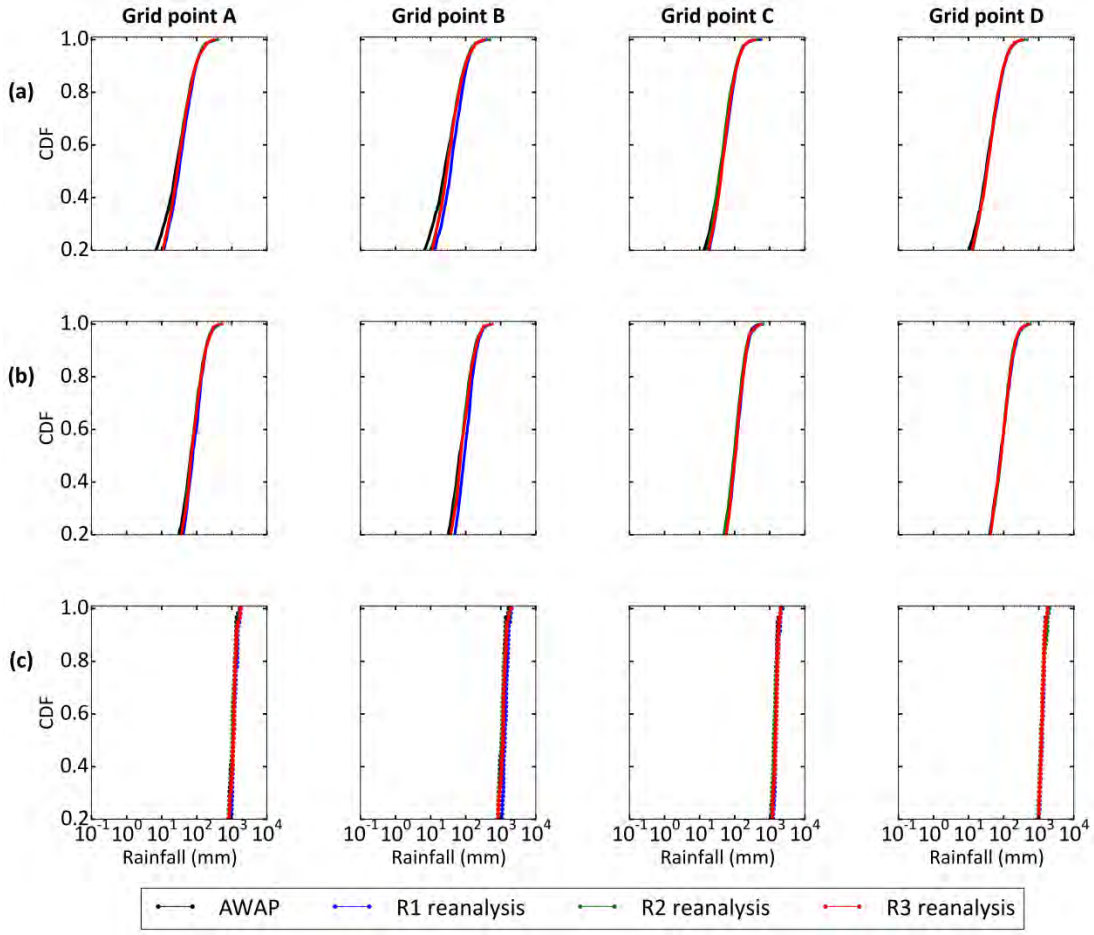

Figure A. 15.2 Cumulative probability distributions of bias corrected reanalyses and AWAP across the Williams River site for (a) fortnightly, (b) monthly and (c) annual resolutions at grid points A, B, C and D. Note that daily rainfall are in log scale and only values greater than 0.2 mm are plotted.

A.2 Chapter 9 - Section 9.2

The CDFs of the mean annual and daily rainfall for Richmond River and Sydney sites are presented in Figures A.3 to A.10.

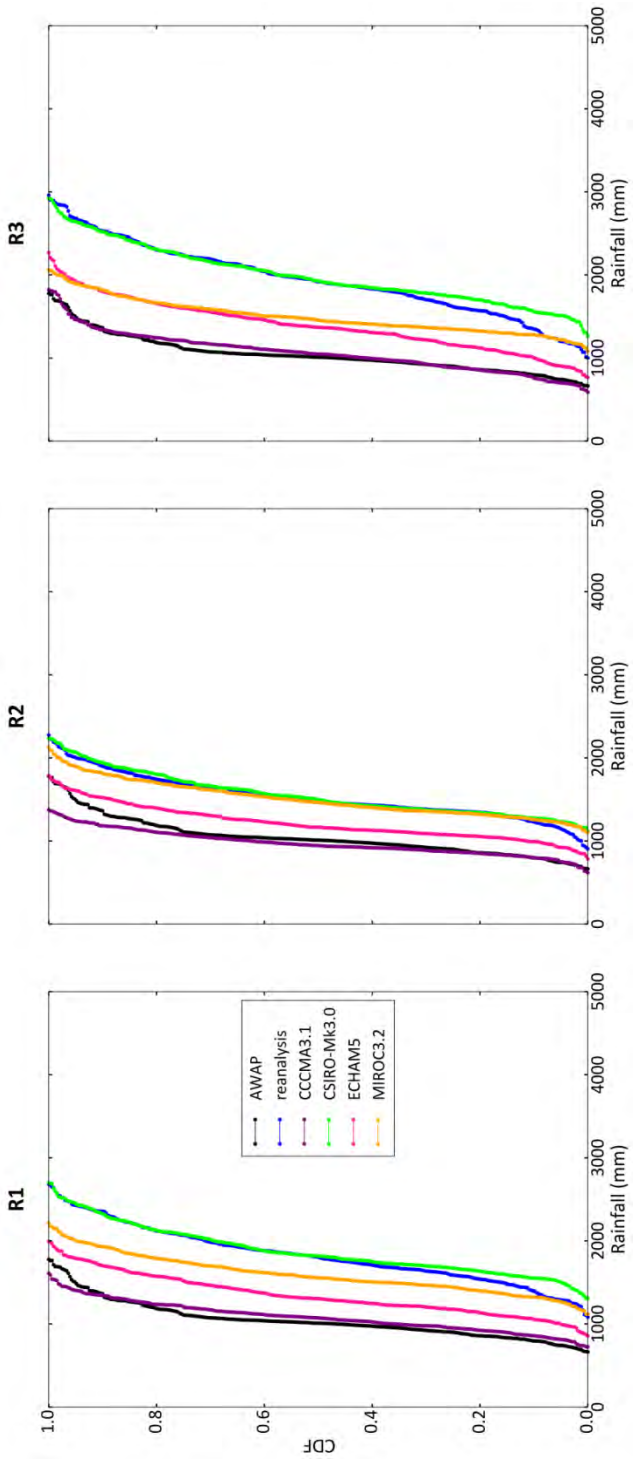

Figure A. 15.3 Cumulative probability distributions of mean annual rainfall of uncorrected NARCliM GCMs and AWAP across the Richmond River site. R1, R2 and R3 (columns) are three RCM configurations

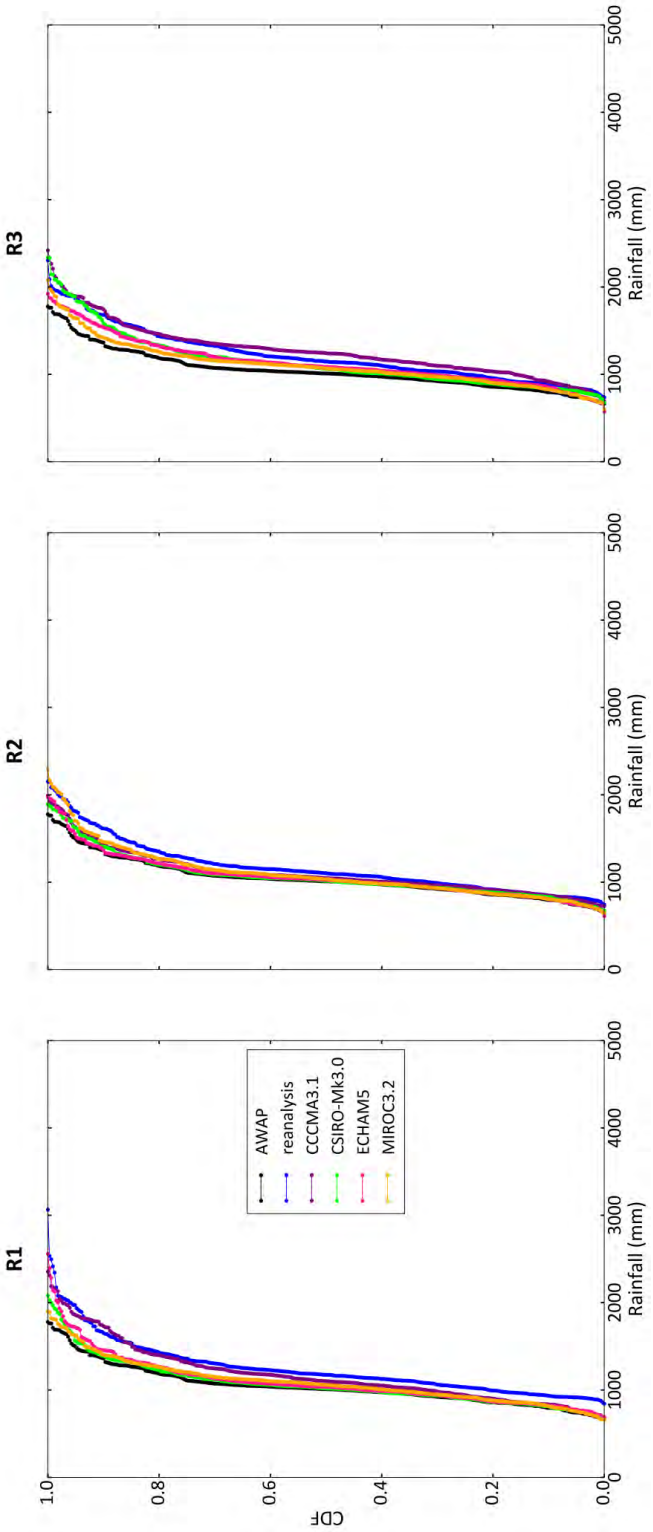

Figure A.15.4 Cumulative probability distributions of mean annual rainfall of bias corrected NARCliM GCMs and AWAP across the Richmond River site. R1, R2 and R3 (columns) are three RCM configurations

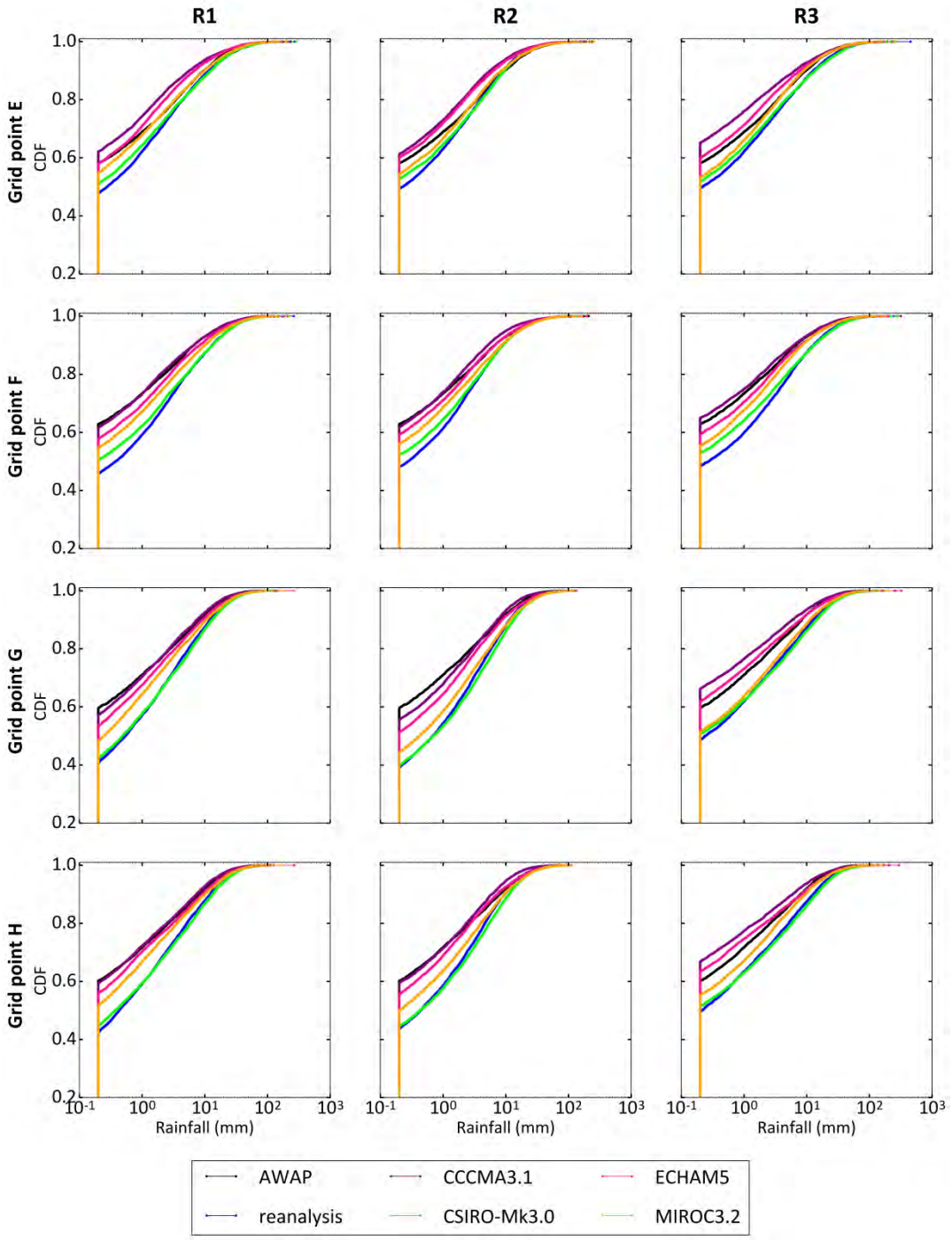

Figure A.15.5 Cumulative probability distributions of daily rainfall of uncorrected NARCliM GCMs and AWAP at Grid point E, F, G and H of Richmond River site. Note that daily rainfall is in log scale and only values greater than 0.2 mm are plotted. Points E and F are low elevation, G and H high elevation.

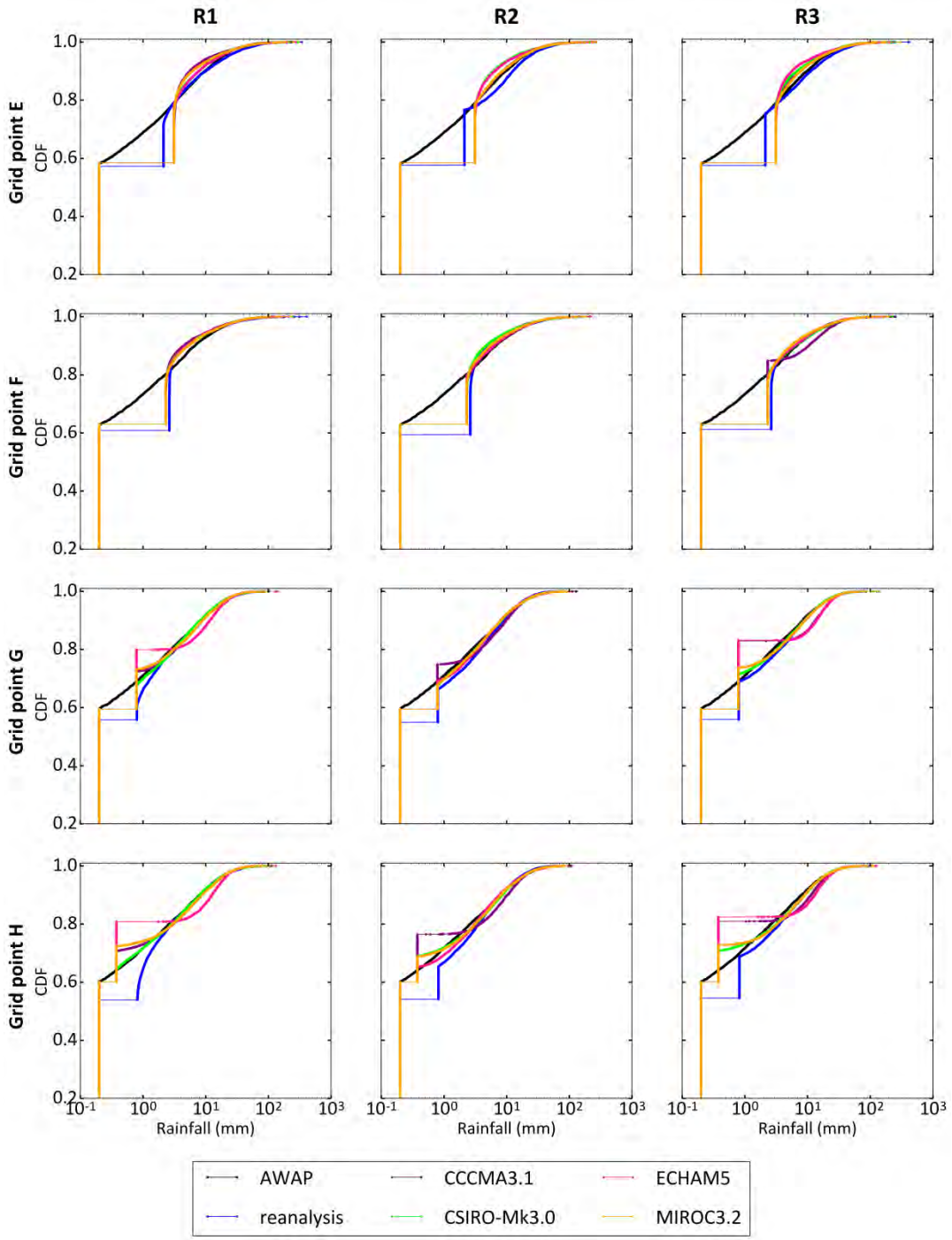

Figure A.15.6 Cumulative probability distributions of daily rainfall of bias corrected NARCliM GCMs and AWAP at Grid point E, F, G and H of Richmond River site. Note that daily rainfall is in log scale and only values greater than 0.2 mm are plotted. Points E and F are low elevation, G and H high elevation.

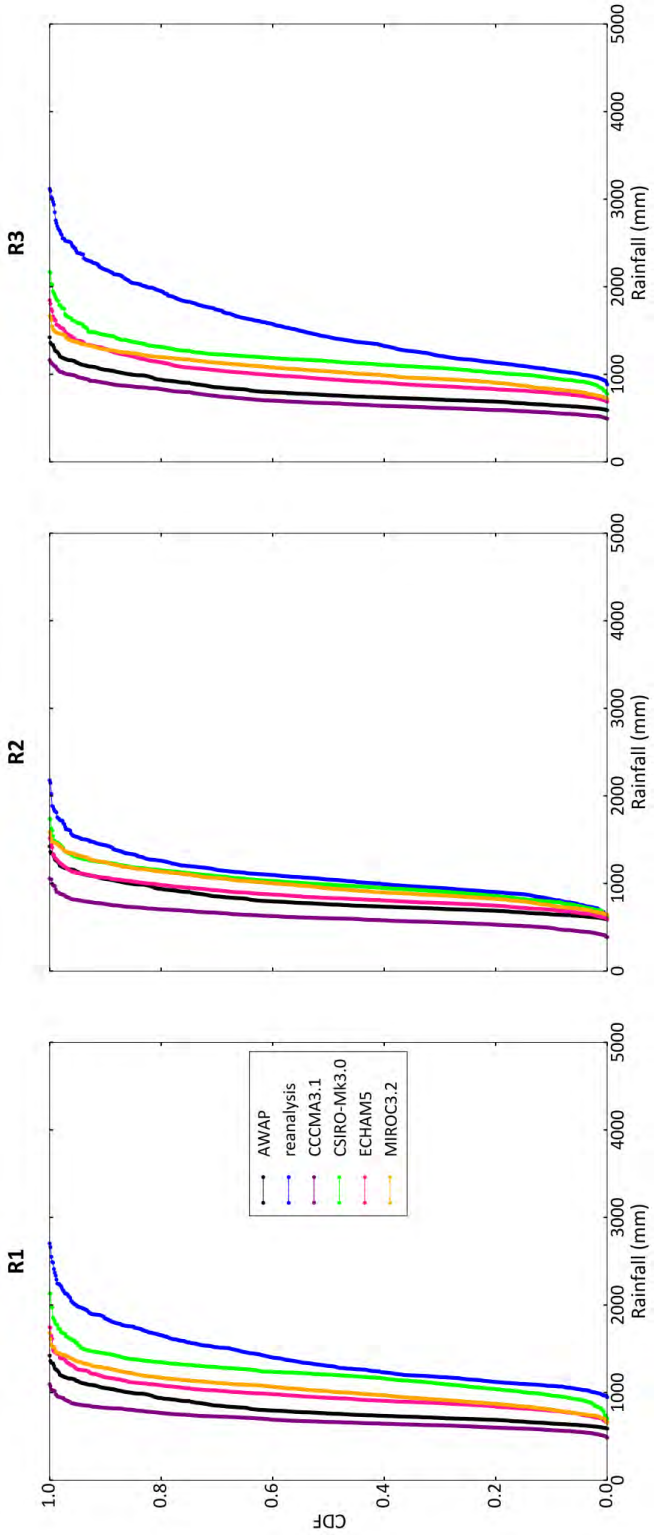

Figure A.15.7 Cumulative probability distributions of mean annual rainfall of uncorrected NARCliM GCMs and AWAP across the Sydney site. R1, R2 and R3 (columns) are three RCM configurations

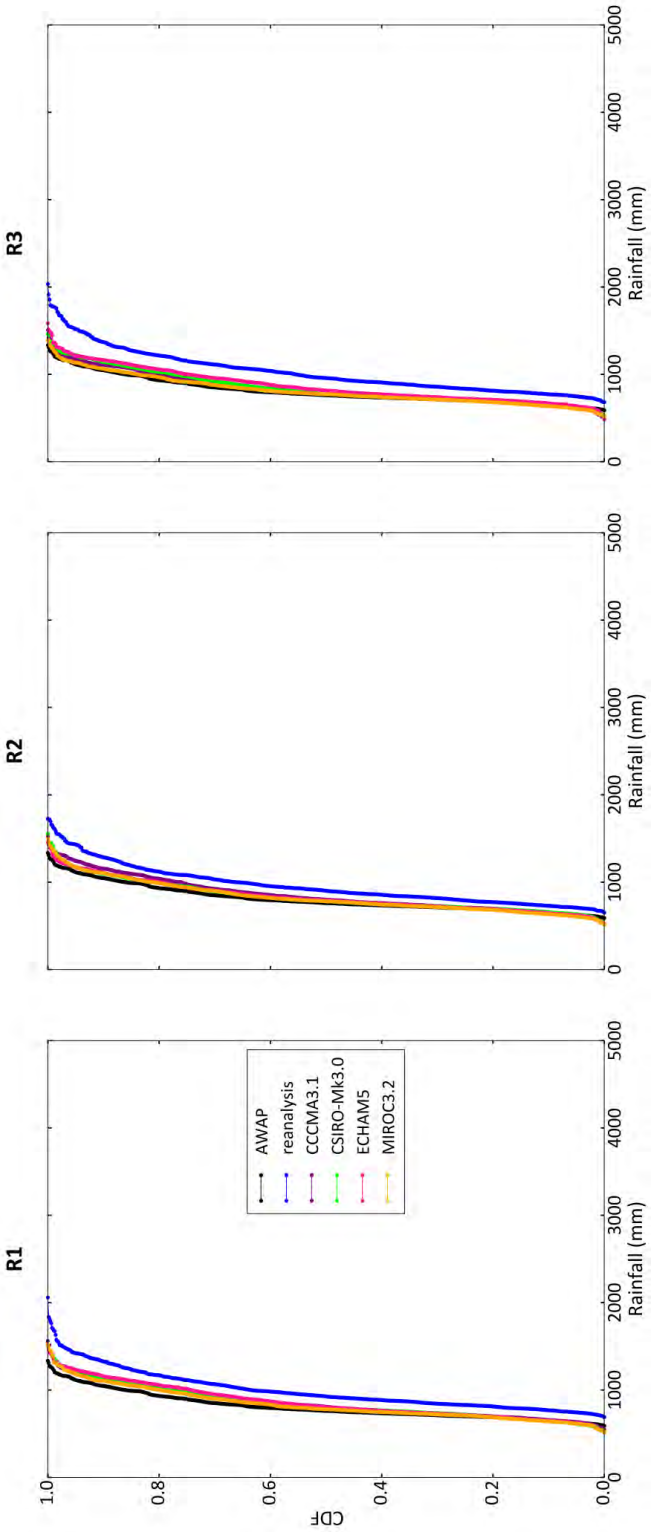

Figure A.15.8 Cumulative probability distributions of mean annual rainfall of bias corrected NARCliM GCMs and AWAP across the Sydney site. R1, R2 and R3 (columns) are three RCM configurations

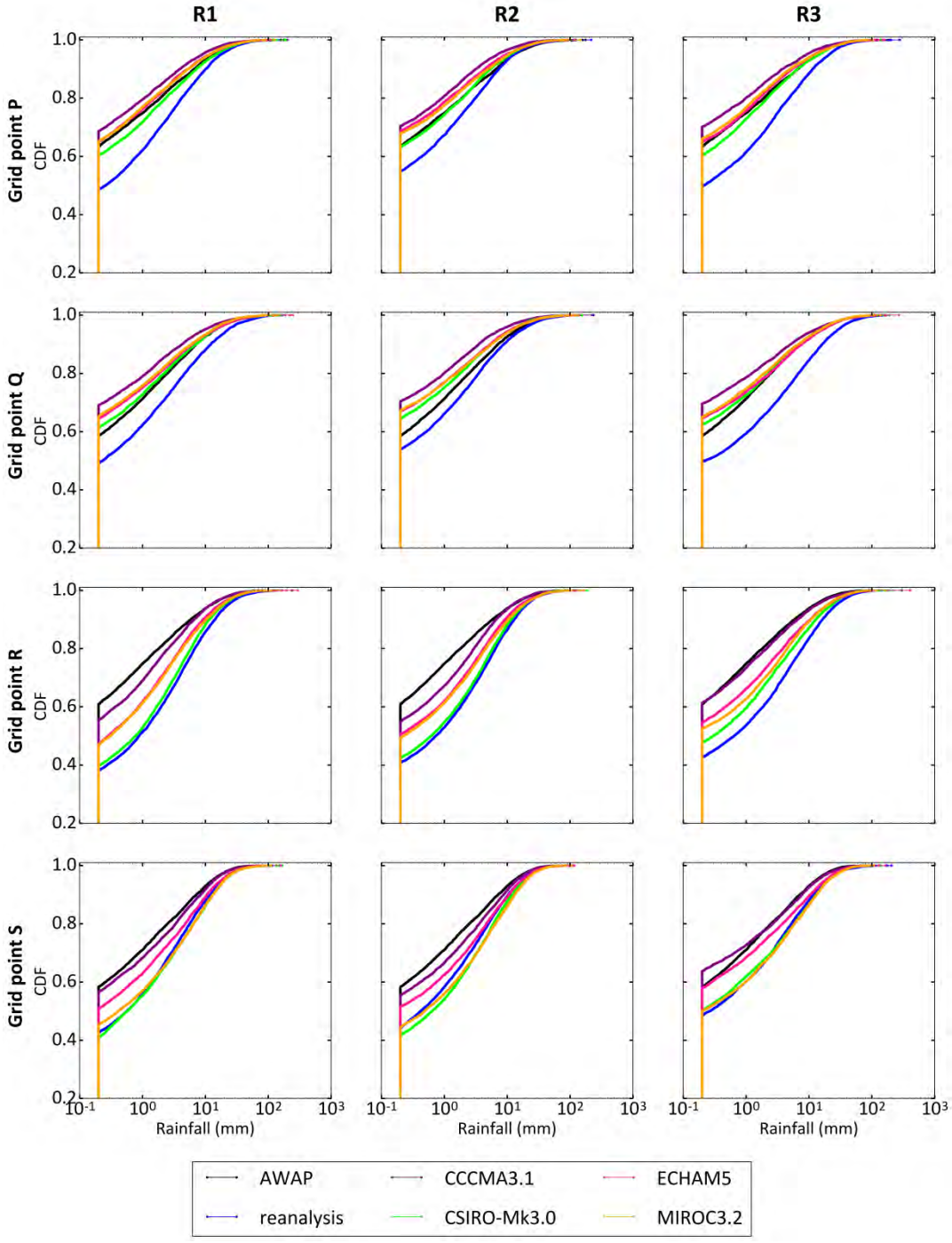

Figure A.15.9 Cumulative probability distributions of daily rainfall of uncorrected NARCliM GCMs and AWAP at Grid point P, Q, R and S of Sydney site. Note that daily rainfall is in log scale and only values greater than 0.2 mm are plotted. Points P and Q are low elevation, R and S high elevation.

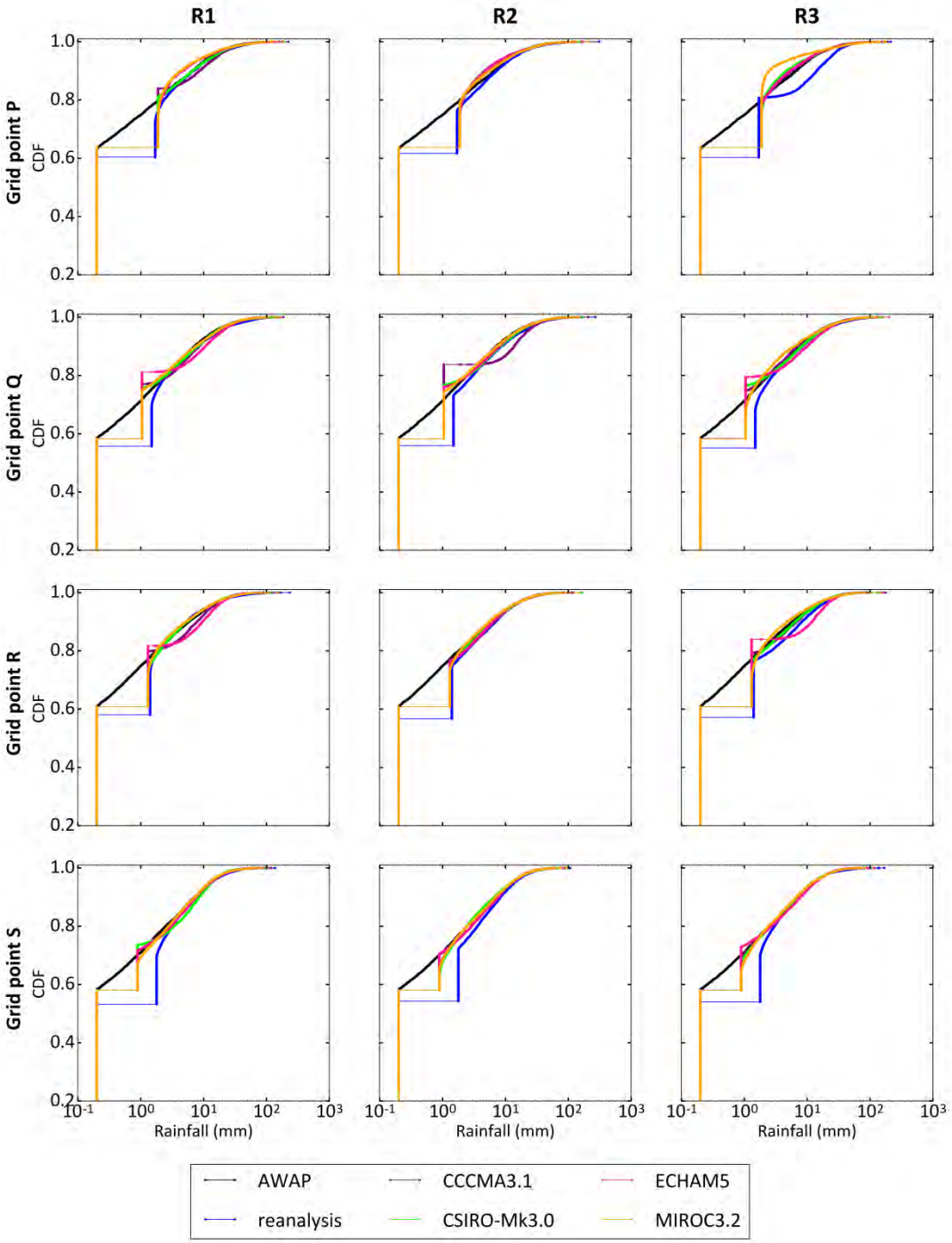

Figure A.15.10 Cumulative probability distributions of daily rainfall of bias corrected NARCliM GCMs and AWAP at Grid point P, Q, R and S of Sydney site. Note that daily rainfall is in log scale and only values greater than 0.2 mm are plotted. Points P and Q are low elevation, R and S high elevation.

A.3 Chapter 10 - Section 10.2

The mean annual rainfall of uncorrected reanalyses and AWAP for the Bega River and Sydney sites are shown in Figures A.11 to A.12.

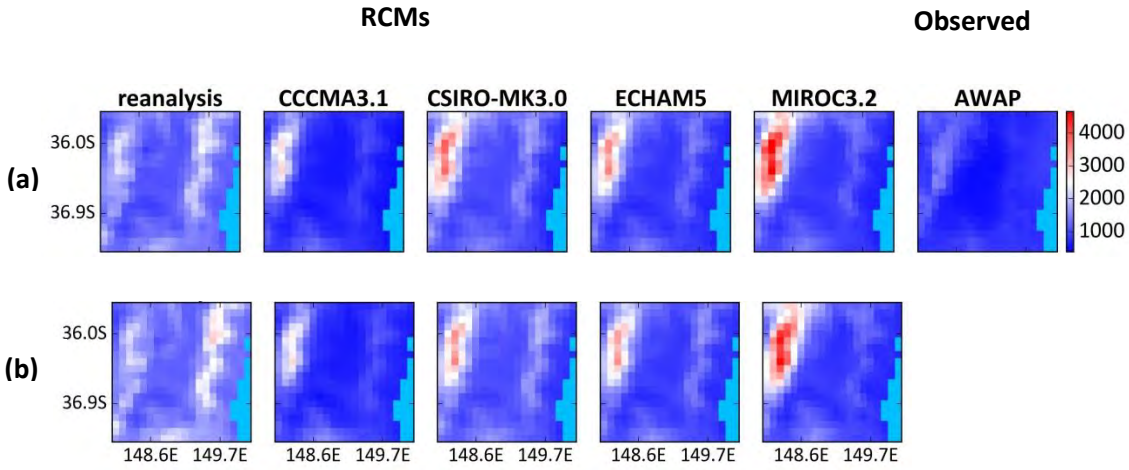

Figure A.15.11 Spatial distribution of the mean annual rainfall (1990-2009) of the Bega River site: The plots are for the uncorrected simulations of (a) R1 and (b) R3, and AWAP.

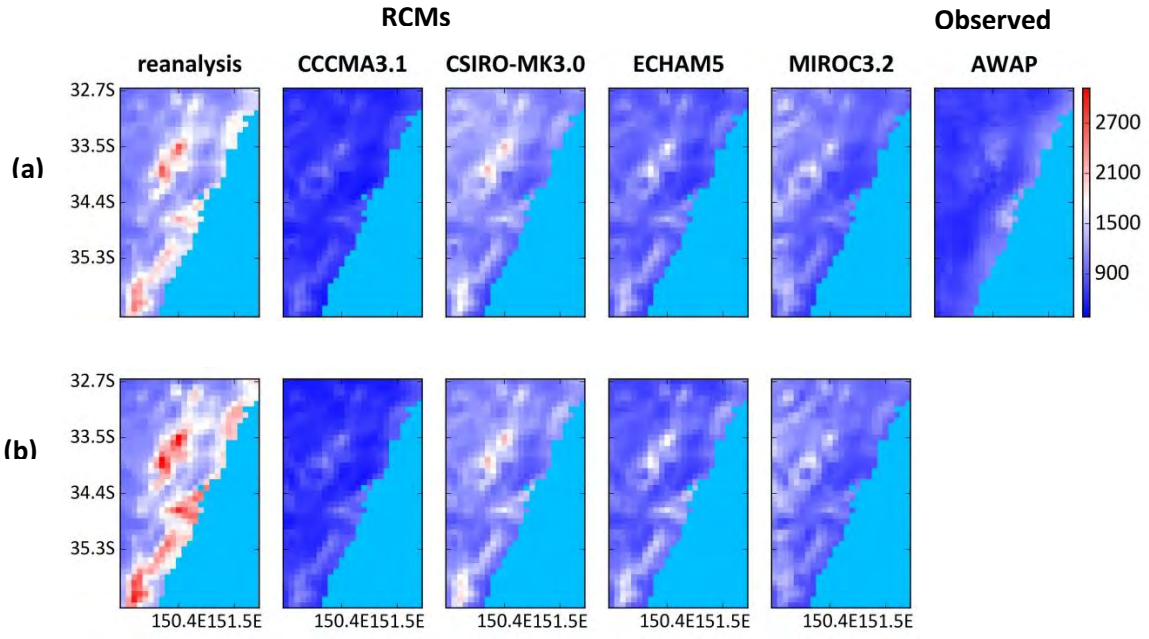

Figure A.15.12 Spatial distribution of the mean annual rainfall (1990-2009) of the Sydney site: The plots are for the uncorrected simulations of (a) R1 and (b) R3, and AWAP.

A.4 Chapter 10, Section 10.2.3

The spatial variability of C_v of the uncorrected and bias corrected NARCliM RCMs compared with AWAP for the Williams River and Bega River sites are shown in Figures A.13 to A.24.

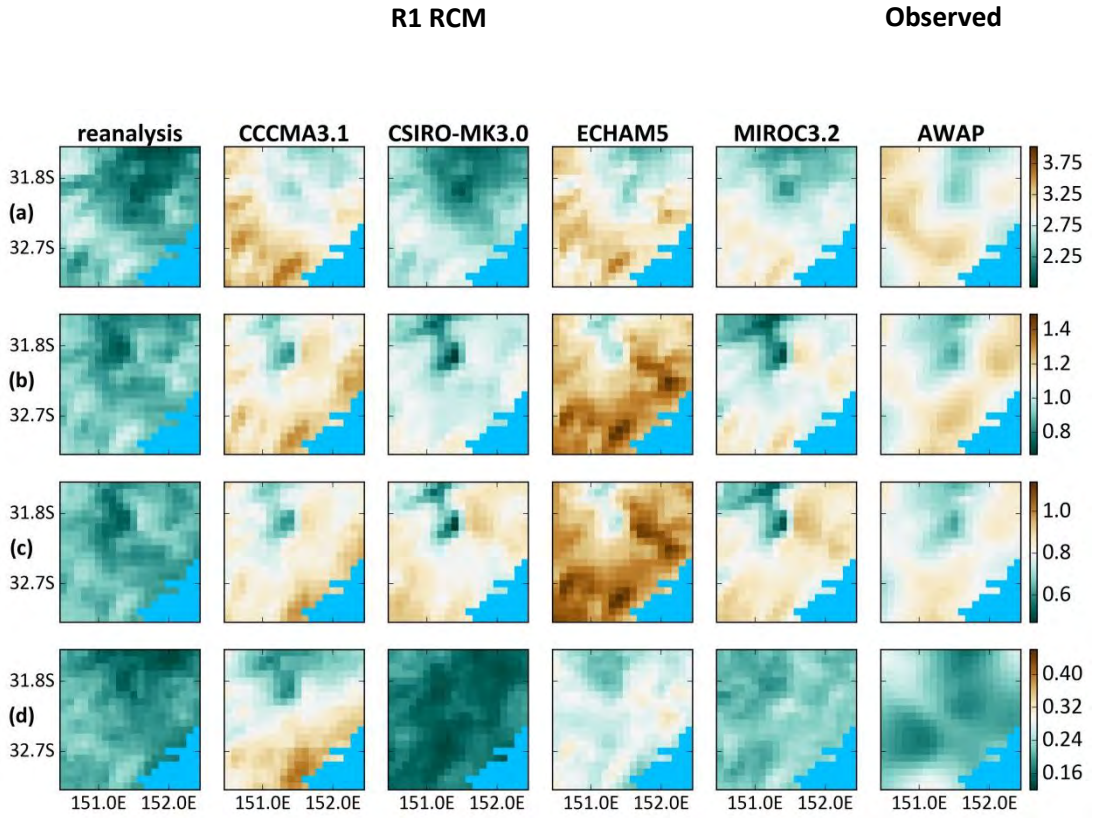

Figure A.15.13 Spatial distribution of the C_v of the rainfall (1990-2009) of the Williams River site: The plots are for the uncorrected simulations of R1, and AWAP. Time resolutions are; (a) daily, (b) fortnightly, (c) monthly, and (d) annual.

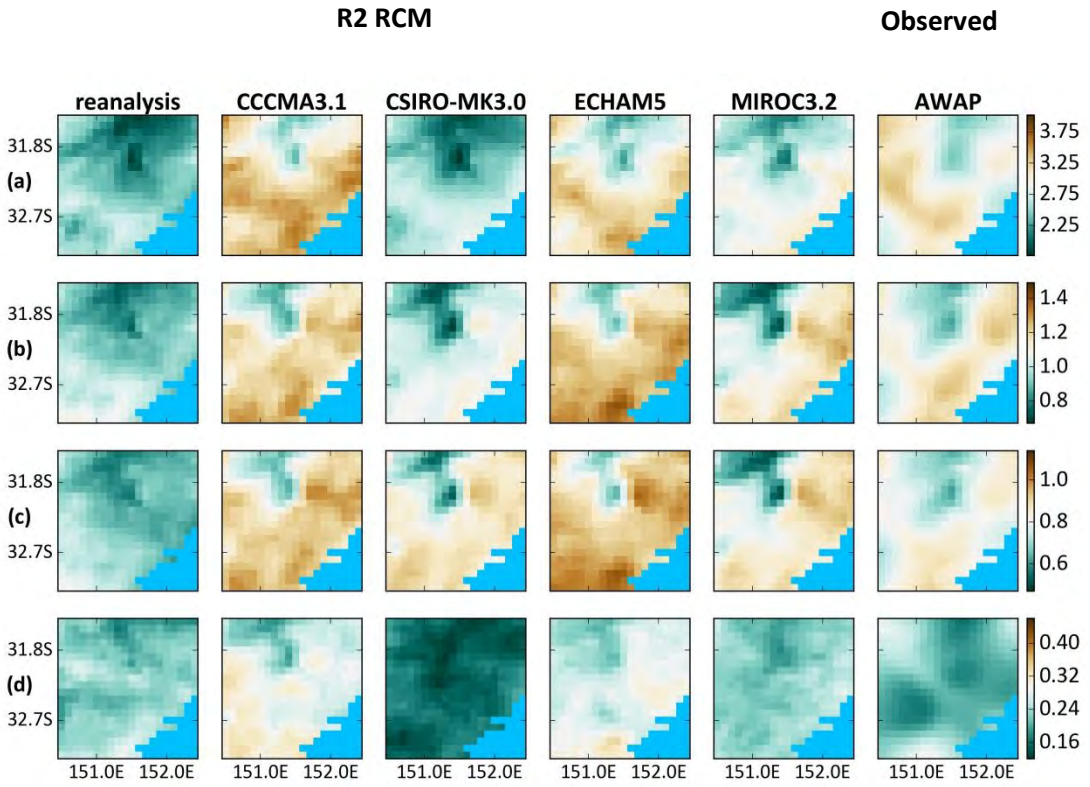

Figure A.15.14 Spatial distribution of the C_v of the rainfall (1990-2009) of the Williams River site: The plots are for the uncorrected simulations of R2, and AWAP. Time resolutions are; (a) daily, (b) fortnightly, (c) monthly, and (d) annual.

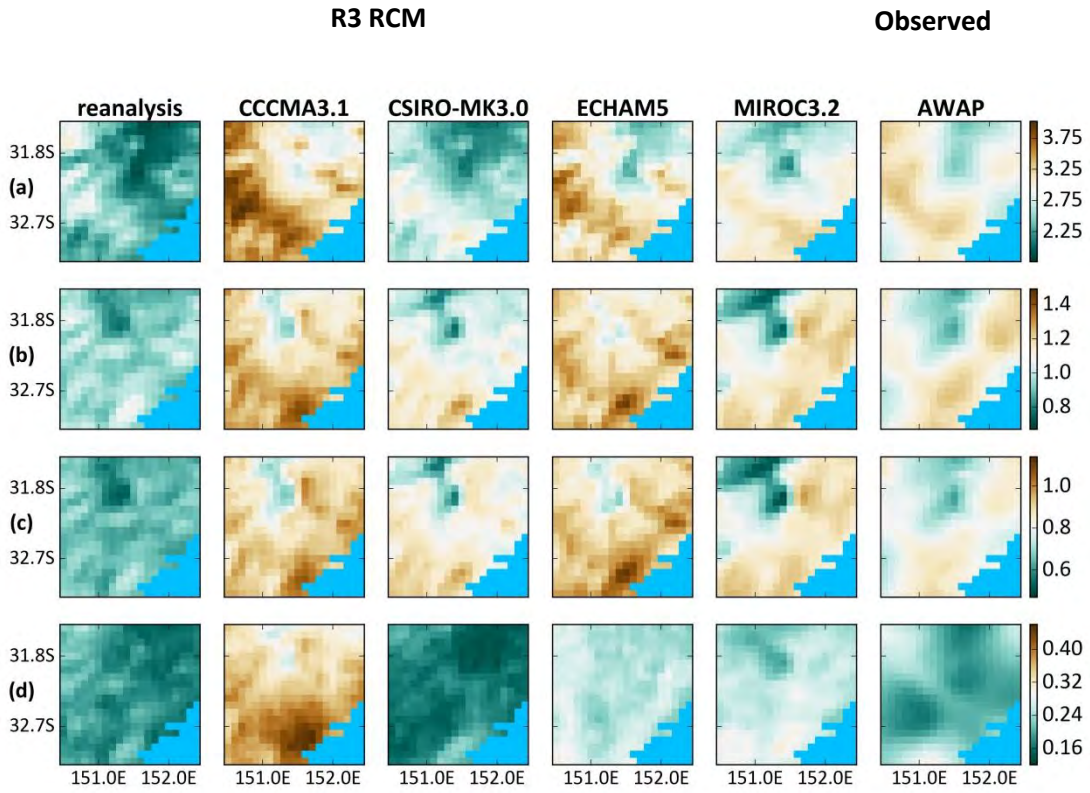

Figure A.15.15 Spatial distribution of the C_v of the rainfall (1990-2009) of the Williams River site: The plots are for the uncorrected simulations of R3, and AWAP. Time resolutions are; (a) daily, (b) fortnightly, (c) monthly, and (d) annual.

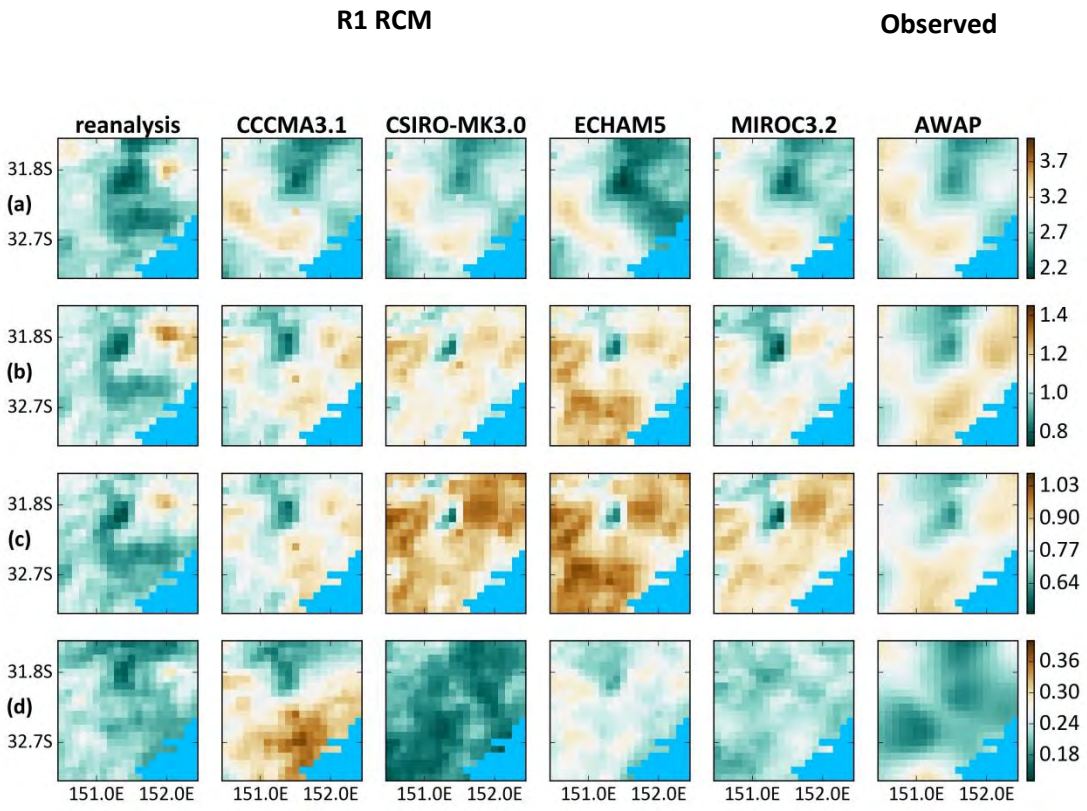

Figure A.15.16 Spatial distribution of the C_v of the rainfall (1990-2009) of the Williams River site: The plots are for the bias corrected simulations of R1, and AWAP. Time resolutions are; (a) daily, (b) fortnightly, (c) monthly, and (d) annual.

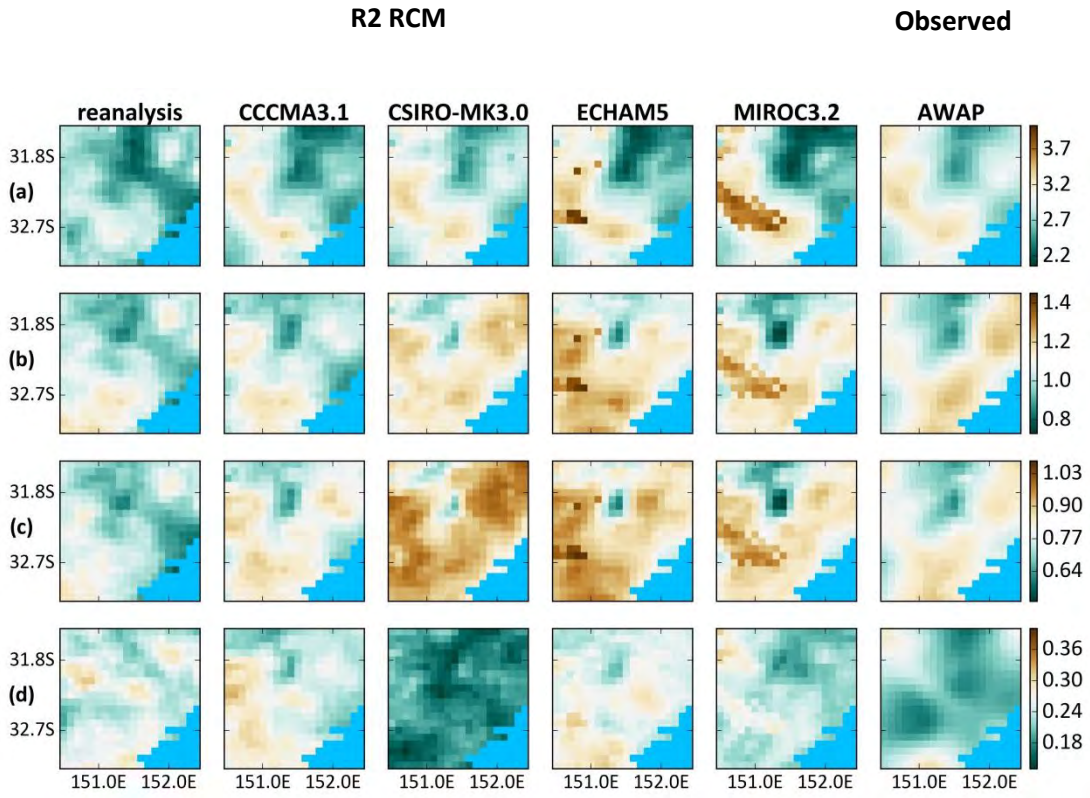

Figure A.15.17 Spatial distribution of the C_v of the rainfall (1990-2009) of the Williams River site: The plots are for the bias corrected simulations of R2, and AWAP. Time resolutions are; (a) daily, (b) fortnightly, (c) monthly, and (d) annual.

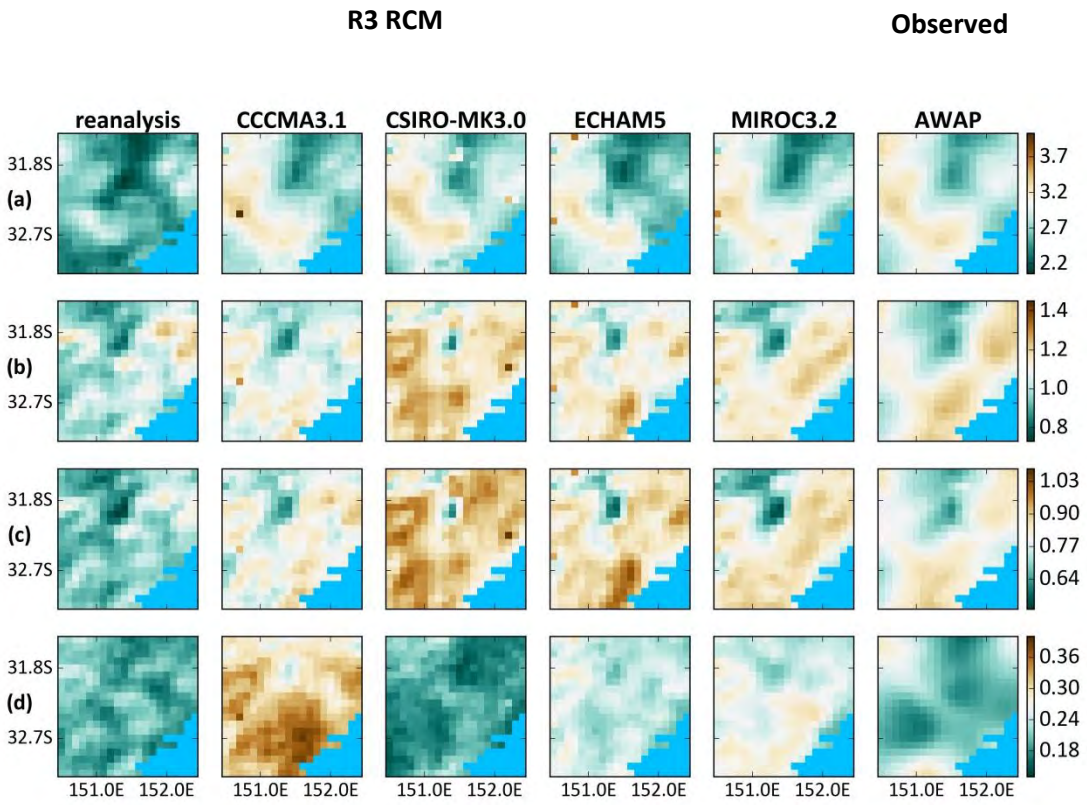

Figure A.15.18 Spatial distribution of the C_v of the rainfall (1990-2009) of the Williams River site: The plots are for the bias corrected simulations of R3, and AWAP. Time resolutions are; (a) daily, (b) fortnightly, (c) monthly, and (d) annual.

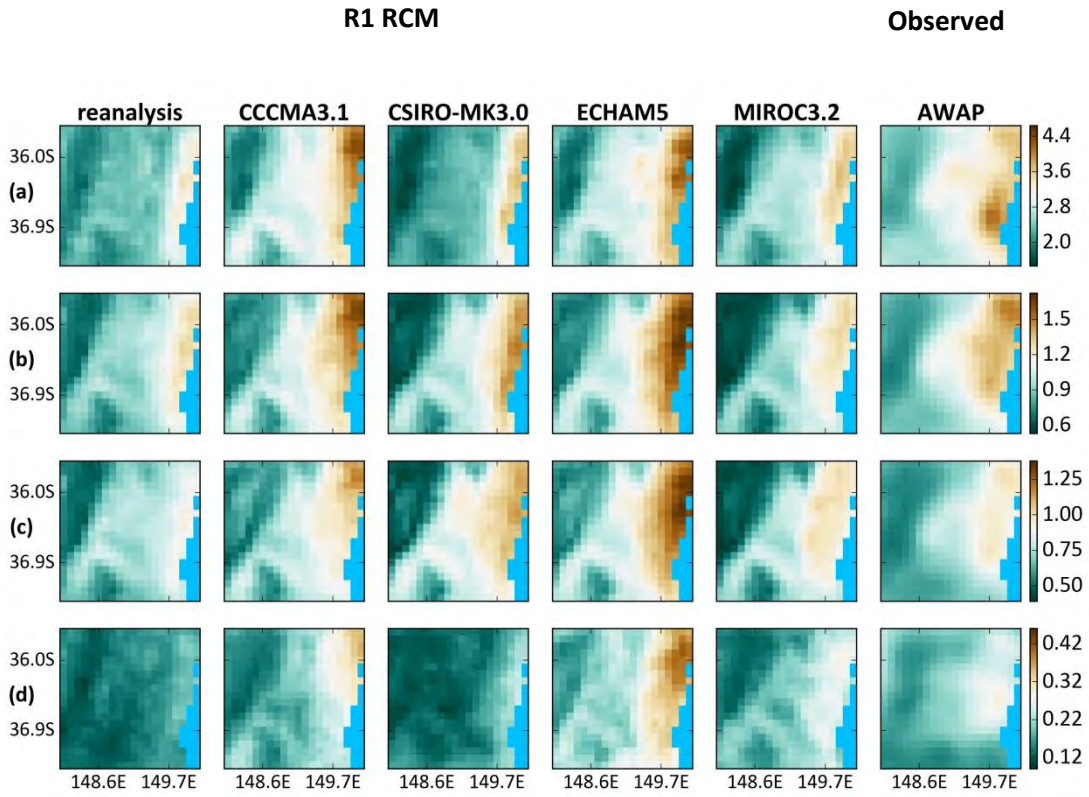

Figure A.15.19 Spatial distribution of the C_v of the rainfall (1990-2009) of the Bega River site: The plots are for the uncorrected simulations of R1, and AWAP. Time resolutions are; (a) daily, (b) fortnightly, (c) monthly, and (d) annual.

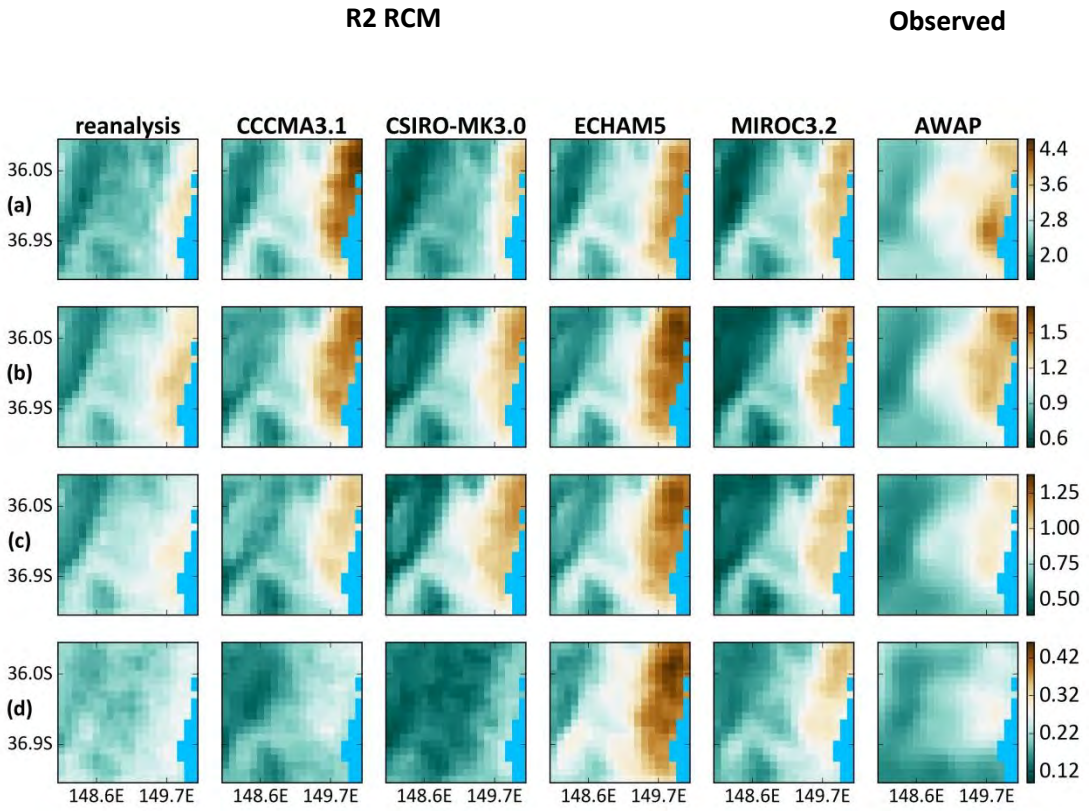

Figure A.15.20 Spatial distribution of the C_v of the rainfall (1990-2009) of the Bega River site: The plots are for the uncorrected simulations of R2, and AWAP. Time resolutions are; (a) daily, (b) fortnightly, (c) monthly, and (d) annual.

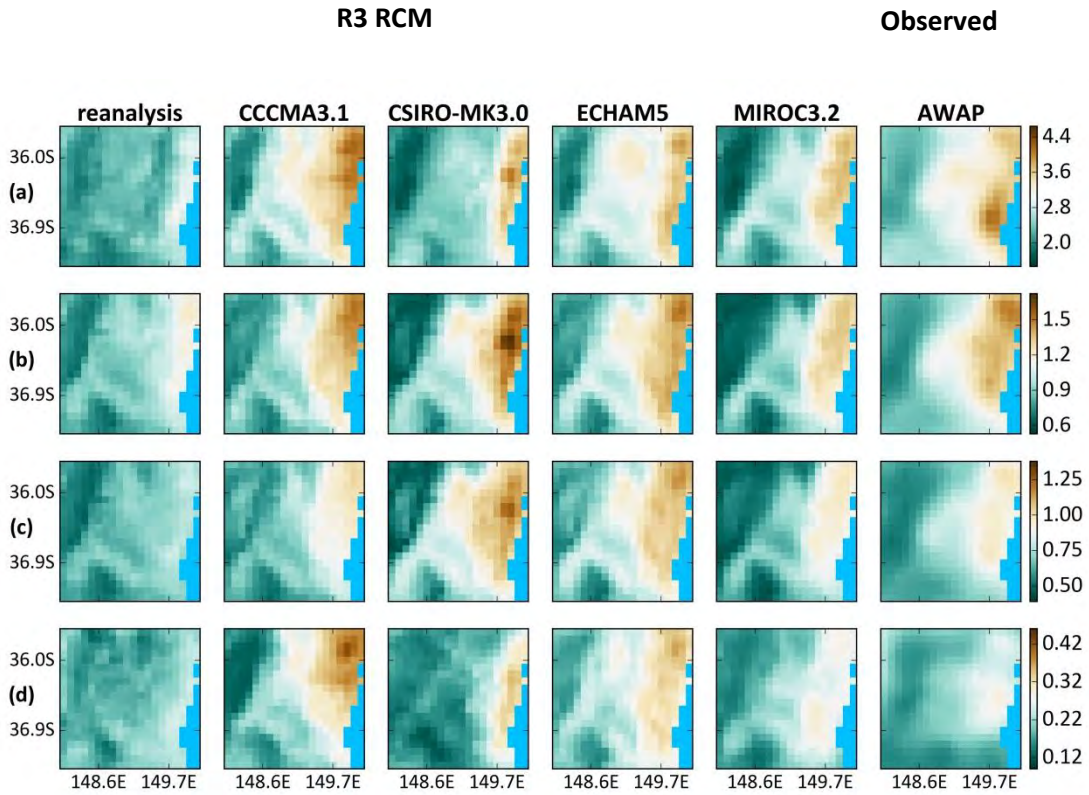

Figure A.15.21 Spatial distribution of the C_v of the rainfall (1990-2009) of the Bega River site: The plots are for the uncorrected simulations of R3, and AWAP. Time resolutions are; (a) daily, (b) fortnightly, (c) monthly, and (d) annual.

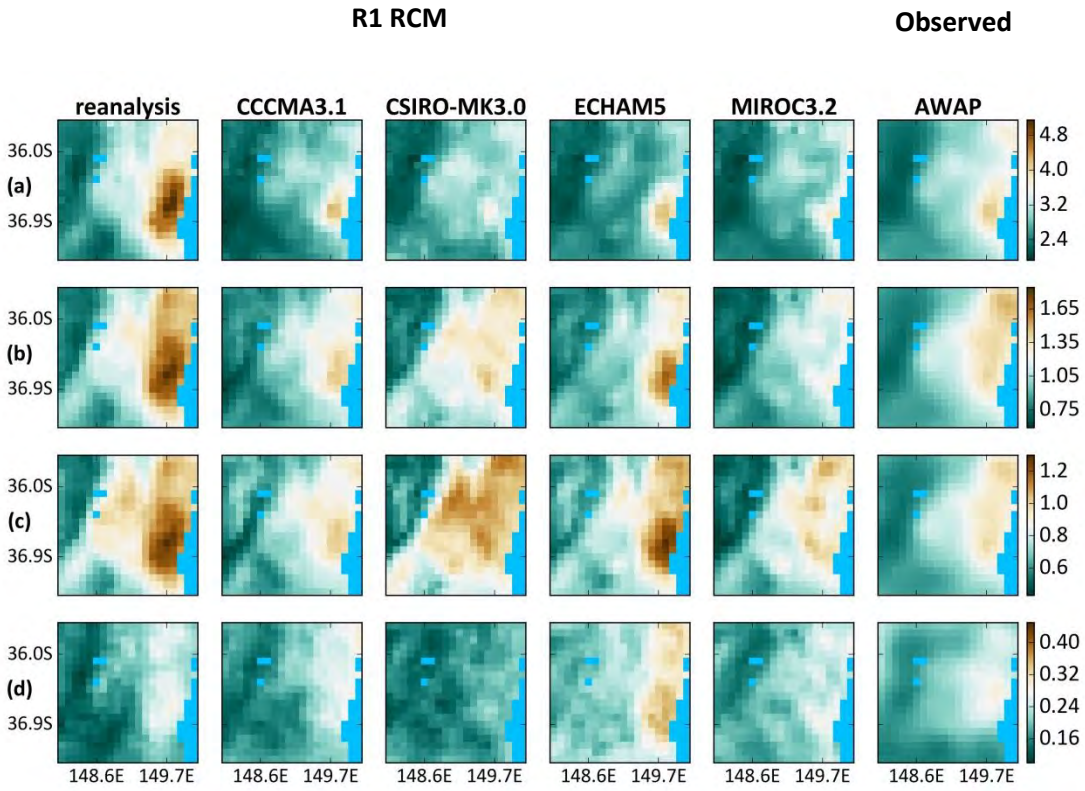

Figure A.15.22 Spatial distribution of the C_v of the rainfall (1990-2009) of the Bega River site: The plots are for the bias corrected simulations of R1, and AWAP. Time resolutions are; (a) daily, (b) fortnightly, (c) monthly, and (d) annual.

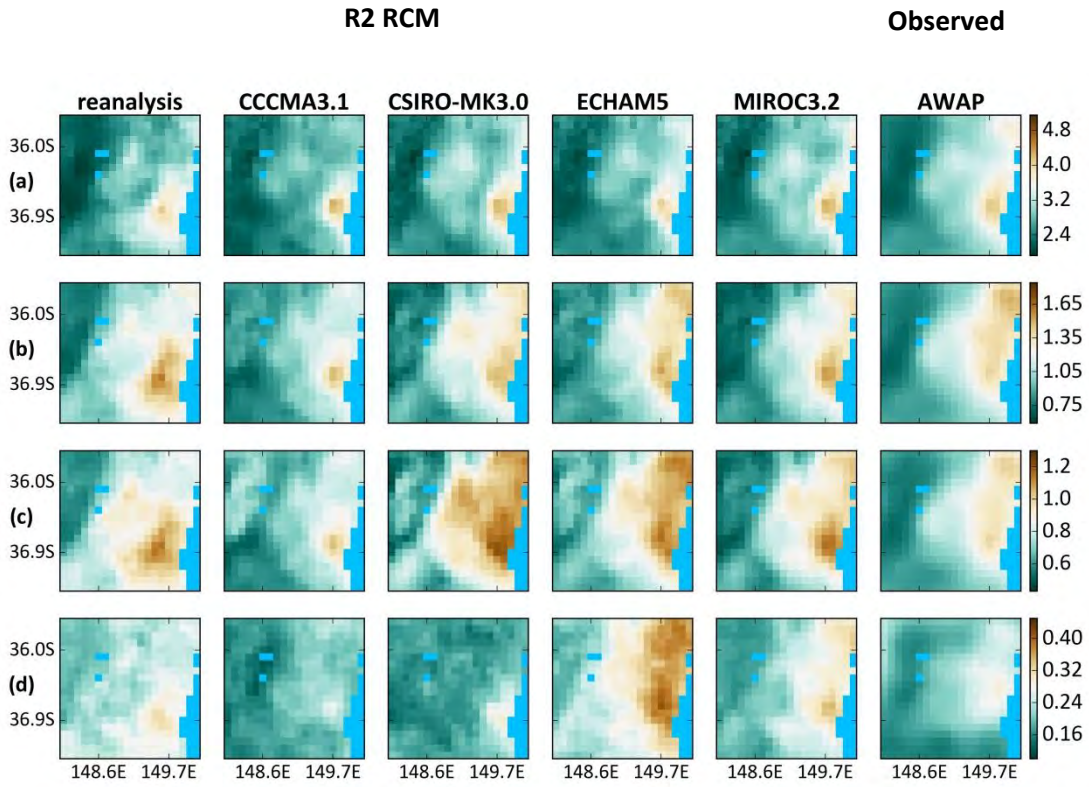

Figure A.15.23 Spatial distribution of the C_v of the rainfall (1990-2009) of the Bega River site: The plots are for the bias corrected simulations of R2, and AWAP. Time resolutions are; (a) daily, (b) fortnightly, (c) monthly, and (d) annual.

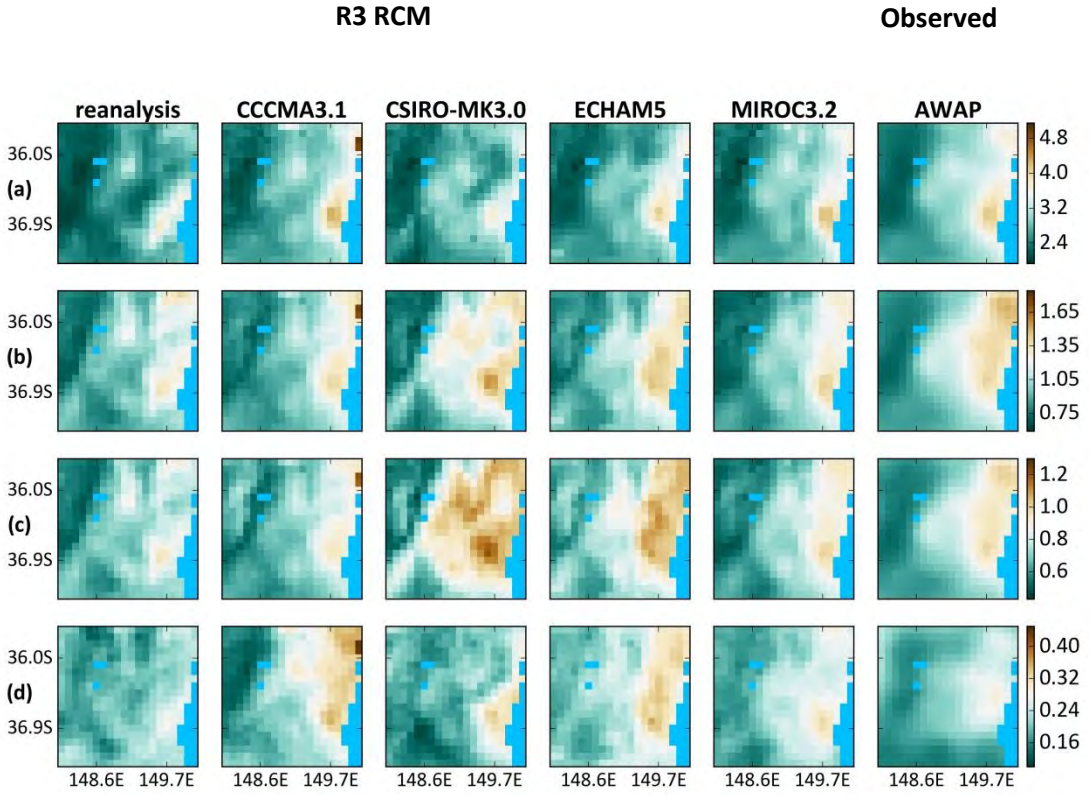

Figure A.15.24 Spatial distribution of the C_v of the rainfall (1990-2009) of the Bega River site: The plots are for the bias corrected simulations of R3, and AWAP. Time resolutions are; (a) daily, (b) fortnightly, (c) monthly, and (d) annual.

A.5 Chapter 10 - Section 10.2.4

The spatial variability of lag-1 correlations of the uncorrected and bias corrected NARCliM RCMs compared with AWAP for the Williams River and Bega River sites are shown in Figures A.25 to A.36.

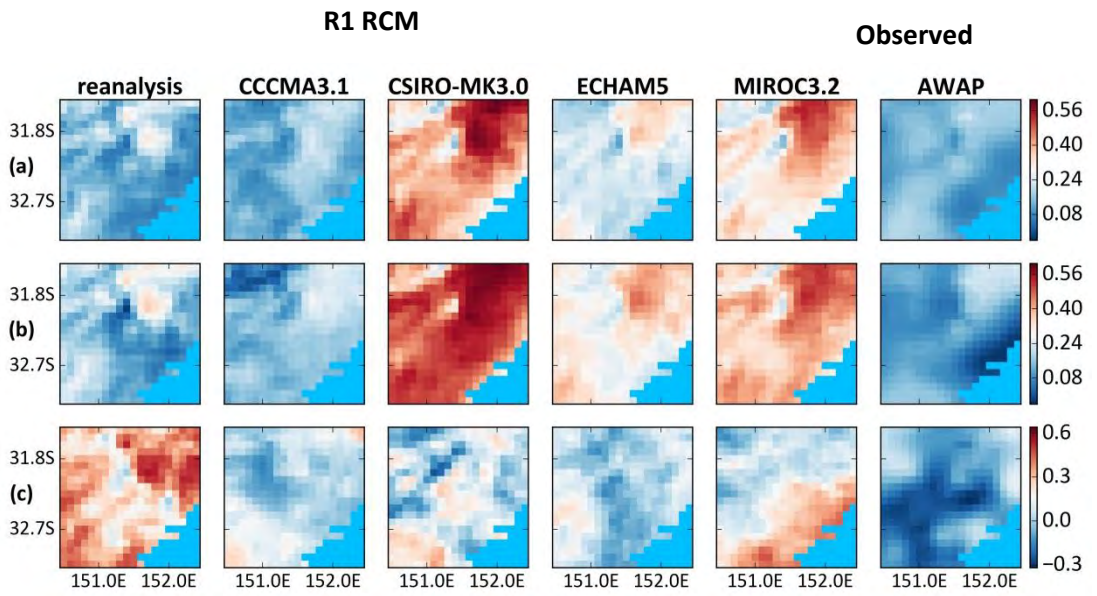

Figure A.15.25 Spatial distribution of the lag-1 autocorrelation of the rainfall (1990-2009) of the Williams River site: The plots are for the uncorrected simulations of R1, and AWAP. Time resolutions are; (a) fortnightly, (b) monthly, and (c) annual.

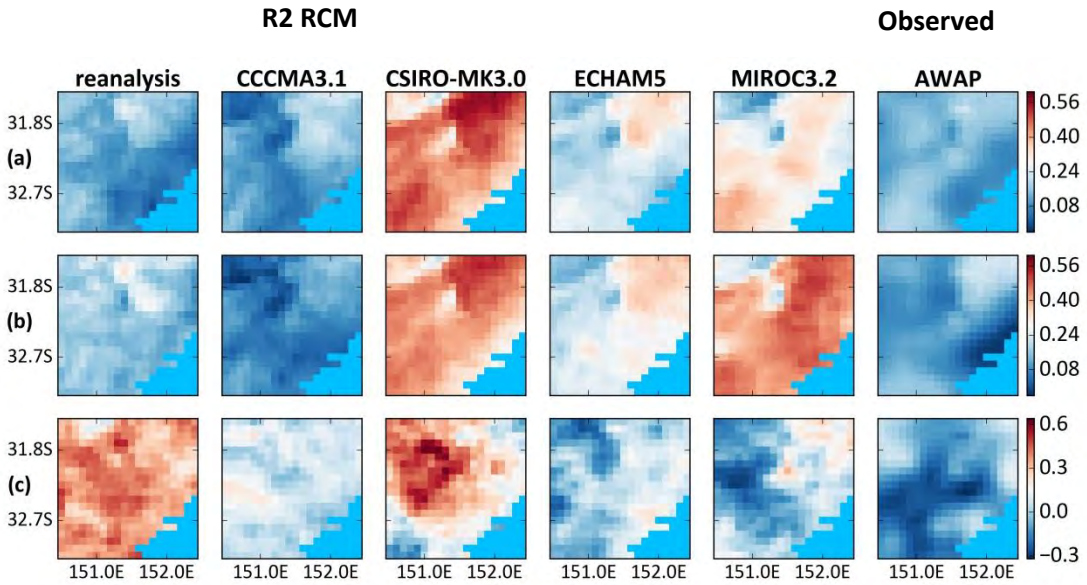

Figure A.15.26 Spatial distribution of the lag-1 autocorrelation of the rainfall (1990-2009) of the Williams River site: The plots are for the uncorrected simulations of R2, and AWAP. Time resolutions are; (a) fortnightly, (b) monthly, and (c) annual.

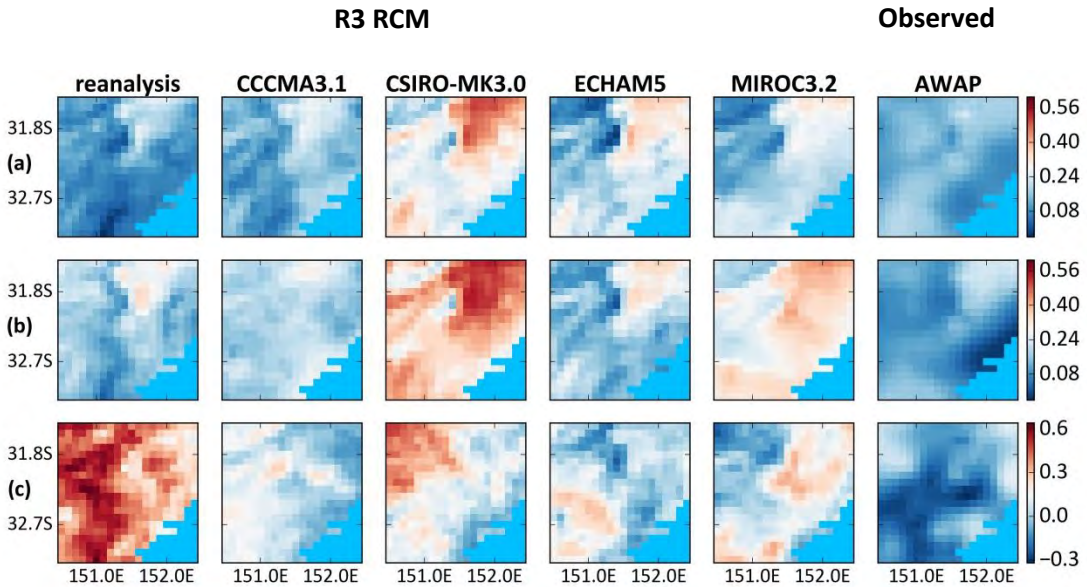

Figure A.15.27 Spatial distribution of the lag-1 autocorrelation of the rainfall (1990-2009) of the Williams River site: The plots are for the uncorrected simulations of R3, and AWAP. Time resolutions are; (a) fortnightly, (b) monthly, and (c) annual.

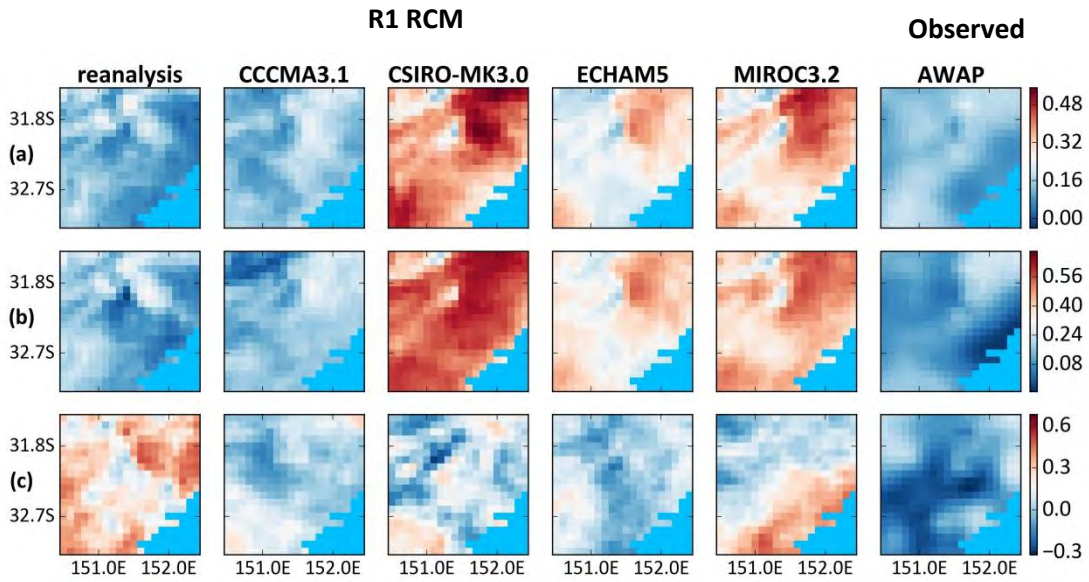

Figure A.15.28 Spatial distribution of the lag-1 autocorrelation of the rainfall (1990-2009) of the Williams River site: The plots are for the bias corrected simulations of R1, and AWAP. Time resolutions are; (a) fortnightly, (b) monthly, and (c) annual.

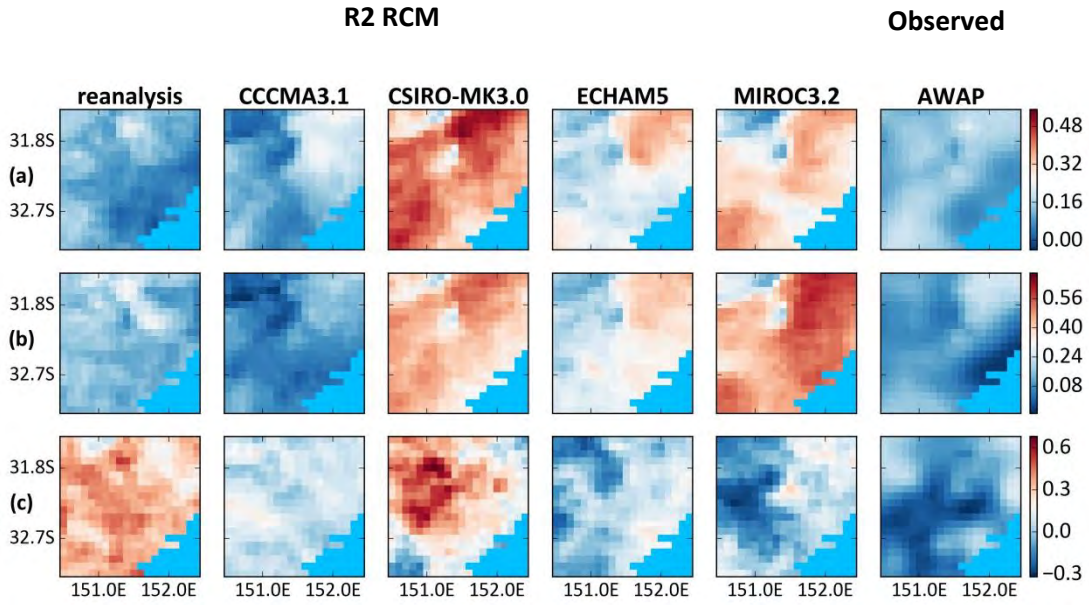

Figure A.15.29 Spatial distribution of the lag-1 autocorrelation of the rainfall (1990-2009) of the Williams River site: The plots are for the bias corrected simulations of R2, and AWAP. Time resolutions are; (a) fortnightly, (b) monthly, and (c) annual.

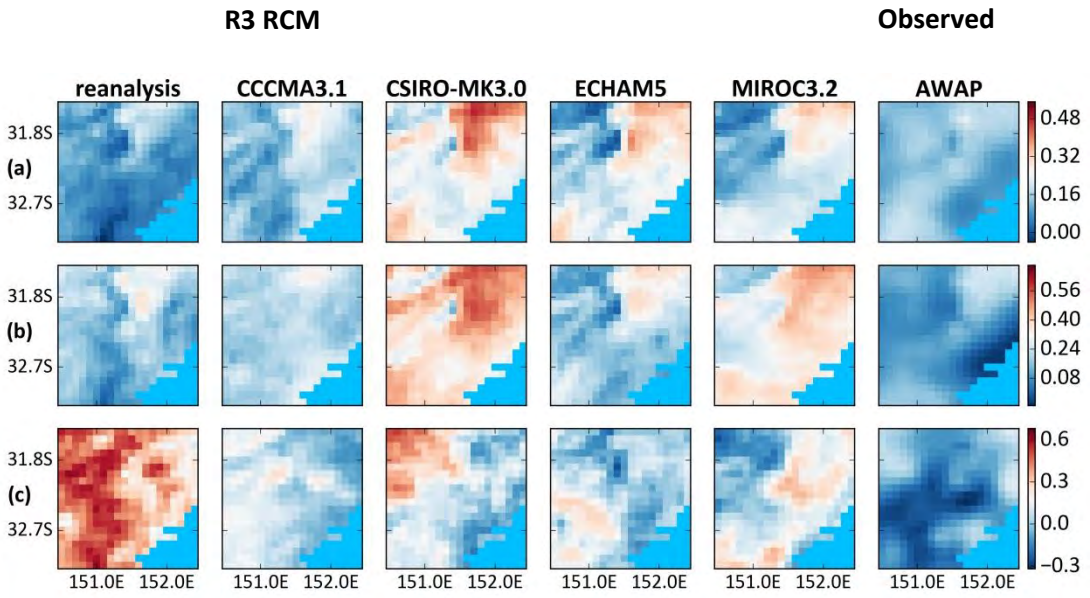

Figure A.15.30 Spatial distribution of the lag-1 autocorrelation of the rainfall (1990-2009) of the Williams River site: The plots are for the bias corrected simulations of R3, and AWAP. Time resolutions are; (a) fortnightly, (b) monthly, and (c) annual.

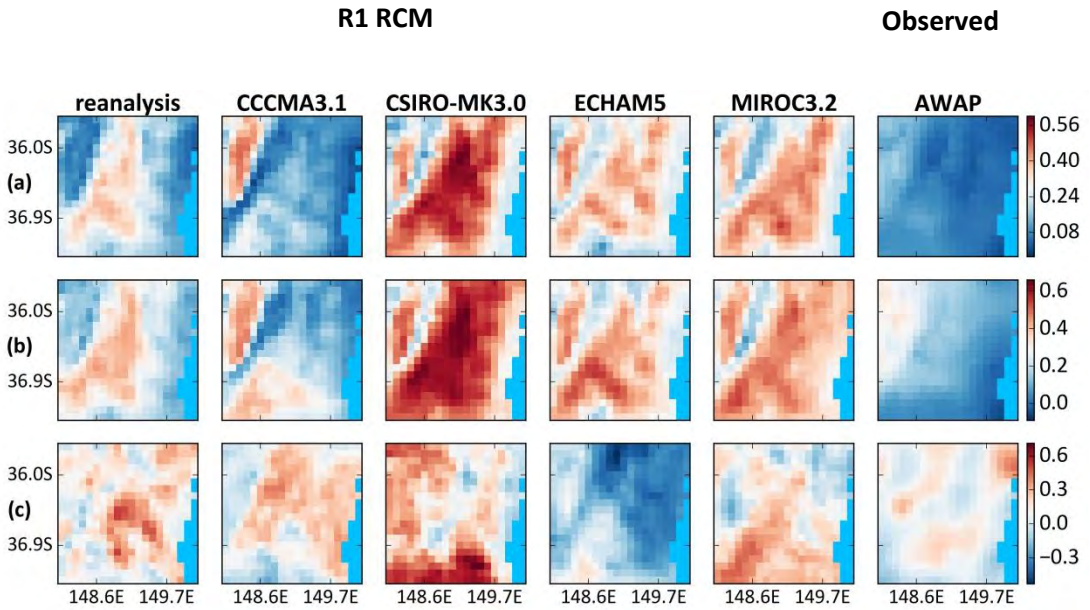

Figure A.15.31 Spatial distribution of the lag-1 autocorrelation of the rainfall (1990-2009) of the Bega River site: The plots are for the uncorrected simulations of R1, and AWAP. Time resolutions are; (a) fortnightly, (b) monthly, and (c) annual.

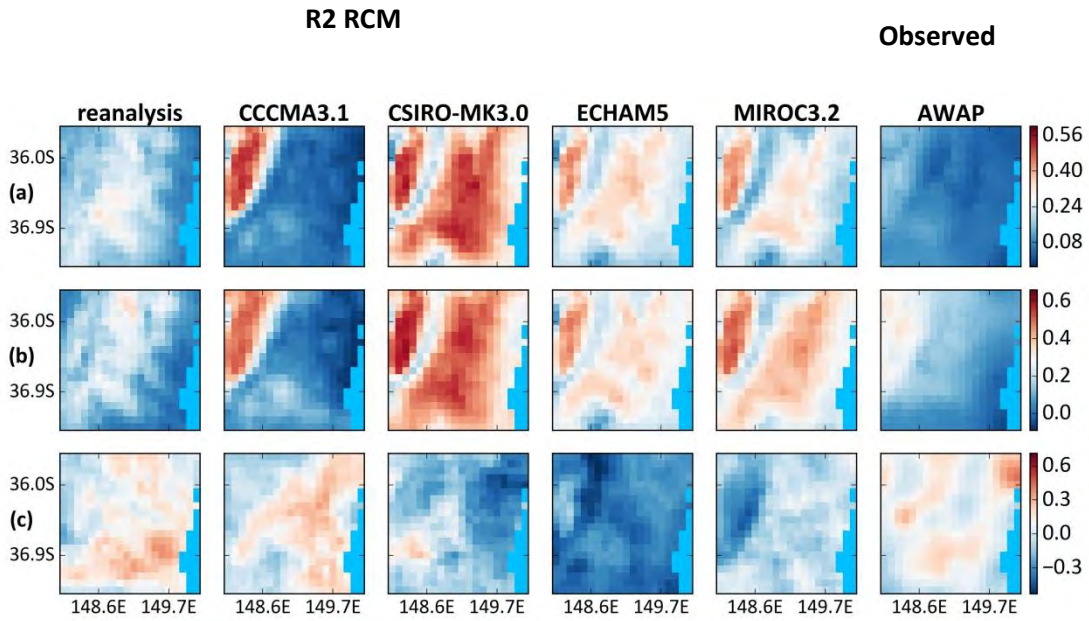

Figure A.15.32 Spatial distribution of the lag-1 autocorrelation of the rainfall (1990-2009) of the Bega River site: The plots are for the uncorrected simulations of R2, and AWAP. Time resolutions are; (a) fortnightly, (b) monthly, and (c) annual.

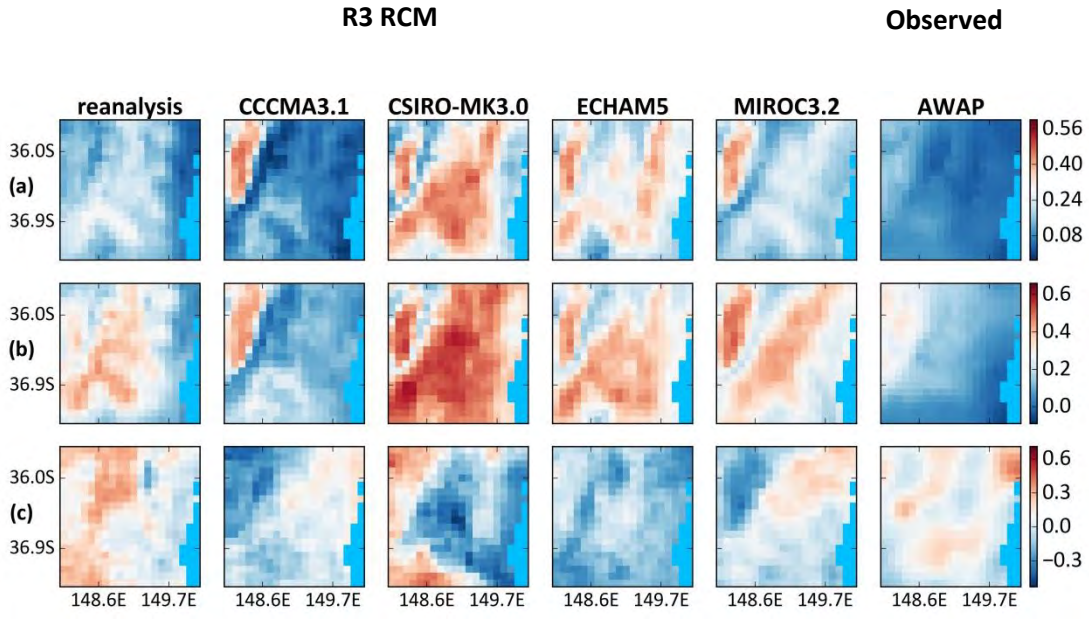

Figure A.15.33 Spatial distribution of the lag-1 autocorrelation of the rainfall (1990-2009) of the Bega River site: The plots are for the uncorrected simulations of R3, and AWAP. Time resolutions are; (a) fortnightly, (b) monthly, and (c) annual.

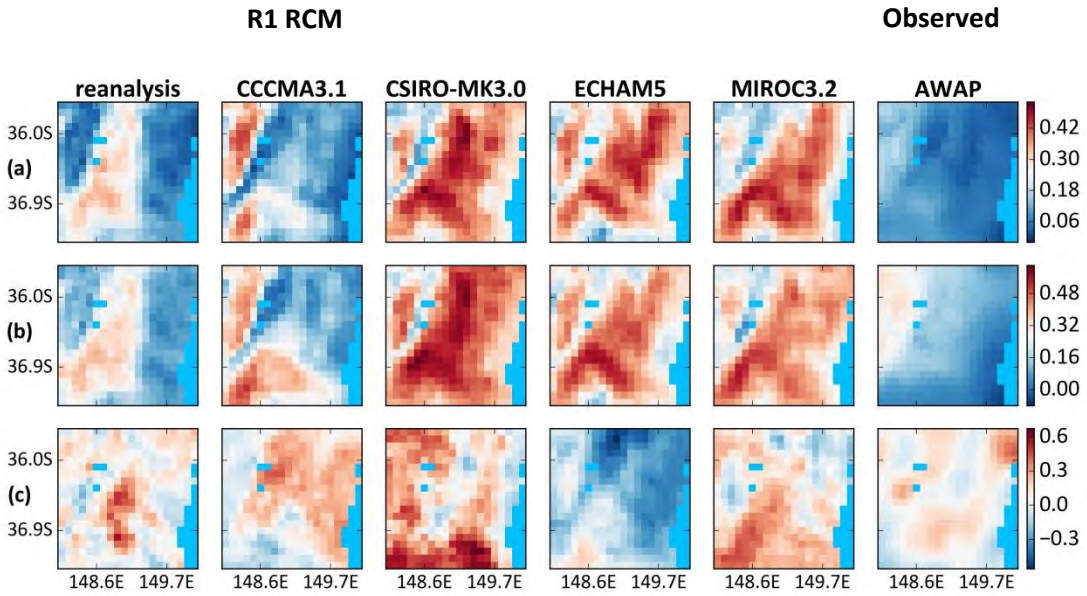

Figure A.15.34 Spatial distribution of the lag-1 autocorrelation of the rainfall (1990-2009) of the Bega River site: The plots are for the bias corrected simulations of R1, and AWAP. Time resolutions are; (a) fortnightly, (b) monthly, and (c) annual.

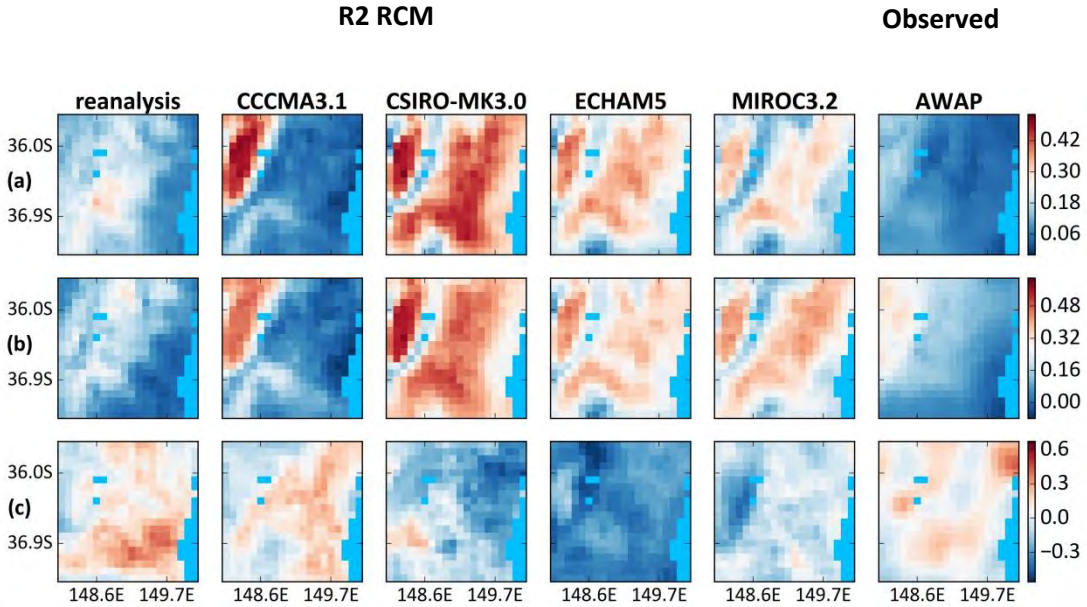

Figure A.15.35 Spatial distribution of the lag-1 autocorrelation of the rainfall (1990-2009) of the Bega River site: The plots are for the bias corrected simulations of R2, and AWAP. Time resolutions are; (a) fortnightly, (b) monthly, and (c) annual.

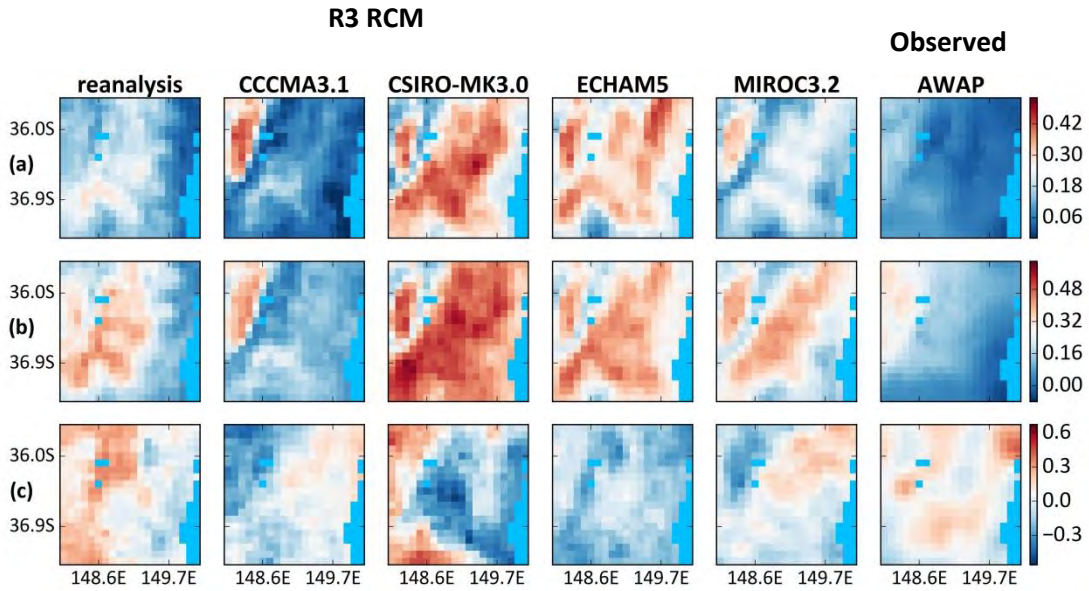

Figure A.15.36 Spatial distribution of the lag-1 autocorrelation of the rainfall (1990-2009) of the Bega River site: The plots are for the bias corrected simulations of R3, and AWAP. Time resolutions are; (a) fortnightly, (b) monthly, and (c) annual.

A.6 Chapter 12 - Section 12.2

The spatial correlation of the uncorrected and bias corrected NARCliM RCMs compared with AWAP for the Bega River and Sydney sites are shown in Figures A.37 to A.68.

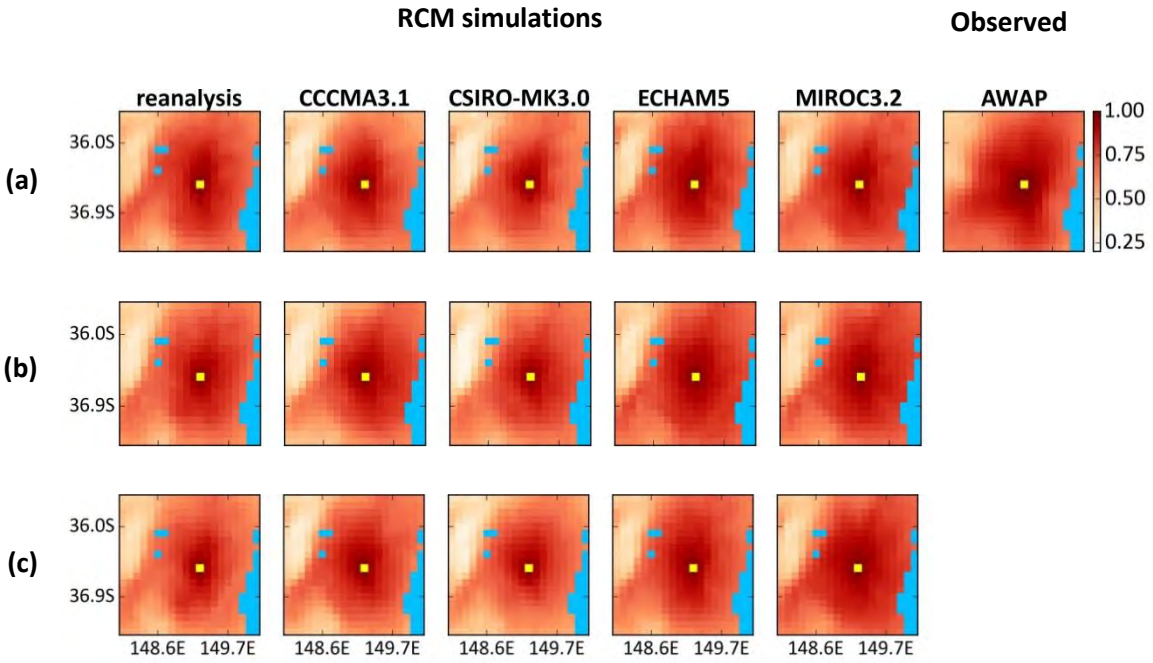

Figure A.15.37 Spatial correlations of daily rainfall between the reference grid point and all other grid points in the Bega River site. The plots are for the uncorrected simulations of (a) R1, (b) R2, and (c) R3 RCMs, and AWAP. The reference is Q12, a high elevation grid point (shown in yellow boxes).

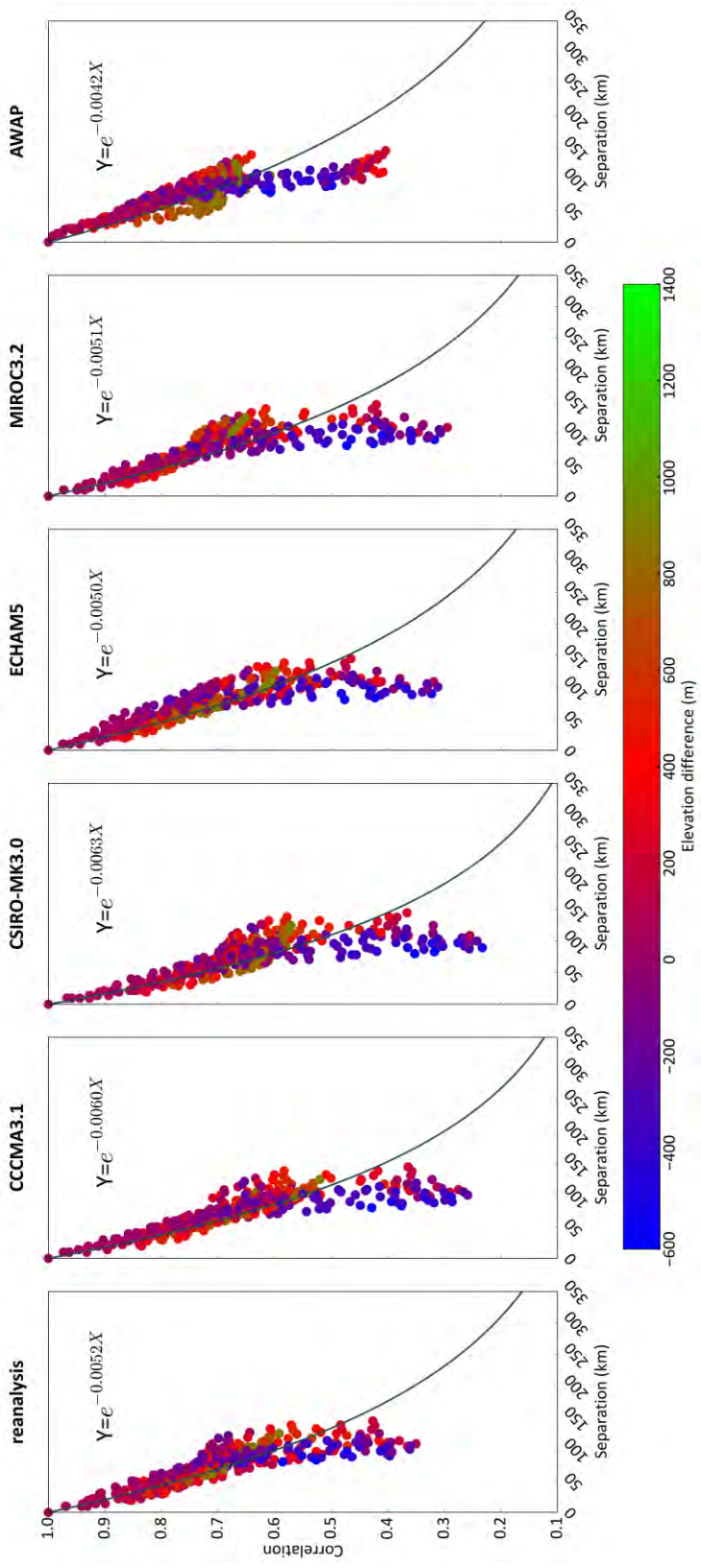

Figure A.15.38 Spatial correlations function (1990-2009) of the Bega River site. The reference is Q12 high elevation grid point. The plots are for the uncorrected GCM simulations of R1 RCM and AWAP.

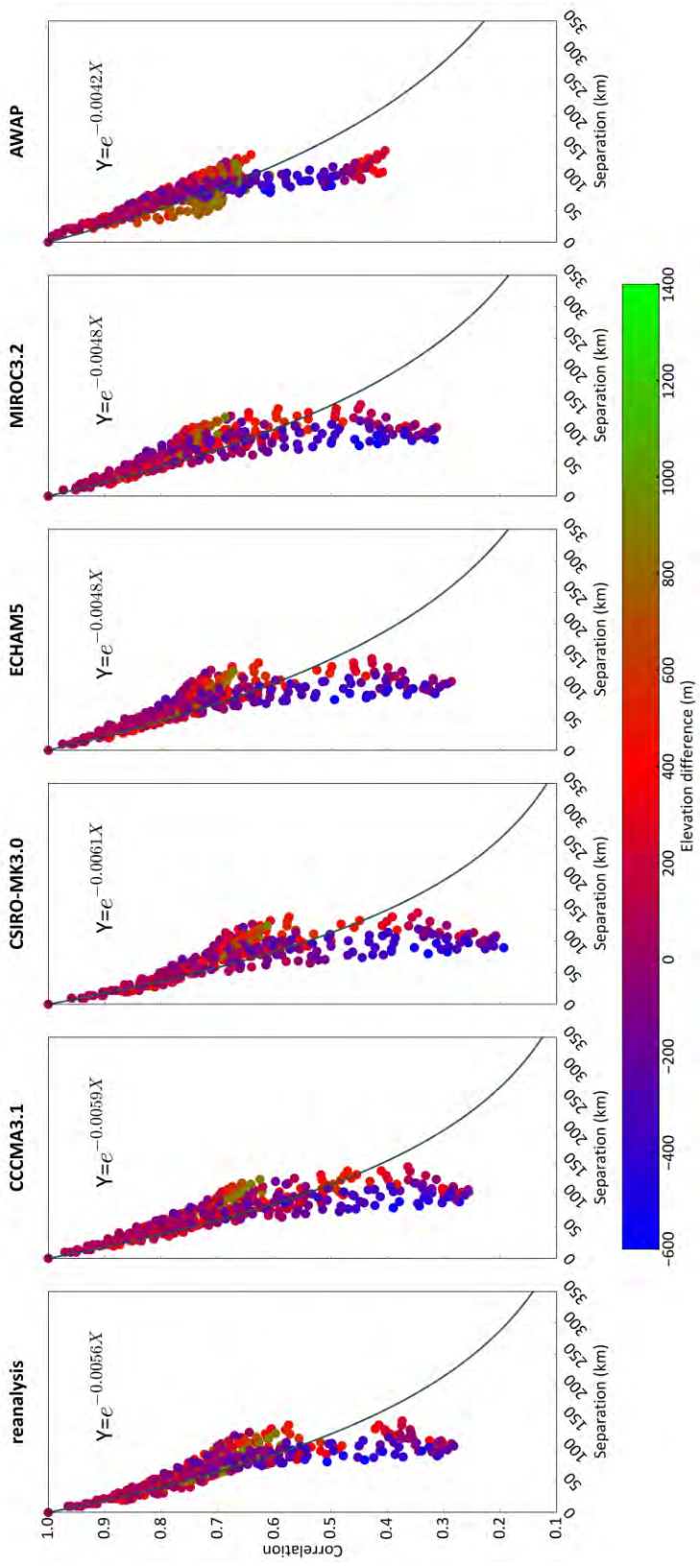

Figure A.15.39 Spatial correlations function (1990-2009) of the Bega River site. The reference is Q12 high elevation grid point. The plots are for the uncorrected GCM simulations of R2 RCM and AWAP.

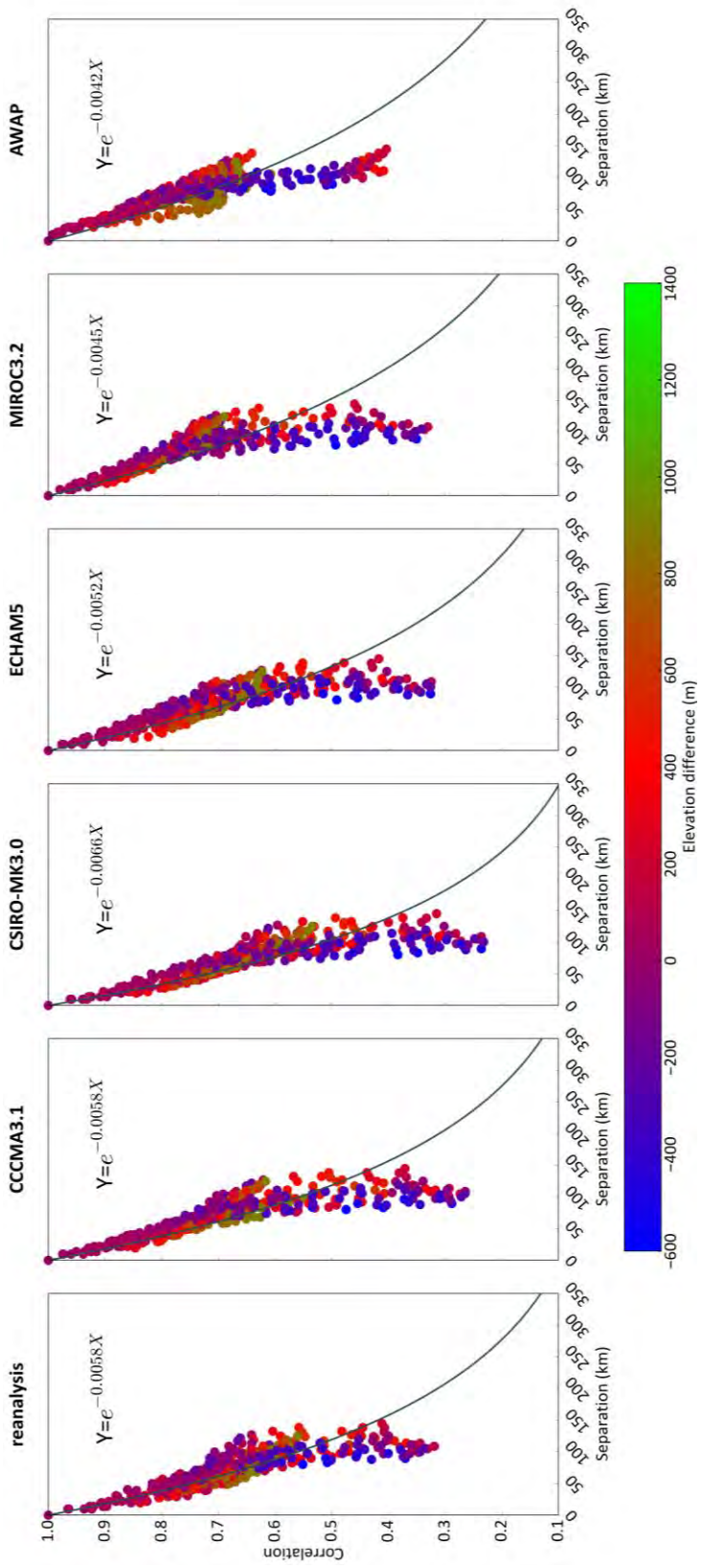

Figure A.15.40 Spatial correlations function (1990-2009) of the Bega River site. The reference is Q12 high elevation grid point. The plots are for the uncorrected GCM simulations of R3 RCM and AWAP.

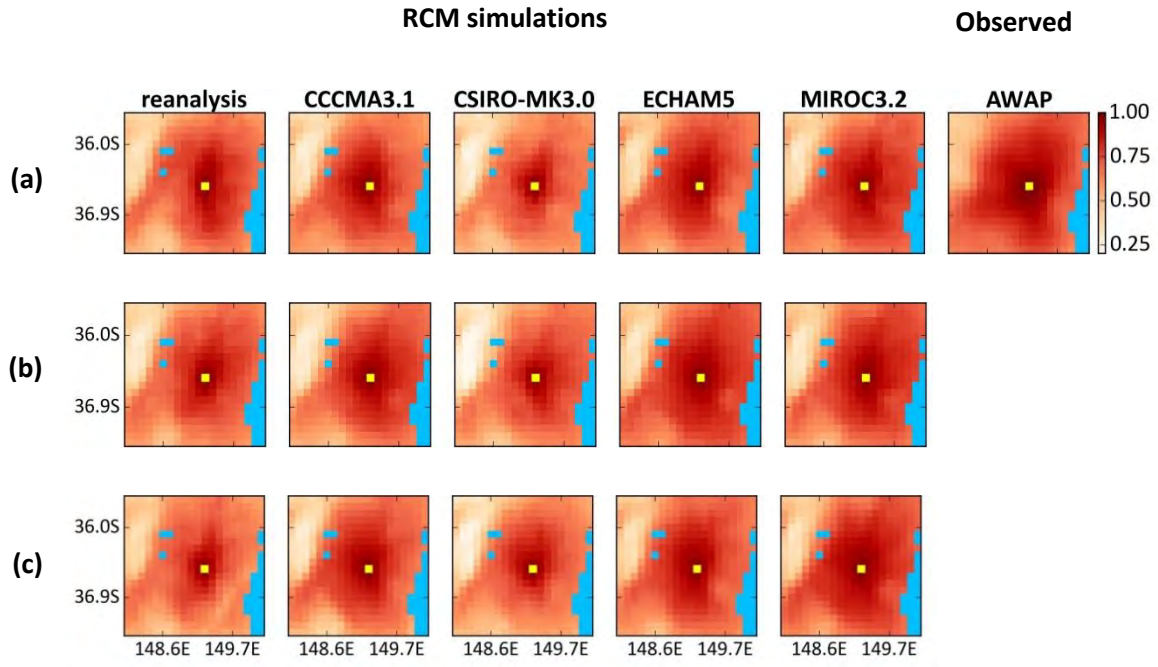

Figure A.15.41 Spatial correlations of daily rainfall between the reference grid point and all other grid points in the Bega River site. The plots are for the bias corrected simulations of (a) R1, (b) R2, and (c) R3 RCMs, and AWAP. The reference is Q12, a high elevation grid point (shown in yellow boxes). The sky blue grid points inside the site are inland reservoirs updated with the bias correction.

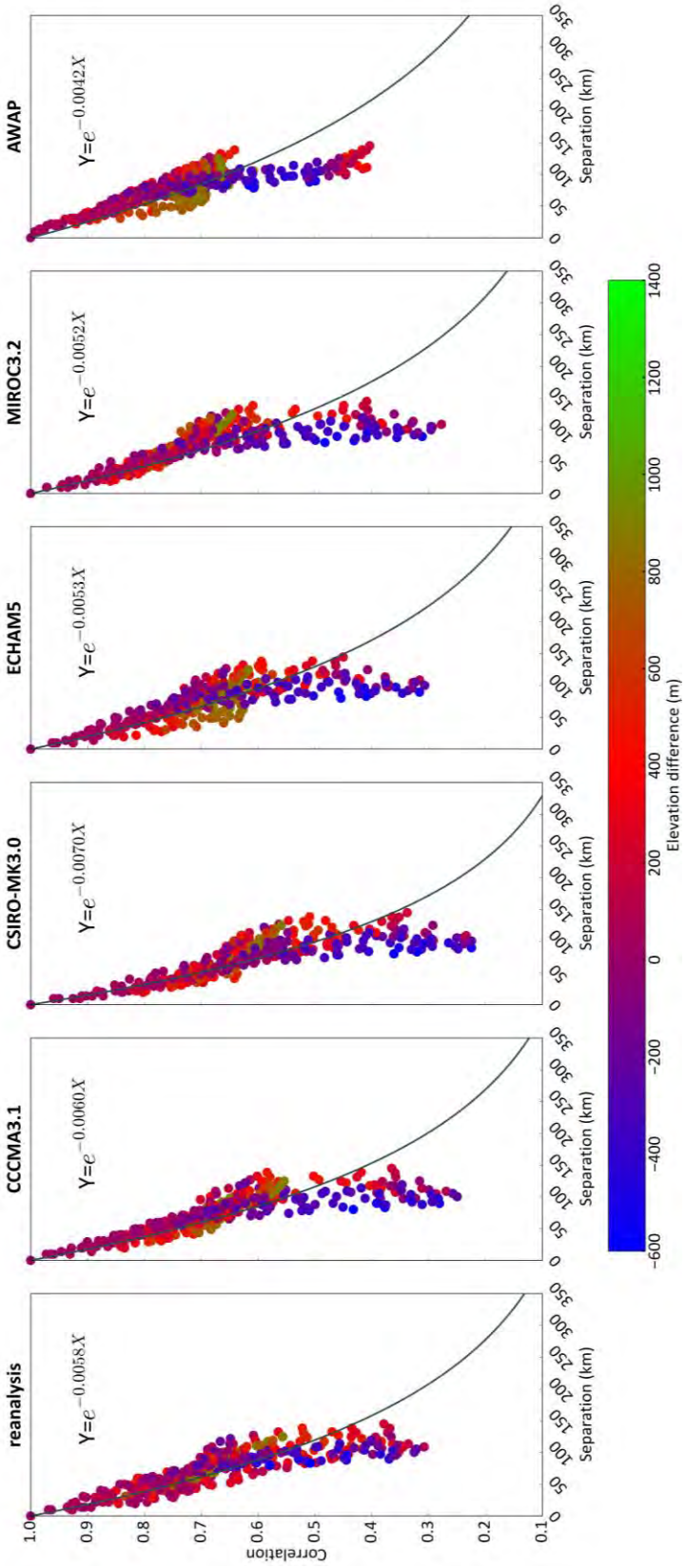

Figure A.15.42 Spatial correlations function (1990-2009) of the Bega River site. The reference is Q12 high elevation grid point. The plots are for the bias corrected GCM simulations of R1 RCM and AWAP.

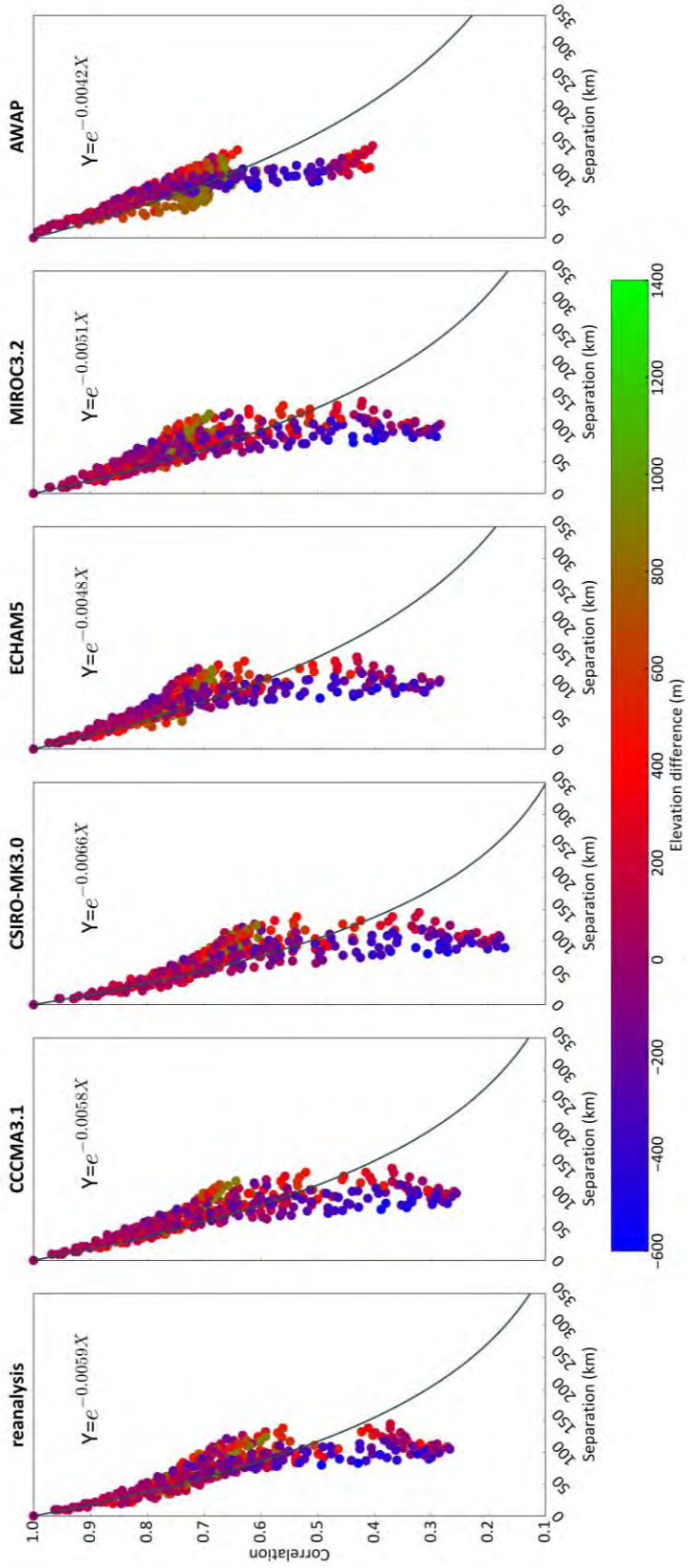

Figure A.15.43 Spatial correlations function (1990-2009) of the Bega River site. The reference is Q12 high elevation grid point. The plots are for the bias corrected GCM simulations of R2 RCM and AWAP.

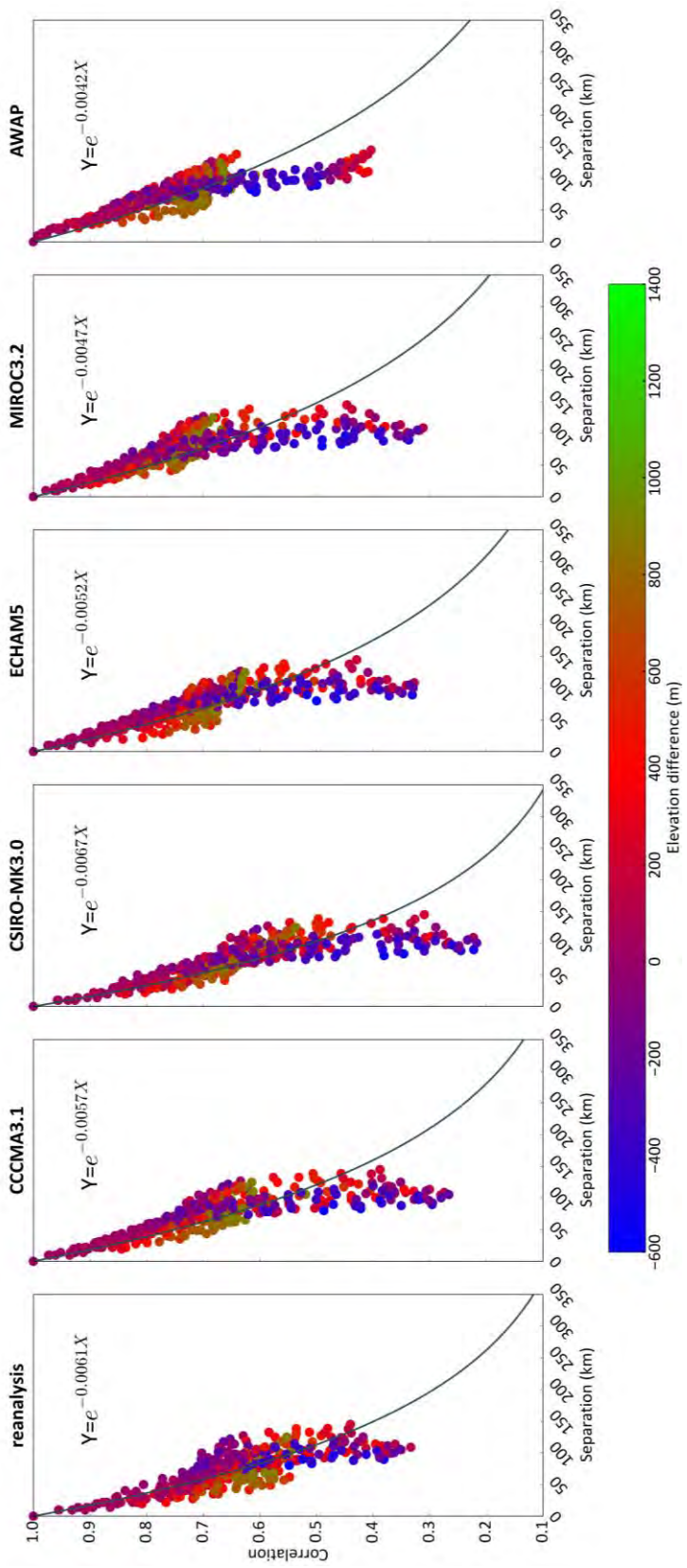

Figure A.15.44 Spatial correlations function (1990-2009) of the Bega River site. The reference is Q12 high elevation grid point. The plots are for the bias corrected GCM simulations of R3 RCM and AWAP.

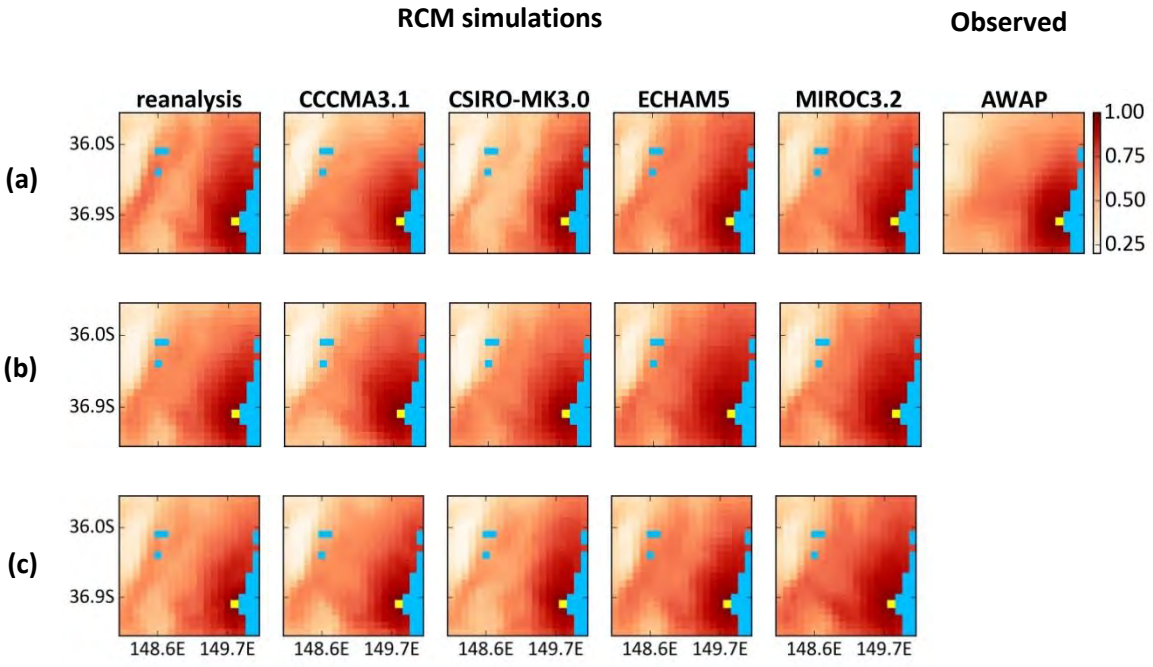

Figure A.15.45 Spatial correlations of daily rainfall between the reference grid point and all other grid points in the Bega River sitesite. The plots are for the uncorrected simulations of (a) R1, (b) R2, and (c) R3 RCMs, and AWAP. The reference is Q3, a low elevation grid point (shown in yellow boxes).

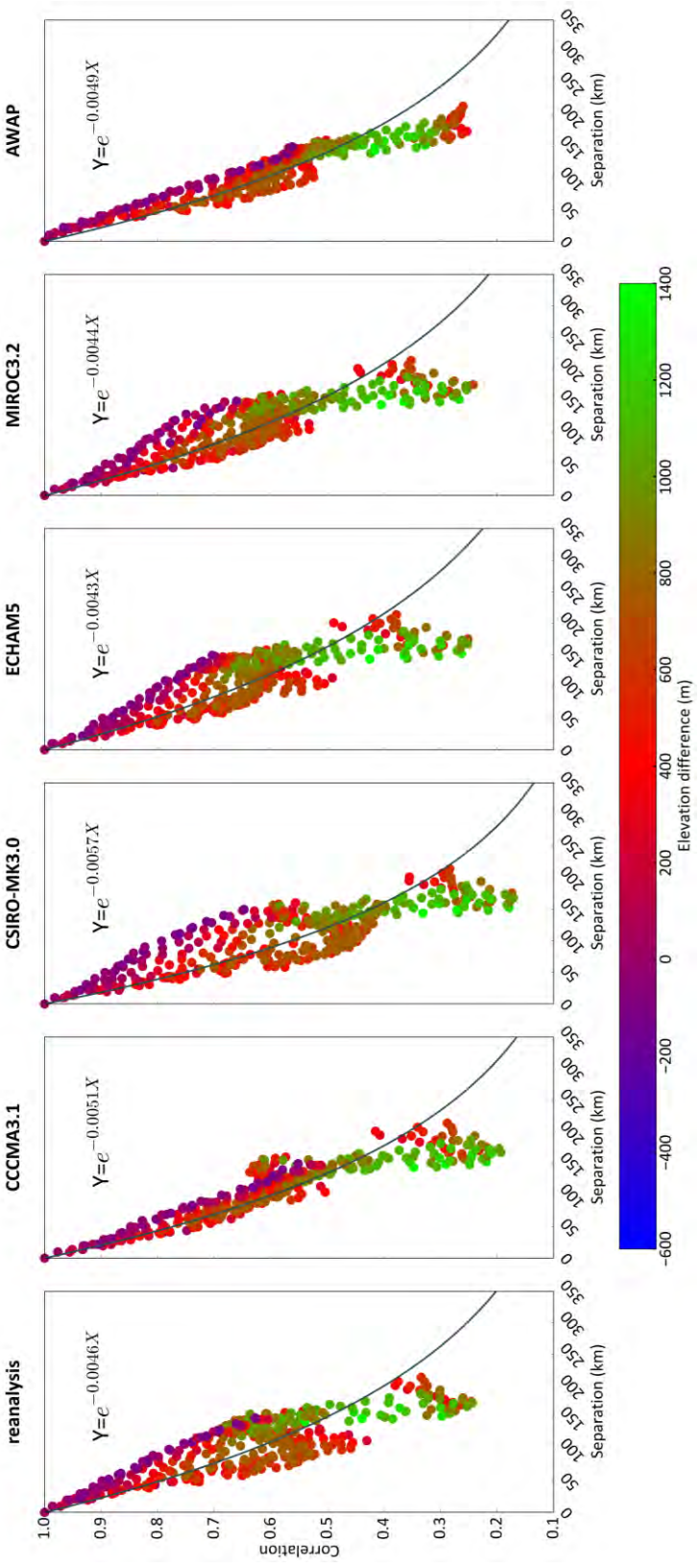

Figure A.15.46 Spatial correlations function (1990-2009) of the Bega River site. The reference is Q3 low elevation grid point. The plots are for the uncorrected GCM simulations of R1 configuration of the WRF RCM and AWAP.

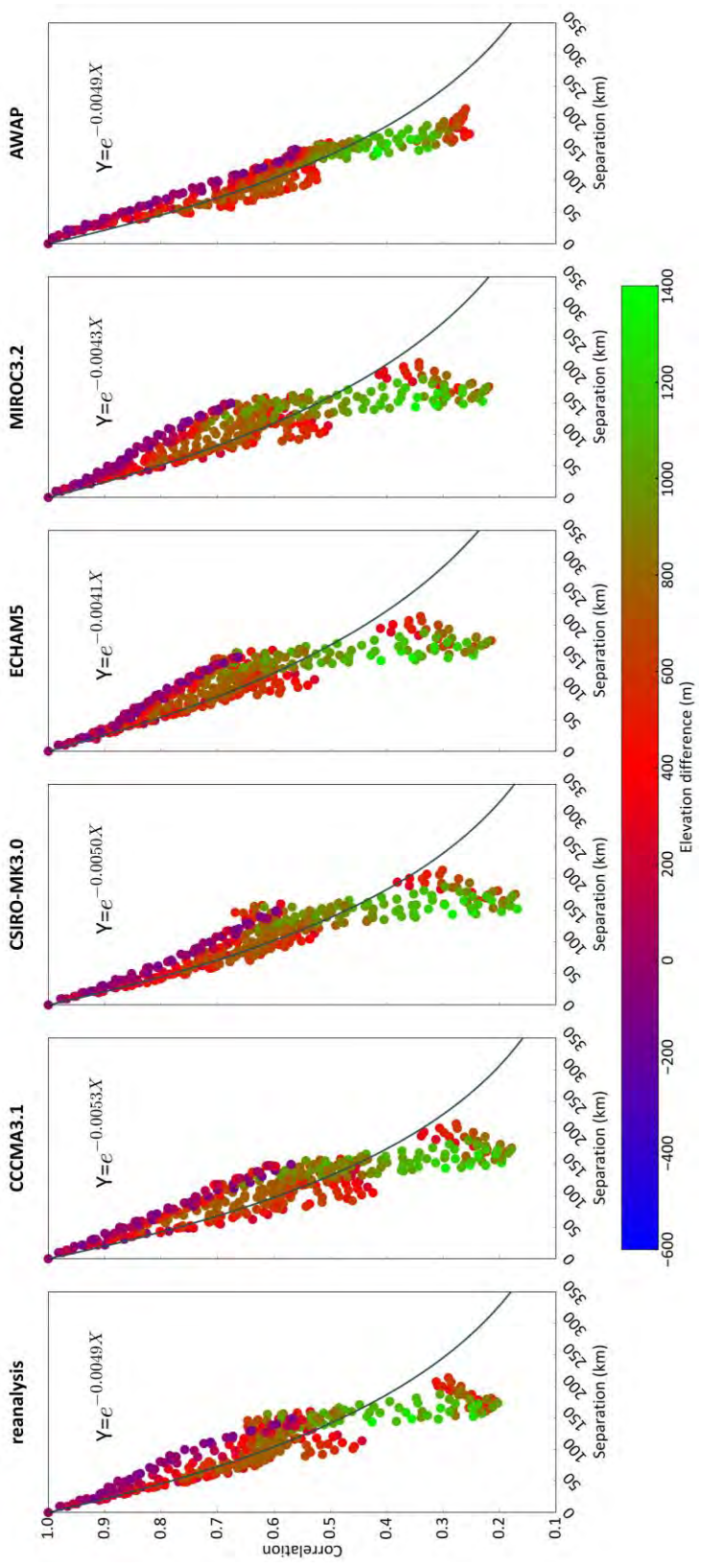

Figure A.15.47 Spatial correlations function (1990-2009) of the Bega River site. The reference is Q3 low elevation grid point. The plots are for the uncorrected GCM simulations of R2 configuration of the WRF RCM and AWAP.

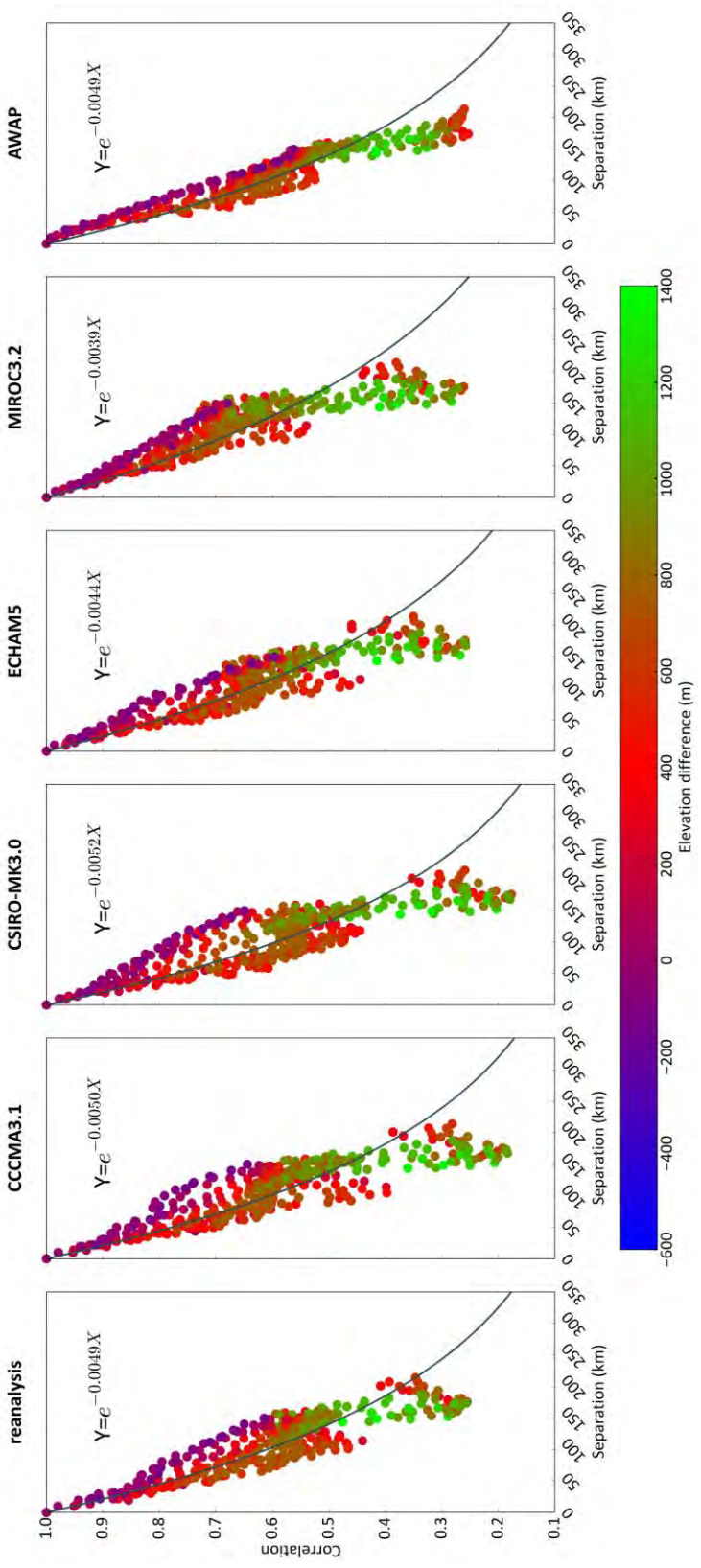

Figure A.15.48 Spatial correlations function (1990-2009) of the Bega River site. The reference is Q3 low elevation grid point. The plots are for the uncorrected GCM simulations of R3 configuration of the WRF RCM and AWAP.

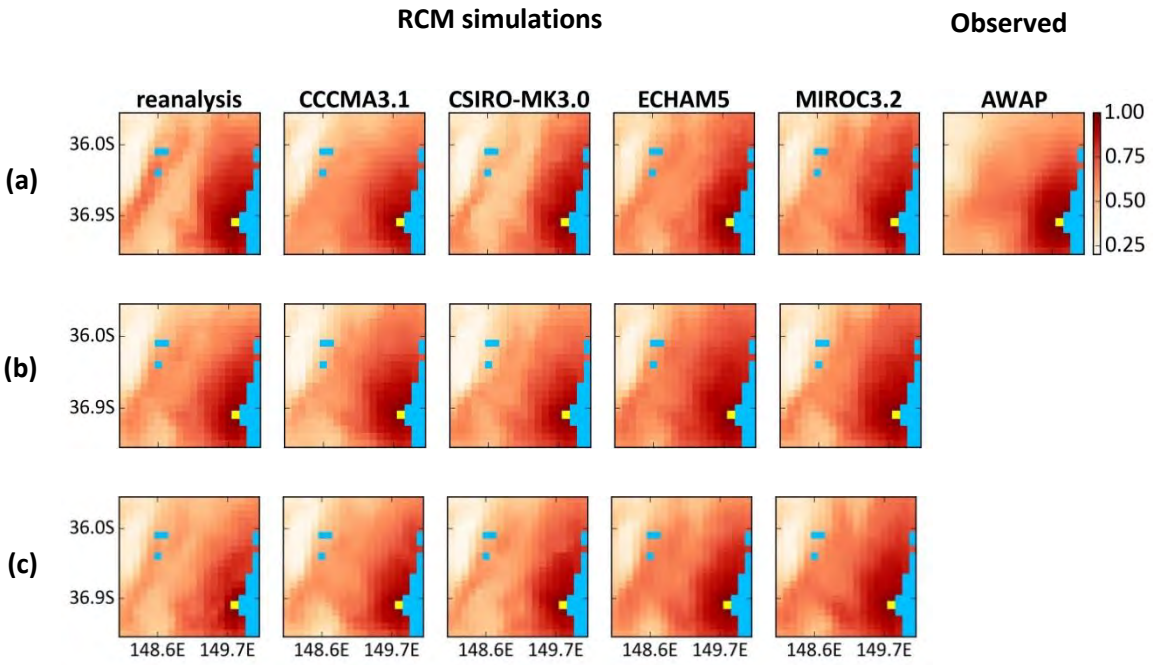

Figure A.15.49 Spatial correlations of daily rainfall between the reference grid point and all other grid points in the Bega River site. The plots are for the bias corrected simulations of (a) R1, (b) R2, and (c) R3 RCMs, and AWAP. The reference is Q3, a low elevation grid point (shown in yellow boxes). The sky blue grid points inside the site are inland reservoirs updated with the bias correction.

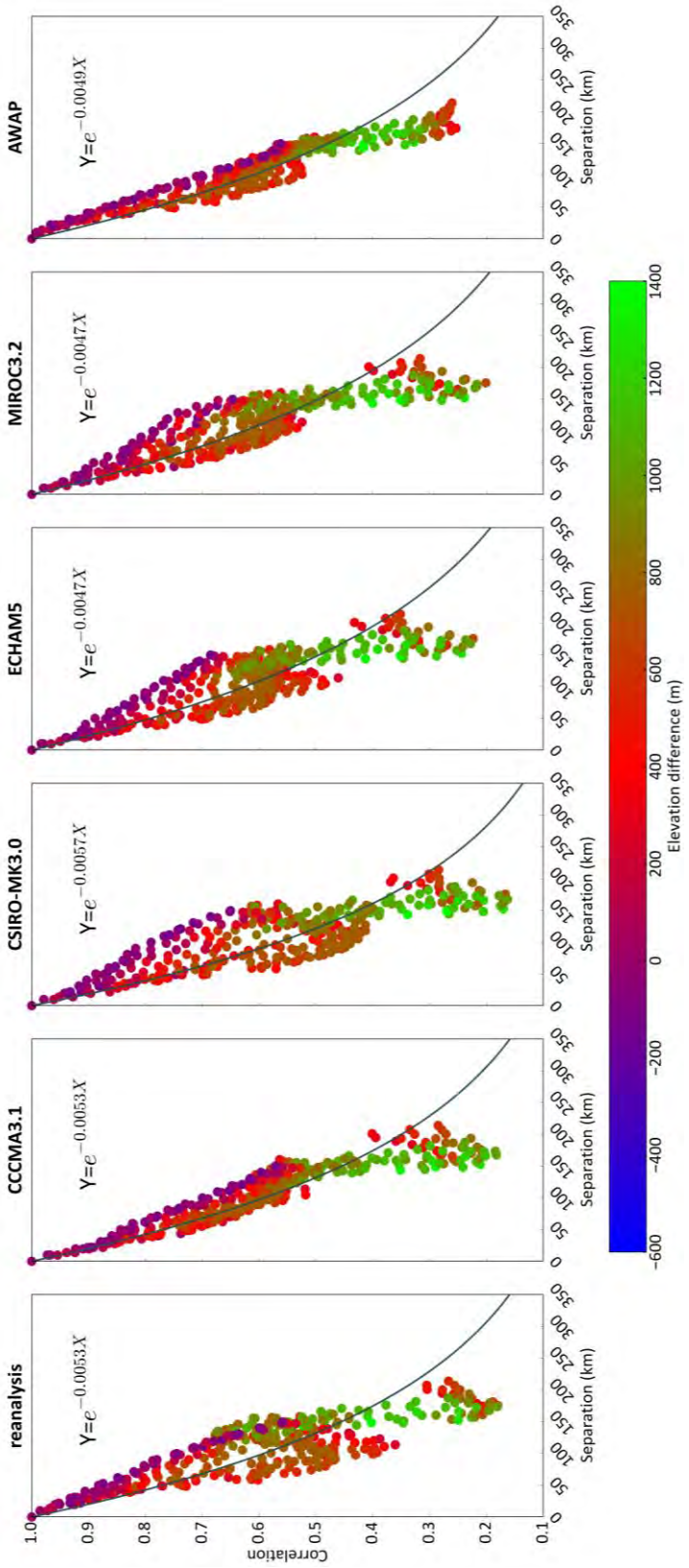

Figure A.15.50 Spatial correlations function (1990-2009) of the Bega River site. The reference is Q3 low elevation grid point. The plots are for the bias corrected GCM simulations of R1 RCM and AWAP.

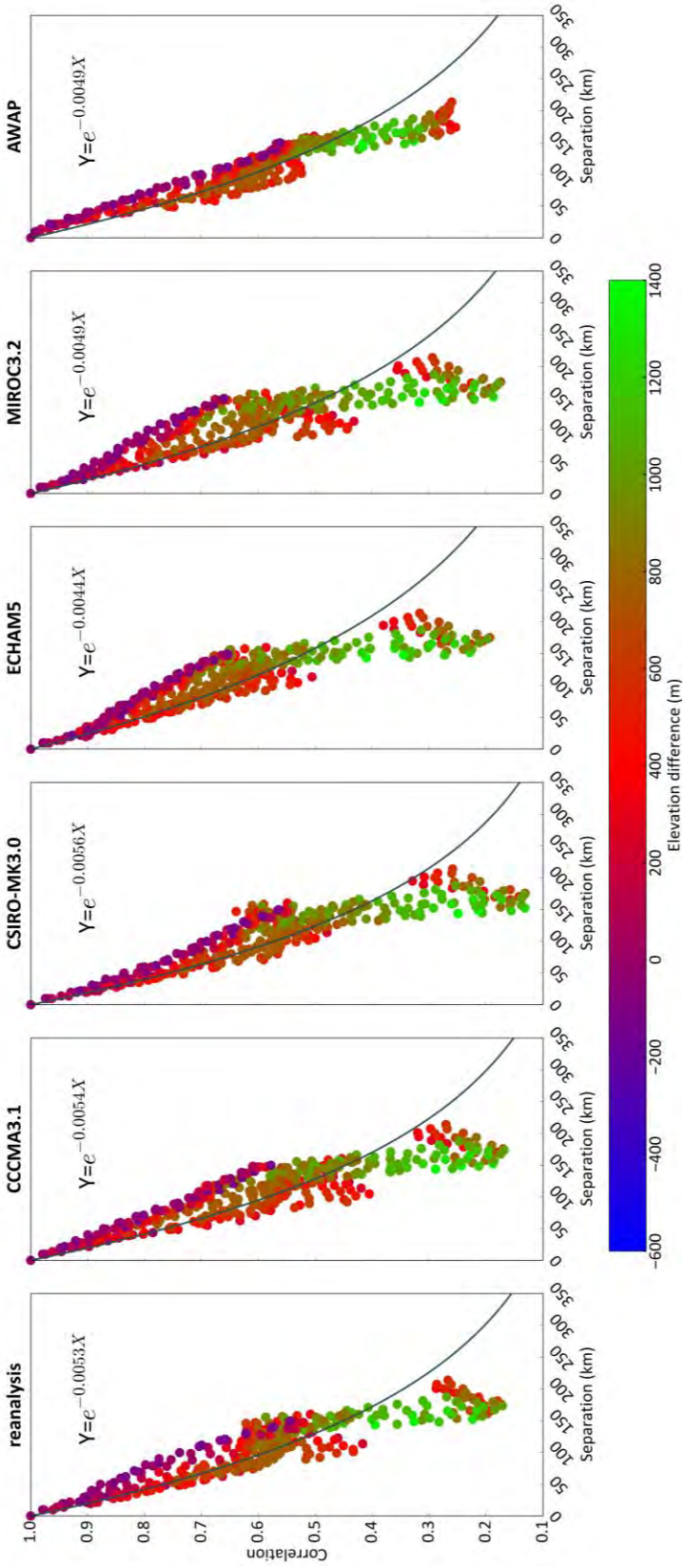

Figure A.15.51 Spatial correlations function (1990-2009) of the Bega River site. The reference is Q3 low elevation grid point. The plots are for the bias corrected GCM simulations of R2 RCM and AWAP.

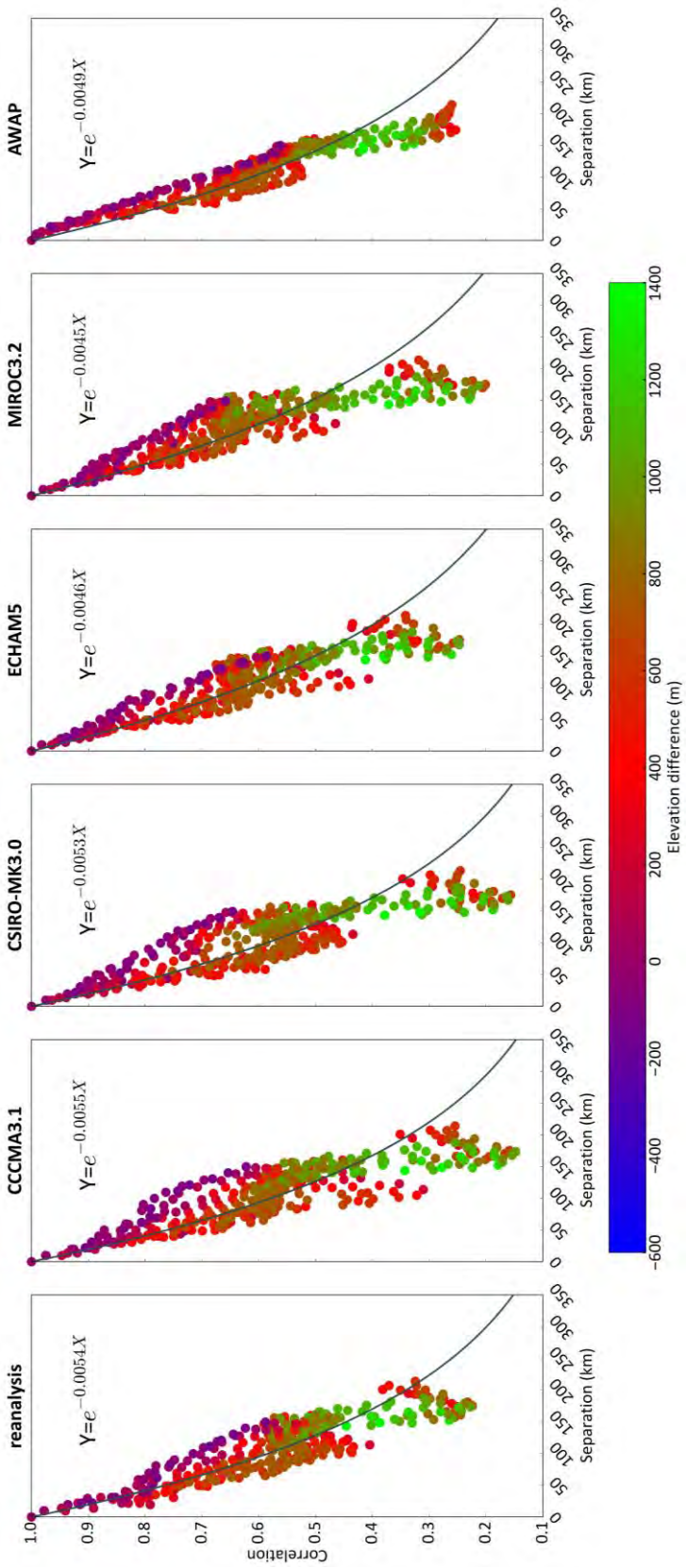

Figure A.15.52 Spatial correlations function (1990-2009) of the Bega River site. The reference is Q3 low elevation grid point. The plots are for the bias corrected GCM simulations of R3 RCM and AWAP.

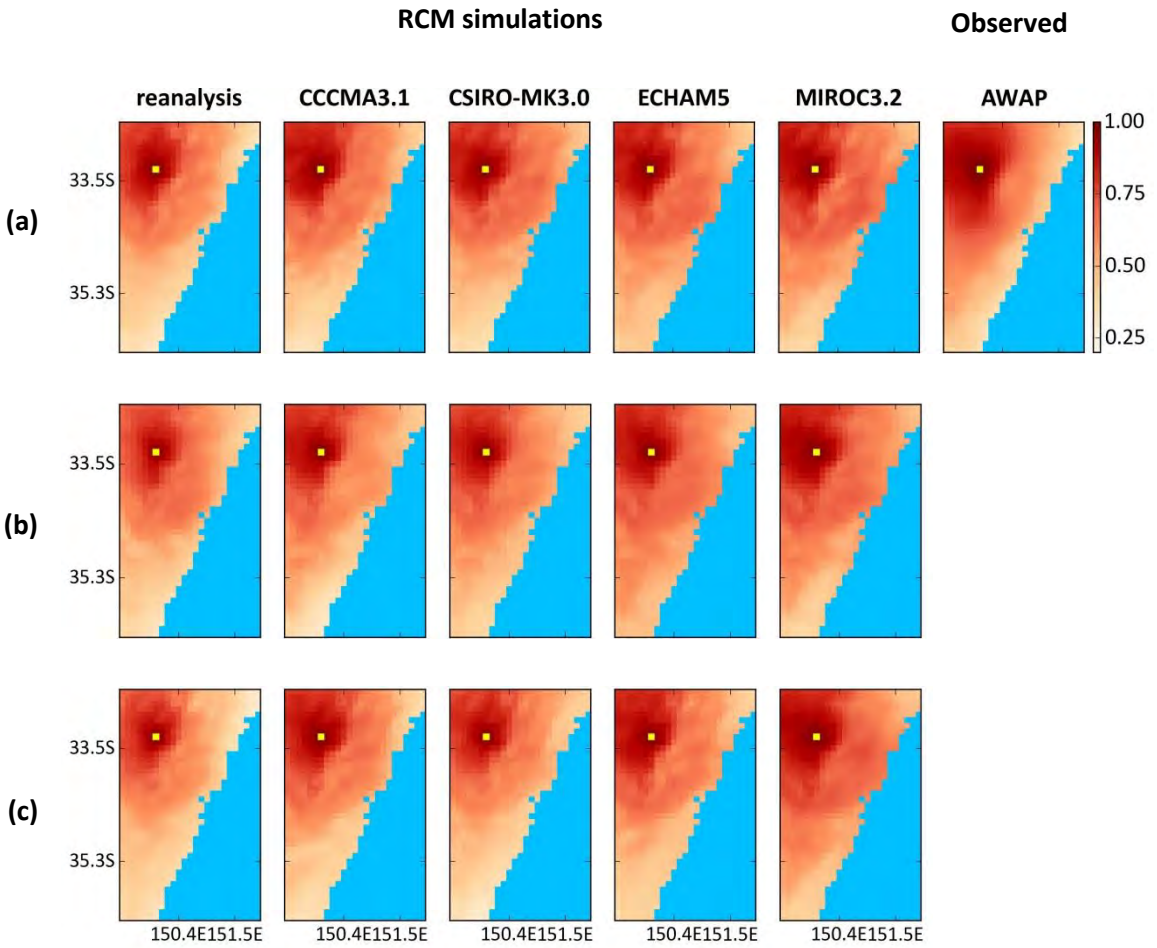

Figure A.15.53 Spatial correlations of daily rainfall between the reference grid point and all other grid points in the Sydney sitesite. The plots are for the uncorrected simulations of (a) R1, (b) R2, and (c) R3 RCMs, and AWAP. The reference is S22, a high elevation grid point (shown in yellow boxes).

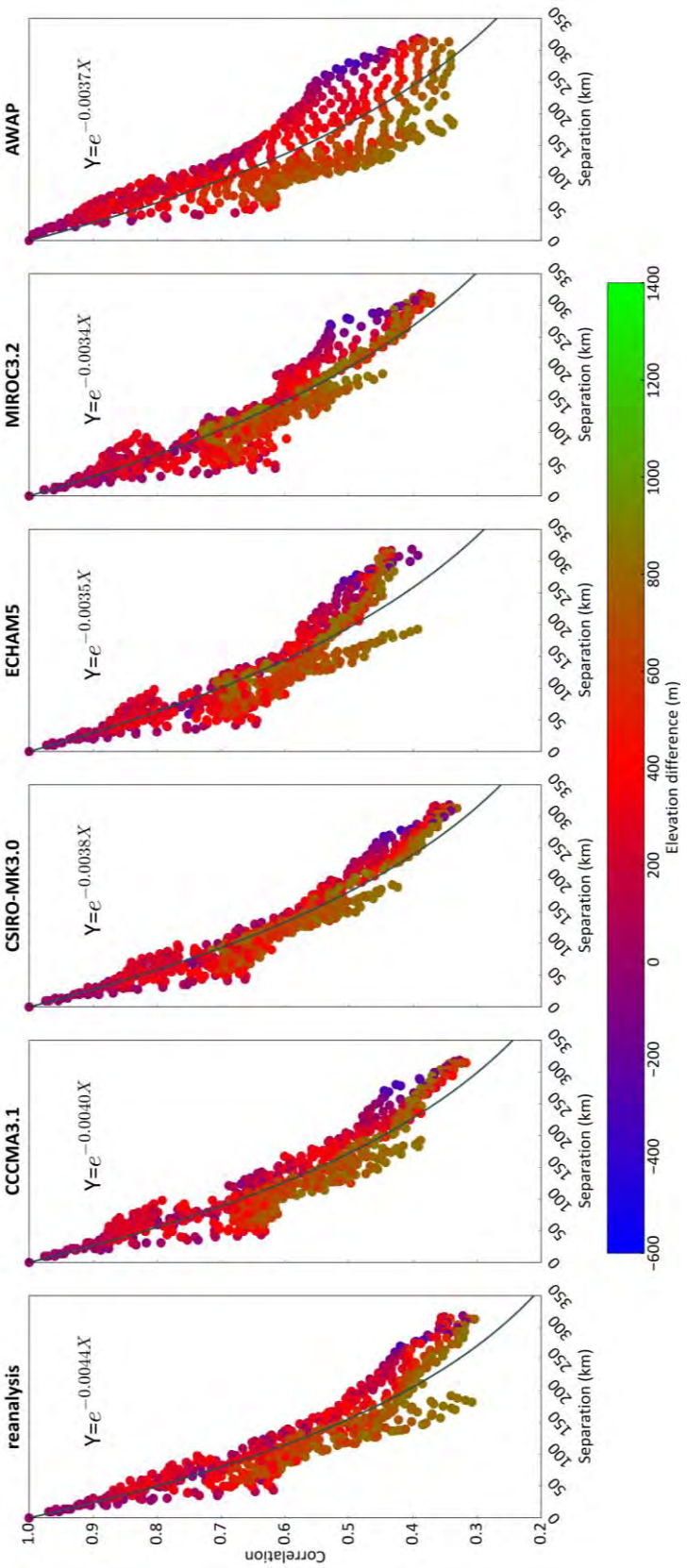

Figure A.15.54 Spatial correlations function (1990-2009) of the Sydney site. The reference is S22 high elevation grid point. The plots are for the uncorrected GCM simulations of R1 RCM and AWAP.

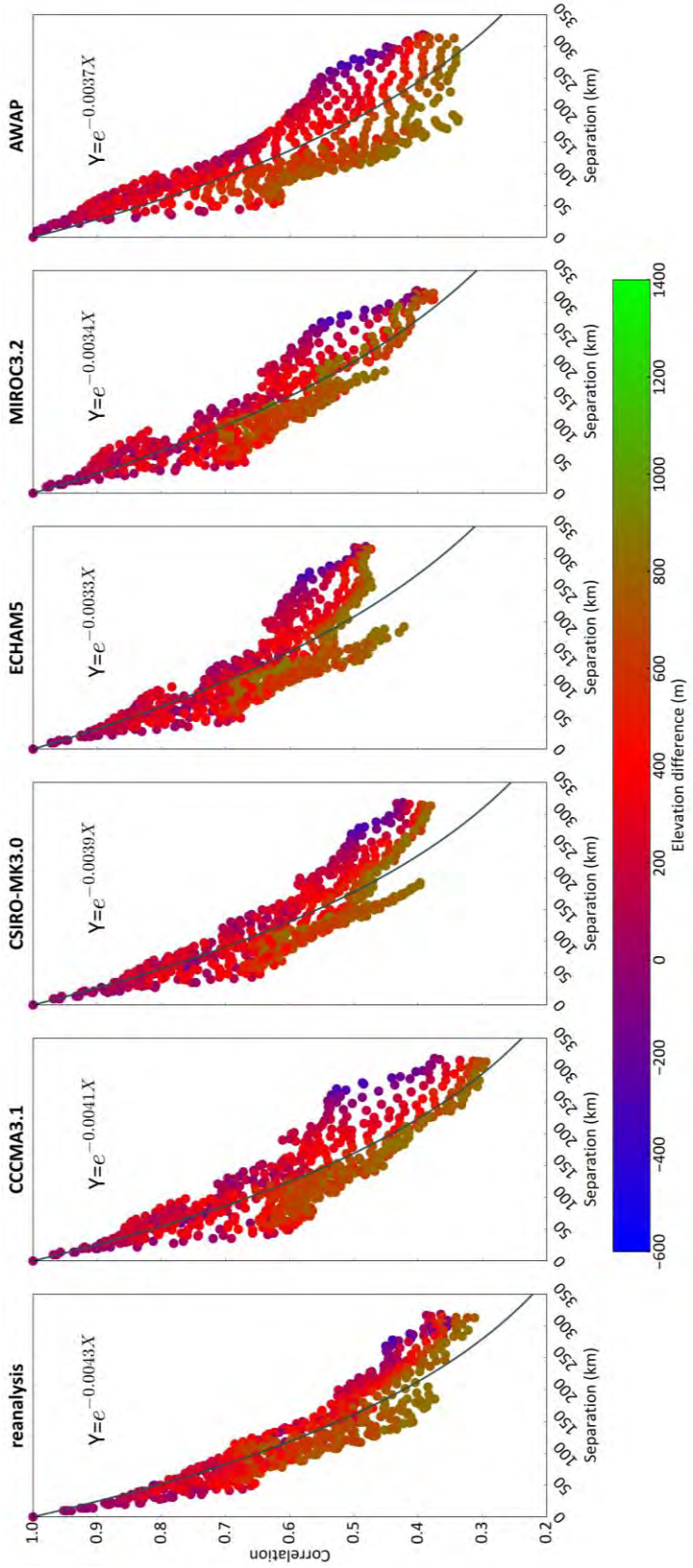

Figure A.15.55 Spatial correlations function (1990-2009) of the Sydney site. The reference is S22 high elevation grid point. The plots are for the uncorrected GCM simulations of R2 RCM and AWAP.

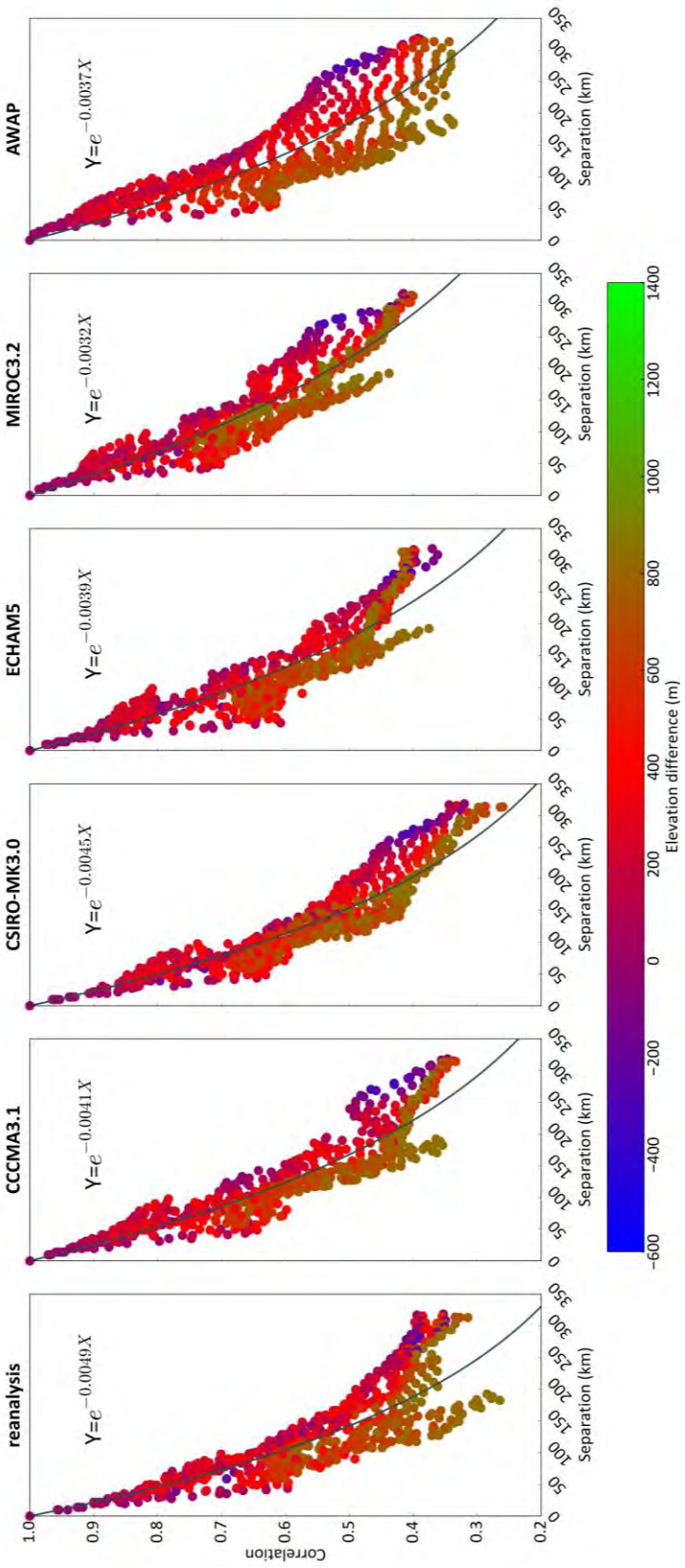

Figure A.15.56 Spatial correlations function (1990-2009) of the Sydney site. The reference is S22 high elevation grid point. The plots are for the uncorrected GCM simulations of R3 RCM and AWAP.

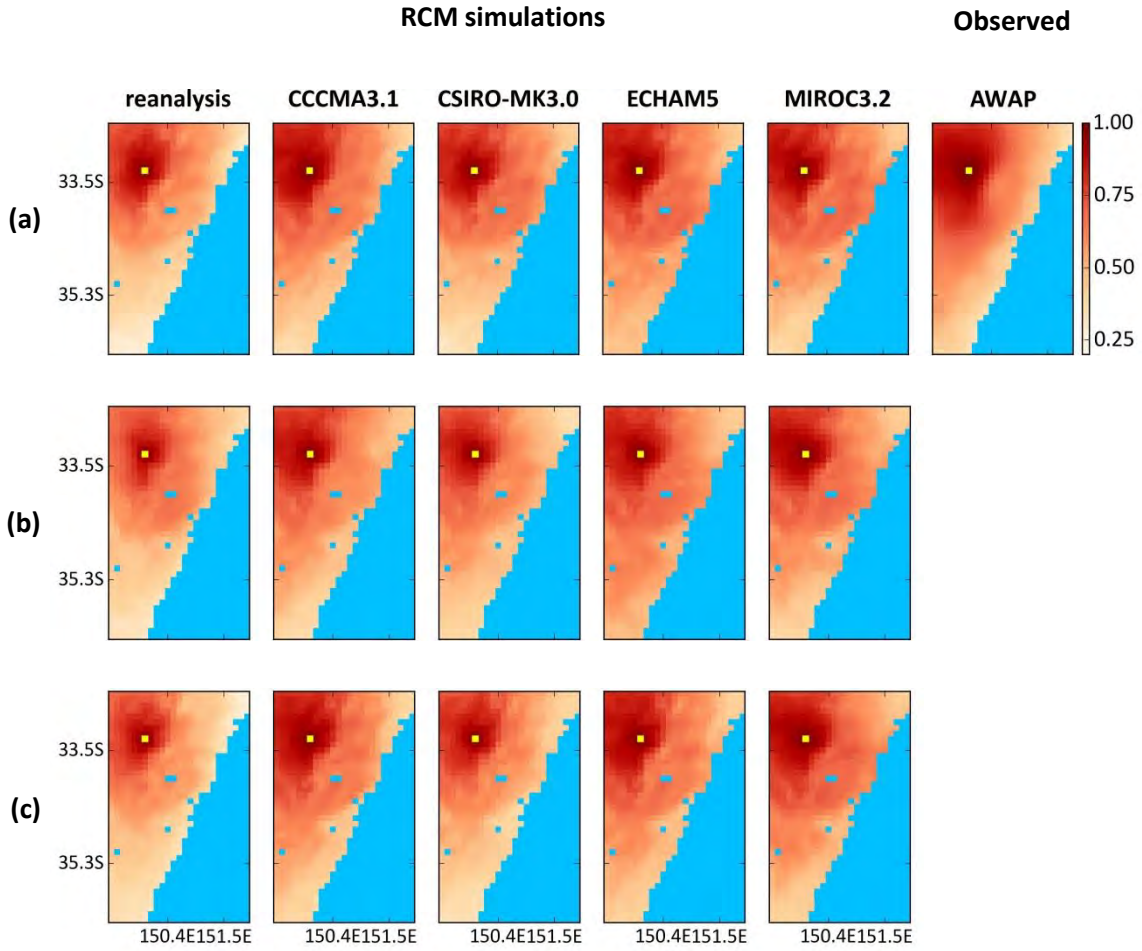

Figure A.15.57 Spatial correlations of daily rainfall between the reference grid point and all other grid points in the Sydney site. The plots are for the bias corrected simulations of (a) R1, (b) R2, and (c) R3 RCMs, and AWAP. The reference is S22, a high elevation grid point (shown in yellow boxes). The sky blue grid points inside the site are inland reservoirs updated with the bias correction.

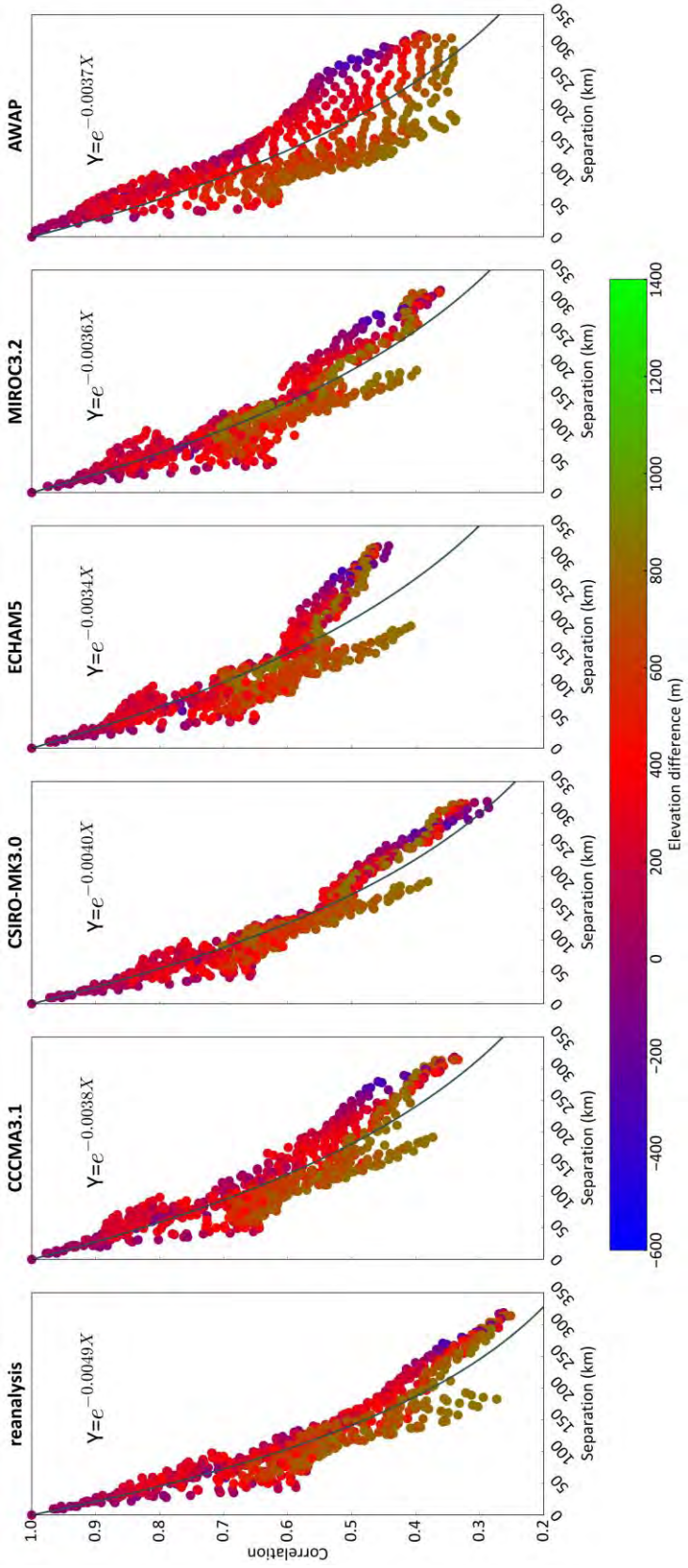

Figure A.15.58 Spatial correlations function (1990-2009) of the Sydney site. The reference is S22 high elevation grid point. The plots are for the bias corrected GCM simulations of R1 RCM and AWAP.

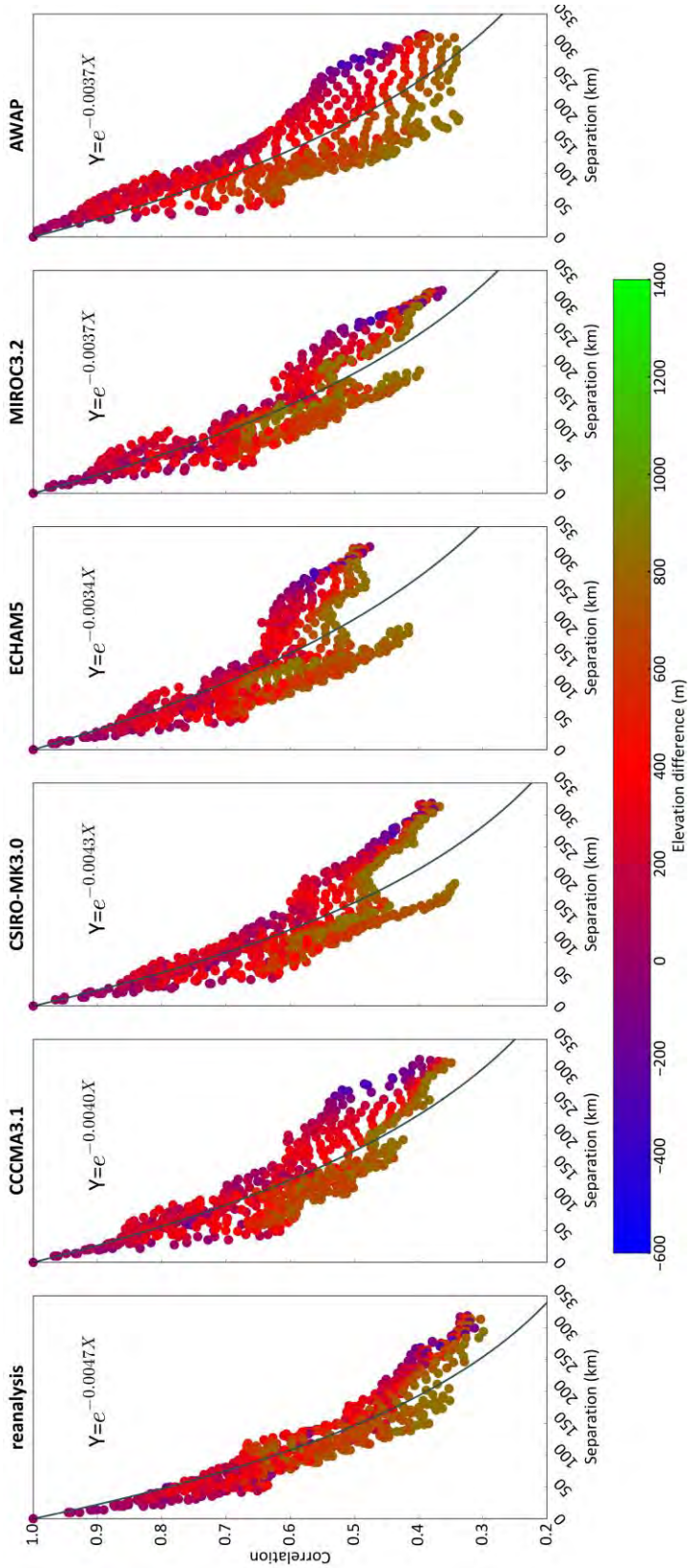

Figure A.15.59 Spatial correlations function (1990-2009) of the Sydney site. The reference is S22 high elevation grid point. The plots are for the bias corrected GCM simulations of R2 RCM and AWAP.

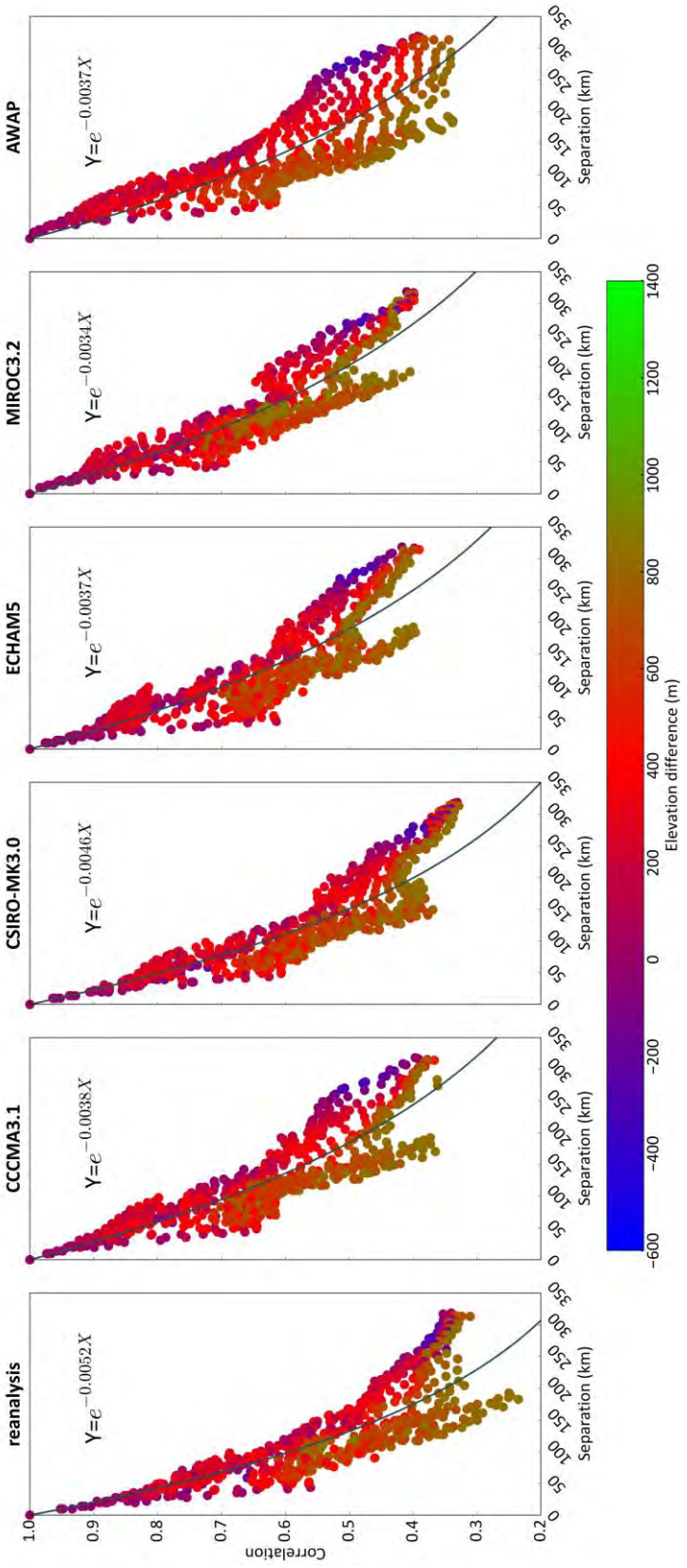

Figure A.15.60 Spatial correlations function (1990-2009) of the Sydney site. The reference is S22 high elevation grid point. The plots are for the bias corrected GCM simulations of R3 RCM and AWAP.

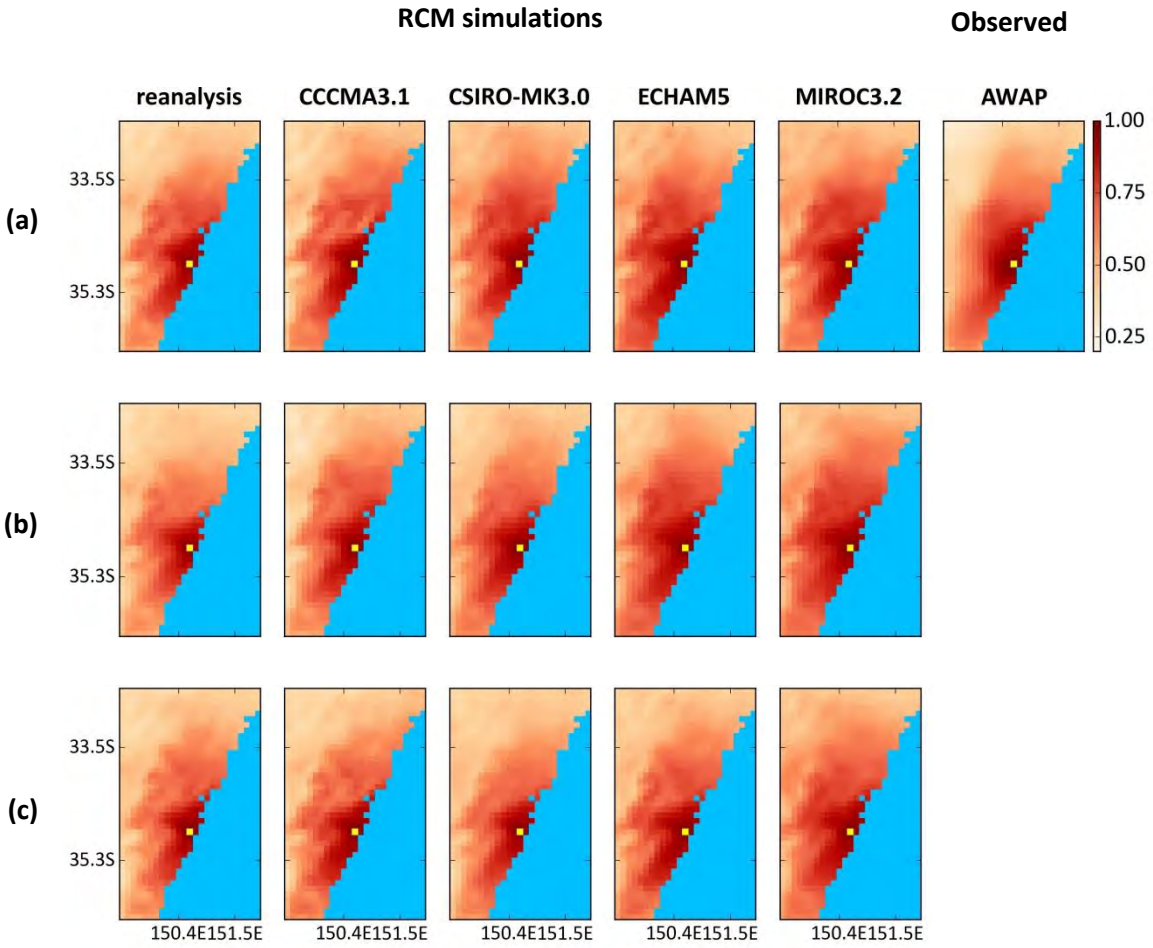

Figure A.15.61 Spatial correlations of daily rainfall between the reference grid point and all other grid points in the Sydney sitesite. The plots are for the uncorrected simulations of (a) R1, (b) R2, and (c) R3 RCMs, and AWAP. The reference is S8, a low elevation grid point (shown in yellow boxes).

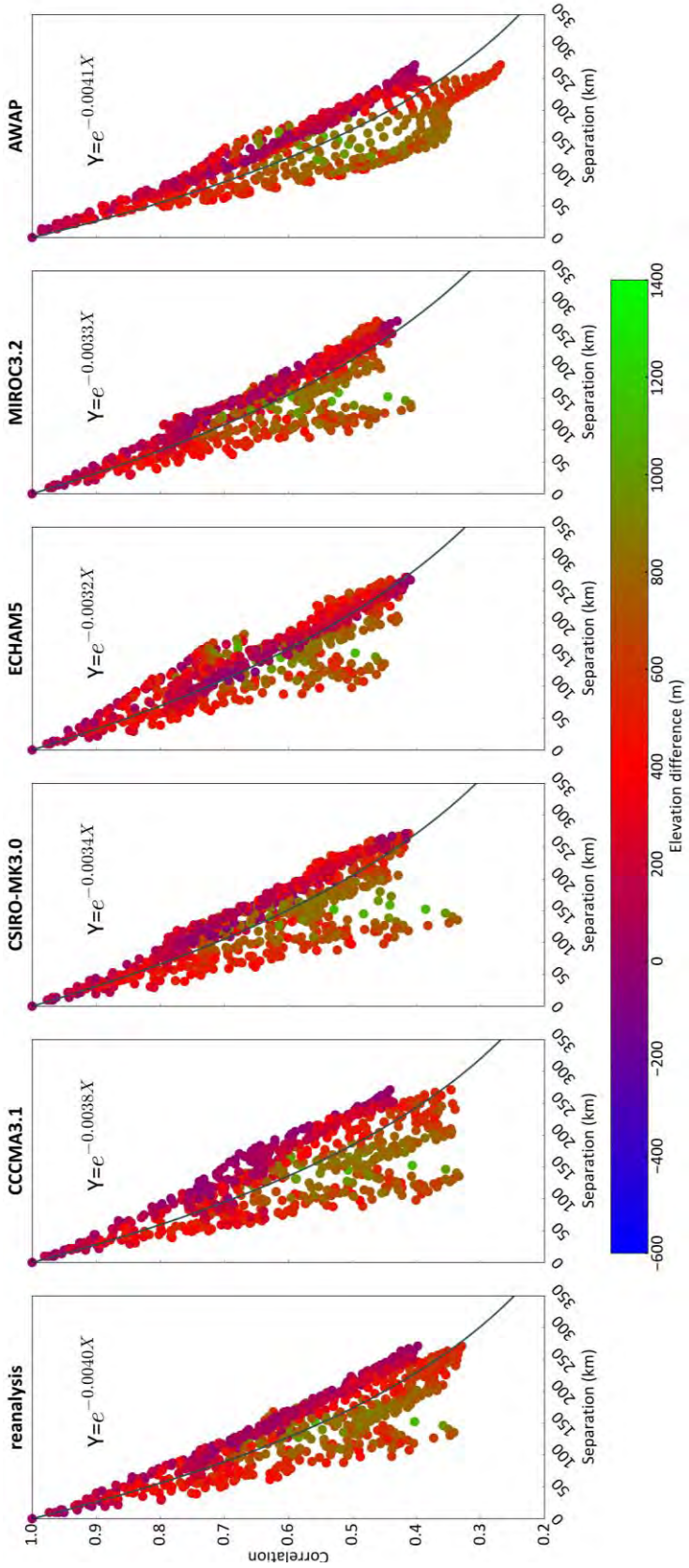

Figure A.15.62 Spatial correlations function (1990-2009) of the Sydney site. The reference is S8 low elevation grid point. The plots are for the uncorrected GCM simulations of R1 RCM and AWAP.

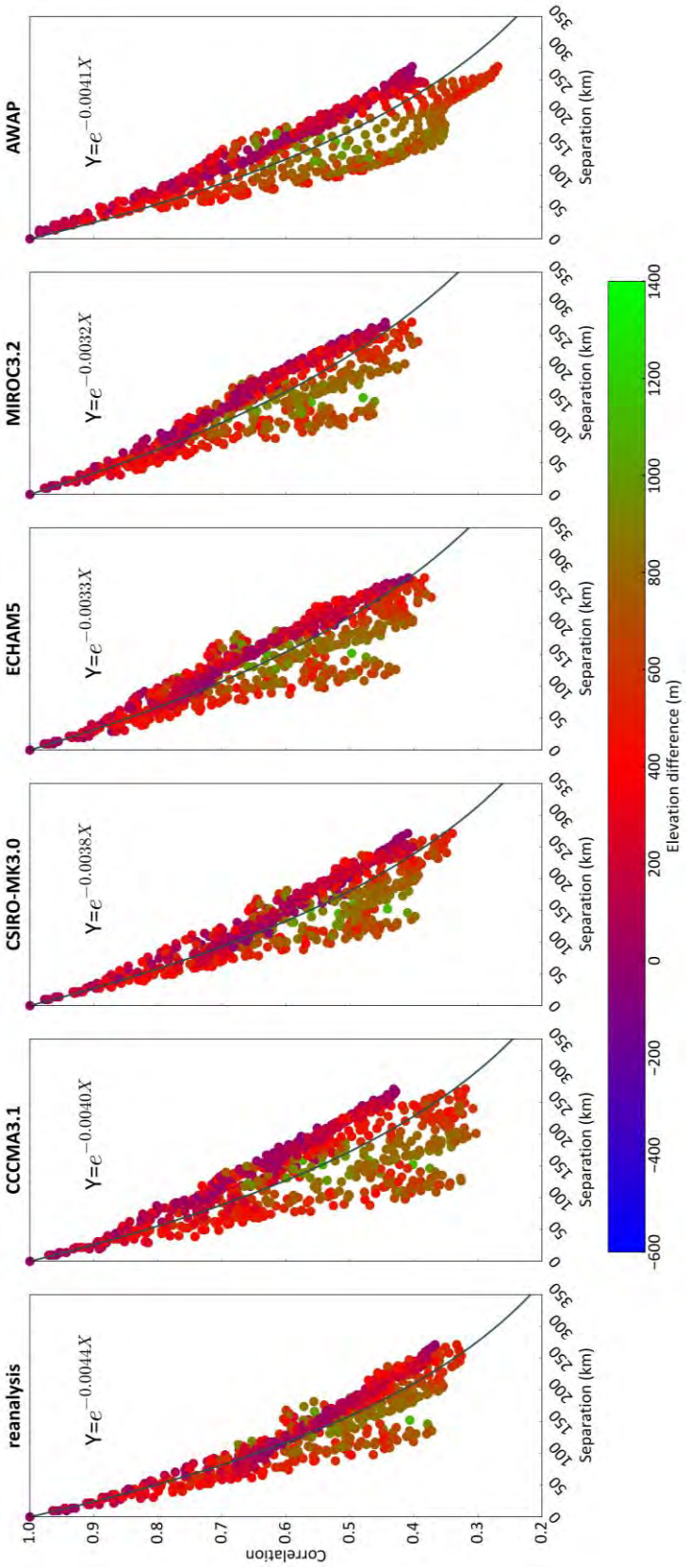

Figure A.15.63 Spatial correlations function (1990-2009) of the Sydney site. The reference is S8 low elevation grid point. The plots are for the uncorrected GCM simulations of R2 RCM and AWAP.

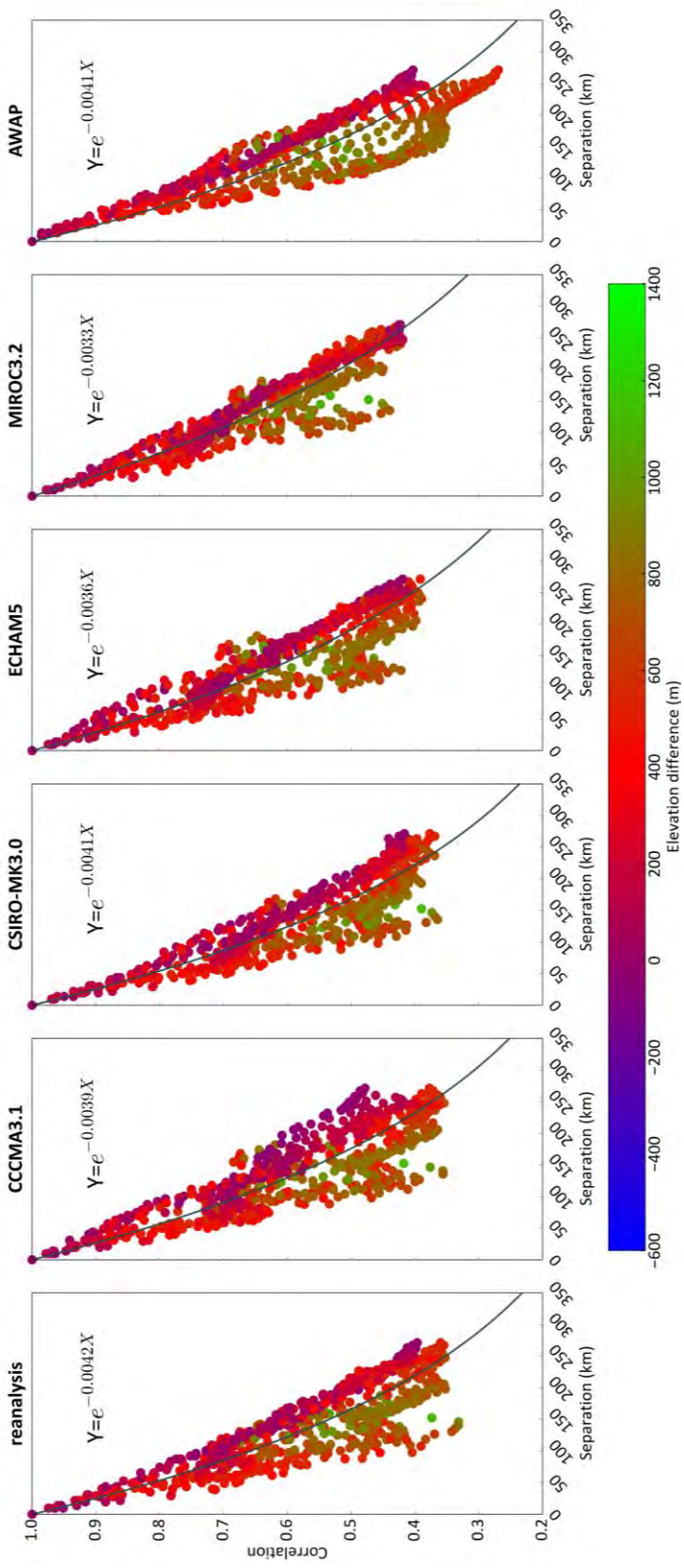

Figure A.15.64 Spatial correlations function (1990-2009) of the Sydney site. The reference is S8 low elevation grid point. The plots are for the uncorrected GCM simulations of R3 RCM and AWAP.

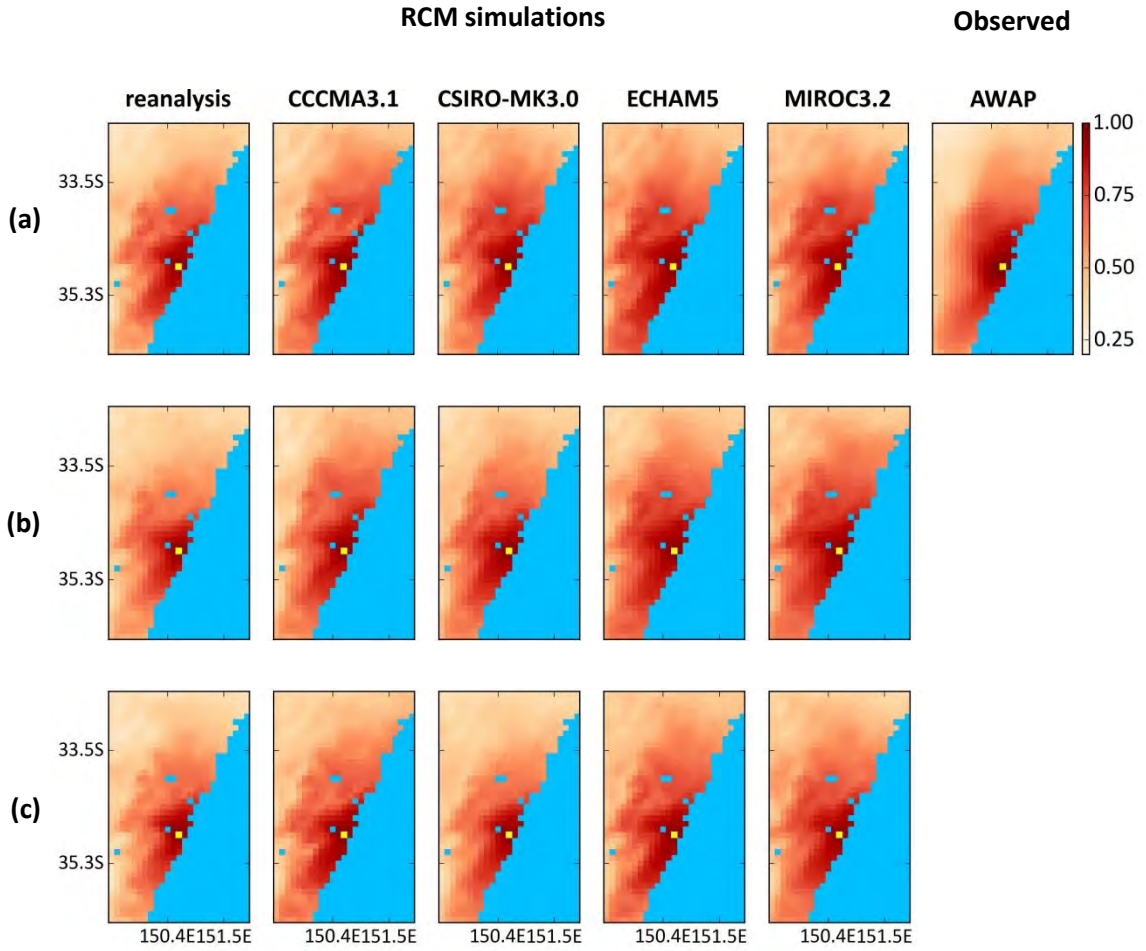

Figure A.15.65 Spatial correlations of daily rainfall between the reference grid point and all other grid points in the Sydney site. The plots are for the bias corrected simulations of (a) R1, (b) R2, and (c) R3 RCMs, and AWAP. The reference is S8, a low elevation grid point (shown in yellow boxes). The sky blue grid points inside the site are inland reservoirs updated with the bias correction.

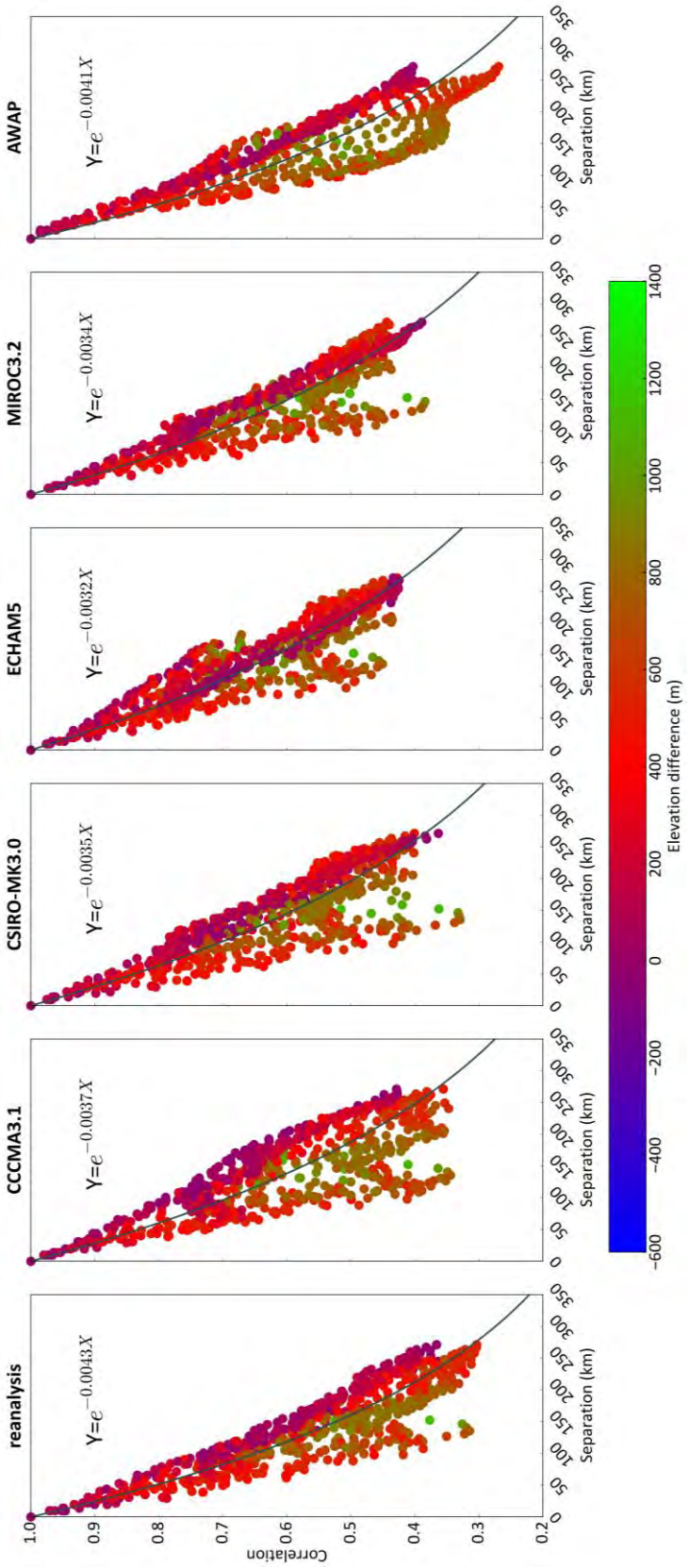

Figure A.15.66 Spatial correlations function (1990-2009) of the Sydney site. The reference is S8 low elevation grid point. The plots are for the bias corrected GCM simulations of R1 RCM and AWAP.

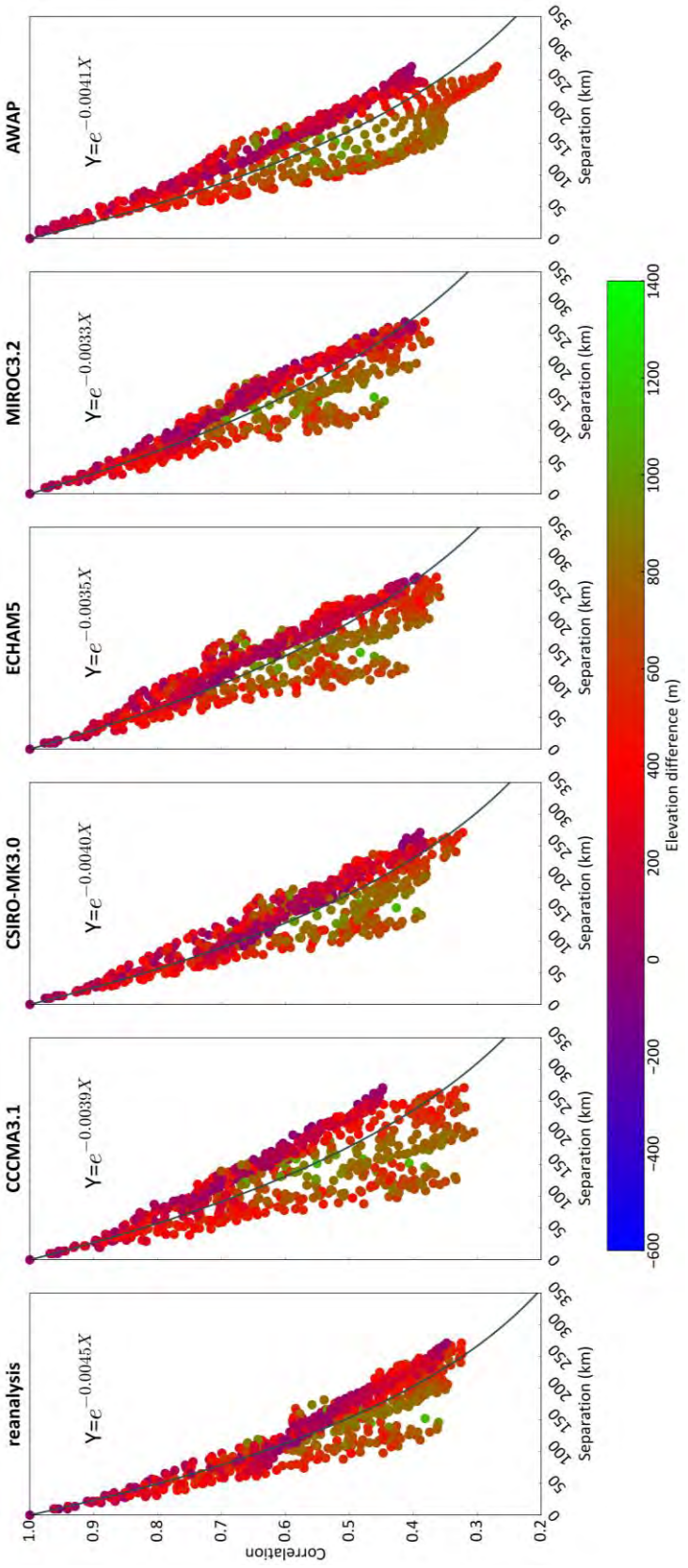

Figure A.15.67 Spatial correlations function (1990-2009) of the Sydney site. The reference is S8 low elevation grid point. The plots are for the bias corrected GCM simulations of R2 RCM and AWAP.

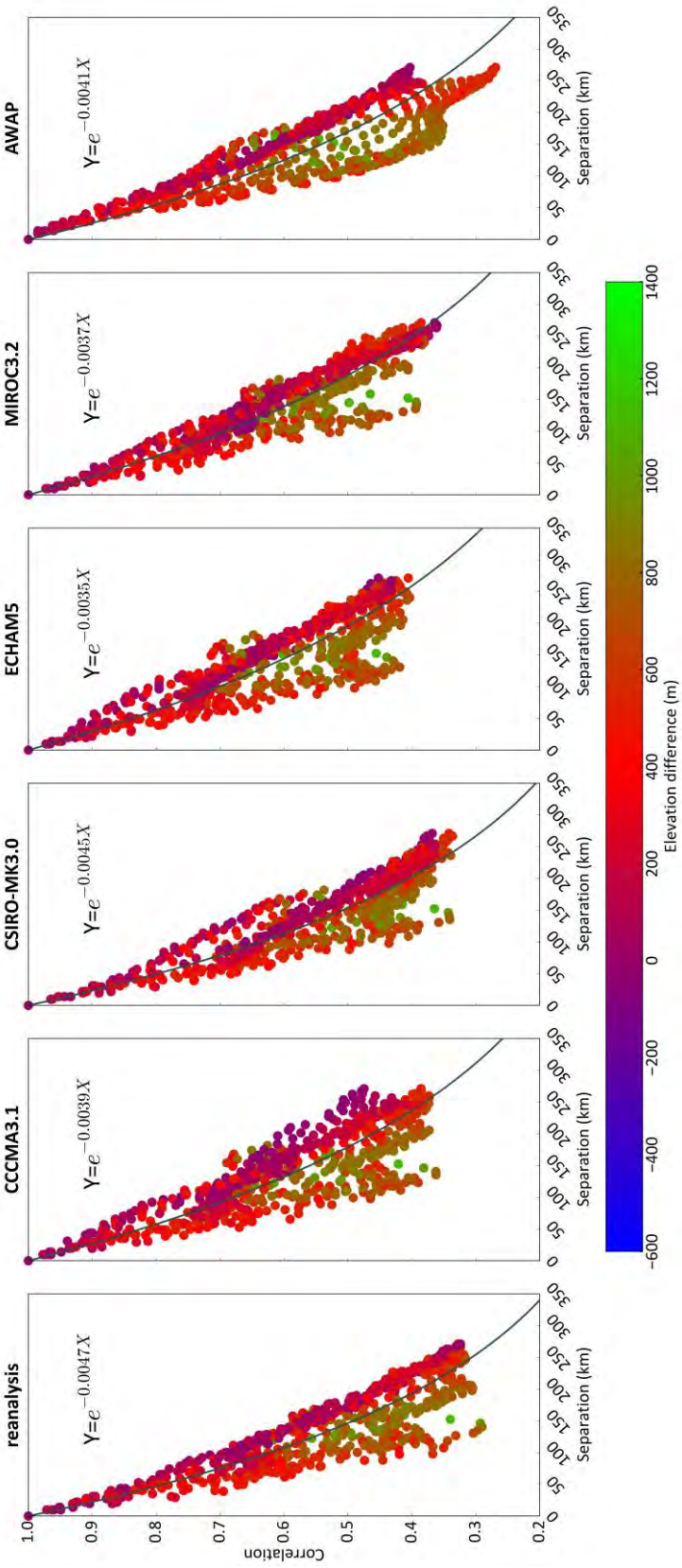

Figure A.15.68 Spatial correlations function (1990-2009) of the Sydney site. The reference is S8 low elevation grid point. The plots are for the bias corrected GCM simulations of R3 RCM and AWAP.

References

Anders, A. M. and Nesbitt, S. W. (2015), Altitudinal Precipitation Gradients in the Tropics from Tropical Rainfall Measuring Mission (TRMM) Precipitation Radar. *Journal of Hydrometeorology,* 16, 441–448, doi: 10.1175/JHM-D-14-0178.1.

Argüeso, D., Evans, J.P. and Fita, L. (2013), Precipitation bias correction of very high resolution regional climate models. *Hydrology and Earth System Sciences Discussions*, doi:10.5194/hessd-10-8145-2013.

Argüeso, D., Hidalgo-Muñoz, J.M., Gámiz-Fortis, S.R., Esteban-Parra, M.J., Castro Díez, Y. (2012), Evaluation of WRF Mean and Extreme Precipitation over Spain: Present Climate (1970–99), *Journal of Climate,* 25, 4883– 4897.

Bishop, C. H. and Abramowitz, G. (2013), Climate model dependence and the replicate Earth paradigm, *Climate Dynamics*, 41, 885–900, doi:10.1007/s00382-012-1610-y, 2013.

Bhend, J and Whetton, P .(2015), Evaluation of simulated recent climate change in Australia, *Journal of Southern Hemisphere Earth System Science,* 65, 4-18.

Box, G.E.P. and Cox, D.R. (1964), An Analysis of Transformations. *Journal of the Royal Statistical Society Series B-Statistical Methodology*, 26(2), 211–252.

Brooks, A.P. and Brierley, G.J. (1997), Geomorphic Responses of lower Bega River to catchment disturbance, 1851-1926, *Geomorphology*, 18, 291-304.

Browning, S.A. and Goodwin, I.D. (2013), Large-scale influences on the evolution of winter subtropical maritime cyclones affecting Australia's east coast. *Monthly Weather Review*, 141, 2416–2431, doi:10.1175/MWR-D-12-00312.1.

Browning, S.A. and Goodwin, I.D (2016). Large scale drivers of Australian East Coast Cyclones since 1871. *Journal of Southern Hemisphere Earth System Science*, 66, 125–151.

Callaghan J. and Power S.B. (2014), Major coastal flooding in southeastern Australia 1860-2012, associated deaths and weather systems. *Australian Meteorological and Oceanographic Journal, 64, 183–213.*

Caya, D., Laprise, R. (1999), A semi-implicit semi-lagrangian regional climate model: the Canadian RCM. *Monthly Weather Review*, 127:341–362.

Charles, A., Timbal, B., Fernandez, E., and Hendon, H. (2013), Analog downscaling of seasonal rainfall forecasts in the Murray darling basin, *Monthly Weather Review*, 141, 1099–1117, doi:10.1175/MWR- D-12-00098.1.

Chen, M. (2013), *On the Predictability of Hydrology Using Land Surface Models and Field Soil Moisture Data*, PhD thesis, The University of Newcastle, Callaghan, Australia.

Chen, J., Brissette, F. P. and Leconte, R. (2012), Coupling statistical and dynamical methods for spatial downscaling of precipitation, *Climatic Change*, 114(3-4), 509-526.

Chiew, F. H. S. (2006), Estimation of rainfall elasticity of streamflow in Australia, *Hydrological Sciences Journal-Journal Des Sciences Hydrologiques*, *51(4)*, 613-625.

Chiew, F. H. S., Potter, N.J., Vaze, J., Petheram, C., Zhang, L., Teng, J. and Post, D.A. 2014. Observed hydrologic nonstationarity in far south-eastern Australia: implications for modelling and prediction. *Stochastic Environmental Research and Risk Assessment*, 28(1), 3–15.

Chiew, F. H. S., Teng, J., Vaze, J. and Kirono, D. G. C. (2009), Influence of global climate model selection on runoff impact assessment, *Journal of Hydrology*, 379, 172–180.

Chowdhury,A.F.M.K. (2016), *Development and evaluation of stochastic rainfall models for drought security assessment*, PhD thesis, The University of Newcastle, Callaghan, Australia.

Chubb, T. H., Manton, M. J., Siems, S. T. and Peace, A. D. (2016), Evaluation of the AWAP daily precipitation spatial analysis with an independent gauge network in the Snowy Mountains, *Journal of Southern Hemisphere Earth Systems Science*, *66*, 55-67.

CSIRO and Bureau of Meteorology (2007), Climate Change in Australia. *Technical Report*. Australia. www.climatechangeinaustralia.gov.au.

CSIRO and Bureau of Meteorology (2015), Climate Change in Australia, *Technical Report*. Melbourne, Australia. www.climatechangeinaustralia.gov.au

de Szoeke, S. and Xie, S. (2008), The tropical eastern Pacific seasonal cycle: Assessment of errors and mechanisms in IPCC AR4 coupled ocean - Atmosphere

general circulation models, *Journal of Climate*, 21(11), 2573-2590, doi:10.1175/2007JCLI1975.1.

Daly, C., Neilson, R. P. and Phillips, D. L. (1994), A statistical–topographic model for mapping climatological precipitation over mountainous terrain. *Journal of Applied* Meteorology, 33, 140–158.

Diffenbaugh, N., Giorgi, F. and Pal, J. (2008), Climate change hotspots in the United States, *Geophysical Research Letters*, 35(16), doi:10.1029/2008GL035075.

Di Luca, A., Evans, J.P., Pepler, A., Alexander, L. and Argüeso, D. (2016), Comparing the model representation of East Coast Lows at various resolutions. *Journal of Southern Hemisphere Earth System Science*, 66, 108–124.

Dowdy, A.J., Grose, M.R., Timbal, B., Moise, A., Ekström, M., Bhend, J. and Wilson, L. (2015), Rainfall in Australia's eastern seaboard: areview of confidence in projections based on observations and physical processes*, Australian Meteorological and Oceanographic Journal*, 65, 107–126.

Evans, J.P. (2009a), 21st century climate change in the Middle East, *Climatic Change*, 92(3-4), 417-432.

Evans, J. P. (2009), Global warming impact on the dominant precipitation processes in the Middle East, *Theoretical and Applied Climatology*, *99(3)*, 389-402.

Evans, J.P. and Argüeso, D. (2014), Guidance on the use of bias corrected data, NARCliM Technical Note 3, 7pp., NARCliM Consortium, Sydney, Australia.

Evans, J.P., Argüeso, D., Di Luca, A., Olson, R., Ji, F., Lee, C., Riley, M. and Scorgie, Y. (2014a), *NSW Coastal Conference*, Ulladalla, NSW.

Evans, J. P., Ekström, M., and Ji, F. (2012), Evaluating the performance of a WRF physics ensemble over South-East Australia. *Climate Dynamics, 39*, 1241–1258, doi:10.1007/s00382-011-1244-5

Evans, J. P., Fita, L., Argüeso, D., and Liu, Y. (2013), Initial NARCliM Evaluation, *20th International Congress on Modelling and Simulation*, Adelaide, Australia, 1–6 December 2013

Evans, J. P., Ji, F., Lee, C., Smith, P., Argüeso, D., and Fita, L. (2014), Design of a regional climate modelling projection ensemble experiment – NARCliM, *Geoscientific Model Development* , *7(2)*, 621-629.

Evans, J. P., and McCabe, M. F. (2010), Regional climate simulation over Australia's Murray-Darling basin: A multitemporal assessment, *Journal of Geophysical Research-Atmospheres*, *115*, D14114, doi:10.1029/2010JD013816.

Evans, J. P., and McCabe, M. F., (2013), Effect of model resolution on a regional climate model simulation over southeast Australia, *Climate Research*, *56*, 131–145, doi:10.3354/cr01151.

Evans, J.P., Oglesby, R.J. and Lapenta, W.M. (2005), Time series analysis of regional climate model performance, Journal of Geophysical Research D: Atmospheres, 110(4), 1-23.

Evans, J. P., Smith, R.B., and Oglesby, R.J. (2004), Middle East climate simulation and dominant precipitation processes, *International Journal of Climatology*, *24(13)*, 1671-1694.

Evans, J.P. and Westra, S. (2012) Investigating the Mechanisms of Diurnal Rainfall Variability Using a Regional Climate Model*, Journal of Climate*, 25, 7232–7247, doi:10.1175/JCLI-D-11-00616.1.

Fu, G. B., Charles, S. P., Chiew, F. H. S. and Teng, J. (2011), Statistical downscaling of daily rainfall for hydrological impact assessment, *19th International Congress on Modelling and Simulation (Modsim 2011)*, 2803-2809.

Gallant, A. J. E., Kiem, A. S., Verdon-Kidd, D. C., Stone, R. C., and Karoly, D. J. (2012), Understanding hydroclimate processes in the Murray-Darling Basin for natural resources management. *Hydrology and Earth System Sciences,* 16, 2049-2068, doi:10.5194/hess-16-2049-2012.

Gleckler, P., Taylor, K. and Doutriaux, C. (2008), Performance metrics for climate models. *Journal of Geophysical Research: Atmospheres*, 113, D06104, doi: 10.1029/2007JD008972.

Giorgi, F., Jones, C. and Asrar, G.R. (2009) Addressing climate information needs at the regional level: the CORDEX frame work, *World Meteorological Organization – Bulletin*, 58: 175−183

Giorgi, F., Marinucci, M. R., and Bates, G. T. (1993a), Development of a second generation regional climate model (RegCM2). I. Boundary layer and radiative transfer processes, *Monthly Weather Review, 121*, 2794–2813.

Grose, M.R., Bhend, J., Argueso, D., Ekström, M., Dowdy, A.J., Hoffmann, P., Evans, J.P. and Timbal, B. (2015), *Australian Meteorological and Oceanographic Journal*, 65, 72–89.

Hawkins, E. and Sutton, R. (2009), The potential to narrow uncertainty in regional climate predictions, *Bulletin of the American Meteorological Society,* 90,1095e1107.

Hegerl, G., and Zwiers, F. (2011), Use of Models in Detection and Attribution of Climate Change. *Wiley Interdisciplinary Reviews: Climate Change*, 2, 570–591. http://dx.doi.org/10.1002/wcc.121.

Hutchinson, M. F. (1995) Interpolating mean rainfall using thin plate smoothing splines. *International Journal of Geographic Information Systems*, 9(4), 385–403.

Hutchinson, M. F. (1998a). Interpolation of rainfall data with thin plate smoothing splines: I Two dimensional smoothing of data with short range correlation. *Journal of Geographic Information and Decision Analysis*, 2, 139-151.

Hutchinson, M. F. (1998b). Interpolation of rainfall data with thin plate smoothing splines: II analysis of topographic dependence. *Journal of Geographic Information and Decision Analysis*, 2, 152 -167.

Hopkins, L. C., and Holland, G. J. (1997), Australian heavy-rain days and associated east coast cyclones: 1958-92, *Journal of Climate*, *10(4)*, 621-635.

Irving, D. B., Whetton, P. and Moise, A. F. (2012), Climate projections for Australia: a first glance at CMIP5, *Journal of Southern Hemisphere Earth System Science,* 62, 211-225.

IPCC (2007), *Climate Change 2007: The Physical Basis*. Contributions of Working Group 1 to the Fourth Assessment Report of the Intergovernmental Panel on Climate Change, Cambridge University Press. http://www.ipcc.ch

IPCC (2013), *Climate Change 2013*. The Physical Science Basis. Contribution of Working Group I to the Fifth Assessment Report of the Inter- governmental Panel on Climate Change. Cambridge University Press. http://www.ipcc.ch

Jeffrey, S. J., Carter, J. O., Moodie, K. B. and Beswick, A. R. (2001), Using spatial interpolation to construct a comprehensive archive of Australian climate data, *Environmental Modelling and Software*, 16(4), 309-330.

Ji, F., Ekström, M., Evans, J. P., and Teng, J. (2014), Evaluating rainfall patterns using physics scheme ensembles from a regional atmospheric model. *Theoretical and Applied Climatology*, *115*, 297–304, doi:10.1007/s00704-013-0904-2.

Ji, F., Riley, M., Clarke, H. , Evans, J.P., Argüeso, D. and Fita, L. (2013), High resolution rainfall projections for the Greater Sydney Region, *20th International Congress on Modelling and Simulation*, Adelaide, Australia, 1–6 December 2013 www.mssanz.org.au/modsim2013

Johns, T. C., and Coauthors (2006), The new Hadley Centre Climate Model (HadGEM1): Evaluation of coupled simulations. *Journal of Climate*, 19, 1327–1353.

Jones, D.A., Wang, W. and Fawcett, R. (2009), High-Quality Spatial Climate Data-Sets for Australia. *Australian Meteorological and Oceanographic Journal, 58*(4): 233–48.

Kalnay, E., Kanamitsu, M., Kistler, R., Collins, W., Deaven, D., Gandin, L., Iredell, M., Saha, S., White, G.,Woollen, J., Zhu, Y., Chelliah, M., Ebisuzaki, W., Higgins, W., Janowiak, J., Mo, K. C., Ropelewski, C., Wang, J., Leetmaa, A., Reynolds, R., Jenne, R., and Joseph, D. (1996), The NCEP/NCAR 40-year reanalysis project, *Bulletin of the American Meteorological Society*, *77*, 437–471.

Kendon, E., Jones, R., Kjellstrom, E. and Murphy, J. (2010), Using and Designing GCM-RCM Ensemble Regional Climate Projections, *Journal of Climate*, 23(24), 6485-6503, doi:10.1175/2010JCLI3502.1.

Kiem, A.S. and Franks, S.W. 2001. On the identification of ENSO-induced rainfall and runoff variability: a comparison of methods and indices. *Hydrological Science Journal*, 46(5), 715–727.

Kiem, A. S., and Verdon-Kidd, D. C. (2010), Towards understanding hydroclimatic change in Victoria, Australia – preliminary insights into the "Big Dry". *Hydrology and Earth System Sciences*, 14, 433–445, www.hydrol-earth-syst-sci.net/14/433/2010/.

Kiem, A. S., and Verdon-Kidd, D. C. (2011), Steps towards 'useful' hydroclimatic scenarios for water resource management in the Murray-Darling Basin. *Water Resources Research*, 47, W00G06, doi:10.1029/2010WR009803.

Kiem, A. S., Twomey, C., Lockart, N., Willgoose, G., Kuczera, G., Chowdhury, A.F.M.K., Parana Manage, N. and Zhang, L. (2016). Links between East Coast Lows and the spatial and temporal variability of rainfall along the eastern seaboard of Australia. *Journal of Southern Hemisphere Earth System Science*, 66, 162–176.

Kirono, D.G.C. and Kent, D.M. (2011). Assessment of rainfall and potential evaporation from global climate models and its implications for Australian

regional drought projection. *International Journal of Climatology*, 31, 1295-1308.

Knutti, R., Abramowitz, G., Collins, M., Eyring, V., Gleckler, P. J., Hewitson, B. and Mearns, L. O. (2010), Good practice guidance paper on assessing and combining multi model climate projections, *Meeting Report of the Intergovernmental Panel on Climate Change Expert Meeting on Assessing and Combining Multi Model Climate Projections*, edited by T. F. Stocker, D. Qin, G.-K. Plattner, M. Tignor, and P. M. Midgley, IPCC Working Group I Technical Support Unit, University of Bern, Bern, Switzerland.

Knutti, R., Meehl, G. A., Allen, M. R. and Stainforth, D. A. (2006), Constraining climate sensitivity from the seasonal cycle in surface temperature. *Journal of Climate*, 19, 4224–4233.

Kostopoulou, E., Tolika, K., Tegoulias, I., Giannakopoulos, C., Somot, S., Anagnostopoulou, C., and Maheras, P. (2009), Evaluation of a regional climate model using in situ temperature observations over the Balkan Peninsula, *Tellus Series A: Dynamic Meteorology and Oceanography*, *61(3)*, 357-370.

Koutsoyiannis, D., Efstratiadis, A., Mamassis, N., and Christofides, A. (2008), On the credibility of climate predictions. *Hydrological Sciences Journal,* 53(4), 671–684.

Kundzewicz, Z. W., Mata, L. J., Arnell, N., Döll,P., Kabat, P., Jiménez, B., Miller, K., Oki, T.,Şen, Z. and Shiklomanov, I. (2007) Freshwater resources and their management. Climate Change 2007: Impacts, Adaptation and Vulnerability. Contribution of Working Group II to the Fourth Assessment Report of the Intergovernmental Panel on Climate Change(ed. by Parry, M. L., Canziani, O. F. , Palutikof, J. P., van der Linden, P.J. and Hanson, C. E.), 173–210. Cambridge University Press, UK.

Lavery, B., Joung, G., and Nicholls, N. (1997), An extended high-quality historical rainfall dataset for Australia. *Australian Meteorological and Oceanographic Journal, 46,* 27-38.

Liu, Z., Mehran, A., Phillips, T. J. and AghaKouchak. A. (2014), Seasonal and regional biases in CMIP5 precipitation simulations, *Climate Research*, 60, 35-50.

Lockart, N., Willgoose, G.R., Kuczera, G.A., Kiem, A.S, Chowdhury, A.F.M., Parana Manage, N., Zhang, L. and Twomey, C. (2016). Case study on the use of dynamically downscaled climate model data for assessing water security in the

Lower Hunter region of the eastern seaboard of Australia. *Journal of Southern Hemisphere Earth System Science*, 66, 177–202.

Liu, D. L. and Zuo, H. P. (2012), Statistical downscaling of daily climate variables for climate change impact assessment over New South Wales, Australia, *Climatic Change*, 115(3-4), 629-666.

McMahon, T.A. 1964. *Hydrological features of the Hunter Valley, NSW*. The Hunter Valley Research Foundation Monographs, 20. Newcastle, NSW.

McMahon, T. A., Murphy, R. E., Peel, M. C., Costelloe, J. F., and Chiew, F. H. S. 2008. Understanding the surface hydrology of the Lake Eyre Basin: Part 1—Rainfall. *Journal of Arid Environments*, 72(10), 1853-1868.

Mariotti, A., Zeng, N., Yoon, J., Artale, V., Navarra, A., Alpert, P. and Li, L. (2008), Mediterranean water cycle changes: transition to drier 21st century conditions in observations and CMIP3 simulations, *Environmental Research Letters*, 3(4), doi:10.1088/1748-9326/3/4/044001.

Maxino,C. C., McAvaney, B. J., Pitman, A. J. and Perkins, S. E. (2008), Ranking the AR4 climate models over the Murray-Darling Basin using stimulated maximum temperature, minimum temperature and precipitation . *International Journal of Climatology*, 28(7), 983-983.

Meehl, G. A., Covey, C., Delworth, T., Latif, M., McAvaney, B., Mitchell, J. F. B., Stouffer, R. J., and Taylor, K. E. (2007), The WCRP CMIP3 multimodel dataset - A new era in climate change research, *Bulletin of the American Meteorological Society, 88(9)*, 1383-1394.

Mielke, P. W., Jr. (1985), Geometric concerns pertaining to applications of statistical tests in the atmospheric sciences, *Journal of Atmospheric Sciences*, 42, 1209-1212.

Mielke, P. W., Jr. (1991), The application of multivariate permutation methods based on distance functions in the earth sciences, *Earth Science Review*, 31, 55-71.

Min, S. K., Legutke, S., Hense, A., and Kwon,W.-T. (2005), Internal variability in a 1000-yr control simulation with the coupled climate model ECHOG –II. El niño Southern Oscillation and North Atlantic Oscillation, *Tellus A: Dynamic Meteorology and Oceanography*, 57, 622– 640.

Moise, A. and coauthors (2015), Evaluation of CMIP3 and CMIP5 Models over the Australian Region to Inform Confidence in Projections, *Journal of Southern Hemisphere Earth System Science,* 65, 19-53.

Murphy, B. and Timbal, B. (2008), A review of recent climate vari- ability and climate change in southeastern Australia. . *International Journal of Climatology*, 28, 859−879

Pal, J.S, Giorgi, F., Bi, X., Elguindi, N. and 16 others (2007) Regional climate modelling for the developing world: the ICTP RegCM3 and RegCNET. *Bulletin of the American Meteorological Society*, 88,1395–1409.

Pearson, K. 1895. Notes on regression and inheritance in the case of two parents. *Proceedings of the Royal Society of London*, 58, 240–242.

Pepler, A.S., Imielska, A., Coutts-Smith, A., Gamble, F. and Schweitzer, M. (2016), Identifying East Coast Lows with climate hazards on the eastern seaboard, *Journal of Southern Hemisphere Earth System Science*, 66, 97–107.

Parkinson, G. 1986. *Atlas of Australian Resources: Vol. 4, Climate.* Australian Surveying and Land Information Group, Australian Government Publishing Service: Canberra.

Parry, M. L., Canziani, O. F., Palutikof, J. P., van der Linden, P. J., and Hanson, C.E. (2007), *"Climate Change 2007: Impacts, Adaptation and Vulnerability. Contribution of Working Group II to the Fourth Assessment Report of the Intergovernmental Panel on Climate Change",* Cambridge University Press, Cambridge, UK, 976.

Perkins, S. E., Pitman, A. J., Holbrook, N. J. and McAneney, J. (2007), Evaluation of the AR4 Climate Models' Simulated Daily Maximum Temperature, Minimum Temperature, and Precipitation over Australia Using Probability Density Functions, *Journal of Climate*, 20(17), 4356-4376.

Piani, C., Frame, D. J., Stainforth, D. A. and Allen, M. R. (2005), Constraints on climate change from a multi-thousand member ensemble of simulations. *Geophysical Research Letters*, 32, L23825, doi:10.1029/2005GL024452.

Piani, C., Haerter, J., and Coppola, E. (2010a), Statistical bias correction for daily precipitation in regional climate models over Europe, *Theoretical and Applied Climatology*, 99, 187–192.

Piani, C.,Weedon, G. P., Best, M., Gomes, S. M., Viterbo, P., Hage- mann, S., and Haerter, J. O. (2010b), Statistical bias correction of global simulated daily

precipitation and temperature for the application of hydrological models, *Journal of Hydrology*, 395, 199–215.

Randall, D. A., Wood, R. A., Bony, S., Colman, R., Fichefet, T., Fyfe, J., Kattsov, V., Pitman, A., Shukla, J., Srinivasan, J., Stouffer, R. J., Sumi, A., and Taylor, K. E. (2007), Climate Models and Their Evaluation. In *"Climate Change 2007: The Physical Science Basis. Contribution of Working Group I to the Fourth Assessment Report of the Intergovernmental Panel on Climate Change"* (Eds: Solomon, S., Qin, D., Manning, M., Chen, Z., Marquis, M., Averyt, K.B., Tignor, M. and Miller, H.L.), Cambridge University Press, Cambridge, United Kingdom and New York, USA.

Raupach, M.R., Briggs, P.R., Haverd, V., King, E.A., Paget, M. and Trudinger, C.M. (2009), Australian Water Availability Project (AWAP): CSIRO Marine and Atmospheric Research Component: Final Report for Phase 3. *CAWCR Technical Report 13*. Centre for Australian Weather and Climate Research, Melbourne, 67.

Raupach, M.R., Briggs, P.R., Haverd, V., King, E.A., Paget, M. and Trudinger, C.M. (2012), *Australian Water Availability Project*. CSIRO Marine and Atmospheric Research, Canberra, Australia.

Reichler, T. and Kim, J. (2008), How well do coupled models simulate today's climate?, *Bulletin of the American Meteorological Society*, 89, 303–311.

Risbey, J.S., Pook, M.J., McIntosh, P.C., Wheeler, M.C., Hendon, H.H. (2009), On the remote drivers of rainfall variability in Australia.Mon Weather Rev 137: 3233−3253

Rodriguez-Iturbe, I. and Mejía, J. M. (1974), On the transformation of point rainfall to areal rainfall, *Water Resources Research*, 10(4), 729–735, doi:10.1029/WR010i004p00729.

Salon, S., Cossarini, G., Libralato, S., Gao, X., Solidoro, C., and Giorgi, F. (2008), Downscaling experiment for the Venice lagoon. I. Validation of the present-day precipitation climatology, *Climate Research*, *38(1)*, 31- 41.

Sankarasubramaniam, A., Vogel, R.M., and Limburner, J. F. (2001), Climate elasticity of streamflow in the United States, *Water Resources Research*, 37, 1771–1781.

Shand, T. D., Goodwin, I. D., Mole, M. A., Carley, J. T., Coghlan, I. R., Harley, M. D., and Peirson, W. L. (2010), NSW Coastal Inunda- tion Hazard Study: Coastal

Storms and Extreme Waves, *WRL Technical Report*, UNSW Water Research Laboratory, Sydney, Australia.

Shukla, J., DelSole, T., M. Fennessy, M., Kinter, J. and Paolino, D. (2006), Climate model fidelity and projections of climate change. *Geophysical Research Letters*, 33, L07702, doi:10.1029/2005GL025579.

Siriwardena, L., Finlayson, B. L. and McMahon, T. A. (2006), The impact of land use change on catchment hydrology in large catchments: The Comet River, Central Queensland, Australia. Journal of Hydrology, 326(1–4), 199-214.

Skamarock,W. C., Klemp, J. B., Dudhia, J., Gill, D. O., Barker, D. M., Duda, M. G., Huang, X.-Y.,Wang,W., and Powers, J. G. (2008), A Description of the Advanced Research WRF Version 3, NCAR Technical Note, NCAR, Boulder, CO, USA.

Smith, R. B. (1979), The influence of mountains on the atmosphere, *Advances in Geophysics,* 21, 87–230

Smith, I., Syktus, J., McAlpine, C. and Wong, K. (2013), Squeezing information from regional climate change projections – results from a synthesis of CMIP5 results for south-east Queensland, Australia. *Climatic Change*, 121, 609-619, doi: 10.007/s10584-013-0956-4.

Smith, I. and Chandler, E. (2010), Refining rainfall projections for the Murray Darling Basin of south-east Australia-the effect of sampling model results based on performance, *Climatic Change*, 102, 377– 393, doi:10.1007/s10584-009-9757-1.

Solman, S. and Nunez, M. (1999) Local estimates of global climate change: a statistical downscaling approach, *International Journal Climatology*, 19:835–861

Solomon, S., D. Qin, M. Manning, Z. Chen, M. Marquis, K. B. Averyt, M. Tignor, and H. L. Miller, Eds., 2007: *Climate Change 2007*: The Physical Science Basis. Cambridge University Press, 996 pp.

Song, R., Gao, X., Zhang, H., and Moise, A. (2008), 20 km resolution regional climate model experiments over Australia: Experimental design and simulations of current climate, *The Australian Meteorological Magazine*, *57(3)*, 175–193

Speer, M.S., Wiles, P. and Pepler, A.S. (2009). Low pressure systems off the New South Wales coast and associated hazardous weather: Establishment of a database. *Australian Meteorological and Oceanographic Journal*,58, 29–39

Stainforth, D. A., Allen, M. R., Tredger, E. R., and Smith, L. A. (2007), Confidence, uncertainty and decision-support relevance in climate predictions. *Philosophical Transactions of the Royal Society A, 365,* 2145-2161; doi:10.1098/rsta.2007.2074.

Stephens, E.M., Edwards, T.L., and Demeritt, D. (2012), Communicating probabilistic information from climate model ensembles—lessons from numerical weather prediction. *Wiley Interdisciplinary Reviews- Climate Change 2012, 3(5)*, 409–426, doi:10.1002/wcc.187.

Stott, P. A., Gillett, N. P., Hegerl, G. C., Karoly, D. J., Stone, D. A., Zhang, X. and Zwiers, F. (2010), Detection and Attribution of Climate Change: A Regional Perspective. *Wiley Interdisciplinary Reviews Climate Change*, 1, 192–211.

Sun, Y., Solomon, S., Dai, A., and Portmann, R. W. (2007) How often will it rain? *Journal of Climate*, 20, 4801–4818, doi:10.1175/JCLI4263.1.

Suppiah, R., Hennessy, K., Whetton, P. H., McInnes, K., Macadam, I., Bathols, J., Ricketts, J. and Page, C. M. (2007), Australian climate change projections derived from simulations performed for the IPCC 4th Assessment Report, *Journal of Southern Hemisphere Earth System Science* (formerly known as Australian Meteorological Magazine), 56(3), 131-152.

Taylor, K. E. (2001), Summarizing multiple aspects of model performance in a single diagram, *Journal of Geophysical Research*, 106 (D7), 7183–7192.

Taylor, K.E., Stouffer, R.J. and Meehl, G.A. (2012), An Overview of CMIP5 and the Experiment Design, *Bulletin of the American Meteorological Society*, 93, 485-498.

Tebaldi, C and Knutti, R. (2007), The use of themulti-model ensemble in probabilistic climate projections, *Philosophical Transactions of the Royal Society,* A365, 2053–2075

Thompson, G., Rasmussen, R. M. and Manning, K. (2004), Explicit forecasts of winter precipitation using an improved bulk microphysics scheme. Part I: Description and sensitivity analysis, *Monthly Weather Review*, 132(2), 519–542.

Timbal, B., (2010), The climate of the Eastern Seaboard of Australia: a challenging entity now and for future projections, *IOP Conference Sereis: Earth Environ. Science (EES)*, 11, 012013.

Timbal, B. and W. Drosdowsky, (2013), The relationship between the decline of South-eastern Australia rainfall and the strengthening of the sub- tropical ridge. *International Journal of Climatology*., 33, 1021:1034, doi:10.1002/joc.3492.

Trenberth, K. E. (1998), Atmospheric moisture residence times and cycling: Implications for rainfall rates with climate change. *Climatic Change*, 39, 667–694.

Tozer, C.R., Kiem, A.S. and Verdon-Kidd, D.C. (2012), On the uncertainties associated with using gridded rainfall data as a proxy for observed. Hydrology and Earth System Sciences, 16, 1481–1499, doi:10.5194/hess-16-1481-2012.

van Oldenborgh, G. J., Philip, S. Y., and Collins, M. (2005), El Niño in a changing climate: a multi-model study*, Ocean Science*, 1, 81–95, doi:10.5194/os-1-81-2005.

Vaze, J., Teng, J. and Chiew, F.H.S. (2011). Assessment of GCM simulations of annual and seasonal rainfall and daily rainfall distribution across south-east Australia. *Hydrological Processes*, 25, 1486-1497.

Vavrus, S., Waliser, D., Schweiger, A. and Francis, J. (2009), Simulations of 20th and 21st century Arctic cloud amount in the global climate models assessed in the IPCC AR4, *Climate Dynamics*, 33(7-8), 1099- 1115, doi:10.1007/s00382-008-0475-6.

Verdon-Kidd, D. C., Kiem, A. S., Willgoose, G., and Haines, P. (2010), *East Coast Lows and the Newcastle/Central Coast Pasha Bulker storm*, Report for the National Climate Change Adaptation Research Facility (NCCARF), Gold Coast, Australia

Verdon-Kidd, D.C., Kiem, A.S. and Willgoose, G. (2016) East Coast Lows and the Pasha Bulker storm – lessons learned eight years on. Journal of Southern Hemisphere Earth System Science, 66, 152–161.

Verdon, D. C., Wyatt, A.M., Kiem, A.S. and Franks, S.W. (2004). Multi-decadal variability of rainfall and streamflow - Eastern Australia. Water Resources Research.,40(10), W10201, doi:10.1029/2004WR003234

Woldemeskel, F. M., Sharma, A., Sivakumar, B. and Mehrotra, R. (2012), An error estimation method for precipitation and temperature projection for future climates, *Journal of Geophysical Research - Atmospheres*, 117.

Watterson, I. G. (1996), Non-dimensional measures of climate model performance, *International Journal of Climatology*, 16, 379–391.

Watterson, I. G. (2008), Calculation of probability density functions for temperature and precipitation change under global warming, *Journal of Geophysical Research: Atmospheres*, 113, D12106, doi:10.1029/2007JD009254.

Whetton, P.H., McInnes, K.L., Jones, R.N., Hennessy, K.J., Suppiah, R., Page, C.M., Bathols, J. and Durack, P. (2005), Climate change projections for Australia for impact assessment and policy application: *A review. CSIRO Technical Paper*. 001, Aspendale, Vic., CSIRO Marine and Atmospheric Research, 34p. http://www.cmar.csiro.au/e-print/open/whettonph_2005a.pdf

Wigley, T. M. L., and Jones, P. D. (1985), Influence of precipitation changes and direct CO_2 effects on stream flow, *Nature 314*, 149–152.